AD NUMBER:	AD0520957
CLASSIFICATION CHANGES	
TO:	Unclassified
FROM:	Confidential
LIMITATION CHANGES	
TO:	Approved for public release; distribution is unlimited.
FROM:	Distribution authorized to U.S. Gov't. agencies and their contractors; Critical Technology; 1 Oct 1970. Other requests shall be referred to Air Force Rocket Propulsion Laboratory, Edwards AFB, CA 93523.
AUTHORITY	
	C to U, 31 Oct 1982, Group 4, DoDD 5200.10; ST-A per AFRL ltr dtd 5 Feb 1986

SECURITY MARKING

The classified or limited status of this report applies to each page, unless otherwise marked.
Separate page printouts MUST be marked accordingly.

CONFIDENTIAL

AFRPL-TR-70-127

(UNCLASSIFIED TITLE)

ADVANCED MANEUVERING PROPULSION TECHNOLOGY PROGRAM--INTERIM FINAL REPORT (VOLUME I: FLUORINE/HYDROGEN ENGINE SYSTEM ANALYSIS AND DESIGN)

Rocketdyne
A Division of North American Rockwell Corporation
6633 Canoga Avenue
Canoga Park, California

Technical Report AFRPL-TR-70-127

October 1970

Group 4
Downgraded at 3-Year Intervals
Declassified After 12 Years

In addition to security requirements which must be met, this document is subject to special export controls and each transmittal to foreign governments or foreign nationals may be made only with prior approval of AFRPL(RPPR/STINFO), Edwards, California, 93523.

Air Force Rocket Propulsion Laboratory
Air Force Systems Command
United States Air Force
Edwards Air Force Base, California

CONFIDENTIAL

CONFIDENTIAL

AFRPL-TR-70-127

(UNCLASSIFIED TITLE)

ADVANCED MANEUVERING PROPULSION TECHNOLOGY PROGRAM--INTERIM FINAL REPORT (VOLUME I: FLUORINE/HYDROGEN ENGINE SYSTEM ANALYSIS AND DESIGN)

ROCKETDYNE
A Division of North American Rockwell Corporation
6633 Canoga Avenue
Canoga Park, California

Technical Report AFRPL-TR-70-127

October 1970

Group 4
Downgraded at 3-Year Intervals
Declassified After 12 Years

Air Force Rocket Propulsion Laboratory
Air Force Systems Command
United States Air Force
Edwards Air Force Base, California

CONFIDENTIAL

FOREWORD

(U) This technical report presents the results of Task I, Engine System Analysis and Design, and Task II, Engine Critical Component Demonstration Testing, conducted as part of the Advanced Maneuvering Propulsion Technology (AMPT) Program. The program conducted by Rocketdyne, a Division of North American Rockwell, during the period of November 1967 to June 1970, was authorized by the USAF Rocket Propulsion Laboratory under contract F04611-67-C-0116.

(U) The Air Force program manager was Mr. R. L. Wiswell and the Air Force project engineer was Mr. W. W. Wells. Mr. R. R. Morin was the Rocketdyne program manager, Mr. H. G. Diem the Rocketdyne assistant program manager, and Mr. D. H. Huang the Rocketdyne project engineer.

(U) This report was submitted on 31 July 1970 as Rocketdyne report number R-8280, Volumes I and II. These volumes are:

- I. Engine System Analysis and Design
- II. Engine Critical Component Demonstration Testing

(U) Task III of the program, Propellant Feed System Analysis and Design, was conducted by two vehicle company subcontractors (General Dynamics/Convair and Lockheed Missiles and Space Company), and the results are published separately as reports AFRPL-TR-70-103 and AFRPL-TR-70-104, respectively.

(U) A separate Materials and Processes report was published as AFRPL-TR-70-126.

(U) This technical report has been reviewed and is approved.

R. L. Wiswell,
AFRPL AMPT Program Manager,
RPRES

ABSTRACT

(U) The analysis and design studies conducted on the fluorine/hydrogen engine system of the Advanced Maneuvering Propulsion System (AMPS) are presented. The work included the engine system, thrust chamber assemblies, turbopump assemblies, and controls. Design requirements, design tradeoffs, operating characteristics, and layout drawings are shown for the major components and system.

CONTENTS

ILLUSTRATIONS

TABLES

ABBREVIATIONS AND SYMBOLS

AMPS	Advanced Maneuvering Propulsion System
B-4A	test stand designation at the Nevada Field Laboratory
C_p	specific heat
CRES	corrosion-resistant steel
C_u	pump volute diffuser change in tangential component of velocity
C_2	pump volute diffuser inlet velocity
C_3	pump volute diffuser outlet velocity
D	pump diffusion factor
FTV	fuel turbine valve
FMEA	failure mode and effects analysis
GD/C	General Dynamics Convair
h_g	heat transfer coefficient
ID	inside diameter
k	thermal conductivity
K_{FTV}	fuel turbine valve slew rate response to current
K_{OTV}	oxidizer turbine valve slew rate response to current
LMSC	Lockheed Missiles and Space Company
MFV	main fuel valve
MOV	main oxidizer valve
MR	mixture ratio
0	solidity = chord length/spacing
OD	outside diameter
OTV	oxidizer turbine valve

SECTION I

(U) INTRODUCTION

(U) The Advanced Maneuvering Propulsion Technology (AMPT) Program is being conducted to provide technology advancements applicable to future high-energy advanced maneuvering propulsion systems. The first portion of the program, reported in this volume, was conducted during the period of November 1967 to June 1970, and was devoted to a fluorine/hydrogen (F_2/H_2) propulsion system. A typical system is illustrated in Fig. 1 with some of the basic design parameters for the Advanced Development Program (ADP), together with some of the design variations that were also considered.

(C) The fluorine/hydrogen engine configuration (Fig. 2) utilized concentric thrust chambers. The outer main thrust chamber (30,000 pounds thrust) incorporated the toroidal-aerodynamic spike design concept. The inner secondary thrust chamber (3300 pounds thrust) was a bell-type design. The thrust chambers were fed from independent turbopumps that are driven by hot gases from each thrust chamber. Each thrust chamber can be throttled over a 9:1 thrust range, which gives the engine system an overall throttle ratio of 81:1. The normal mode of operation was for the thrust chambers to fire one at a time.

(C) The fluorine/hydrogen propellant feed system consists of the main propellant tankage; thermal conditioning and support structure; zero-gravity expulsion system; fill, vent, feed, and drain lines; propellant management system; and a pressurization system. The 18,000-pound weight for the complete propulsion system, together with a 2000-pound payload (20,000 pounds total), is compatible with the present Titan III-D launch vehicle for polar orbit launches from the Air Force Western Test Range. A gimbal angle of ±10 degrees was selected to provide the capability for rapid turning maneuvers. System thermal design provides the capability of at least 14 days in orbit with no fluorine loss and with very little hydrogen loss, depending on the mission duty cycle.

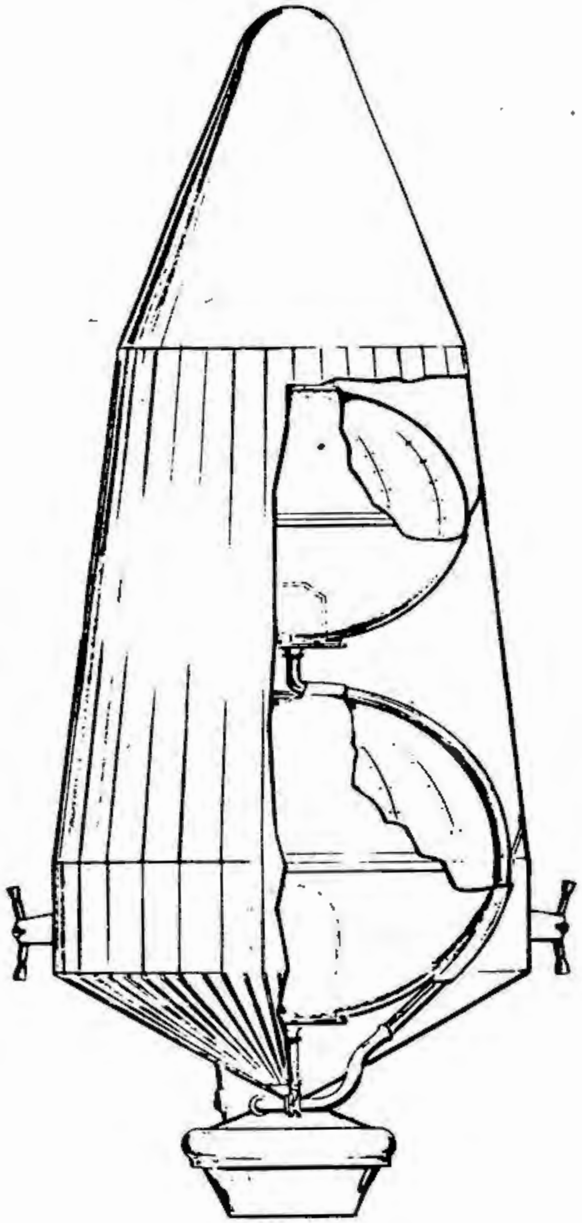

	DESIGN POINT FOR ADP	DESIGN VARIATIONS BEING CONSIDERED
PROPULSION SYSTEM WEIGHT, LB	18,000	10,000 TO 75,000
PAYLOAD WEIGHT, LB	2,000	1,000 TO 25,000
THRUST (MAXIMUM), LB	30,000	VARIATIONS WITH STAGE SIZE & APPLICATION
LAUNCH VEHICLE	TITAN III D	FAMILY OF LAUNCH VEHICLES
SPACE RESIDENCE TIME	14 DAYS (NO F_2 VENTING)	UP TO 180 DAYS
RESTARTS	30 MINIMUM	VARIATIONS WITH MISSION REQUIREMENTS
PAD HOLD CAPABILITY	• NO F_2 VENTING • H_2 VENTING & TOPPING	NEAR INSTANT LAUNCH READINESS
FLIGHT PLAN	• NO SUBORBITAL BURN • 100 NM, CIRCULAR POLAR ORBIT	DEPENDENT ON APPLICATION

CONFIDENTIAL

Figure 1. System Characteristics (U)

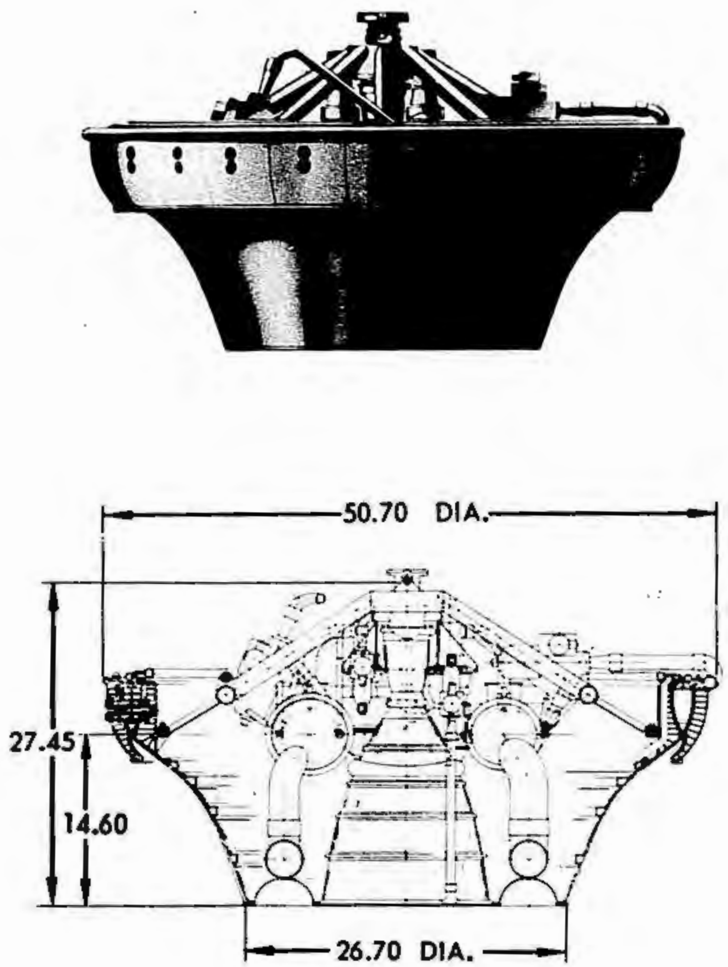

PARAMETER	MAIN ENGINE	SECONDARY ENGINE
THRUST, POUNDS	30,000	3,300
CHAMBER PRESSURE, PSIA	650	750
VACUUM SPECIFIC IMPULSE, SECONDS	460	457.5
MIXTURE RATIO, O/F	12:1	12:1
THROTTLE RATIO	9:1	9:1
AREA RATIO	60:1	60:1

Figure 2. Engine System for Advanced Maneuvering Propulsion System (U)

(C) The AMPT Program for the fluorine/hydrogen propulsion system originally consisted of two phases. Phase I of the program, which was for a 32-month period, included the following three tasks:

Task I: Engine Analysis and Design

Task II: Engine Critical Component Demonstration Testing

Task III: Propellant Feed System Analysis and Design

(U) Tasks I and II were accomplished by Rocketdyne, and Task III was performed by two vehicle company subcontractors--General Dynamics/Convair and Lockheed Missiles and Space Company.

(U) Phase II of the program was to provide for detail design, fabrication, and demonstration test of the complete propulsion system. The system, of flight-type design, was to be based on engine and propellant feed system design analyses and layout drawings generated in Phase I. Phase II of the program was not accomplished, however, because of redirection of the program by the Air Force. This volume of the report covers the work performed on the engine analysis and design (Task I) for the fluorine/hydrogen propulsion system.

SECTION II

(U) SUMMARY

(U) This volume of the report summarizes the work performed on Task I of the AMPT Program. This task provided for design and analysis of the complete engine system. Maximum use was made of the test results obtained during the critical component testing (Task II) in arriving at the final optimized engine design. The engine system design and analysis included those propellant feed system considerations necessary to ensure the compatibility of the total propulsion system. The status of high-energy F_2/H_2 propulsion technology was assessed and, with the results of tradeoff studies and comparisons, a recommended high-energy system design was defined. Mode of failure analyses were conducted on the final design of all critical engine components. The Task I effort was divided into four areas: engine system, thrust chamber assemblies, turbopump assemblies, and controls. The approach used is illustrated in Fig. 3 .

1. ENGINE SYSTEM DESIGN

(C) The engine system was designed to deliver the maximum performance practically attainable, using advanced technology and staying within the engine design constraints listed in Table 1 . The engine design allows for high reliability and a minimum of required maintenance. For maximum effectiveness, the engine is capable of rapid starting and operation with a minimum of time lost for chilldown or thermal conditioning of the engine between firing cycles. Tradeoff studies were conducted for the pump drive cycle method (hot combustion gas tapoff versus H_2 tapoff drive). An additional design goal was that the engine system include provisions for long life (10 hours), refurbishment, and reuse. The basic engine design is suitable for unmanned and manned missions.

2. THRUST CHAMBER ASSEMBLIES

(U) Analyses were conducted to determine the operational requirements for the thrust chambers and injectors. Flowrates, pressure drops, chamber contours, cooling requirements, and operating temperatures were determined

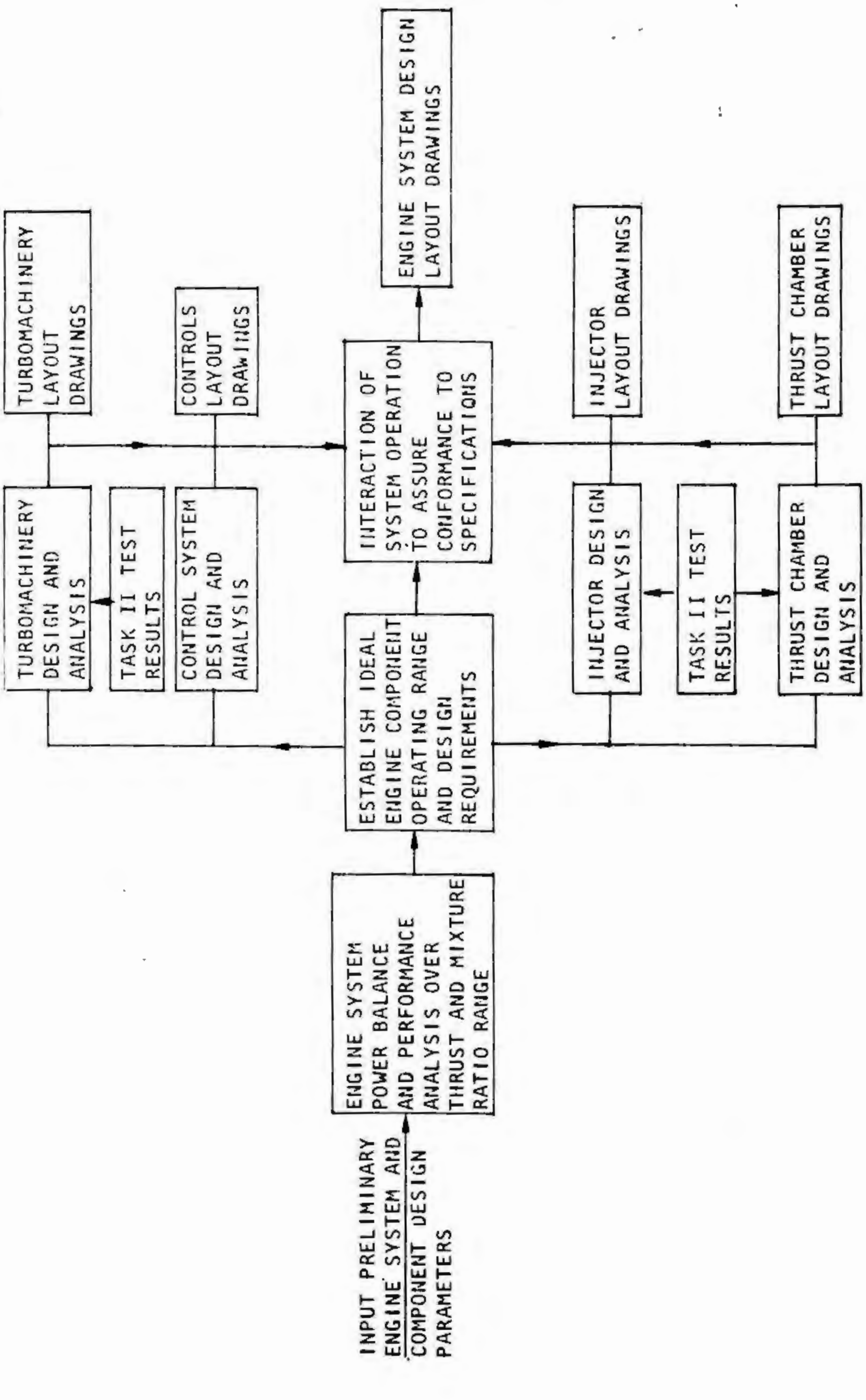

Figure 3. Flow Chart for Task I Engine System Analysis and Design Effort (U)

TABLE 1

BASIC PROPULSION SYSTEM OPERATING PARAMETERS (U)

Propulsion System Weight, pounds	18,000
Payload Weight, pounds	2000
Maximum Thrust, pounds	30,000
Thrust/Weight Ratio At maximum thrust and maximum gross weight of propulsion system plus payload	1.5
Minimum Delivered Performance, c* (shifting), percent	97
Throttling Range	81:1
Restart Capability (minimum)	30
Engine Life, hours	10
Gimbal Angle, degrees	±10
Propellants	LF_2/LH_2
Space Residence Time, days (minimum)	14
Pad Hold Capability (no fluorine loss)	Indefinite
Launch Criteria	
Maximum Diameter, feet	10
Environment and Loads	Titan III-C without Transtage

Mission

Intercept

Rendezvous

Evasive maneuvers with reconnaissance maneuvering capability

(U) for both maximum and minimum thrust for both the main and secondary thrust chambers. Thermal conditioning requirements for the thrust chamber and the injectors, together with associated nonpropulsive propellant losses, were determined. Maximum use of Task II test results was made in arriving at the final thrust chamber and injector designs.

3. TURBOPUMPS

(U) The design and operational requirements of the complete turbopump assemblies over the design throttling range, including turbines, pumps, inducers, seals, and bearings, were defined. Tradeoff studies were conducted and included pump hydrodynamics, turbine gas dynamics, and throttling. The analysis and design studies included materials selection, stress analysis, dynamics studies, and turbopump and component layout drawings. Thermal conditioning studies and life and reliability studies were also conducted.

4. CONTROLS

(U) The engine control system was defined as those components which control the engine system mixture ratio, the thrust level, and the start and shutdown sequences. Analyses were conducted to determine the operational requirements for all of the engine control system components. The analyses included defining the start and shutdown sequences, throttling control system, valves, and engine control components. Computer models of the engine system were synthesized, and transient aspects of the engine control system were investigated.

SECTION III

ENGINE SYSTEM

1. ENGINE SYSTEM DESCRIPTION

(C) The AMPS engine system design consists of a concentric thrust chamber arrangement with a main aerospike engine and a secondary bell engine, which is located in the center of the main engine (Fig. 4). The main engine provides a maximum thrust of 30,000 pounds and is throttleable to 3330 pounds. The secondary engine provides a maximum thrust of 3330 pounds and a minimum thrust of 370 pounds. The main engine has a maximum operating chamber pressure of 650 psia, and the secondary engine has a maximum operating chamber pressure of 750 psia.

(C) Both engines are pump-fed and regeneratively cooled, and both engines operate on a liquid bipropellant combination of fluorine (oxidizer) and hydrogen (fuel). The main engine turbopumps are driven by hot hydrogen gas which is tapped off from the thrust chamber just before the fuel enters the injector. The hydrogen is heated in the regenrative cooling jacket. The secondary engine turbopumps are driven by fuel-rich gas which is tapped directly from the combustion chamber.

(C) The main and secondary engine turbopumps are centrifugal types which are directly driven by velocity-compounded turbines operated in parallel by the drive gases. Heat exchangers for helium pressurant can be located in the turbine exhaust gas ducts if required. Warm hydrogen for tank pressurization may be drawn from the exit of the coolant circuit if desired.

(C) The engines operate sequentially and provide for a continuous thrust variation of 81:1. The system is designed for multiple starts at altitude. The main engine start is accomplished by tank pressure-fed operation, with the turbine drive gases bled from the cooling jacket exit to provide power to accelerate the turbopumps. The secondary

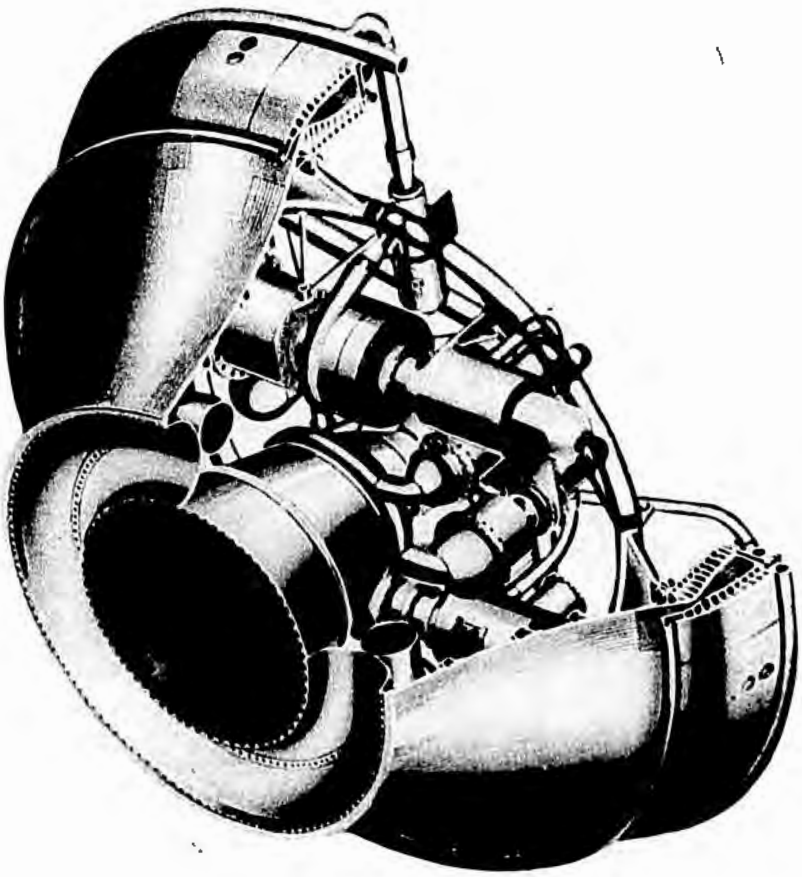

Figure 4. Engine Assembly (U)

engine utilizes helium gas supplied at a constant pressure from the engine-mounted helium regulator to provide power to accelerate the turbopumps. Transfer to hot-gas tapoff drive gases is accomplished after combustion has been established in the thrust chamber.

(C) The control system for each engine consists of main propellant valves (two valves) located upstream of the turbopumps, and turbine control valves (two valves) in the turbine feed lines just upstream of the turbines. Engine operation is controlled by a system which receives guidance system commands and engine parameter feedback, and then computes the engine control signals. An engine system layout drawing is shown in Fig. 5. The system is depicted schematically in Fig. 6. The major engine design parameters are shown in Table 2.

CONFIDENTIAL

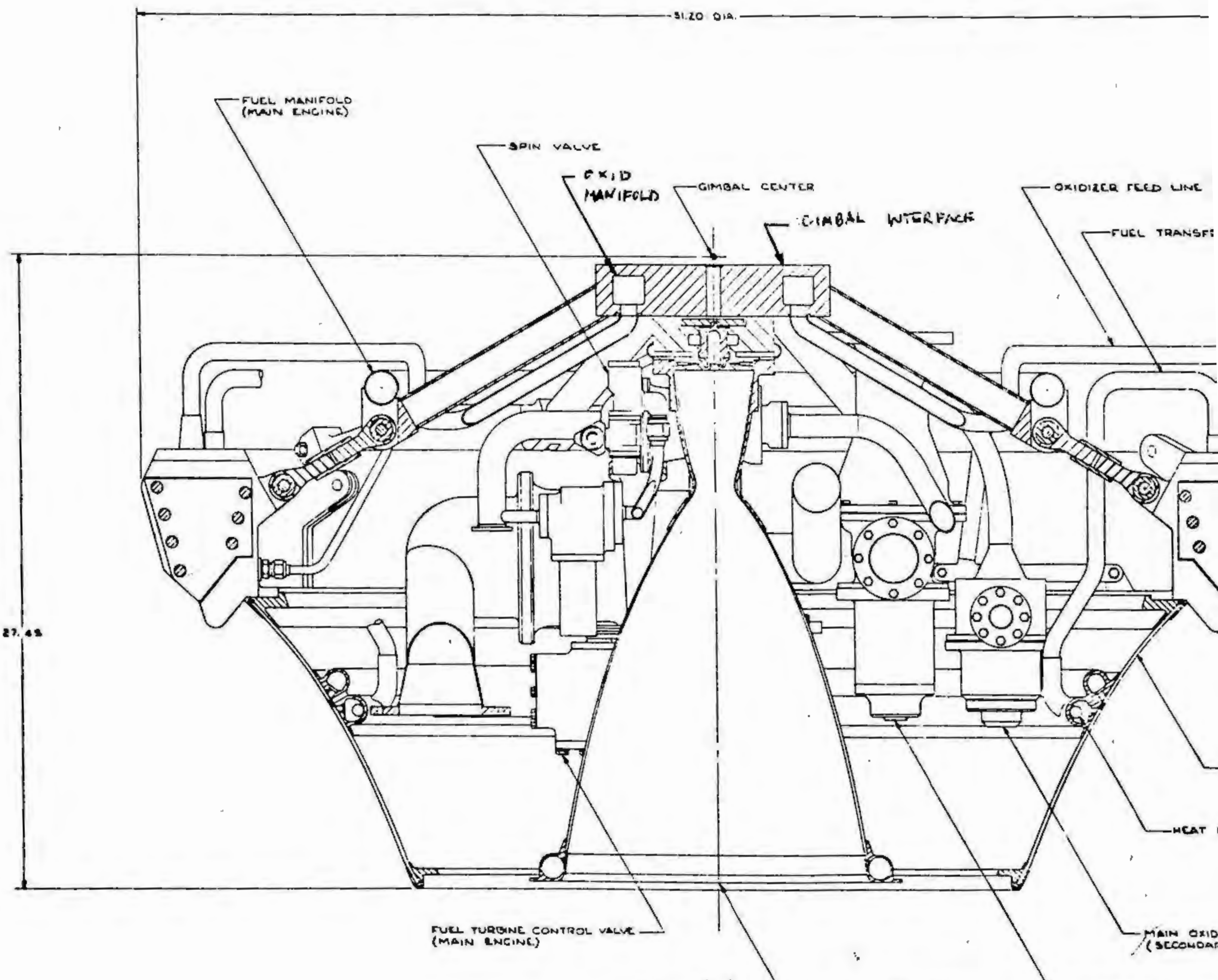

SECTION A-A

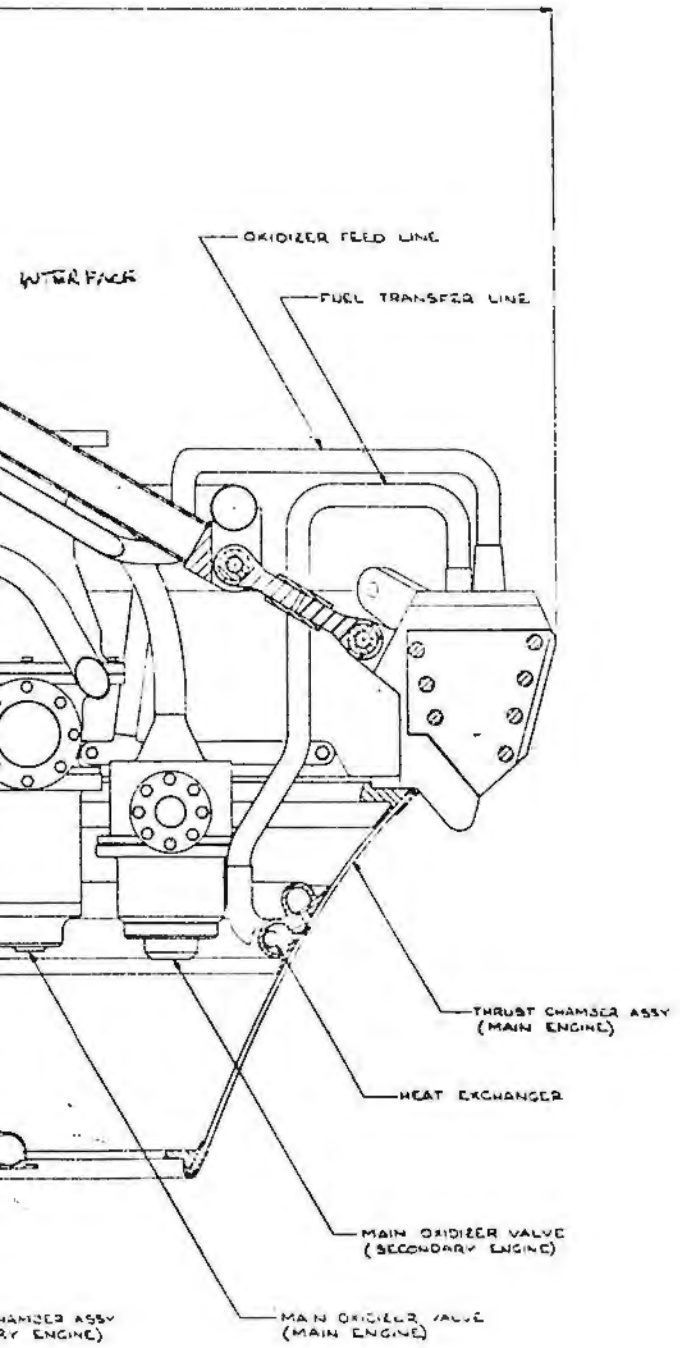
INTERFACE
OXIDIZER FEED LINE
FUEL TRANSFER LINE
THRUST CHAMBER ASSY
(MAIN ENGINE)
HEAT EXCHANGER
MAIN OXIDIZER VALVE
(SECONDARY ENGINE)
MAIN OXIDIZER VALVE
(MAIN ENGINE)

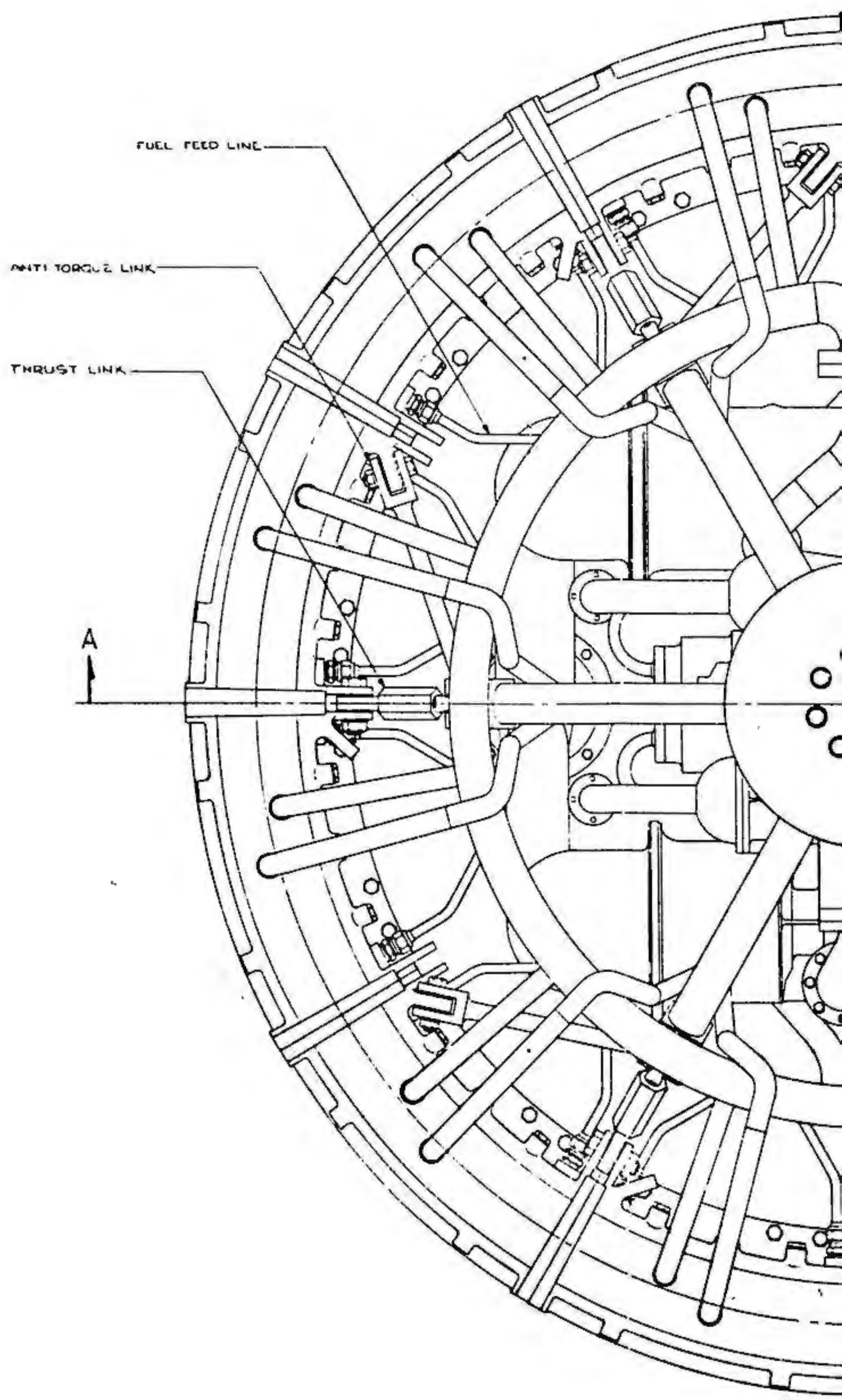
FUEL FEED LINE
ANTI TORQUE LINK
THRUST LINK
A

2

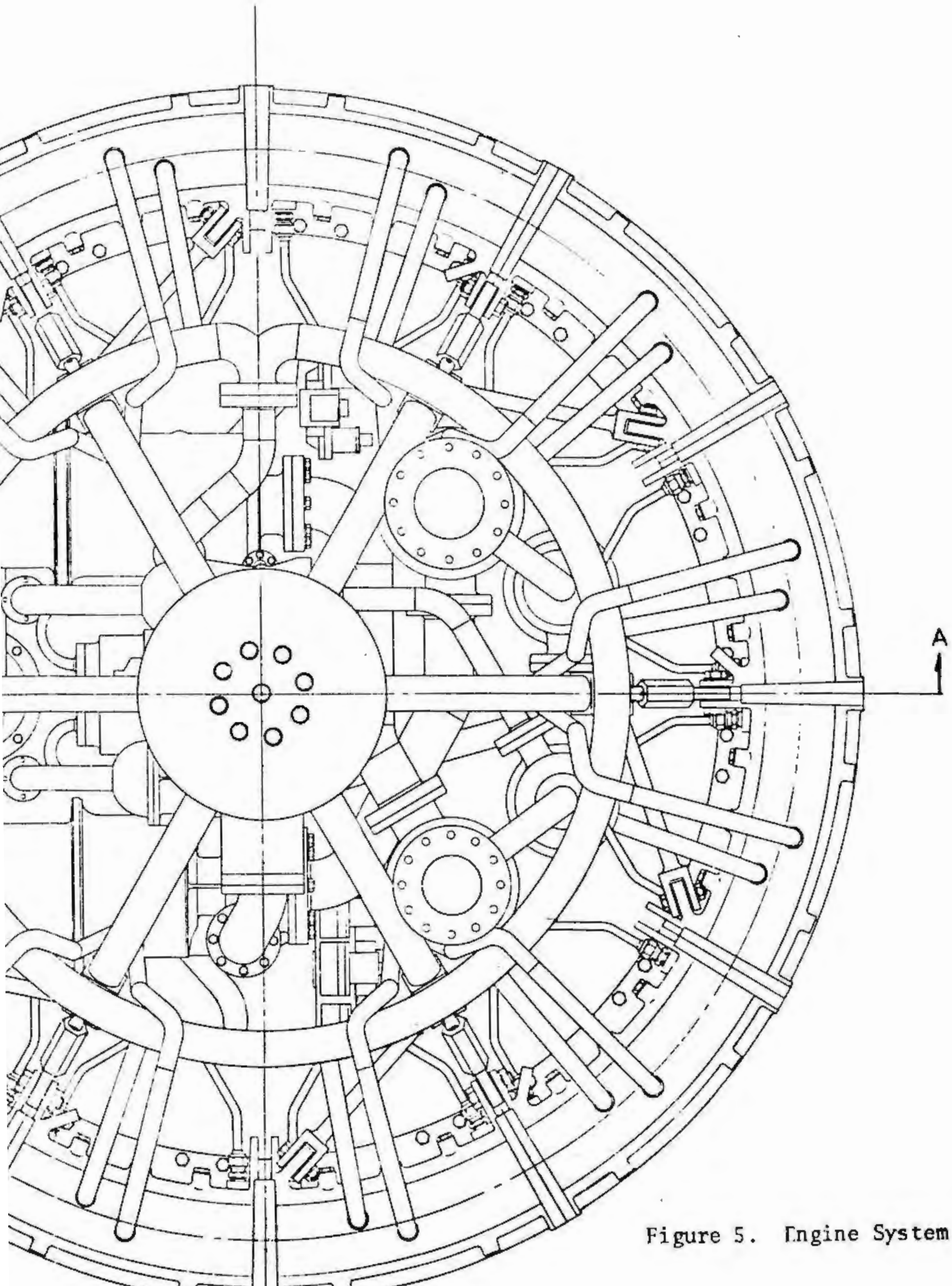

Figure 5. Engine System Assembly (U)

3

CONFIDENTIAL

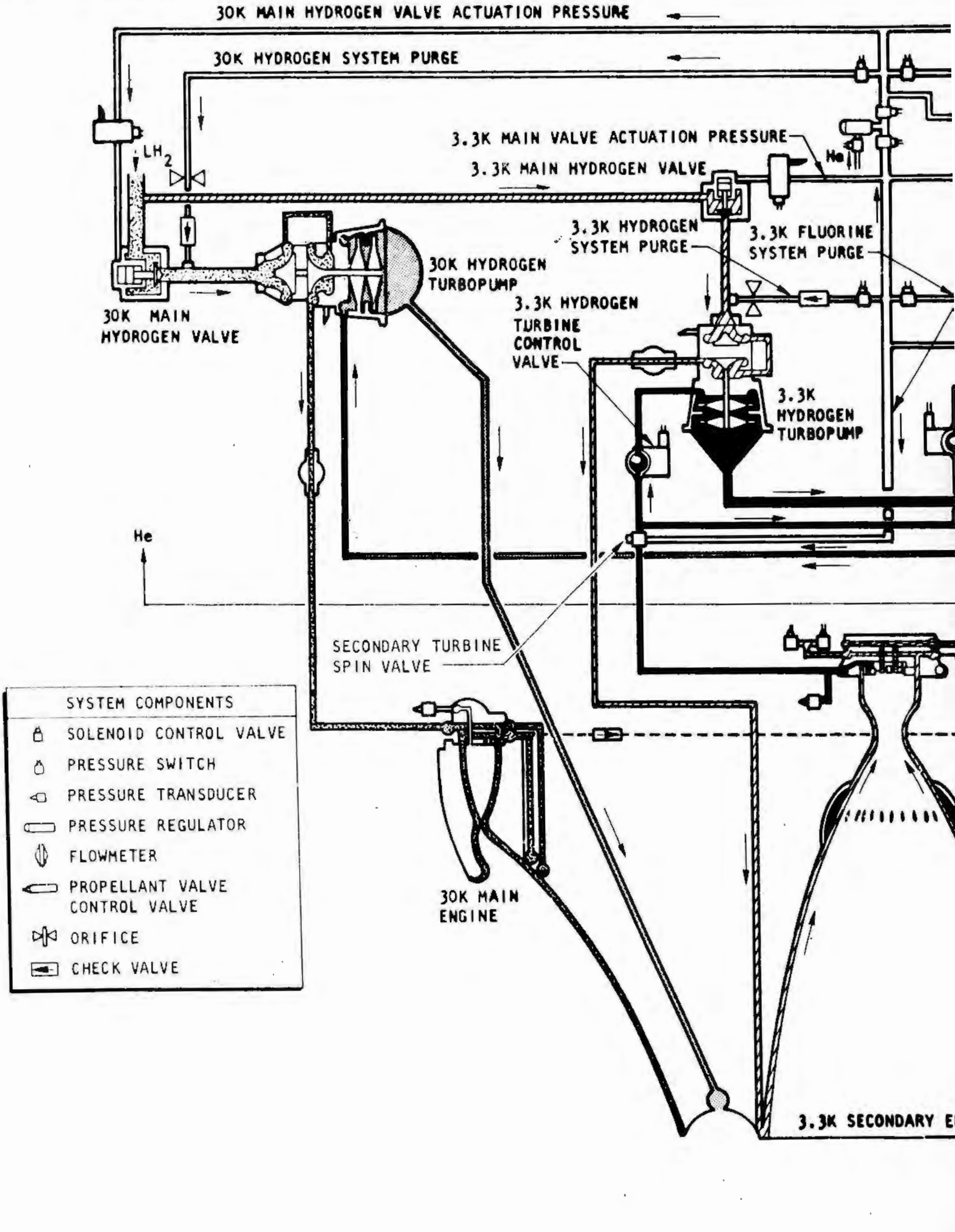

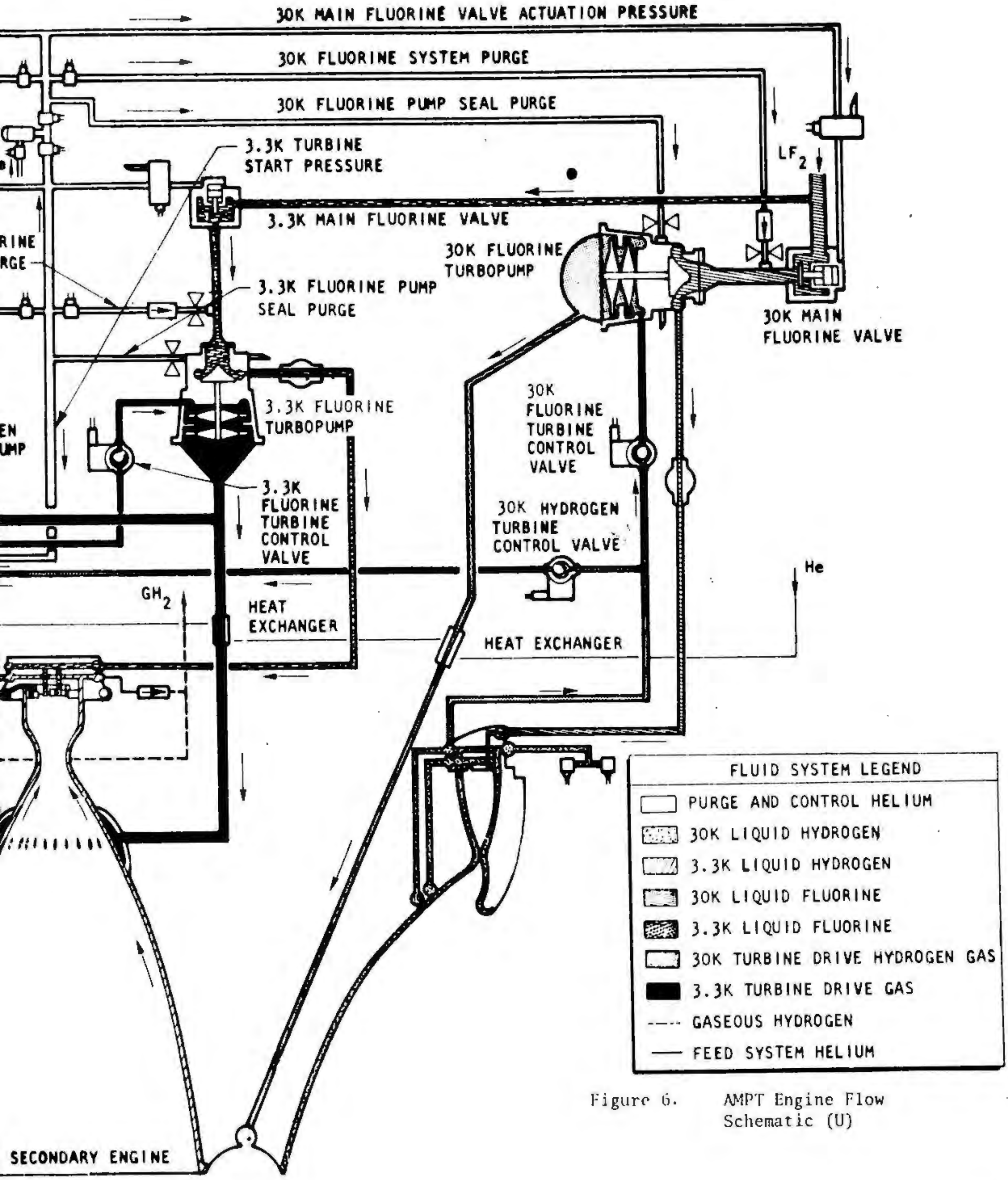

Figure 6. AMPT Engine Flow Schematic (U)

TABLE 2

BASIC ENGINE SYSTEM DESIGN PARAMETERS (U)

Parameter	Main Engine	Secondary Engine
Design Thrust, pounds	30,000	3330
Propellants	LF_2/LH_2	LF_2/LH_2
Chamber Pressure (Nozzle Stagnation), psia	650	750
Expansion Area Ratio	60:1	60:1
Engine Mixture Ratio, o/f	12:1	12:1
Turbine Drive-Gas Source	Hydrogen Tapoff	Thrust Chamber Tapoff
Throttling Ratio	9:1	9:1
Gimbal Angle, degrees	±10.0	±10.0
Thrust Chamber Design	12 supersonic baffles segmented combustion chamber (aerospike nozzle)	Cylindrical chamber (bell nozzle)
Geometric Throat Area, sq in.	25.13	2.42
Characteristic Length, inches	24.2	13.8
Injector-to-Throat Distance, inches	3.5	5.0
Injector Width, inches	2.0	---
Engine Diameter at Center of Throat, inches	45.83	---
Nozzle Percent Length	20	80
Contraction Ratio	11.4	4.0:1
Contour	G_c	---
Throat Gap, inch	0.175	---
Injector Type	Fan	Fan
Nominal Specific Impulse at Maximum Thrust, seconds	460.0	458.5

CONFIDENTIAL

CONFIDENTIAL

2. ENGINE SYSTEM ANALYSIS AND DESIGN

a. Pump Drive Cycle Selection

(U) The three candidate pump drive cycles were evaluated to determine their impact on the turbopump design configurations and system operational features. The three selected candidates were: (1) thrust chamber tapoff, (2) hydrogen tapoff, and (3) expander topping. Previous AMPS studies (Ref. 1 and 2) have shown these power cycles to have the greatest potential for this application. The three candidate cycles as employed in the main engine are illustrated in Fig. 7.

(C) The system design and operational parameters were established for each of the candidate drive cycles as applied to both the main and secondary engines. The candidate drive cycles were also compared on the basis of other operational features such as complexity, engine start, and dynamic throttling. The major design parameters are shown below:

	Main Engine	Secondary Engine
Nozzle Type	Aerospike (20 percent length)	Bell (80 percent length)
Design Thrust, pounds	30K	3.3K
Chamber Pressure, psia	650	750
Area Ratio	60:1	60:1
Engine Mixture Ratio	12:1	12:1
Throttle Ratio	9:1	9:1

(1) Thrust Chamber Tapoff

(U) The thrust chamber tapoff cycle previously had been tentatively selected for the AMPS main and secondary engines. The turbine drive gases are tapped directly from a low mixture ratio, low temperature region of the combustion chamber (Fig. 7). After the gases pass through the turbines, they are

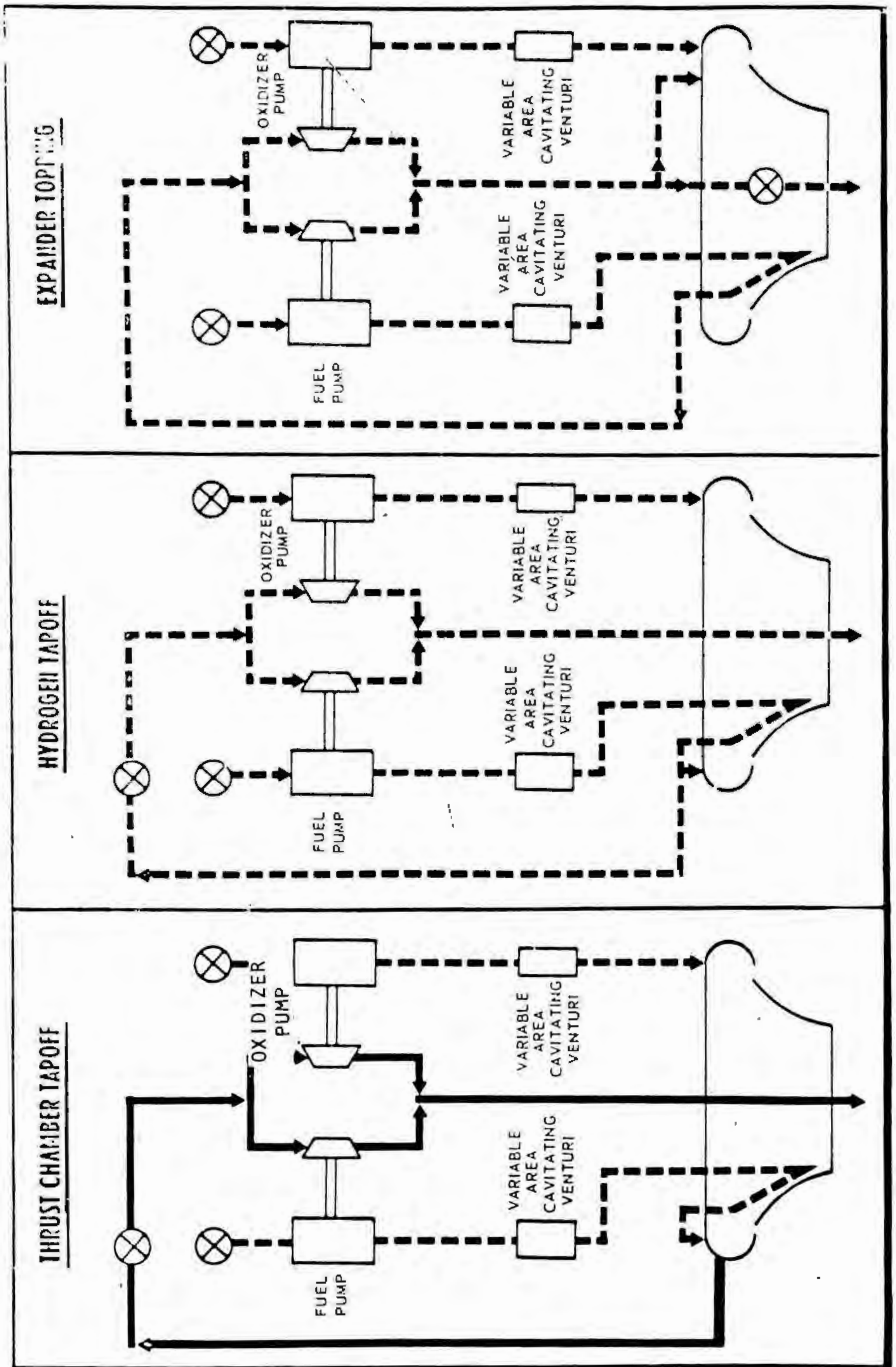

Figure 7. Engine Cycles

(U) ducted to the base region of the aerospike nozzle to augment the base pressure thrust contribution. There are numerous variations to this basic cycle concept such as turbine arrangement and the disposition of the turbine exhaust gases. In the secondary engine the turbine exhaust can be ducted into the primary nozzle or expanded through a separate nozzle.

(2) Hydrogen Tapoff

(U) The hydrogen tapoff cycle (Fig. 7) extracts a relatively small turbine flow (secondary flow) from the main hydrogen fuel flow after it passes through the thrust chamber cooling jacket. The major portion of the total hydrogen flow (primary flow) is then injected into the combustion chamber. For the main engine, the secondary flow is directed into the base of the aerospike nozzle after passing through the turbine. If the turbine flowrate requirement is greater than the optimum base flow for the aerospike nozzle, the excess hydrogen can be used for propellant tank pressurization, or recirculated back into the pump inlet. For this comparison, all of the turbine flow was ducted to the nozzle base.

(3) Expander Topping

(U) In the expander topping cycle (Fig. 7) all of the hydrogen leaving the thrust chamber cooling jacket is expanded through the turbines and then directed to the injector. For the main engine, a small percentage of the turbine flow is extracted before entering the injector for secondary flow into the base of the aerospike nozzle.

(4) Selection Criteria

(U) The major areas for investigation of the candidate cycles were first established. Items that did not exhibit a significant difference between the candidate cycles were excluded from the comparison. The selection criteria provided a comprehensive comparison of the important system and component considerations. Some of the basic criteria and items of consideration are summarized in Table 3 .

TABLE 3

TURBINE DRIVE CYCLE SELECTION CONSIDERATIONS (U)

General	Engine Start
Engine Performance	Thermal Conditioning Requirements
Turbine Drive Gas Inlet Temperature	Response
Turbine Inlet Pressure	Repeatability
Thrust Chamber Mixture Ratio	Overtemperature Condition
Thrust Chamber Heat Flux	**Mainstage**
Injector Flowrate	Thrust and Mixture Ratio Control
Pump Discharge Pressure Requirements	Transition of Control From Start
Thermal Isolation	Variation in Turbine Drive
Stability	Gas Inlet Condition
Materials Limitations	**Shutdown**
Engine Weights	Cutoff Impulse
System Packaging	Repeatability
	Purge Requirement

(U) A comparison of delivered engine performance was the most important single item. Closely associated with engine performance was the resulting thrust chamber mixture ratio and its influence on combustion chamber heat flux and injector cooling capabilities. The turbine drive gas inlet temperature and pressure are important considerations from the standpoint of material selection, component size and weight, and engine system performance. Pump discharge pressure requirements dictate pump design restrictions or limitations and overall engine system performance. Other engine system considerations such as thermal isolation between the turbine and pump and turbine and thrust chamber, engine power cycle stability characteristics, the performance vs system weight tradeoff, and system packaging may result in significant advantages or disadvantages in the candidate engine power cycles.

(U) To satisfy the rapid engine start requirements of the AMPS, a study of start transient characteristics of the candidate cycles was required with consideration given to thermal conditioning requirements, repeatability of start over a range of engine environmental and thermal conditions, and the possibility of an overtemperature condition occurring in the turbine.

(U) During mainstage operation, items such as thrust and mixture ratio control, the transition of control from start to mainstage, and the possible variation in turbine drive gas inlet conditions during throttling operations were evaluated.

(5) Main Engine

(a) Design and Operating Parameter Comparison

(C) Prior to determining the potential delivered engine performance of the candidate cycles, the major turbopump design parameters were established for a nominal engine mixture ratio of 13:1. The resulting engine system requirements are presented in Table 4 for the three candidate cycles. The effective cooling jacket mixture ratio is the same as the engine mixture ratio and is equal for the three cycles. Thus, all of the hydrogen pumped passes through the cooling jacket for each of the cycles; the cycle selection is not influenced by regenerative-cooling considerations.

(U) The pump discharge pressure requirements are equivalent for the thrust chamber tapoff and hydrogen tapoff cycles, while the fuel pump discharge pressure is approximately 13 percent higher for the expander topping cycle. The higher value is primarily because of the fact that all of the hydrogen is expanded through the turbine before injection into the chamber.

CONFIDENTIAL

TABLE 4

COMPARISON OF MAIN ENGINE DESIGN AND OPERATING PARAMETERS FOR CANDIDATE TURBINE DRIVE CYCLES (FULL-THRUST CONDITION) (U)

Operating or Design Parameter	Thrust Chamber Tapoff	Hot Hydrogen Tapoff	Hydrogen Expander Topping
Engine Mixture Ratio	13:1	13:1	13:1
Effective Cooling Jacket Mixture Ratio	13:1	13:1	13:1
Thrust Chamber Mixture Ratio	14.56	13.20	13.97
Thrust Chamber Heat Flux, percent of value for thrust chamber tapoff cycle	--	-1.0	+0.6
Pump Discharge Pressure, psi			
Oxidizer	1250	1250	1250
Fuel	1902	1902	2156
Turbine Drive Gas Inlet Temperature, F	1500	1000	1000
Turbine Inlet Pressure, psi			
Oxidizer	210	210	1178
Fuel	300	300	1028
Turbine Pressure Ratio			
Oxidizer	7	7	1.206
Fuel	10	10	1.206
Nominal Start Time (to 90 percent), seconds	~2.75	~2.0	~2.5

CONFIDENTIAL

CONFIDENTIAL

(C) The selected turbine drive gas inlet temperatures are based on the previous selection studies (Ref. 1 and 2) with respect to the thrust chamber tapoff cycle and on the available hydrogen temperature for the two hydrogen drive cycles. To illustrate the influence of turbine inlet temperature (previously selected as 1500 F) on the thrust chamber tapoff system performance, results are presented for a 1200 F inlet temperature. The lower temperature is representative of a minimum achievable for the combustion gas tapoff concept.

(U) The turbine inlet pressures were selected to provide fast engine start characteristics (low pressure) and still achieve a reasonable discharge pressure and base flow characteristics. The turbine pressure ratios were selected from design considerations for the thrust chamber tapoff and hydrogen tapoff. The turbine pressure ratios for the expander topping cycle were derived from a power balance where the entire hydrogen flow is expanded through the turbines.

(b) Performance Comparison

(C) The engine performance analysis for the three candidate turbine drive cycles was conducted over a range of engine mixture ratios to ensure that any interrelationship that exists between the engine power cycle and the engine mixture ratio would be included in the final design selection. The delivered main engine performance for continuous operation at full thrust vs engine mixture is shown in Fig. 8 for each of the candidate cycles. The specific impulse for the thrust chamber tapoff cycle is shown for turbine inlet temperatures of 1200 and 1500 F. All of the power cycles exhibit a slight increase in engine performance as the engine mixture ratio is decreases. At an engine mixture ratio of 13:1, the thrust chamber tapoff cycle (T_W = 1500 F) achieves 1.3 second higher specific impulse than the hydrogen tapoff cycle. At a turbine inlet temperature of 1200 F, the performance advantage is reduced to 0.3 second. The expander topping cycle achieves a 2.0-second performance advantage over the hydrogen tapoff cycle.

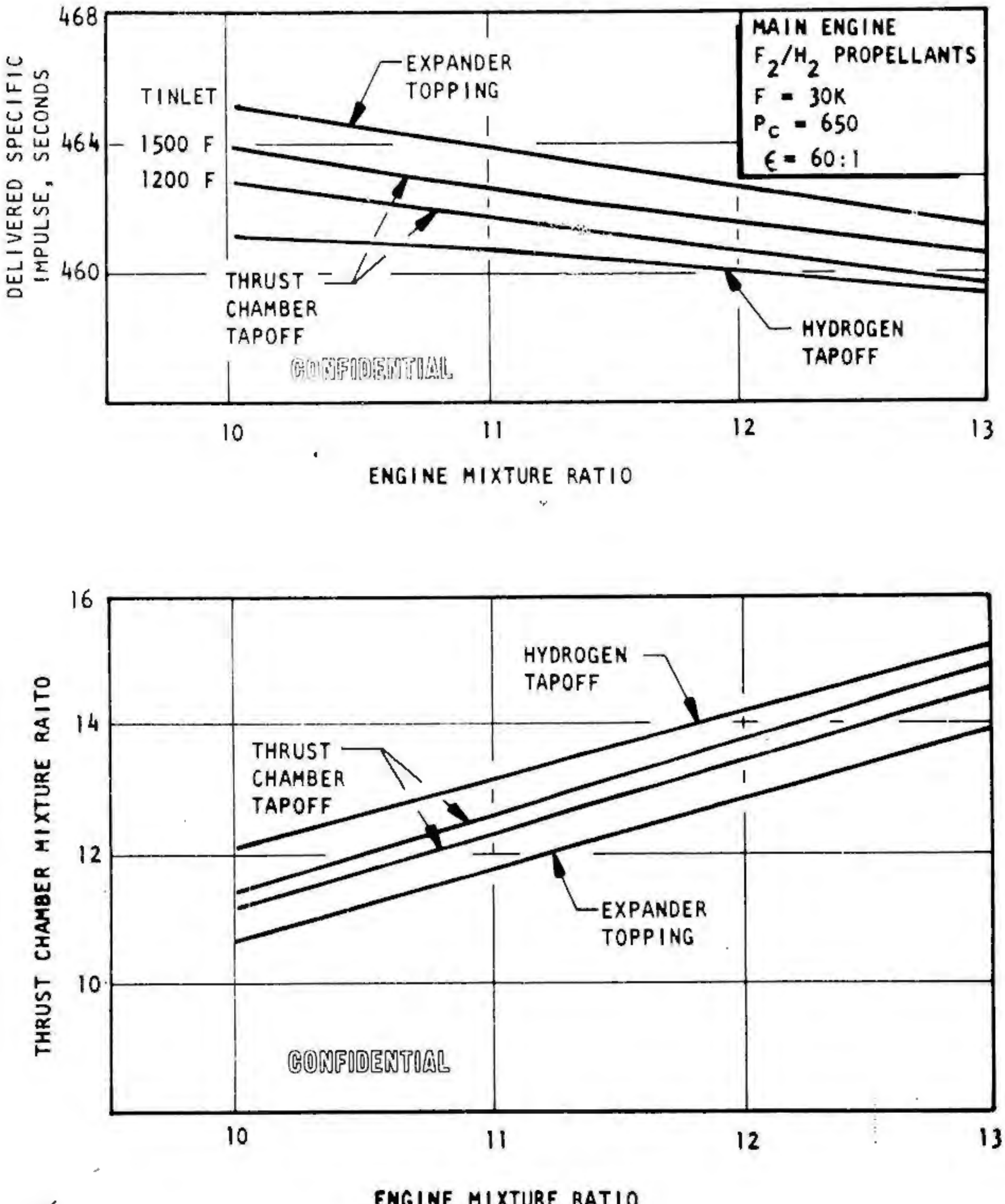

Figure 8. Performance Comparison of Candidate Turbine Drive Cycles (Full-Thrust Operation) (U)

(U) The thrust chamber mixture ratio vs engine mixture ratio is also shown in Fig. 8 for each of the cycles. The expander topping cycle has the lowest thrust chamber mixture ratio because only the optimum amount of base bleed (all of which is hydrogen) is subtracted from the primary flow. The hydrogen tapoff cycle has the highest thrust chamber mixture ratio because all of the turbine flow is hydrogen and is ducted into the nozzle base. The resulting thrust chamber mixture ratios are the primary cause for the spread in engine performance for the various turbine drive cycles because at the estimated hydrogen injection temperature, the peak theoretical performance occurs at a mixture ratio of approximately 8:1.

(C) The delivered engine specific impulse vs engine mixture ratio for 9:1 throttled operation is shown in Fig. 9 for the candidate cycles. The corresponding thrust chamber mixture ratio is also shown. At the throttled operating condition, little difference is seen in the performance capabilities of the three cycles because the thrust chamber mixture ratios are nearly equal.

(c) Operational Features

(U) A qualitative comparison of the system operational features for the three cycles was also conducted and is discussed in the following outline.

- Operational
  - Stability
  - Thermal Conditioning
  - Possible Overtemperature During Start
  - Variation in Drive Gas Temperature With Throttling
- Environment
  - Corrosivity
  - Valves
- Structural
  - Materials Limitations
  - Estimated System Weight
  - System Packaging
  - Complexity

(U) Turbine drive cycle stability was seen to be a potential problem area for the expander topping cycle because of the low pressure ratio turbines that are required. This would result in subsonic flow in the turbine nozzles and a direct coupling of any instability between the turbine and thrust chamber.

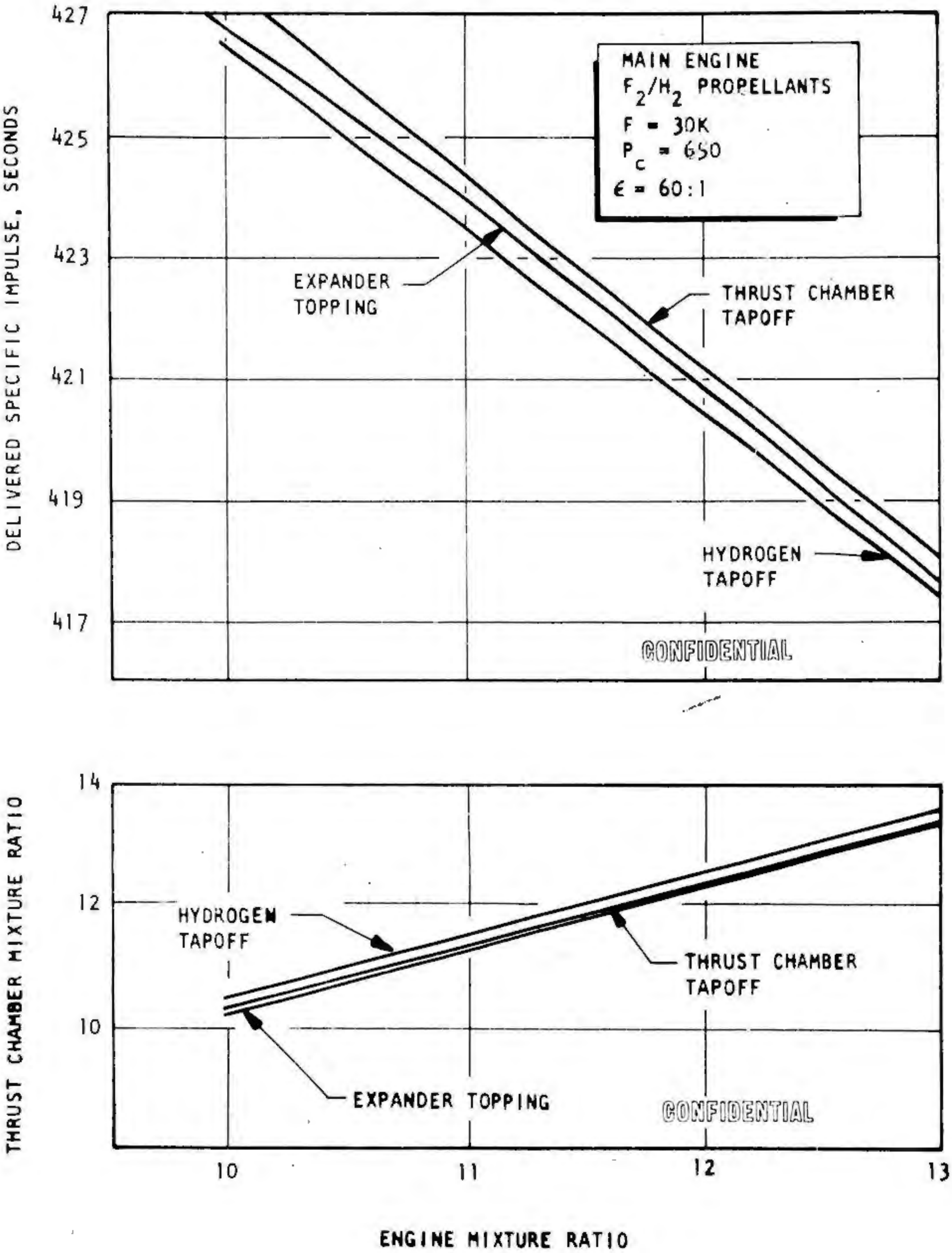

Figure 9. Performance Comparison of Candidate Turbine Drive Cycles (9:1 Throttled Operation) (C)

(U) The higher turbine operating temperature of the thrust chamber tapoff cycle results in a higher residual heat capacity for the turbomachinery and a greater thermal conditioning requirement under certain start conditions.

(U) The thrust chamber tapoff concept could result in an uncertain tapoff gas mixture ratio, and therefore temperature during the engine start transient and also during throttling operations because of dynamic characteristics of the propellant feed system. The uncertain tapoff gas mixture ratio could result in an overtemperature condition occurring in the turbine drive system during nonsteady-state operation. The gaseous hydrogen drive cycles would eliminate this potential problem area because turbine drive gas temperature is controlled by the bulk temperature rise of the thrust chamber jacket coolant.

(U) From a hardware operating environment standpoint, the thrust chamber tapoff cycle is at a disadvantage because of the higher gas temperatures and corrosivity of the HF content of the combustion gas. These factors result in limitations in materials that are suitable for the turbine and ducting fabrication.

(C) A preliminary comparison of engine system weights for the candidate cycles indicated that there would not be a significant difference in system weight between the thrust chamber tapoff and hydrogen tapoff cycles. However, the expander topping cycle would result in an approximate 10-percent increase in engine system weight (46 pounds). This is primarily a result of the increased turbine inlet pressure and the larger ducting and valves required to accommodate the larger turbine flowrate. Using the propulsion system weight-specific impulse exchange factor of 15 lb/sec, this weight increase is equivalent to 3 seconds of specific impulse. (Ref. 1).

(U) The larger hot-gas ducting and valves required in the expander topping cycle would also make engine component packaging problems more difficult.

(U) The injector design criteria associated with the thrust chamber tapoff concept would result in increased complexity in design and development efforts. The accomplishment of a uniform tapoff gas mixture ratio during steady-state and transient operation would be a significant development task.

(U) There would also be a complexity disadvantage for the expander topping cycle in that turbine bypass ducting would be required to reduce pump power for throttled operation.

(d) Engine Start Characteristics

(C) The engine system start characteristics for each of the candidate cycles were investigated to compare start times and other items related to the start system. The analysis was conducted with the aid of the digital computer model that was developed for the AMPS main engine. For this analysis, the pumps were assumed to be primed at initiation of the start sequence. All engine starts were tank-head starts with oxidizer and fuel tank pressures of 65 and 70 psia, respectively. A parallel turbine configuration was used for the three cycles. For this analysis, no attempt was made to optimize the start sequence for any of the cycles. Because this study was concerned only with the available start energy of each cycle, all starts were made using the following engine sequence. The main oxidizer valve was opened to the 20-percent position 150 milliseconds after engine start. This position was held until fuel turbopump speed reached 30,000 rpm, at which time the valve was sequenced to ramp to its mainstage position in 1.0 second.

(C) The hot-gas tapoff and hydrogen bleed cycles were started with the tapoff valve at 200 percent of mainstage position. The tapoff valve was then closed to its mainstage position in 100 milliseconds when the main oxidizer valve was sequenced to begin to ramp open.

(C) Starts were made for each cycle with the thrust chamber thermally conditioned to its predicted maximum and minimum temperature (1460 and 400 R, respectively).

(U) By comparing turbopump speed buildup for each of the cycles under identical start conditions, the power cycle which had the highest potential start energy was determined. Fuel turbopump speed for each cycle at both extremes of thrust chamber conditioning is shown in Fig. 10 . As can be seen, the hydrogen tapoff cycle has the fastest tank-head start under both extremes of thrust chamber thermal conditioning. Main chamber pressure buildup for each of these starts is shown in Fig. 11. The nominal start times to 90 percent of full thrust for each of the cycles are shown in Table 4 .

(e) Selection Summary

(C) A review of the cycle comparisons in the various areas led to the selection of the hydrogen tapoff cycle as the most favorable candidate for the main engine. A summary of the major considerations influencing this selection is outlined below.

1. The hydrogen tapoff cycle has the fastest start time; 0.5 and 0.75 seconds faster than the expander topping and thrust chamber tapoff, respectively.
2. The hydrogen tapoff cycle is the least complex.
3. Predictable turbine drive gas temperatures during start and transient operation
4. Low turbine operating temperature (1000 F)
5. Desirable system stability characteristics (provides decoupling of thrust chamber and turbine)
6. Noncorrosive turbine drive gas
7. The hydrogen tapoff cycle results in a small performance penalty relative to other candidates; 1.3 seconds less than thrust chamber tapoff with a tapoff temperature of 1500 F, and 0.3 second with a tapoff temperature of 1200 F. The expander topping

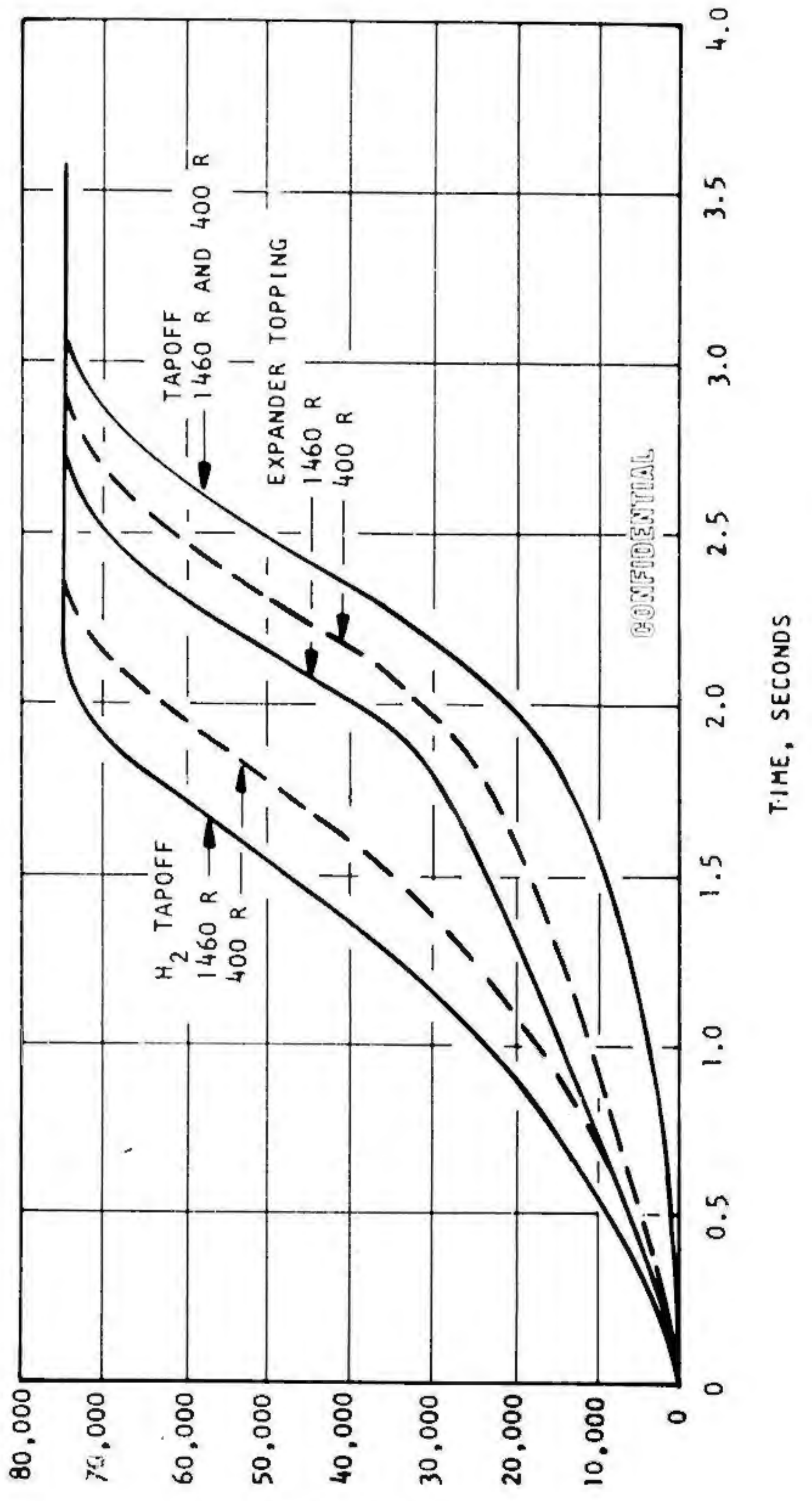

Figure 10. Fuel Pump Speed (U)

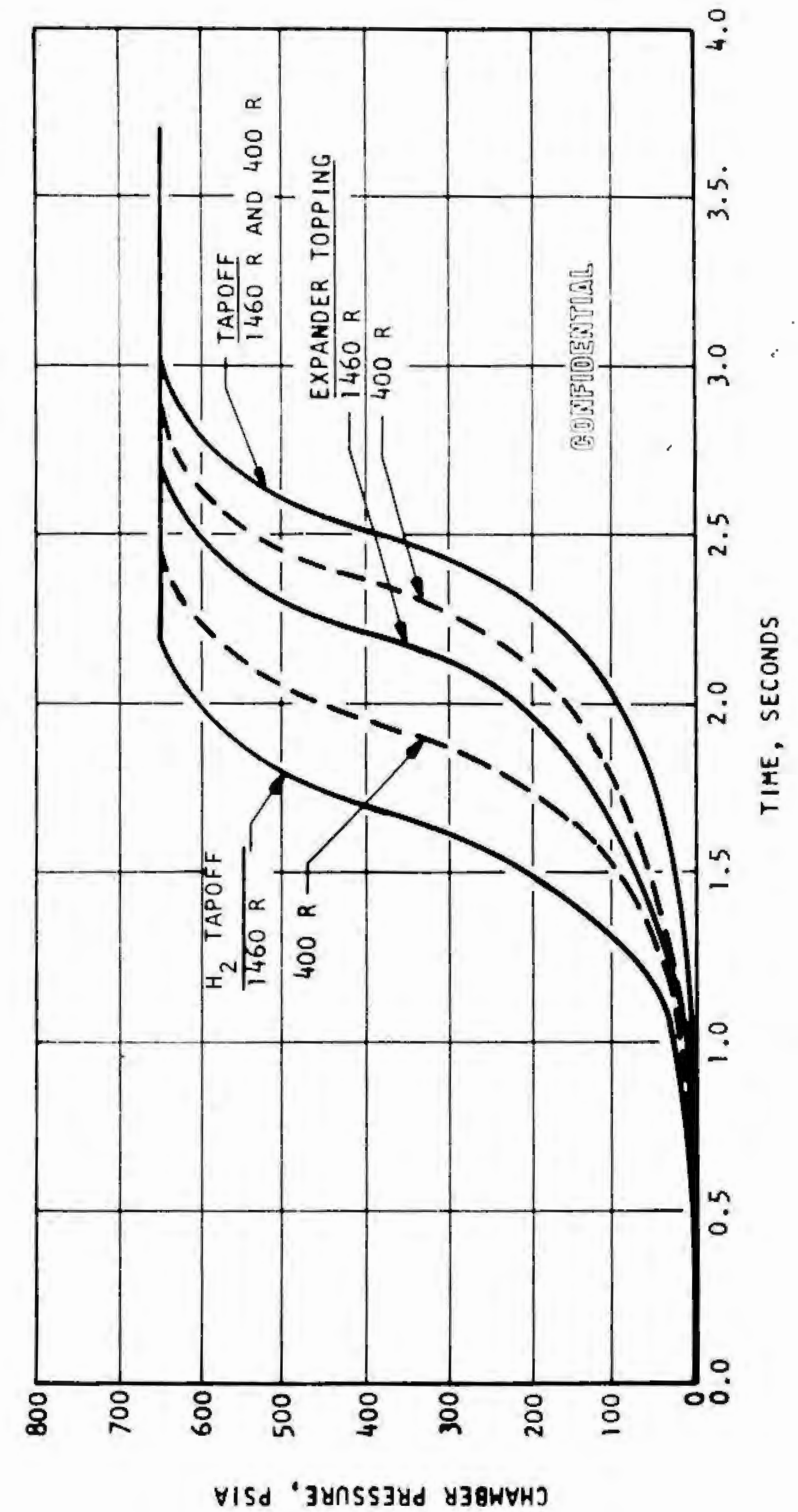

Figure 11. Main Chamber Pressure (U)

(C) cycle has a 2.1-second performance advantage but when system weight differences are included, the hydrogen tapoff has only an equivalent 1.0-second advantage. There is a negligible difference in throttled engine performance between the three cycles.

8. The excess hydrogen secondary flow, over the optimum amount required in the nozzle base, has other potential uses (tank pressurization, etc.).

(6) Secondary Engine

(U) All of the selection criteria established for the main engine were then applied to the secondary engine to select the most favorable engine power cycle. Many of the conclusions stated for the qualitative considerations on the main engine cycle comparisons are also valid for the secondary engine. However, certain engine system characteristics peculiar to the secondary engine resulted in a greatly different relative comparison of the candidate cycles.

(a) Design and Operating Parameter Comparison

(C) The major engine system and turbopump operating parameters were established to provide a comparison of the turbine drive cycle effects. This comparison is presented in Table 5 for an engine mixture ratio of 13:1. The two tapoff cycles have identical pump discharge pressure requirements while the expander topping cycle, fuel pump discharge pressure is approximately 65 percent higher. The higher fuel pump discharge pressure is because of the fact that all of the hydrogen must be expanded through the turbine nozzles. One of the major differences between the main engine and the secondary engine is the temperature of the gaseous hydrogen available for turbine drive. The bulk temperature rise in the

TABLE 5

COMPARISON OF SECONDARY ENGINE DESIGN AND OPERATING PARAMETERS
FOR CANDIDATE TURBINE DRIVE CYCLES (FULL THRUST) (U)

Operating Design Parameter	Thrust Chamber Tapoff	Hot Hydrogen Tapoff	Hydrogen Expander Topping
Engine Mixture Ratio	13:1	13:1	13:1
Effective Cooling Jacket Mixture Ratio	13:1	13:1	13:1
Thrust Chamber Mixture Ratio	14.5	18.5	13.1
Pump Discharge Pressure, psi			
Oxidizer	1454.4	1454.4	1454.4
Fuel	1571.9	1571.9	2594
Turbine Drive Gas Inlet Temperature, F	1500	207	207
Turbine Inlet Pressure, psi			
Oxidizer	600	600	2145
Fuel	600	600	1900
Turbine Pressure Ratio			
Oxidizer	20	20	1.842
Fuel	20	20	1.842

CONFIDENTIAL

CONFIDENTIAL

(C) cooling jacket of the secondary engine is considerably lower than in the main engine. For the gaseous hydrogen drive cycles, the maximum available turbine inlet temperature is 207 F. However, the thrust chamber tapoff system can provide considerably higher energy gases. As a result of the lower hydrogen temperatures, the hydrogen tapoff cycle requires a higher percentage of the fuel flow to produce the required turbine horsepower and this results in a very high thrust chamber mixture ratio (above stoichiometric). In the expander topping cycle, all of the hydrogen is injected into the chamber after being expanded through the turbines.

(U) The indicated turbine inlet pressures and pressure ratios for the two tapoff cycles are based on the previous design for the secondary engine turbomachinery (Ref. 1). Those values shown for the expander topping cycle were derived from an engine power balance.

(b) Engine Performance Comparison

(C) A comparison of the delivered engine specific impulse vs engine mixture ratio at full thrust for the three candidate cycles is shown in Fig. 12 along with the resulting thrust chamber mixture ratio variation. The hydrogen tapoff cycle has the lowest performance over the mixture ratio range primarily because of the high thrust chamber mixture ratio. The thrust chamber tapoff cycle achieves approximately 6.5 seconds higher specific impulse. Less than 1.0-second difference results between combustion gas tapoff temperatures of 1200 and 1500 F.

(C) The expander topping cycle obtains 11.0 seconds higher specific impulse than the hydrogen tapoff cycle at an engine mixture ratio of 15:1. However, there is insufficient energy available in the heated hydrogen to drive the hydrogen pump at lower mixture ratios. As the hydrogen flowrate

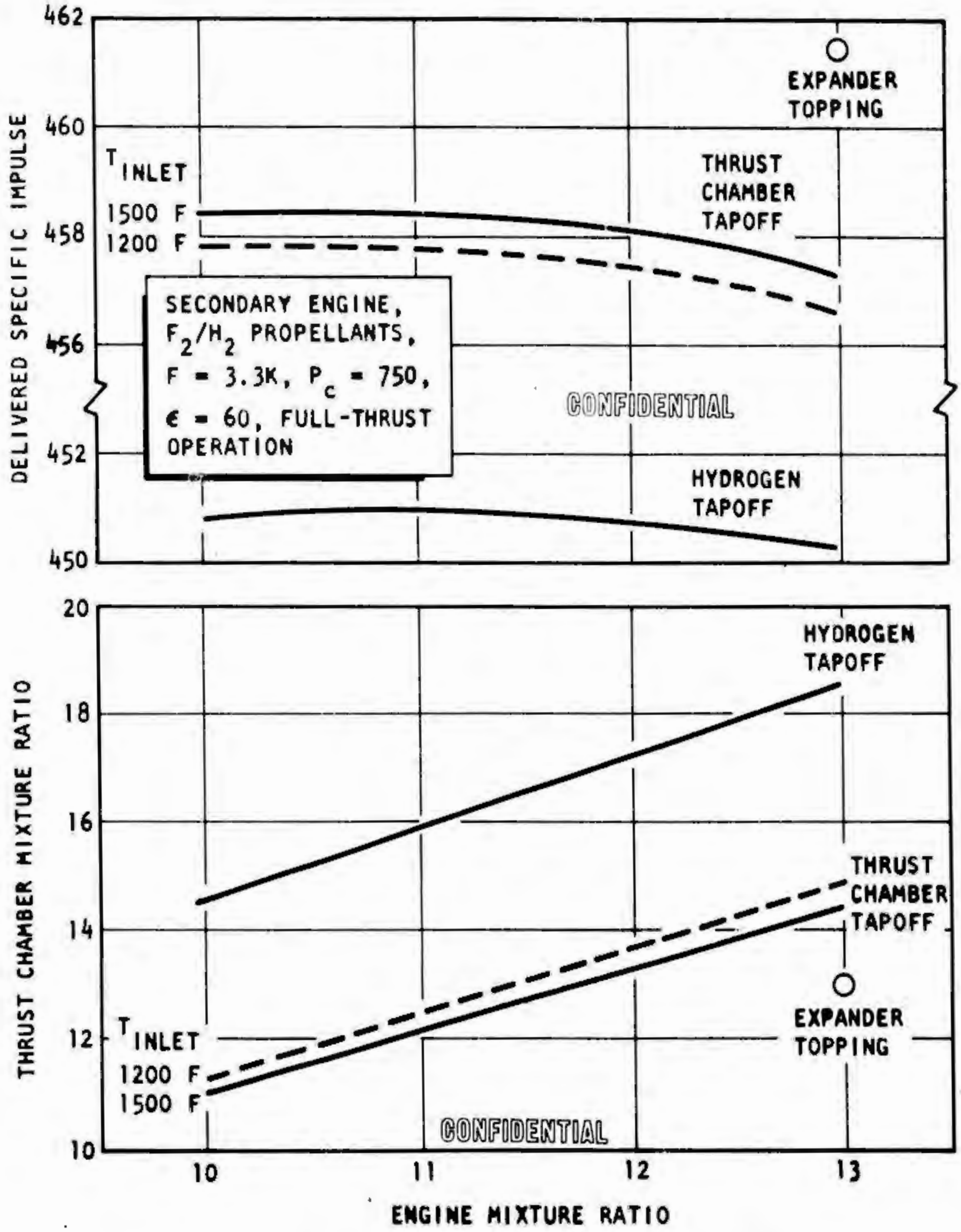

Figure 12. Performance Comparison of Candidate Turbine Drive Cycles (U)

(C) is increased (lower mixture ratios), the pump horsepower requirements are increased and the hydrogen bulk temperature rise in the cooling jacket is reduced. If the turbine pressure ratio is increased to compensate for the increased horsepower requirement, the pump discharge pressure also increases. The net result is that the basic expander topping cycle will not operate at engine mixture ratios below 13:1 for this engine.

(C) The delivered engine specific impulse for 9:1 throttled operation of the secondary engine is shown in Fig. 13. The thrust chamber tapoff cycle obtains the highest performance over the engine mixture ratio range. The expander topping cycle is power limited below an engine mixture ratio of 13:1.

(c) Selection Summary

(C) A review of the cycle comparisons for the secondary engine resulted in the selection of the thrust chamber tapoff system. The same disadvantages (corrosivity, material limitations, injector complexity, etc.) that were listed for the main engine also exist for the secondary engine; however, the disadvantages associated with the alternative cycles are far more critical. In summary, the major factors are that the thrust chamber tapoff cycle achieves significantly higher performance than the hydrogen tapoff cycle and the expander topping cycle is restricted to high mixture ratio operation. Also, by reducing the tapoff temperature from 1500 to 1200 F, many of the potential difficulties of the thrust chamber tapoff cycle can be alleviated. The resulting mixture ratio of the tapoff gases will be low (~0.8:1), thus reducing the corrosivity factor. The injector complexity and development problems associated with the thrust chamber tapoff concept in conjunction with the bell-type chamber are considered to require a lesser effort than with the segmented toroidal chamber.

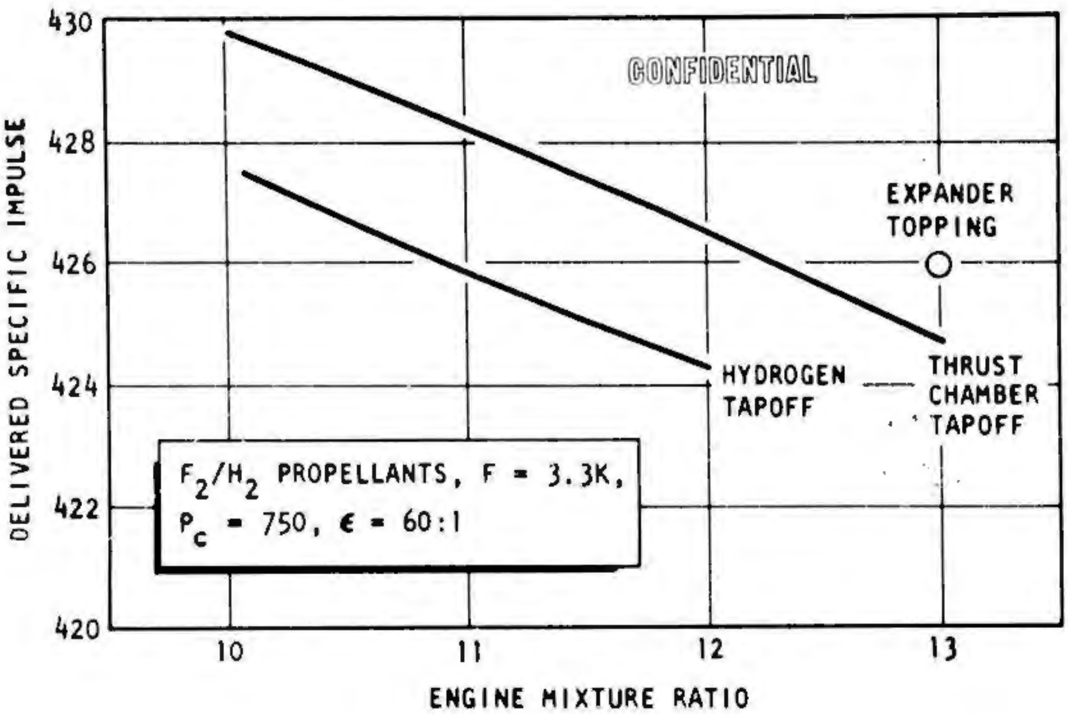

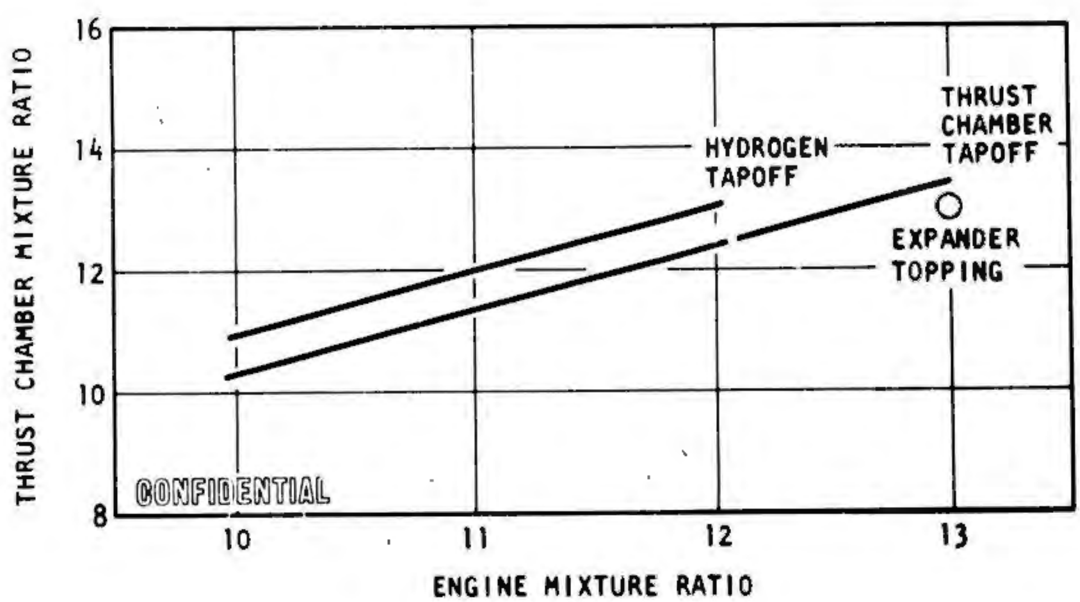

Figure 13. Performance Comparison of Candidate Turbine Drive Cycles, Secondary Engine (9:1 Throttled Operation) (C)

b. Series Versus Parallel Turbine Arrangement

(U) A study was conducted to determine and compare the design and operational advantages that are inherent in the series or parallel turbine arrangements in conjunction with the hydrogen tapoff turbine drive cycle. In previous AMPS component selection studies (Ref. 1 and 2), the parallel turbine arrangement was selected in conjunction with the thrust chamber tapoff turbine drive gas source. A re-evaluation of these previous selection studies was considered to be necessary in this program because the turbine drive gas was changed to hot hydrogen tapoff for the main engine. Items of consideration in this re-evaluation included engine performance, engine start characteristics, control system complexity, advantages in turbine design, and off-design operation.

(U) Preliminary design and operating parameters were determined for the series turbopump designs. The previously established parallel turbine parameters were then used for a comparison of the turbine design requirements. A summary of the primary turbine design requirements is presented in Table 6.

TABLE 6

TURBINE DESIGN REQUIREMENTS
(FULL THRUST; MAIN ENGINE) (U)

CONFIDENTIAL	Series Arrangement		Series Arrangement	
Parameter	Oxidizer	Fuel	Oxidizer	Fuel
Turbine Pressure Ratio	2.3	4.5	10	10
Inlet Pressure Ratio, psia	66	300	300	300
Turbine Flowrate, lb/sec	0.684	0.684	0.260	0.539
Effective Turbine Nozzle Area, in.^{2}	2.22	0.545	0.275	0.394
Polar Moment of Inertia, lb-ft-sec^2	0.00186	0.00262	0.00186	0.00262

(U) The turbine pressure ratios and inlet pressures were selected to provide a fast engine start transient. The required flowrates were approximated from an engine power balance analysis, and the turbine nozzle effective areas were computed as a function of flowrates and inlet pressure. The estimated turbopump polar moments of inertia shown in Table 6 were used in the engine start model analysis.

(1) Engine Performance

(C) An engine balance analysis was conducted for the main engine at full thrust and 9:1 throttled operation with the series and parallel turbine arrangement. At full thrust operation, the series turbine arrangement provided a 0.7-second higher delivered specific impulse. This advantage was reduced to 0.5 second at the throttled operating condition. These differences in engine performance are considered to be negligible, and, for the purposes of this comparison, the two turbine arrangements provide equal engine performance.

(2) Engine Operational Features

(U) A tradeoff study was conducted to investigate and compare the engine start characteristics of the two turbine arrangements. The analysis was conducted with the computerized AMPS engine start model.

(C) The comparison of engine start characteristics is made at altitude conditions. The series turbine, with a fuel inlet pressure of 300 psia, produces faster engine start (approximately 100 milliseconds) than the parallel cycle. At higher inlet pressures, this relatively slight advantage is sacrificed and, depending on the selected pressure, the series turbine arrangement start time may be slower than the parallel turbine

(C) arrangement. The parallel system start time can likely be shortened by optimizing the start sequence and initially directing the entire turbine flow to the fuel turbine to increase the fuel turbine starting torque. This option does not exist for the series arrangement.

(3) Design Considerations

(U) A preliminary evaluation of engine packaging and control system requirements was conducted for the two turbine arrangements. The larger hot-gas ducting and valve required between the fuel and oxidizer turbine in the series arrangement will result in greater difficulty in component packaging and a probable system weight increase. A cursory analysis of the engine throttling characteristics indicated that the series arrangement will require a bypass system around the oxidizer turbine to accomplish the required engine throttling. The probable system weight increase incurred with larger ducting and bypass system would more than compensate for the slight performance advantage of the series turbine arrangement.

(U) Based on the findings of these studies, significant reason does not exist to justify a change to the series turbine arrangement. The parallel system provides essentially equivalent engine performance and equivalent start time, greater system flexibility, and a less complex control system for off-design point operation.

c. Mixture Ratio Selection

(C) Previous mixture ratio selection studies (Ref. 1 and 2) were conducted for the AMPS and led to the selection of an engine design mixture ratio of 13:1. These studies were primarily based on the optimization

(C) of vehicle performance, and showed that there was only a slight variation in ΔV capability over a relatively wide range of system mixture ratios. These previous studies included the influence of the predicted engine performance, engine system component operating restrictions, and propellant feed system weight variations with mixture ratio.

(U) In re-evaluation of the mixture ratio selection, refinements in the engine performance calculations and engine design parameters are considered along with propellant feed systems with ellipsoidal tanks.

(U) The purposes of this analysis were to determine the influence of these recent system refinements and to include additional considerations such as orbital propellant storage, propellant utilization requirements, and engine durability.

(1) Selection Criteria

(U) The major considerations in the mixture ratio selection are engine performance, system weight, and the resulting mission ΔV capability. Additional factors that ultimately influence the ΔV performance are propellant storage capabilities and propellant utilization system requirements. Other independent considerations are engine component operating and design restrictions and durability or life.

(a) Engine Performance

(C) The delivered engine performance information used in this evaluation was generated in conjunction with the turbine drive cycle selection studies and is shown in Fig. 8 through 13. Two possible engine design philosophies may be assumed in determining the influence of engine mixture ratio

(C) on specific impulse. One approach is to choose a maximum combustion chamber wall temperature and vary the coolant tube size and outlet pressure as the hydrogen flowrate is varied. The other approach is to maintain a constant tube size, letting wall temperature and pump outlet pressure become the variables. The later approach was used in this study for engine durability considerations. Thus, as engine mixture ratio is decreased from the nominal design of 13:1, the thrust chamber wall temperature decreases but the pump discharge pressure increases. If constant tube bundle design is assumed, the thrust chamber is capable of operation at all mixture ratios shown. In general, engine specific impulse increases as the engine mixture ratio is reduced. This trend was exhibited for all thrust levels and for each of the candidate pump drive cycles.

(b) Feed System Weight

(U) The propellant feed system subcontractors, Convair Division of General Dynamics (GD/C) and Lockheed Missiles and Space Company (LMSC), provided preliminary feed system weight data for their respective design concepts. These relative stage inert weight trends are shown in Fig. 14 along with the curve labeled Rocketdyne which was the propellant feed system weight trend developed in Ref. 1 and used in the mixture ratio optimization studies conducted for Ref. 1 and 2. Each weight curve is referenced to the nominal design value of 13:1 because only the weight variation with change in mixture ratio is important.

(c) Mission Performance Capabilities

(U) The combining of the engine performance and propellant feed system weight information into the system ΔV capabilities provided the ultimate comparison of the effect of mixture ratio variation.

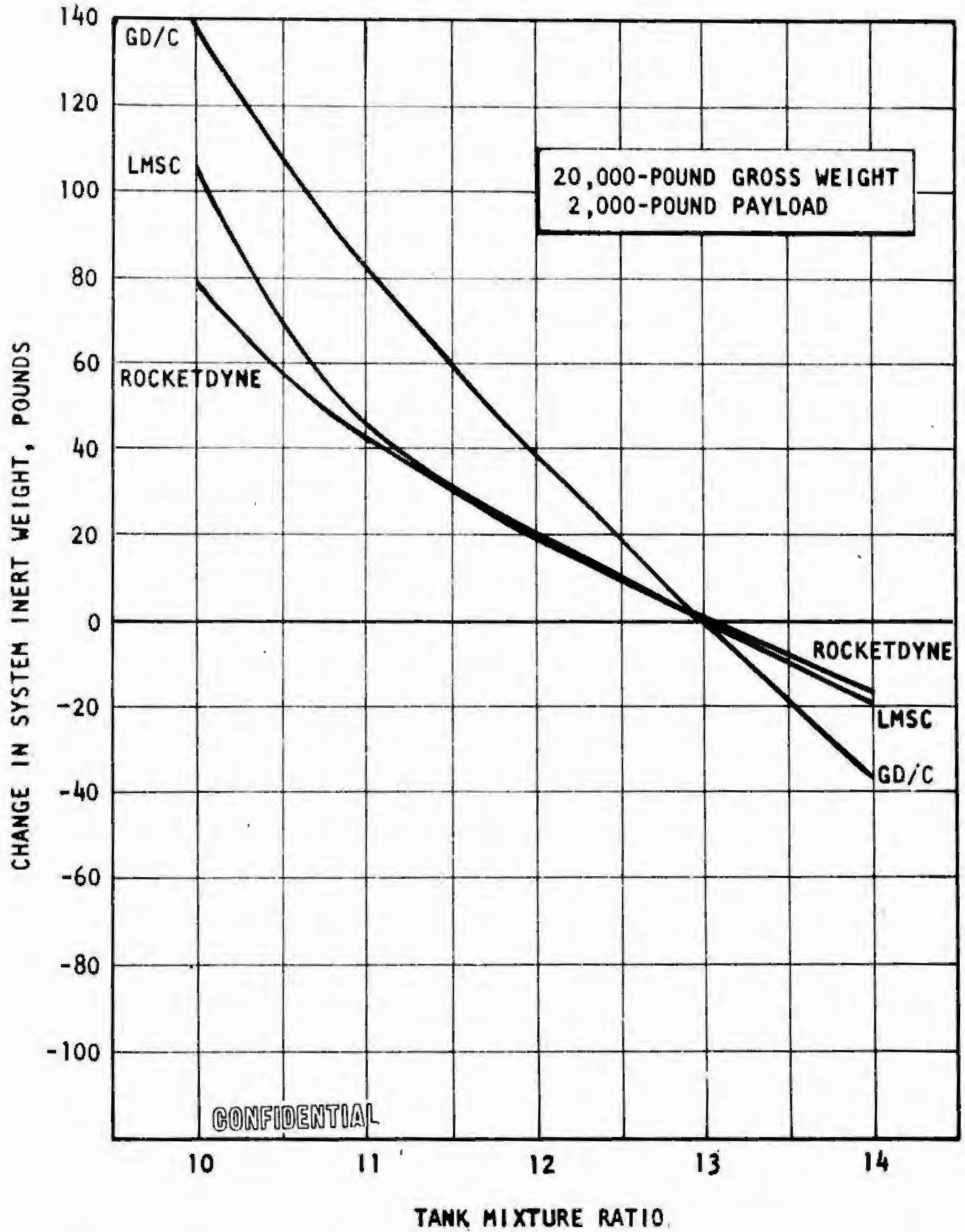

Figure 14. Change in AMPS Inert Weight as a Function of Tank Mixture Ratio (U)

(U) A number of possible mission profiles were considered (Table 7). The equal thrust use case (all thrust levels used equally) was approximated by assuming that one quarter of the propellant load was used at each of the four end points of the throttling curves: the main engine at maximum and minimum thrust, and the secondary engine at maximum and minimum thrust. The rendezvous missions were performed in the standard manner with the interceptor following an optimum trajectory on the range--range rate plane (Ref. 1).

TABLE 7

POSSIBLE MISSION THRUST PROFILES (U)

1.	Aerospike thrust chamber at full thrust
2.	Aerospike thrust chamber at minimum thrust
3.	Secondary thrust chamber at full thrust CONFIDENTIAL
4.	Secondary thrust chamber at minimum thrust
5.	Equal propellant usage at all thrust levels
6.	Series of rendezvous with passive targets with a 2000 ft/sec plane change between rendezvous
7.	Series of rendezvous with passive targets
8.	Series of rendezvous with evading targets having F/W = 0.7
(F/W = Thrust/Weight)	

(U) The ΔV data are presented as a limit region of loss or gain and an average loss or gain. This method of averaging all cycles and weight estimates together would be questionable if actual hardware were involved, because the probability of actually operating at the average point would be zero. However, because parametric data are being used and it is the slopes of the weight and specific impulse curves that are of interest, the use of an average value is justified by the fact that the final designs are not firmly established.

(U) The ΔV variations with mixture ratio for the ellipsoidal tank vehicle are shown in Fig. 15 and 16 for typical mission profiles. The average change in ΔV and the limits within which all cycles fall are given. In the case of equal thrust level use (Fig. 15), the limits represent the average of the limits at each thrust level. In the case of the rendezvous missions, the limits at each mixture ratio represent the limiting cycle, mission, and weight estimate. Thus, all variations calculated are enclosed within the limit region.

(C) The maximum change in ΔV for any possible mission thrust profile is shown in Fig. 17. This range represents all cycles considered for the ellipsoidal tank vehicles. The lower limit line is of primary importance because it indicates the maximum possible loss in performance that could be incurred by changing the nominal engine mixture ratio. For the ellipsoidal tank vehicle, the nominal mixture ratio could be reduced to 11.5 with less than a 1-percent (approximately 200 to 220 ft/sec) loss in ΔV and with a possible gain in performance for some missions and weight estimates. However, as shown in Fig. 15 and 16 by the average variation, the loss in ΔV even at mixture ratio 10 would probably be less than 1 percent for most missions.

(U) The corresponding curves for the performance including the spherical tank vehicle in addition to the previous weight values are shown in Fig. 18, 19, and 20. Because the spherical tank vehicle has a shallower weight slope with mixture ratio (Fig. 14), the addition of this weight estimate raises the average change in ΔV and the upper limit curve. The lower limit curve remains the same.

(U) The analysis showed that the variation in ΔV capability between the three engine power cycles was negligible and well within the limitations established by the feed system weight effects and mission duty cycle effects.

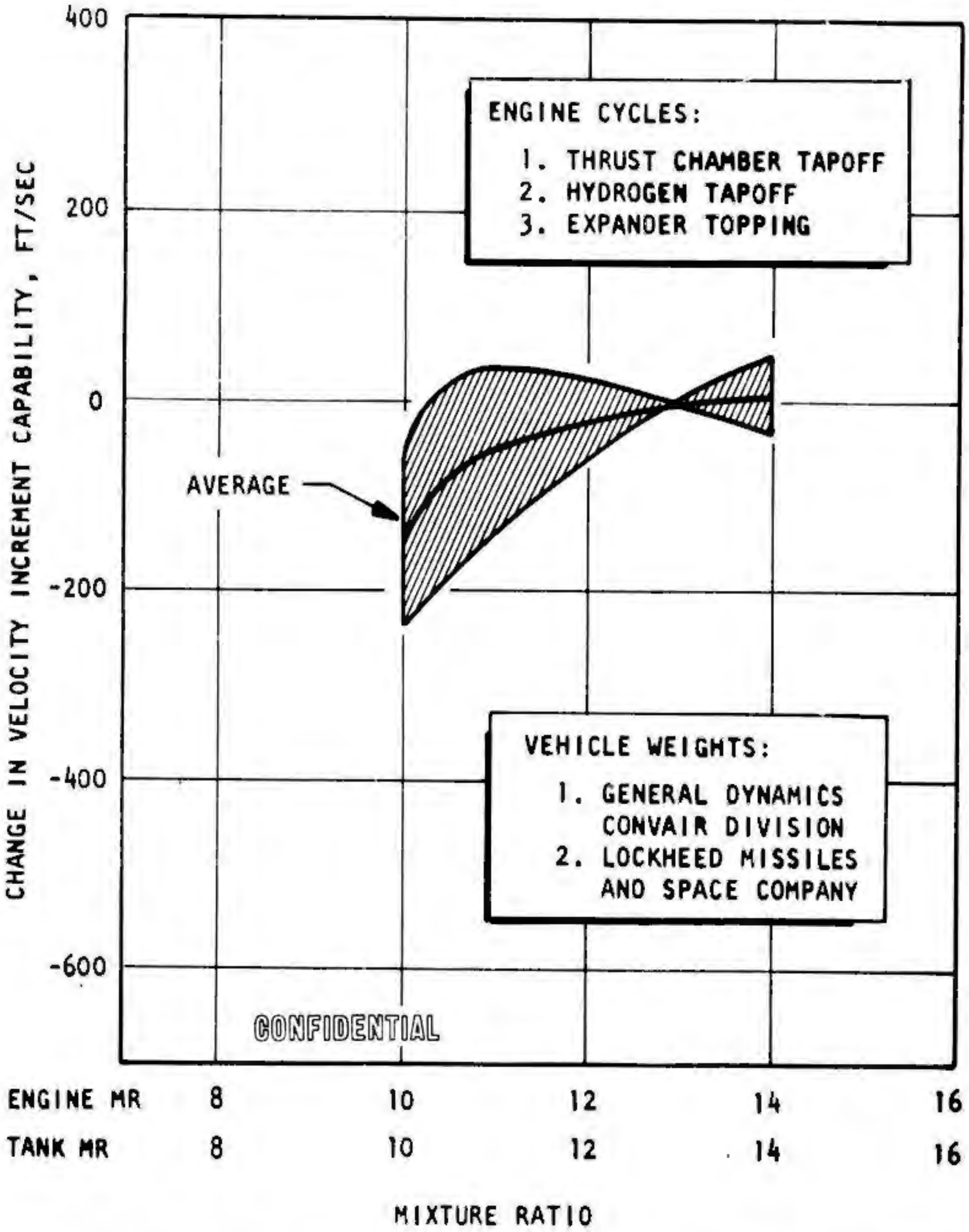

Figure 15. Range of Possible Velocity Increment Changes With Engine Mixture Ratio (Approximately Equal Use of All Engine Thrust Levels, Ellipsoidal Tank Systems) (U)

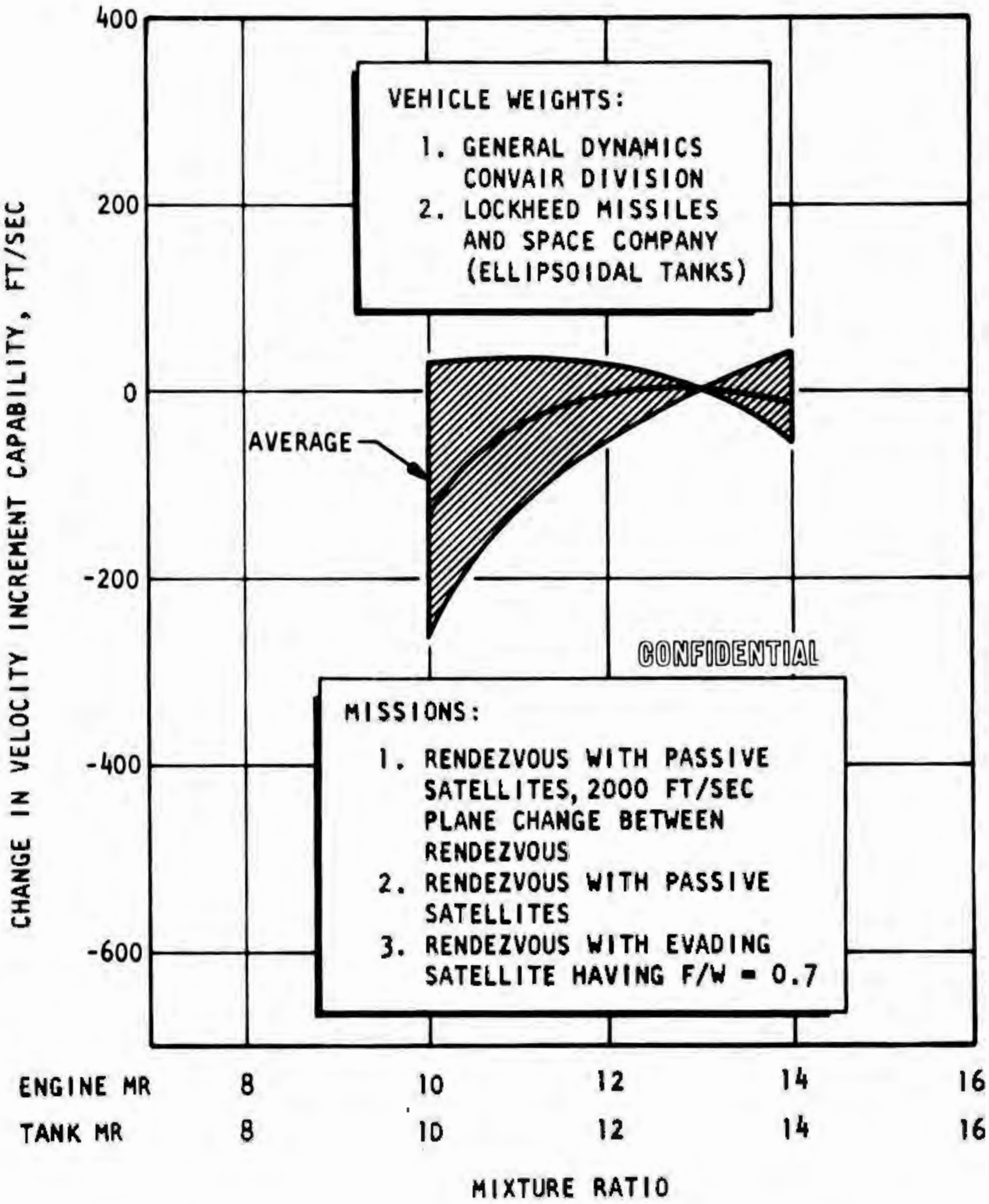

Figure 16. Range of Possible Velocity Increment Changes With Engine Mixture Ratio for Ellipsoidal Tank Vehicles (U)

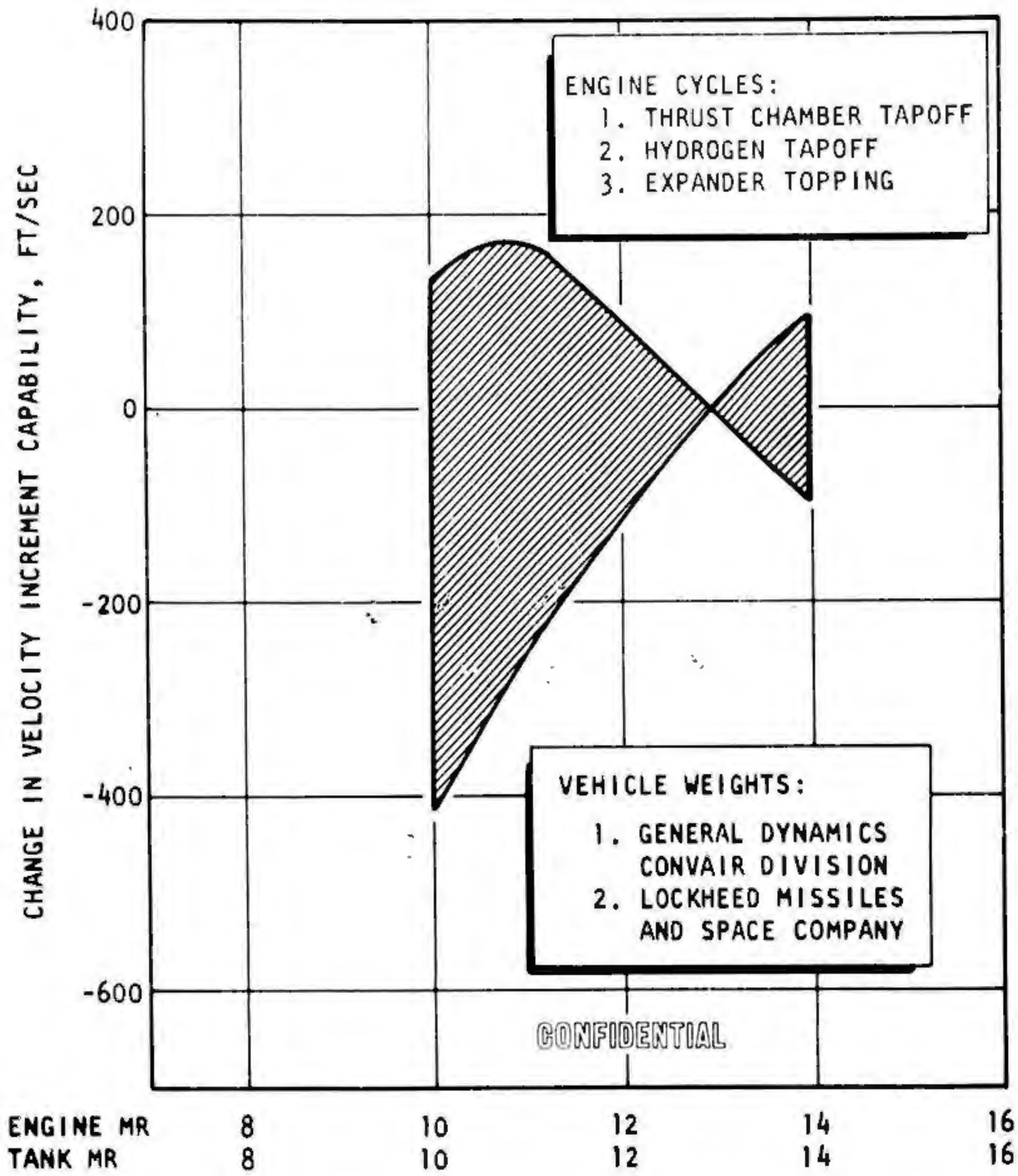

Figure 17. Maximum Possible Change in Velocity Increment Capability for Any Mission Thrust Profile (Ellipsoidal Tank Systems) (U)

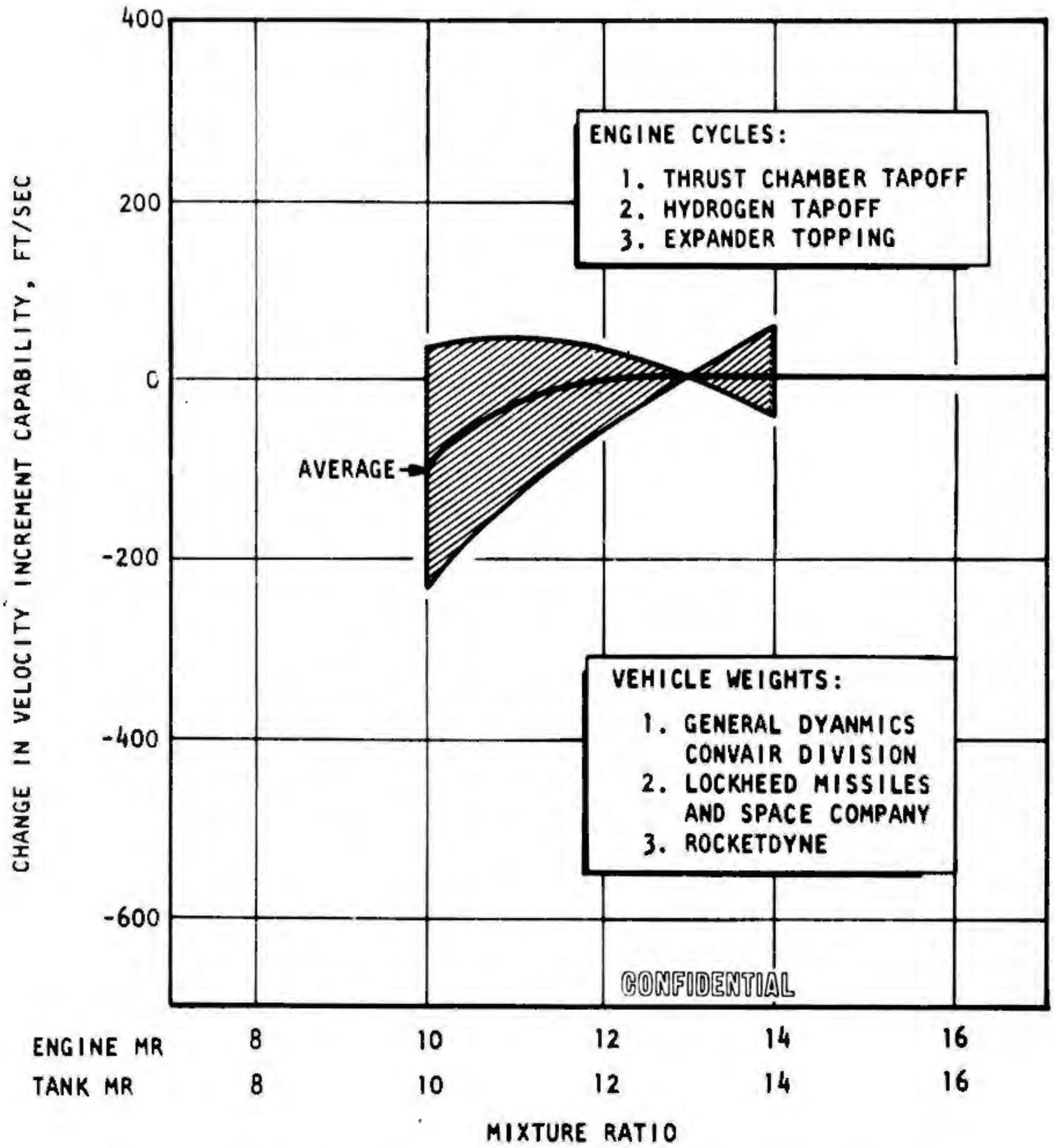

Figure 18. Range of Possible Velocity Increment Changes With Engine Mixture Ratio for Approximately Equal Use of all Engine Thrust Levels (U)

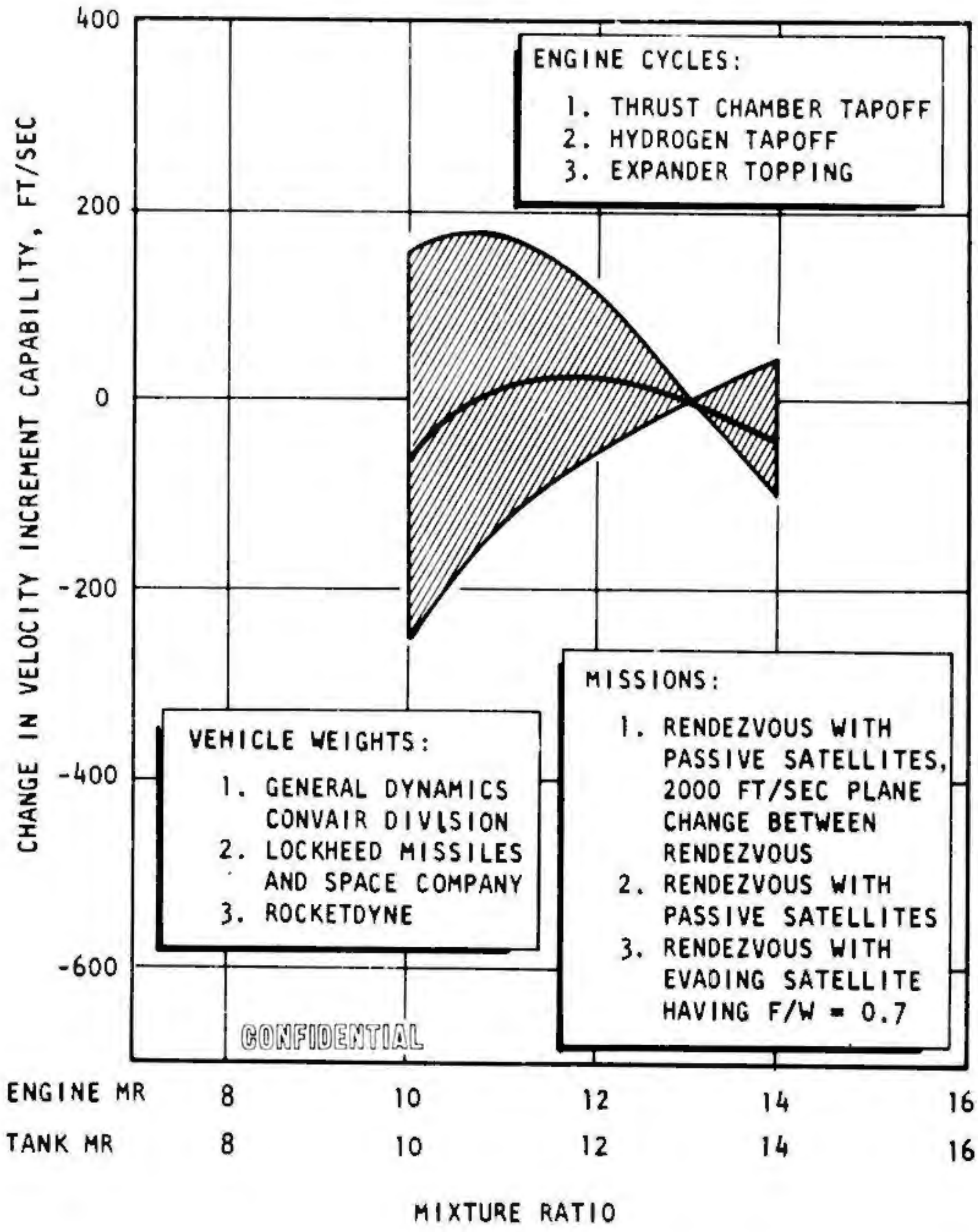

Figure 19. Range of Possible Velocity Increment Changes With Engine Mixture Ratio for Several Mission Profiles (U)

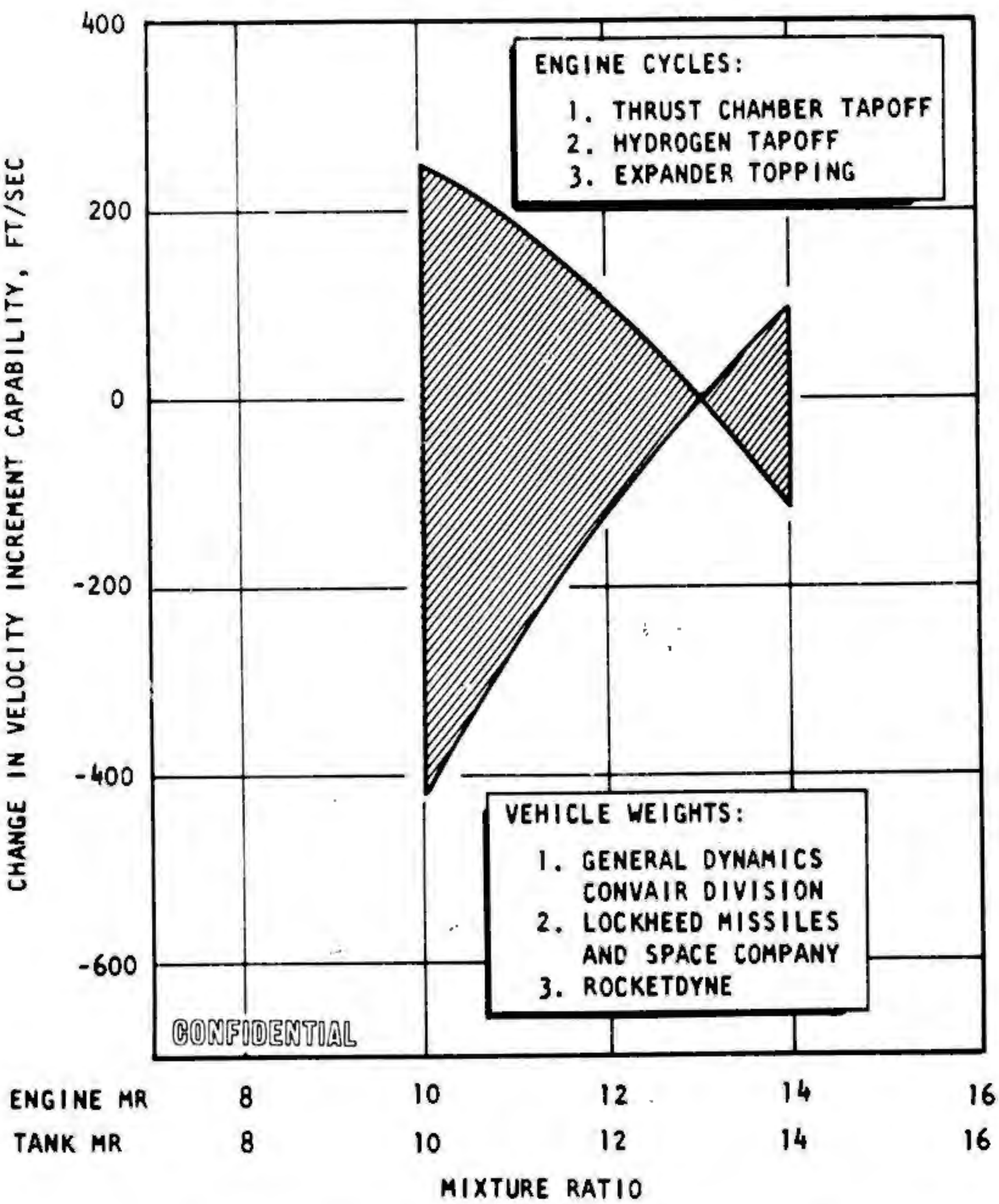

Figure 20. Maximum Possible Change in Velocity Increment Capability for Any Mission Thrust Profile (U)

(U) A comparison of the performance estimates using the ellipsoidal tank weights is shown in Fig. 21 for the tapoff cycle and a variety of thrust profiles. The Lockheed estimates tend to give a ΔV peak at lower mixture ratios than do the Convair estimates.

(d) Propellant Storage Effects

(C) The orbital lifetime of the AMPS can be increased by utilizing tank mixture ratios lower than the present original value of 13:1. This effect is shown in Fig. 22. For extended missions in which the ullage volume is increased and the hydrogen tank is vented to refrigerate the fluorine tank, the gains available in ΔV performance obtained by reducing the tank mixture ratio become even more significant. The amount of hydrogen that is vaporized during a representative mission profile is illustrated in Fig. 23. The selected mission was a 90/10 duty cycle which was determined (Ref. 1) to be critical from a hydrogen storage standpoint. This mission was defined by a propulsive maneuver immediately upon achieving orbit in which approximately 90 percent of the propellant is consumed. The propulsive maneuver is followed by a 14-day orbital coast after which the remaining propellants are burned. In Fig. 23, the weight of unvaporized hydrogen remaining in the tanks is shown at the beginning of the coast period and at the end of the 14-day coast versus tank design mixture ratio. The difference between these curves indicates the amount of hydrogen vaporized and unavailable for propulsion. These calculations are based on the orbital propellant storage analysis presented in Ref. 2. There are various approaches which may be followed to compensate for these storage losses and effect simultaneous depletion of the oxidizer and fuel. All of these approaches may be defined as a form of propellant utilization strategy.

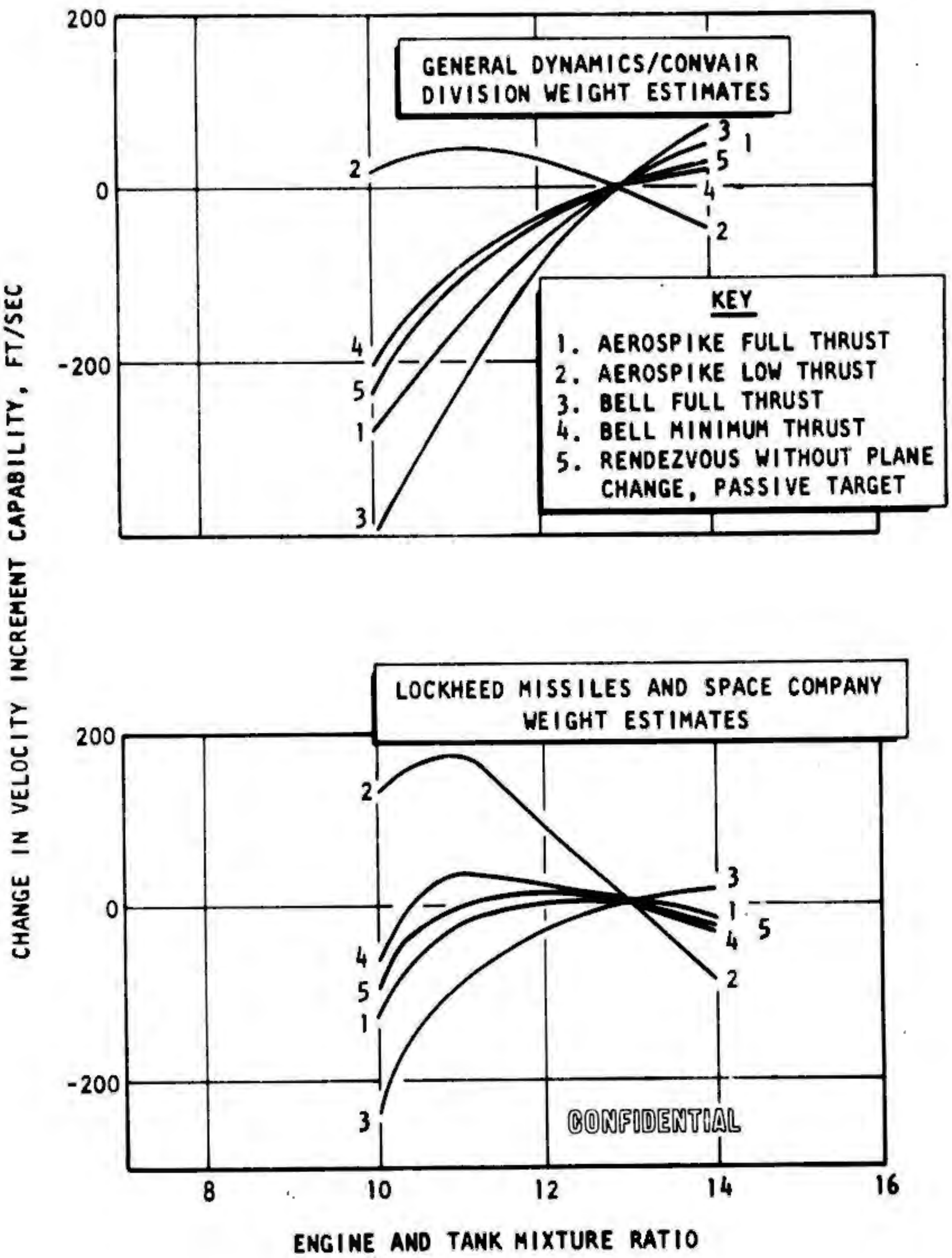

Figure 21. Effect of Weight Variation Upon Velocity Increment Variation (U)

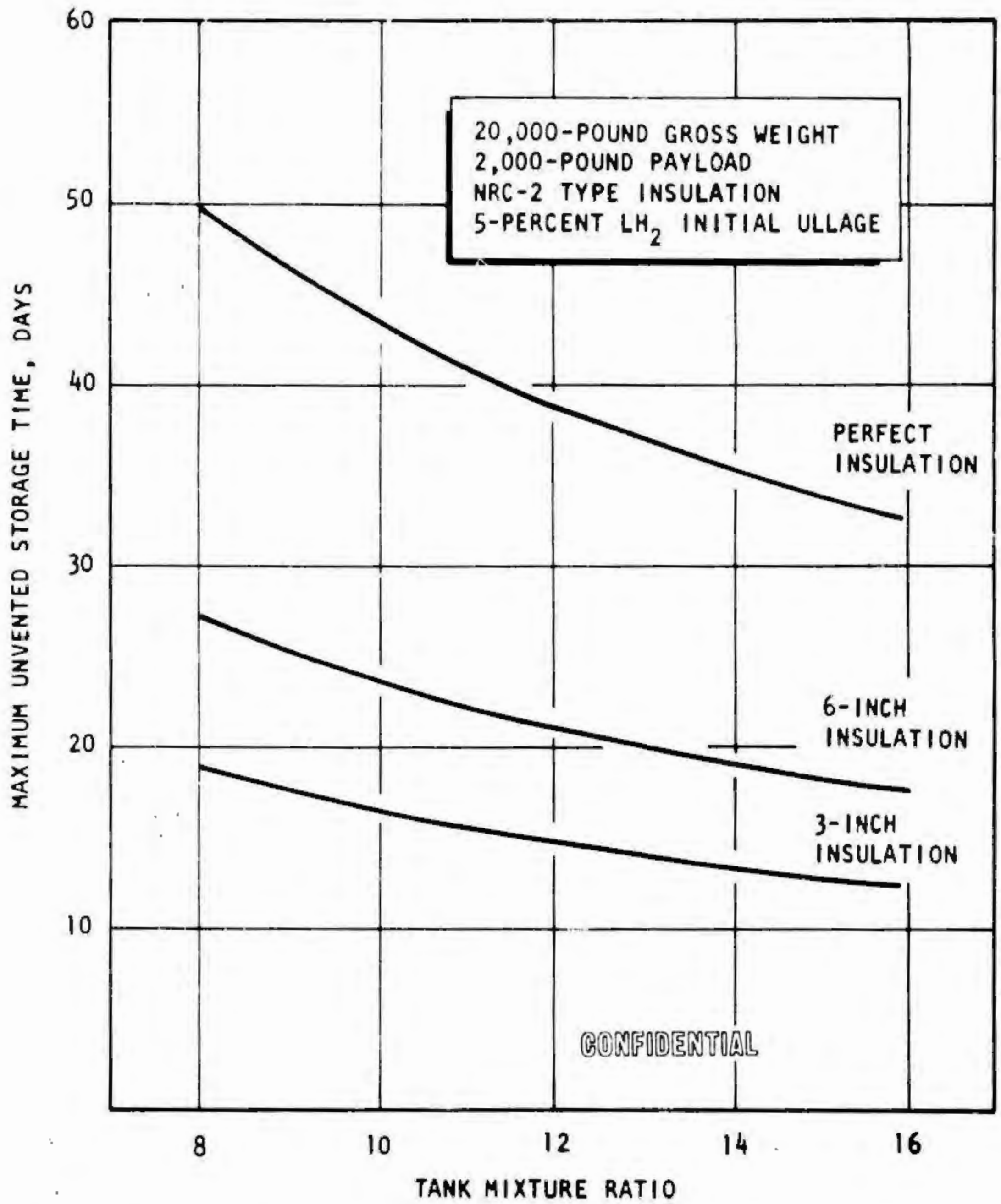

Figure 22. Effect of Tank Mixture Ratio Upon the Storability of Hydrogen (U)

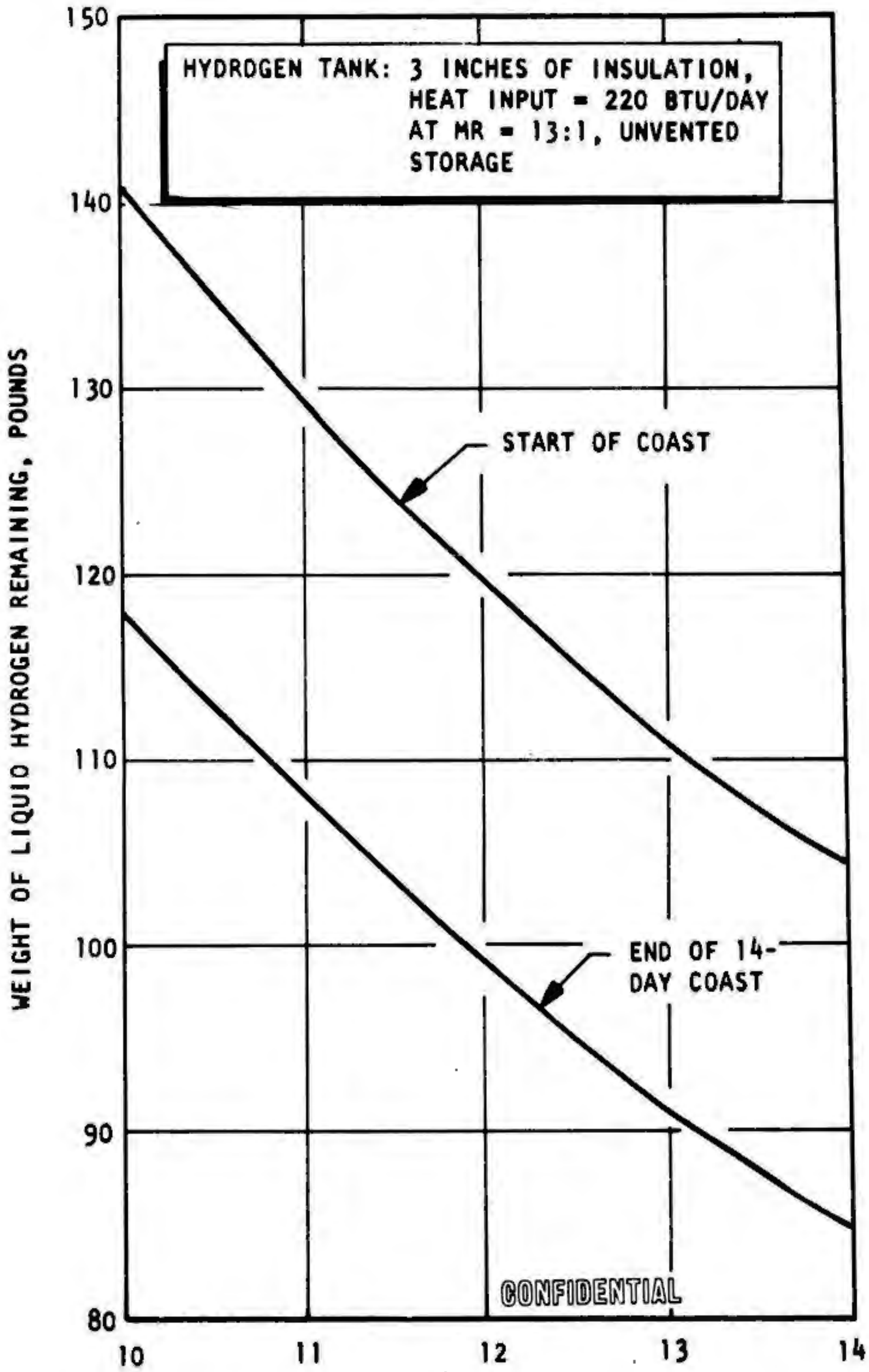

Figure 23. Residual Fuel as a Function of Engine Mixture Ratio and Duty Cycle (U)

(e) Propellant Utilization Effects

(U) To maximize the propellant utilization for all missions, the system must have a fuel bias to offset hydrogen vaporization losses. This bias can be achieved either by setting the tank design mixture ratio equal to the nominal engine mixture ratio and off-loading oxidizer for some missions, or by designing the tanks for a lower mixture ratio than the nominal. The latter method makes the most efficient use of the system's capacity but requires the capability of operating the engines at lower than nominal mixture ratio for some missions.

(U) Two approaches to propellant utilization strategy were considered in this study.

(U) In the single mode propellant utilization system, the tank design mixture ratio is equal to the nominal engine design mixture ratio, and the engine operating mixture ratio is constantly adjusted to correspond to the propellant mixture ratio existing in the tank. In those missions where large amounts of hydrogen are vaporized, very high engine operating mixture ratios could result for the final propulsive maneuvers and may be intolerable from an engine cooling standpoint.

(U) The second approach has been termed a dual mode propellant utilization system and is defined by loading the system with an excess of hydrogen to compensate for the maximum vaporization that might be expected to occur. The tanks would be designed for a lower mixture ratio than the nominal engine design mixture ratio corresponding to the amount of hydrogen bias. The engine would then be operated at the nominal design mixture ratio for the first 90 percent of the propellant consumed for all mission profiles. The remaining 10 percent of the propellants would be consumed at the then existing mixture ratio of the propellants in the tanks.

(U) The advantage of the dual mode propellant utilization system is illustrated in Fig. 24 for a range of nominal engine and tank design mixture ratios for the previously described 90/10 mission profile. The engine operating mixture ratio for the last firing is shown for both propellant utilization strategies versus the nominal tank design mixture ratio. In the case of the dual mode system, the engine mixture ratio during the last firing is also the nominal design engine mixture ratio because the hydrogen tank was biased with exactly the amount that was to be vaporized. The single mode system results in intolerably high engine mixture ratios during the last firing.

(U) Since the AMPS must be capable of a wide range of mission profiles, the propellant utilization schemes must be examined at the opposite operational extreme where all of the propellants are consumed immediately upon achieving orbit and a minimum of hydrogen vaporization has occurred. In the case of the single-mode system, the engine would operate at its nominal design mixture ratio. The situation is illustrated in Fig. 25 for the dual-mode propellant utilization.

(U) The upper curve in Fig. 25 is the same as that shown in Fig. 24 for engine operation with dual-mode propellant utilization. The lower curve in Fig. 25 shows the mixture ratio at which the engine must be operated to effect simultaneous propellant depletion on the first day. These results show that the dual-mode propellant utilization method requires that the engine be capable of operation at three mixture ratio units below its nominal design value.

(U) Relatively high nominal mixture ratios are desirable for propellant utilization because of the excursions to lower mixture ratios that are required with the dual mode of operation. The lower the nominal value, the lower must be the minimum allowable mixture ratio to achieve complete depletion. A desirable design feature, however, is to provide a thrust chamber regenerative-cooling system design that will permit operation at

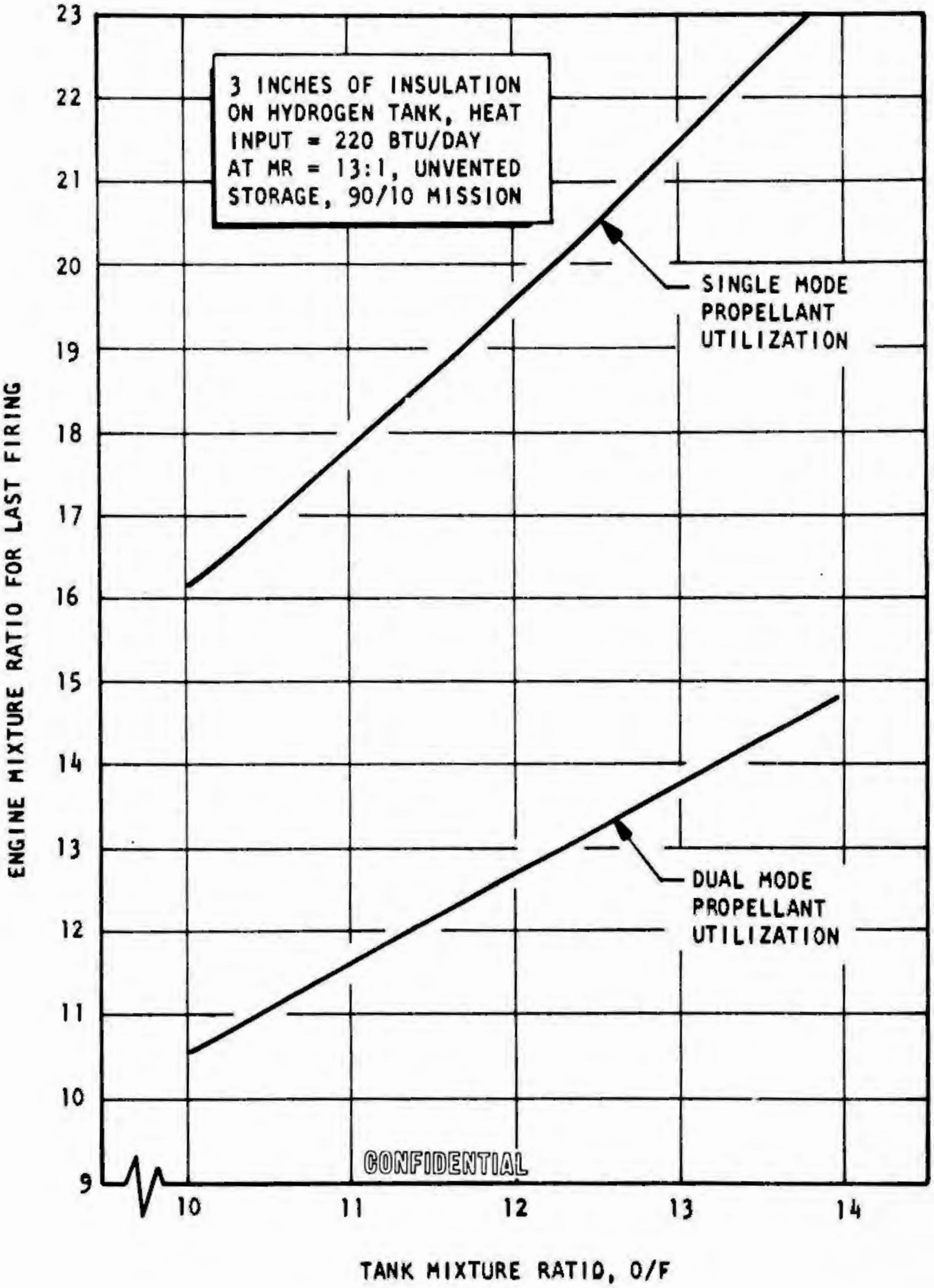

Figure 24. Propellant Utilization Comparison; Single Mode Versus Dual Mode (U)

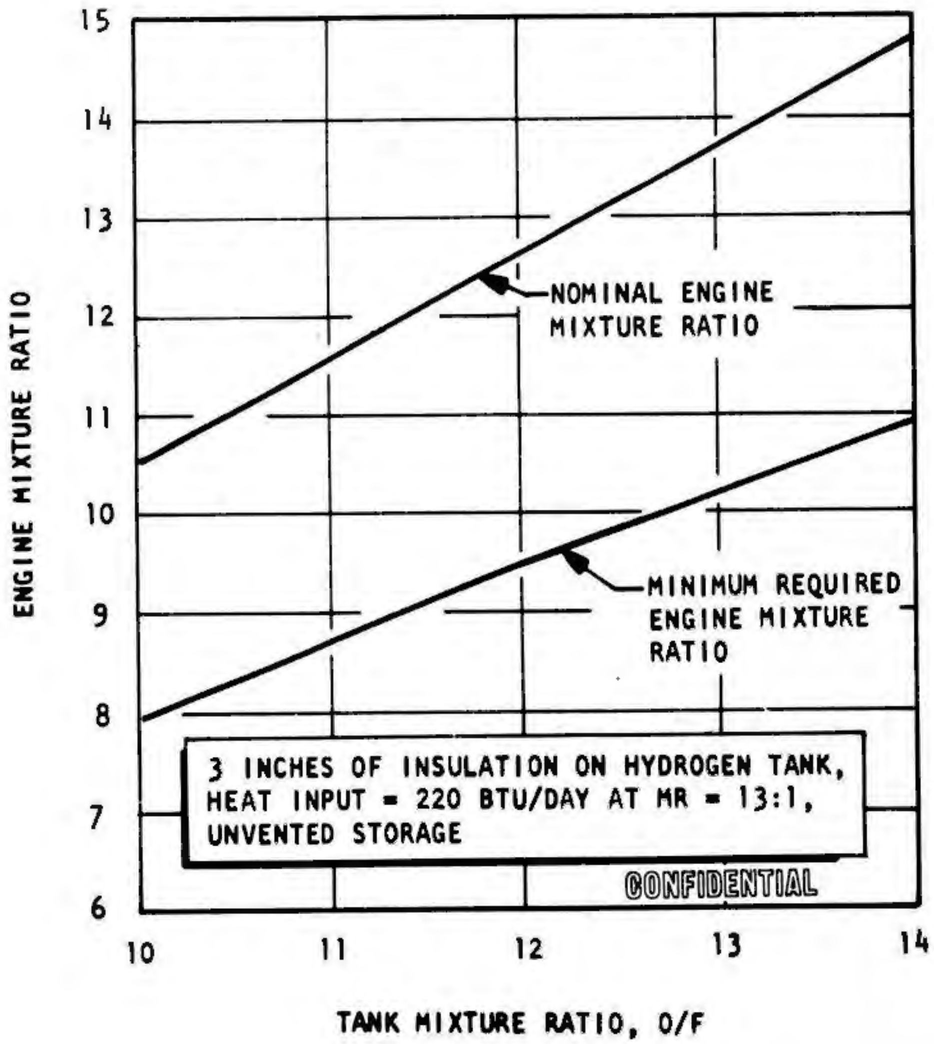

Figure 25. Dual Mode Propellant Utilization for a 1-Day Mission (U)

mixture ratios above the nominal design value. Often the capability of operation slightly above nominal is required to ensure complete propellant depletion. Also, maintaining engine mixture ratio precisely on a throttling engine is difficult, and excursions above nominal could be unavoidable.

(C) The effect of the dual mode propellant utilization on mission performance capabilities was approximated by setting the tank design mixture ratio to a value lower than the nominal engine design mixture ratio and repeating the previously described relative ΔV calculations. The results are shown in Fig. 26 and 27, and again the maximum possible performance loss is less than 1 percent for nominal engine design mixture ratios above 11.5:1.

(C) An alternate variation to the dual mode propellant utilization system might be considered. The oxidizer tank could be off-loaded to provide the hydrogen bias to compensate for storage losses. In this case, the tank design mixture ratio would be equal to the nominal engine design mixture ratio, but the dual mode propellant utilization system would otherwise function as previously described. As a result, less propellant would be available for propulsion and the tank weight associated with this unfilled oxidizer tank volume must be carried through the propulsive maneuver as inert weight. A degradation in system ΔV capability would result in comparison with the fuel bias tank design. The magnitude of the ΔV loss is illustrated in Fig. 28 versus nominal engine design mixture ratio for the 90/10 mission duty cycle. The ΔV values have been normalized to the ΔV achieved with a single firing at a mixture ratio of 13:1. The off-loaded oxidizer tank results in an approximate 2.5-percent loss in ΔV in comparison with the fuel bias tank design.

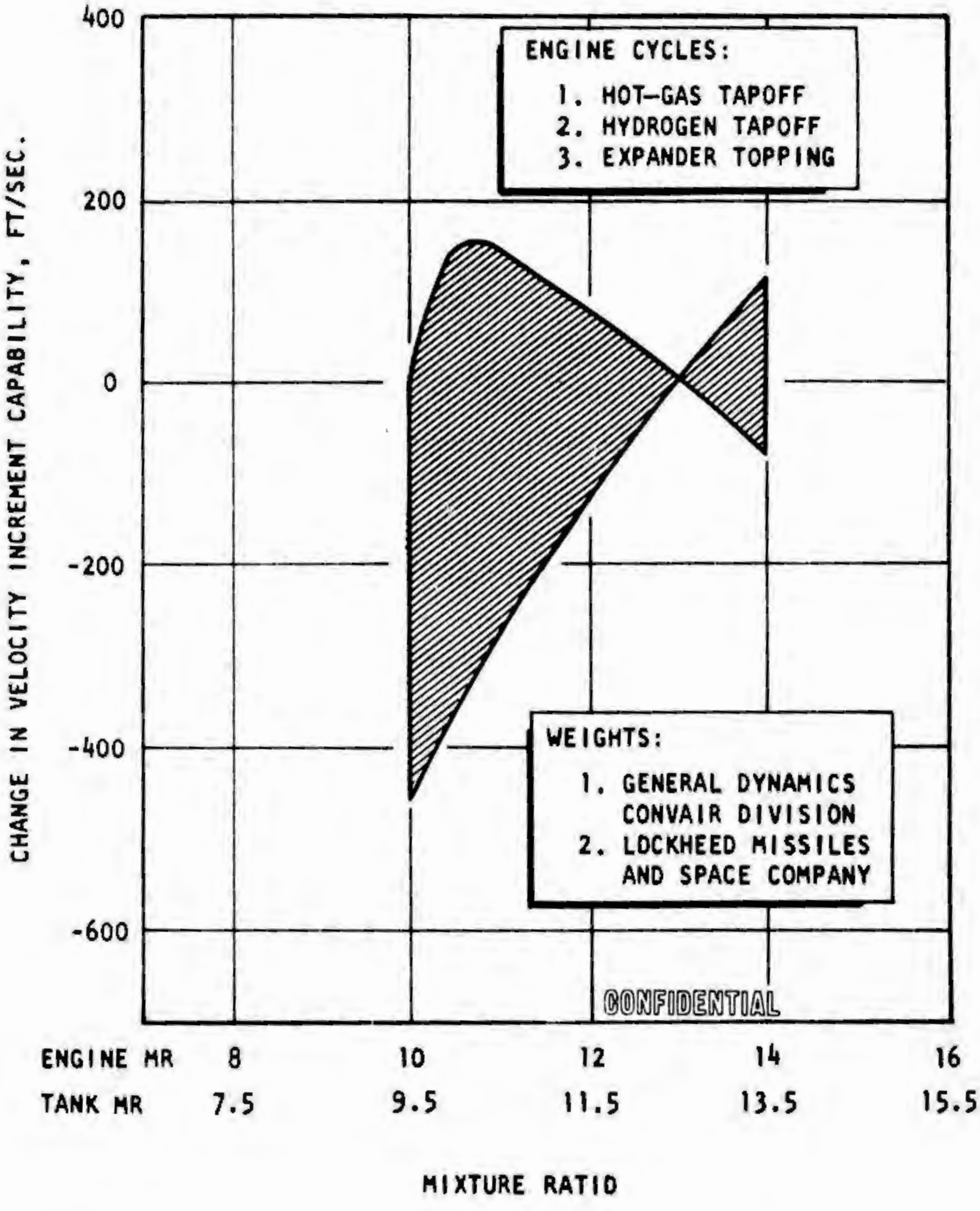

Figure 26. Maximum Possible Change in Velocity Increment Capability for Any Mission Thrust Profile With Ellipsoidal Tank Systems (MR_{tank} = MR_{engine} -0.5) (U)

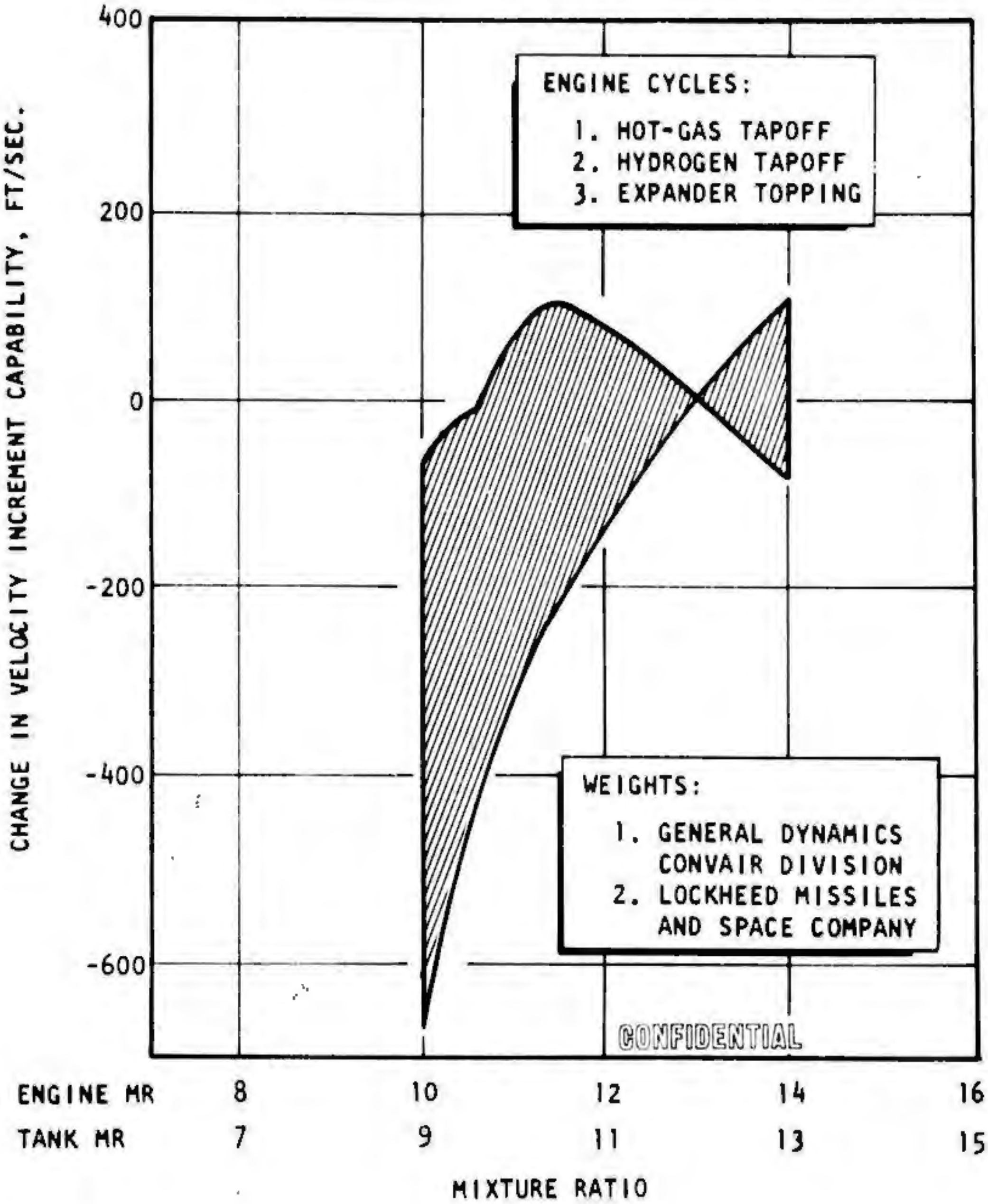

Figure 27. Maximum Possible Change in Velocity Increment Capability for Any Mission Thrust Profile With Ellipsoidal Tank Systems ($MR_{tank} = MR_{engine} - 1.0$) (U)

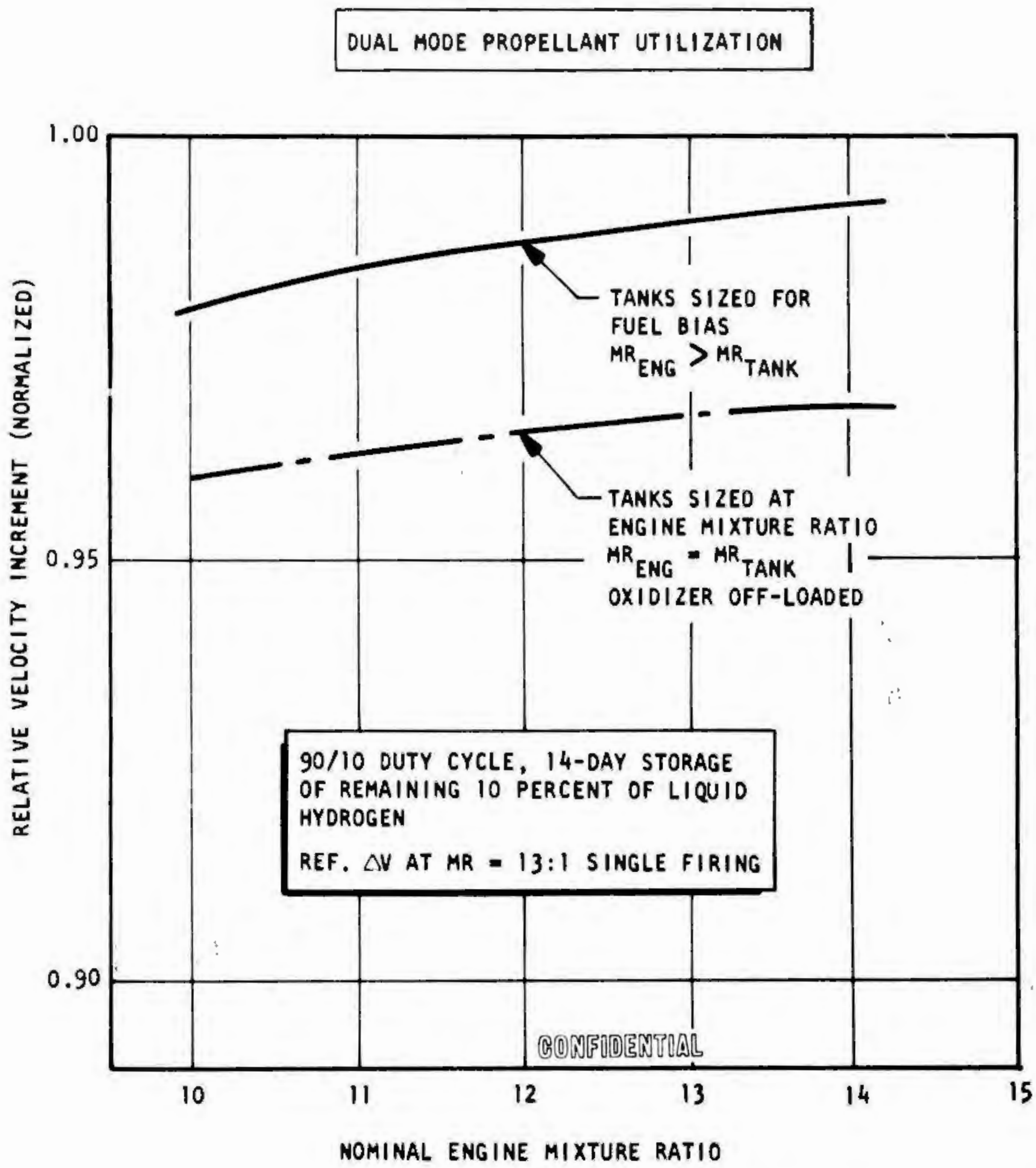

Figure 28. Effect of Engine Mixture Ratio on Relative Velocity for Two Tank Sizing Schemes (U)

(..) Engine Durability

(C) As was previously discussed, the engine design philosophy assumed for reduced engine design mixture ratios was to let the thrust chamber gas side wall temperature become the variable. As the mixture ratio is reduced, the wall temperature decreases, but the tube bundle pressure drops and, thus, the pump discharge pressure is increased. The reduced thrust chamber wall temperature would result in an improvement in engine durability with the presently selected tube material.. The effect of reducing the nominal engine design mixture ratio with a constant tube design, on wall temperature and tube bundle pressure drop, is shown in Fig. 29 for the main engine. These results show that the wall temperature is reduced 100 F for each unit reduction in mixture ratio. The pressure drop is increased 30 psi for each unit reduction in mixture ratio.

(3) Mixture Ratio Selection Summary

(U) A summary of the major results of this analysis is outlined below.

1. Generally, decreasing mixture ratio results in increasing specific impulse.
2. Decreasing tanked mixture ratio results in increasing stage weight.
3. Mission ΔV is only slightly affected over the mixture ratio range considered.
4. A propellant storage advantage exists for lower tank mixture ratios.
5. The propellant utilization system requires that the engine be capable of operation at 3 mixture ratio units below the nominal design value (dual mode).
6. Thrust chamber hot-gas side tube-wall temperature is 100 F lower per unit of mixture ratio decrease.

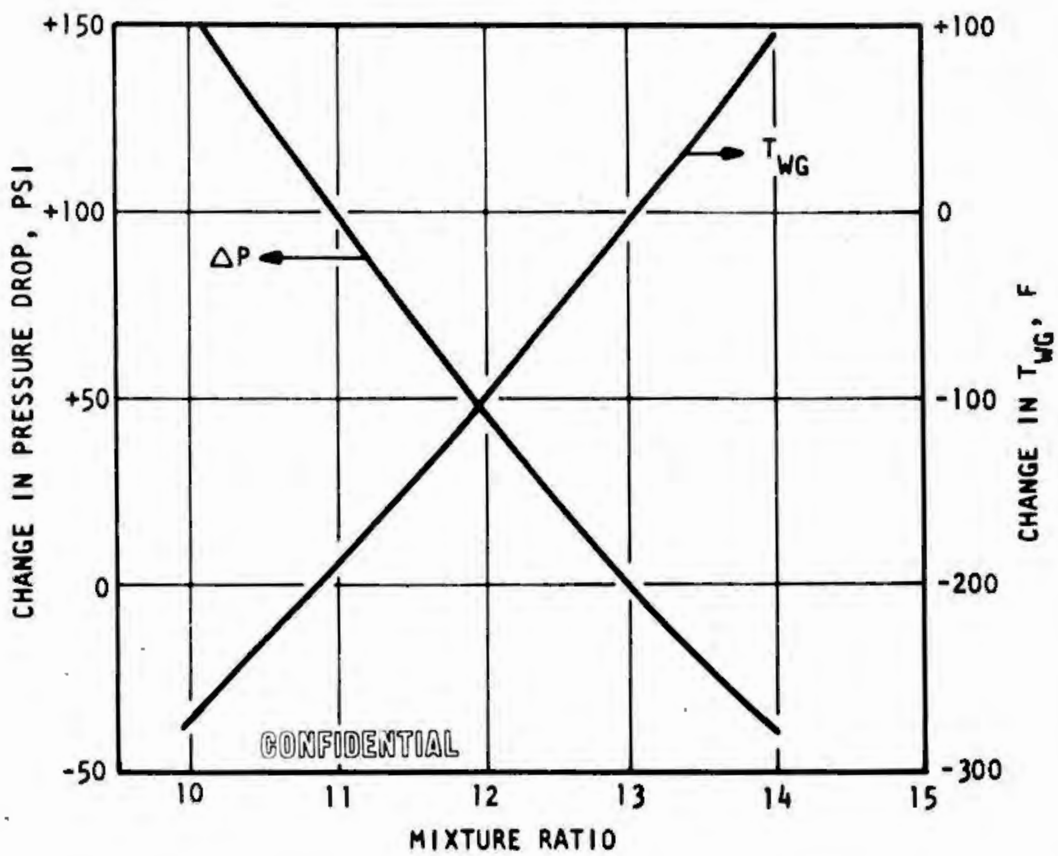

Figure 29. Effect of Mixture Ratio Variation on Wall Temperature and Pressure Drop (U)

(C) A review of these system studies has led to the selection of a nominal engine design mixture ratio of 12:1. This engine mixture ratio provides near maximum ΔV capability, reasonable mixture ratio excursions (both higher and lower) for propellant utilization, and increased engine durability over the previously selected value of 13:1.

(C) A propellant tank design mixture ratio of 11.5:1 is recommended based on the Rocketdyne orbital propellant storage studies (Ref. 1). Propellant feed system subcontractor experience or analysis may indicate lower hydrogen tank heating rates which may alter the recommended tank design mixture ratio. Also, a lower tank design mixture ratio may result from the consideration of fuel-rich start and cutoff transients and the wide variations in expected engine restart requirements.

d. Basic Engine Design Parameter Definition

(U) The basic engine design parameters for the engine were defined, and are presented in Table 8. Primary changes from the original design parameters at the start of the program include the main engine thrust chamber pressure, expansion area ratio, turbine drive cycle, thrust chamber design configuration, and engine mixture ratio for the main and secondary engines. Other differences between the original parameters and current design parameters listed in Table 8 are either related to the differences listed above or are the result of refinements in the description of components, lines, and manifolds. Pressure and temperature distributions throughout the main and secondary engine systems are presented in Fig. 30 and 31.

CONFIDENTIAL

Parameter	9:1 Engine Mixture				
	Main Engine				
Thrust at Vacuum, pounds	30,000		3330		33
Nozzle Stagnation Pressure, psia	654.3		77.4		75
Total Oxidizer Flowrate, lb/sec*	58.80		6.86		6.
Total Fuel Flowrate, lb/sec*	6.53		0.76		0.
Thrust Chamber Mixture Ratio, o/f	11.52		9.44		10
Thrust Chamber Oxidizer Flowrate, lb/sec	58.80		6.86		6.
Thrust Chamber Fuel Flowrate, lb/sec	5.11		0.727		0.
Oxidizer Turbine Flowrate, lb/sec	0.431		0.0055		0.
Fuel Turbine Flowrate, lb/sec	0.997		0.0295		0.
Turbine Inlet Temperature, R	798		1440		15
Hydrogen Injection Temperature, R	848		1490		51
Nominal Specific Impulse, seconds	459.2		436.8		45
	Oxid.	Fuel	Oxid.	Fuel	Oxid.
System Pressure Losses, psid					
Injector	194	405	25	90	364
Cooling Jacket, Manifolds, and Ducts	--	1249	--	202	--
Line and Manifolds	--	--	--	--	38
Line	39	15	0.1	0.1	38
Pump Discharge Pressure, psia	887	2319	102	370	1235
Pump Inlet Pressure, psia	45	60	45	60	45
Pump Horsepower	195.7	1205.6	2.16	25.8	42.3

*Nominal propellant inlet temperatures to the pumps are 157 and 47 R for

TAB.E 8

ENGINE SYSTEM OPERATING PARAMETERS (U)

ixture Ratio				12:1 Engine Mixture Ratio (Nominal Design)									
Secondary Engine				Main Engine				Secondary Engine				Ma	
3330		370		30,000		3330		3330		370		30,000	
757.0		88.4		650.0		77.8		749.4		87.9		647.2	
6.53		0.771		60.20		7.21		6.70		0.799		60.72	
0.725		0.086		5.02		0.60		0.559		0.066		4.67	
10.26		9.21		14.81		12.50		13.62		12.30		15.91	
6.47		0.769		60.20		7.21		6.66		0.797		60.72	
0.630		0.083		4.06		0.57		0.489		0.065		3.82	
0.055		0.0018		0.342		0.0045		0.055		0.0017		0.325	
0.100		0.0016		0.610		0.0189		0.059		0.0010		0.529	
1535		1775		1038		1870		1660		1980		1108	
517		729		1088		1920		642		960		1158	
459.0		431.9		460.0		426.5		458.5		427.5		458.8	
Oxid.	Fuel	Oxid.	Fuel	Oxid.	Fuel	Oxid.	Fuel	Oxid.	Fuel	Oxid.	Fuel	Oxid.	Fu
364	316	43	37	200	335	25	90	375	244	44	29	204	32
--	257	--	30	--	1036	--	167	--	198	--	23	--	87
38	188	0.5	2.2	--	--	--	--	40	105	0.6	1.5	--	--
38	34	0.5	0.4	39	12	0.1	0.1	40	20	0.6	0.2	39	11
1235	1591	137	163	889	2033	103	335	1240	1354	138	146	890	18
45	60	45	60	45	60	45	60	45	60	45	60	45	60
42.3	125.8	0.61	1.02	201.9	808.8	2.27	18.0	43.6	73.8	0.61	0.72	204.7	68

' R for the oxidizer and fuel

2

inal Design)				13:1 Engine Mixture Ratio							
Secondary Engine				Main Engine				Secondary Engine			
330		370		30,000		3330		3330		370	
49.4		87.9		647.2		77.9		745.9		87.7	
.70		0.799		60.72		7.31		6.75		0.806	
.559		0.066		4.67		0.56		0.519		0.062	
3.62		12.30		15.91		13.51		14.77		13.33	
.66		0.797		60.72		7.31		6.71		0.805	
.489		0.065		3.82		0.53		0.454		0.060	
.055		0.0017		0.325		0.004		0.055		0.0017	
.059		0.0010		0.529		0.0171		0.052		0.0009	
660		1980		1108		1970		1705		2045	
42		960		1158		2020		686		1030	
58.5		427.5		458.8		423.0		457.9		425.9	
.	Fuel	Oxid.	Fuel	Oxid.	Fuel	Oxid.	Fuel	Oxid.	Fuel	Oxid.	Fuel
	244	44	29	204	320	25	85	377	226	45	27
	198	--	23	--	876	--	158	--	184	--	22
	105	0.6	1.5	--	--	--	--	40	89	0.6	1.1
	20	0.6	0.2	39	11	0.1	0.1	40	17	0.5	0.2
)	1354	138	146	890	1857	103	321	1241	1300	138	142
	60	45	60	45	60	45	60	45	60	45	60
,	73.8	0.61	0.72	204.7	685.3	2.30	1.60	44.0	64.4	0.61	0.65

3

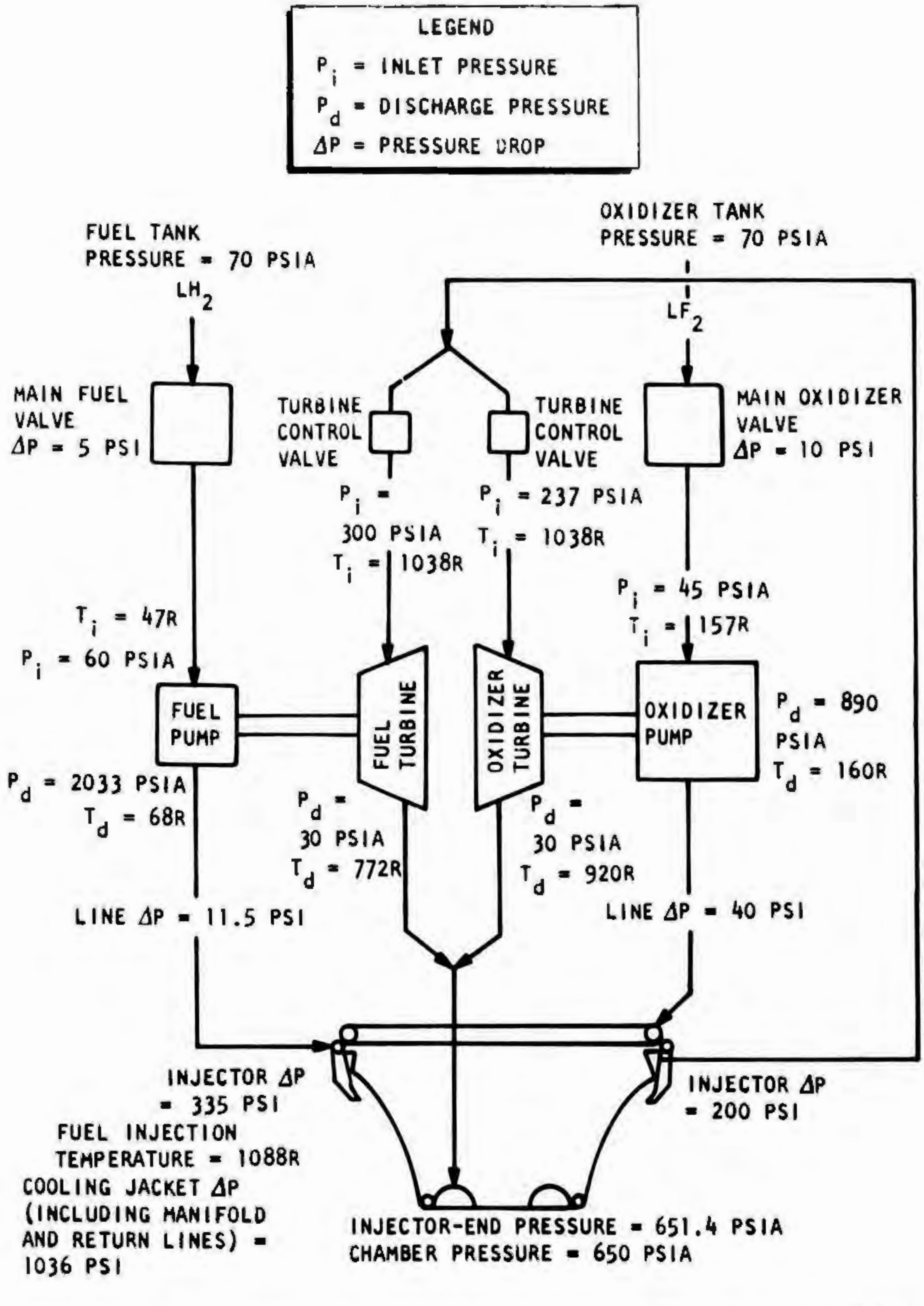

Figure 30. Pressure and Temperature Values for Main Engine at Full Thrust and 12:1 Mixture Ratio (C)

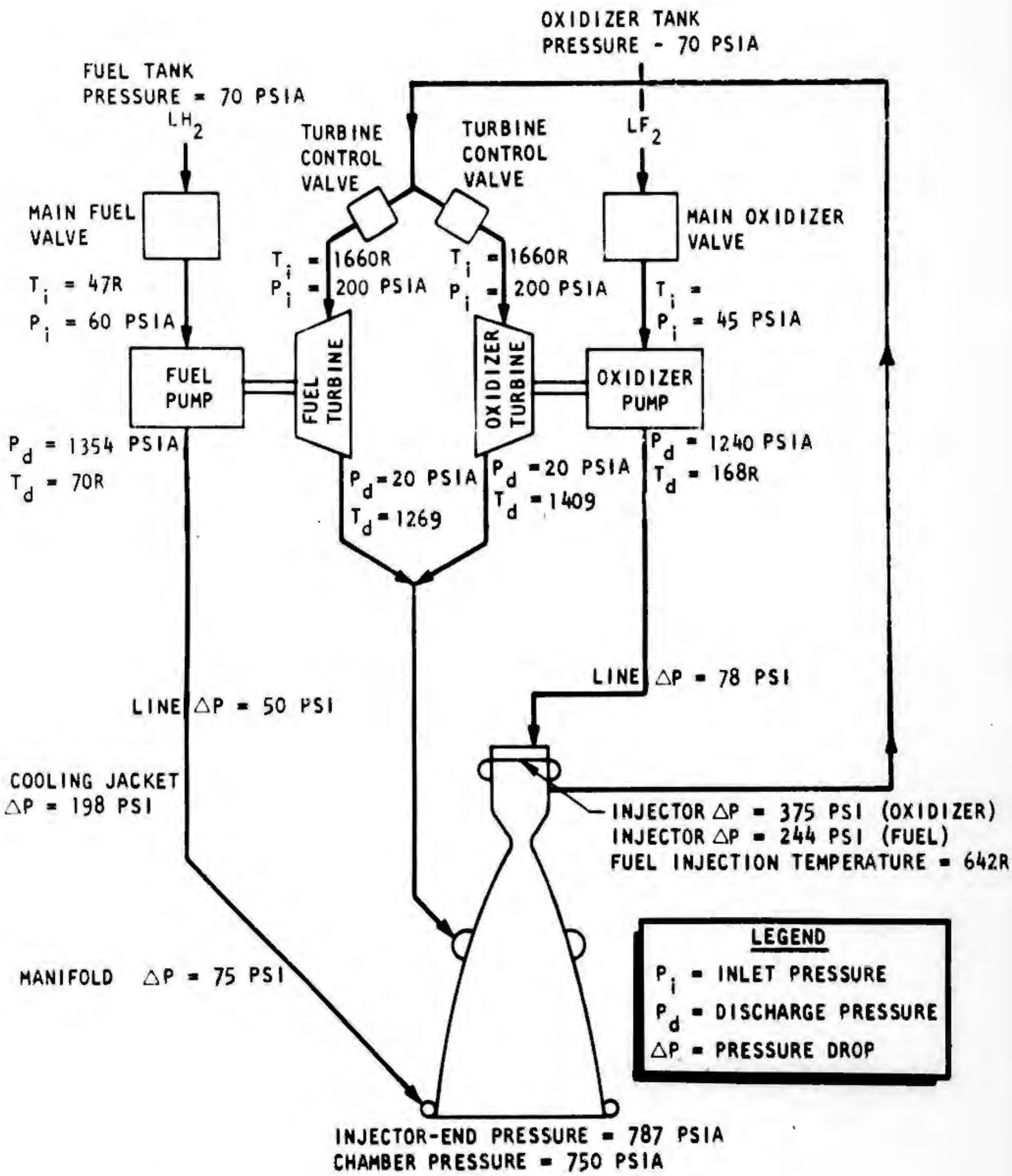

Figure 31. Pressure and Temperature Values for Secondary Engine at Full Thrust and 12:1 Mixture Ratio (C)

e. Thrust and Mixture Ratio Envelope

(C) An engine system study was conducted to define the range of thrust and mixture ratios within which the engine is capable of operation. Previous component and engine system design and operational studies have been conducted at the nominal engine mixture ratio of 12:1 and over the required throttling thrust range. However, mixture ratio selection and propellant storage studies have indicated that off-design mixture ratio operation will be required to accomplish the range of possible mission applications with a maximum performance capability. As a result, the engine system must be capable of operation over a range of mixture ratios at any thrust level within the required throttling range. The exact limits of the required mixture ratio excursions were not known at the time of this study because the propellant management subsystem studies had not been completed. However, previous studies concerned with AMPS mixture ratio selection, propellant storage capability, and propellant utilization requirements, have indicated that for efficient propellant utilization, the engine must be capable of operating three mixture ratio units below the nominal design. The analysis also determined that the capability of operating slightly above nominal mixture ratio is also required to ensure complete propellant depletion.

(C) Based on these earlier findings, engine and component thrust and mixture ratio envelope studies were conducted over a mixture ratio range of from 9:1 to 13:1 and over the required thrust range for both the main and secondary engine. This mixture ratio range is anticipated to be adequate for the propellant utilization requirements.

(1) Method of Analysis

(U) A flow chart describing the various steps involved in this study is shown in Fig. 32 . The analysis was begun by conducting an engine system power balance and performance analysis for a range of engine thrust levels and mixture ratios. The current engine and component design and operating

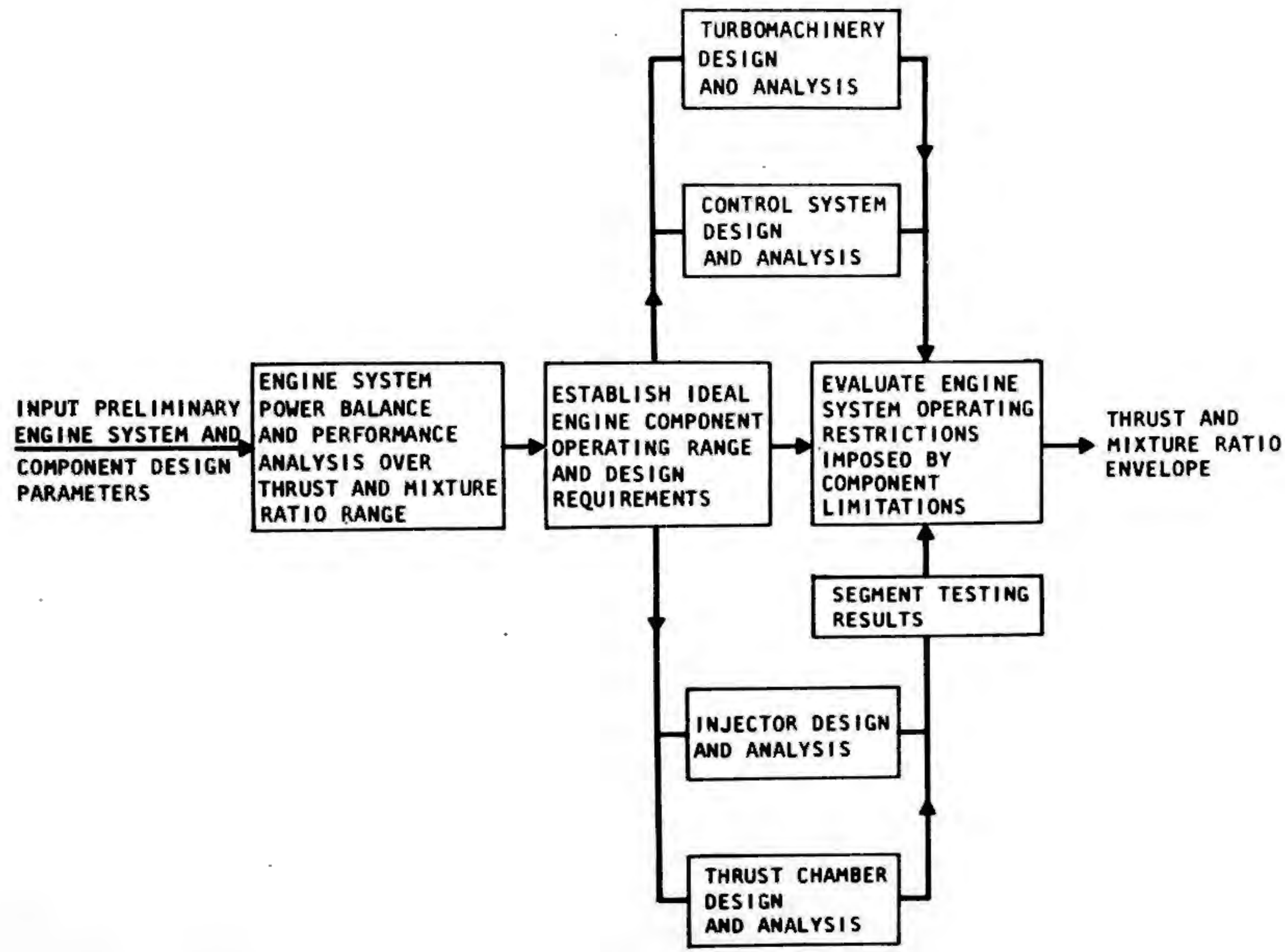

Figure 32. Flow Chart for Thrust and Mixture Ratio Envelope Evaluation (U)

(U) parameters were input to this analysis along with the current pump and turbine operating maps, predicted thrust chamber efficiencies, and regenerative cooling heat transfer values.

(U) The results of this analysis provide detailed information pertaining to the engine system and component operating range, such as, propellant flowrates, turbine flowrates, valve pressure drop requirements, and turbine speeds vs thrust and mixture ratio. This information then establishes the ideal or desired range of operating conditions for each of the engine system components over the range of thrust and mixture ratio considered. This information is then fed into the individual component design and analysis studies to indicate the desired operating range in speed, pressure drop, flowrate, and pump head rise. Where this operating range cannot be satisfied without seriously compromising the design, the restrictions imposed by that specific component are imposed on the engine system operating range. The net result will be to define the thrust vs mixture ratio envelope within which the overall engine system is capable of operation.

(2) Results

(U) The engine power balance and performance analysis was completed for the main and secondary engines over their respective thrust and mixture ratio ranges. The results of this analysis have been evaluated to determine the range of operating conditions and design requirements for each of the system components. An example of the type of information that is obtained from this analysis is presented in Fig. 33 through 38, which show the operating ranges of the main engine fuel and oxidizer pumps and the turbine hot-gas valve to satisfy the required range of thrust and mixture ratio.

(C) The main engine pump design studies have furnished pump maps (head vs flow curves) indicating permissible regions of operation. The required operating regions from the engine power balance analysis were then superimposed on these maps. The results are shown in Fig. 39 for the main engine oxidizer and fuel pumps. The required operating regions are shown for the oxidizer pump with either single or dual turbine hot-gas control

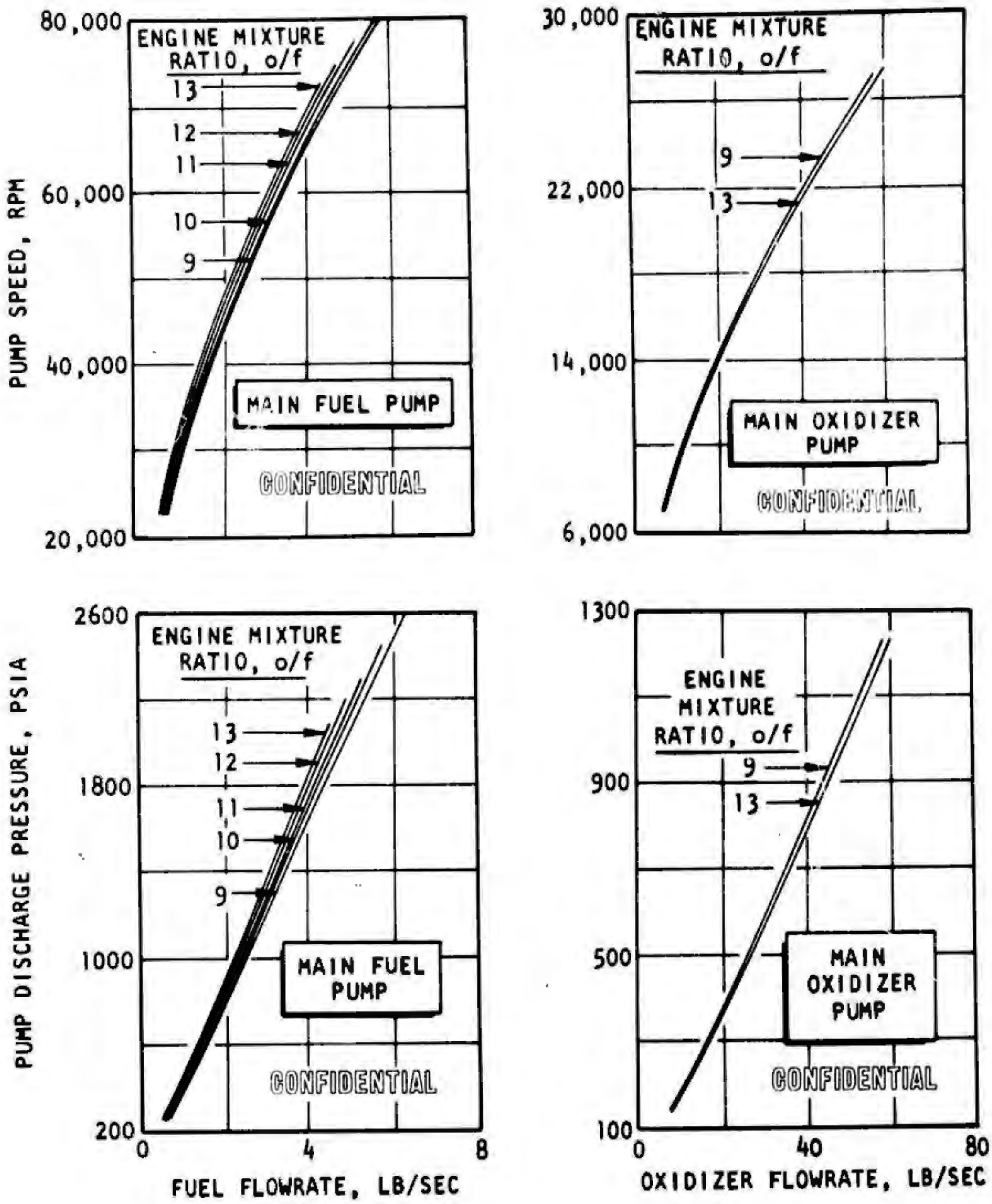

Figure 33. Operating Requirements for Main Engine Pumps (U)

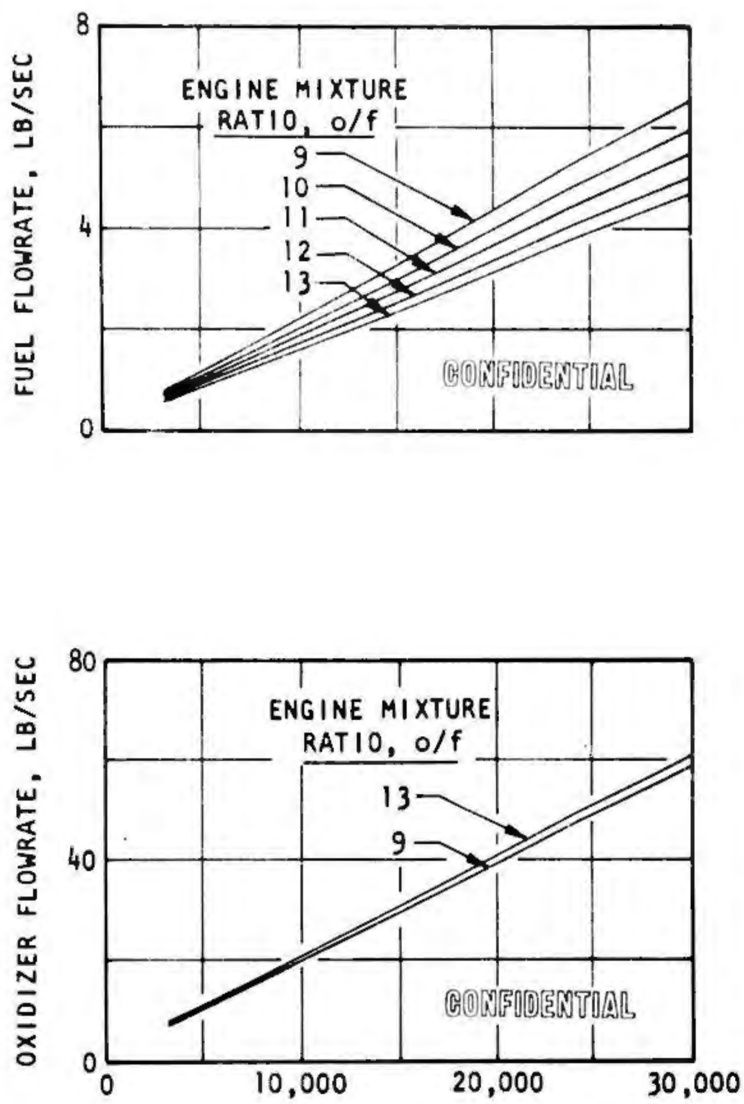

Figure 34. Flowrate Requirements for Main Engine Propellants (U)

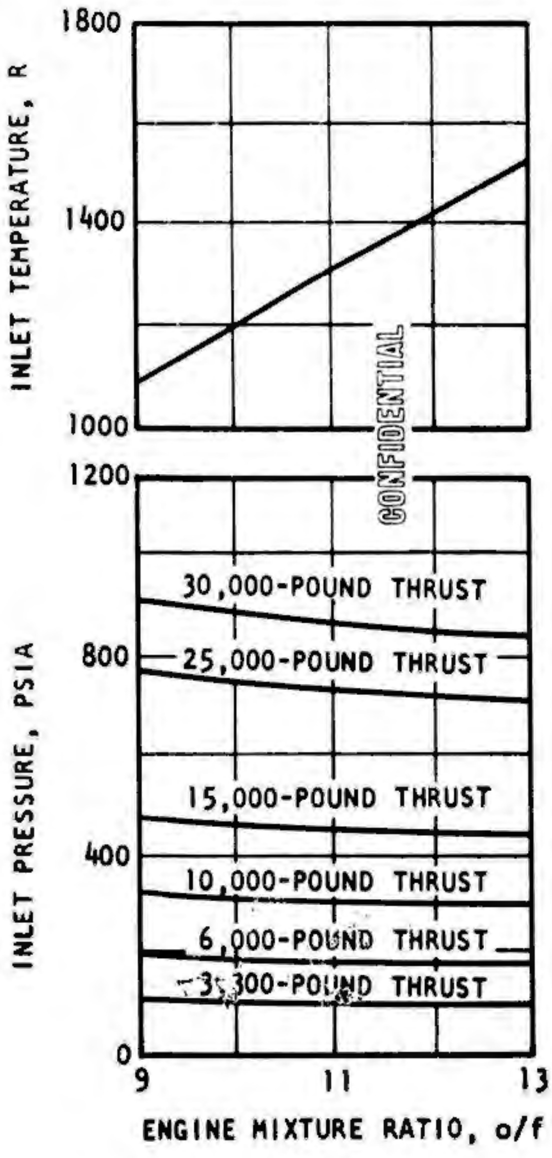

Figure 35 . Inlet Conditions for Main Engine Hot-Gas Valve (U)

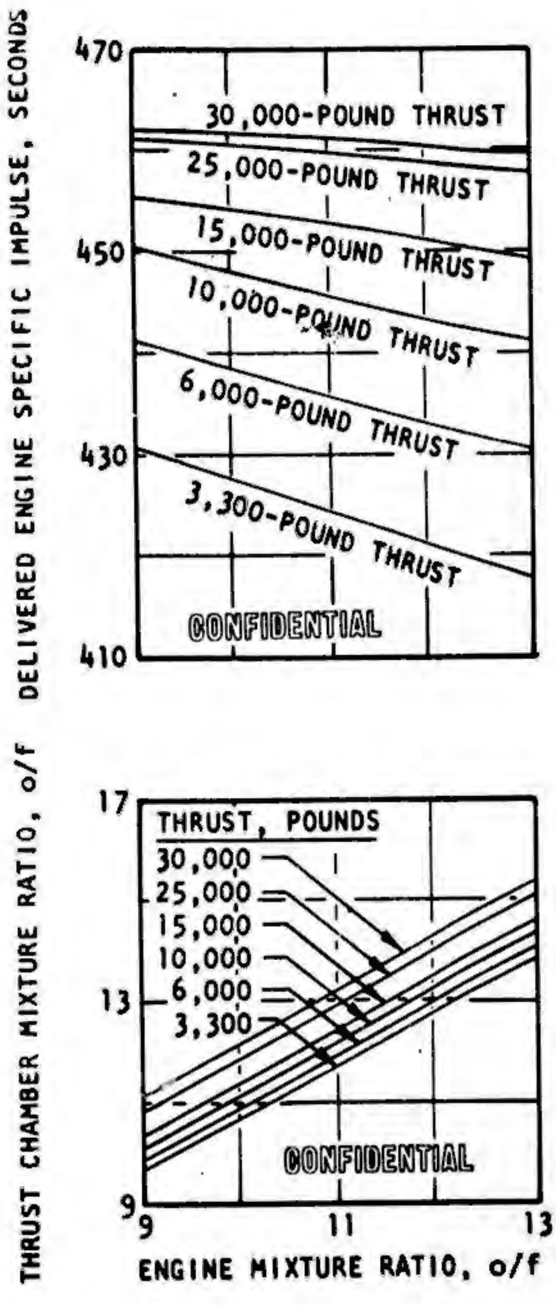

Figure 36 . Main Engine Performance (U)

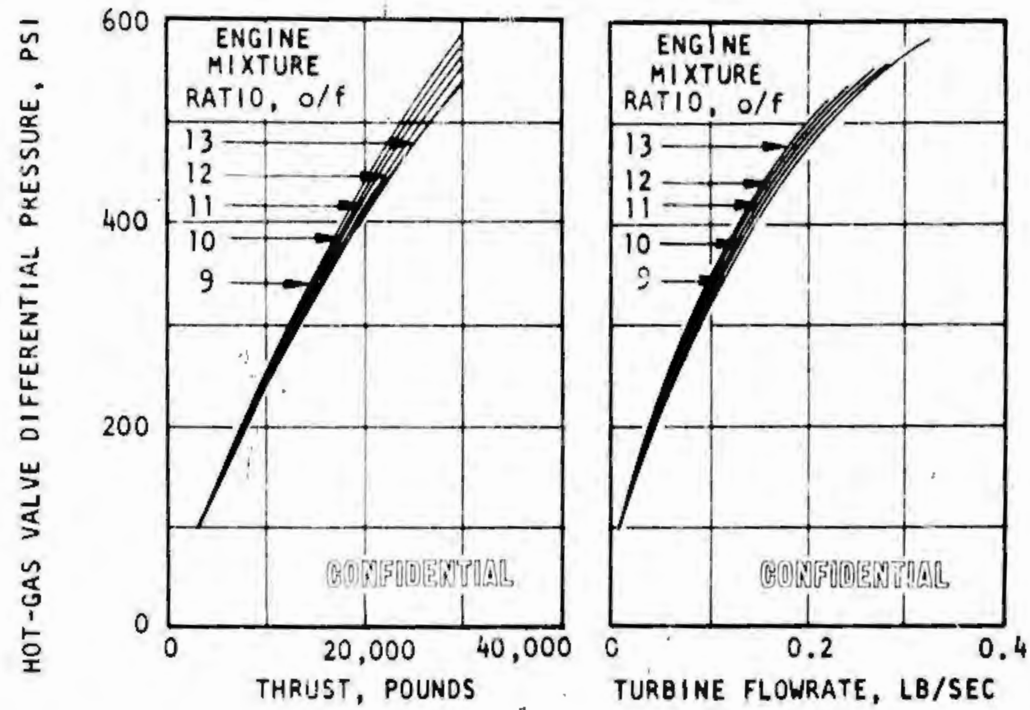

Figure 37. Differential Pressure Requirements for Main Engine Oxidizer Turbine Hot-Gas Valve (U)

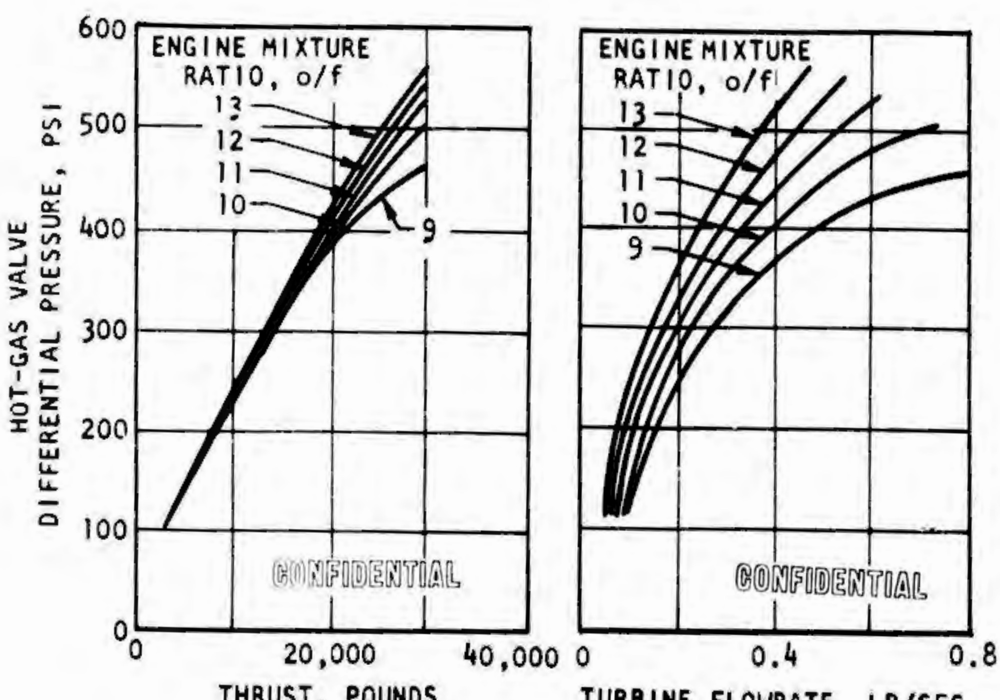

Figure 38. Differential Pressure Requirements for Main Engine Fuel Turbine Hot-Gas Valve (U)

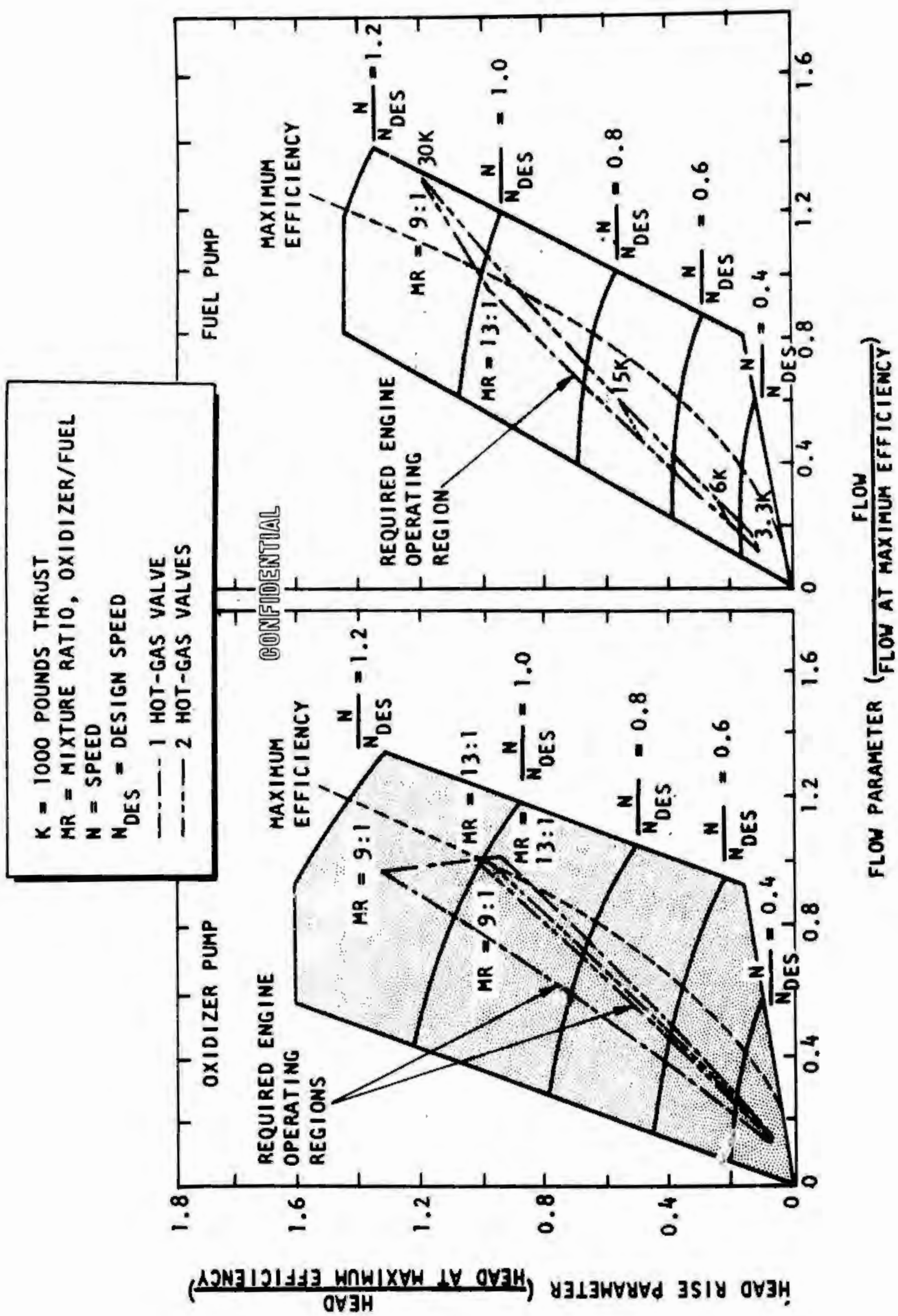

Figure 39. Operating Envelopes for Main Engine Propellant Pumps (U)

(C) valves. The fuel pump is unaffected by this option. The results shown in Fig. 39 indicate that the oxidizer and fuel pumps will not impose any restrictions on engine operation between thrust levels of 30,000 and 3330 pounds and mixture ratios of 9:1 to 13:1.

(C) The fuel and oxidizer turbopump assemblies are capable of operation throughout the desired operating envelope. The oxidizer pump is capable of operating over a wide range of mixture ratios and at flowrates corresponding to a thrust level of approximately 33,000 pounds (curve 1, Fig. 40). The maximum thrust achievable with the fuel pump (curve 2, Fig. 40) is more dependent on the operating mixture ratio. These pump limitations are due to the combined effect of pump cavitation and maximum speed restrictions. The pump speed has been limited to 113 percent of the nominal design speed (nominal design at 30,000 pound thrust and 12:1 mixture ratio).

(U) The main engine thrust and mixture ratio will be controlled by a valve located at the inlet of each turbine. The turbine-control valves are limited only by total flow area available. The engine system operating limitations with respect to the fuel and oxidizer turbine-control valves were determined from data obtained with the analog control model.

(U) The thrust/mixture ratio envelope for the secondary engine is similar to that of the main engine. Preliminary analyses indicate that there are no component limitations which restrict the envelope within the required range. Verification of the analyses is to be made as further detailed design of the hardware is accomplished.

(U) f. Main and Secondary Engine Performance

(1) Main Engine Balance

(C) A main engine system power balance and performance analysis was conducted to determine the effects of component modifications and experimental results that have occurred since the initiation of the program. The system performance analysis was conducted for maximum and minimum thrust and for engine mixture ratios of 9:1 to 13:1. The system changes that

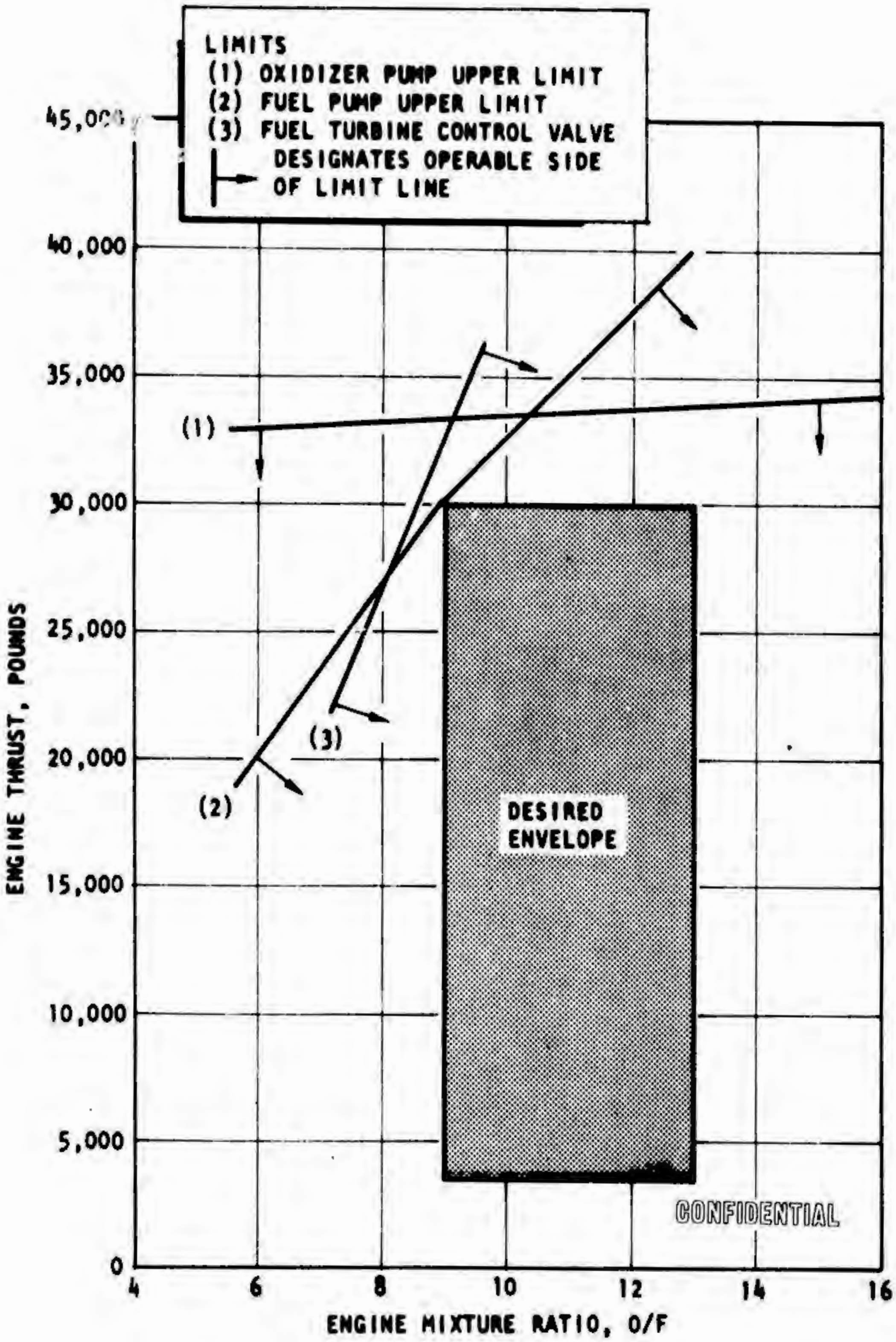

Figure 40. Engine System Operating Envelope (U)

(C) were incorporated into the revised performance estimates are an accumulation of design modifications and refinements in the predicted operating characteristics of various components. A list of the accumulated changes that were included in this analysis is as follows:

1. Refinements in fuel and oxidizer turbine and pump efficiency estimates
2. Decrease in oxidizer turbine pressure ratio by the use of identical fuel and oxidizer turbines
3. Removal of cavitating venturis from propellant high-pressure feed system
4. Slight increase in theoretical values of c* and specific impulse from a revision in the heat of formation of HF
5. The change to a single-pass channel-wall chamber cooling circuit, resulting in a change to the coolant circuit pressure loss and bulk temperature rise, with a subsequent effect on fuel injector inlet and turbine drive gas inlet conditions and pump discharge pressure requirements.

These changes or refinements in engine component design or operating characteristics were input to the computerized turbopump power balance and engine system performance analysis. The results of the main engine system performance analysis are shown in Table 9 for full thrust and minimum thrust operation over the intended range of mixture ratio. Some of the major operating conditions of the components also are presented.

(U) (2) Secondary Engine Balance

(C) The secondary engine performance estimates and operating parameters were revised to include changes incorporated since the initiation of the program. The revision to the analysis included the most recent turbopump operating parameters, slight refinements in chemical properties used in the theoretical propellant performance calculations (HF heat of formation), and the reduced pump discharge pressure requirements due to the elimination of the cavitating venturis from the high-pressure propellant feed lines. The engine balance was conducted with a constant tapoff gas mixture ratio over the operating range.

TABLE 9

MAIN ENGINE SYSTEM OPERATING PARAMETERS AND PERFORMANCE ESTIMATES (U)

Engine Mixture Ratio	9:1		10:1		11:1		12:1		13:1	
Thrust, pounds	30K	3.33K	30K	3.33K	30K	3.33K	30K	3.33K	30K	3.33K
Total Oxidizer Flowrate, lb/sec	58.80	6.86	59.30	6.99	59.78	7.11	60.20	7.21	60.72	7.31
Total Fuel Flowrate, lb/sec	6.53	0.76	5.93	0.70	5.43	0.65	5.02	0.60	4.67	0.56
Injector Fuel Flowrate, lb/sec	5.11	0.727	4.71	0.67	4.37	0.62	4.06	0.57	3.82	0.53
Total Turbine Flowrate, lb/sec	1.428	0.035	1.22	0.030	1.06	0.028	0.952	0.023	0.854	0.021
Thrust Chamber Mixture Ratio	11.52	9.44	12.59	10.48	13.67	11.50	14.81	12.50	15.91	13.51
Fuel Injection Temperature, R	848	1490	938	1560	1018	1720	1088	1930	1158	2020
Fuel Pump Discharge Pressure, psia	2319	370	2217	358	2116	338	2033	335	1857	321
Oxidizer Pump Discharge Pressure, psia	887	102	887	102	888	103	889	103	890	103
Delivered Engine Specific Impulse, seconds	459.2	436.8	459.9	433.1	460.0	429.5	460.0	426.5	458.8	423.0

CONFIDENTIAL

CONFIDENTIAL

(C) The injector and tapoff system design that has been established for the secondary engine has been analyzed to determine the tapoff gas properties and flow characteristics over the intended operating range of thrust and mixture ratio for the thrust chamber. The simplest and most practical approach was to design for a constant tapoff gas mixture ratio at all thrust chamber operating conditions. However, the hydrogen temperatures at the exit of the thrust chamber cooling jacket varies with thrust and mixture ratio. This influences the combustion gas temperature and the diluent (H_2) temperature which compose the tapoff gases. Therefore, even with a constant tapoff gas mixture ratio, the turbine inlet gas temperature will vary. The anticipated range of turbine inlet temperatures has been established as 1200 to 1500 F over the thrust and mixture ratio range. Actually, it is difficult to predict accurately what the tapoff gas properties will be over the operating range due to the many possible variables. The exact information will be available only after thrust chamber test experience is obtained. At this time, the constant tapoff gas mixture ratio and 1200 to 1500 F turbine inlet temperature appear to be the most accurate theoretical model.

(C) The results of the engine performance analysis, over the intended range of operating mixture ratios, are presented in Table 10 for full-thrust operation and Table 11 for minimum-thrust operation. Only very minor variations in the flowrates and operating conditions have resulted due to the above revisions. Figures 41 and 42 show the variation in tapoff flowrate and its influence on thrust chamber mixture ratio for a constant engine mixture ratio of 12:1.

g. Engine Influence Coefficients

(C) A set of preliminary engine influence coefficients (Tables 12 through 15) were prepared for the main and secondary engine at their respective full and 9:1 throttled thrust operating levels and, in both cases, at the nominal design mixture ratio of 12:1. The selected independent variables include external engine effects such as propellant inlet pressure and temperature conditions, and internal engine design or operating conditions such as system pressure drop and coolant bulk temperature rise.

TABLE 10. SECONDARY ENGINE FULL THRUST OPERATING CONDITIONS (U)

Engine Mixture Ratio	9:1		10:1		11:1		12:1		13:1	
Thrust at Vacuum, lbs.	3330		3330		3330		3330		3330	
Nozzle Stagnation Pressure, psia	757.0		754.5		752.1		749.4		745.9	
Total Oxidizer Flowrate, lb/sec	6.53		6.59		6.65		6.70		6.75	
Total Fuel Flowrate, lb/sec	0.725		0.659		0.605		0.559		0.519	
Thrust Chamber Mixture Ratio	10.26:1		11.38:1		12.49:1		13.62:1		14.77:1	
Thrust Chamber Oxidizer Flowrate, lb/sec	6.47		6.54		6.60		6.66		6.71	
Thrust Chamber Fuel Flowrate, lb/sec	0.630		0.574		0.529		0.489		0.454	
Oxidizer Turbine Flowrate, lb/sec	0.055		0.0556		0.055		0.055		0.055	
Fuel Turbine Flowrate, lb/sec	0.100		0.0825		0.069		0.059		0.052	
Turbine Flow Mixture Ratio	0.618:1		0.618:1		0.618:1		0.618:1		0.618:1	
Turbine Inlet Temperature, R	1535		1580		1630		1660		1705	
Hydrogen Injection Tempature, R	517		552		597		642		686	
Nominal Specific Impulse, sec	459.0		459.2		458.9		458.5		457.9	
	OXID	FUEL	OXID	FUEL	OXID	FUEL	OXID	FUEL	OXID	FUEL
System Pressure Losses, psid										
Injector	364	316	368	287	372	264	375	244	377	226
Cooling Jacket, Manifolds and Ducts	-	257	-	233	-	214	-	198	-	184
Line and Manifolds	76	222	79	178	79	147	80	125	80	96
Pump Discharge Pressure, psia	1235	1591	1238	1492	1240	1425	1240	1354	1241	1300
Pump Inlet Pressure	45	60	45	60	45	60	45	60	45	60
Pump Horsepower	42.3	125.8	42.8	102.8	43.3	86.7	43.6	73.8	44.0	64.4
Turbine Inlet Pressure	-	-	-	-	-	-	200	200	-	-
Turbine Discharge Pressure	-	-	-	-	-	-	20	20	-	-
Turbine Discharge Temperature	1292	1138	1336	1187	1380	1237	1409	1269	1452	1313
Turbine Pressure Ratio	10	10	10	10	10	10	10	10	10	10

TABLE 11. SECONDARY ENGINE MINIMUM THRUST OPERATING CONDITIONS (U)

Engine Mixture Ratio	9:1		10:1		11:1		12:1		13:1	
Thrust at Vacuum, lbs.	370		370		370		370		370	
Nozzle Stagnation Pressure, psia	88.4		88.2		68.0		87.9		87.7	
Total Oxidizer Flowrate, lb/sec	0.771		0.781		0.789		0.799		0.806	
Total Fuel Flowrate, lb/sec	0.086		0.078		0.072		0.066		0.062	
Thrust Chamber Mixture Ratio	9.21:1		10.23:1		11.27:1		12.30:1		13.33:1	
Thrust Chamber Oxidizer Flowrate, lb/sec	0.769		0.779		0.788		0.797		0.805	
Thrust Chamber Fuel Flowrate, lb/sec	0.083		0.0761		0.070		0.065		0.060	
Oxidizer Turbine Flowrate, lb/sec	0.0018		0.0018		0.0018		0.0017		0.0017	
Fuel Turbine Flowrate, lb/sec	0.0016		0.0013		0.0012		0.0010		0.0009	
Turbine Flow Mixture Ratio	0.618:1		0.618:1		0.618:1		0.618:1		0.618:1	
Turbine Inlet Temperature, R	1775		1845		1910		1980		2045	
Hydrogen Injection Temperature, R	752		822		890		960		1030	
Nominal Specific Impulse, sec	431.9		430.9		429.4		427.5		425.9	
System Pressure Losses, psid	OXID	FUEL	OXID	FUEL	OXID	FUEL	OXID	FUEL	OXID	FUEL
Injector	43	37	43	34	44	31	44	29	45	27
Cooling Jacket, Manifolds and Ducts	-	30	-	27	-	25	-	23	-	22
Line and Manifolds	1.0	2.6	1.1	2.2	1.1	1.9	1.2	1.7	1.1	1.3
Pump Discharge Pressure, psia	137	163	137	156	137	151	138	146	138	142
Pump Inlet Pressure	45	60	45	60	45	60	45	60	45	60
Pump Horsepower	0.61	1.02	0.60	0.89	0.60	0.80	0.61	0.72	0.61	0.65
Turbine Inlet Pressure	-	-	-	-	-	-	22	15	-	-
Turbine Discharge Pressure	-	-	-	-	-	-	2.2	1.5	-	-
Turbine Discharge Temperature	1670	1573	1741	1639	1805	1700	1875	1768	1939	1829
Turbine Pressure Ratio	10	10	10	10	10	10	10	10	10	10

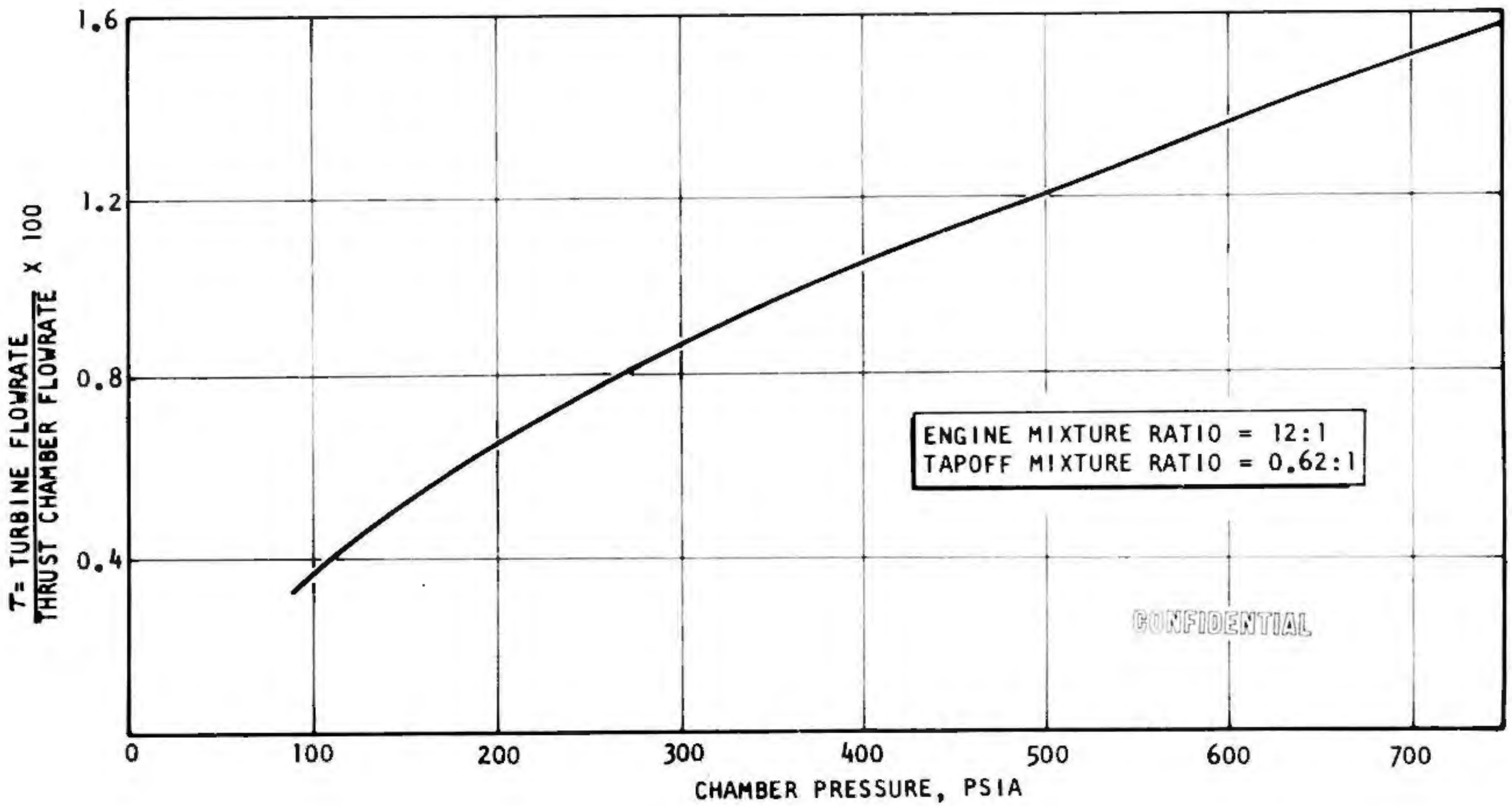

Figure 41. Secondary Engine Turbine Flowrate as a Percentage of Chamber Flowrate vs Chamber Pressure (U)

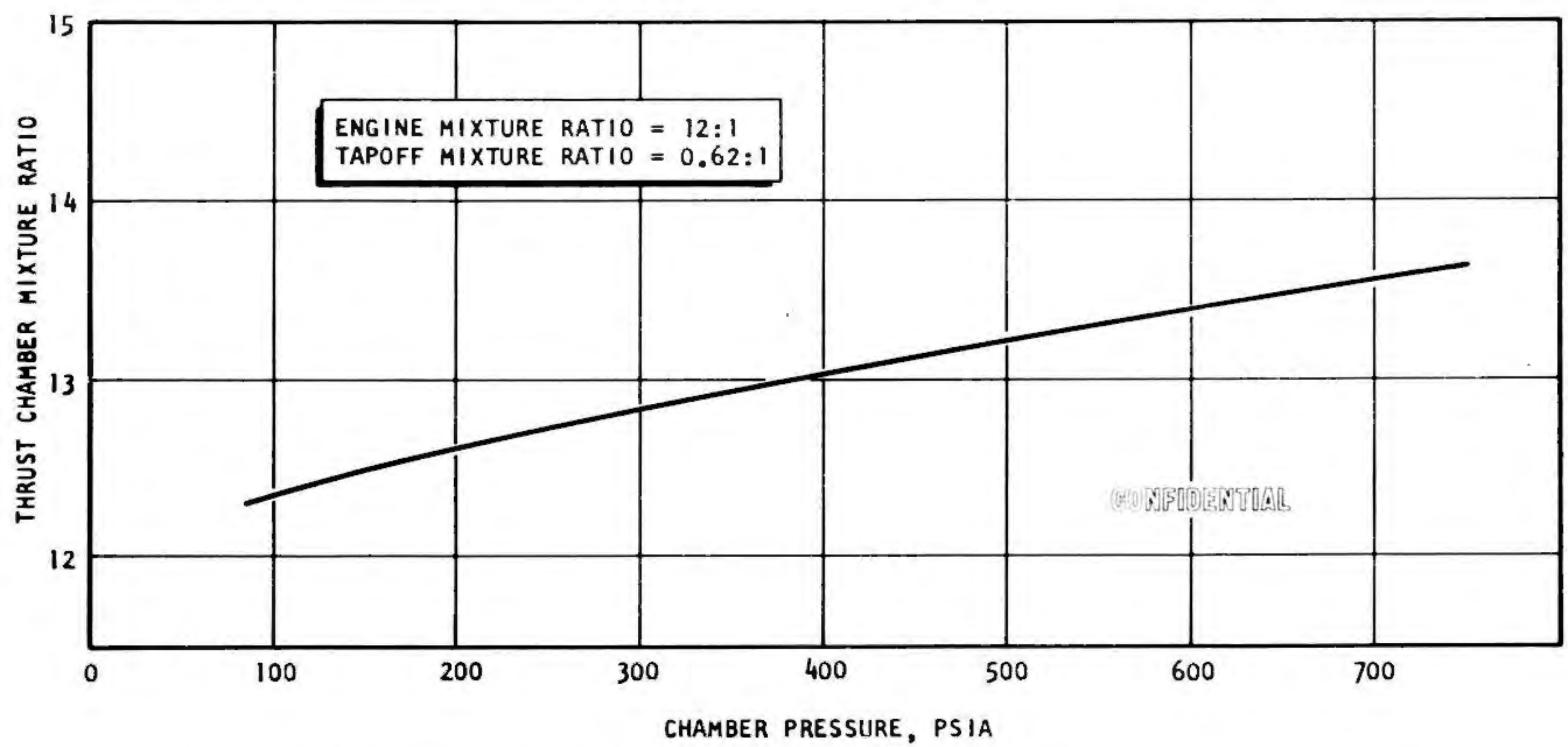

Figure 42. Secondary Engine Thrust Chamber Mixture Ratio vs Chamber Pressure (U)

TABLE 12

MAIN ENGINE INFLUENCE COEFFICIENTS FOR FULL THRUST OPERATION (U)

Independent Variable	Nominal Value	Remarks
Fuel Pump Inlet Pressure, psia	60	A 1-percent increase in any independent variable causes a percentage change in each dependent variable. The magnitude of change in dependent variables is listed below.
Oxidizer Pump Inlet Pressure, psia	45	
Fuel Pump Inlet Temperature, R	40	
Oxidizer Pump Inlet Temperature, R	153	
Fuel Injector Pressure Drop, psi	201.3	
Oxidizer Injector Pressure Drop, psi	325.7	
Coolant Bulk Temperature Rise, R	1432	

CONFIDENTIAL

Dependent Variable	Percent Change Caused by 1-Percent Increase In: Fuel Pump Inlet Pressure	Oxidizer Pump Inlet Pressure	Fuel Pump Inlet Temperature	Oxidizer Pump Inlet Temperature	Fuel Injector Pressure Drop	Oxidizer Injector Pressure Drop	Coolant Bulk Temperature Rise
Engine Specific Impulse	0.000	0.000	-0.002	-0.001	-0.001	-0.001	0.014
Thrust Chamber Mixture Ratio	-0.003	-0.001	0.022	0.017	0.009	0.014	-0.119
Oxidizer Pump Speed	-0.003	-0.015	0.000	0.262	0.000	0.126	-0.004
Fuel Pump Speed	-0.016	0.000	0.214	0.000	0.045	0.000	0.000
Oxidizer Pump Horsepower	0.000	-0.038	0.001	0.452	0.000	0.317	-0.017
Fuel Pump Horsepower	-0.034	0.000	0.361	0.000	0.104	0.000	-0.009
Oxidizer Pump Discharge Pressure	0.000	0.000	0.000	0.029	0.000	0.309	-0.003
Fuel Pump Discharge Pressure	0.000	0.000	0.021	-0.001	0.107	-0.001	0.005
Oxidizer Turbine Flowrate	-0.004	-0.022	0.000	0.216	0.017	0.181	-0.638
Fuel Turbine Flowrate	-0.019	-0.003	0.164	0.031	0.065	0.025	-0.641

TABLE 13

MAIN ENGINE INFLUENCE COEFFICIENTS FOR 9:1 THROTTLED OPERATION (C)

Independent Variable	Nominal Value	Remarks
Fuel Pump Inlet Pressure, psia	60	A 1-percent increase in any independent variable causes a percentage change in each dependent variable. The magnitude of change in dependent variables is listed below.
Oxidizer Pump Inlet Pressure, psia	45	
Fuel Pump Inlet Temperature, R	40	
Oxidizer Pump Inlet Temperature, R	153	
Fuel Injector Pressure Drop, psi	27.3	
Oxidizer Injector Pressure Drop, psi	39.5	
Coolant Bulk Temperature Rise, R	1407	

Dependent Variable	Percent Change Caused by 1-Percent Increase In: Fuel Pump Inlet Pressure	Oxidizer Pump Inlet Pressure	Fuel Pump Inlet Temperature	Oxidizer Pump Inlet Temperature	Fuel Injector Pressure Drop	Oxidizer Injector Pressure Drop	Coolant Bulk Temperature Rise
Engine Specific Impulse	0.001	0.001	0.000	0.000	0.000	-0.001	0.006
Thrust Chamber Mixture Ratio	-0.011	-0.009	0.003	0.002	0.006	0.009	-0.034
Oxidizer Pump Speed	0.000	-0.227	0.000	0.219	0.000	0.234	-0.002
Fuel Pump Speed	-0.157	0.001	0.202	0.000	0.082	-0.001	0.000
Oxidizer Pump Horsepower	0.000	-0.631	0.000	0.285	0.000	0.653	-0.008
Fuel Pump Horsepower	-0.394	0.001	0.273	0.000	0.210	-0.001	-0.003
Oxidizer Pump Discharge Pressure	0.000	0.000	0.000	0.004	0.000	0.333	-0.075
Fuel Pump Discharge Pressure	0.001	0.001	0.002	0.000	0.123	-0.001	0.000
Oxidizer Turbine Flowrate	-0.046	-0.346	-0.004	0.063	0.020	0.352	-0.542
Fuel Turbine Flowrate	-0.225	-0.036	0.065	0.010	0.124	0.042	-0.540

TABLE 14

SECONDARY ENGINE INFLUENCE COEFFICIENTS FOR FULL THRUST OPERATION (U)

Independent Variable	Nominal Value	Remarks
Fuel Pump Inlet Pressure, psia	60	A 1-percent increase in any independent variable causes a percentage change in each dependent variable. The magnitude of change in dependent variables is listed below.
Oxidizer Pump Inlet Pressure, psia	45	
Fuel Pump Inlet Temperature, R	40	
Oxidizer Pump Inlet Temperature, R	153	
Fuel Injector Pressure Drop, psi	243.8	
Oxidizer Injector Pressure Drop, psi	374.7	
Coolant Bulk Temperature Rise, R	576	

	Percent Change Caused by 1-Percent Increase In:						
Dependent Variable	Fuel Pump Inlet Pressure	Oxidizer Pump Inlet Pressure	Fuel Pump Inlet Temperature	Oxidizer Pump Inlet Temperature	Fuel Injector Pressure Drop	Oxidizer Injector Pressure Drop	Coolant Bulk Temperature Rise
Engine Specific Impulse	0.000	0.000	0.001	0.000	0.000	0.000	0.002
Thrust Chamber Mixture Ratio	-0.002	-0.001	0.028	0.012	0.008	0.010	0.017
Oxidizer Pump Speed	0.000	-0.013	0.000	0.264	0.000	0.120	-0.002
Fuel Pump Speed	-0.019	0.000	0.268	0.000	0.063	0.000	-0.001
Oxidizer Pump Horsepower	0.002	-0.032	0.001	0.456	0.000	0.299	-0.003
Fuel Pump Horsepower	-0.028	0.012	0.525	0.012	0.147	0.012	0.008
Oxidizer Pump Discharge Pressure	0.000	0.000	-0.002	0.024	-0.001	0.303	-0.001
Fuel Pump Discharge Pressure	-0.001	0.000	0.041	0.041	0.178	0.000	-0.001
Oxidizer Turbine Flowrate	-0.002	0.014	0.014	0.209	0.006	0.180	-0.117
Fuel Turbine Flowrate	-0.024	-0.001	0.282	0.282	0.082	0.010	-0.126

TABLE 15

SECONDARY ENGINE INFLUENCE COEFFICIENTS FOR 9:1 THROTTLED OPERATION (C)

Independent Variable	Nominal Value	Remarks
Fuel Pump Inlet Pressure, psia	60	A 1-percent increase in any independent variable causes a percentage change in each dependent variable. The magnitude of change in dependent variables is listed below.
Oxidizer Pump Inlet Pressure, psia	45	
Fuel Pump Inlet Temperature, R	40	
Oxidizer Pump Inlet Temperature, R	155	
Fuel Injector Pressure Drop, psi	28.9	
Oxidizer Injector Pressure Drop, psi	44.4	
Coolant Bulk Temperature Rise, R	890	

Dependent Variable	Percent Change Caused by 1-Percent Increase In: Fuel Pump Inlet Pressure	Oxidizer Pump Inlet Pressure	Fuel Pump Inlet Temperature	Oxidizer Pump Inlet Temperature	Fuel Injector Pressure Drop	Oxidizer Injector Pressure Drop	Coolant Bulk Temperature Rise
Engine Specific Impulse	0.000	0.000	0.000	0.000	0.000	0.000	0.001
Thrust Chamber Mixture Ratio	-0.011	-0.008	0.004	0.002	-0.006	0.009	0.014
Oxidizer Pump Speed	0.000	-0.192	0.000	0.208	-0.001	0.222	-0.001
Fuel Pump Speed	0.267	0.000	0.217	0.000	0.147	-0.001	-0.001
Oxidizer Pump Horsepower	0.001	-0.518	0.000	0.274	-0.001	0.601	-0.002
Fuel Pump Horsepower	-0.648	0.001	0.359	0.000	0.362	-0.001	-0.001
Oxidizer Pump Discharge Pressure	0.001	0.000	-0.001	0.003	0.000	0.677	-0.001
Fuel Pump Discharge Pressure	0.000	0.000	0.005	0.000	0.197	-0.001	-0.001
Oxidizer Turbine Flowrate	-0.022	-0.310	0.005	0.067	0.014	0.359	-0.160
Fuel Turbine Flowrate	-0.371	-0.020	0.118	-0.004	0.207	0.023	-0.162

(C) The system pressure drop effect is characterized by the oxidizer or fuel injector ΔP, and may be interpreted to have the same percentage effect on the dependent variables as ΔP variations in other parts of the system. The analysis was conducted based on the assumption that the control system would always maintain the command thrust and mixture ratio value with any system perturbation. Based on this assumption, engine thrust and mixture ratio remain constant, and the delivered engine specific impulse becomes the primary dependent variable. Other dependent variables are presented to indicate the effect of the independent variables on engine system component operating characteristics such as pump and turbine speeds, flowrates, and horsepower requirements. The data in Tables 12 through 15 show that there is minimal effect realized by varying any one independent variable. This should be expected with an engine utilizing both thrust and mixture ratio control.

h. Engine Start and Cutoff Analysis

(1) Preliminary Sequence Selection

(U) Start and cutoff sequence logic analyses were conducted for the main engine. Although differences existed in the secondary engine transients, they were considered to be inconsequential for this preliminary analyses.

(C) The basic philosophy adopted for start and cutoff engine sequences was that the transitions would be accomplished without exposing the thrust chamber to excessive temperatures that may result in shortened service life. Because mainstage oxidizer/fuel mixture ratio (12:1) operation is planned to be on the fuel-rich side of stoichiometric (18:1), it was concluded that start must be accomplished with a fuel lead and cutoff must be accomplished with a fuel lag. In this way, the maximum mixture ratio experienced during the start or cutoff transient would be less than 12:1, and the high temperature associated with stoichiometric mixture ratio would be averted.

(U) With the fuel lead during start, measures are required to prevent the oxidizer system from becoming primed with gaseous fuel. With this condition present, propellant ignition would probably occur in the oxidizer injector, ducting, manifolds, valves, and or pump when the oxidizer valve opened. Consequently, a helium purge was defined to provide a positive pressure in the oxidizer system and block the fuel flow from the combustion chamber through the oxidizer injector.

(U) With these considerations, a flow diagram for the start sequence was defined (Fig. 43). From the flow diagram, and the preliminary data generated from the mathematical start model used in the cycle selection studies, the start sequence shown in Fig. 44 and 45 were defined.

(U) The major difference in the preliminary model work presented and the final start sequence analysis that is presented later in this section is that of unprimed turbopumps at start. The preliminary model analysis assumed primed pumps.

(U) A flow diagram of the cutoff sequence was prepared (Fig. 46) on the basis of realizing a fuel-rich cutoff transient. From this diagram, a cutoff sequence was estimated and is shown in Fig. 47 and 48.

(C) Because the engine is to be designed for rapid restart capability, the engine requires the necessary conditioning following cutoff to prepare for an immediate restart or, in the other limiting case, for a restart after an extended coast period. An evaluation was made, using the predicted volumes for the oxidizer system, from which it was determined that a 100-scfm helium purge initiated coincident with main oxizier valve closure and introduced upstream of the oxidizer pump would purge the residual oxidizer (exclusive of traps) from the main engine system in approximately 1.0 second. This purge should fulfill the restart conditioning requirement.

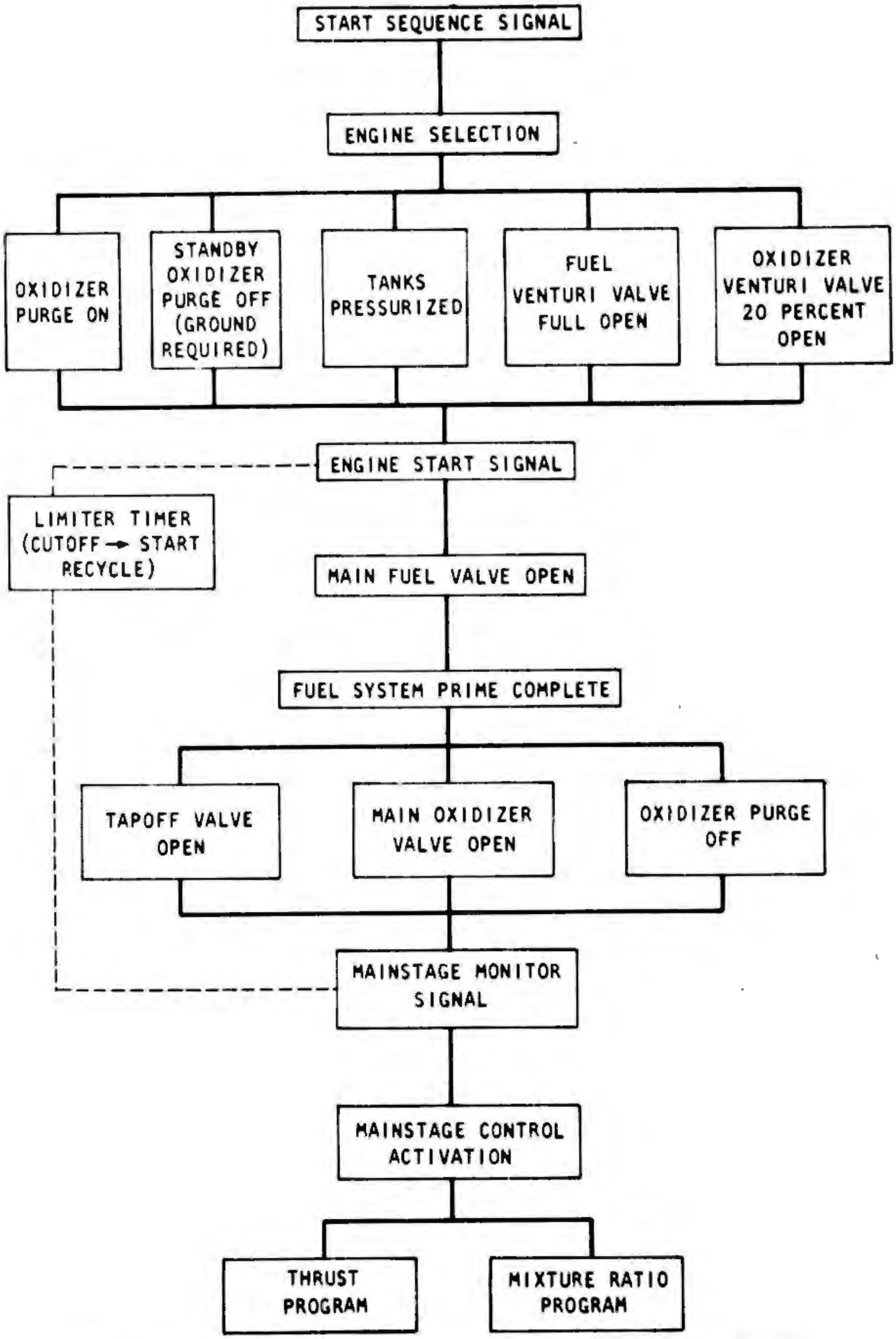

Figure 43. Start Sequence Flow Diagram (Preliminary) (U)

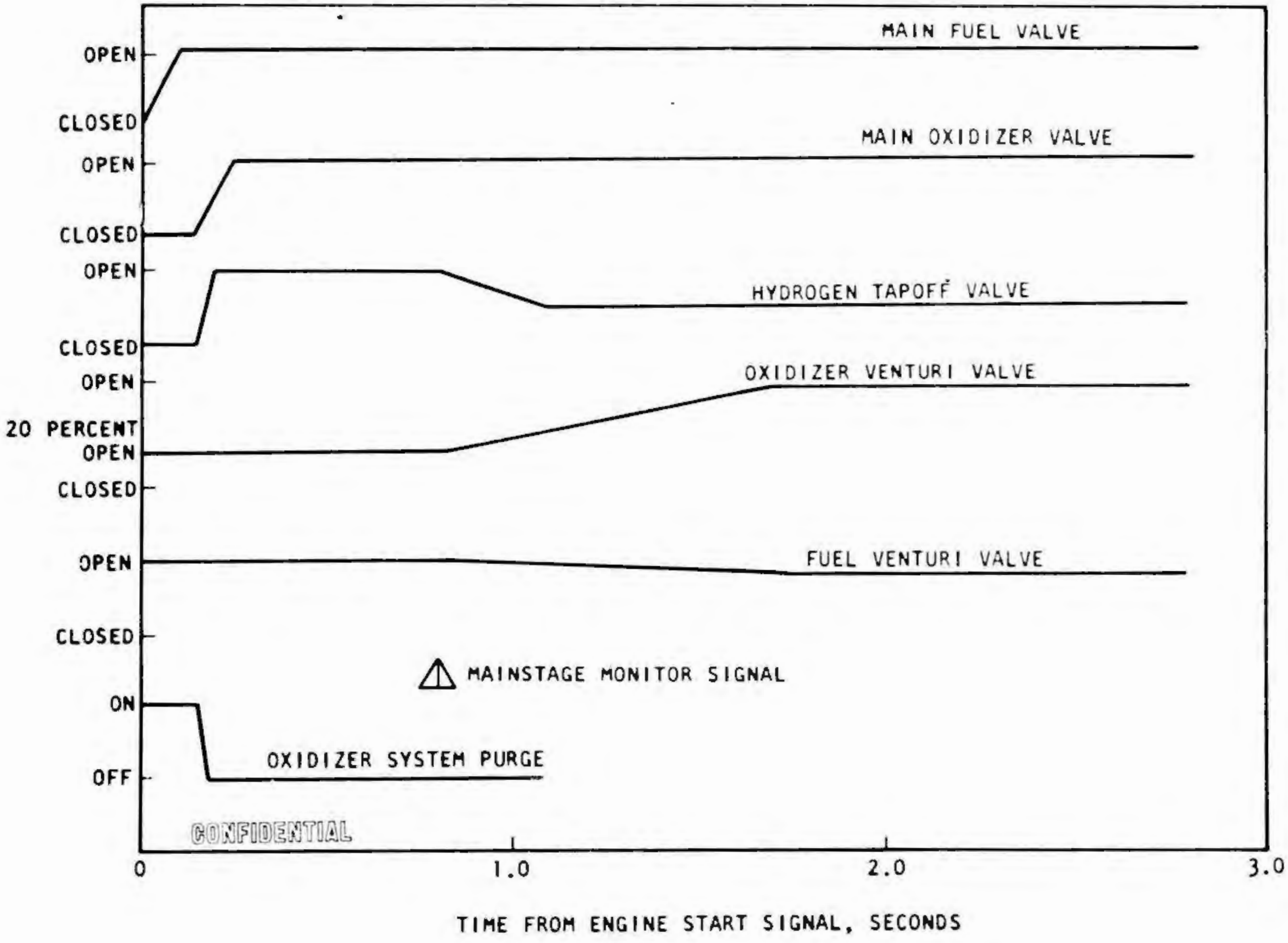

Figure 44. Engine Start Sequence (Preliminary) (U)

CONFIDENTIAL

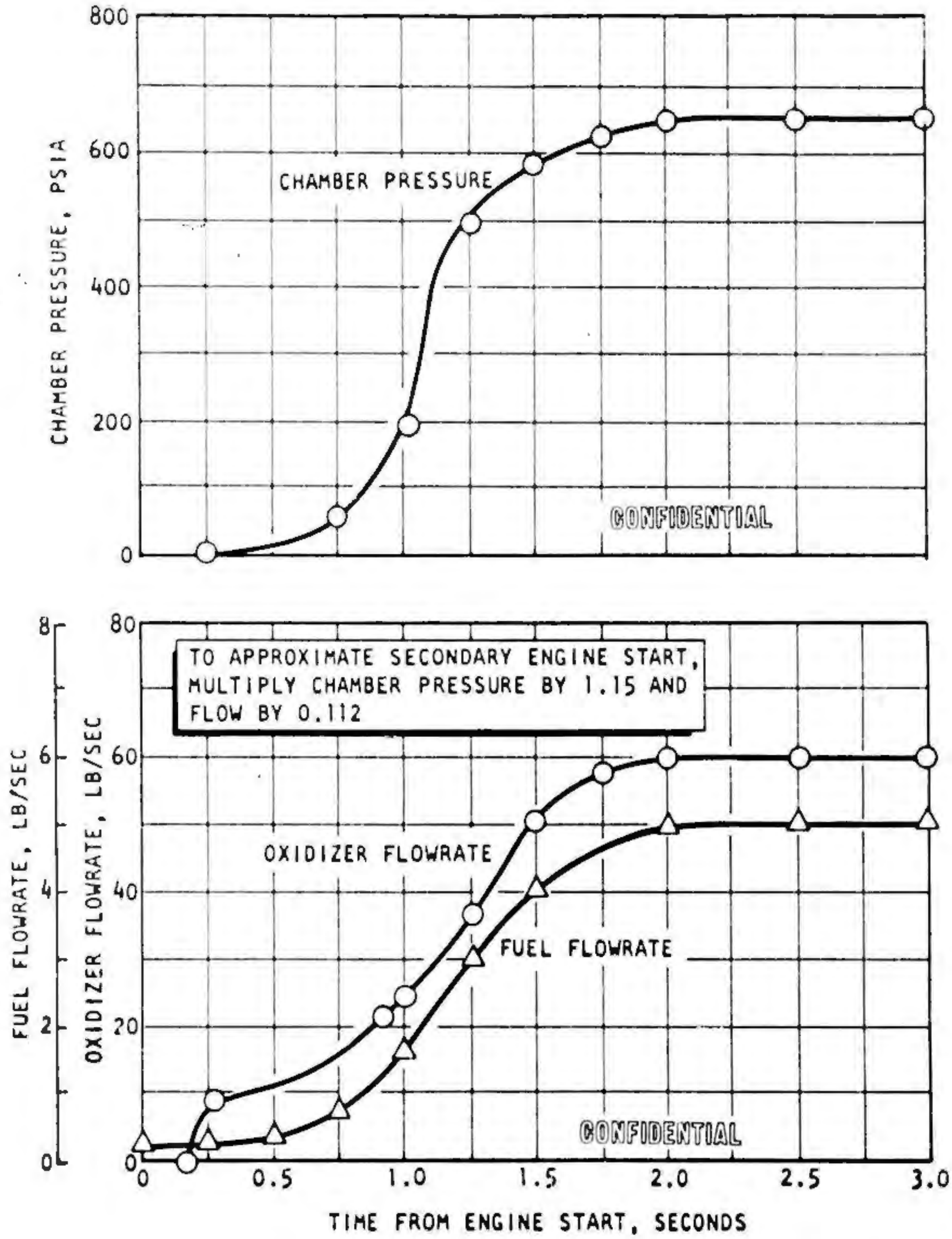

Figure 45. Main Engine Start Transient (Preliminary) (U)

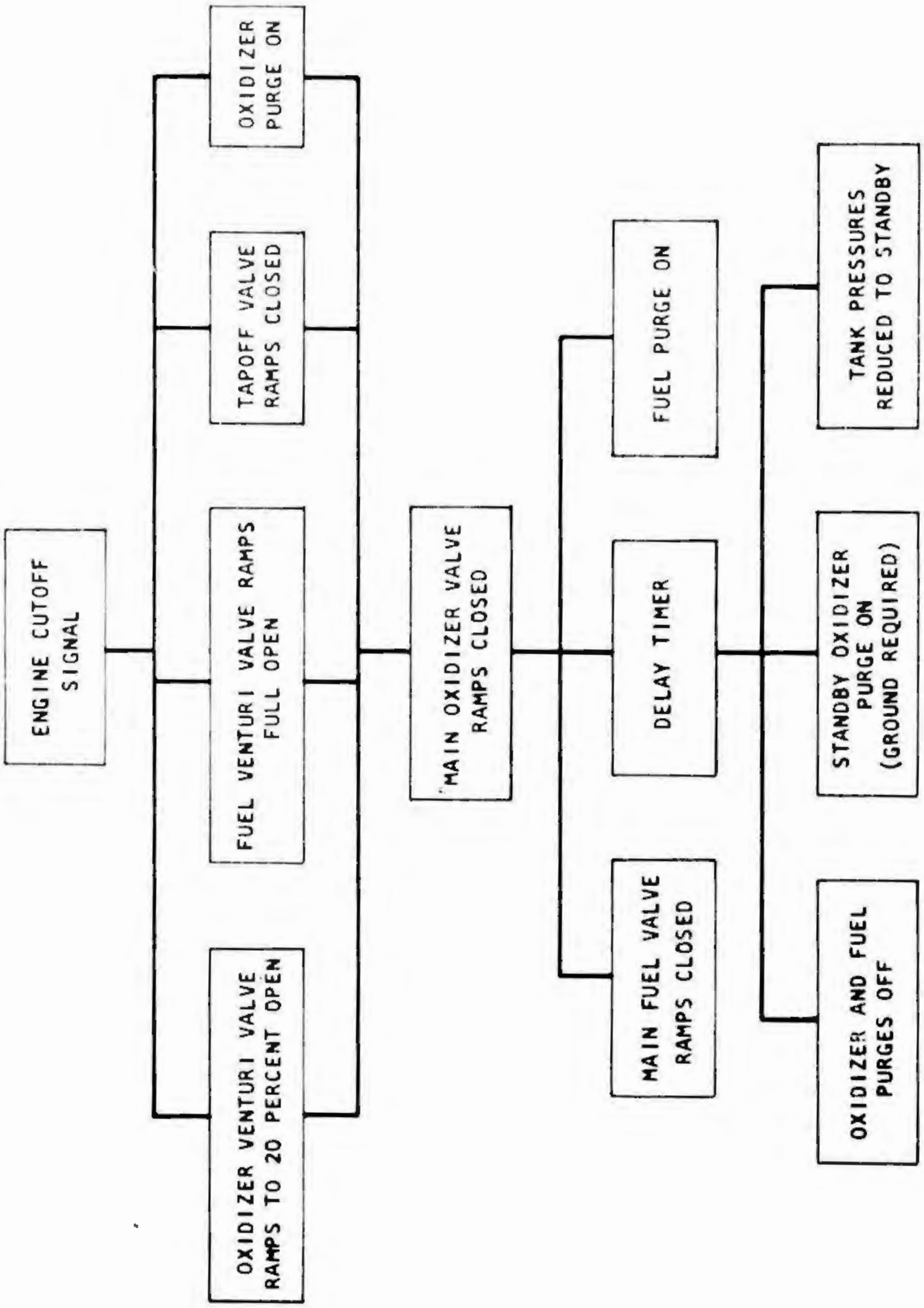

Figure 46. Cutoff Sequence Flow Diagram (Preliminary) (U)

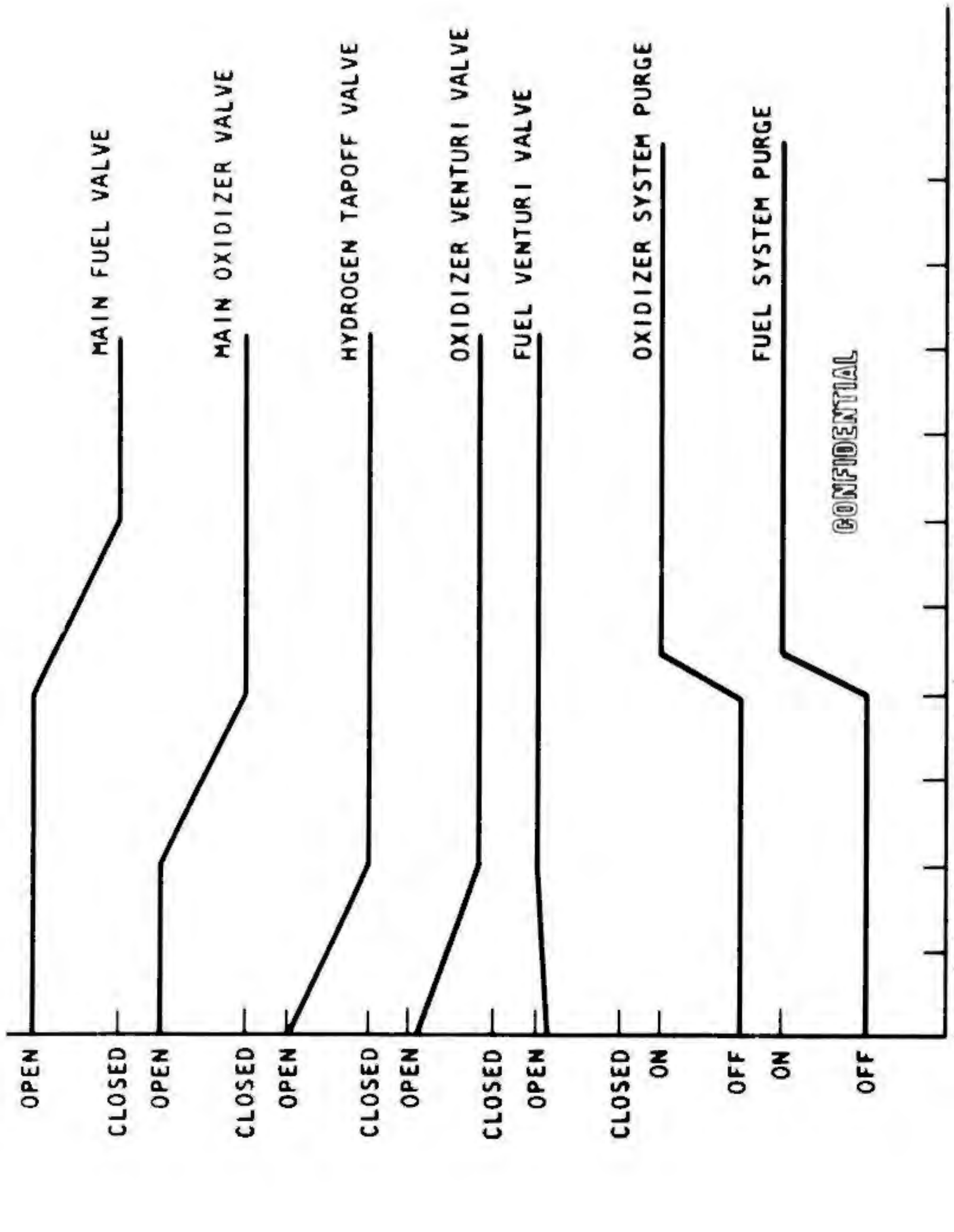

Figure 47. Engine Cutoff Sequence (Preliminary) (U)

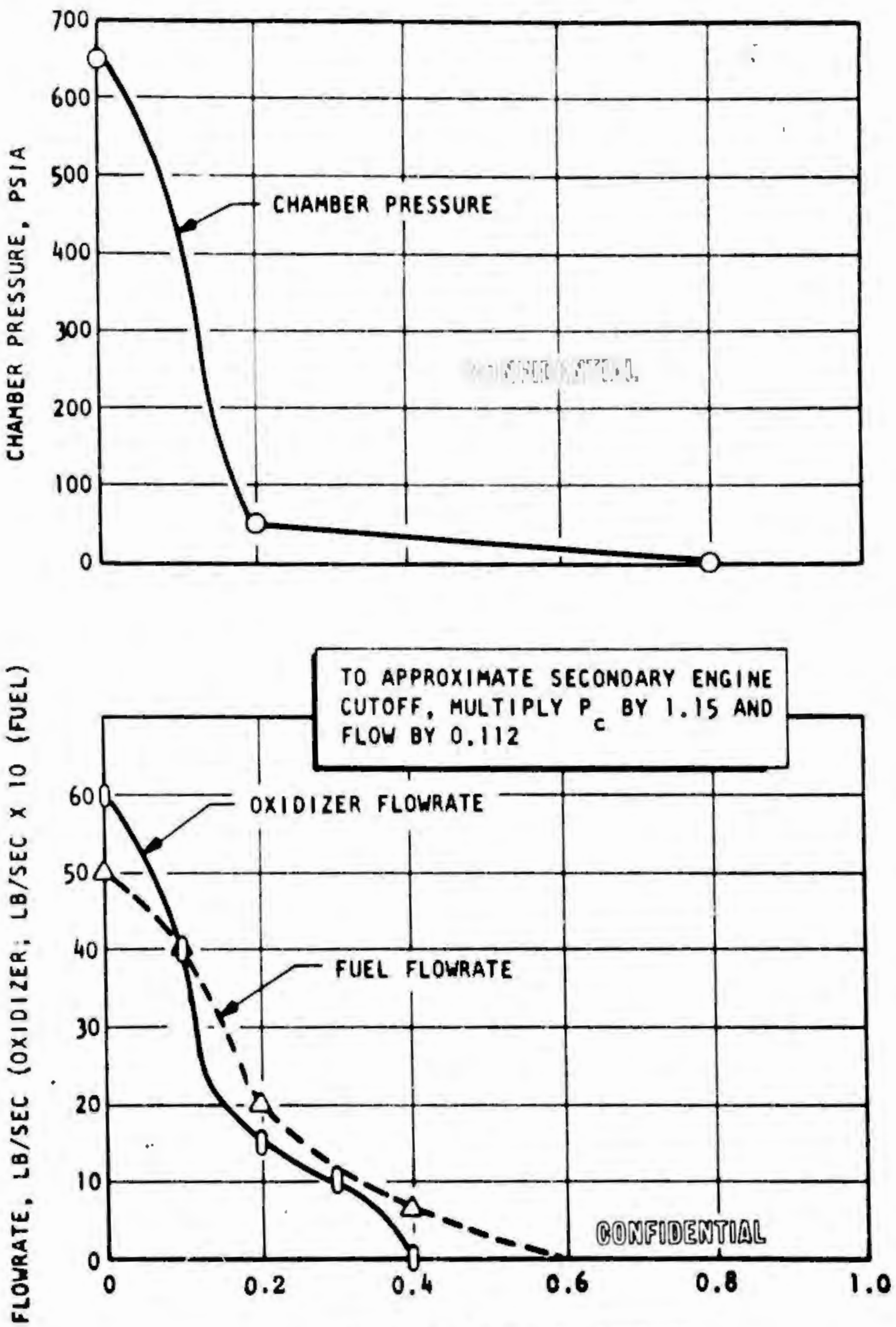

Figure 48. Main Engine Cutoff Transient (Preliminary) (U)

(U) A control logic for the main engine was defined that would provide the start and cutoff sequences previously described, together with the conditioning purges, and is discussed in the Controls section, page 416. A fuel system purge at cutoff is included in the logic to produce positive fuel expulsion to the combustion chamber during the cutoff transient.

(2) Transition Between Main and Secondary Engine

(U) In certain mission applications there is a requirement for continuous engine throttling in thrust regions where it is necessary to switch from the main engine to the secondary engine. A brief evaluation of the impact of this consideration on the control system start and cutoff logic and sequencing was conducted.

(U) Under the most severe of engine operating conditions, there could be a significant time lag between the time when the main engine is shut down and the secondary engine is brought up to full thrust unless special provisions are made. This time lag is due to the possible requirement for engine childown, a helium purge of the secondary engine feed system before startup, and the nominal start transient time.

(C) An estimate was made of the AMPS engine switching time lag for a rendezvous mission application based on the preliminary engine start and cutoff transients presented in the previous quarterly report. This estimate assumed that the secondary engine start signal would occur simultaneously with the main engine cutoff signal. An estimate of the delivered engine thrust vs time is shown in Fig. 49 for the main and secondary engines. The dotted line indicates the total thrust produced during the overlap period when both engines are producing thrust. The total time lag between cutoff and the re-establishment of thrust is seen to be approximately 2 seconds. This time lag is satisfactory for a near-optimum rendezvous approach trajectory based on the studies of Ref. 1 and 3. The results of this study for these type missions indicate that special control system provisions are unnecessary for the main/secondary engine throttling transition; however, they would be provided if other type missions dictate the need.

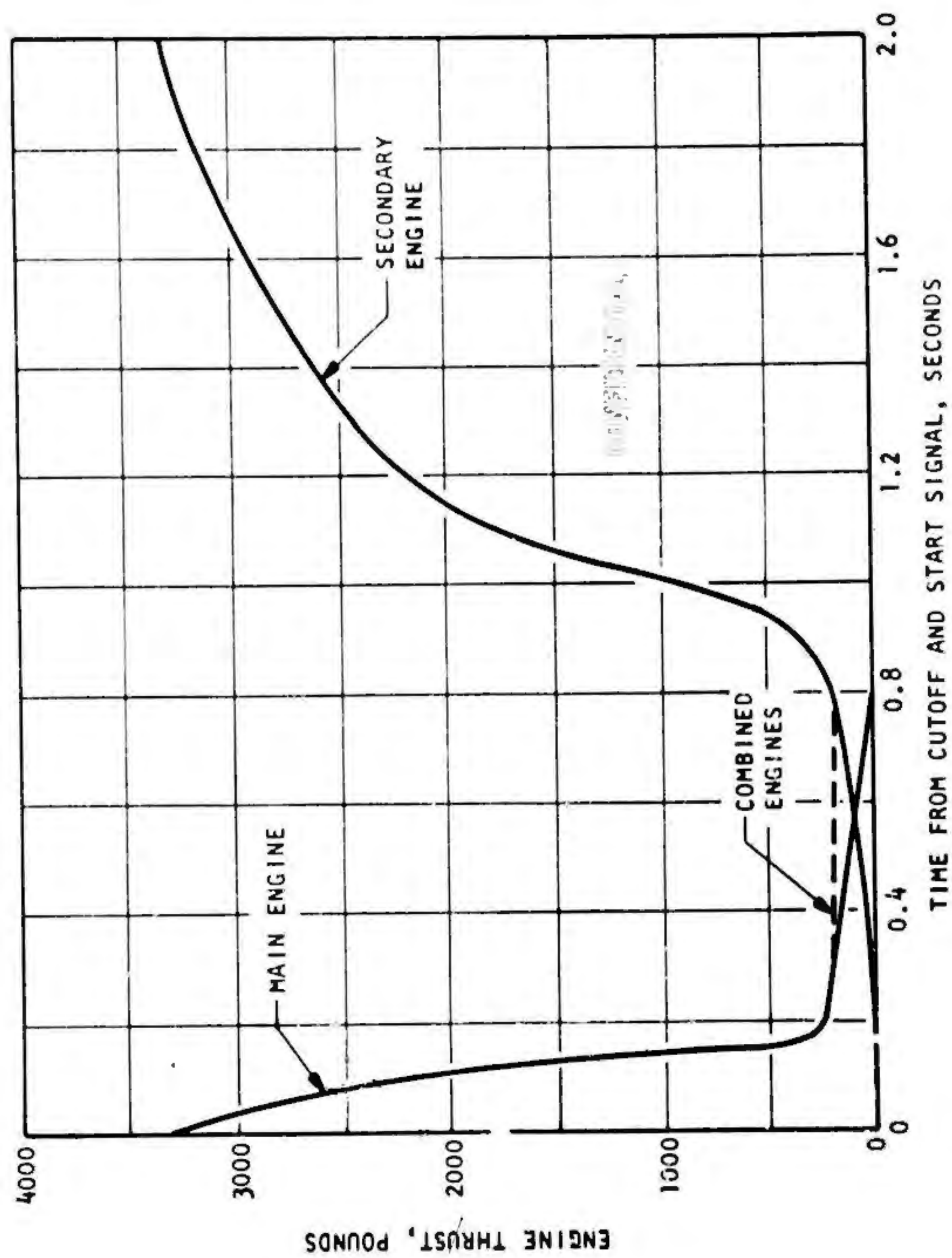

Figure 49. Predicted Thrust During Transition from Main to Secondary Engines (U)

(3) Main Engine Thermal Conditioning Requirements

(U) A study was conducted to determine the effects of fuel feed system thermal conditioning upon the main engine's start transient.

(C) The analysis was conducted with the use of the digital computer model of the engine start dynamics. Simulated tank-head engine starts were made with fuel and oxidizer tank pressures of 70 psia and 65 psia, respectively. The lower oxidizer tank pressure was used to prevent high mixture ratio excursions during priming of the oxidizer feed system. The main stage tank pressures were assumed to be 70 psia in both tanks.

(U) Engine thermal conditioning requirements were investigated for two extremes of initial feed system thermal conditions. The first case simulated an immediate restart; the pumps would be at the propellant liquid temperatures and the thrust chamber would be at an average bulk temperature of approximately 1000 F. The second case simulated the engine thermal conditions after attaining equilibrium during an orbital coast period. This latter case represents the most stringent thermal conditioning requirements, because the pumps and thrust chamber temperature would be approximately 60 F. It has been determined that the initial pump temperatures will always be within these approximate extremes. The analytical model used in establishing the pump thermal conditions was verified by comparison with analytical predictions and actual engine firings studied under contract NAS 8-20324, "Thermodynamic Improvements in Liquid Hydrogen Turbopumps." The results of the current AMPS analysis were found to correlate closely with the results of the previous studies.

(C) With the fuel pump and ducting at liquid hydrogen temperatures, the engine will reach full mainstage in approximately 2.0 seconds. However, with the warm pump and ducting, the engine will require approximately 4.3 seconds to reach mainstage. The warmer pump and ducting increases the engine start time by lengthening the time before the pump begins to generate positive head and by reducing the fuel flowrate through the system.

(U) The vaporization of the hydrogen entering the "warm" pump results in increased resistance to liquid flow by the downstream feed system components such as the hydrogen control valves and cooling jacket tube bundle. Thermal conditioning requirements of the oxidizer feed system were found to be nonrestrictive relative to the fuel feed system.

(U) Several methods were considered to reduce the magnitude of the heat flux transferred to the fuel and/or reduce the effect of the hardware temperature upon the start time. Methods of reducing the downstream resistance to flow were also investigated. The following system variations were considered:

1. A 0.002-inch Kel-F coating on the rotating parts of the fuel pump
2. A 0.010-inch Kel-F coating on the high-pressure ducting and nonrotating parts of the fuel pump
3. A 0.002-inch Kel-F coating on the rotating parts of the fuel pump plus a 0.010-inch Kel-F coating on the ducting and nonrotating parts of the fuel pump
4. Replacement of the fuel cavitating venturi with a large flow area valve

(U) Figure 50 shows that the amount and location of the Kel-F coating, or any other low-conductivity coating, determines how effectively the fuel is thermally isolated from the metal and how quickly the fuel reaches liquid temperatures. Once the fuel has reached liquid temperatures, the fuel density in the feed system is dependent upon the pressure generated by the pump. Thus, pump speed buildup will influence how quickly liquid densities are attained. Figure 50 also shows fuel density at the pump discharge for each of the system alterations considered.

(U) Chilldown and priming of the fuel system is hampered by choking of the cavitating venturi with gaseous and two-phase flow. Thus, a chilldown was made with the cavitating venturi replaced by a low-resistance butterfly valve. The results of this change are included in Fig. 50 .

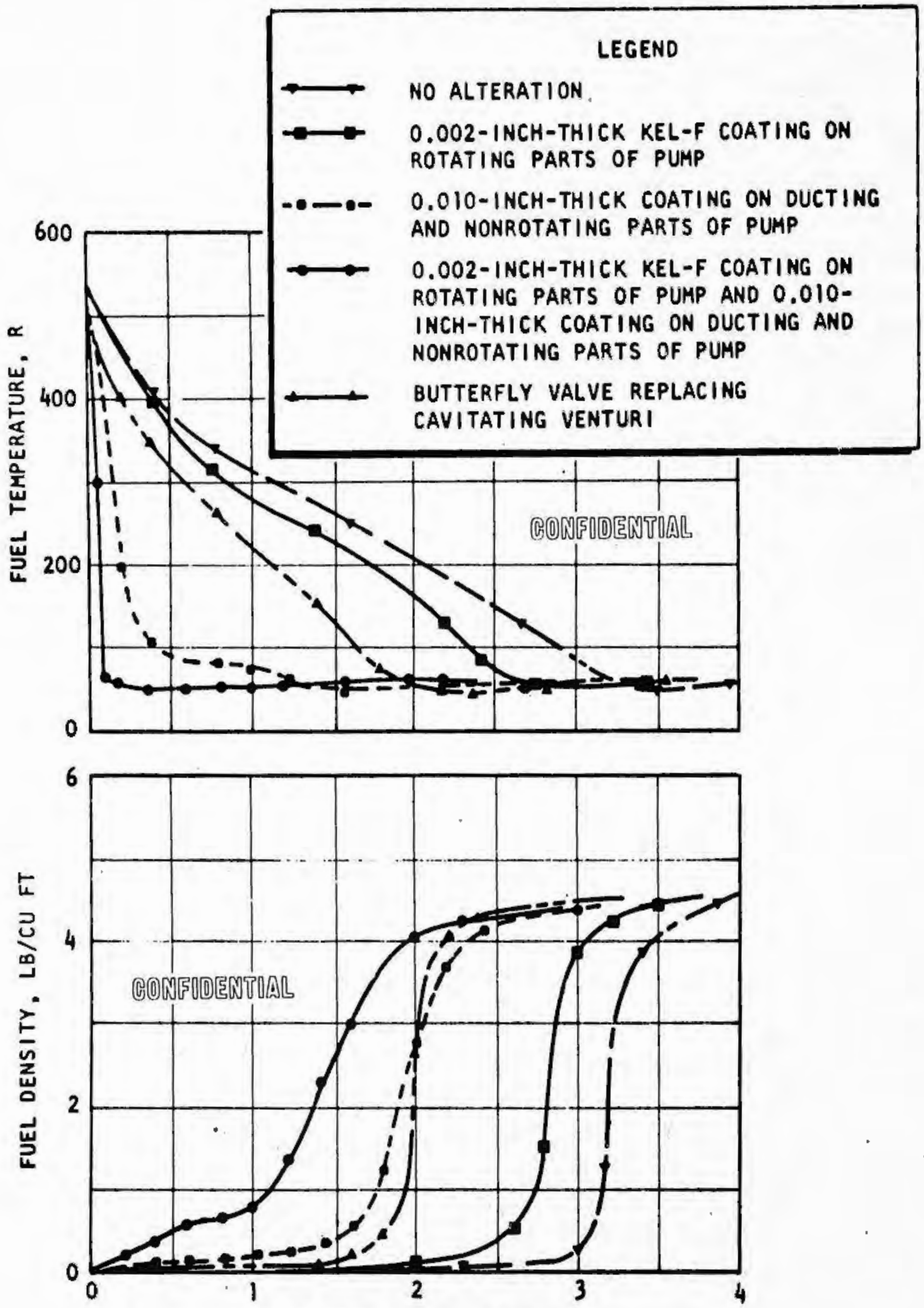

Figure 50. Fuel Temperature and Density at Pump Discharge During Main Engine Start (U)

(U) Use of the butterfly valve instead of the cavitating venturi reduced childdown and fuel pump prime by approximately 1.0 second. The 1.0-second gain in start time was achieved by increasing the amount of fuel flow through the system in the early phase of engine start.

(U) Using the same engine sequence for each of the above system variations, the total elapsed time from start to mainstage is given in Table 16.

(U) An alternate control system configuration, using two hot-gas turbine control valves, may also provide a benefit for the "warm" start condition through greater sequencing flexibility during the start transient.

(4) Preliminary Start Sequencing Optimization

(U) A start sequencing control system optimization was completed for the main engine using a single hot-gas turbine control valve. The optimization analysis had the primary objectives of providing a rapid start with little or no overshoot of pump speed or chamber pressure, maintaining engine mixture ratio within a tolerable range for thrust chamber cooling considerations, and providing control function signals that are independent of initial engine thermal conditions. That is, the control system will automatically compensate for variations in initial thermal conditions by taking the sequencing function signals from selected engine system operating parameters. A further requirement is that the above engine starting features be achieved at starts to any thrust level within the throttling range.

(C) The analysis was started by assuming the basic start sequencing control logic that was previously discussed. Tank-head starts were simulated with the aid of the computerized engine dynamic start model. Start characteristics were evaluated with both cold and warm initial conditions. Full-thrust chamber pressure was 650 psia with a mixture ratio of 12:1. A cavitating venturi was used for the oxidizer flow-control valve, and a large flow area valve was used for the fuel flow valve. Both oxidizer and fuel turbine flow was controlled by a single hot-gas valve.

TABLE 16

EFFECT OF FUEL SYSTEM THERMAL VARIATIONS
ON ENGINE START TIME (U)

Fuel System Variation	Engine Start Time, seconds	
	Instant Restart	Start After Long Coast Period
No Alteration	2.0	4.3
0.002-Inch-Thick Kel-F Coating on Rotating Parts of Pump	2.0	3.9
0.010-Inch-Thick Kel-F Coating on Ducting and Nonrotating Parts of Pumn	2.0	3.0
0.002-Inch-Thick Kel-F Coating on Rotating Parts of Pump, and 0.010-Inch-Thick Kel-F Coating on Ducting and Nonrotating Parts of Pump	2.0	2.49
Butterfly Valve		2.81

CONFIDENTIAL

(C) The main chamber pressure and pump flowrates as a function of time during the start transient are shown in Fig. 51. The results shown in Fig. 51 are representative of the optimized start sequence for the single hot-gas valve system. The following sequence was established for the illustrated starts.

1. Main fuel and oxidizer valves opened at engine start
2. Fuel-control valve opened to mainstage position at engine start
3. Hot-gas valve opened to +200 percent of mainstage at engine start
4. Oxidizer control valve opened to 35 percent of mainstage when fuel injection pressure reaches 50 psia (liquid is in pump)
5. Fuel control valve, oxidizer control valve, and hot-gas valve turned over to mainstage controls when oxidizer injection pressure reaches 200 psia (oxidizer ducting primed)

(U) The results shown in Fig. 51 indicate that the following basic engine start objectives can be achieved with this sequence.

1. Rapid starts can be achieved.
2. Warm pump starts can be achieved, which are faster than shown, by utilizing the previously discussed feed system variations to improve thermal conditioning effects.
3. Good thrust control is obtained.
4. No overshoot occurs.
5. Engine mixture ratio is maintained at or below the mainstage command valve through the start transient.

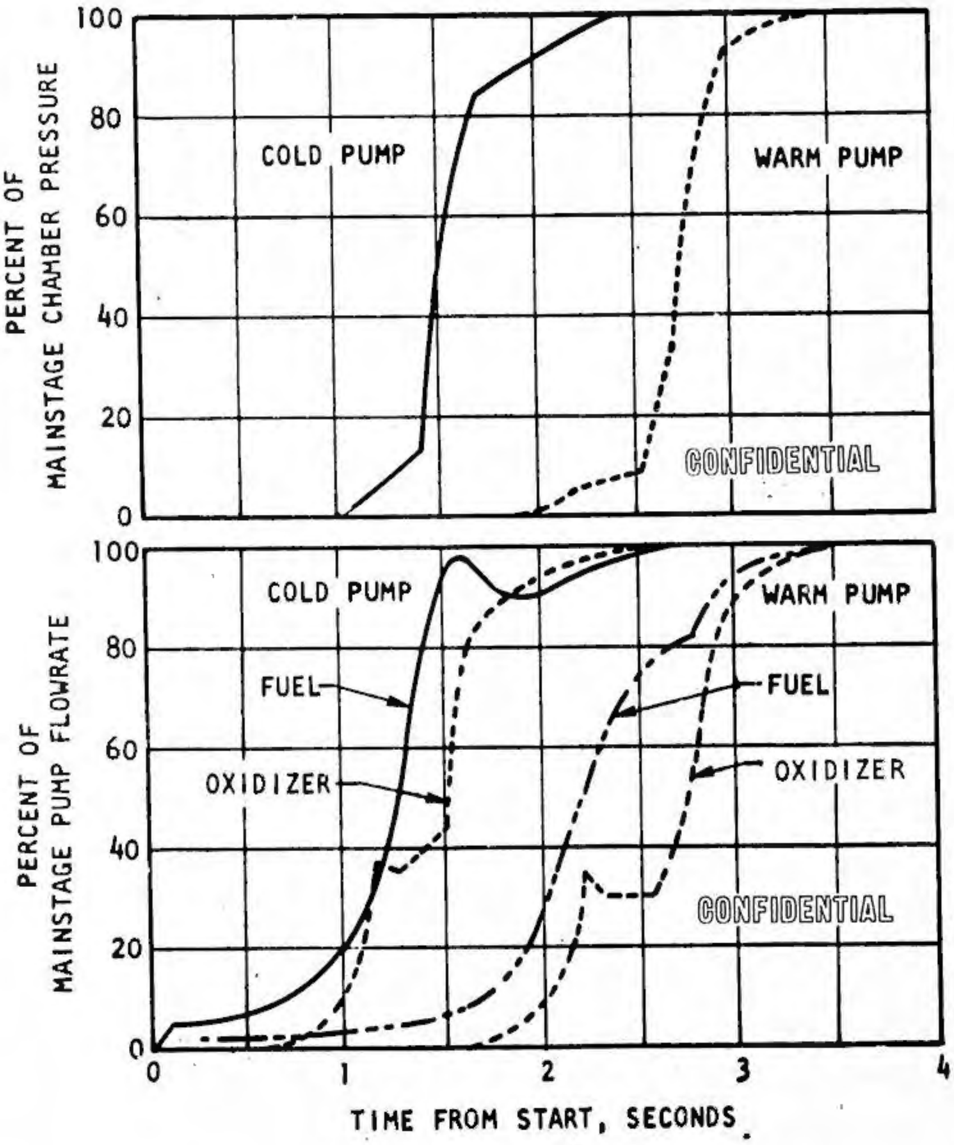

Figure 51. Main Engine Chamber Pressure and Pump Flowrates During Start (U)

(5) Engine Control Configuration Selection

(C) The control systems for the AMPS engines is required to control thrust over a throttle range of 9:1 and over a mixture ratio range of 12:1 to 9:1 (oxidizer weight:fuel weight). The original configuration at the start of the program utilized liquid control valves located in the high-pressure propellant duct and a single turbine control valve located in a line common to both oxidizer and fuel turbine inlets.

(U) In the original engine start sequence analysis (Ref. 1), some major limitations existed. As a result, several variations in the number of valves used, together with the location of the valves in the engine, were defined for control of the AMPS engines, and a tradeoff analysis was conducted. The analysis was made for the main engine, but the results are equally applicable to the secondary engine.

(U) The variations (Fig.52) included combinations of one turbine control valve with one and two liquid control valves, and two turbine control valves with one, two, and no liquid control valves.

(C) In addition to thrust and mixture ratio control, the objectives for the AMPS engine control system were established in terms of thrust ramp rate between 10 and 100 percent thrust, and engine restart capability. An objective of 90-percent thrust per second was established as a realistic ramp rate objective for either increasing or decreasing thrust. The maximum throttle rate required for a passive target intercept was found to be 0.2 percent per second for an initial range rate of 2000 ft/sec and a range of 50 n mi (Ref. 1). Similarly, the equivalent ramp rate at start is 45 percent per second (the start sequence to 90-percent thrust is accomplished in 2 seconds). However, during a portion of the start sequence the thrust ramp is in the order of 90 percent per second. Also, rapid restart of the engines or switching from one engine to the other is considered a primary objective. In this respect, a cutoff sequence objective in the order of 2.0 seconds and a switching time objective of 2.0 seconds were established.

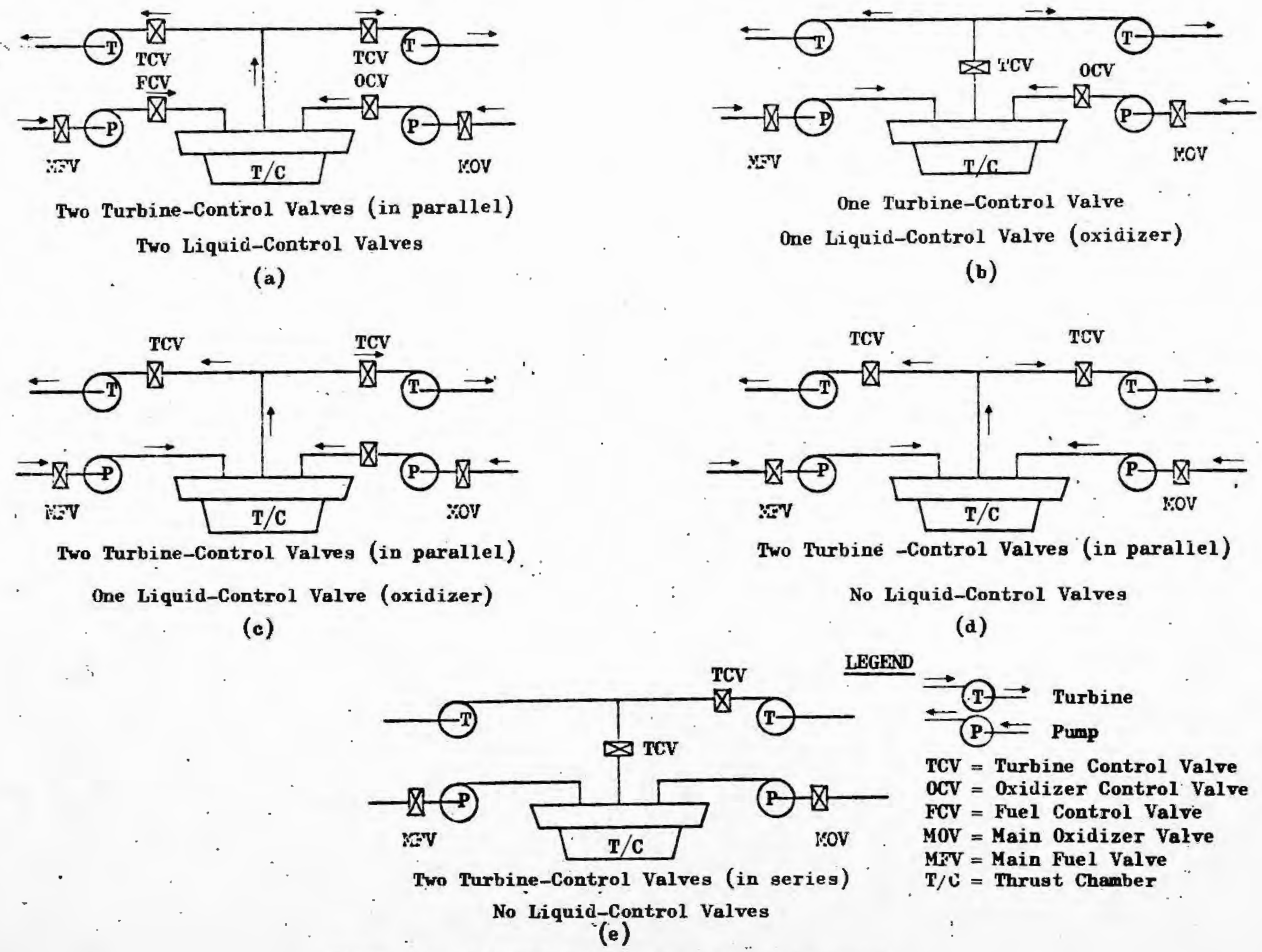

Figure 52. Alternate Control Systems Considered (Simplified Main Engine Flow Schematics) (U)

(U) In addition to satisfying these objectives, it was considered important that a relatively simple control system be defined. To be consistent with the start and cutoff sequence objectives, the ramp rate of 90 percent per second was established.

(U) At the outset of the tradeoff analysis, major influencing factors were found to be the number and location of turbine control valves. The turbine control valve arrangements are discussed below.

(a) Single Turbine Control Valve System

(U) The original configuration consisting of a single turbine control valve and oxidizer and fuel liquid control valves was found to have more than adequate thrust and mixture ratio control. Results from the mainstage control analog model indicated that a thrust ramp rate in excess of 200 percent per second is achievable while maintaining engine mixture ratio within 1 unit of targeted. Although the configuration was not tested, similar results are predicted for a control system consisting only of a single turbine control valve and a single oxidizer liquid control valve (Fig. 52b).

(U) The liquid control valves defined for the original configuration were variable area cavitating venturi valves. In addition to providing engine control, the valves were expected to provide decoupling of the engine manifold and thrust chamber fluid systems from the pump and feed system and also provide the mechanism to determine flow for engine mixture ratio control. The model tests showed that with the cavitating venturi valves in cavitation during increasing thrust, the maximum ramp achievable from 10-percent thrust to 100-percent thrust was approximately 60 percent per second. The limitation was generated by inability to accelerate the fuel pump at a rate sufficient to provide adequate venturi valve inlet pressure for cavitation during higher ramp rates. Conversely, the design of the engine and feed system can likely be accomplished to minimize the probability of fluid system coupling (e.g., high injection velocities and system

(U) tuning), and the cavitating venturi valves would not be needed for that purpose. In this case, the operating level of the pumps would be reduced by ≈15 percent; that amount of pressure required to maintain the liquid valves in cavitation.

(C) Considering mainstage operation while using a single turbine control valve, the analysis showed that at low mixture ratio the oxidizer pump would be required to operate at a level ≈30 percent above nominal operation. The turbine feed system would be balanced to provide optimum pump discharge pressures during nominal engine operation. However, at low engine mixture ratio (9:1) the single turbine control valve would be opened additionally to produce the higher fuel flowrate. At the same time the oxidizer pump speed would be increased, requiring that the oxidizer liquid control valve compensate for the corresponding increase in pump discharge pressure.

(U) The single turbine control valve was found to cause considerable restrictions in the operation and sequencing associated with engine start and cutoff. The analyses showed that the small area of the fuel cavitating venturi valve would restrict the thermal conditioning rate of the fuel pump. The predicted effect on start was to increase the sequence during a warm pump start in excess of 4.0 seconds. No appreciable effect was predicted for a cold pump start.

(U) Even more serious was the requirement that with the single turbine configuration, the oxidizer and fuel pumps start spinning together. A fuel-rich start was considered mandatory to maintain reasonable thrust chamber wall temperatures (and therefore maintain hardware integrity) during the engine start sequence. To accomplish this, the fuel system must be fully primed and at a reasonable operating mass flowrate prior to entry of the oxidizer into the combustion chamber. To accomplish this in a 2 second start, fuel pump power is required to pump the fuel through the engine during the fuel system prime. With a common turbine control valve these conditions require that the oxidizer turbine and pump spin with no fluid in the pump. This prospect is completely unsatisfactory because the

(C) condition could be catastrophic either as the result of unusual rotating-parts deflection or as a result of a detonation in the heated bearing cavity when the coolant (oxidizer) is admitted to the pump.

(U) At cutoff, the single turbine control valve restrains the rate in which the residual propellants can be expelled. The method to expel the residual propellants was with the use of gaseous purges after cutoff had been initiated. To do this without causing hardware damage, the thrust chamber wall temperatures must be maintained at a low level (i.e., coolant flowrate must be sufficient to cool the walls). This probably could be accomplished by maintaining a sufficiently low mixture ratio (i.e., adequate fuel flow) during residual propellant expulsion.

(C) After the single turbine control valve closes there are two options available to expel the residual propellants. The first option is to simultaneously close both oxidizer and fuel shutoff valves and purge both systems free of propellant. By computing the comparitive residual weights it was estimated that the weight ratio was $\approx$20:1 (oxidizer/fuel). Consequently, a low mixture ratio could not be maintained for the entire expulsion. Additionally, helium has less heat capacity than that of hydrogen; thereby, the thrust chamber cooling would be reduced when helium entered the tubes.

(C) The second option would be to permit fuel to continue to flow under tank-head pressure until the oxidizer was expelled, then purge the fuel residual from the engine. In this case, as in the first option, the cutoff time (including purges) would be long ($\approx$ 5 seconds). Also, in both options, the injection velocity of the propellants would be extremely low. Heat transfer analyses have indicated that, at excessively low injection velocities, the injector heat flux is correspondingly high and is undesirable.

(U) Combining all the factors associated with the single turbine control valve, the conclusion was made that the restraints were excessive and could cause serious compromises in the engine design and operation.

(b) Two Turbine Control Valve System With Liquid Propellant Control

(U) The AMPS engine control system consisting of two turbine control valves and liquid propellant control valves (Fig. 52a and 52b) has all the advantages of the single turbine control valve configuration. Additionally, during mainstage operation individual turbine control permits near-optimum operation of the fuel and oxidizer pumps at all thrust and mixture ratio operating levels.

(U) The greatest advantages of individual turbine control are realized in the operational factors associated with the start and cutoff sequences. With the use of two turbine control valves, the fuel and oxidizer pumps would be operated independently of each other at start and cutoff. At start, the fuel system could be primed, and sufficient pressure could be established prior to opening the oxidizer shutoff valve and oxidizer turbine control valve. Also, the oxidizer would be admitted to the pump prior to opening the turbine control valve, thereby avoiding operation of the oxidizer pump prior to providing bearing coolant.

(C) At cutoff, the fuel turbine would continue to operate at approximately the throttled thrust level until the residual oxidizer was purged free of the engine. In this way, the oxidizer expulsion time would be reduced to less than 2.0 seconds, and the issue of overheating the injector face because of low injection velocities would be avoided.

(U) The major disadvantage of adding a second turbine control valve would be that of adding control system and engine complexity. The configuration could result in four control valves in the engine where two liquid propellant control valves were also used. The conclusion was, however, that two turbine control valves were required to provide the flexibility needed in development of the AMPS engines.

(c) Two Turbine Control Valves Without Liquid Propellant Control

(U) Because a simple engine control system was a primary objective for the AMPS engines, and individual turbine control was apparently a requirement to accomplish satisfactory start and cutoff sequences, the decision was made to evaluate the possibility of eliminating the liquid propellant control valves from the system. Two configurations were initially considered (Fig. 52d and 52e); however, the dual (parallel) configuration was found to have more positive mainstage control; therefore, the major analysis was made on the configuration shown in Fig. 52d.

(C) The analysis showed that the thrust ramp rate capability for this configuration was in excess of 100 percent per second while maintaining mixture ratio within ±1 mixture ratio unit. The turbine-control-only configuration has all the advantages of the turbine and liquid propellant control except that provisions would be required to determine and control engine mixture ratio if the venturi valves were removed from the system. An analysis on this subject is presented in section III, 2, n of this volume.

(U) Because fluid system coupling of the engine system frequencies with feed system critical frequencies may be avoided by engine design considerations, the penalty in control system complexity attendant with the addition of two variable area cavitating venturi valves (four control valves) is not warranted. As a result, the control system consisting of two turbine-control-valves-only was adopted for the AMPS engines. Figure 53 persents the flow schematic for this configuration for the main and secondary engines.

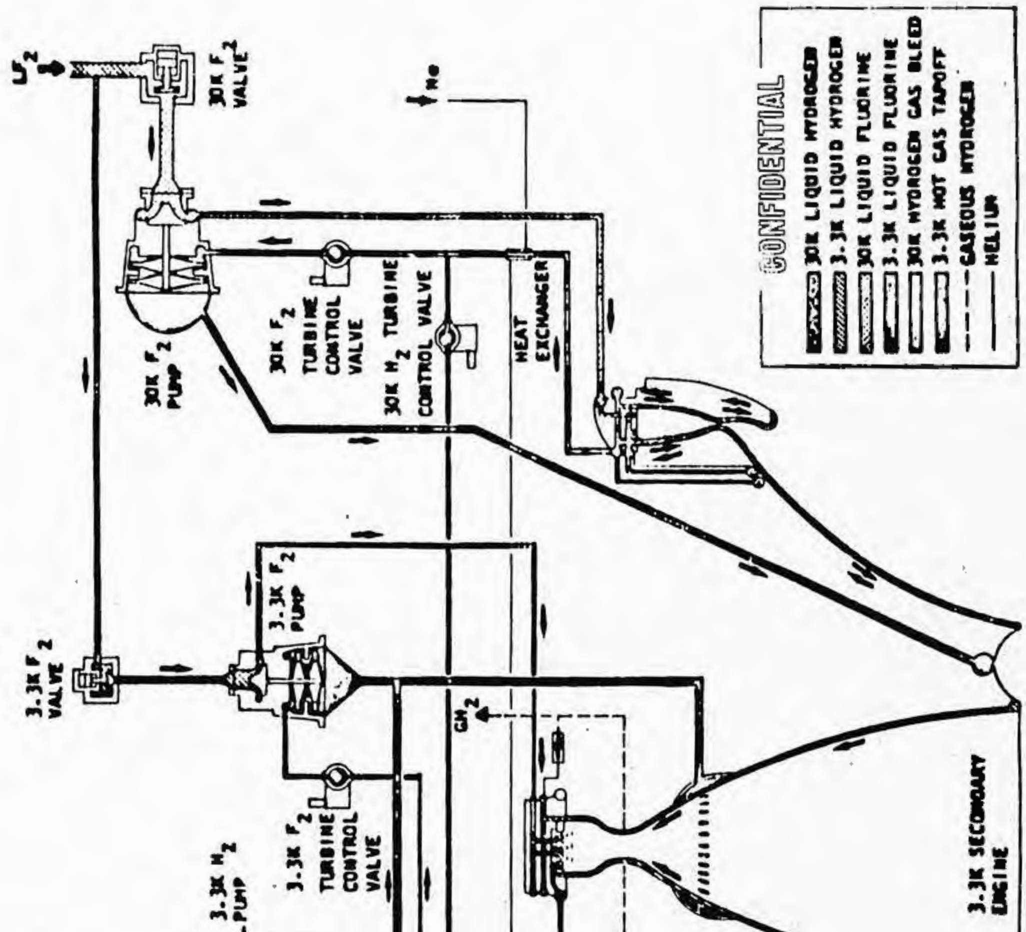

Figure 53. AMPS Engine Flow Schematic Showing Turbine Control Arrangement (U)

(6) Optimization of Start and Cutoff Sequence for Selected Control Configuration

(a) Main Engine Start Sequence

(U) The first series of model tests conducted using the two turbine-control valve configuration also utilized a two-position, high-pressure oxidizer propellant valve. A block diagram of the model for this configuration is shown in Fig. 54.. The opening sequence for the valves is shown in Fig. 55. At engine start signal the main fuel valve and the fuel turbine-control valve were opened. When the fuel injection pressure increased to 50 psi, indicating that the fuel system was primed, the main oxidizer valve and the oxidizer turbine control valves were opened. The mainstage control system was activated by a chamber pressure monitoring switch. The chamber pressure transient predicted by this start sequence is shown in Fig. 56. The analysis showed that there was an overshoot in chamber pressure of approximately 8 percent.

(C) Several attempts to optimize the start sequence were made by changing the open setting of the two-position valve, but these had no appreciable effect on the magnitude of overshoot. The decision was then made that the turbine-control valves could possibly be used to control both overshoot and the rate of thrust buildup. With this philosophy, the use of the two-position oxidizer valve was not necessary. A block diagram for the model of this configuration is shown in Fig. 57. The sequence evaluated (Fig. 58) consisted of simultaneous opening of the main fuel valve and fuel turbine-control valve. The signal to open the main oxidizer valve and oxidizer turbine valve was initiated when the chamber pressure reached 50 psi, which indicated pump and fuel system priming were completed. In this test sequence, all valves except the oxidizer turbine valve were opened fully during start. This valve was held at the 10-percent open position until chamber pressure reached 80 psia. At this point, the mainstage control was activated, and the valves were driven by the respective thrust and mixture ratio commands. The resulting start sequences to full thrust and throttled thrust, as reflected in chamber pressure and pump flowrates for

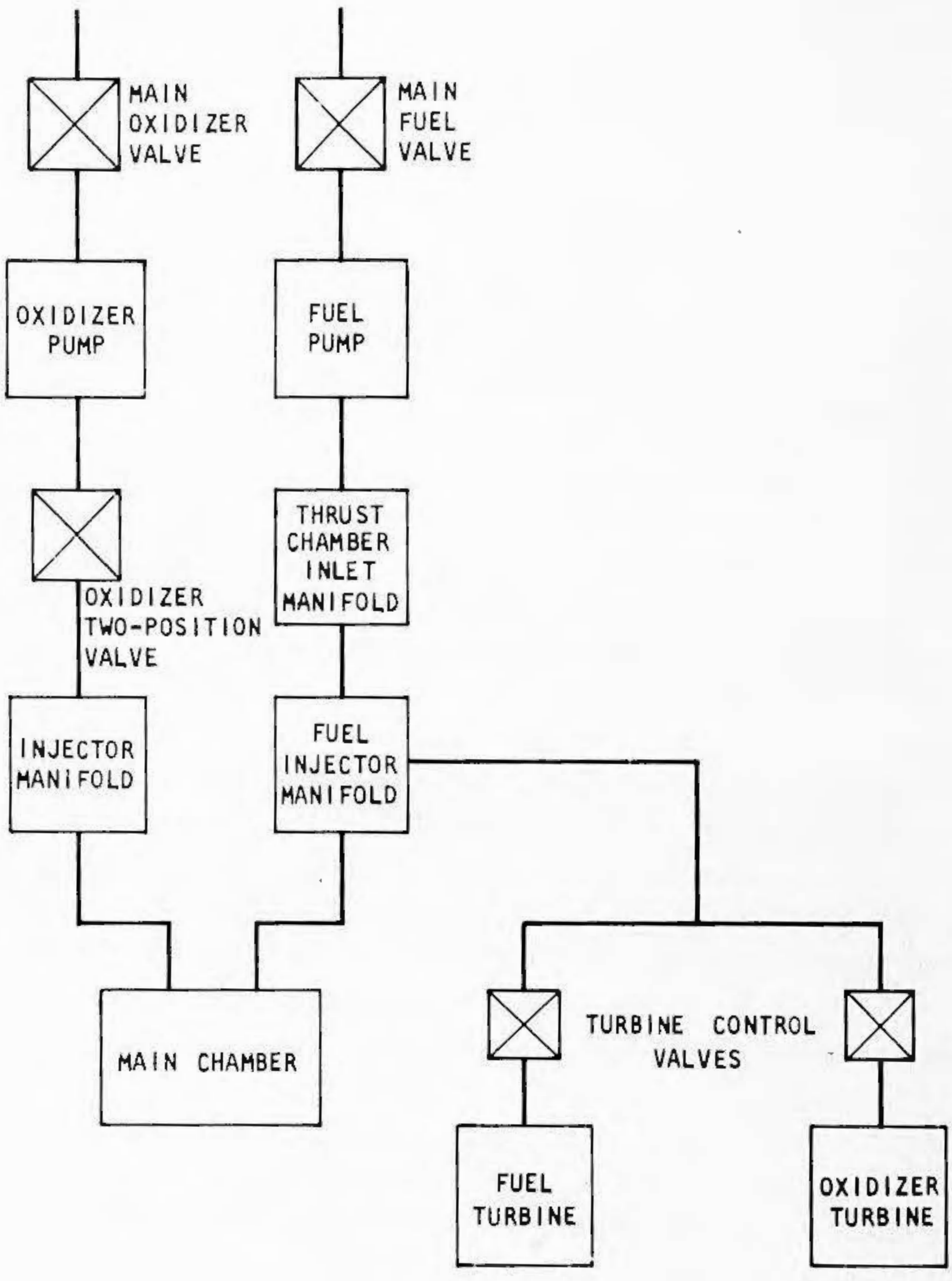

Figure 54. Main Engine Control System Consisting of Two Hot-Gas Control Valves and One Liquid-Line Valve (U)

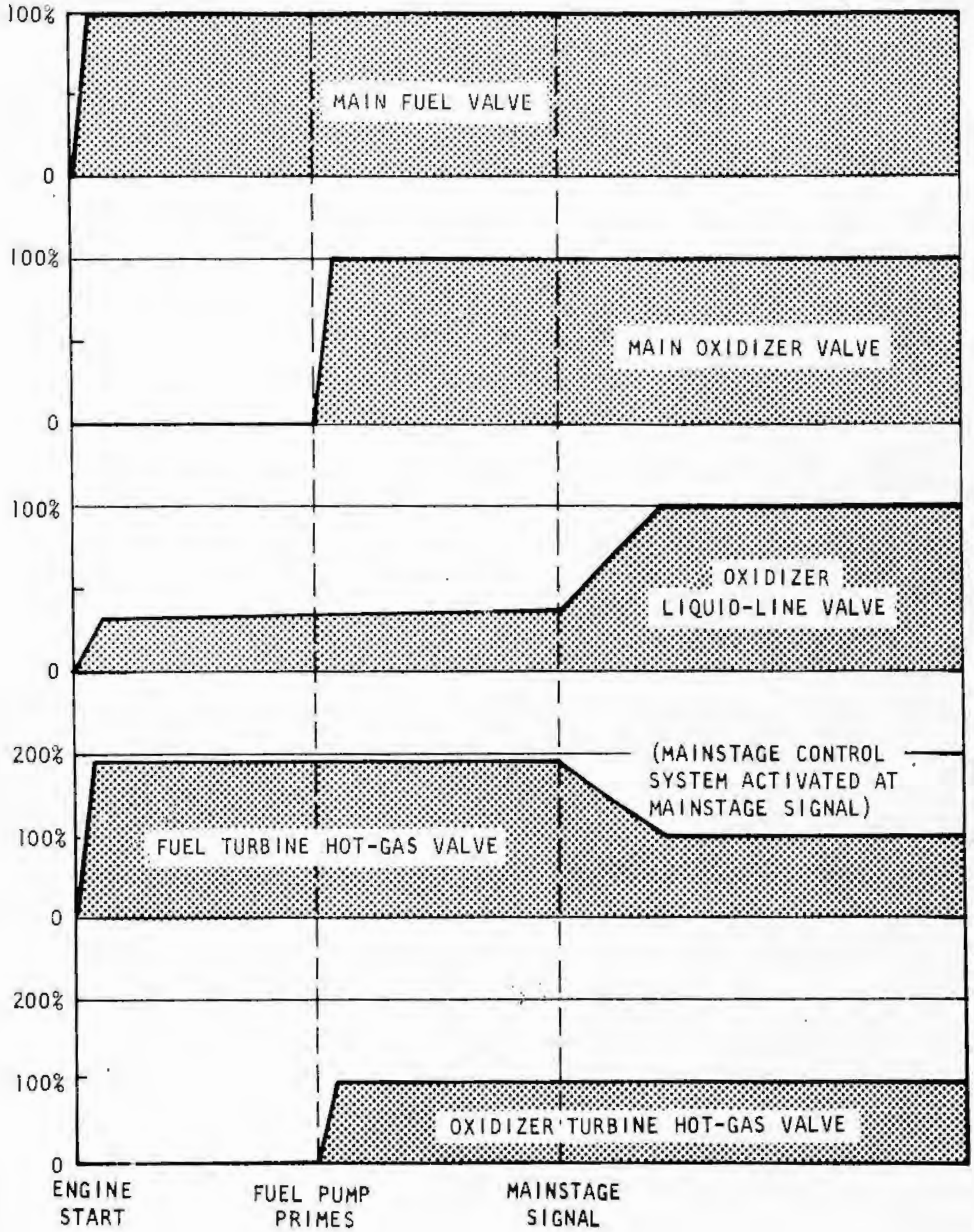

Figure 55. Sequence Used for Main Engine Control System With Two Turbine-Control Valves and One Liquid Line Valve (U)

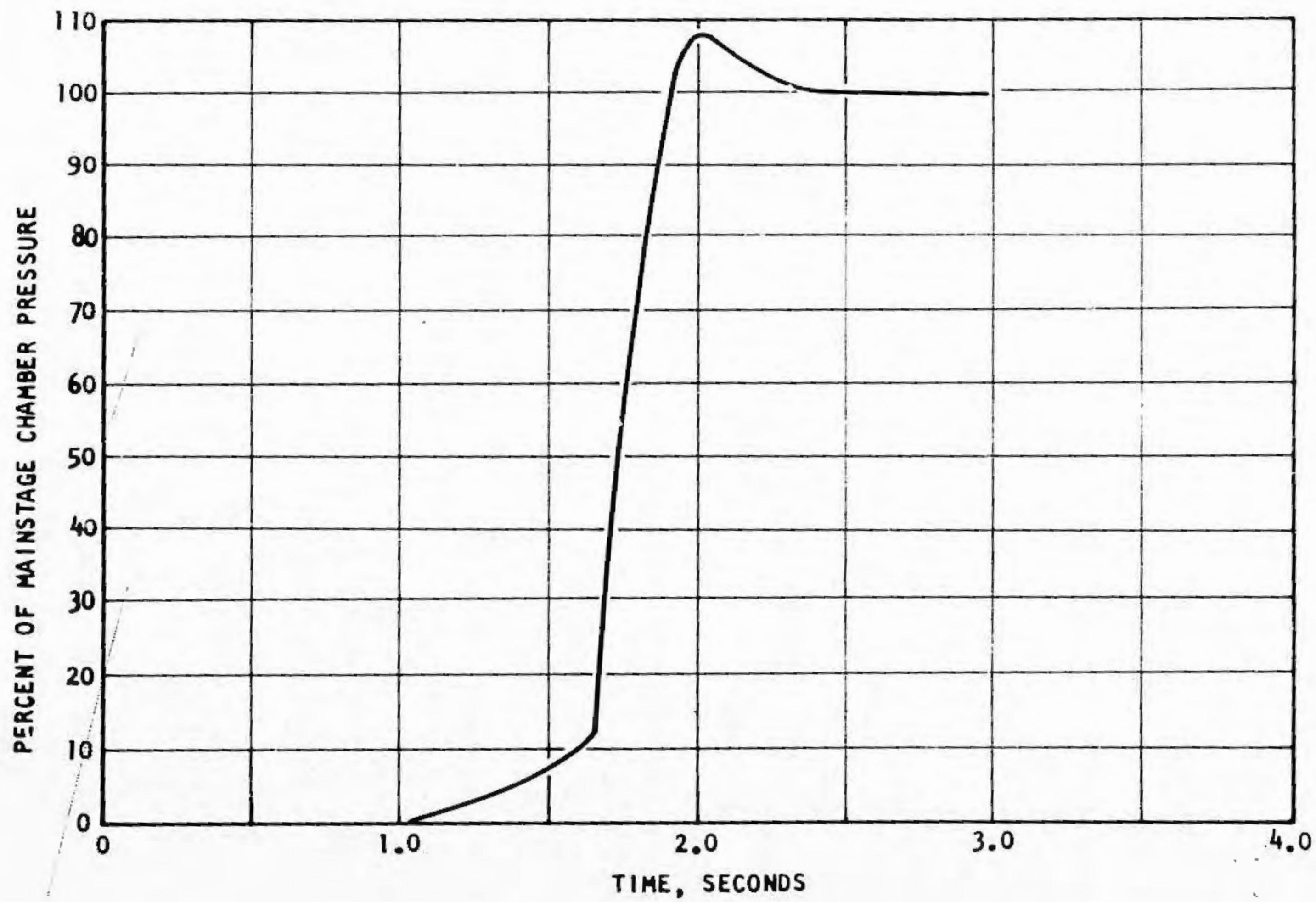

Figure 56. Percent of Mainstage Chamber Pressure for Cold-Pump Start, Two Turbine-Control Valves With One Two-Position Oxidizer Valve, Main Engine (U)

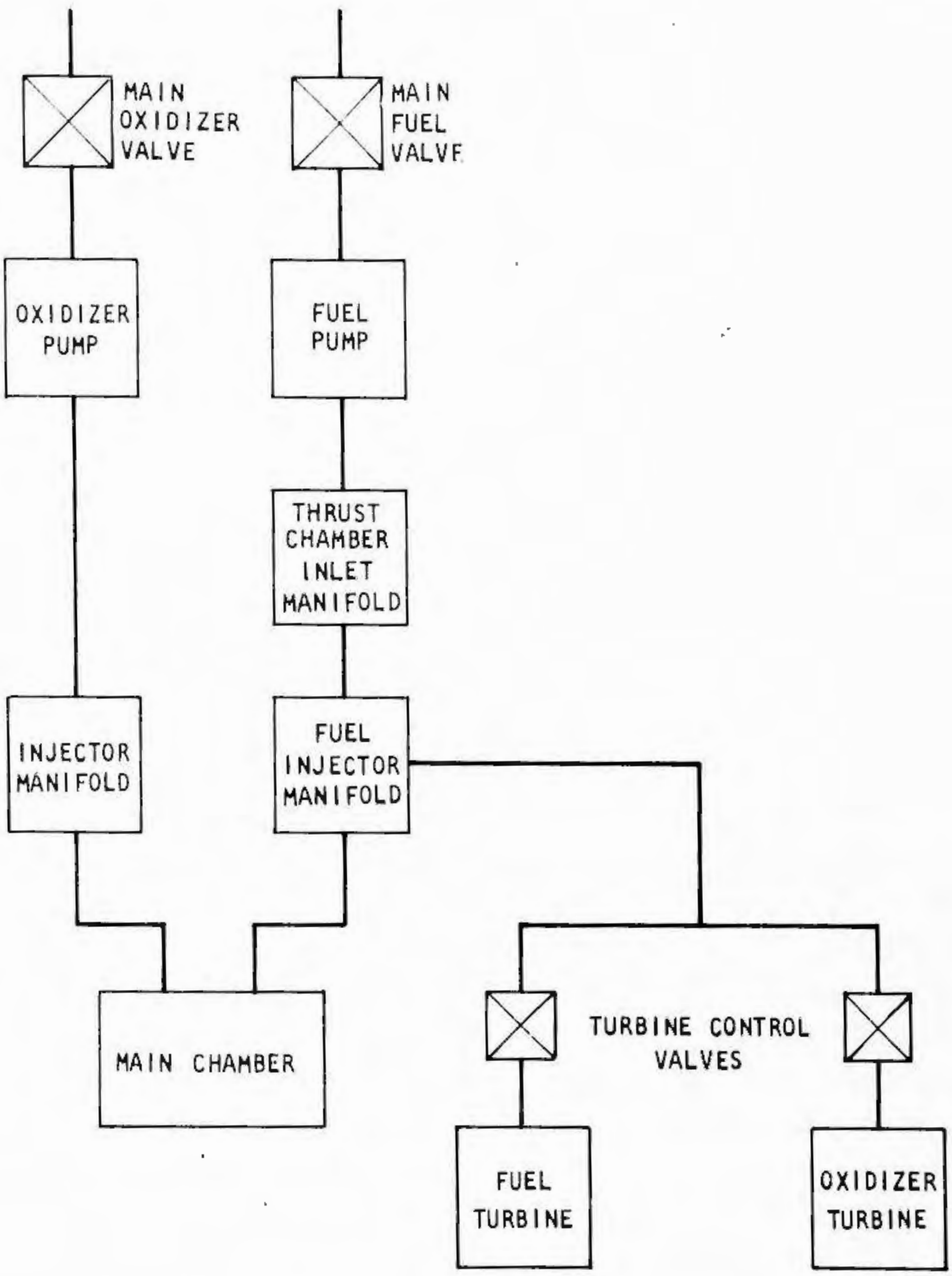

Figure 57. Main Engine Control System Consisting of Two Turbine-Control Valves (U)

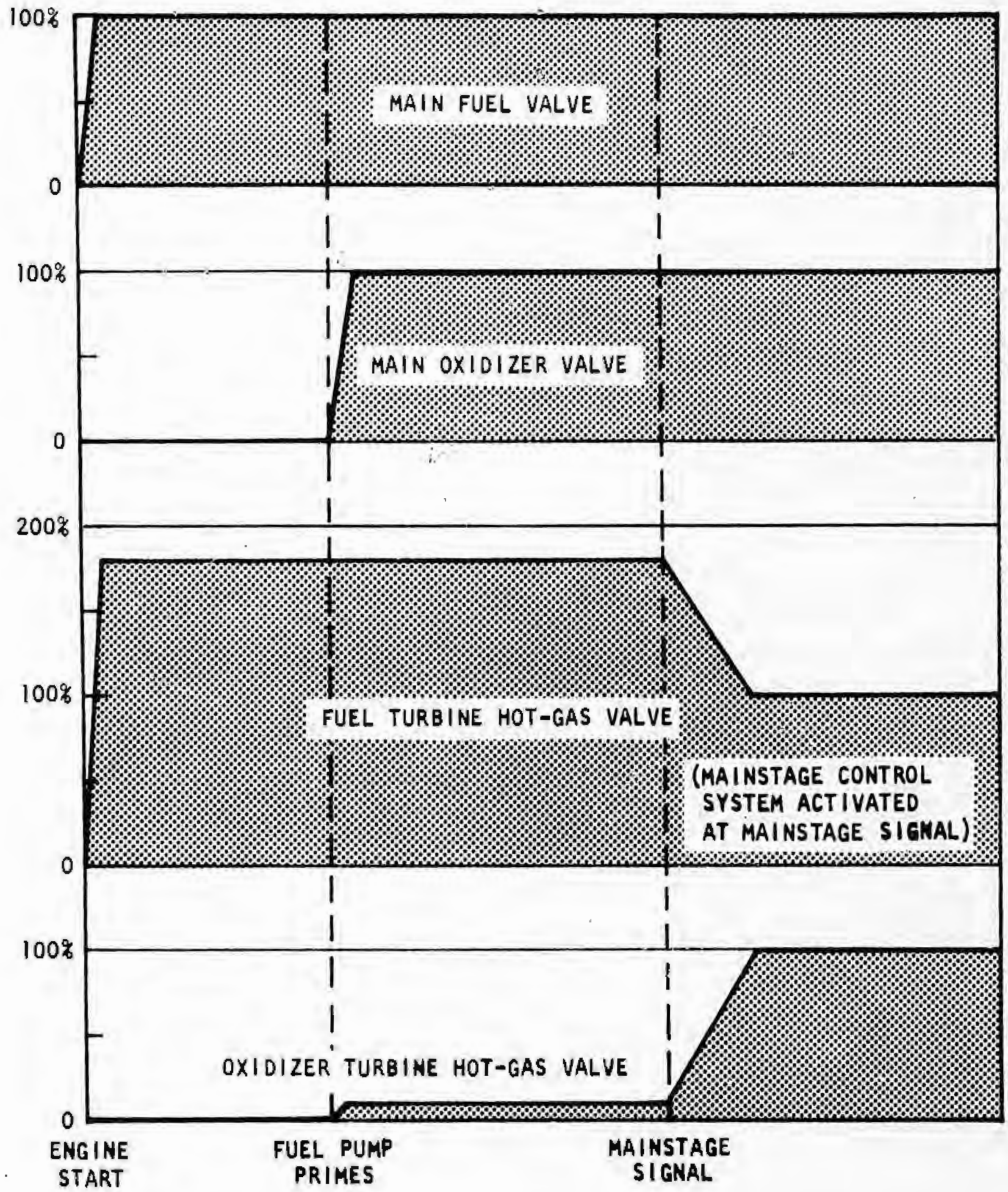

Figure 58. Sequence Used for Main Engine Control System Consisting of Two Turbine-Control Valves (U)

(C) cold pumps and warm pumps, are shown in Fig. 59 and 60. Figure 59 shows that an overshoot to approximately 40 percent of full thrust was experienced during the start to the throttled thrust level for both cold and warm pumps; otherwise, the start predicted for each of the four extreme cases was satisfactory.

(C) The cause of the overshoot was the result of the oxidizer control valve opening in an attempt to correct the mixture ratio error. Therefore, the fuel control valve was programmed to close down from 180 percent of the full-thrust position to the desired mainstage position at the time the fuel system primed. The mainstage control was activated at the time chamber pressure achieved 80 psia. (The pressure level used to actuate mainstage control was later changed to 50 psia.) This sequence completely eliminated the overshoot during start to the full-throttled thrust level. However, when the same sequence was attempted to the full-thrust level the chamber mixture ratio (MR) became excessive. The cause was a result of the fact that the fuel turbine control valve closed to correct the minus MR error and the turbine speed slowed below the mainstage value. After the MR error was reversed, the high fuel pump inertia (relative to the oxidizer pump) prevented the fuel pump from accelerating sufficiently to avoid a large position mixture ratio error. Also, the time to 90 percent of full thrust was extended to approximately 4.0 seconds. This start sequence is shown in Fig. 61 and 62.

(C) Because the mixture ratio control crossfeed compensation was strong enough to override the thrust command during the start transients, the decision was made that the solution would be either to reduce the crossfeed compensation gain during the start transient, or merely to program the valves to the desired thrust and mixture ratio levels and delay the control system activation until the error was reduced to an acceptable level. The initial approach was to utilize the latter method. The mainstage signal used in this case was reduced to a P_c of 50 psia, and this signal initiated programming of both fuel and oxidizer turbine control valves to the desired thrust and mixture ratio operating levels. Significant in this

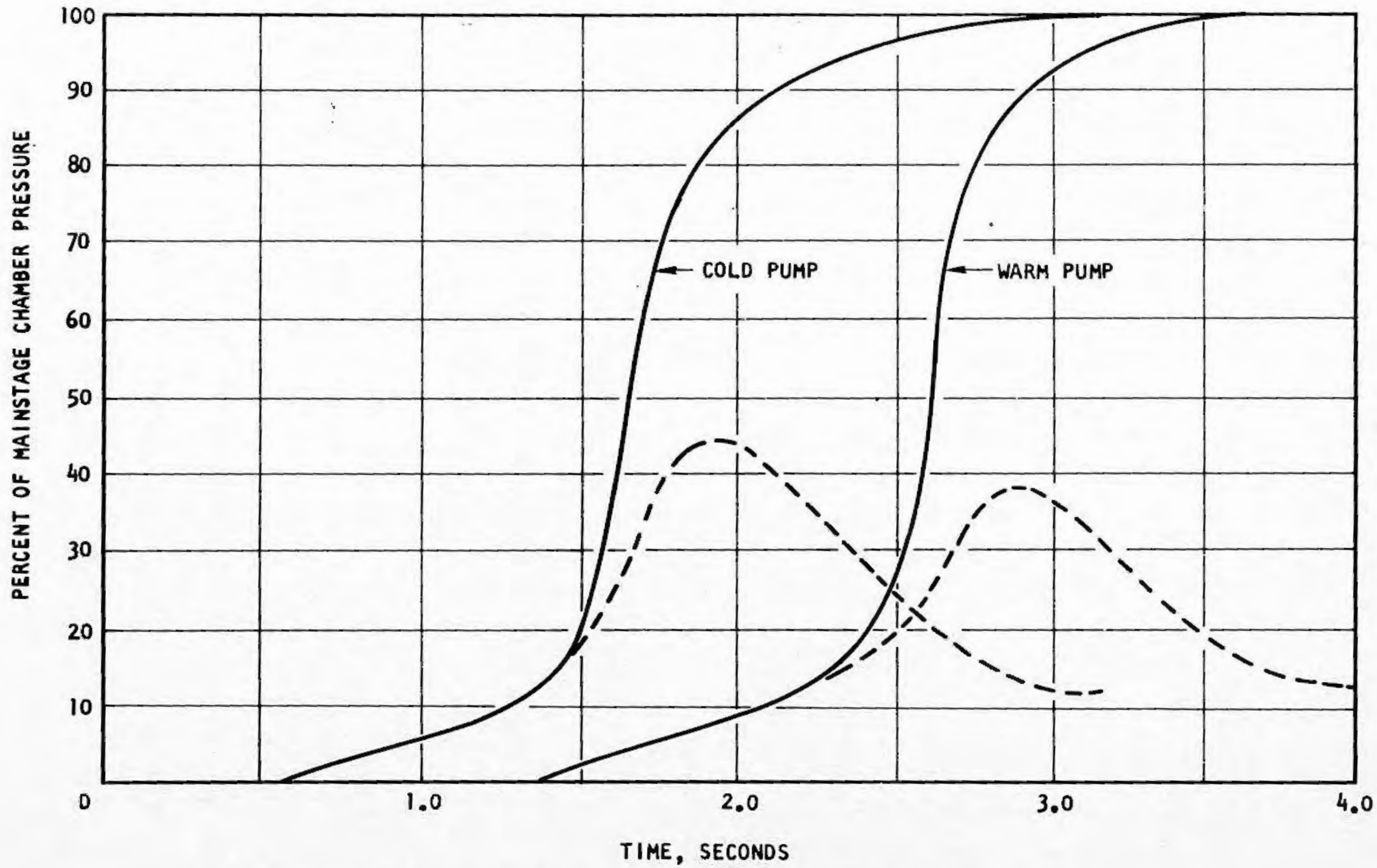

Figure 59. Percent of Main Chamber Pressure for Warm- and Cold-Pump Starts to Maximum and Minimum Thrust (U)

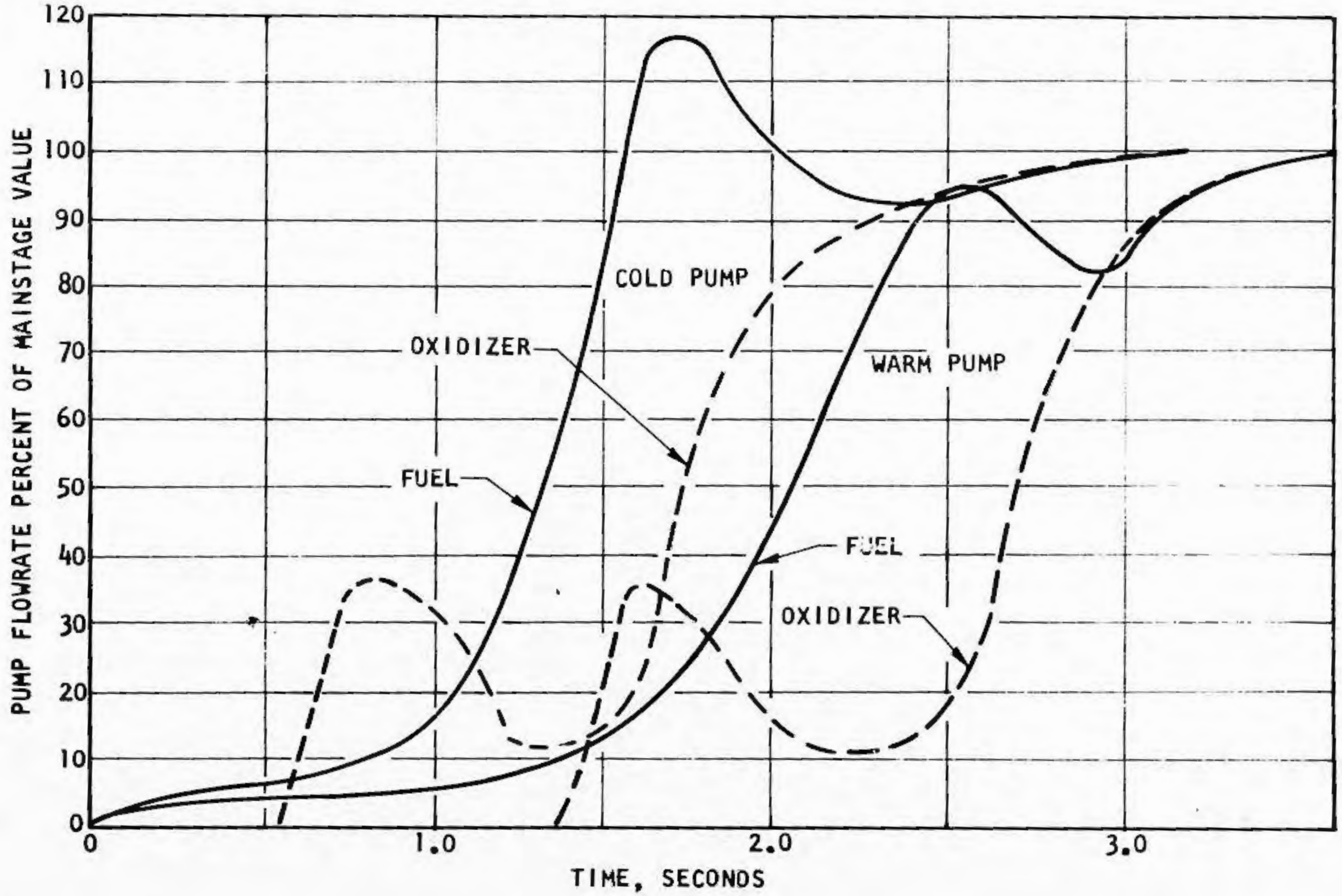

Figure 60. Main Engine Propellant Flowrates During Engine Start (U)

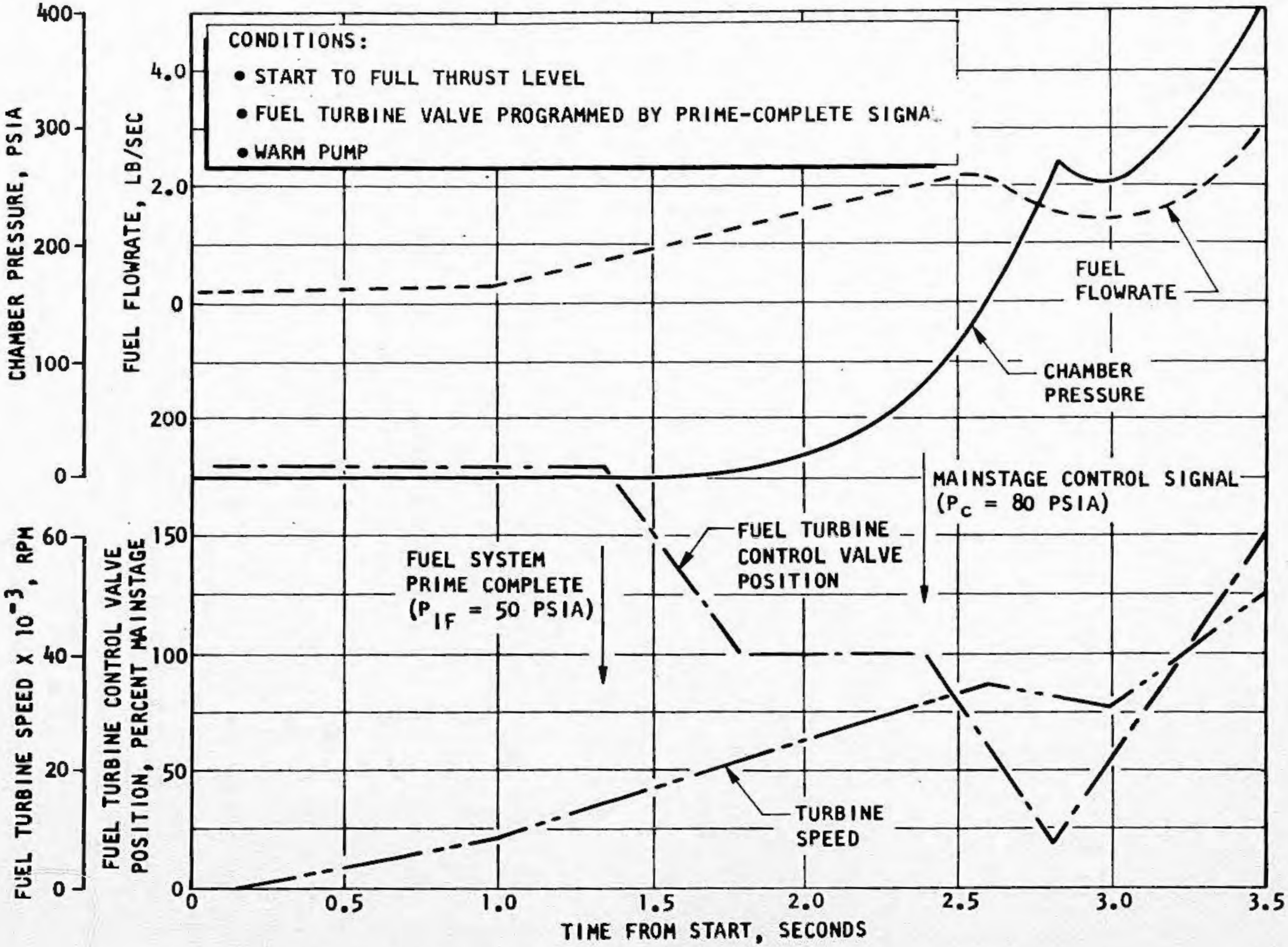

Figure 61. AMPS Main Engine Start Sequence, Fuel Parameters (U)

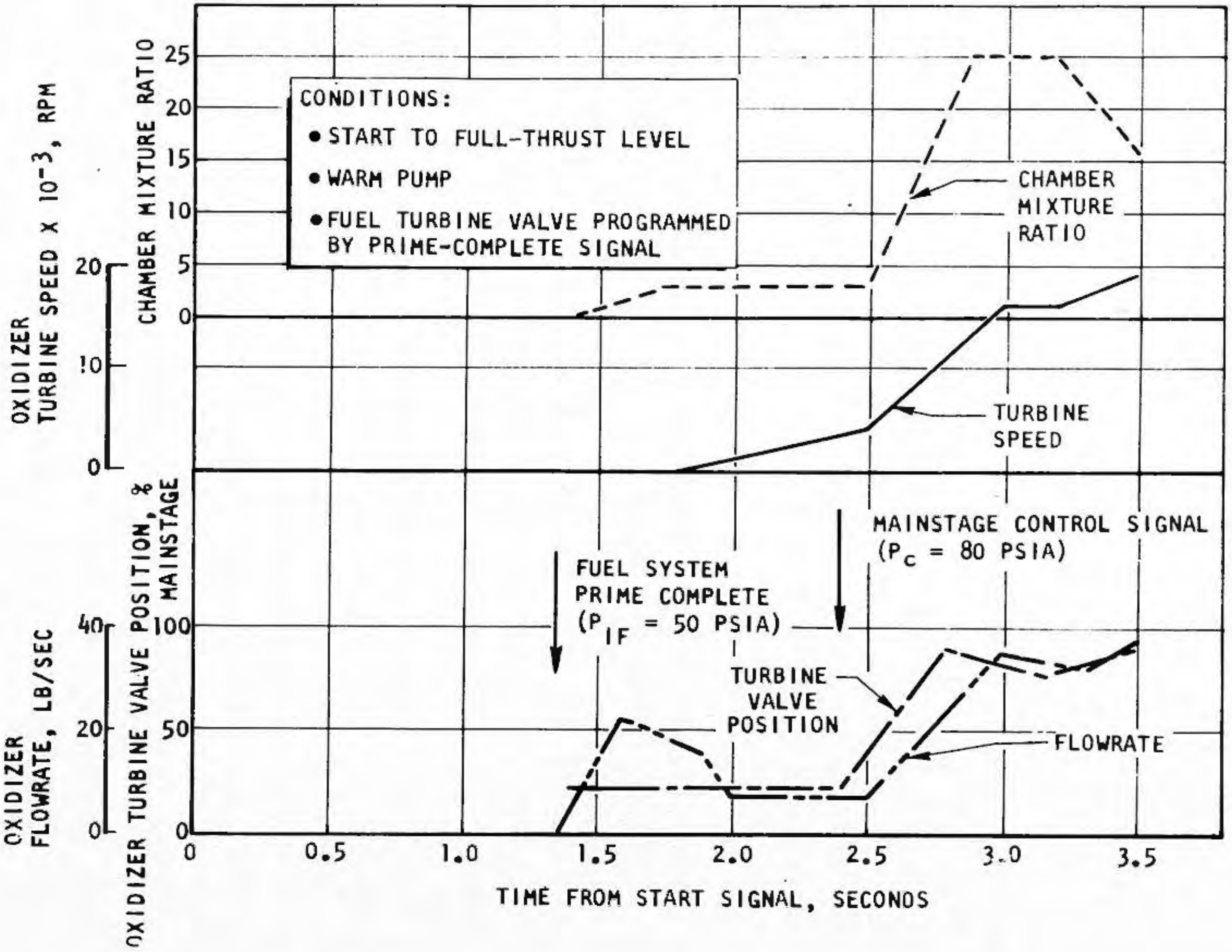

Figure 62. AMPS Main Engine Start Sequence, Oxidizer Parameters (U)

(C) sequence is the fact that the travel time of the fuel control valve was the same for programming to the full-thrust level and the throttled-thrust level. This sequence produced a predicted start time to 90-percent full thrust of approximately 2.7 seconds for a start following an extended coast period (warm pumps), and there was a fuel-rich mixture ratio throughout the transient period. The start sequence is shown in Fig. 63 through 65.

(U) Using the same basic sequence, a start was made to the full-throttled thrust level (again with warm pumps). This test is shown also in Fig. 63 through 65. As in the case of the full thrust start, mixture ratio during the entire transient period was fuel rich.

(C) The developed start model was then used to predict the start transient to full thrust for the main engine considering an immediate restart (cold pumps). The resulting transients in chamber pressure and propellant flowrates are shown in Fig. 66 together with the starts to full and throttled thrust levels after an extended coast period (warm pumps). The relatively large oxidizer pump flows shown at start (between 0.5 and 1.0 second for cold pumps) in Fig. 66 are the result of priming the oxidizer system.

(b) Secondary Engine Start Model

(U) The secondary engine utilizes hot combustion gases tapped from the thrust chamber to drive the parallel turbopump system. A digital start model describing the configuration was constructed to investigate the start transients for this turbine drive.

(C) Requirements placed on the start of the secondary engine were as follows:

1. The engine must be able to start satisfactorily with either warm or cold turbopumps (a factor dependent on the length of time elapsed since the last engine firing).

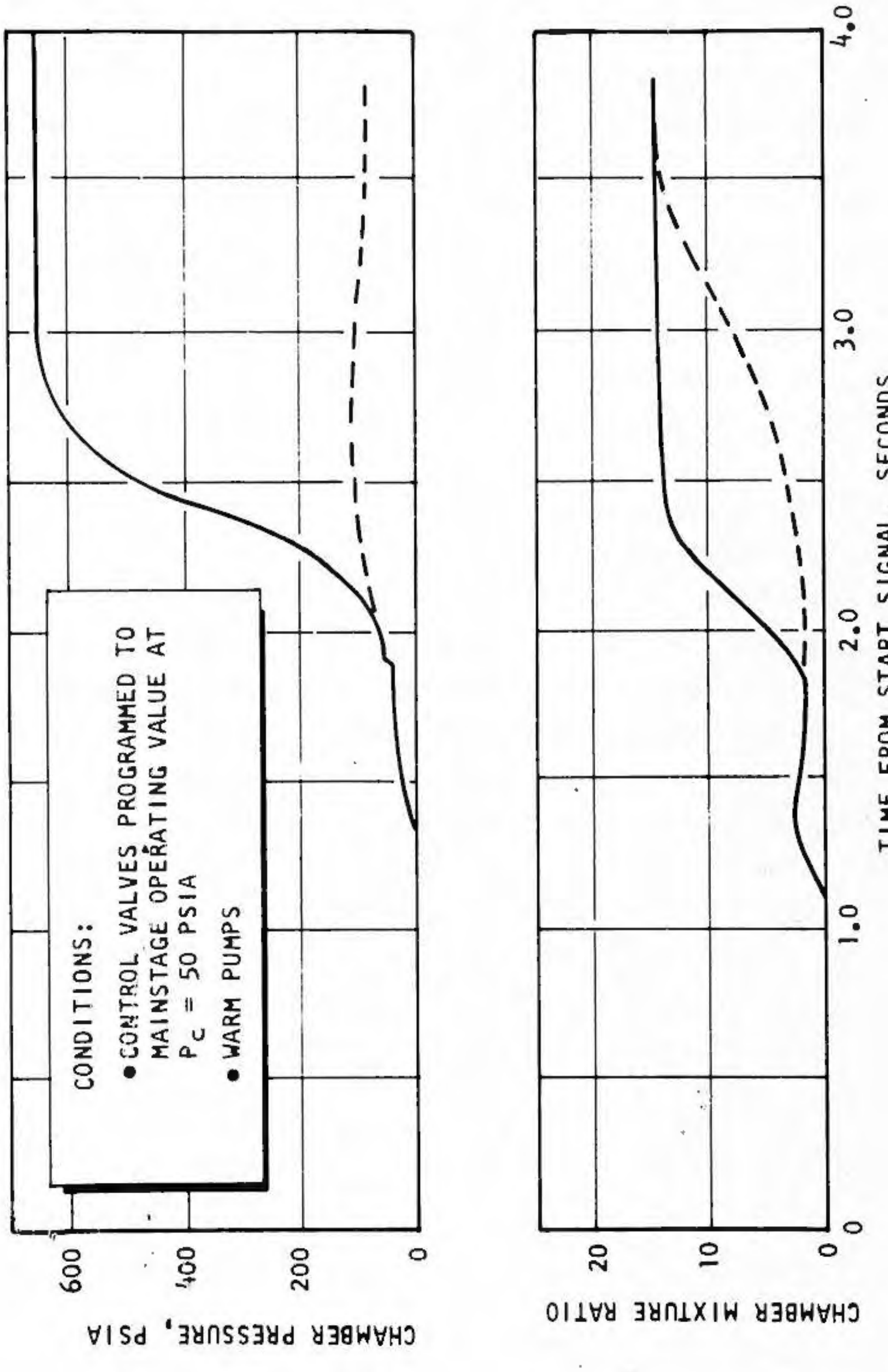

Figure 63. AMPS Main Engine Start to Maximum and Minimum Thrust (U)

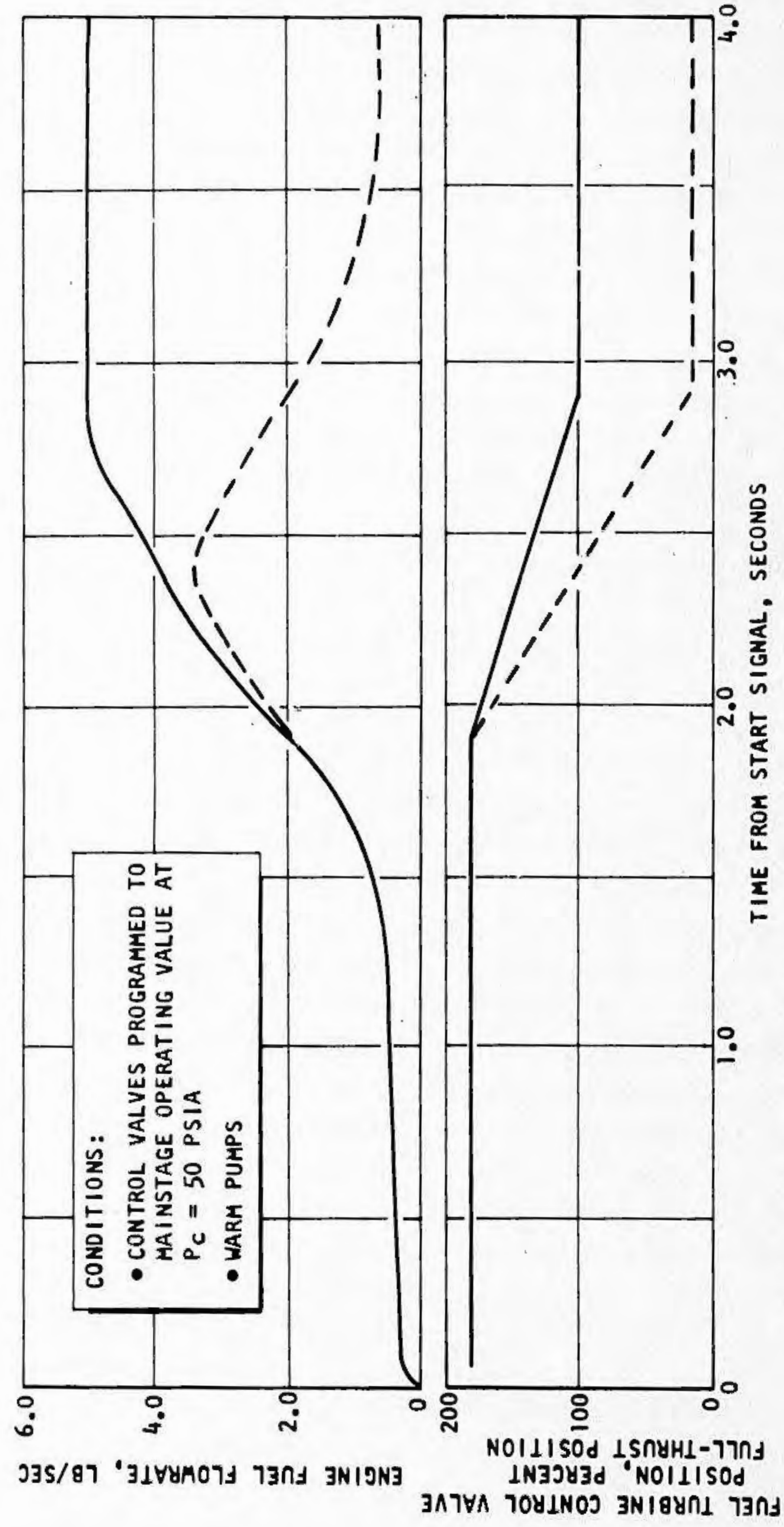

Figure 64. AMPS Main Engine Start to Maximum and Minimum Thrust (U)

CONFIDENTIAL

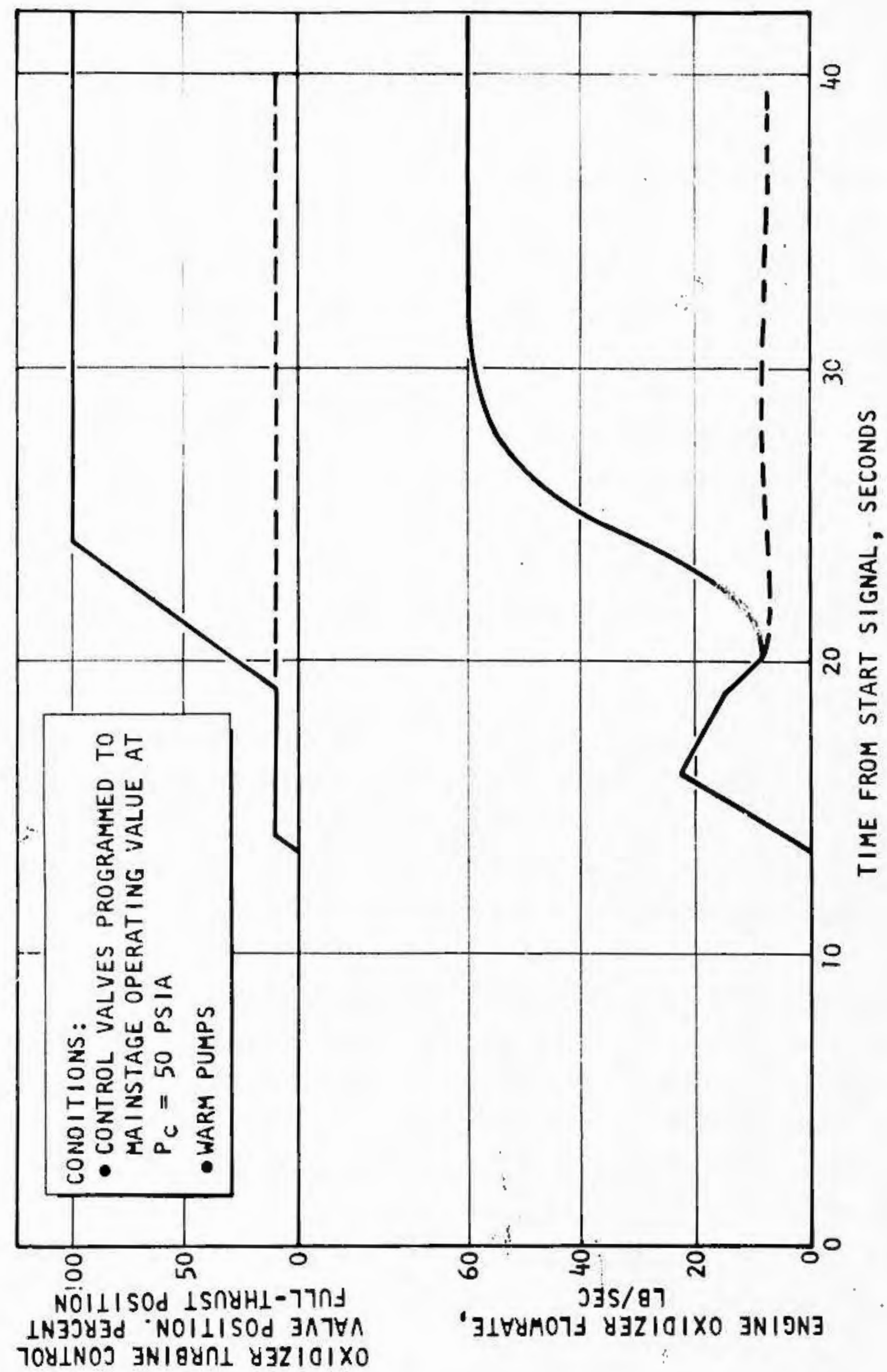

Figure 65. AMPS Main Engine Start to Maximum and Minimum Thrust (U)

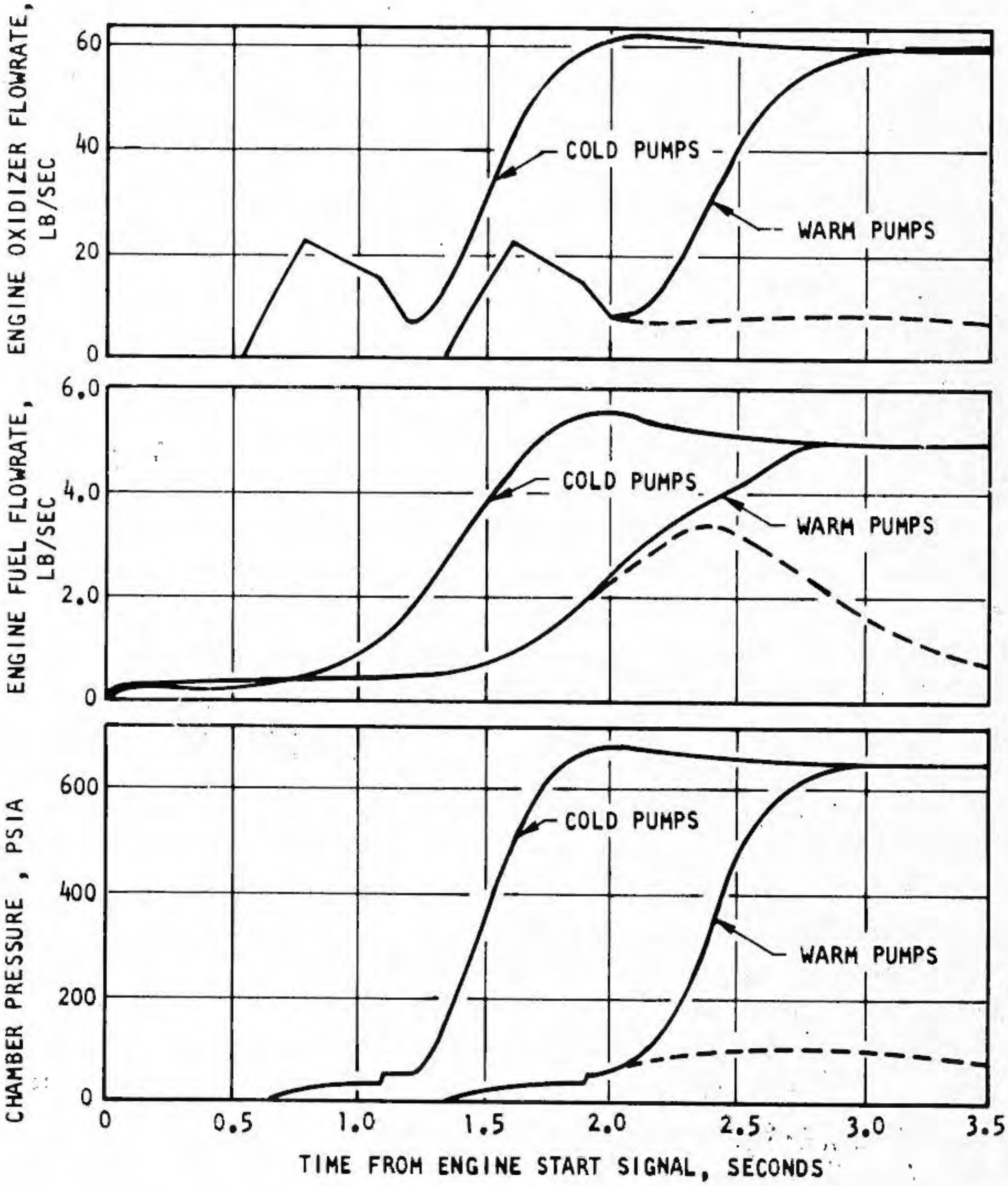

Figure 66. Main Engine Start to Full and Throttled Thrust (U)

(C) 2. Start under tank-head conditions

3. The oxidizer turbopump must not rotate until oxidizer is in the pump.

4. Start times on the order of 2.0 seconds maximum

(U) The secondary engine control system is basically the same as the main engine, consisting of main shutoff valves upstream of the fuel and oxidizer pumps, plus two parallel hot-gas valves upstream of the turbines that control turbopump speed. This system is shown schematically in Fig. 67a.

(C) The following sequence was used to obtain the fastest start possible with the basic engine configuration:

1. Main fuel valve opened full and fuel turbine hot-gas valve opened to +200 percent of mainstage position at engine start.
2. Main oxidizer valve opened full and oxidizer turbine hot-gas valve opened to 10 percent of mainstage position at fuel system prime.

(C) All starts were made with fuel and oxidizer tank pressures of 70 and 65 psia, respectively.

(C) For a hot-gas tapoff engine, the power available to drive the turbines is proportional to main chamber pressure which, in turn, is primarily a function of the amount of oxidizer flowing into the chamber. As a result, the hot-gas tapoff engine starting under tank-head conditions realized a slow buildup rate because of the low power available to drive the turbines during the initial fuel-lead portion of the start. Thus, because of low fuel turbopump speed, a relatively long time was required to prime the fuel pump and high-pressure ducting. The resulting time required for main chamber pressure to reach 100 psia was approximately 5.0 and 2.8 seconds, respectively, for warm and cold pump start conditions.

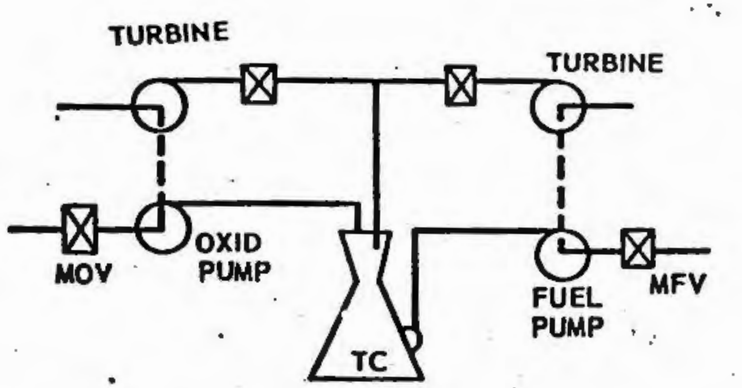

(a) THRUST CHAMBER HOT-GAS TAPOFF FOR START AND MAINSTAGE TURBINE DRIVE

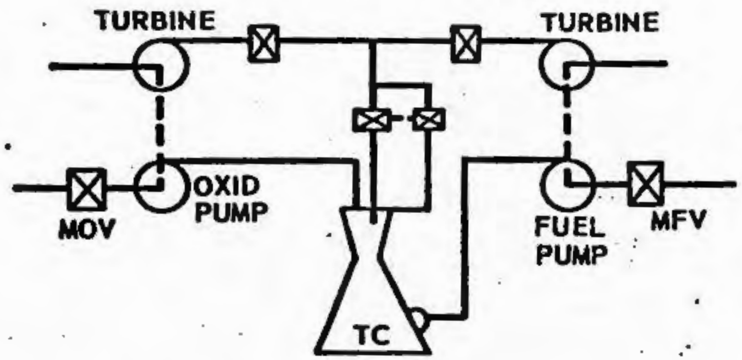

(b) FUEL INJECTOR BYPASS FOR TURBINE DRIVE DURING START TRANSIENT ONLY (HOT-GAS TAPOFF DURING MAINSTAGE)

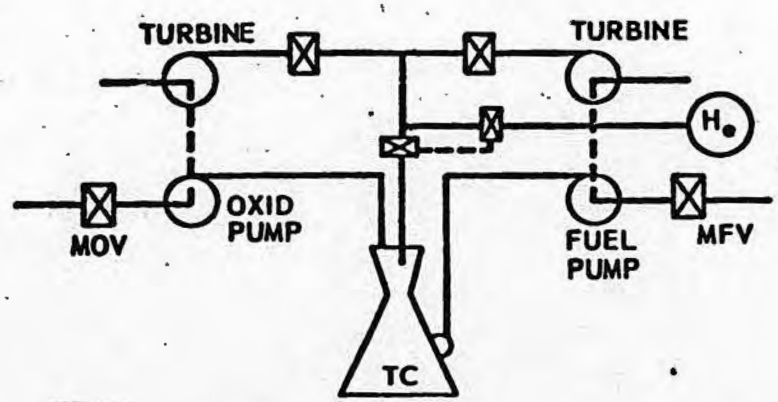

(c) PNEUMATIC (HELIUM) POWER FOR TURBINE DRIVE DURING START TRANSIENT ONLY (HOT-GAS TAPOFF DURING MAINSTAGE)

Figure 67. Secondary Engine Turbine Power Sources Considered for Starting (U)

(C) As a result of the long start times required with the hot-gas tapoff engine system, modifications to the system were investigated to shorten the start time. The first system modification investigated utilized a bypass from the fuel injector manifold to the fuel turbine inlet manifold (Fig. 67b). This bypass would be used only during the initial part of the start to increase the power available to the fuel turbine (additional gas flowing through the turbine at a higher pressure) and, also, to help speed up thermal conditioning of the fuel feed system (resistance of the fuel injector is bypassed). The bypass would be closed as the oxidizer side primes. Start times with this system modification were found to be approximately 4.0 and 1.9 seconds, respectively, for the warm and cold pump conditions.

(U) A second bypass system (a bypass from the pump discharge duct to the fuel turbine inlet manifold) also was considered; however, no start transient data were obtained for this system.

(U) The third system change that was considered utilized helium from the helium purge bottle to drive the turbines during the initial part of the start (Fig. 67c). For this system, helium at a constant pressure was provided to the fuel turbine inlet at engine start. When the fuel feed system primed, the oxidizer turbine control valve opened and helium was used to drive the oxidizer turbopump. When main chamber pressure reached a predetermined level, the helium supply was shut off, and hot gas from the chamber was directed to the turbines to complete the start.

(U) As in the case of the main engine sequence, programming of the valves through start was required to achieve a repeatable and rapid start sequence. This type of start was slightly more difficult to achieve for the secondary engine because of relatively large pump and turbine inertias. Consequently, the valve sequences for the secondary engine were not the same as those for the main engine. The valve sequences for the secondary engine are shown in Fig. 68 for a warm pump start (start after an extended coast period).

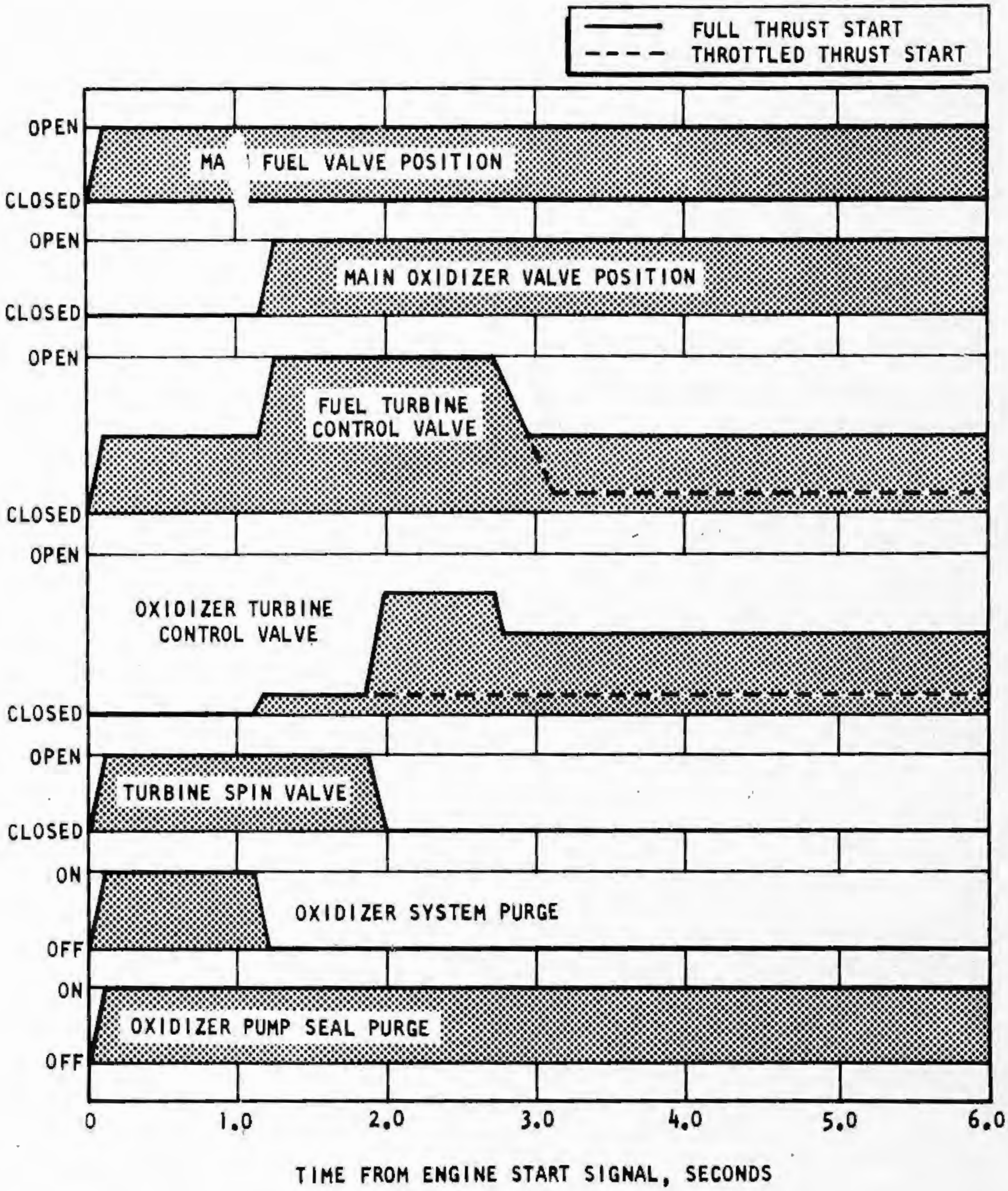

Figure 68. Secondary Engine Start Sequence (U)

(U) A programmed two-step fuel turbine valve was required to control the rate of buildup of the fuel turbine speed and, at the same time, accelerate the pump to mainstage to effect a rapid start sequence. The two steps were to the mainstage position (100 percent) and to 200 percent of mainstage position.

(C) Overdriving the oxidizer turbine valve also was required. For the case shown (Fig. 68), the valve was opened to 150 percent of the mainstage value. In practice, the degree of valve opening will be required on the basis of the error signal to the valve. Both valves were signaled to the desired mainstage position by a timer referenced to the time at which chamber pressure reached 80 psia. The start transients for chamber pressure and propellant flowrates are shown in Fig. 69 for starts to full thrust considering warm and cold pumps, and for a start to throttled thrust considering warm pumps. The propellant usage for the warm pump start condition to 90 percent of full thrust was computed to be 4.61 pounds oxidizer and 0.570 pound fuel. This results in an excess of 0.186-pound fuel for the start. The 90-percent value coincides approximately with the predicted point at which the mixture ratio error was reduced to less than 0.5 unit. For the start to throttled thrust, 0.71 pound fuel and 3.28 pounds oxidizer were used before the mixture ratio error was reduced to within 0.5 unit. The excess fuel in this case was 0.44 pound. No correlation was made with the thrust buildup in this case because near achievement of target thrust was realized rather early in the sequence, and a relatively large mixture ratio error existed considerably beyond this point (Fig. 69). Helium usage for the start sequence was predicted to be 0.12 pound per start and was found to be approximately the same for both start to full thrust and throttled thrust.

(c) Main Engine Cutoff

(U) In the previous work, the mathematical start model was developed for the main engine, and a start sequence was developed. The same computerized mathematical model was used to develop a cutoff sequence for the main engine. The model utilized the basic sequence shown in Fig. 70. The factors considered important in the sequence were to expel all residual oxidizer from the engine in a controlled manner and accomplish cutoff without exposing the thrust chamber to a marginal cooling situation.

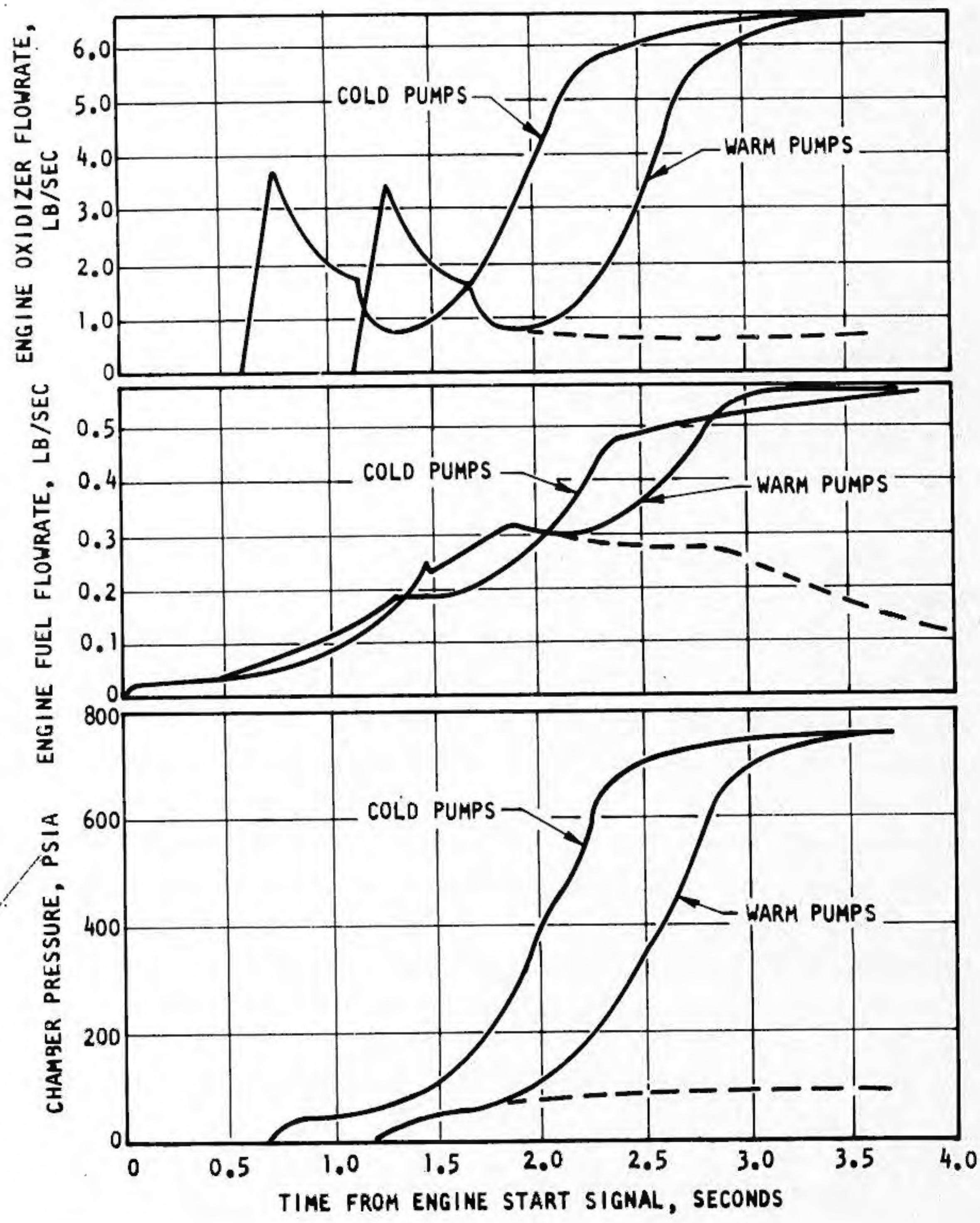

Figure 69. Secondary Engine Start Transients (U)

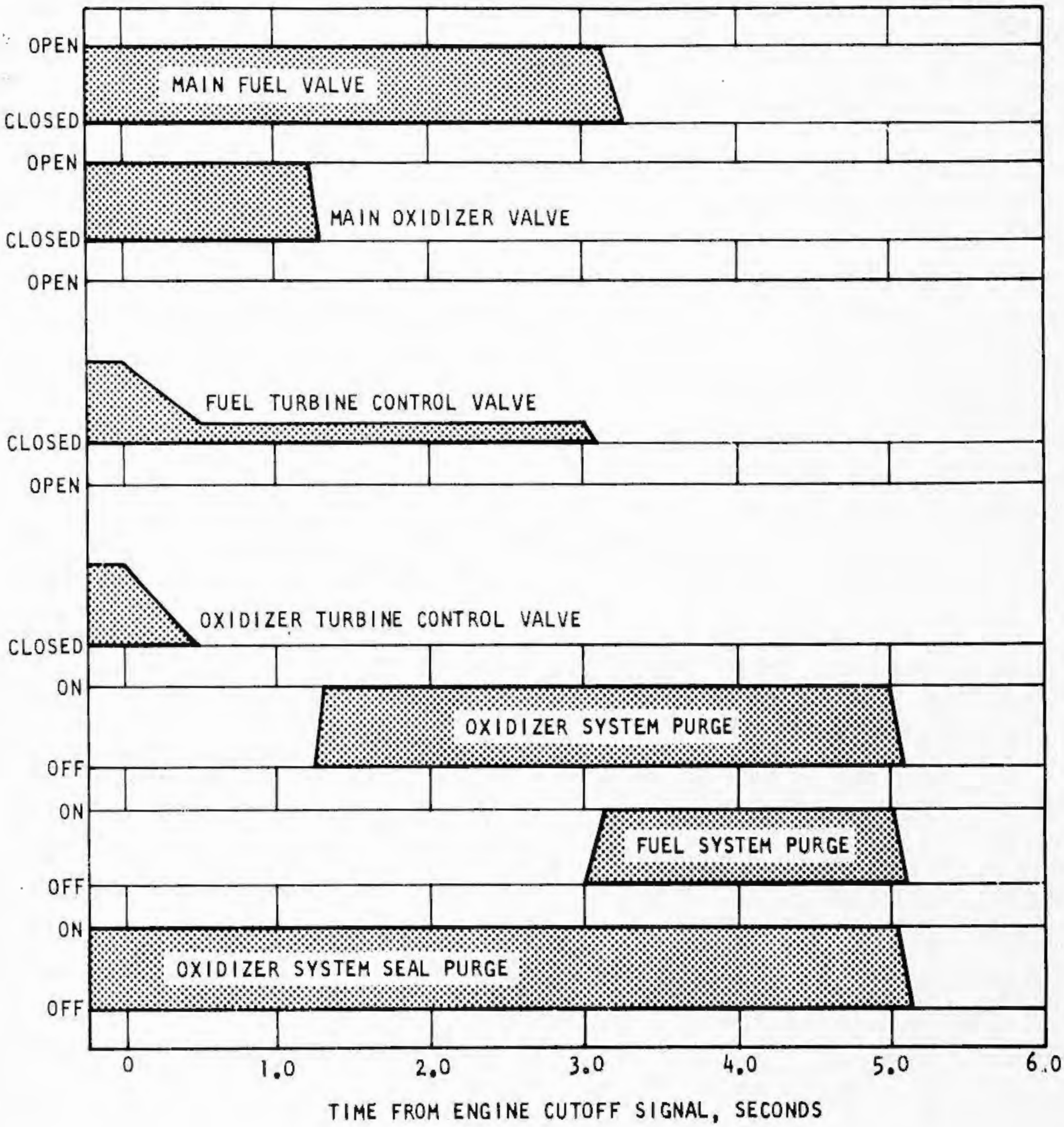

Figure 70. Main Engine Cutoff Sequence for Valves (U)

(C) To accomplish these objectives, the engine thrust is ramped to the full throttled thrust level, at which time the main oxidizer valve is closed and the oxidizer in the engine downstream of the shutoff valve is purged through the injector and burned at the throttled thrust level. The fuel turbine and pump are driven at a compatible level until the residual oxidizer is expelled. The resulting cutoff transients are shown for the engine flowrates and chamber pressure in Fig. 71. The predicted quantity of propellants that will flow into the engine during the cutoff from full thrust was computed from the curves of Fig.71 and were found to be approximately 33 pounds of oxidizer and 5 pounds of fuel. The time required for full decay of chamber pressure was predicted by the model to be approximately 3.0 seconds. This decay time, however, does not restrict the engine restart capability because the cutoff and start sequences are designed so that the cutoff could be interrupted at any point in the sequence and the engine restarted in a normal sequence from the point of interruption.

(C) Assuming a linear relationship between thrust and chamber pressure, and using the chamber pressure decay in Fig. 71, the cutoff impulse for the main engine from full thrust was predicted to be approximately 20,000 lb-sec. The cutoff impulse for the full-throttled-thrust case was predicted to be that impulse represented from the point of oxidizer purge "on" to oxidizer expulsion. This impulse value is approximately 5000 lb-sec.

(C) The impulse value associated with full thrust and the amount of propellants used during cutoff were predicted by the model to be slightly greater than those predicted previously in Ref. 2 . The primary differences in the predictions were the rate of slowdown of the oxidizer and fuel pumps and the logic in sequencing the main oxidizer valve closed. The previous predictions had been made strictly on the basis of the predicted pump response to a step input while the computer model considers the residual power available to the turbines during the shutdown. In the case of the main oxidizer valve sequencing, the valve was closed in the previous prediction as soon as the oxidizer turbine valve reached the full-closed position. In the cutoff sequence shown in Fig. 70, the main oxidizer valve was closed when

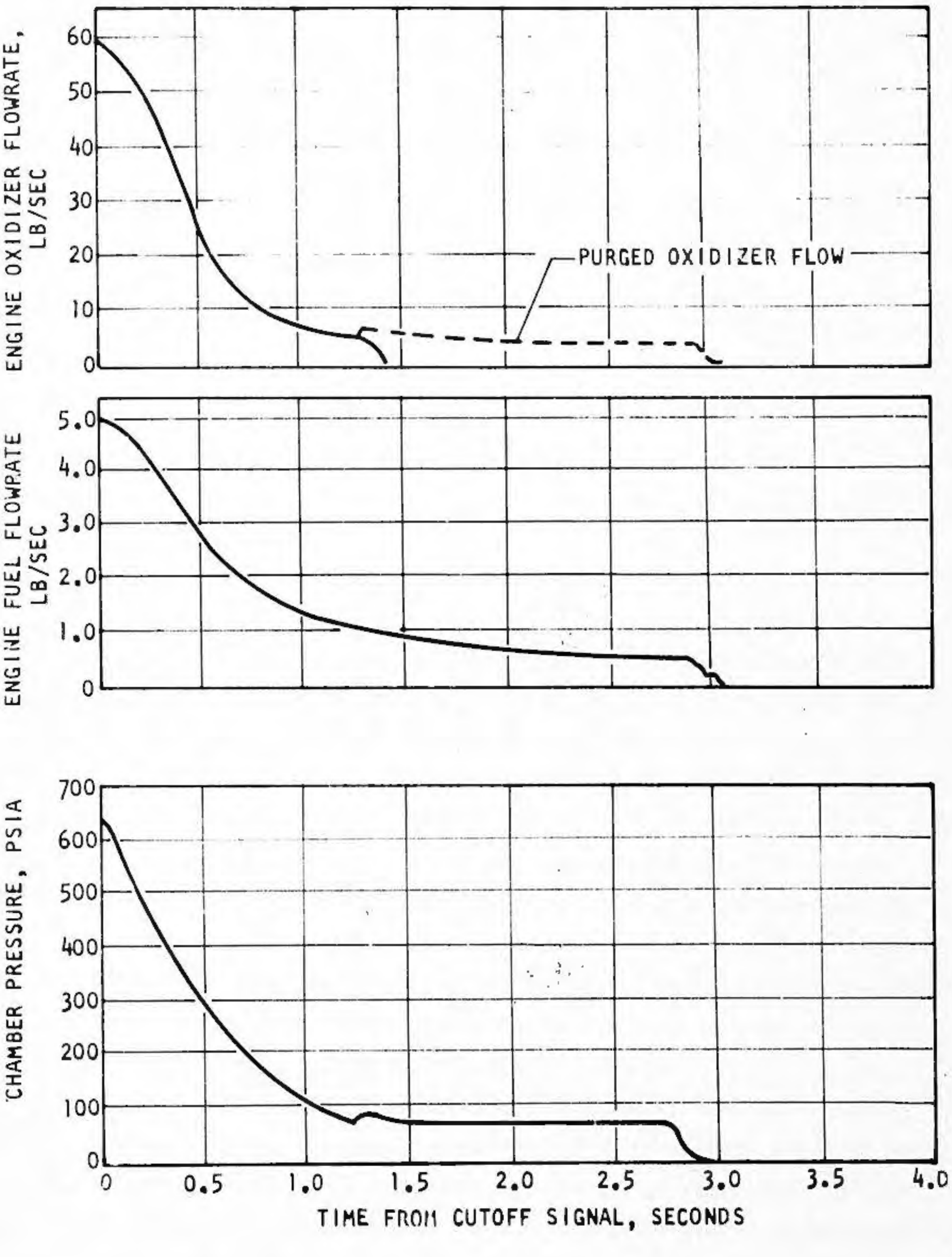

Figure 71. Main Engine Cutoff From Full Thrust (U)

chamber pressure reached 80 psia. Both variations resulted in lengthening the cutoff sequence slightly, and, at the same time, increased the propellant consumption and cutoff impulse. The amount of excess fuel usage (used at less than 12:1 MR) was virtually unchanged in the two predictions. Previously, an excess of 2.2 pounds fuel was predicted compared to 2.1 pounds excess fuel predicted by the cutoff model.

(d) Secondary Engine Cutoff

(C) The developed secondary engine cutoff sequence (Fig. 72) was essentially the same as the main engine sequence. Engine thrust was ramped to the full-throttled level, and the residual oxidizer was purged and burned at the throttled thrust level. The propellant flows and chamber pressure transients for cutoff from the full thrust level are shown in Fig. 73. The total propellant flow into the engine during shutdown was computed to be 2.8 pounds of oxidizer and 0.8 pound of fuel. An excess fuel usage of approximately 0.5 pound results (compared to a 12:1 mixture ratio).

(C) The cutoff impulse for the secondary engine shutdown from full thrust was estimated to be approximately 3300 lb-sec. For cutoff from the throttled thrust level, the value was determined to be 500 lb-sec.

(7) Effect of Unprimed Feed System Lines

(U) There have been indications that maintaining fully primed feed system lines during extended coast periods may be a difficult objective to achieve. As a result, a brief analysis was made to evaluate the effect of unprimed lines on the main engine start sequence. The main engine digital start model was used for this investigation.

(U) All previous start analysis and control system optimization of the main engine have been performed with the assumption that liquid propellants

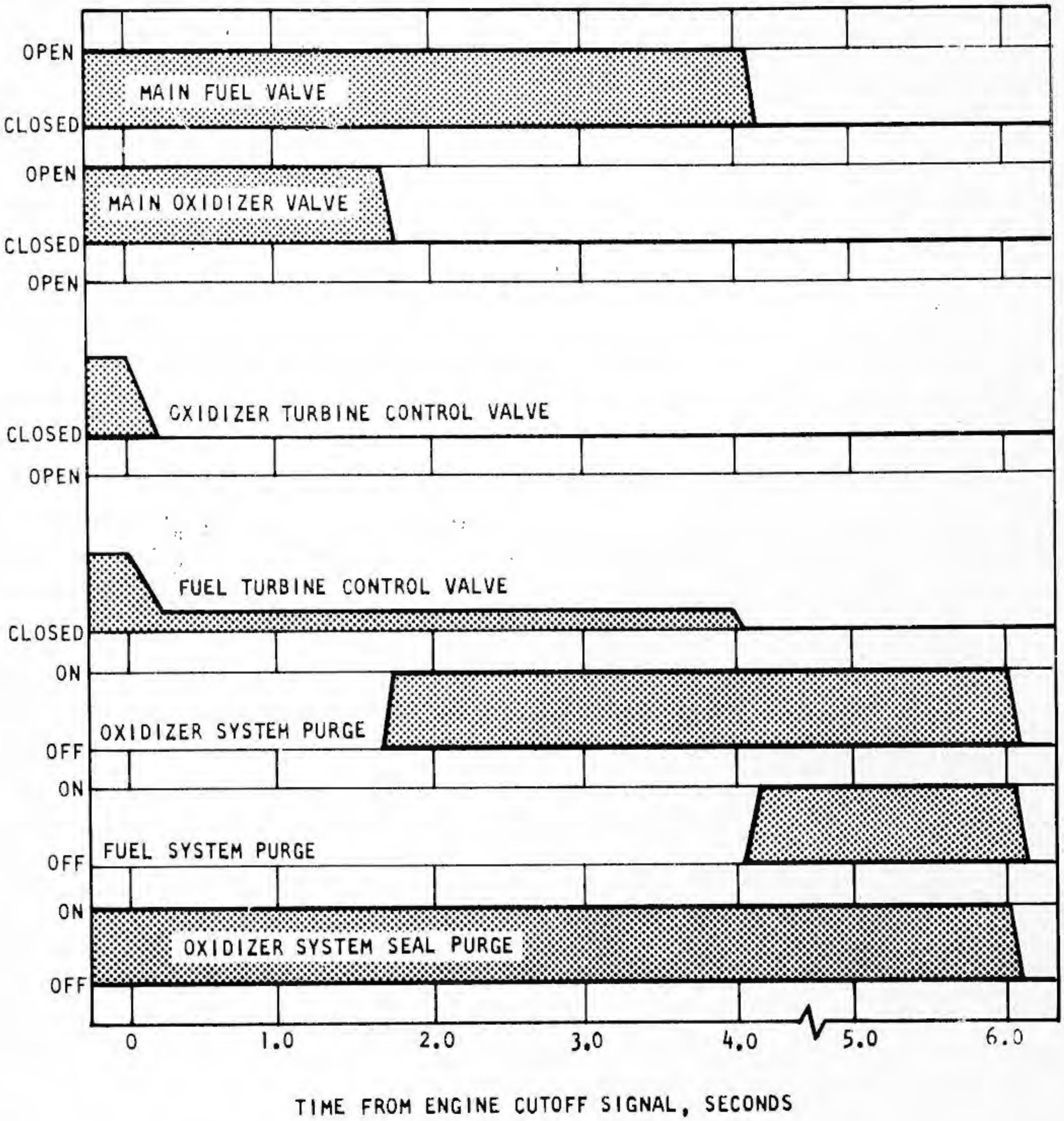

Figure 72. Secondary Engine Cutoff Sequence (U)

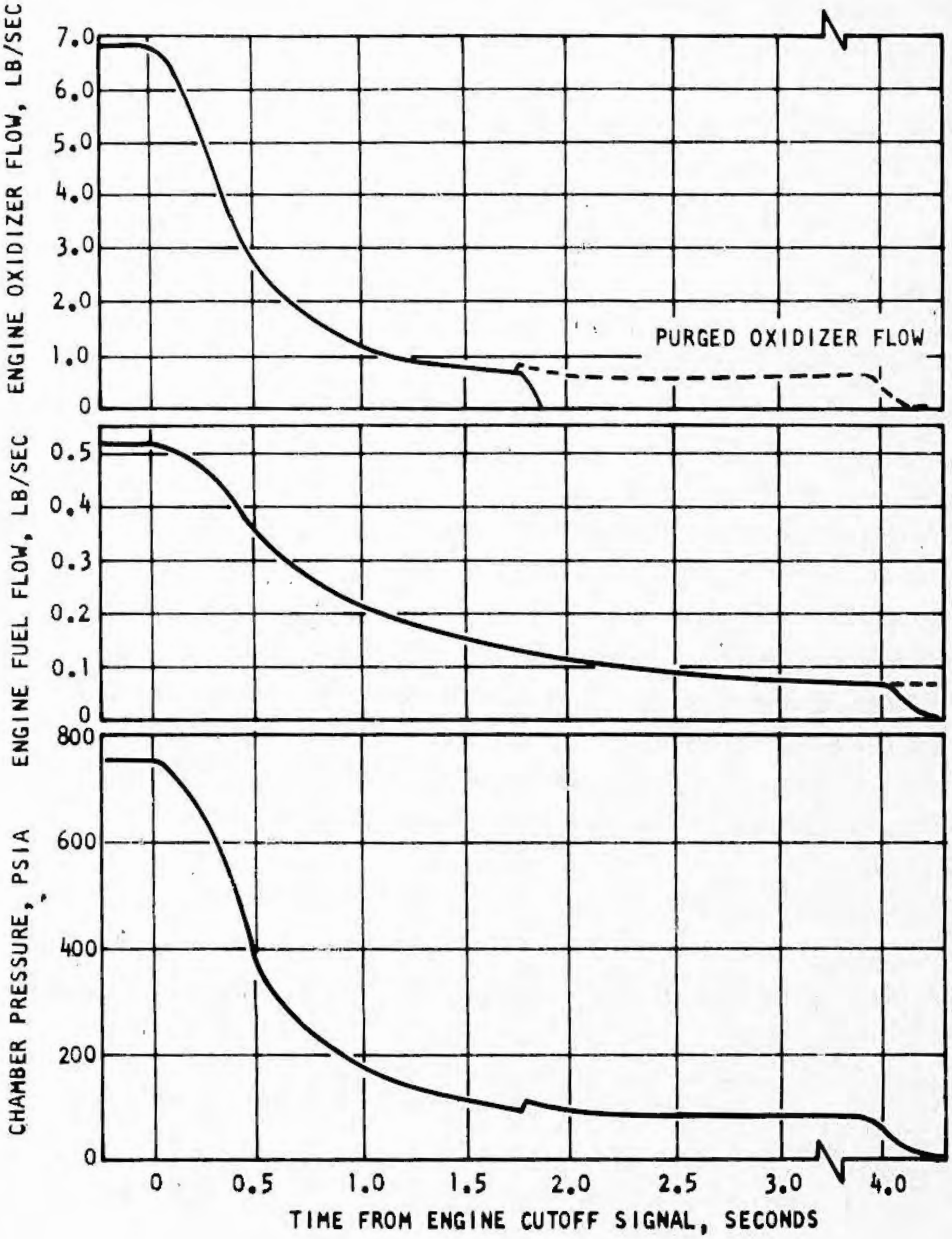

Figure 73. Secondary Engine Cutoff Sequence (U)

(U) would be present at the inlet to both engines at engine start. If, however, liquid could be maintained only at the inlets to the propellant prevalves, then the inlet lines for both propellants would have to be thermally conditioned and primed before the engine could be programmed into mainstage.

(C) **The following inlet lines were programmed into the start model:**

Fuel Inlet Line	**90-inch length**
	2.5-inch outer diameter
	0.02-inch wall (Inconel)
Oxidizer Inlet Line	**46.6-inch length**
	3.0-inch outer diameter
	0.02-inch wall (Inconel)

(U) **Exterior line insulation was not considered because the times involved made the effects independent of insulation.**

(C) **Two computer model starts were made with these lines warm (530 R) and unprimed at engine start. One run assumed the internal surface of the lines to be coated with a low thermal conductivity material (0.002-inch Kel-F on the fuel side, 0.002-inch ceramic coating on the oxidizer side). The second run was made assuming the lines to be bare.**

(C) The start times from engine start to 90 percent of mainstage P_c for a warm start with coated lines were predicted to be approximately 4.0 seconds. The start time for the coated, unprimed lines was predicted to be approximately 5.0 seconds. The analysis showed that, at best, the unprimed feed system line would extend the main engine start by 1 to 2 seconds, or 50- to 100-percent longer than the start time objective. Extrapolating to predict the effect on the secondary engine start sequence, the impact was concluded to be even greater.

i. Final Definition Main and Secondary Engine Start and Cutoff Sequences

(U) The major portion of the engine system start and cutoff model analyses has been discussed in the previous section of this report; however, some final analysis and refinements were accomplished during subsequent portions of the Task I efforts, therefore an updated or final discription of the engine start and cutoff procedures is presented along with the selection of sequencing signal sources and values.

(U) The engine system start and cutoff signals are initiated through the vehicle guidance system. The guidance system supplies thrust and mixture ratio command values to the engine selection circuit. Depending on the command thrust value, either the main or secondary engine is selected and a start signal is fed to the proper engine. There is no direct feedback from the engine system to the vehicle guidance system. However, there is an implicit feedback because the guidance system monitors vehicle thrust and mixture ratio of the remaining tanked propellants. The actual feedback is done within the engine controller package by comparing the delivered thrust and mixture ratio (determined from chamber pressure and propellant flowrate measurements) with the command values from the guidance system (Fig. 74).

(1) Main Engine Start Sequence

(C) Further refinements were made to the main engine start sequence. A flow schematic of the engine system and a diagram of the main engine start procedures and functions are shown in Fig. 75 and 76. A limiter timer is used to initiate a cutoff procedure if a mainstage monitor signal is not achieved in 5 seconds. The engine start and valve sequencing is illustrated in Fig. 77 for a start following an extended coast period (H_2 pump temperature of 550 R). The engine employs a tank-head start. The start signal opens the pneumatic system isolation valve which activates the pneumatic system, and the oxidizer pump seal cavity purge is

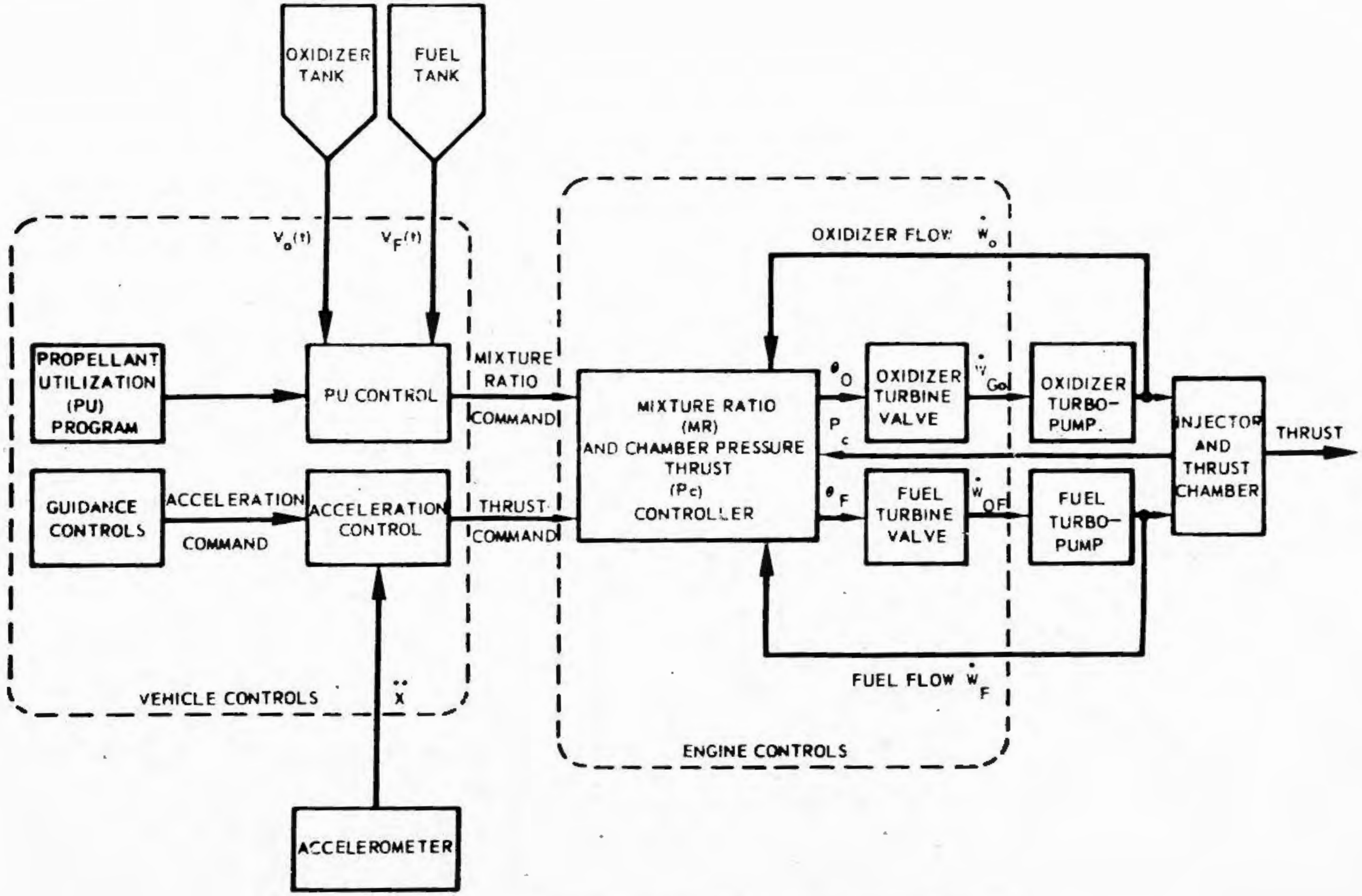

Figure 74. Vehicle-to-Engine Dynamic Control Interface (U)

CONFIDENTIAL

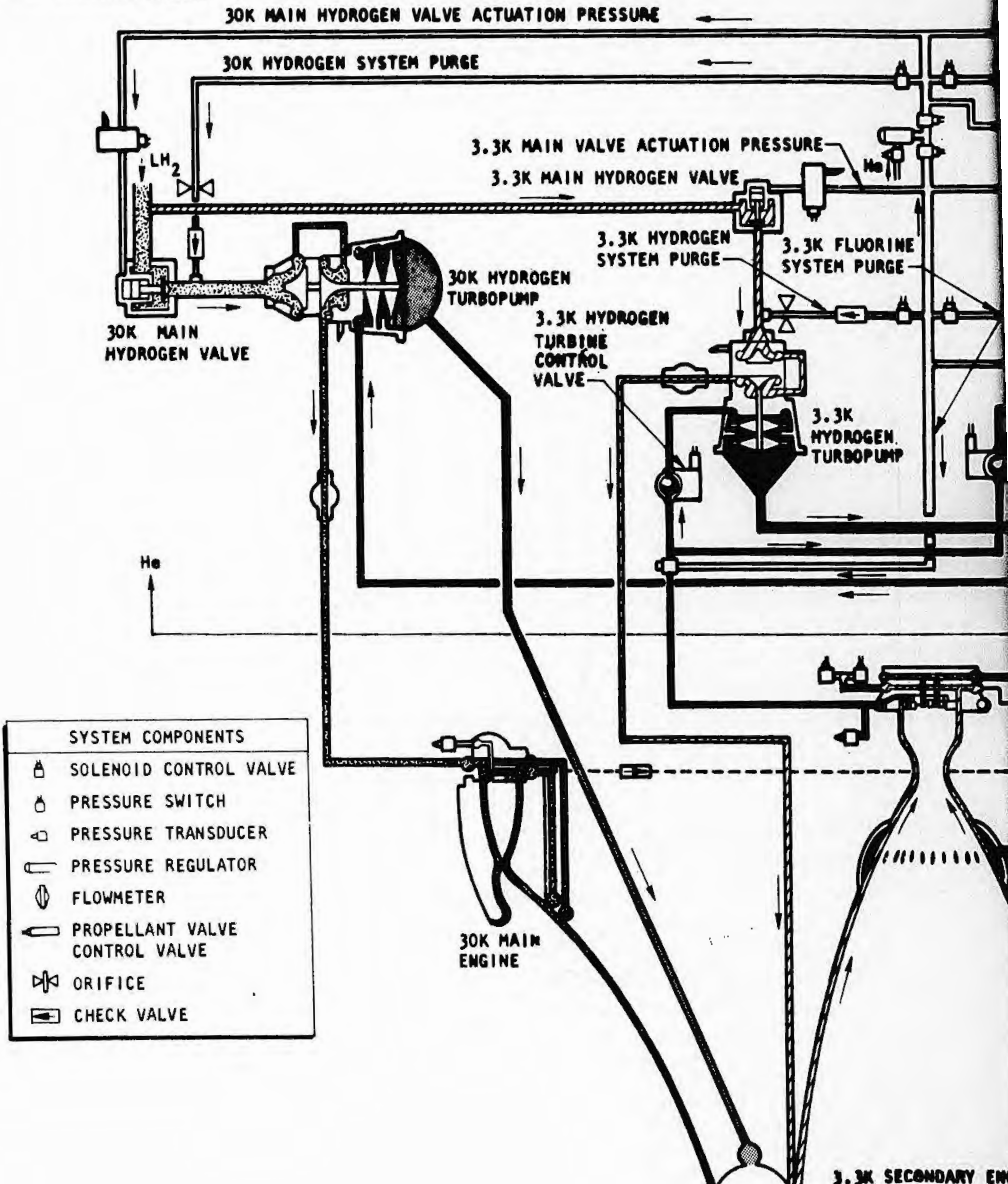

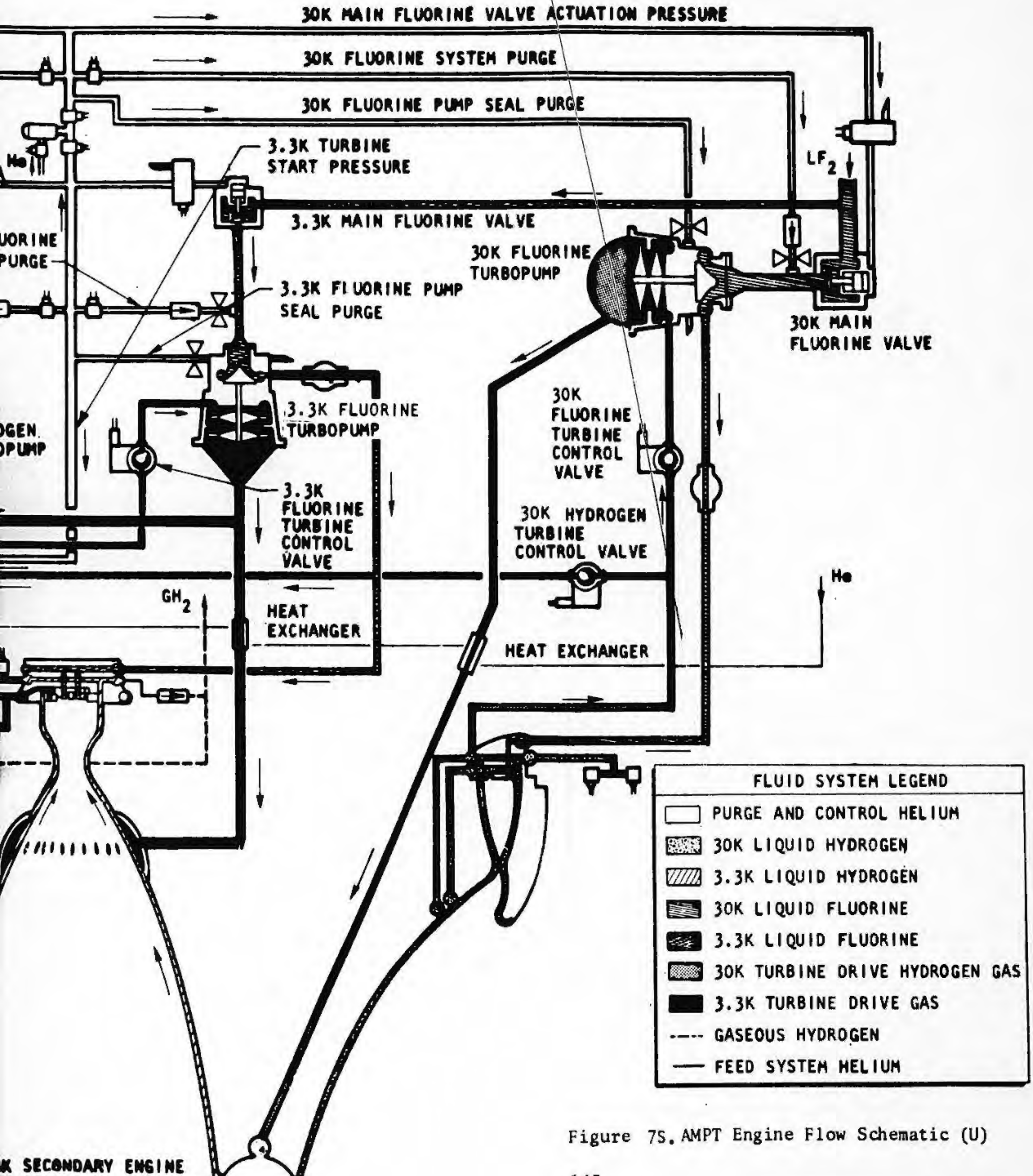

Figure 7S. AMPT Engine Flow Schematic (U)

 2

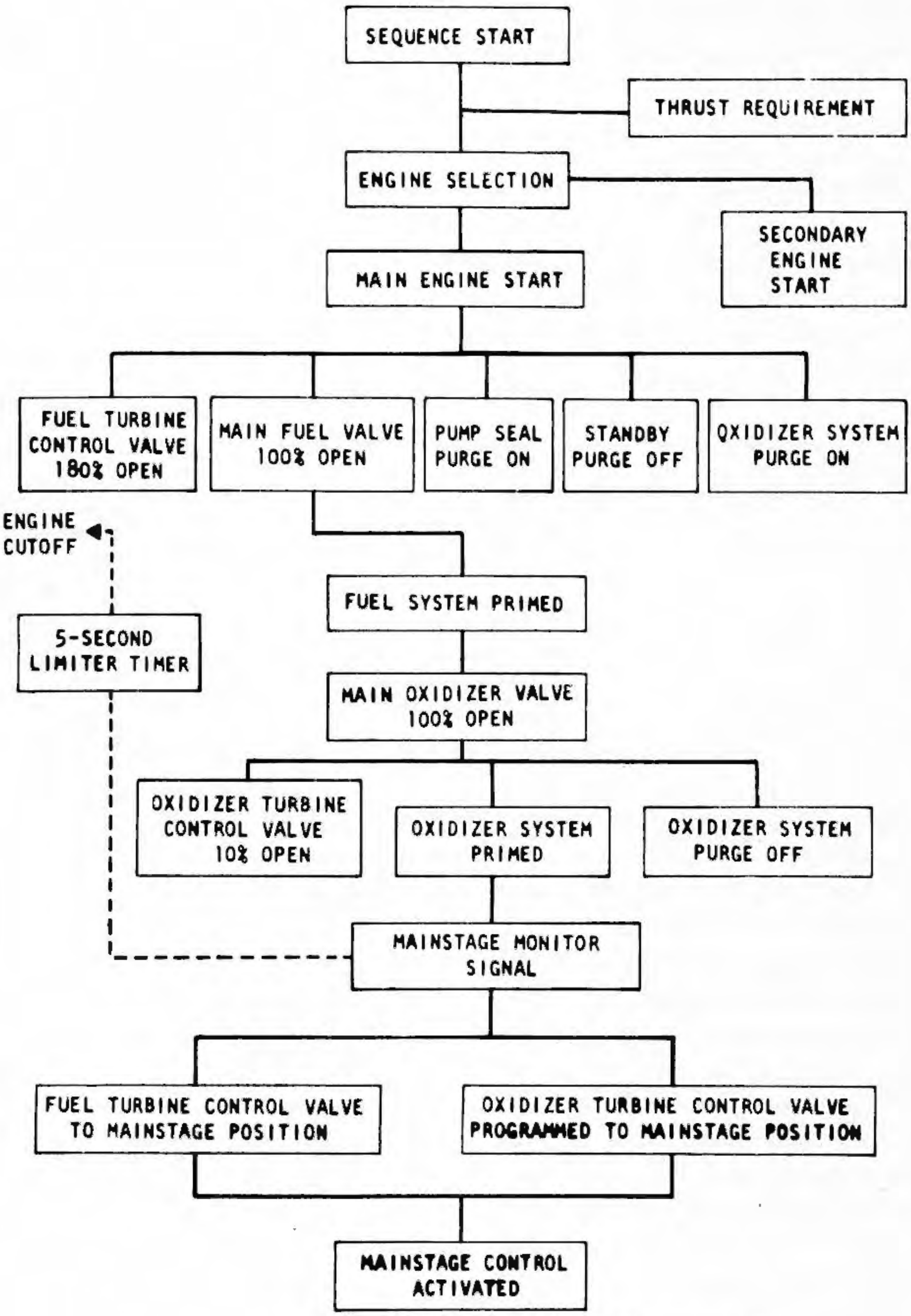

Figure 76. Main Engine Start Sequence (U)

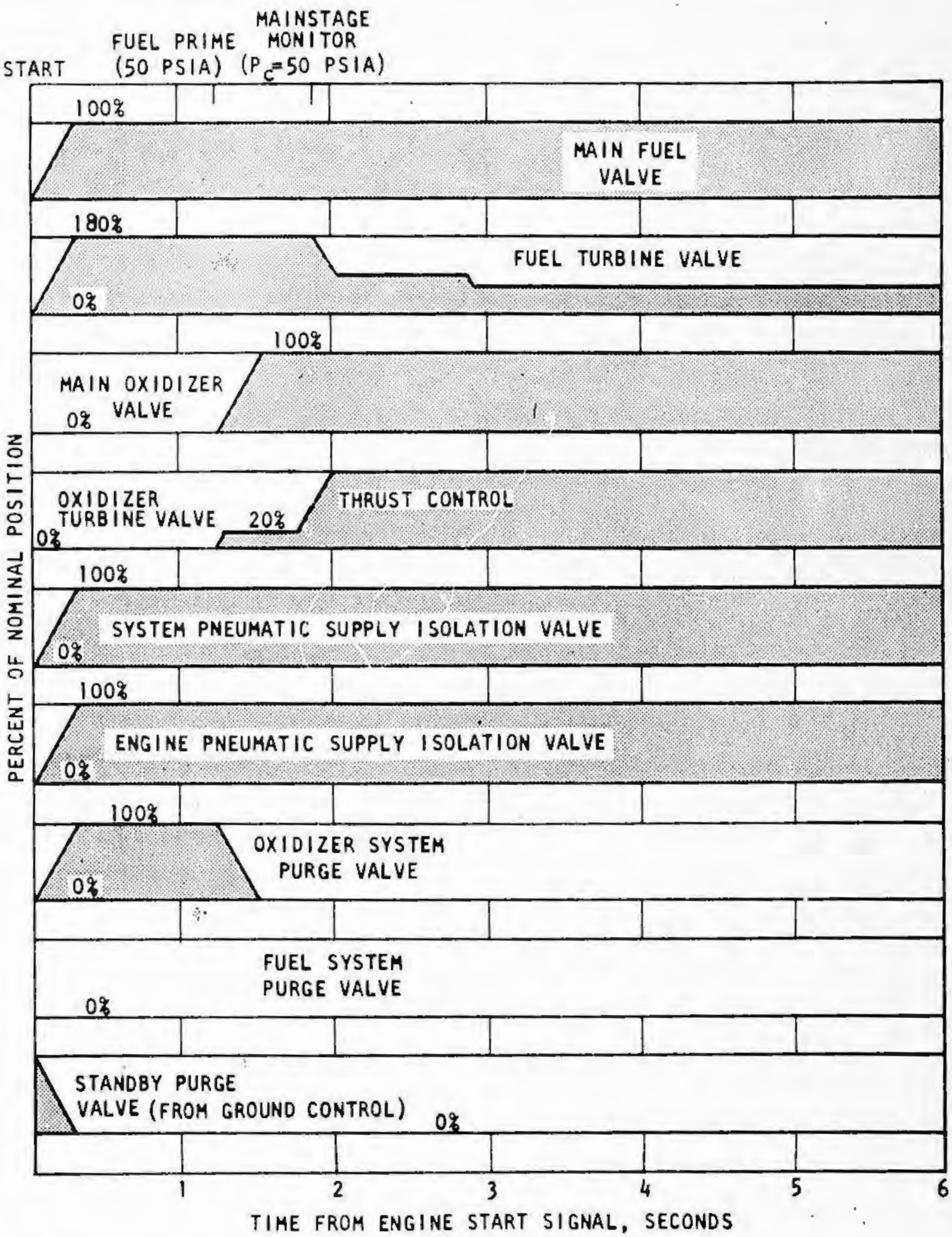

Figure 77. Main Engine Start (U)

initiated automatically when the pneumatic system is activated. The main fuel valve is ramped to full open, the fuel turbine control valve is opened to 180 percent of its full thrust position, and the oxidizer system purge solenoid valve is opened. The main engine fuel turbine control valve is designed with a maximum flow area that is 180 percent of the required flow area for the full-thrust operating condition.

(C) The full-thrust operating position is, therefore, termed the 100-percent position. These valve positions are held until the fuel side primes, indicated by a pressure switch which is triggered at a fuel injection pressure of 50 psia or greater. When the pressure switch senses fuel-side prime, the oxidizer main valve is ramped to full open, and the oxidizer system purge solenoid valve is closed. Also, the oxidizer turbine control valve opens to a position of 20 percent of its full-thrust operating position.

(C) The valves are then maintained in this position until a mainstage monitor signal is received (pressure switch indicating 50 psia or greater chamber pressure). This signal indicates oxidizer side prime. At this point, both turbine control valves are ramped to a position corresponding to the command thrust value at nominal mixture ratio (12:1); mixture ratio control is not initiated at this point. A 1-second time delay is then employed before mixture ratio control is activated. Computer start model analysis has shown that if mixture ratio control is introduced simultaneously with thrust control, there is a tendency for a thrust overshoot before the command thrust value is obtained. This thrust overshoot is caused by the oxidizer turbine control valve going full open in an attempt to rapidly increase the oxidizer flowrate and achieve the nominal or command engine mixture ratio value. The delay in introducing mixture ratio control results in a low engine mixture ratio for a slightly longer portion of the start transient. The start time or buildup of chamber pressure and propellant flowrates to mainstage are shown in Fig. 78 for an immediate restart and a start after an extended coast period. The start procedures and valve sequencing shown in Fig. 77 are for a start following an extended coast period (H_2 pump temperature of 550 R). A sequence corresponding to an immediate restart (cold H_2 pump) can be obtained by subtracting 0.7 second from the time to the fuel system prime complete signal and all subsequent events in the sequence. Starts to lower thrust levels are made using the identical sequence.

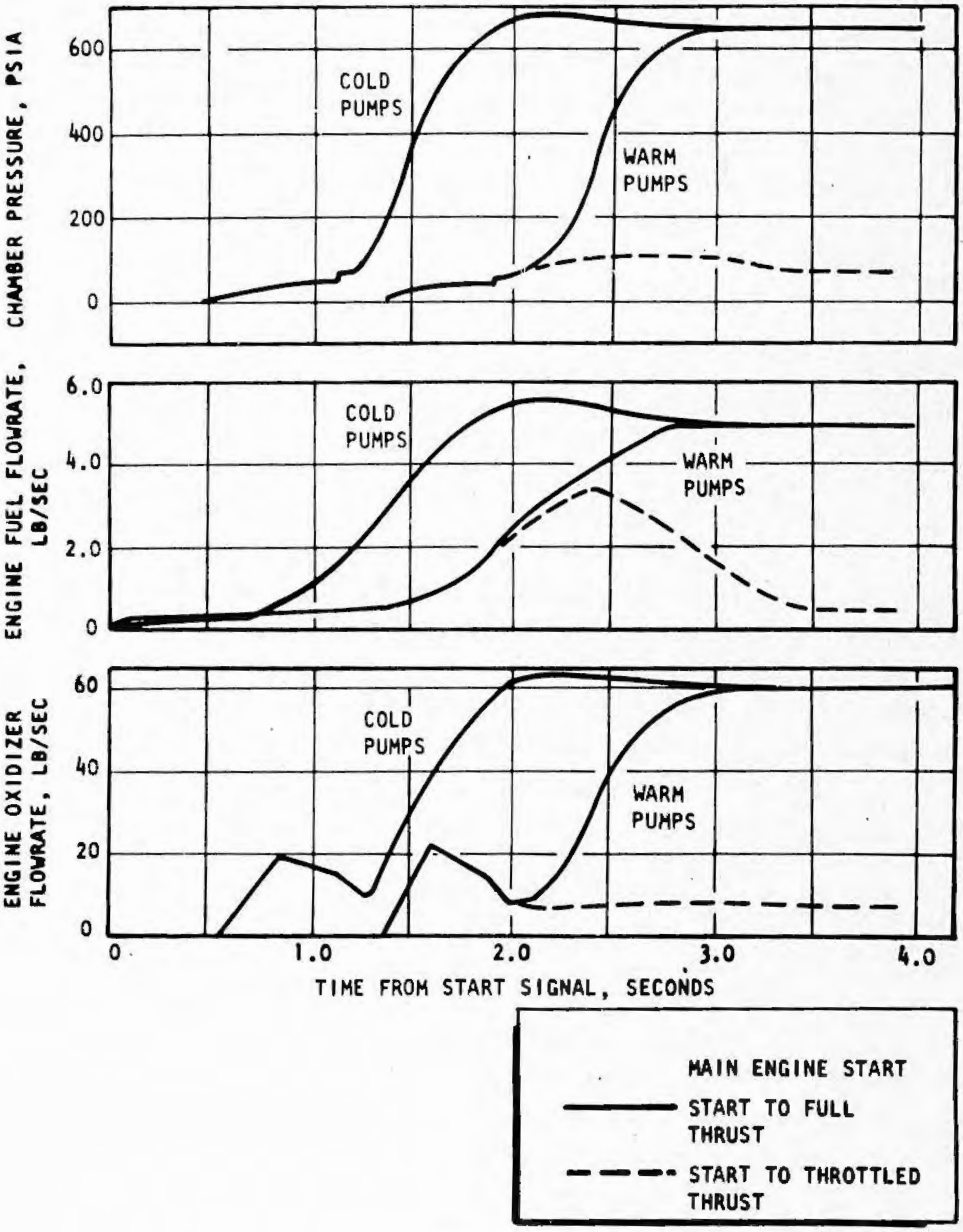

Figure 78. Main Engine Start Transients (U)

(2) Main Engine Cutoff Sequence

(C) A flow diagram for the main engine cutoff functions and procedures is shown in Fig. 79. The cutoff sequence is shown in Fig. 80. At cutoff signal, both the fuel and oxidizer turbine control valves begin to ramp closed. The oxidizer turbine control valve travels to the fully closed position, and the fuel turbine control valve is stopped and held at 20 percent of its full-thrust position. When the chamber pressure is reduced to 80 psia, a pressure switch signals the main oxidizer valve closed, and a helium purge (85-psia injection pressure) of the oxidizer systen is initiated.

(U) Because the purge pressure is greater than the oxidizer tank pressure, the main oxidizer valve must be closed to prevent the helium purge from blowing back into the main oxidizer tank. For this reason, the purge should be activated by a delayed signal so that the main valve will be closed prior to initiation of the purge. This actuation is accomplished with a 100-millisecond delay timer. A 2-second timer switch is then activated at the time the oxidizer purge is started to close the main fuel valve and the fuel turbine control valve. A 100-millisecond time delay is then employed before opening the fuel system purge valve. This delay allows time for the fuel main valve to reach the fully closed position before introducing the higher pressure fuel system purge. The fuel system purge may not be necessary in the flight engine as the fuel will quickly vaporize and disperse through the injector in the vacuum environment. However, the fuel system purge is considered to be a necessary safety precaution for ground testing. The purge injection pressure was determined by making the conservative assumption that minimum thrust chamber pressure exists in the chamber at the time the fuel purge is introduced. The purge pressure requirement then continuously decreases as chamber pressure decays. The higher pressure also provides a fast, positive purge of the residual fuel. However, thrust chamber testing will

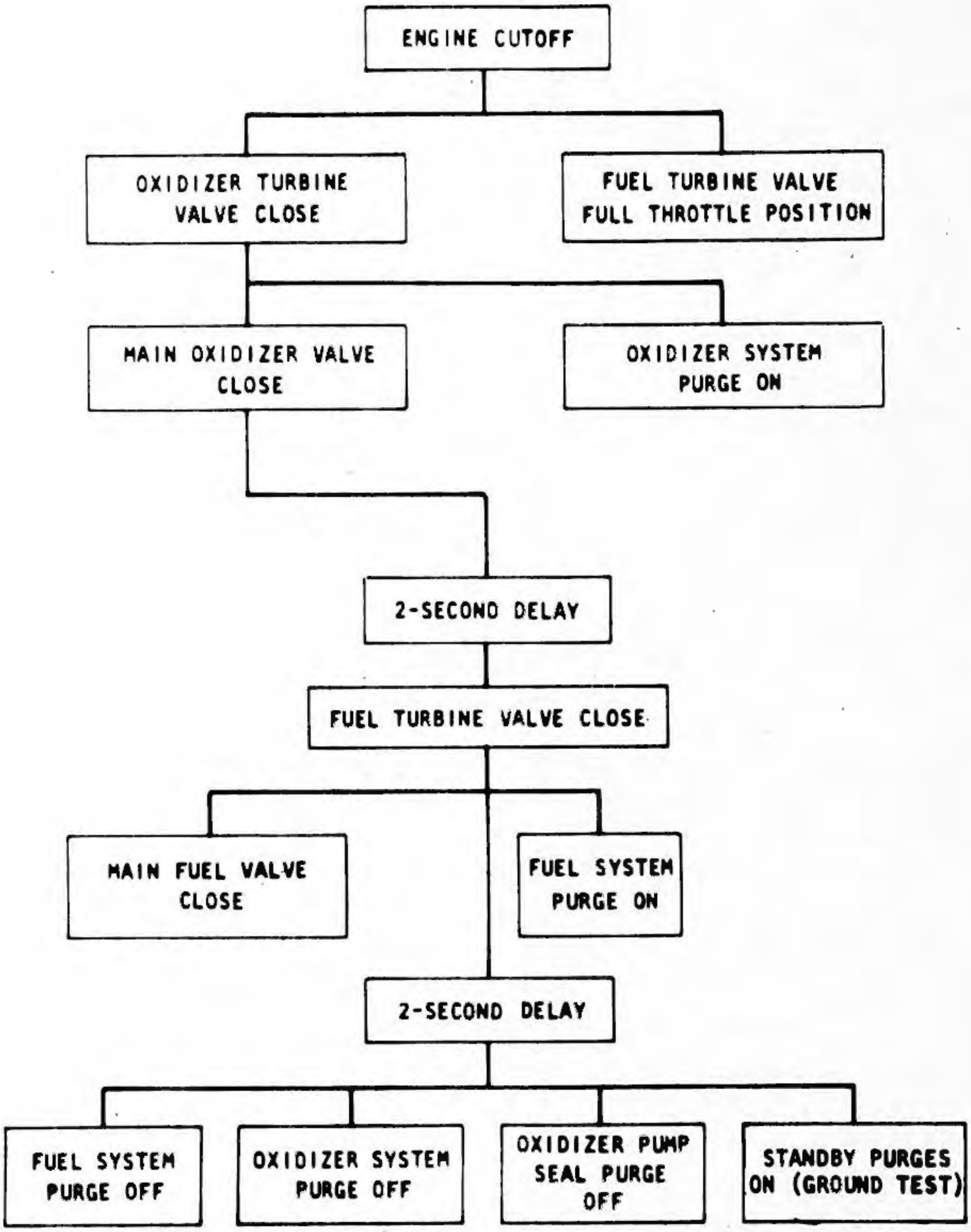

Figure 79. Main and Secondary Engine Cutoff Sequence (U)

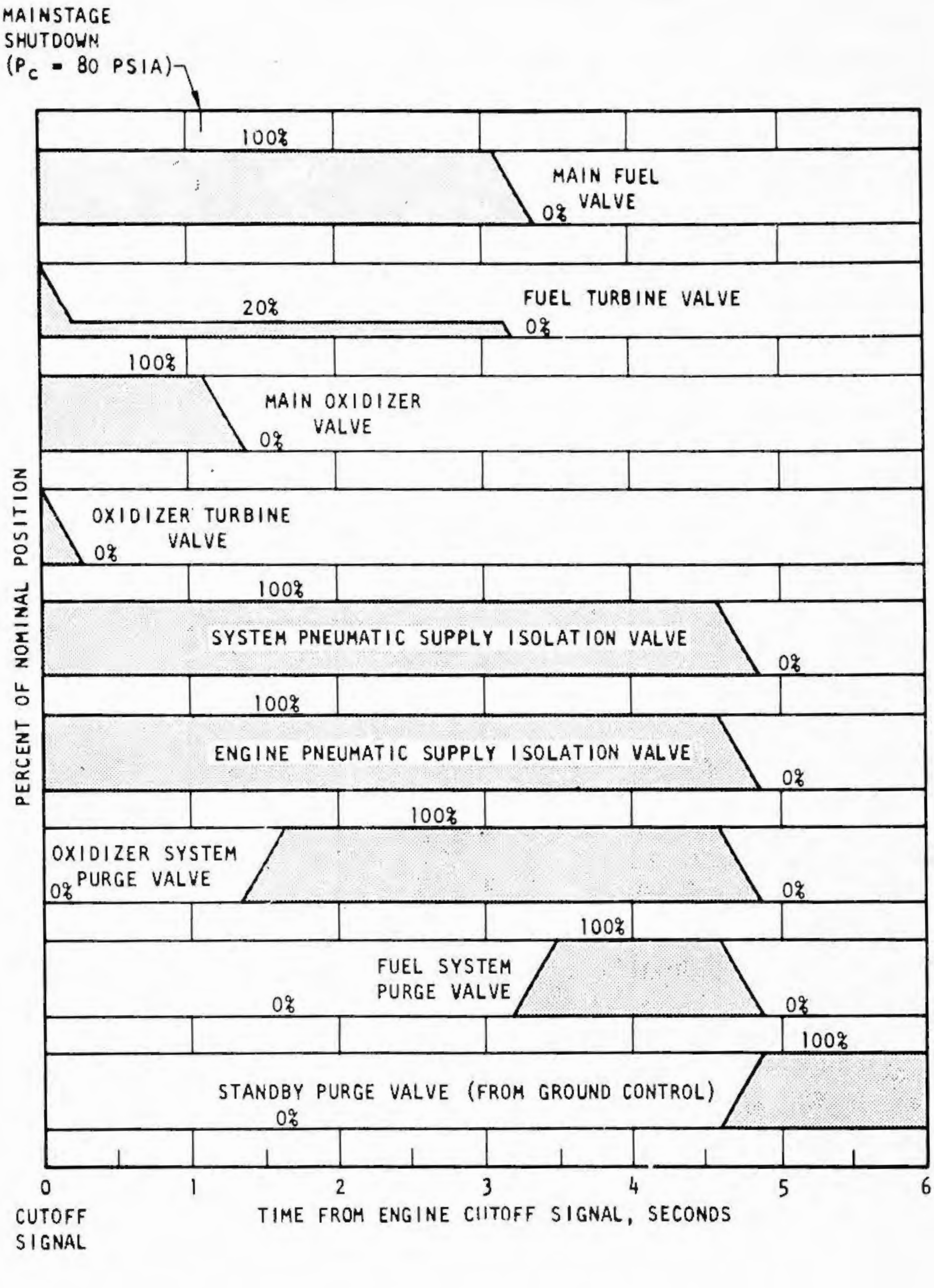

Figure 80. Main Engine Cutoff (U)

(U) provide more detailed information which may indicate that the fuel purge injection pressure can be reduced. If the pressure can be reduced below tank pressure, the need for the delay timer between closing of the main fuel valve and opening of the fuel purge solenoid valve would be eliminated. A delay timer will then close both fuel and oxidizer system purge control valves approximately 1.5 seconds after the fuel turbine control valve is closed. The transient values of propellant flowrate and chamber pressure are shown in Fig. 81 as a function of time from the cutoff signal.

(3) Secondary Engine Start Sequence

(U) An auxiliary energy source is required to provide power to the turbines during the early part of the start to speed up the thermal conditioning and priming of the fuel pump and high-pressure ducting. Helium from the pneumatic system is used as this energy source. The tank-head start used with the main engine resulted in excessively long start transient times with the smaller thrust chamber configuration and the thrust chamber tapoff turbine drive used in the secondary engine. A flow diagram of the secondary engine start sequence is shown in Fig. 82. The engine start and valve sequencing as a function of time is shown in Fig. 83 for the warm pump initial condition. A sequence corresponding to an immediate restart (cold pumps) can be obtained by subtracting 0.65 second from the time to the fuel system prime complete signal and all subsequent events. The transient values of propellant flowrate and chamber pressure during the start transient are shown in Fig. 84.

(C) At engine start, the fuel main valve is opened full and the fuel turbine control valve is opened to its full-thrust operating condition (100 percent). The pneumatic system supply valves and the turbine start valve (helium turbine spin supply) also are opened at the engine start signal. The helium is introduced (turbine start valve) at a pressure of 200 psia and a nominal temperature of 530 R upstream of both of the

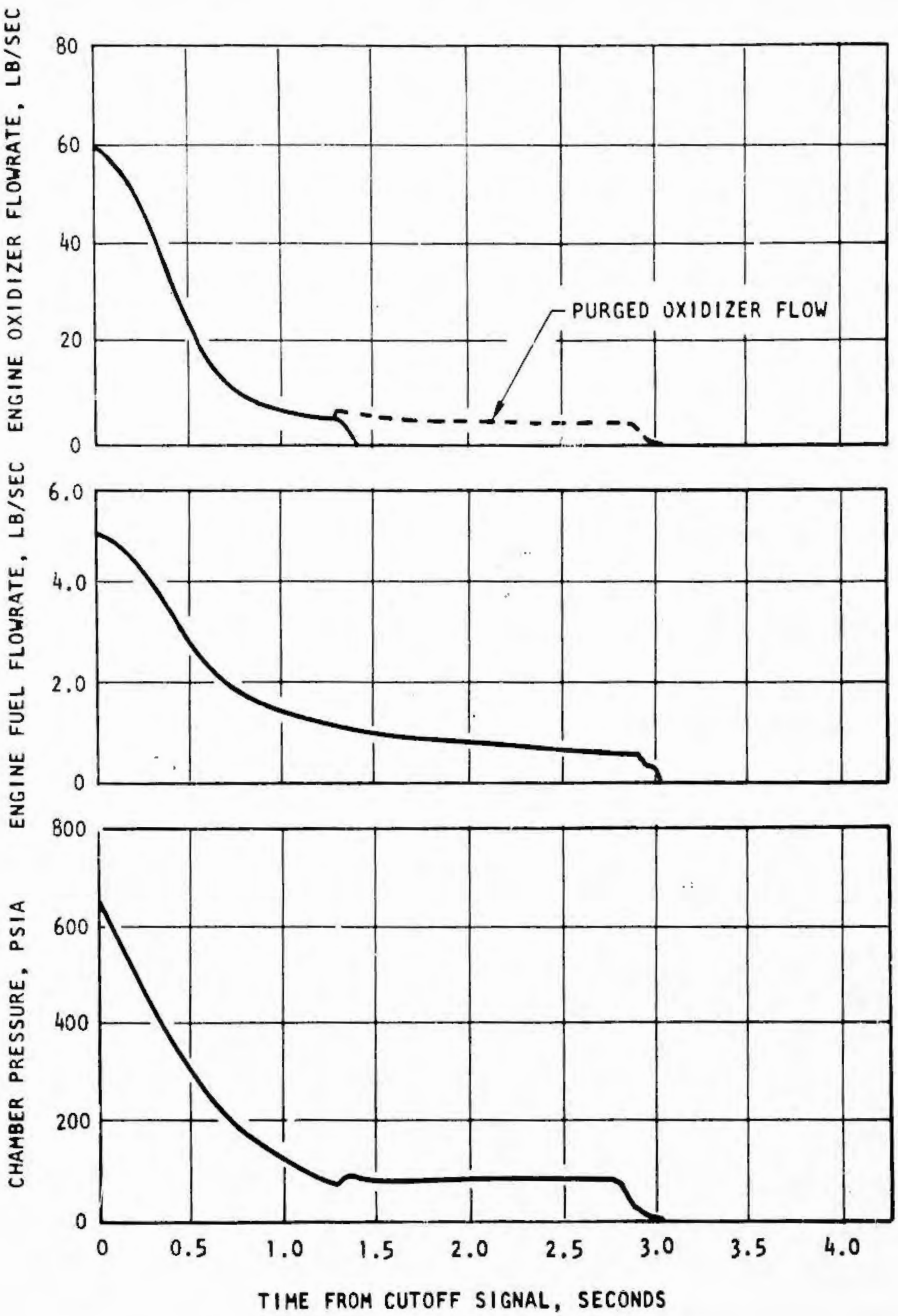

Figure 81. Main Engine Cutoff From Full Thrust (U)

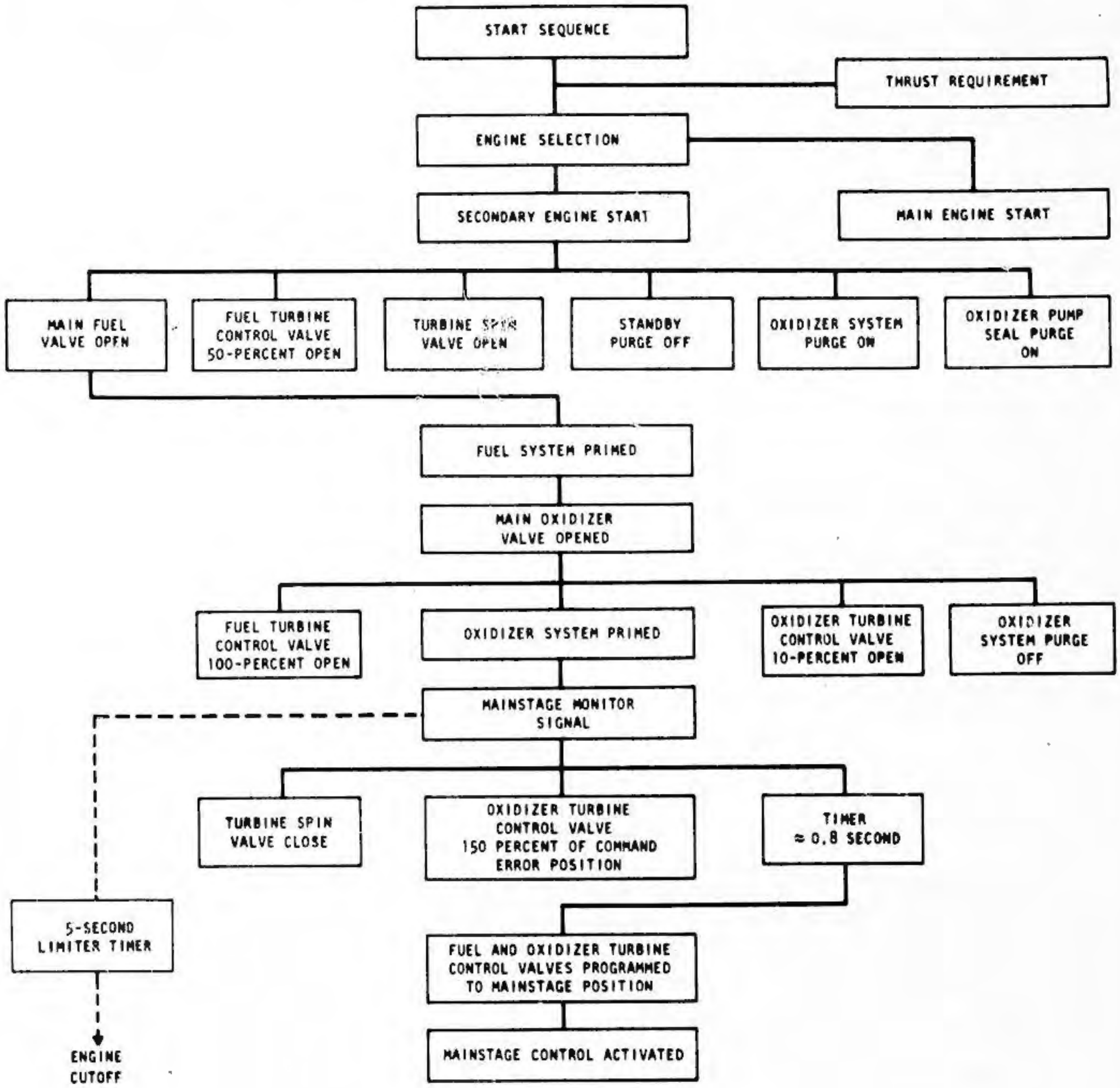

Figure 82. Secondary Engine Start Sequence (U)

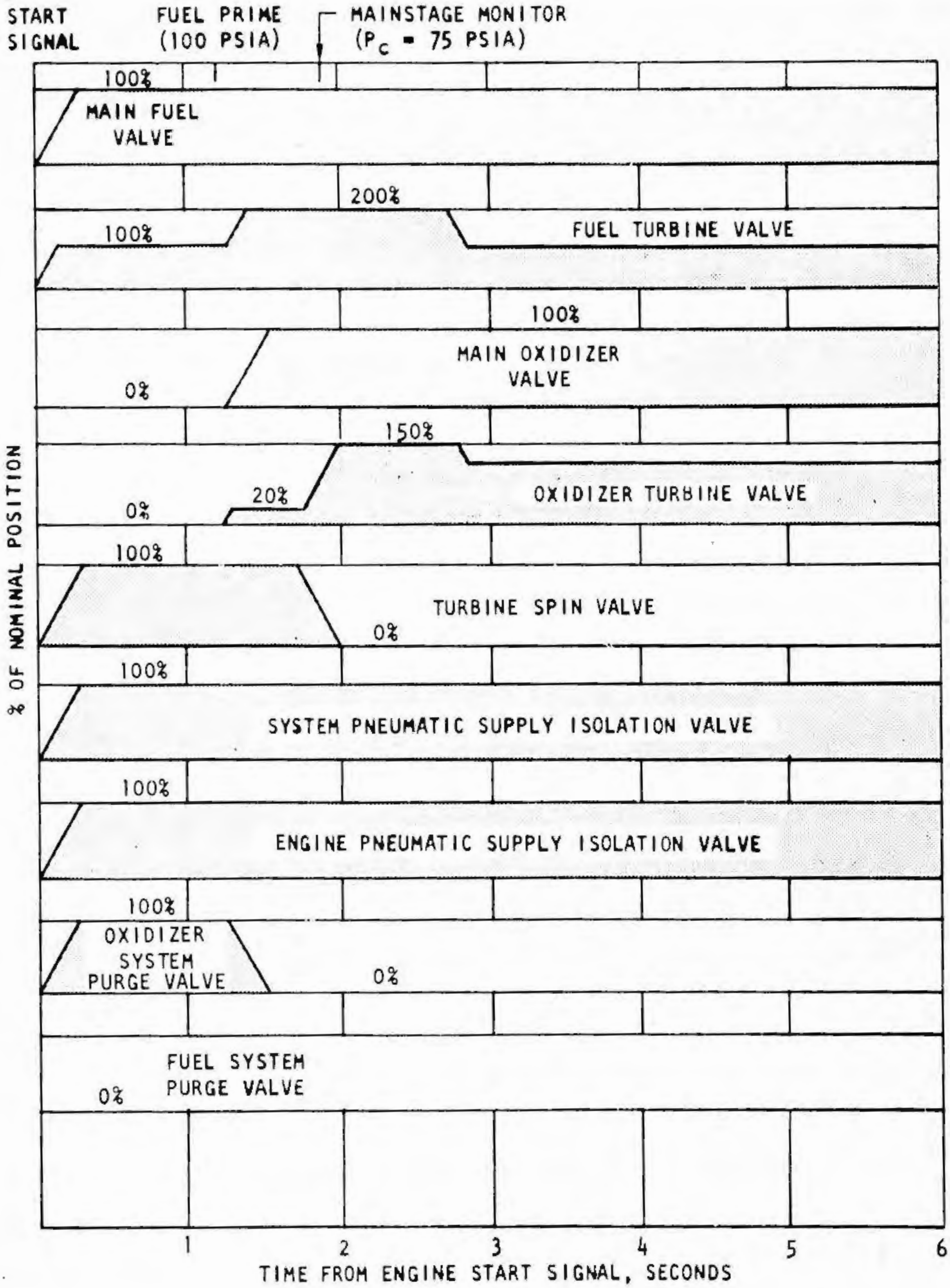

Figure 83. Secondary Engine Start (U)

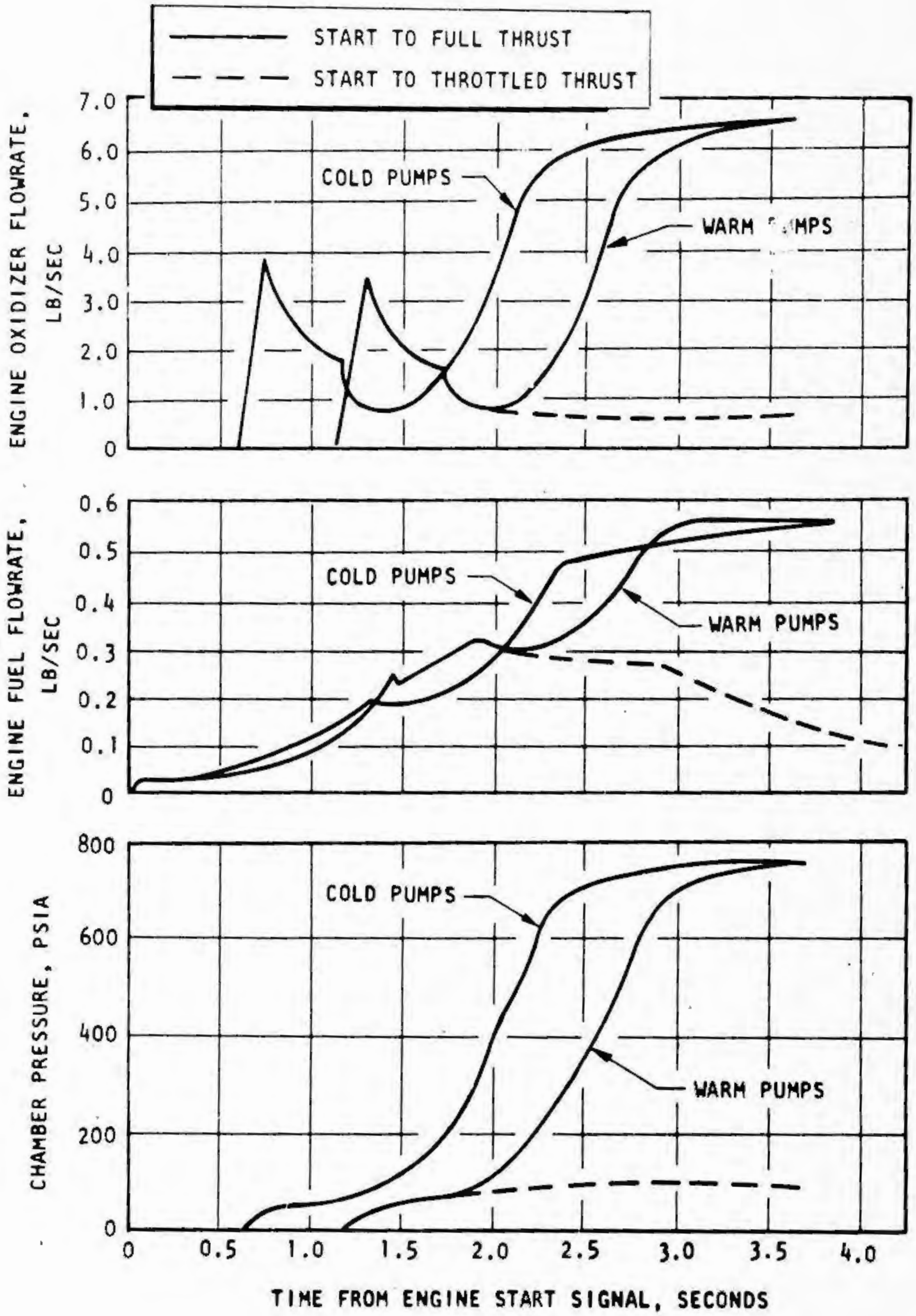

Figure 84. Secondary Engine Start Transients (U)

(C) turbine control valves. Ambient helium was used in the start model analysis. However, if lower temperature helium is introduced at the same pressure but at a lower temperature ($\geq$200 R), the estimated effect on the start transient will be negligible. The turbine start valve is designed so that the hot-gas flow passage to the thrust chamber is closed and the helium will flow only to the two turbine control valves. The turbine control valves are then used to control the helium flow to the proper turbine.

(C) These valve positions are held until the fuel side primes, indicated by a fuel injection manifold pressure signal of $\geq$100 psia. When the pressure switch signals fuel side prime, the oxidizer main valve opens full, the oxidizer system purge valve is closed, and the oxidizer turbine control valve opens to 20 percent of its full-thrust operating position. When the oxidizer turbine control valve is opened to the 20-percent position, the turbine drive helium begins to power the oxidizer turbine. The valves are held in these positions until the oxidizer side primes. Oxidizer prime is indicated by the mainstage monitor signal which occurs when the combustion chamber pressure reaches 75 psia. At this point, the helium supply to the turbine is shut off, and the turbine spin valve is positioned so that the turbines are driven by thrust chamber tapoff gases. The mainstage monitor initiates a 1-second timer and also signals the oxidizer turbine control valve to be ramped to a second or intermediate position which is determined by the following equation:

(U)

$$\underset{\text{(percent of mainstage)}}{\text{second position}} = \underset{\text{(percent of mainstage)}}{\text{first position}} +$$

$$130 \text{ percent} \left[\frac{P_c \text{ command} - P_c \text{ minimum thrust}}{P_c \text{ full thrust} - P_c \text{ minimum thrust}} \right]$$

(U) Using the above equation, the control system will select a second position of 150 percent of mainstage for a full-thrust start while, for a minimum-thrust start, the valve remains in its initial position. This

(C) method of determining the intermediate position for the oxidizer turbine control valve allows the oxidizer pump to be overpowered during the latter portion of the start, thus reducing required start time. The fuel turbine control valve remains in its initial position, and the valves are held in this position until the termination of the 1-second timer which was initiated by the mainstage monitor signal. At this point, the turbine control valves are ramped to their mainstage command values. Engine starts to throttled thrust levels are made using the same start sequence as a full-thrust start. The only differences are the calculated value for the oxidizer turbine control valve intermediate position and the final positions for the turbine control valves which are dictated by the command thrust value.

(4) Secondary Engine Cutoff Sequence

(C) The flow diagram for the secondary engine cutoff procedures is identical to that shown in Fig. 79 for the main engine. The secondary engine valve sequencing, propellant flowrates, and chamber pressure values as a function of time from the cutoff signal are shown in Fig. 85 and 86. At the cutoff signal, both the fuel and oxidizer turbine hot-gas valves begin to ramp closed. The oxidizer turbine control valve ramps full closed, and the fuel turbine control valve stops at 20 percent of its full-thrust operating position. The valves are held in this position until the main chamber pressure is reduced to 100 psia. At this point, the main oxidizer valve is ramped closed, and a 100-millisecond timer is activated which then signals the oxidizer system purge on (100-millisecond delay allows sufficient time for the main oxidizer valve to close before introducing oxidizer system purge). This purge, at a pressure of 80 psia, is introduced upstream of the oxidizer pump and results in an oxidizer purge flowrate approximating that required for minimum thrust operating flowrate. The fuel turbine and pump are still driven at the minimum thrust power level. A second timer is initiated when the oxidizer purge is started to provide an approximate 2.5-second delay (oxidizer system purge

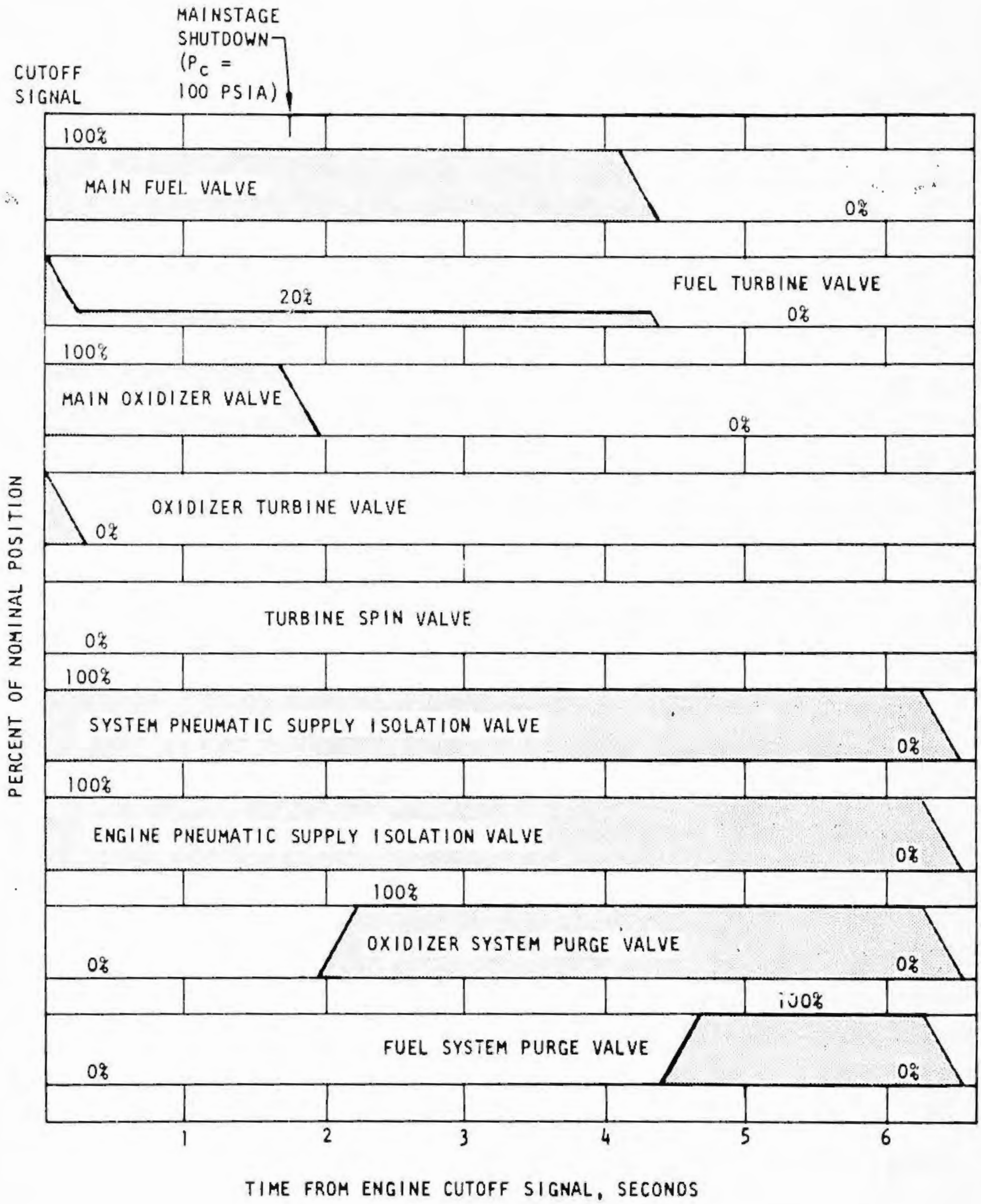

Figure 85. Secondary Engine Cutoff (U)

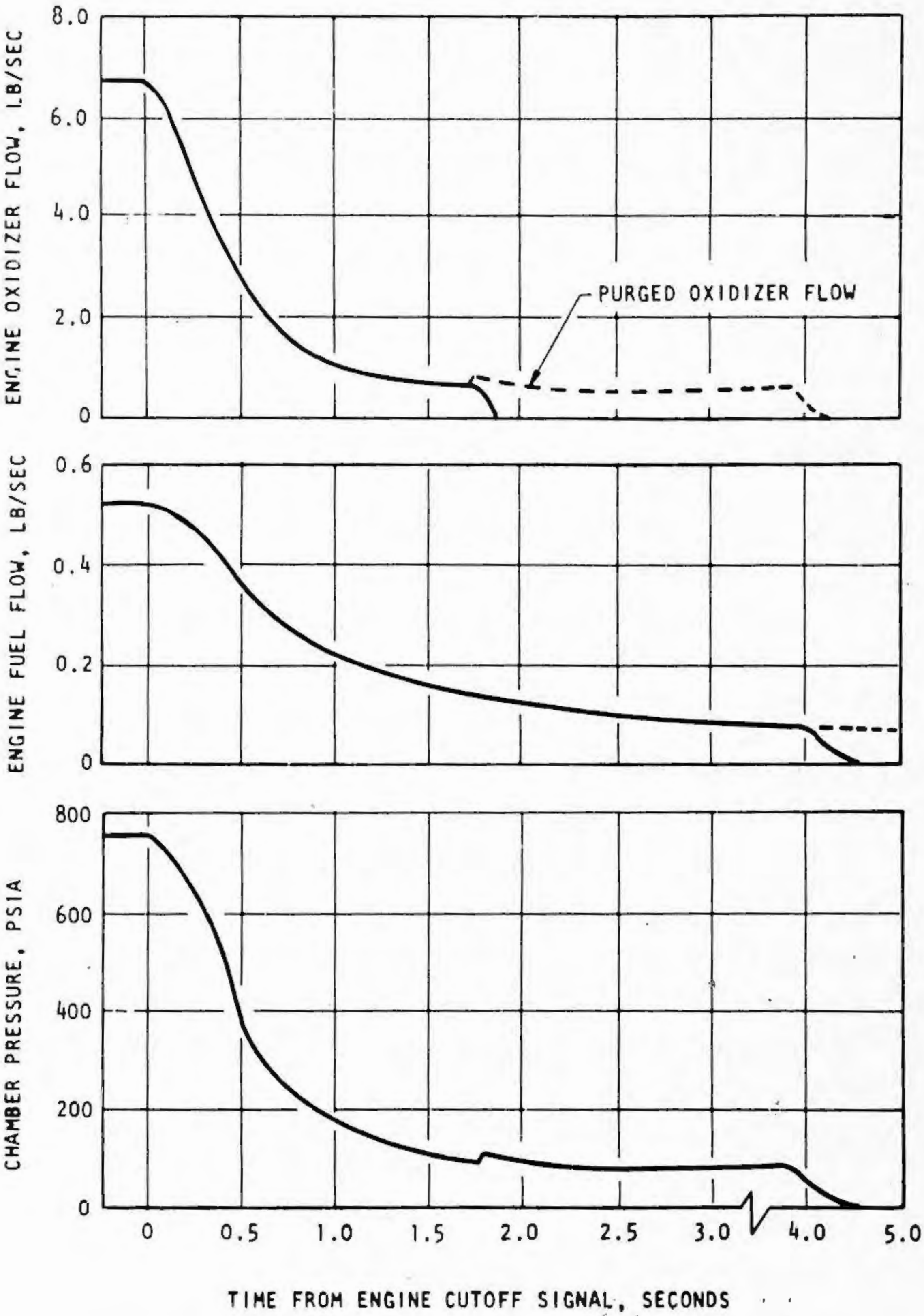

Figure 86. Secondary Engine Cutoff From Full Thrust (U)

(C) requires approximately 2.5 seconds) before the main fuel valve and turbine control valves are ramped closed and the fuel system purge is introduced. A third timer then closes both the oxidizer and fuel system purge valves approximately 2 seconds after the fuel system purge is started.

(5) Future System Variations

(U) As thrust chamber and engine system test experience is obtained, more information will be available to define the engine start and sequencing requirements more accurately. Also, further design and analysis of the control system components may indicate possible areas of improvement. Consideration will be given to using the thrust control chamber pressure readout for those sequence functions that are currently being signaled by individual chamber pressure taps. This would greatly reduce the number of pressure taps required in the engine system.

(U) The times specified for the various delay timers are approximate values based on theoretical calculations or estimates. As test results become available, revisions will probably be made in the specified time delays, with possibly some additions or exclusions to the present number of delay time functions.

j. Engine Base Flow Analysis

(U) An investigation was conducted to evaluate the effect of recirculation of the main engine thrust chamber primary combustion gas into the bell thrust chamber when the main thrust chamber is firing.

(U) The flow field of a typical aerospike engine firing at high altitude is illustrated in Fig. 87. Low-velocity gases in the nozzle base region cannot negotiate the pressure rise at the recompression shock, and, as a result, these gases are turned back toward the base. The gas in the base region forms a natural recirculation pattern, with the central core of the flow moving toward and stagnating at the center of the base. Cold-flow model tests investigating base recirculation have been performed on a number of aerospike configurations. Also, an extensive water table study investigating base recirculation phenomena has been performed.

(U) From these studies, it has been concluded that, if no low-temperature secondary bleed gas is exhausted into the aerospike base, the temperature of the recirculating gas is near the primary combustion temperature. Introduction of low-temperature secondary gas into the base strongly affects the base recirculation pattern and influences the temperature of the gas in the base cavity. With the proper secondary flow and orientation of injection for a particular base configuration, the base temperature can be maintained near the temperature of the secondary flow.

(U) To evaluate the effect of the secondary flow (1 percent of primary) on the recirculation pattern of the main engine thrust chamber, Rocketdyne's water table facility (located at the Rocket Nozzle Test Facility at Los Angeles Division of North American Rockwell Corporation) was used. In previous water table tests, the results showed that directing the secondary flow to oppose the natural recirculation of the fluid in the base region tended to retard entry into the base cavity of the mixture

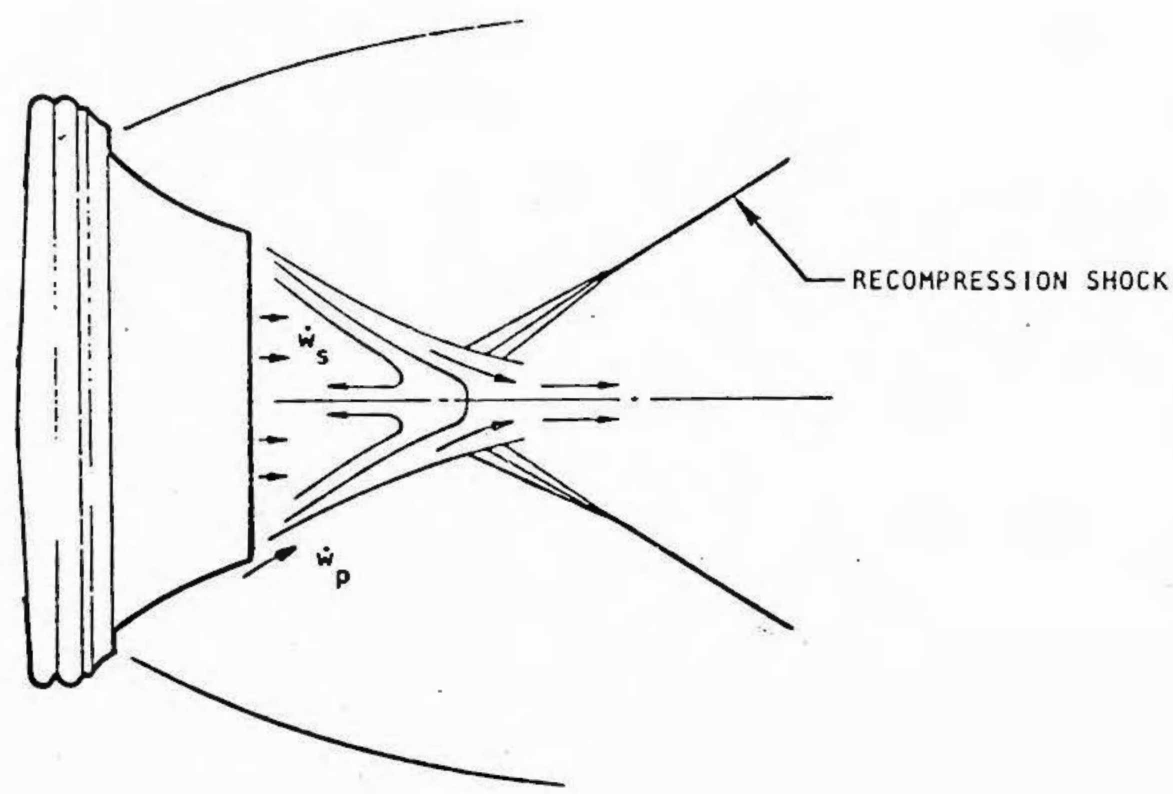

Figure 87. Flow Field of Typical Aerospike Nozzle (U)

of primary and secondary fluids circulating from the base jet boundary shear layer. The success of this test method to qualitatively reproduce trends observed with cold-flow air testing suggested that the water table could be used quickly and successfully to simulate the circulation of gases in the secondary engine bell chamber and base region.

(U) The water table (Fig. 88) can be used to simulate two-dimensional supersonic flow of a gas, because of the properties of surface waves on a sheet of shallow water. The hydraulic analogy to compressible gas flow rests on a similarity of equations of a constant-density inviscid liquid flowing in a shallow, horizontal, open channel of rectangular cross section, where the free surface curvature is small compared with the depth; and the isentropic flow of a perfect gas with specific heat ratio $\gamma = 2$, in a two-dimensional channel of rectangular cross section with no discontinuities in the flow.

(U) To simulate gas recirculation in the main engine base region, an AMPS model (Fig. 89) was installed on the water table. The model was placed on the glass floor plate as shown in Fig. 90 and 91. Two strips of formed aluminum were inserted into the base cavity; the inner strip to simulate the secondary engine bell chamber and the outer strip to form a channel which would permit injection of secondary flow. Weights were placed on the aluminum strips to prevent movement during water flow conditions. During flow conditions, white foam particles were scattered over the water surface, and still photographs were taken from which flow paths could be identified. A 2.5-inch head of water was established upstream of the model. This head simulates the primary stagnation pressure associated with the combustion chamber of a real engine. A variable-height sluice gate permitted the establishment of the model primary flow field with proper Mach number simulation. The primary flow path can be observed in Fig. 90.

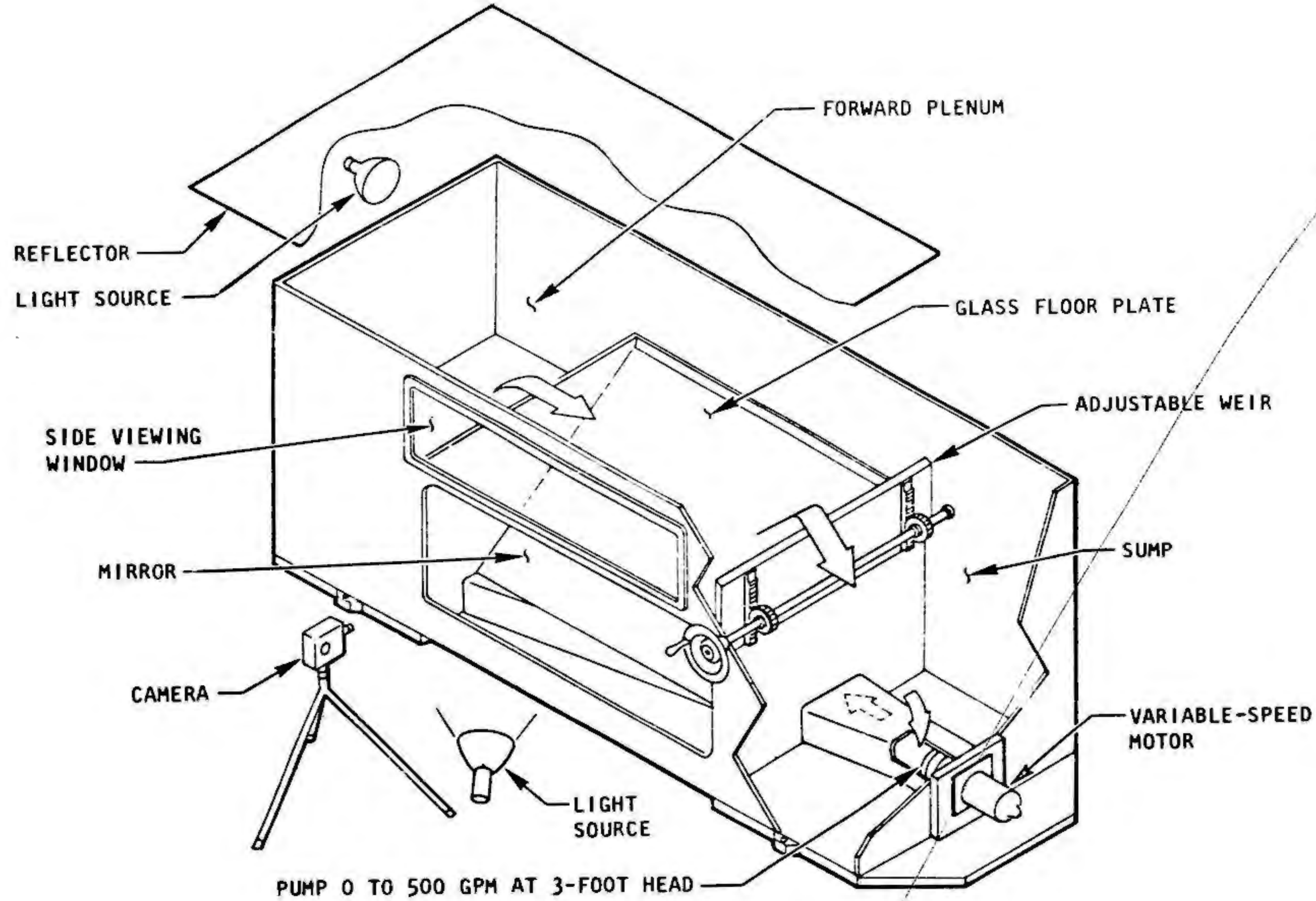

Figure 88. Water Table (U)

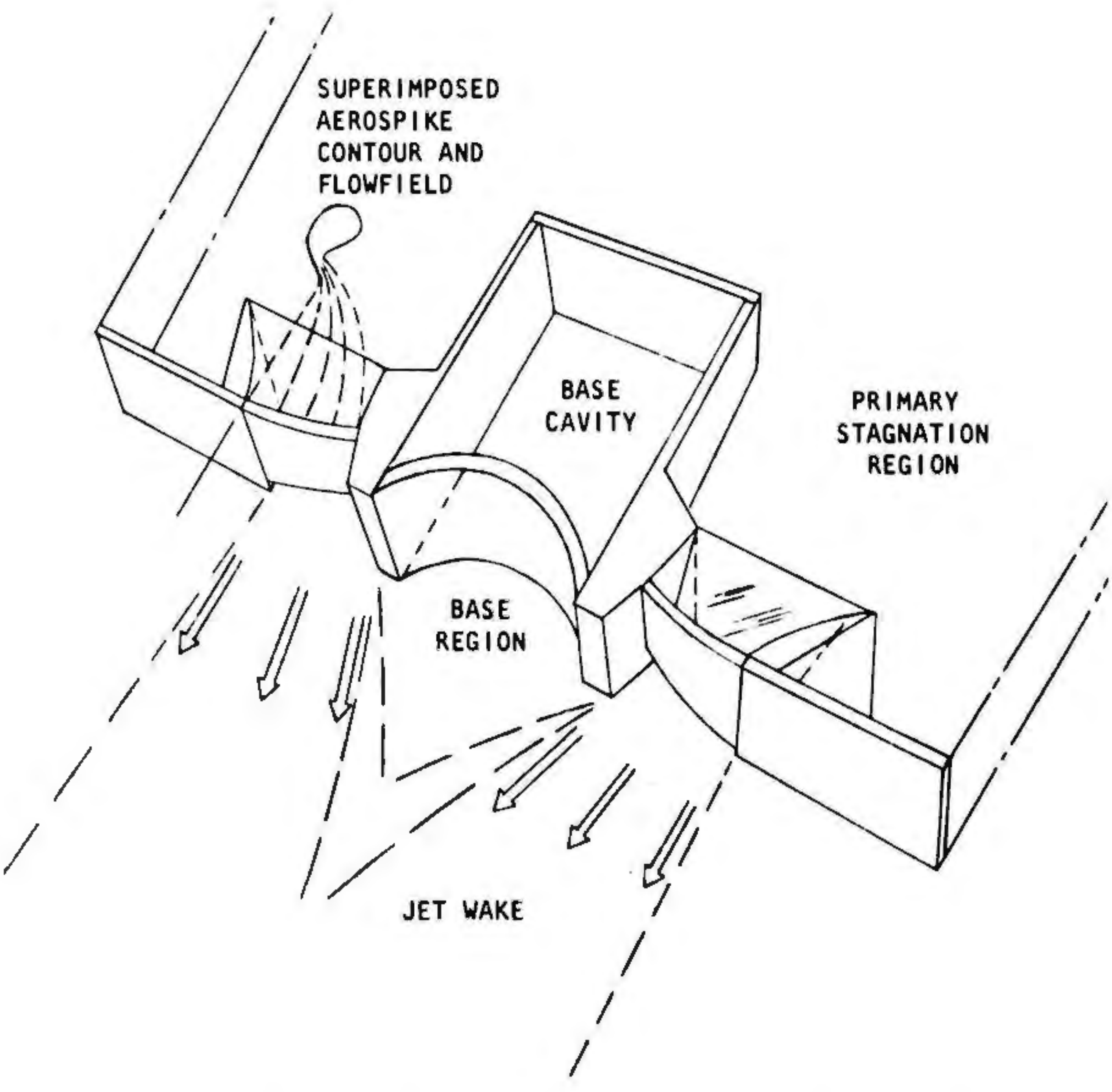

Figure 89. AMPS Model Installed in Water Table With Sluice-Generated Primary Flow (U)

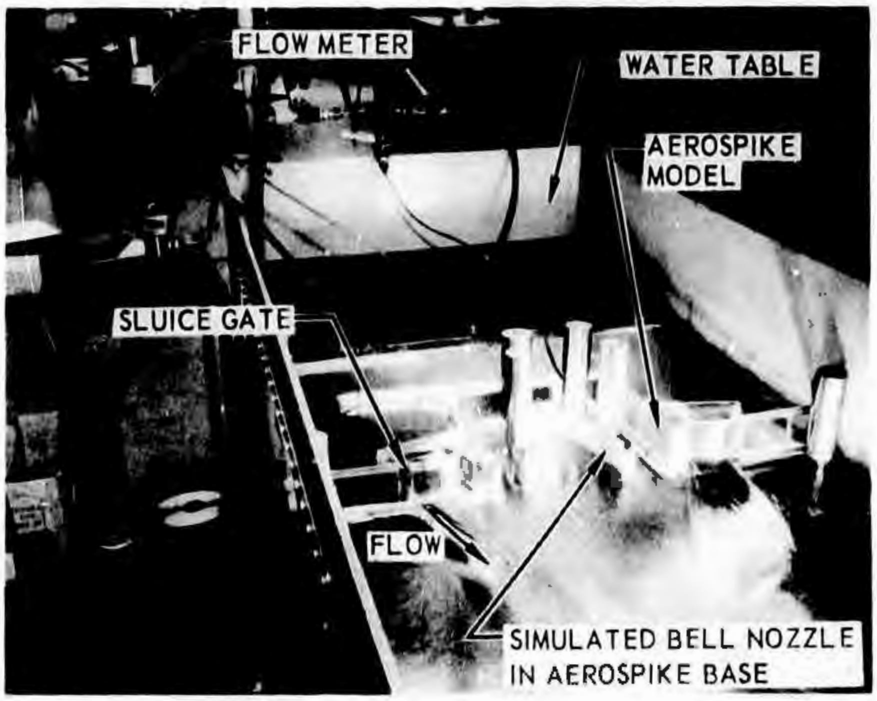

Water Table With Simulated AMPS Engine Base Region

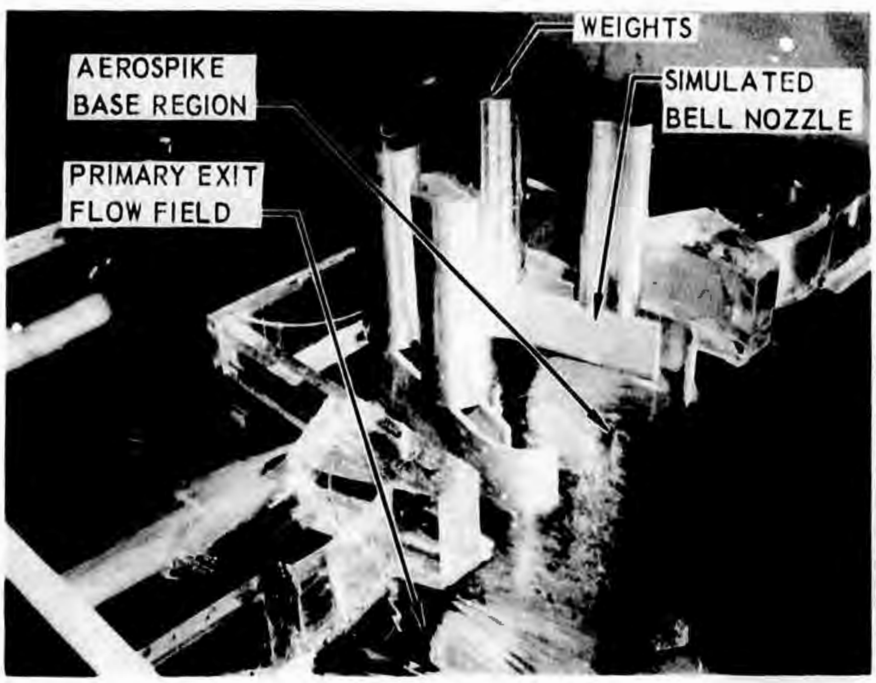

AMPS Engine Base Region

Figure 90. Primary Flowpath for AMPS Engine Base Region (U)

(U) Four secondary flow combinations were used: (1) zero secondary flow, (2) annular (or axial) bleed, (3) inward (radial) bleed, and (4) a combination of the two bleed flows. Figure 91 shows a sketch of the flow paths associated with these combinations.

(U) In the case of no secondary flow, although a strong natural recirculation pattern was established, very little motion occurred within the bell. In the case of pure axial secondary flow (1 percent of primary flow), the primary gas circulated into the region that simulates the secondary thrust chamber cavity. Comparing the case of axial secondary flow with no secondary flow, the results show that the presence of pure axial flow may actually promote penetration of the recirculation gases into the bell chamber region. The actual gases in the recirculation flow would be a mixture of secondary gases and primary gases. The temperature of these gases is not known since there are no data to identify the amount of mixing. The temperature, however, would likely be excessive.

(C) Figure 91 shows a simulation of 1-percent secondary flow directed radially toward the thrust chamber centerlines. The natural recirculation, still a mixture of primary and secondary fluids, has been forced away from the bell cavity. As shown in Fig. 91, the particles are nearly motionless in the bell and in the region immediately aft the bell. The pattern suggests that the temperature of the gases in the bell chamber cavity would be approximately equal to the stagnation temperature of the secondary gas ($\approx$ 640 F).

(U) On other aerospike thrust chamber test programs, the base region has been successfully protected with the use of secondary flow; however, there have been no gas temperature data obtained to define the environment. It has been generally assumed from the test results that, where secondary flow has provided a buffer zone, the gas temperature at the base plate has been near the secondary gas temperature.

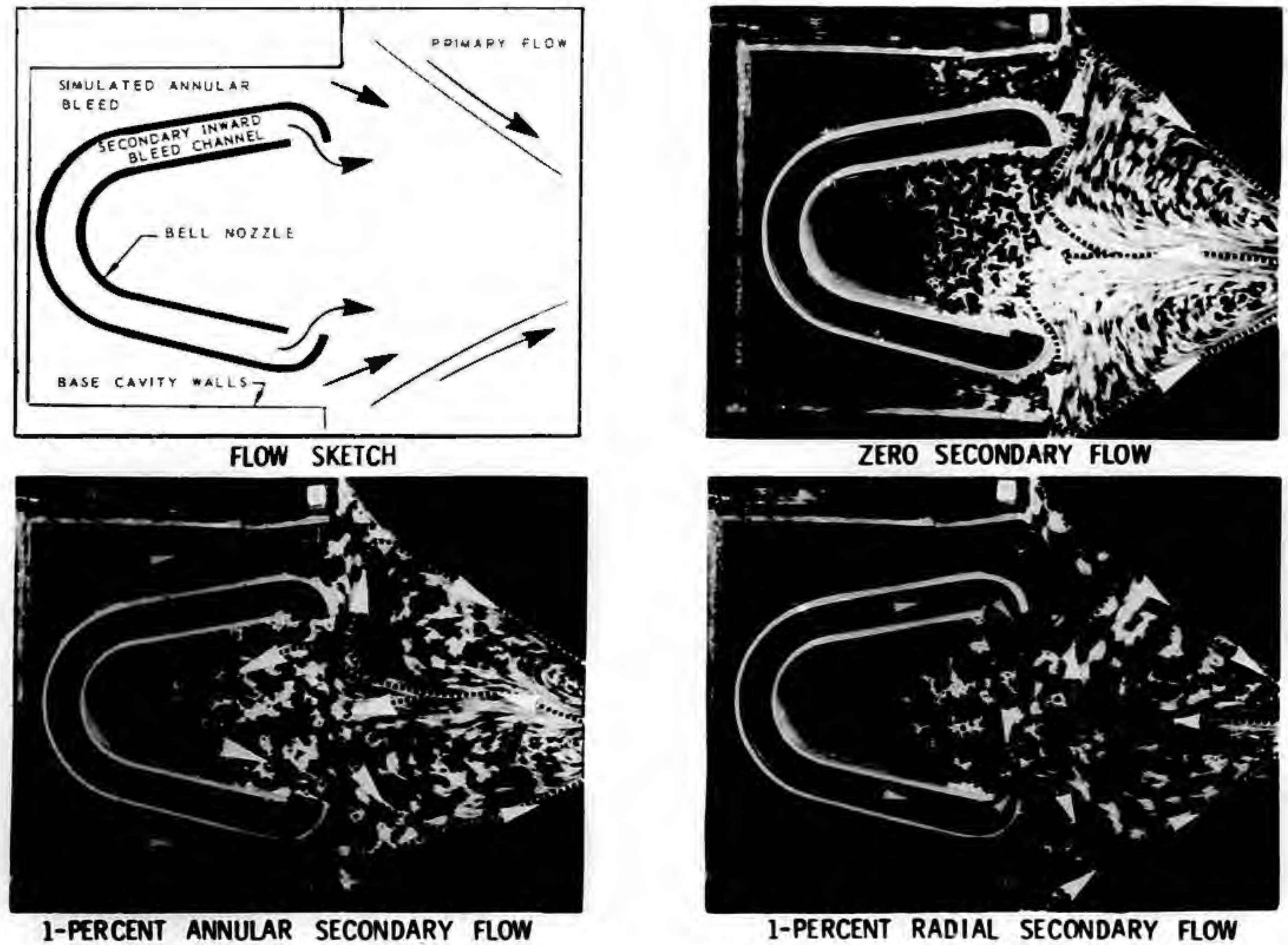

Figure 91. Secondary Flow Paths for AMPS Engine Base Region (U)

(C) From this study, the conclusion was that to maintain the gas temperature at the base of the AMPS engine at a relatively low temperature (640 F) during firing of the main engine, it will be necessary to provide a secondary flow which has a radial injection component (Fig. 92).

k. Engine Exhaust Plume Heating Effects on Thrust Chamber Tubes

(C) Because the radiation heating to the thrust chamber tubes of the nonfiring engine from the exhaust plume of the firing engine could present a serious problem, an analysis was performed to evaluate this condition. Instead of attempting to compute the radiation from a rigorous analysis of the exothermal plume, the heat source was assumed to be an isothermal cylindrical (constant diameter) extension of the thrust chamber. The temperature of the cylindrical surface was assumed to be the mean temperature between the thrust chamber exit plane and the M = 6 (Mach No.) isotherm. This isotherm approximates the cylindrical extension. The heat transferred to the nonfiring engine thrust chamber tube walls was assumed to be the same as that radiated to a projection of the thrust chamber tubes on the thrust chamber exit plane. The resulting heat flux to the main engine thrust chamber as the result of the secondary engine plume was computed to be 43 Btu/hr-ft^2. Because the tubes do not store all heat absorbed, but irradiate to space and conduct heat to adjacent parts, an equilibrium temperature is approached for any given heat flux. Assuming the tube-wall equilibrium temperature to be 1000 R without the plume heating effects, the analysis showed that the maximum increase in temperature would be 10 R for the additional 43 Btu/hr-ft^2. With higher tube-wall temperatures, the effect is even less significant.

(C) Using the same approach for the situation of the main engine exhaust plume radiating to the secondary thrust chamber, the analysis showed that the maximum heat flux on the secondary thrust chamber walls was 282 Btu/hr-ft^2. The resulting increase to a 1000 R tube-wall temperature would be 60 R.

(U) Because the heating effects predicted from the qualitative analyses were negligible and the analyses assumed "worst conditions," a more rigorous analysis was not considered.

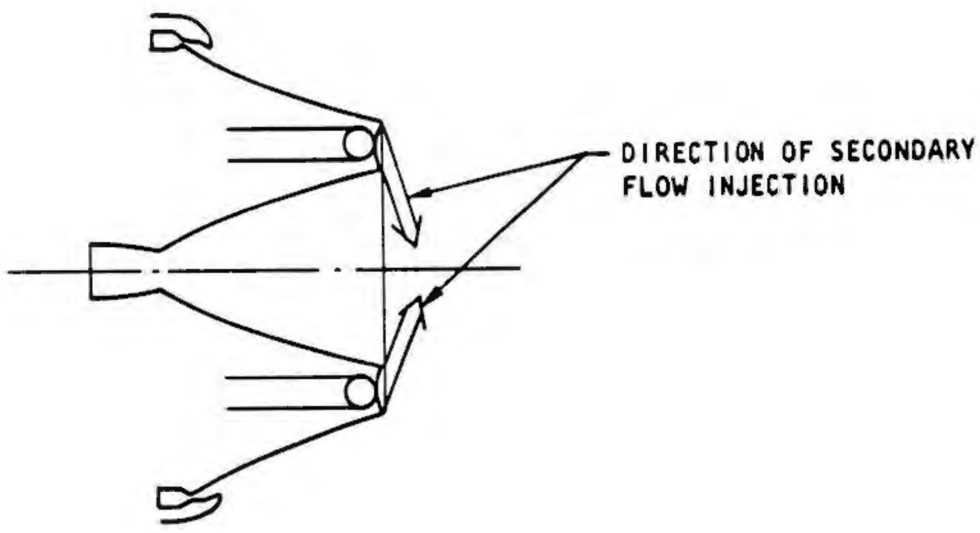

Figure 92. Turbine Exhaust Base Injection Technique to Restrict Base Flow Recirculation Into the Bell Chamber (U)

1. Purge Requirements

(U) To define the inert fluid requirements for the engine system, a purge requirements analysis of the engine system was conducted. This analysis necessitated consideration of the properties of the propellants used, engine operational requirements, serviceability, engine and component configurations, orientation of hardware, and residual propellant expulsion rates.

(U) From the analysis, the total purge fluid requirements were estimated. These are summarized in Table 17. The following discussion presents the analysis conducted in arriving at these estimates.

TABLE 17

ENGINE SYSTEM PURGE REQUIREMENTS (U)

Item	Purge Medium	Regulated Purge Pressure, psia	Purge Flowrate, scim	Purge Temperature, R
Main Engine Operation				
Oxidizer System	Helium	750	75	>180
Fuel System	Helium	750	100	
Oxidizer Pump Seal	Helium	750	4.4	>180
Secondary Engine Operation				
Oxidizer System	Helium	750	Not defined	>180
Fuel System	Helium	750	Not defined	
Oxidizer Pump Seal	Helium	750	1.0	>180
Main and Secondary Engine Ground Test				
Fuel System Standby	Gaseous Nitrogen	750	~1	Ambinet
Oxidizer System Standby	Gaseous Nitrogen	750	~1	Ambient

(U) The approach taken in the analysis was to define the hardware decontamination necessary strictly on the basis of hardware storage, then to define the requirements necessary to restart the engine and, finally, to evaluate various methods of minimizing the impact of these requirements on the restart capability of the engine.

(1) Decontamination for Storage

(U) As the fuel and oxidizer are cryogenic, no major problem is expected with regard to decontamination for purposes of hardware storage. However, the propellants exhausting into the thrust chamber would result in finite thrust until all propellants were dissipated. Given sufficient time, both propellants in the propellant feed system would dissipate to the atmosphere through the thrust chamber and leave no residual which would require special treatment (i.e., draining, flushing, etc.) to expel. Also, there are sufficient sources in all situations of operation to provide the necessary heat to vaporize the residual. The ground operation presents the greatest problem in this regard because of the gravitational conditions which tend to "puddle" the fluids at low points. As the result of "puddling" evaporation of residuals would be retarded because of the increased amount of heat transfer required at the low points. In a zero gravity environment, the evaporation would be uniform throughout uniform volumes. A hypothetical case was assumed where all of the residual oxidizer for the main engine (0.116 cu ft)was contained in 1-inch x 0.085-inch stainless steel tubes with a zero gravity field. Under the probable environment imposed following engine shutdown, it would require in excess of 100 seconds for the oxidizer to evaporate. Less time would be required for evaporating the fuel because the majority of the residual fuel would be in the vapor state at engine shutdown, and the heat input required to vaporize the remainder would be much less than that required to vaporize the oxidizer.

(2) Engine Start Conditions

(U) From the standpoint of the start sequences contemplated for the AMPS engines, where a significant fuel lead is to be used, the possibility exists that the oxidizer system could become primed with fuel before the oxidizer valve opened. The result would be that combustion would occur upstream of the oxidizer injector. This problem could be avoided if a gas purge was introduced into the oxidizer system during the period of fuel lead. The magnitude or location of entry for this purge is not critical as its purpose is to merely provide a positive pressure at the oxidizer injector; however, both magnitude and location become important if one engine has been operating and the other engine is started. Because the turbine gas is to be expelled into the base region, the atmosphere in the nonoperating engine fuel and oxidizer systems is expected to be fuel rich. Consequently, the entire oxidizer system must be purged free of fuel prior to opening the main oxidizer valve (MOV). In the case of restarting the engine immediately after shutdown, virtually no propellant evaporation was assumed to occur, and the engine propellant system would be fully primed at the time engine start would be required. To avert preignition with the residual propellants, procedures are required which would produce an inert chamber atmosphere during fuel system prime.

(3) Effect of Purges on Restart

(U) Analyses were made to evaluate and reduce the impact of the required purges on the restart capability. An initial analysis was made to determine the rate at which oxidizer expulsion could occur. For this analysis a 100-scfm helium purge, with an entry point immediately downstream of the main oxidizer shutoff valve, was assumed. In this configuration, the entire engine oxidizer system ($\approx$0.116 cu ft) would be purged free of oxidizer. For the calculation, the assumption was made that the properties of the oxidizer would be the same as mainstage until the expulsion was complete, and there would be virtually no mixing of the oxidizer and purge gas. In a zero gravity field, the assumption would probably be valid. With the influence of gravity (or axial thrust), the purge would probably not be as effective. A calculation was made to estimate the effect of heat transfer on the effectiveness of the purge. The assumption was made that the purge gas was supplied at a temperature of 400 F and a pressure of 750 psia and dropped to 150 R and 25 psia upon entering the engine. The change in enthalpy between the two conditions is 400 Btu/lb. On the basis of the 100-scfm (0.0174 lb/sec) purge flowrate, the heat available for heating the oxidizer is 7 Btu/sec. Since the heat of vaporization for the oxidizer is approximately 80 Btu/lb, the heat input from the purge gas is relatively insignificant.

(C) A potential problem in the purge procedure is that, to expel all the oxidizer with a zero chamber pressure, there must be no fuel flow. Consequently, the mixture ratio must increase through stoichiometric and, thereby, expose the chamber to a short period of high combustor chamber temperature. To assess the magnitude of this problem, a heat balance was made using the data (film coefficient, heat flux, etc.) derived from the 5-inch (G_c contour) segment testing. The data used was that produced during 70-psia chamber pressure operation. The tube wall temperatures (gas and coolant) and coolant wall film coefficients were computed on the basis of combustion temperature, coolant temperature, and heat flux at the nominal mixture ratio. The assumption was made that the coolant temperature and gas and coolant film coefficients would remain the same, and the heat balance was computed for stoichimetric mixture ratio. The gas-side tube wall temperature increase as a result of the mixture ratio increase was computed to be 20 R (1680 R to 1700 R). The assumption of constant wall film coefficients is probably optimistic; however, the case may be approached if the main fuel valve is left open until the oxidizer purge is completed.

(C) Because of the uncertainty associated with the oxidizer-rich purge, an analysis was made to define a purge which would avoid the high mixture ratio condition. A fuel flowrate is required during the oxidizer expulsion which will maintain the thrust chamber mixture ratio at or below the nominal operating mixture ratio. The maximum fuel weight contained in the fuel system volume (0.26 cu ft) is approximately 0.6 pound and could be as little as 0.5 pound. The residual propellant mixture ratio would then be in the range of approximately 17:1 to 20:1. To maintain the mixture ratio during purging at, or below, the nominal operating mixture ratio, the fuel shutoff valve cannot be closed simultaneously with the oxidizer shutoff valve.

(C) The approach considered for providing adequate fuel flow during the purge involves the use of the two turbine hot-gas valves. Since allowable expulsion flowrate of the residual oxidizer following cutoff is a function

(C) of the fuel flowrate (lower than nominal mixture ratio), the fuel flowrate could be maintained at the full throttled thrust level during the period of oxidizer expulsion if the hot-gas valve controlling the fuel turbine flowrate was left open until the oxidizer was expelled. With this fuel flowrate, the oxidizer flowrate could also be maintained at a compatible flowrate during residual expulsion. Computations revealed that under these conditions the oxidizer expulsion time would be less than 2.0 seconds. During the purge, the injection velocities of the propellants would be comparable to the velocities achieved during full throttled operation. Therefore, injector face heating would be no problem with this purge configuration. The restart would be faster than normal; however, no problems are anticipated as a result of the condition.

(U) The conclusion was that the two hot-gas valve configurations of the control system provide a method for unlimited restart capability and, at the same time, avoid the question of the effect of low injection velocities on injector heating.

(U) Total fluid requirements for the oxidizer system purge were computed as a function of the maximum number of starts and restarts required of the main engine. With these criteria, an estimated 250 scf of helium is required (Table 18). The thermal conditioning of the purge is to be such that the oxidizer does not freeze ($\approx$82 R) when helium gas is introduced into the oxidizer system. The calculations were made with an assumed temperature of 200 R. The purge is to be supplied to the engine from a regulated pressure source combined with proper orificing to meet the flow requirements.

(U) Because secondary engine volumes had not been defined, similar analyses were not possible with respect to the oxidizer system purge requirements. However, in the interest of determining preliminary requirements, a volume of 100 cu in. was estimated. By scaling the purge requirement from the main engine as a linear function of volume, the total purge fluid requirements for the secondary engine were estimated to be 125 scf.

TABLE 18

TOTAL ENGINE SYSTEM OPERATIONAL PURGE FLUID REQUIREMENTS
FOR EXTREME DUTY CYCLES (U)

	Helium Purge Volume, scf
Main Engine (31 Starts; Maximum Duration)	
Oxidizer System	250
Fuel System	100
Pump Seal Purge	150
Total	500
Secondary Engine (31 Starts; Maximum Duration)	
Oxidizer System	125
Fuel System	50
Pump Seal Purge	300
Total	475
Total AMPS Engine (29 Short Main Engine Burns With 1 Long Secondary Engine Burn)	~650

(U) Although the pressure value of the regulated source is not particularly critical, the number of accessory requirements should be maintained at a minimum. Consequently, a regulated pressure source of 750 psia was identified as the purge source because the pneumatic pressure planned for engine valve actuators is 750 psia. The same regulator could possibly be used for both purposes.

(4) Fuel System Purge Requirements

(U) Although there is no requirement for purging the fuel system from the standpoint of hardware storage, the use of a purge after shutdown is advantageous to minimize the time interval in which the residual fuel expels from the thrust chamber. If the propellant is permitted to boil off, a finite residual thrust will be present until the boiloff is completed. Using the same approach that was used for the oxidizer system, the time required for the residual fuel (225 cu in. at 3.9 lb/cu ft) to evaporate was estimated to be in excess of 90 seconds. By supplying a 100-scfm helium purge, expulsion of residual fuel could be accomplished in slightly more than 1.0 second.

(U) Inclusion of the fuel system purge in the cutoff sequence puts no restraint on the restart capability, and the purge can be overridden by an engine start signal.

(C) The fluid requirements of the purge were computed based on the maximum number of starts required (31 starts) and for a 2-second purge following each engine shutdown sequence (Table 18). The total volume requirement was 100 scf for the main engine.

(U) Estimating the fuel system volume for the secondary engine to be half that of the main engine results in a 50-scf fluid requirement for the secondary engine fuel purge.

(U) There is no temperature requirement for the purge (50 R was used for the calculations). The purge is to be supplied from a regulated source pressure and combined with proper orificing to meet the flow requirements. The entry point of the purge to the engine is to be immediately downstream of the fuel shutoff valve.

(S) Turbopump Seal Cavity Purge

(U) Purge requirements for scavenging and pressurizing the cavity between the main engine oxidizer pump seal and turbine seal have been specified to be 7500 scim helium during operation and 1500 scim helium during static conditions with propellants in the pump. The resulting seal cavity pressure for these flowrates was computed to be approximately 50 psia. Analyzing these requirements with respect to the anticipated start and cutoff sequences of the main engine, a dual requirement for operation of the engine was concluded to be not warranted. This conclusion is based on the fact that, under present operating concepts, fuel and oxidizer will be present in the seal area only while the pumps are turning, except for brief periods during start and cutoff. However, to attempt to program a static purge of different magnitude than the operating purge for these brief periods (on the order of 1.0 second) would be unpractical. Consequently, a 7500-scim helium purge was identified for the main engine oxidizer pump seal cavity. To program the purge "on" and "off", consistent with the engine sequencing, the purge is to be sequenced "on" with the signal to pressurize the propellant tanks, and "off" with termination of the oxidizer system purge following engine cutoff. The control would provide 750-scim helium flow at any time that oxidizer was in the pump.

(U) The secondary engine oxidizer pump seal purge logic would be the same, but the magnitude would be 1500 scim.

(U) Maximum fluid requirements for providing the purge are based on the possibility of only secondary engine starts combined with maximum duration (minimum thrust) of operation. With these conditions, approximately 300 scf helium would be required for operation (Table 18). If the main engine operated for a maximum duration (minimum thrust), 150 scf would be required. The conditioning requirements for the purge prior to entry into the seal cavity are that the supply pressure is a regulated pressure and, to avoid formation of fluid in the cavity, the gas temperature of the purge must be above the saturation temperature of the oxidizer. In the case of a 50 psia cavity pressure, the temperature would be above 180 R (200 R was assumed for the calculations).

(6) Ground Requirements

(U) An aspect of the engine system purge requirements was the procedures unique to the ground testing. The altitude environment (100,000 feet) of the engine is to be simulated during the actual ground test firing. The environment was assumed to be maintained sufficiently long before and after engine start to permit utilization of the operational purges defined previously. Since ground testing of the AMPS engine is to be accomplished in the confinement of an environment chamber, the atmosphere inside the chamber must be maintained at a neutral atmosphere as nearly as possible to reduce the possibility of damage to the facility. To accomplish this, both oxidizer and fuel systems of the engine are to be purged free of propellants prior to shutdown of the altitude environment. The purges defined for the fuel and oxidizer systems in previous paragraphs will satisfy this requirement.

(U) Since both purge systems will be cold following engine tests and the environment exposure of the systems will eventually be that of the test site environment, continuous purges in both fuel and oxidizer systems during all periods of nonfiring conditions will be necessary to maintain moisture control. Moisture in either system could result in severe damage either as a result of ice formation in the fuel system and ice formation or combustion in the oxidizer system.

(U) Following periods of engine maintenance during which the purges are required to be shut off, other contamination prevention measures will be necessary (e.g., purge and passivation). The magnitude of the standby purges is not critical since their only purpose is to prevent moisture or other contaminants from entering the propellant systems. These purges appear to be the only operational requirement unique to ground testing the AMPS engine.

m. Engine System Pneumatic and Electrical Requirements

(U) Estimates of engine system pneumatic and electrical requirements were established for coordination with the feed system subcontractors. The purpose of this initial effort is to provide a basis for the integration of the overall propulsion system pneumatics and electrical systems. The engine system requirements presented here are estimates of the maximum requirements based on the current engine control system concepts and calculated estimates of engine purge requirements.

(1) Pneumatic Requirements

(U) The engine system pneumatic control package will supply regulated pressure for opening and closing control of the main propellant valves, regulated purge flow to the oxidizer turbopump seal cavity, and regulated purge flow to the ducts downstream of the main propellant valves. One integrated pneumatic package is anticipated for each engine (main and secondary). A schematic of the basic pneumatic system for each engine is shown in Fig. 93 . A single regulator is used for both main and secondary engines and, therefore, an additional two-way solenoid valve is provided for the oxidizer pump seal purge to restrict the purge flow to only the operating engine. The solenoid valve upstream of the regulator will isolate the regulator to reduce helium loss during periods when the engine is not operating. The pneumatic fluid is helium, Bureau of Mines grade "A." The operating conditions are as follows:

Temperature	Fluid Pressures
Fluid Environment 200 to 600 R	Regulator Inlet 800 to 3500 psig Regulator Outlet 750 ±25 psig normal operation 900 psig maximum (relief valve set pressure)

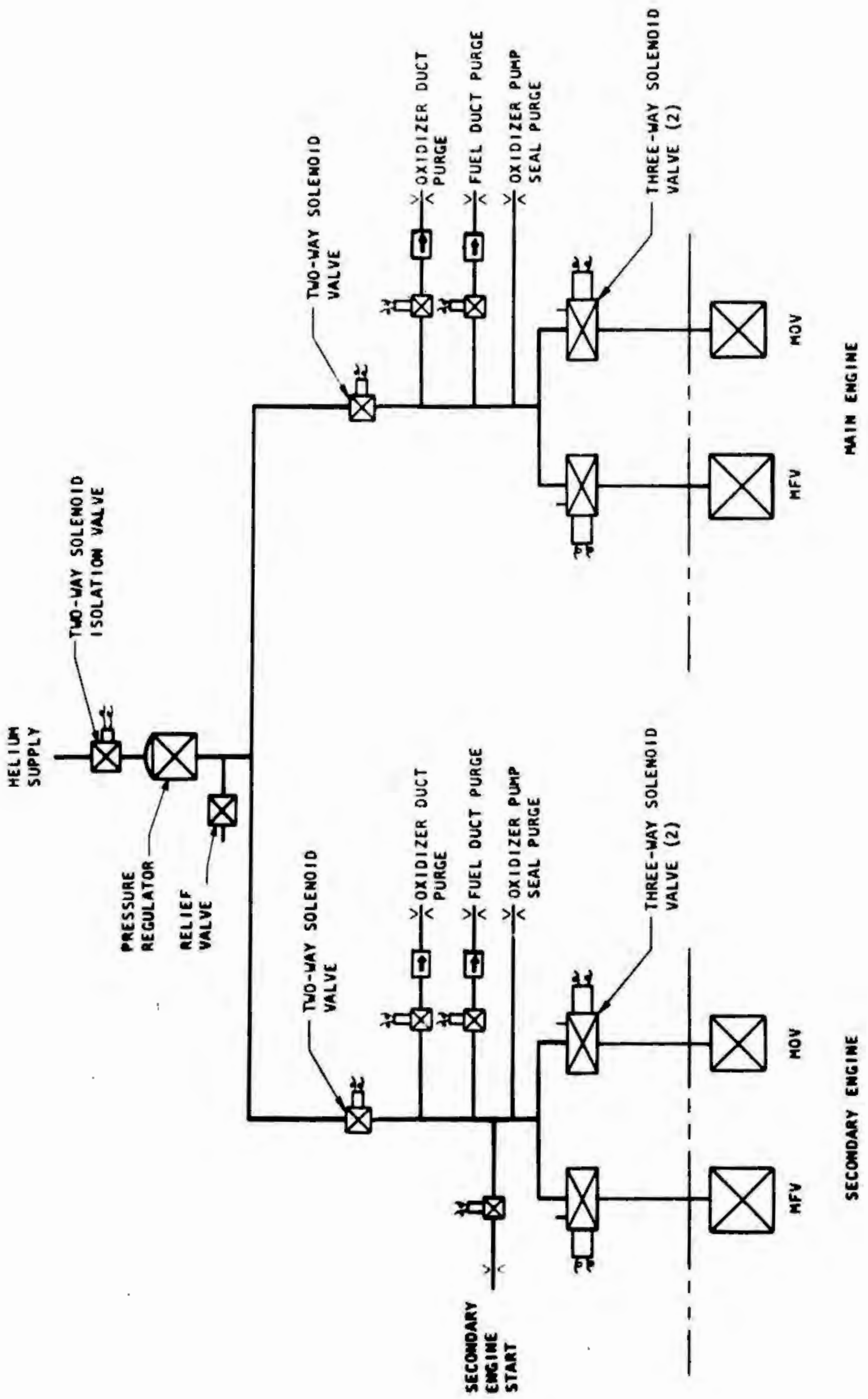

Figure 93. . Basic Pneumatic Control System (U)

(U) The leakage rates for the various pneumatic system components used in the analysis were best estimates of achievable leakage rates based on previous experience. The values used are shown below for upstream helium conditions of 750 psig and 200 R.

Leakage Rates

Three-Way Solenoid Valve	60 scim each
Two-Way Solenoid Valves	10 scim each
Regulator and Relief Valve	50 scim total (external)
Main Valve Actuator	150 scim each

(U) Leakage of the three-way solenoid valves, the two-way solenoid valve used in the purge lines, the external leakage of the regulator and relief valve, and leakage of the main valve actuators will be experienced throughout engine operation. During nonoperative periods (orbital coast), the leakage through the two-way solenoid valve upstream of the regulator is assumed to be lost.

(U) Pneumatic fluid usage for engine start and cutoff is determined from the engine purge requirements and valve actuator system volumes. Pneumatic system volume vented during each valve actuation was estimated from layouts to be 5 cu in. These helium flowrate requirements were then combined to describe the main and secondary engine system pneumatic volumetric flowrate requirements for each engine start and cutoff, per minute of engine operation, and per hour of orbital coast. These volumetric flowrates are presented in Table 19 for each of the pneumatic system functions. All volumes are given for standard temperature and pressure conditions.

(C) The established helium usage rates were then used to determine total pneumatic system helium weight requirements for a range of possible mission applications. The total helium volume requirement is dependent on total engine burn duration, number of engine starts, and total orbital coast duration. Helium flowrate requirements were calculated for maximum and minimum burn duration for both the main and secondary engines. The burn durations shown in Table 20 are based on the entire propellant load (~15,500 pounds) being consumed at the accompanying specified thrust level.

TABLE 19

ENGINE SYSTEM PNEUMATIC REQUIREMENTS* (U)

Function	Volume Per Start, cu in.	Volume Per Minute of Engine Operation, scim	Volume Per Hour of Coast, cu in.	Volume at Maximum Thrust, cu in.	Volume at Minimum Thrust, cu in.	Volume For 31 Starts, cu in.	Volume For 14 Days, cu in.
Main Propellant Valve Actuation							
Main Engine	2,600					80,500	
Secondary Engine	2,600					80,500	
Steady State							
Main Engine		470		1,860	17,200		
Secondary Engine		470		15,850	140,500		
Coast			560				186,000
Spin Start							
Secondary Engine	20,000					620,000	
Oxidizer Duct Purge (5 seconds)							
Main Engine	10,820					335,000	
Secondary Engine	1,900					58,900	
Fuel Duct Purge (2 seconds)							
Main Engine	5,750					178,000	
Secondary Engine	1,750					54,250	
Oxidizer Pump Seal Purge							
Main Engine		7,600		30,100	279,000		
Secondary Engine		1,728		58,000	518,000		
Total							
Main Engine				31,960	296,200	593,500	
Secondary Engine				73,850	658,500	813,750	186,000

*He Gas, 3000-psig Supply Pressure, 750-psig Regulator Pressure, ≥200 R Temperature

TABLE 20

RANGE OF ENGINE BURN DURATIONS (U)

Engine	Burn Duration, seconds	
	Maximum Thrust	Minimum Thrust
Main	238	2,020
Secondary	2200	18,000

CONFIDENTIAL

(2) Electrical Requirements

(U) Engine system electrical requirements also estimated to provide a basis for determining power source and total energy requirements. This analysis also provided a starting point in an effort to maintain commonality between the feed system and engine system electrical requirements. The engine system concept requires electrical power for solenoid valve actuation, turbine-control valve actuation, engine controller package, and engine instrumentation.

(U) The total power requirements for each of the engine system electrical components are shown in Table 21 along with the estimated voltage and current requirements. Values shown for the engine controller electrical package are estimated based on previous experience. The 110-vac source is desired for the indicated components if available, but other power sources may be acceptable. Engine instrumentation requirements were not sufficiently defined to estimate their electrical power requirements; however, these requirements are expected to be very low relative to the other electrical power requirements.

(C) Maximum electrical energy requirements were determined from the established power requirements and the most severe mission duty cycle. Energy requirements for those components requiring continuous power during engine operation were based on the maximum firing duration of 18,000 seconds.

TABLE 21

ENGINE SYSTEM ELECTRICAL REQUIREMENTS (U)

Function	volts	Current Drain, amps	Number of Components	Total Power Requirement, watts	Maximum Energy Requirement, watt-hr
Three-Way Solenoid Valve	26 to 30 dc	3.0	2	120 to 180*	900
Two-Way Solenoid Valve	26 to 30 dc	2.0	3	120 to 180**	300
Turbine Control Valve Actuator	110 ac***	0.3	2	25*	125
Engine Controller	26 to 30 dc	0.5	1	10 to 20*	100
Instrumentation	---	---	---	---	---
Total					1425

*Continuous power during engine firing
**Continuous power to one valve and two valves activated only during purge operation
***Desired if available (26 to 30 vdc acceptable)

(U) The resulting total electrical energy requirement of 1425 watt-hr is considered to be an estimate of the electrical energy required by the engine system.

n. Engine Flow Measurement and Mixture Ratio Control

(U) Propellant utilization for the AMPS requires that the engine control system be capable of sensing and controlling engine mixture ratio over a sufficient range to accomplish simultaneous propellant depletion for all defined mission requirements. The sensing devices used in the propellant utilization system to determine relative propellant liquid level in the tanks could be the accumulative type (measures flow from the tank) or the liquid level type (measures propellant in the tank). Upon determining relative propellant load from either method, the engine would be commanded to operate at a comparative engine mixture ratio. In operation, the value and control of engine mixture ratio is important, while the values of the propellant flowrates are not particularly important unless they are required to determine mixture ratio. Therefore, mixture ratio control is considered a primary engine requirement, and flow determination is not.

(U) In this analysis, methods were considered where operating characteristics or levels of engine components could be used to sense and control mixture ratio. This analysis did not include direct measurement flow devices (i.e., turbine meters, electromagnetic meters, etc.). In some of the methods considered, only a mixture ratio indication feedback signal would be generated by the engine control system, and there would be no accompanying information from the engine which would indicate propellant flowrates. In these cases, the relative propellant tank levels are required to be determined by a feed system device.

(U) In each of the methods considered, calibration of the engine and component would be required during the static tests on the engine. Methods considered included: (1) pressure loss in a component (i.e., injector ΔP) from which flow and eventually mixture ratio could be determined and controlled, (2) fuel-to-oxidizer system pressure balance from which only mixture ratio could be sensed and controlled, (3) thrust chamber coolant temperature rise from which only mixture ratio could be sensed and controlled, (4) pump operating parameters (speed and propellant density) from which flow and mixture ratio can be computed and controlled, and (5) fuel turbine valve position programmed as a function of command mixture ratio for given engine operating level.

(U) In the analysis no attempt was made to predict the resolution of the controller because the value would be comparable with each type of measuring device. The predicted resolution for control of mixture ratio was made on the basis of present capability associated with transducers and, where engine hardware was involved, the repeatability experienced with similar pieces of hardware on existing engines.

(1) Head Loss for Flow Measurement and Mixture Ratio Control

(U) Use of head loss in the propellant systems for determining flow and mixture ratio has been considered a remote possibility for the AMPS engine. The hesitancy to use this type of "meter" stems from the fact that, while the propellant flowrates vary by a factor of 10 over the engine operating range, the ΔP of the meter varies by a factor of 100 (i.e., $\Delta P \sim \dot{w}^2$). Since pressure is the primary indicator, the resolution of flow would become very difficult at low ΔP.

(U) To demonstrate the mixture ratio uncertainty obtained for the above flow measurement scheme, a venturi section was assumed ($d_1 = 1.125d_2$, fuel; $d_1 = 1.167d_2$, oxidizer), and pressure differential measurement was obtained between the two sections of line (diameters, d_1 and d_2). Assuming

(U) both propellants to be liquid at the meter and with the use of the energy equation ($P + V^2/2g$ = constant), the analysis showed that the static pressure differential between the two sections was 198.8 psid and 125.8 psid for the fuel and oxidizer meters, respectively, at full engine thrust. Combining the effects of uncertainty in the pressure measurements, the mixture ratio uncertainty would be ±0.45 unit.

(U) When the computation was made for the throttled thrust case, the ΔP dropped to 2.89 psid an[illegible] 5 psid for the fuel and oxidizer meters, respectively. No resolution of mixture ratio would be possible if the uncertainty of the pressure transducers remained at ±0.5 percent. With these conditions, negative pressure drops could be recorded and cause an uncertainty in mixture ratio ranging from -7.55 units to virtually infinity. The propellant density factors were not included in the analysis and would increase the uncertainty by an additional factor. Obviously, this approach needs considerable instrumentation improvement if it is to be used.

(U) Dual range pressure transducers could be used to reduce some of the uncertainty. One approach would be to calibrate a single transducer for maximum precision at two operating levels. The fact that the transducer is designed for high pressure operation would still limit the degree of precision at low pressure operation, and any significant improvement at the minimum thrust level is doubtful.

(U) A second approach would be to use dual transducers, one transducer designed and calibrated for high pressure operation and the second transducer designed and calibrated for low pressure operation. With this arrangement provision would be required to protect the low pressure range transducers when high pressures were present. Presumably this would be accomplished with the use of isolation valves, sequenced by the engine thrust level feedback signal.

(U) Adding components and accompanying control to the engine is not particularly acceptable. As a result, prediction of the possible mixture ratio resolution was not computed.

(U) Although the analysis was made for the AMPS main engine, the results are equally applicable to the secondary engine.

(2) Injection Differential Pressure for Mixture Ratio Control

(U) Limited mixture ratio control has been accomplished on Rocketdyne fixed-thrust engines by balancing an engine oxidizer pressure with that of a fuel system pressure through a servovalve, which in turn controls the position of one of the propellant valves. Since this approach has proved successful, the approach was considered for the AMPS engines. The method provides only mixture ratio information and has no capability of predicting propellant flowrates.

(U) In the previous experience with this type of control, propellant compressibility and density changes were ignored as both propellants were quasi-incompressible (RP-1 and LOX). In the AMPS application, compressibility cannot be ignored, primarily because of the fuel characteristics.

(U) There are numerous pressures referenced which could be made on an engine to obtain an indication of mixture ratio. In the following analysis injection pressures were used for the AMPS main engine.

(a) Effect of Propellant Density on Mixture Ratio

(C) For the analysis, the assumption was made that the changes from nominal propellant pressure and temperatures at a particular engine thrust level would be small and density could be expressed in each of these regions as a linear function of pressure and temperature. Considering fuel temperature near 1460 R, the density gain over the engine operating pressure range was found to be -0.000268 lb/ft^3-R. The resolution of temperature was assumed to be ±2 R (0.14 percent of reading) for a single reading. Because there is a reading involved with the engine calibration and with the actual test case, two temperature errors are possible. The combined error was predicted to be the sum of squares of the individual uncertainties (≈±3 R).

(U) Considering fuel pressure at a temperature of 1460 R, the density gain was found to be 0.00026 lb/ft^3-psi for the range of engine operation. The resolution of injection pressure was assumed to be ±5 psi (±0.5 percent of transducer range) for each reading. Again a calibration reading and a test reading are involved and produce a total density uncertainty of ±0.0019 lb/ft^3. Combining both temperature and pressure factors ($\sqrt{\Sigma P^2}$) produces an uncertainty in density of ±1.05 percent. The resulting effect on mixture ratio was computed to be ±0.12 unit.

(U) Similar analysis using predicted oxidizer operating temperatures and pressures resulted in density gains of 0.21 lb/ft^3-R and 0.0012 lb/ft-psi. The uncertainty associated with each pressure (±5 psi) and temperature (±0.5 R) measurement resulted in oxidizer density uncertainty of ±0.159 percent and an uncertainty in mixture ratio of ±0.48 unit. Combining the fuel and oxidizer contributions ($\sqrt{\Sigma MR^2}$) produces an uncertainty of ±0.495 mixture ratio unit.

(b) Effect of Differential Pressure Error

(U) At the full-thrust level, the relationship of engine mixture ratio to injection pressure differential ($P_{fuel} - P_{oxidizer}$) at a constant propellant density was found to be 35 psi/mixture ratio unit (Fig. 94). Because the differential would be resolved from individual transducer voltage output (as opposed to a ΔP gage), the total uncertainty of the two transducers would be ±7.07 psi at all thrust levels (±0.5 percent of transducer range). The resulting uncertainty in mixture ratio at full thrust would be ±0.22 unit.

(U) Combining the uncertainty associated with the density (±0.495 unit) with the uncertainty associated with injection pressure differential (±0.22 unit) produces a predicted uncertainty in engine mixture ratio at full thrust of ±0.54 unit.

(U) Similar analysis conducted at the throttled thrust level produces an uncertainty in mixture ratio of ±2.54 units. The loss of resolution was caused by the low injection differential pressure at the low flowrates.

CONFIDENTIAL

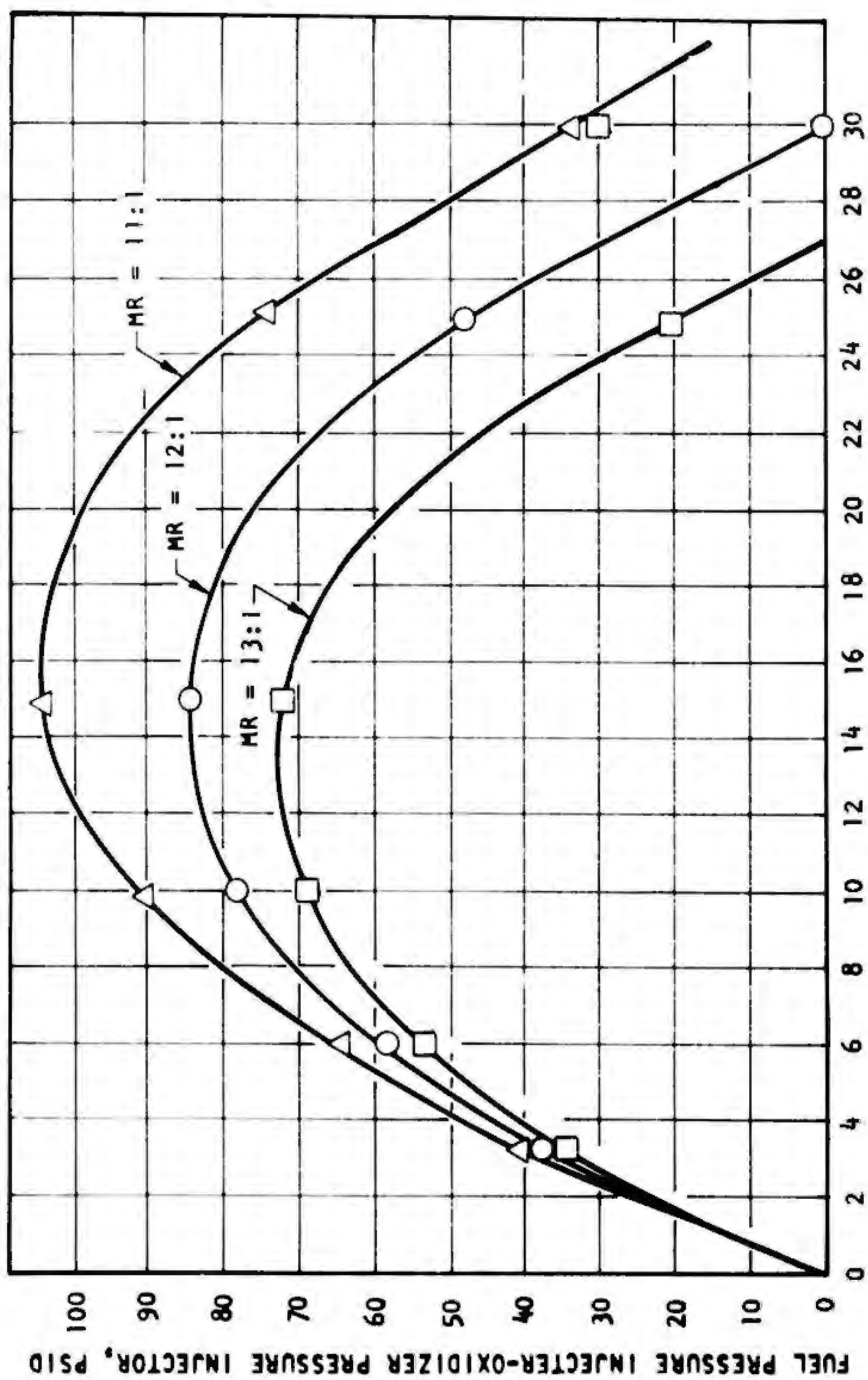

Figure 94. Injection Pressure Difference for Main Engine (U)

CONFIDENTIAL

(U) Therefore, the conclusion was that the use of oxidizer-to-fuel system pressure differentials could not be used for mixture ratio control in the AMPS engines unless better resolution of pressures could be achieved over the full engine operating range.

(c) Thrust Chamber Coolant Temperature Rise for Mixture Ratio Control

(U) Use of thrust chamber coolant temperature rise as an indication of mixture ratio (flowrates are not determined) in a control system has not been previously accomplished at Rocketdyne. Upon examination there are some obvious unknowns which require answers before the approach could be used. Among thse unknowns are: (1) the effect of small amounts of chamber damage on coolant heat load, (2) the effect of a variable thrust level on the linearity relationship of temperature rise and mixture ratio (a study on the J-2 engine revealed a linear relationship over a mixture ratio of approximately 1.5 units), and (3) the degree of instrumentation required to obtain an overall coolant temperature rise, particularly with the segmented thrust chamber. Assuming these questions could be satisfied, an analysis was made to determine the mixture ratio resolution which could be achieved using the presently known factors.

(U) The data from four J-2 engines (36 tests) were analyzed to produce a statistical value (variance) defining the distribution of data about a straight line relating mixture ratio and coolant temperature rise. Assuming the variance of the AMPS data to be comparable, a prediction was made that ±7.75 R represents a 3σ level of dispersion from the straight line.

(U) Combining this value by the sum of squares method with a ±2 R value representing the uncertainty in the measurement produces a total possible error of ±8 R.

(U) From the present heat transfer analysis, the predicted sensitivity of coolant temperature rise for a unit increase in mixture ratio (constant thrust) is 90 R/mixture ratio unit, or conversely 0.0111 mixture ratio unit/R. The uncertainty in mixture ratio as a result of the predicted temperature error is ±0.0888 (approximately 0.1) unit for the main engine.

(U) A similar analysis conducted for the secondary engine produced a sensitivity of 46 R/mixture ratio unit (or 0.0218 mixture ratio unit/R). Assuming the resolution of bulk temperature rise and mixture ratio for the secondary engine is comparable to that presented for the main engine produces an uncertainty in secondary engine mixture ratio of ±0.175 (approximately 0.2) unit. The theoretical values presented in this control method are extremely attractive since the potential resolution of mixture ratio is comparable to that of turbine flowmeters. Additionally, the control system input for mixture ratio is at most a summed voltage input from two temperature measurements.

(3) Pump Parameters for Flow and Mixture Ratio Control

(U) Engine pump performance parameter measurements taken during flight have been used extensively at Rocketdyne to predict propellant flowrates for engine systems flight tested. The method depends or a knowledge of propellant quality going through the pump and the pump speed. The precision with which the engine mixture ratio can be computed and controlled using these data depends on the resolution of propellant conditions, pump speed, the repeatability of pump speed for a given downstream resistance, propellant condition, and operating level. The uncertainty of knowing each of these factors was evaluated in terms of pump speed for the main engine at the full thrust operating level and the throttled-thrust operating level. The pump speed uncertainty factors at each operating level were then combined to produce a factor of uncertainty in knowing engine mixture ratio operating point. The following discussion presents the analysis made in determining the predicted mixture ratio uncertainty at full thrust.

(a) Effect of Pump Inlet Pressure on Pump Speed

(C) The engine influence coefficient table was used to predict the possible error in pump speed as the result of uncertainty in pump inlet pressure. The assumption was made that pressure could be resolved within ±0.5 percent of the transducer range (100 psi). In the case of the fuel pump, this accuracy represents a ±0.835 percent uncertainty in knowing the pump inlet pressure at 60 psia. Using the engine influence coefficient associated with the fuel pump inlet pressure, together with the uncertainty, the analysis showed that the resulting uncertainty in knowing the correct speed required could be ±0.164 rpm for the oxidizer pump and ±10 rpm for the fuel pump.

(U) Similarly, the possible oxidizer pump inlet pressure recording error could cause an uncertainty of ±4.57 rpm in required oxidizer pump speed and ±0.0835 rpm in fuel pump speed. Subsequent discussion shows that the effect of these possible errors in pump speed is not significant.

(b) Effect of Pump Inlet Temperature on Pump Speed

(U) The assumption was made that propellant temperature could be resolved within ±0.5 R for both oxidizer and fuel propellants. For the oxidizer, this accuracy represents ±0.327 percent instrument-recorder precision at the operating temperature. Again, using the engine influence coefficients for the main engine, the analysis showed that the required accompanying pump speed uncertainty would be ±24 rpm for the oxidizer pump and ±0.08 rpm for the fuel pump. Similarly, the effect of a possible fuel temperature error (±1.25 percent) could cause an uncertainty in pump speed of ±0.175 rpm for the oxidizer pump and ±200 rpm for the fuel pump.

(c) Effect of Pump Speed Recording Error

(U) Given enough data points in a revolution, the pump shaft speed could be resolved to virtually no error. In the calculation, the assumption was made that pump speed could be resolved within ±0.05 percent of the actual

(U) speed at full thrust. This could be accomplished with two signals per revolution from the fuel pump shaft and four signals per revolution from the oxidizer pump shaft and could provide a signal each 0.0005 second from each pump. The resulting pump speed uncertainty would be ±14 rpm and ±37.5 rpm, respectively, for the oxidizer and fuel pump shaft speeds.

(d) Effect of Pump Speed Requirement

(U) Pump speed requirement for a given set of hardware and operating conditions is theoretically constant for a particular engine. Any finite change either in the pump operation or in any other hardware operation necessarily causes a change in the required pump operating level. Historically, these factors have been lumped into a single factor for a given rated operating level (thrust and mixture ratio) and defined as run-to-run variation in the required pump speed to meet these conditions. The variance (S^2) obtained from several Rocketdyne engine pumps was examined, and eventually the variance associated with the MK15 pumps was used in estimating the repeatability in required pump speed for a given operating level for the AMPS main engine.

(U) Estimating σ_{R-R} for the AMPS pumps to be equal to $\sqrt{S^2_{R-R}}$ for the MK15 pump and assuming a $3\sigma_{R-R}$ significance level, the uncertainty associated with pump speed requirement was predicted to be ±116 rpm and ±725 rpm, respectively, for the oxidizer and fuel pumps.

(e) Combined Effects

(U) To estimate the total combined uncertainty associated with knowing what pump speed is required and knowing the actual pump speed, a sum of squares approach was taken. The uncertainty in oxidizer pump speed and fuel pump speed was found to be ±120 rpm and ±750 rpm, respectively.

(f) Effect on Engine Mixture Ratio

(U) To equate uncertainty in engine mixture ratio to the uncertainty in pump speed, the approach was taken to relate pump speed to propellant flow for each pump. The method required plotting pump flowrate as a function of

(U) pump speed for the nominal mixture ratio case (Fig. 95), and then computing the slope of the curve at the point of interest (full thrust, etc.). The flow was determined by multiplying the slope by the pump speed uncertainty value. Mixture ratio was computed first by using the nominal fuel flow and the variation in oxidizer flow, then by using nominal oxidizer flow and the variation in fuel flow. The combined mixture ratio uncertainty was determined by the sum of squares of the two components.

(U) Using this method, the total computed mixture ratio uncertainty was found to be ±0.256 unit at the full-thrust operating level. A similar analysis resulted in an uncertainty of ±0.205 mixture ratio unit at the throttled-thrust operating level. The conclusion was therefore reached that with the use of pump calibration, together with propellant pressure and temperature at the pump inlet, main engine mixture ratio could be computed and controlled within ±0.3 mixture ratio unit of the desired value.

(4) Programmed Fuel Turbine Valve Position for Mixture Ratio Control

(U) Calibration of the engine during static test provides the possibility of defining mixture ratio as a function of fuel turbine valve position for a given thrust level, or oxidizer turbine valve position, or a combination of the two (propellant flowrates are not determined). Similar approaches have been successfully used on other Rocketdyne engines where mixture ratio has been expressed as a function of a control valve position for a given thrust level. Although the data are not available to predict the possible mixture ratio resolution with this type of control, the success of the past justifies analysis during engine development work.

(5) Analysis Summary

In summarizing the analysis, the following points are made:

(C) 1. Because $\Delta P \sim \dot{w}^2$, and $\dot{w}$ varies over a range of 10 to 1, flowrates cannot be computed with sufficient precision from propellant system

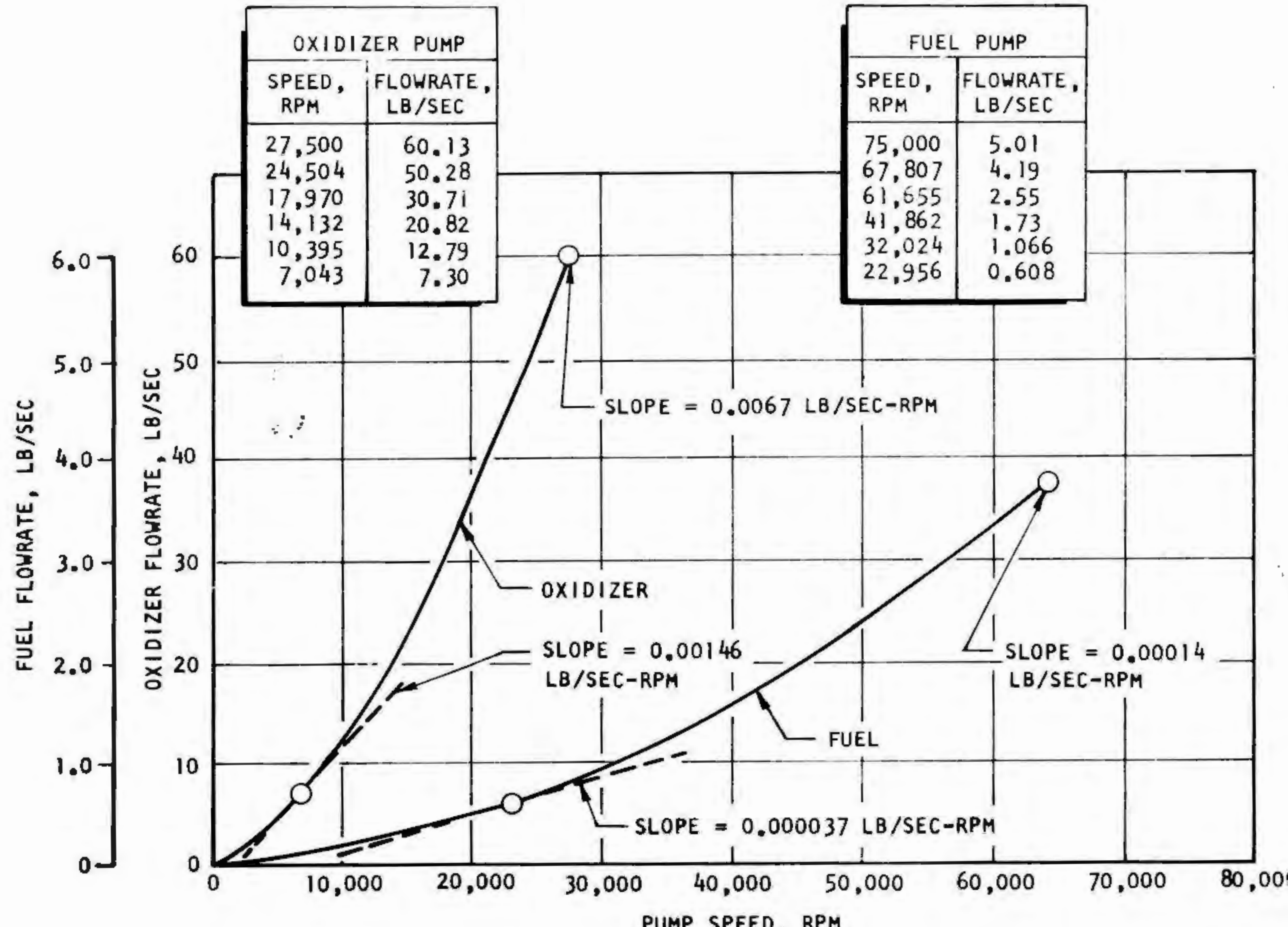

Figure 95. Pump Speed vs Pump Flow (U)

(U) pressure losses or system-to-system pressure differentials to provide adequate mixture ratio control for the AMPS engines.

(U) 2. Calibration of the engine from which use of pump performance, thrust chamber coolant temperature rise, or programmed fuel turbine valve position can be used for mixture ratio control appears feasible; however, all methods require some static test history from which to develop a factor of run-to-run predictability.

(U) 3. For the present, both primary and secondary engine designs include turbine-type flowmeters in the engine control system.

o. Engine Ground Test Checkout Approach

(U) The pretest functional and leak tests, together with the ability to detect malfunctions during hot firing, must be considered prior to attempting ground test of the AMPS engine. Particularly important in the case of the AMPS engine test program is the high reactant nature of the propellants and the confinement of the engine (obscured from view) in the altitude simulation chamber.

(U) The following discussion recognizes the major potential problem areas and offers general solutions or safeguards for overcoming these problems. There is no attempt actually to define detailed procedures but, rather, to bring an awareness of the problems so that design of engine and components will reflect a configuration amenable to functional checkouts, system leak tests, and monitoring for proper operation.

(1) Functional Checkout

(C) There are 28 events presently identified (Table 27) with engine components which can occur during start, mainstage, and cutoff which, if they differ from the normal, would cause some unusual behavior of the engine. Of the

TABLE 22

PRELIMINARY FAILURE EFFECTS ANALYSIS,
AMPS ENGINE GROUND TEST (U)

Event	Result
Main Fuel Valve Fails to Open	Engine will not start.
Main Fuel Valve Fails to Close	Excessive fuel lost after cutoff; no engine damage would result.
Main Fuel Valve Closes Early	Thrust chamber damage and fuel pump overspeed are certainties. This would cause serious engine and facility damage.
Main Fuel Valves Opens Early	No effect if the engine is in the cutoff mode at time propellants are on board and start is not energized.
Main Oxid Valve Fails to Open	Engine will not start.
Main Oxidizer Valve Fails to Close	Main fuel valve and fuel turbine control valve would not close automatically. Engine would operate until residual propellants were depleted or the facility valves closed. Some overspeeding of the fuel pump may occur.
Main Oxidizer Valve Closes Early	Oxidizer pump overspeed, probably causing serious engine and facility damage.
Main Oxidizer Valve Opens Early	Depending on when in the sequence the valve opened, it could cause engine thrust chamber and facility damage.
Fuel Pump Does Not Rotate	Engine does not start.
Fuel Pump Stops Rotating	Engine stops running; may sustain thrust chamber damage. Main oxidizer valve will close and fuel and oxidizer turbine valves will close.
Oxidizer Pump Does Not Rotate	Engine will operate at low level until limiter timer initiates cutoff; probably no other effect.
Oxidizer Pump Stops Rotating	Engine stops running; mainstage switch dropout will initiate an engine cutoff signal.
Fuel Turbine Control Valve Fails to Open	Engine does not start.

TABLE 22

(Continued)

Event	Result
Fuel Turbine Control Valve Opens Early	No effect
Fuel Turbine Control Valve Fails to Close	Pump continues to pump fuel until residuals in fuel feed lines are expelled; no hardware damage.
Fuel Turbine Control Valves Closes Early	Engine stops running; may sustain thrust chamber damage. Main oxidizer valve will close and fuel and oxidizer turbine valves will close; no effect.
Oxidizer Turbine Control Valve Fails to Open	Low-order combustion until limiter timer initiates cutoff; probably no other effect.
Oxidizer Turbine Control Valve Fails to Close	Engine continues to run until propellants in the lines are depleted; either or both pumps could overspeed, causing serious engine and facility damage.
Oxidizer Turbine Control Valve Closes Early	Initiates an early but near-normal cutoff sequence.
Oxidizer Turbine Control Valve Opens Early	Causes overspeed of the oxidizer turbo-pump and may cause pump and other engine damage.
Fuel Jacket Prime Pressure Switches Fail to Actuate	No adverse effect: engine shutdown is affected by limiter timer.
Fuel Jacket Prime Pressure Switches Fail to Deactuate	No effect
Fuel Jacket Prime Pressure Switches Actuate Early	Could cause thrust chamber damage
Fuel Jacket Prime Pressure Switches Deactuate Early	No effect
Mainstage Monitor Pressure Switch Signal Fails to Actuate	Engine cutoff initiated by limiter timer; normal cutoff sequence.
Mainstage Monitor Pressure Switch Fails to Deactuate	No effect

TABLE 22

(Concluded)

Event	Result
Mainstage Monitor Pressure Switch Actuates Early	This effect cannot be evaluated until the switching from start to mainstage control is defined.
Mainstage Monitor Pressure Switch Deactuates Early	Engine cutoff is initiated by limiter timer; normal cutoff sequence.

NOTES:
1. Engine is in cutoff mode at all times during standby when propellants are on board.
2. An emergency shutdown requires that the engine turbine valves close before propellant depletion occurs following closure of the facility prevalves.
3. Fuel system primed pressure switch signal is locked in on actuation.
4. Checkout of the pressure switches during sequence checks would monitor for proper position of switches. Individual checkout for proper actuation would be required prior to installation.
5. No attempt was made in the table to indicate a failure mode and effects analysis for the engine in the AMPS vehicle. This is to be accomplished at a later date.

(U) 28 events, 19 are of a nature that would cause no problem other than the inconvenience of losing the test objectives for that static test. Four events fall into the category of possibly causing some engine damage, but not of a catastrophic nature. The remaining five events could cause not only serious engine damage but, also, facility damage. Extensive checkouts become important for the last two categories. To evaluate each critical event, all possible primary failure modes must be identified that could cause the particular event; then, the appropriate procedure should be defined and implemented that would reduce the possibility of that unscheduled event occurring. In four situations, the malfunction could be the result of that particular component (valve or pump) malfunctioning. The remaining five are of the nature that requires a control system malfunction which causes improper sequencing of valves. Historically, the best way to determine if a component is functional at the time of test is to require the component to perform during checkout under the same conditions the component would perform during hot-fire operation. This performance checkout is obviously impossible in some situations because of the nature of the component and the location of the engine, e.g., actuation of the main fuel or oxidizer shutoff valves would not be possible with propellants at the valves during a checkout because, in so doing, the propellants would be introduced into the engine and altitude chamber. The next best approach would be to perform a checkout of the entire engine, which would go through a simulated start, mainstage, and cutoff sequence. The logic of the AMPS engine requires pressure switch (or equivalent) signals to activate intermediate sequences in the start sequence. Provisions for simulating these would be required in the checkout because the pressure switches themselves would not actuate (no system pressure). Checkout of the pressure switches for proper actuation would be required prior to installation. However, position of the switch could be verified during the sequence checkout procedure. Also, to check the mainstage control, simulated signals for chamber pressure and mixture ratio would be necessary. This can be accomplished at the control panel in much the same way the pressure switch signals are simulated.

(U) The electrical and pneumatic systems automatically receive checkout during the engine start, mainstage, and cutoff checkout procedures. Also, their proper functioning is to be verified by pre-checkout function and continuity checks.

(U) In performing the checkouts, monitoring points and methods must be provided that also identify incipient malfunctions. For example, an increase in the required actuation time or pressure requirement for a valve may indicate the valve would fail to open or, once opened, would fail to close on the next test. Actuation pressure, position, and time would be important measurements in this case.

(U) Emergency engine and facility procedures also are to receive checkouts prior to each test exposure. The objective of these checkouts is to verify proper sequences of facility shutoff valves and engine valves so that a more serious problem is not developed as a result of the procedure. For example, only under the most severe conditions should shutting the facility or engine shutoff valves be considered prior to shutting the turbine control valves. If the reverse is accomplished, overspeeding of the turbopump will occur, and severe damage to the engine and facility could be the end result. Of the five failure modes listed in Table 22 that would cause severe engine and facility damage, four would be the result of overspeeding one of the two turbines. Alternatives must be weighed to determine what the sequence should be to shut down the engine in the case of an emergency during test stand operations to avoid an additional undesirable situation as the result of the emergency shutdown.

(U) Obviously, the key to performing any checkout is the availability of critical function instrumentation (position, etc.) and the recording system itself. Instrumentation that records component functions is to be considered in the original design of each component, with the idea that the component will receive checkouts at each assembly level. An optimum design can be accomplished both from the standpoint of "pure design" and instrumentation.

(2) Leak Check

(C) Measures to prevent propellant leakage from the AMPS engine will be given considerable attention. Several factors unique in the engine design tend to make the problem of leakage even more critical than on other engines. These factors are: (1) the physical behavior of the oxidizer makes an oxidizer system leak virtually prohibitive, and (2) the engine configuration which has both main propellant shutoff valves upstream of the pumps requires that complete engine leak checks will be restricted to low-pressure levels (probably less than 20 psig). To circumvent the situation wherein all joints would receive only the low-pressure check, an assembly procedure can be utilized that will permit leak checking subassembly units at pressures more comparable with the engine operating pressures.

(U) A similar situation arises with passivation of the oxidizer system. Because of the shutoff valves being located upstream of the pumps, it is not possible to utilize the normal passivation procedure recommended for a fluorine system with the assembled engine. The alternative is to passivate individual components prior to engine assembly, and then conduct a flowing passivation of the engine system.

(U) One possible solution to both potential problems would be to make provisions to block off the distribution manifolds of both oxidizer and fuel from the injector and thrust chamber inlets. If flanged joints were used, thin plate blanks could be inserted into the flanges, effecting isolation of the upstream oxidizer and fuel systems. Then a pressure check of all joints between the valve inlets and distribution manifolds could be accomplished at a relatively high pressure ($\approx$200 psia). This pressure check could be accomplished during assembly and, also, during pre-test operations. This approach could also be used in passivating the oxidizer system upstream of the blanked-off flange joints. Subsequently, the only joints depending on a low-pressure leak check are the manifold-to-thrust chamber joints and the joints in the thrust chamber assembly. Also, only the oxidizer injector would depend entirely on a flowing passivation. This approach may appear conservative, but is warranted to avoid hardware and facility risks.

p. Engine/Propellant Feed System Interface Heat Load

(C) Analysis was conducted to define qualitatively the heat load imposed on the thrust structure by the engine system through radiation and conduction heat transfer. These analyses were made to provide the Task III subcontractors a basis for evaluation and design of the thrust structure and propellant feed system. Table 23 summarizes the results of the study. The situation considered to represent the most severe heat load condition was that which is present during main engine operation. Radiation heat transfer sources during this time are the engine hardware and engine exhaust plume. The major source is that of the engine hardware. The inner tubewall temperature ranges from approximately 700 to 1200 R. The turbine feed lines are expected to approach 1500 R, and the turbine exhaust ducts 700 R.

(C) With the use of some simplifying configuration assumptions, it was estimated that the maximum temperature of an imaginary 50-inch-diameter surface formed by the forward end of the main engine injector would be approxmately 1000 R (Fig. 96). For the purpose of determining radiant heat transfer to any surface forward of the injector plane surface, an equivalent emissivity of 0.6 was defined. An 8-inch-diameter occlusion at the center of the 1000 R surface (Fig. 96) is required in the computation to account for the presence of the engine thrust mount and secondary engine thrust chamber.

(C) The radiant energy source of the main engine exhaust plume was estimated in terms of two isothermal surfaces (Fig. 96). The first of these surfaces was a 50-inch-diameter cylinder extending 50 inches aft from the throat plane. A surface temperature for the cylinder of 2200 R was estimated on the basis of an average gas temperature in the cylinder region. The second surface defined was a circular disk at 800 R extending from the outside diameter of the main engine (50-inch diameter) to a diameter of 70 inches. The position of the disk was affixed at the aft end of the main engine thrust chamber. An emissivity of 0.01 was estimated for both surfaces.

TABLE 23

ENGINE/PROPELLANT FEED SYSTEM HEAT INTERFACE DESCRIPTIONS (U)

Engine Thermal Conditions	Engine	Gimbal Block	Propellant Inlet Lines
Equilibrium Temperature During Steady-State Operation of Main Engine	1000 R	200 R	* **
Equilibrium Temperature During Coast	550 R	550 R	550 R
Equivalent Emissivity of Projected Engine Radiant Surface (50-inch-diameter at location 8.5 inches below gimbal point)	0.6	---	---
Plume Radiation (Main Engine)	Dimensions	Emissivity	Temperature
Geometry and Temperatures for Surfaces Approximating Plume Gas Heat Sources			
Disk at Thrust Chamber Exit Plane	50-inch ID; 70-inch OD	0.01	800 R
Cylinder Extending From Chamber Throat Plane	50-inch diameter; 50 inches long	0.01	2200 R

CONFIDENTIAL

*Fuel propellant temperature
**Oxidizer propellant temperature

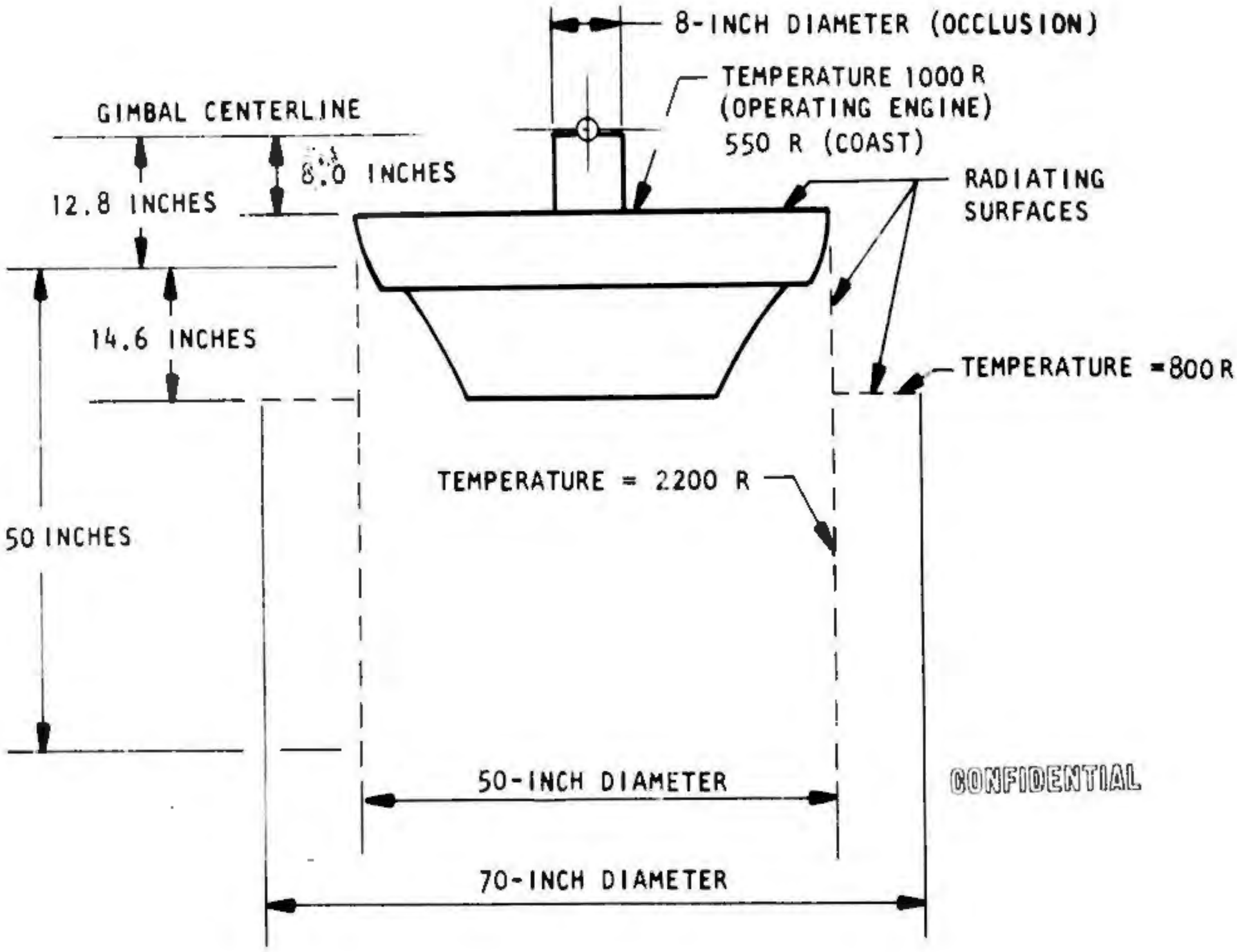

CONFIDENTIAL

Figure 96. Engine Radiation Heat Sources

(C) Conduction heat transfer to the thrust structure and propellant feed system during engine operation is virtually nil. The stabilized temperature of the engine inlet duct where it attaches to the vehicle ducting is expected to be at near propellant temperature as a result of the propellant flow through the ducts. The engine thrust mount temperature also is expected to be near the oxidizer temperature because the thrust mount houses the oxidizer distribution manifold for both engines. The maximum thrust mount conductive heat source was estimated to be 200 R.

(U) Heat conduction through small tubes (i.e., purge and instrumentation lines) that connect to the engine and thrust structure was neglected because these components are, in effect, long fins and would dissipate any temperature gradient rapidly.

(C) The second situation considered was that of vehicle coast. For the worst case, the assumption was made that the engine thrust chamber exit was directed toward the sun. Then, assuming an absorption/irradiation ratio of 1.3, the equilibrium temperature for the engine hardware was computed to be 550 R. In computing the radiant energy from the engine to the thrust structure, the projected area (50-inch diameter) of the main engine at the forward end of the injector should be considered to be at a temperature of 550 R with a 0.6 equivalent emissivity.

q. Engine/Propellant Feed System Line Interface

(U) Because of difficulty anticipated by the propellant feed system contractors in maintaining fully primed propellant feed lines to the engine inlet, a brief evaluation was made to determine the impact of moving the propellant shutoff valves from the present location at the engine inlet to a location upstream within the present thermal conditioning system

(U) As far as the engine start sequence is concerned, this configuration is similar to that of the propellant lines being unchilled downstream of the prevalves. The latter case was tested on the mathematical model (Engine Sequence Analysis section) and was found to extend the start sequence

(U) of the main engine as much as 2.0 seconds. Therefore, the conclusion was that the relocation of the shutoff valve would cause essentially the same result.

(C) The influence of shutoff valve relocation on cutoff, engine purge requirements, and engine/propellant feed system interface were also considered. To evaluate the influence of shutoff valve relocation on engine cutoff and purges, the volumes downstream of the relocated valves were estimated. By assuming that the fuel and oxidizer line diameters are 2.5 and 3.0 inches, respectively, and 36 and 60 inches in length, the total volumes downstream of the shutoff valves were determined to be 0.362 and 0.366 ft^3, respectively, for the main engine, and 0.232 and 0.308 ft^3 for the secondary engine (engine volumes included). These volumes are compared with the volumes downstream of the engine mounted shutoff valves shown in Table 23.

(C) Because the planned engine cutoff sequence utilizes all the residual oxidizer downstream of the shutoff valve to produce impulse during cutoff, the time required to expell the propellants would be proportional to the volume of propellants to be expelled. By this criterion, the cutoff sequence would be extended from the 2-second cutoff presently predicted for the main engine to more than 6 seconds. Also, the secondary engine cutoff sequence would be extended from 2 seconds to more than 10 seconds. This comparison also is shown in Table 23.

(C) Using the same criterion with respect to the engine purge requirements for 31 engine starts, the total helium requirements for the main engine (including valve actuations) would be increased from 593,500 to 1,390,500 sci and would be increased from 347,800 to 1,185,500 sci for the secondary engine. This comparison also is presented in Table 24.

(U) A design ramification attendant with location of the shutoff valves is provision for operating one engine independent of the other engine. As a result, the shutoff valves (engine isolation valves) for both engines must be retained at the engine inlet or separate feed lines installed from each engine to the upstream shutoff valves (two for each engine). In considering all of these factors, the conclusion was that the penalties were too great to consider relocating the shutoff valves from the engine inlet.

TABLE 24

EFFECT OF RELOCATING ENGINE PROPELLANT SHUTOFF VALVES (U)

	Engine Mounted Shutoff Valves		Feed System Mounted Shutoff Valves	
	Oxidizer System	Fuel System	Oxidizer System	Fuel System
Residual Volume, ft^3				
Main Engine	0.120	0.260	0.366	0.362
Secondary Engine	0.06	0.130	0.308	0.232
Cutoff Time, seconds (minimum thrust during oxidizer expulsion)				
Main Engine	$\approx$2.0	$\approx$4.0	$\approx$6.3	$\approx$9.1
Secondary Engine	$\approx$2.0	$\approx$4.0	$\approx$10.6	$\approx$14.2
Helium Purge Requirements, sci				
Main Engine	335,000	178,000	1,060,000	250,000
Secondary Engine	178,000	89,300	945,000	160,000
Total Helium Requirements (including valve actuations), sci				
Main Engine	593,500		1,390,500	
Secondary Engine	347,800		1,185,500	

CONFIDENTIAL

r. Engine Propellant Line Heat Barriers

(1) Heat Barrier Duct

(C) An analysis was made to evaluate and define thermal heat barriers in the propellant lines at the main engine-to-feed system interface. This analysis assumed that the heat barriers would be located in the ducting between the engine shutoff valves and the turbopumps. Ground rules imposed were that the engine-to-feed system heat load be less than 3 Btu/hr for each main propellant duct, that conventional fabrication processes be utilized, that the barrier have a low hydraulic flow resistance, and no auxiliary cooling of the heat harrier flanges would be provided.

(U) To be consistent with the design philosophy of low thermal conductivity, three considerations were made: (1) the material selection should be hased on the coefficient of thermal conductivity and compatibility with the propellants, (2) the wall thickness of the ducting should be minimized while maintaining structural integrity, and (3) the length of the ducts should be maximum to increase the resistance to heat flow through the duct material.

(C) The selected material was Rene 41 which has a coefficient of thermal conductivity of 0.340 Btu-in./hr-F at room temperature and a minimum yield strength of 125,000 psi. The material compatibility of Rene 41, while not as corrosion resistant as the resistant steels or nickel, is suitable for use in the oxidizer and fuel systems.

(C) To determine the minimum harrier wall thickness, a free-body diagram was made for the loading systems as described by the feed system subcontractors. Because both the fuel and oxidizer ducts (barriers) are to be identical, the most severe loading was used to make the analysis. In both cases, the oxidizer lines were subjected to the greater loads. Resolving the largest predicted input loads to the duct resulted in a maximum moment of 5182 lb/in. In terms of barrier wall thickness, 0.0125-inch thickness was required to withstand the loading induced by this propellant feed system load. Because of practical fabrication limitations, a wall thickness of 0.0150 inch was selected for the design. The interconnecting ducts between the propellant shutoff valves and the pumps are shown in Fig. 97.

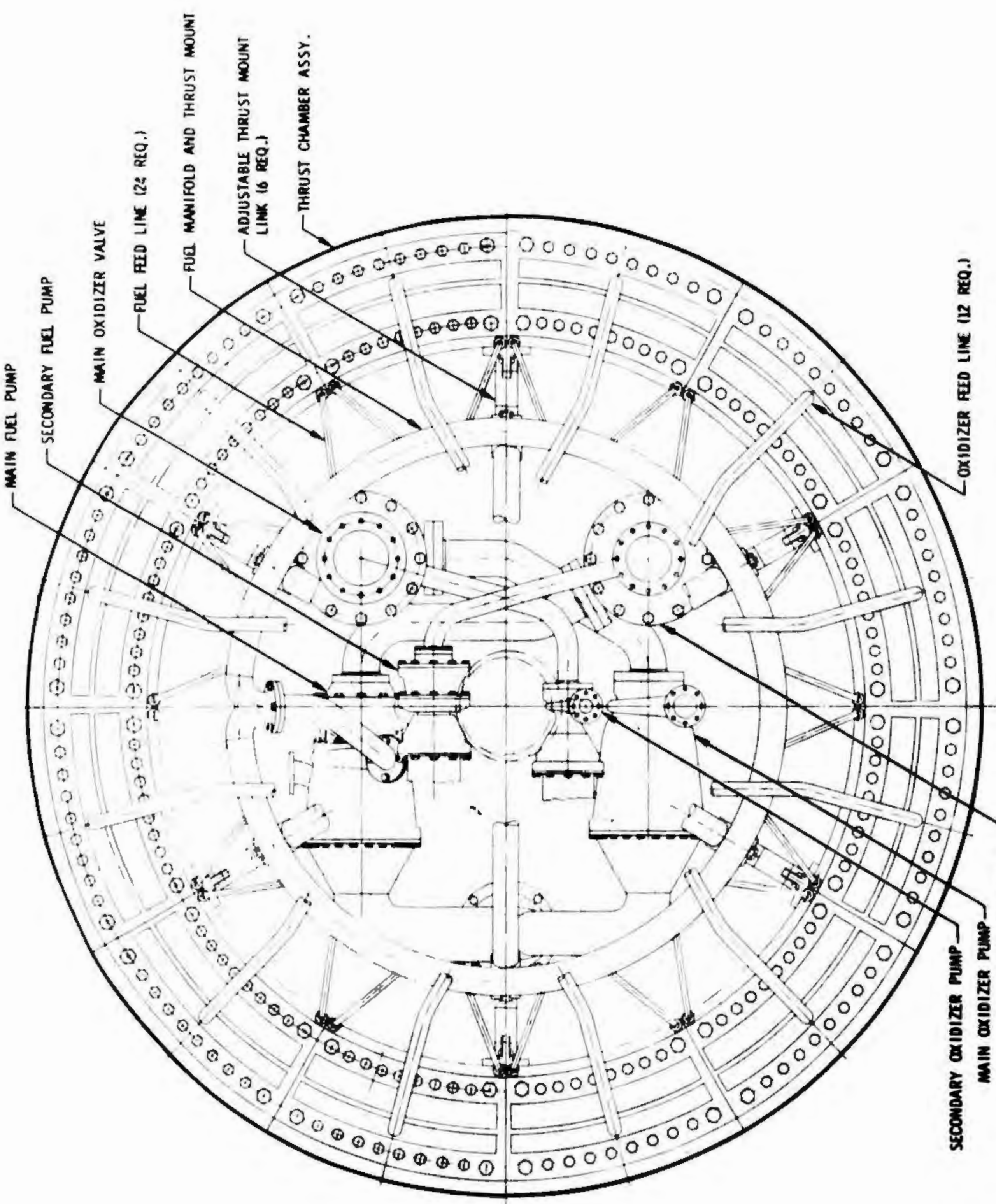

Figure 97. Engine System Packaging (Plan View) (U)

(U) A tabulation defining the heat leak and hydraulic pressure loss of each duct is presented in Table 25. The ducts are designed to be fabricated by standard techniques and practices requiring no special tooling or processes.

TABLE 25

PROPELLANT INLET DUCT PRESSURE LOSSES AND HEAT LEAKS (U)

Engine System	Propellant	Inlet Duct Outside Diameter, inches	ΔP, psi	Q, Btu/hr*
Main	Oxidizer	2.0	2.60	0.63
	Fuel	2.0	0.74	0.78
Secondary	Oxidizer	1.125	2.24	0.24
	Fuel	1.0	0.46	0.45

CONFIDENTIAL

*Not including heat leaks from valve support structure

(2) Fuel Bleed

(U) An analysis was made to evaluate the possibility of using the propellant feed system vent fuel bleed hydrogen for interface cooling, and thus produce an even more efficient heat barrier.

(C) Early in the analysis, use of the vent gas to cool the main and secondary engine fuel pumps was considered. In effect, this would reduce the source temperature on the heat sink side of the fuel line heat barriers. Two benefits would be realized in this approach: (1) a reduction in the heat transfer through the heat barrier, and (2) the fuel pumps would be maintained at a lower temperature during the coast period, thereby reducing the time required to chill the pumps during the start sequence. The secondary engine fuel pump was used in an analysis to evaluate this possibility. Comparing the soakback from the pump discharge duct, turbine exhaust duct, and pump mounts to the total cooling capacity of the coolant for both feed system configurations (GD/C and LMSC) showed that only slight improvements could be obtained.

(C) In the case of the GD/C configuration, where a minimum coolant flowrate of 0.13 lb/hr at 167 R is expected (Ref. 5), the secondary engine fuel pump could be chilled to approximately 300 R using the full flow, but there would be considerably less cooling capacity for chilling the other engine pumps in the series arrangement (Fig. 98). A split-flow arrangement would realize essentially the same results.

(C) In the case of the LMSC configuration, where a coolant flow of 0.0087 lb/hr at 75 R is expected, the effectiveness of the bleed to chill the pumps would be even less. The conclusion was that use of the coolant flow to chill the engine pumps would have a limited benefit.

(C) The second approach evaluated considered using the fuel bleed to intercept all, or a major portion, of the heat load being transported through the barrier. In the current analysis, the heat load considered was that of conduction through the barrier and radiation from the duct interior surfaces. The calculations were conservative in that the entire duct was assumed to be at 500 R for computing the radiated heat addition. Conversely, a linear gradient was considered for computing the heat transferred by conduction. In practice, the heat barrier will require a surface (either insulation or paint) with a low absorbtivity/reflectivity ratio, and the temperature gradient would be approximately linear (i.e., no net heat transfer to or from the surrounding environment).

(C) The heat barriers for the main engine propellant ducts were assumed to be a 7-inch-long, 2-inch-diameter, 0.015-inch-thick wall with a thermal conductivity comparable to that of Rene 41 ($k = 0.00447T + 1.91$ Btu/hr-ft-R). The secondary engine barriers were assumed to be 15 inches long, 1.0 inch diameter, and 0.015 inch wall thickness, of Rene material.

(C) Considering the LMSC configuration, 0.0087 lb/sec of H_2 at a temperature of 75 R is available for cooling the four engine heat barriers. In the case of the oxidizer barriers, the coolant would be at a lower temperature than the desired engine-to-feed system interface (153 R) and could best be

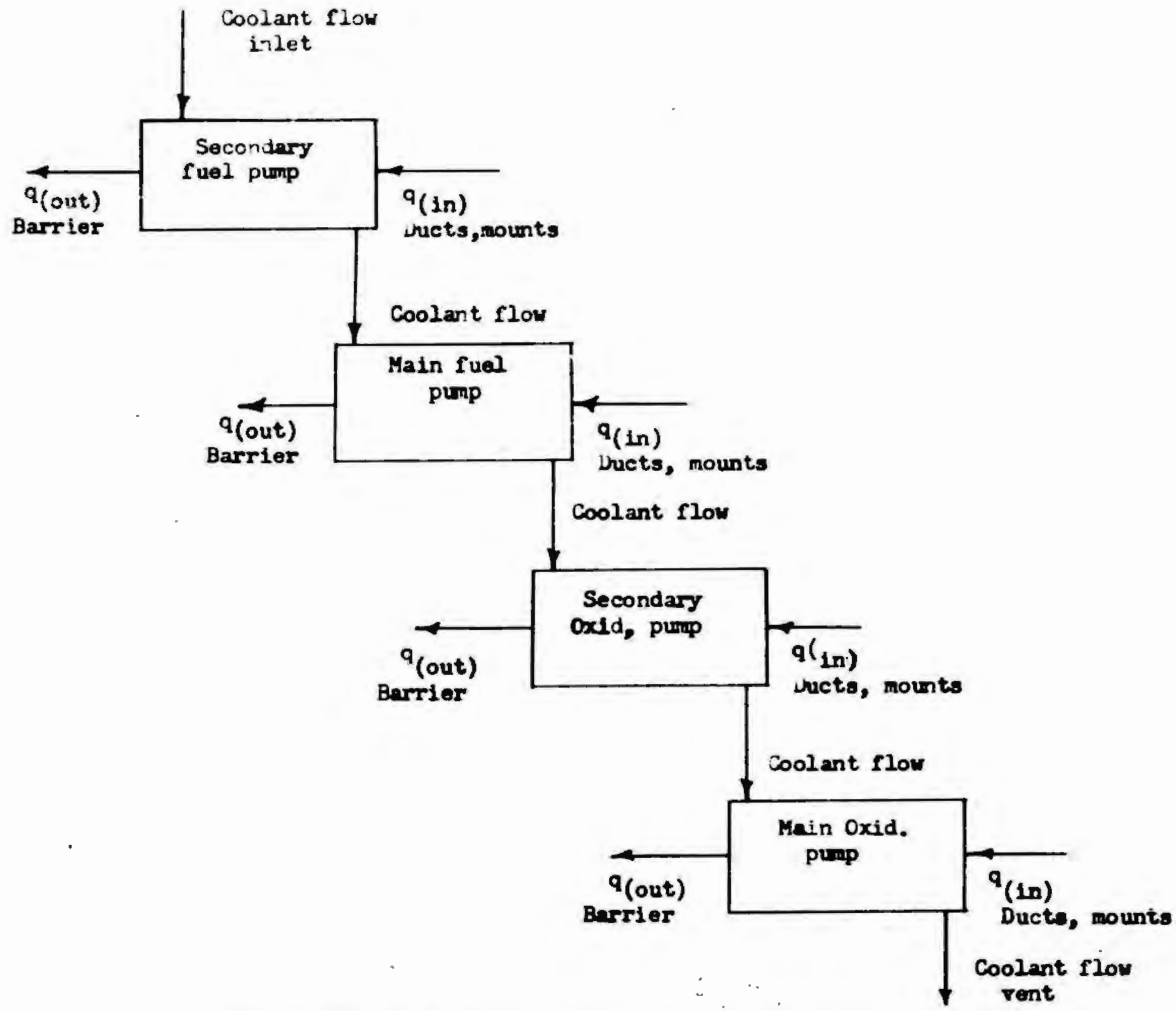

Figure 98. Coolant Flow Utilization for Pump Chill (U)

(C) utilized by chilling the valve end of the heat barriers (cold end) to the 153 R temperature. In doing so, and thereby increasing the coolant temperature to 500 R in the counterflow heat exchanger arrangement (Fig. 100), the analysis showed that approximately 1.43 Btu/hr would be intercepted by conduction from the main engine oxidizer barrier and 0.36 Btu/hr from the secondary engine oxidizer barrier. Also, considering the heat conduction through heat exchanger tubing (0.125-inch diameter, 0.015-inch wall thickness, 15-inch long) added an additional 0.55 and 0.28 Btu/hr to the heat load of the main engine and secondary engine barriers, respectively.

(C) The radiation heat transfer through the duct based on a barrier wall temperature of 500 R was computed to be 2.3 and 0.6 Btu/hr for the main and secondary engine ducts, respectively. Combining the total heat transfer requiring interception (internal duct radiation and wall conduction) totals approximately 5.52 Btu/hr for coolant for both of the oxidizer barriers.

(C) In the case of the fuel duct barriers, the valve and interfaces were assumed to be at 50 R. Because this temperature is less than the available coolant temperature, the total heat load to the fuel interface cannot be intercepted. For the calculation, the heat exchanger chilled half the barrier nearest the pump, making the heat barrier temperature at the mid-point approximately 100 R (Fig. 99). Conduction from the barrier mid-point to the engine/propellant feed system interface was computed to be approximately 0.30 and 0.074 Btu/hr for the main and secondary engine barriers, respectively. The heat load (conduction and radiation) intercepted by the counterflow heat exchangers was computed to be approximately 5.6 Btu/hr (3.3 conduction, 2.3 radiation) and 1.6 Btu/hr (1.0 conduction, 0.6 radiation) for the main and secondary engine barriers.

(C) The total coolant heat load requirement for this approach is the sum of the four individual barriers, or a total of 12.1 Btu/hr. This compares to a 0.0087 lb/hr coolant flow capacity of approximately 12.8 Btu/lh for a temperature rise of from 75 to 500 R.

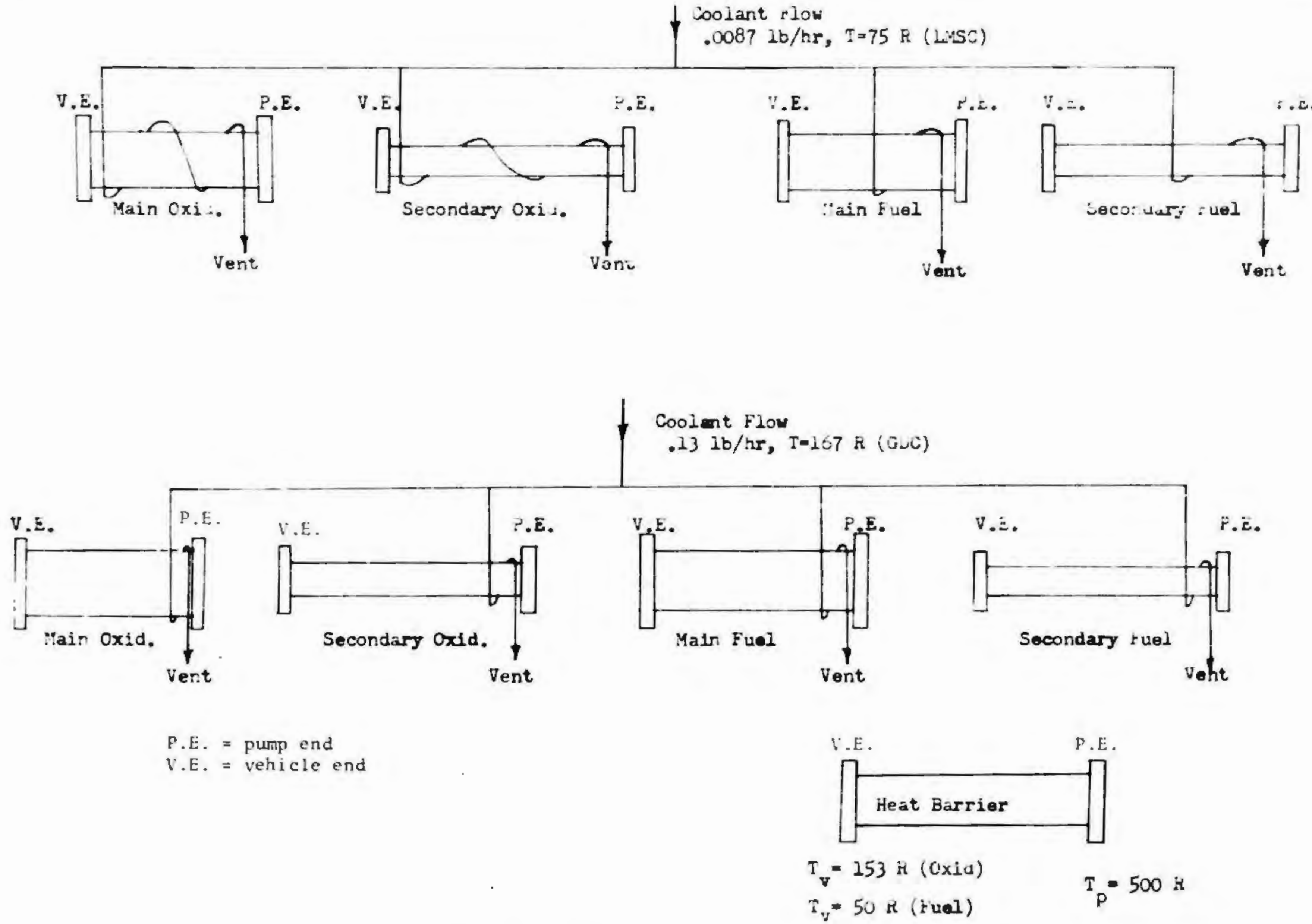

Figure 99. Coolant Flow Utilization for Barrier Chill (U)

(C) In considering the GD/C system, a minimum temperature gradient of 153 to 167 R is achievable in the oxidizer barrier, and 50 to 167 R is available in the fuel barrier. As a result, the analysis considered chilling the pump end of all the barriers (Fig. 99), thereby maximizing the effective length of the barrier temperature gradient and minimizing the heat transfer to the interface. Because of the magnitude of the coolant flowrate (0.13 lb/hr), the pump end of all the barriers could be chilled to approximately 200 R. Consequently, the conduction heat transfer rate to the interface was found to be 0.508 Btu/hr (0.406 main engine, 0.102 secondary engine) for the fuel side and 0.16 Btu/hr (0.13 main engine, 0.03 secondary engine) for the oxidizer side. The internal duct radiation at 200 R produces a negligible heat load contribution at the engine/feed system interfaces.

(U) The conclusion from the analyses was that use of the coolant flows to chill the engine/feed system heat barriers could significantly reduce the heat soakback from the engine to the propellant feed lines. However, based on the propellant feed system analysis conducted by GD/C and LMSC (Ref. 6 and 7), the decision was made to incorporate the heat barriers on the feed system side of the engine/feed system interface. The final engine propellant inlet duct designs, therefore, did not include coolant flow heat exchange devices (Section III,v,5).

s. Static Seal Analysis

(U) The initial engine system concept includes the capability of removing propellant ducting to facilitate inspection and/or removal of components housed in the interior of the main engine thrust chamber torus. With this in mind, an evaluation was made to establish a general philosophy toward seals to be used at the various disconnect joints to permit access

(U) and yet minimize the possibility of leakage. Each joint, however, is to be separately considered during design to determine if the general approach is most suited for the particular joint.

(U) The seals found to best qualify for propellant and turbine system ducting are bobbin seals and pressure-actuated seals (Fig. 100). Both seals produce high unit loads at sealing areas upon installation, which is essential to producing a zero-leakage joint.

(U) The bobbin seal (Fig. 100a) is relatively new at Rocketdyne but has been used with considerable success by other aerospace agencies to produce zero-leakage joints. The major experience with the all-metal bobbin seal has been with duct sizes of 3/4 inch or less. The plastically deformed seal could probably be used in ducts (oxidizer, fuel, and hot gas) with diameters up to 1-1/2 inches.

(U) Pressure-actuated seals (Fig. 100b) have been used extensively at Rocketdyne in virtually all engine system designs. The seals are generally coated with a relatively soft material that deforms plastically on installation. Soft metal coatings would be used on seals for the oxidizer system. Teflon coatings would be used for seals in fuel system applications where temperatures remained below 200 F, and copper coatings would be used for seals in fuel systems where the temperature exceeds 200 F. Some advantage may be realized with the use of pressure-actuated seals because, in some cases, they can be reworked and reused, while the bobbin seal requires replacement after each use.

(U) Standard AN fittings (Fig. 100c) are to be used as instrumentation connections for oxidizer, fuel, and hot-gas systems. Experience with small AN fittings (3/4 inch or less) in these systems has proved satisfactory in previous Rocketdyne and industry applications. The use of standard AN fittings in conjunction with conical copper crush fittings has been particularly successful and would be used in critical locations such as the oxidizer system instrumentation lines.

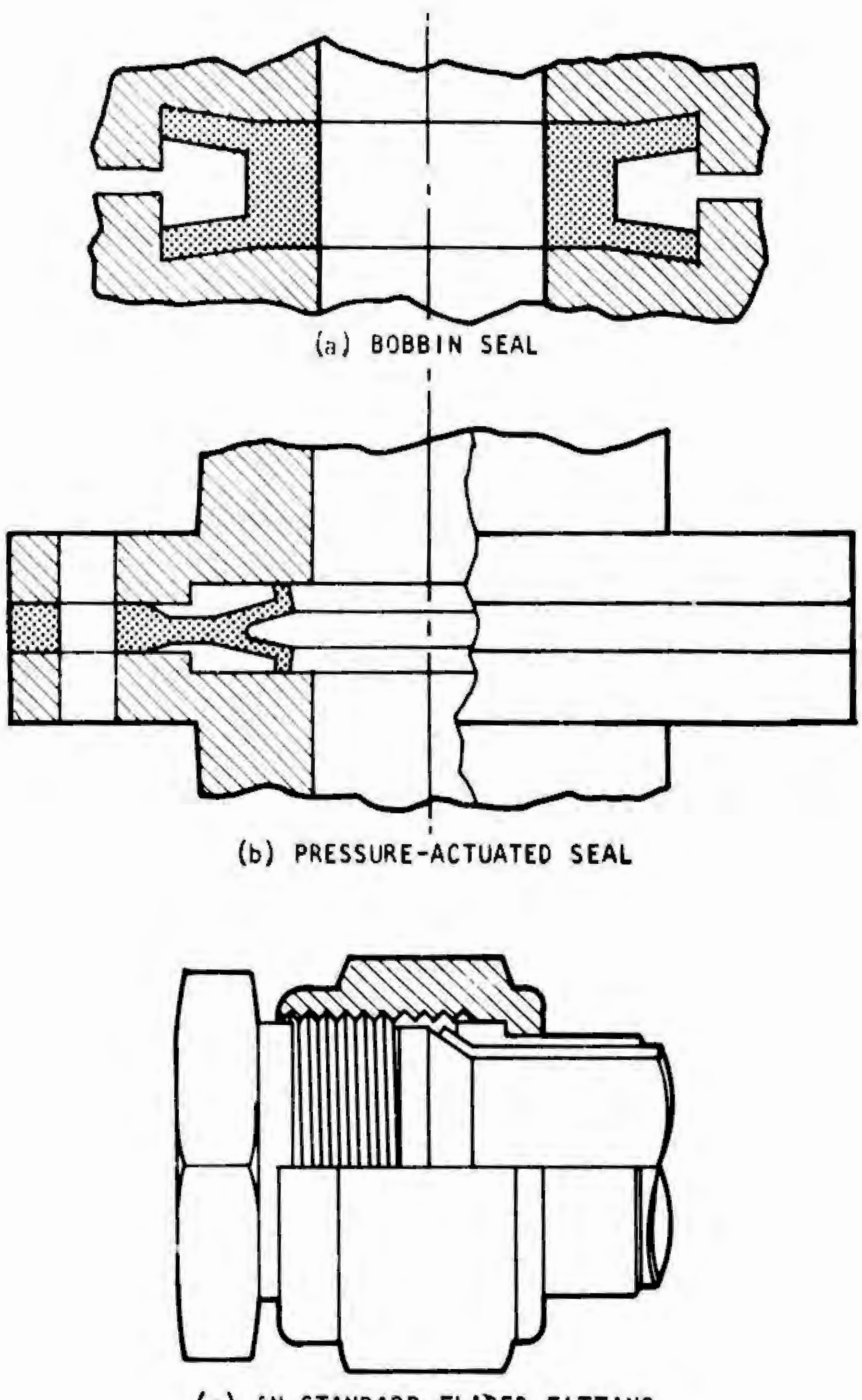

(a) BOBBIN SEAL

(b) PRESSURE-ACTUATED SEAL

(c) AN STANDARD FLARED FITTING

Figure 100. Basic Seal Types Considered for Use in Engine System Connections (U)

(U) Other seals that may have application are metal O-rings and coated, flat, metal gaskets. However, the use of these seals would be limited to special conditions.

t. Heat Exchanger Installations

(U) Analyses were conducted on helium heat exchangers to satisfy the GD/C and LMSC fluorine tank pressurization system requirements. For the LMSC system, a cross-flow heat exchanger was analyzed which fits into the main engine turbine exhaust duct downstream of the Y duct. An analysis was also conducted on a similar type of heat exchanger for the secondary engine. The analysis showed these heat exchangers to be practical and capable of providing the heated helium necessary for fluorine tank pressurization during engine operation.

(U) The Lockheed pressurization system also required heated hydrogen for fuel tank expulsion. The most practical method of supplying this pressurant at the required temperature is to increase the engine hydrogen flowrate, extract a portion of the pressurant flowrate from an appropriate location in the engine cooling circuit, and mix this flow with the remainder of the required pressurant flowrate obtained from the hydrogen pump discharge. The probable locations for obtaining the hot hydrogen are the nozzle coolant inlet manifold and the fuel injection manifold on the main and secondary engine, respectively.

(U) The Convair pressurization system design required a higher helium temperature for fuel tank expulsion. Because of the increased requirement, heat exchangers in either the turbine inlet or exhaust ducts were found to be impractical. A jacket-type heat exchanger on the main engine nozzle coolant exit manifold was investigated and found to be a practical design. This concept takes advantage of the larger flowrate of the hot fluid. The design consists of a single line, through which heated helium flows, which is positioned within the manifold (Fig. 5). Analysis indicates that a similar method can be applied to the secondary engine by placing the tube through the turbine exhaust duct.

u. Oxidizer System Contamination Evaluation

(C) An investigation was made to determine the effects of solid particle contamination of the AMPS engine oxidizer system. The analysis showed that particles larger than 10 microns could cause shutoff valve leakage in excess of the specified allowable value and also could cause damage to the pump seals and bearings. Particles larger than 0.010 inch may also become critical to the injector.

(U) Protection of pump bearings from contamination is important and is accomplished on virtually all other Rocketdyne engine systems. This protection could be accomplished by putting filters (or screens) in the pump bearing coolant passages.

(C) The design practice has generally been not to provide filters in the engine main propellant flow. Instead, manufacturing and transporting processes have been relied upon to produce "clean" propellants for engine use. Considerable effort is also made to ensure engine and feed system cleanliness so that contamination is not self-imposed. This practice was successful during the Rocketdyne Atlas Sustainer Engine FLOX Feasibility Demonstration and during other industry fluorine programs. During one period in the Atlas engine program, a 10-micron absolute filter was used in an oxidizer transfer line for a brief period. Upon removal, no contamination was found in the filter, indicating that the contamination level of a fluorine system can be maintained at a low level.

(U) To provide operational experience with fluorine filters, two 1-inch nominal filters were purchased for the B-4A fluorine test position at the Nevada Field Laboratory. The criteria for this type of filter were established from Ref 8. The filters were designed for low-pressure service and were of the wire-mesh type. The element was fabricated of Nickel 200 wire and had a micron rating of 18 absolute. The housing was fabricated of 300 series CRES. The filters were obtained in a cleaned condition from the Wintec Corporation, Inglewood, California.

(U) One filter was installed in the low-pressure fluorine storage vessel fill line prior to transferring any fluorine into the storage vessel. A total of 4000 pounds of liquid fluorine was transferred through the filter with no problems. The filter was passivated with ambient GF_2 at 60 psig prior to transfer. A transfer flow of 1 lb/sec was maintained with a trailer pressure of 60 psig. The filter was disassembled (Fig. 101) after transfer and some contaminants were found. The contaminants were indicated to be Perlite insulation and Teflon seal material. The success with this type filter indicated that engine system filters can be utilized.

v. Engine System Design

(U) The engine system design (Fig. 102 and 103) was based on a concentric thrust chamber arrangement. The arrangement consists of a main aerospike engine and a secondary bell-type engine. The bell engine is located within the center of the main engine, and both engine exhausts are located along the same axis.

U) As an aid during engine maintenance, maximum accessibility to the engine components has been provided. The engine package has been designed to permit the removal and reinstallation of most components without the task of engine assembly removal.

(U) Wherever possible, the technique of in-place welding of propellant lines has been used. This process has been especially adapted to the oxidizer systems.

(1) Interface Requirements

(U) Interface connections between the main and secondary engines and the propellant feed system may be categorized as structural, fluid, and electrical. The locations and dimensions of the structural mountings and main propellant inlets to the engine system are shown in Fig. 104. Structural connnection for transmission of thrust to the propellant feed system is made at the forward face of the gimbal block. Gimbal actuator attachment is made at two locations 90 degrees apart at locations where the thrust structure attaches to the thrust chamber.

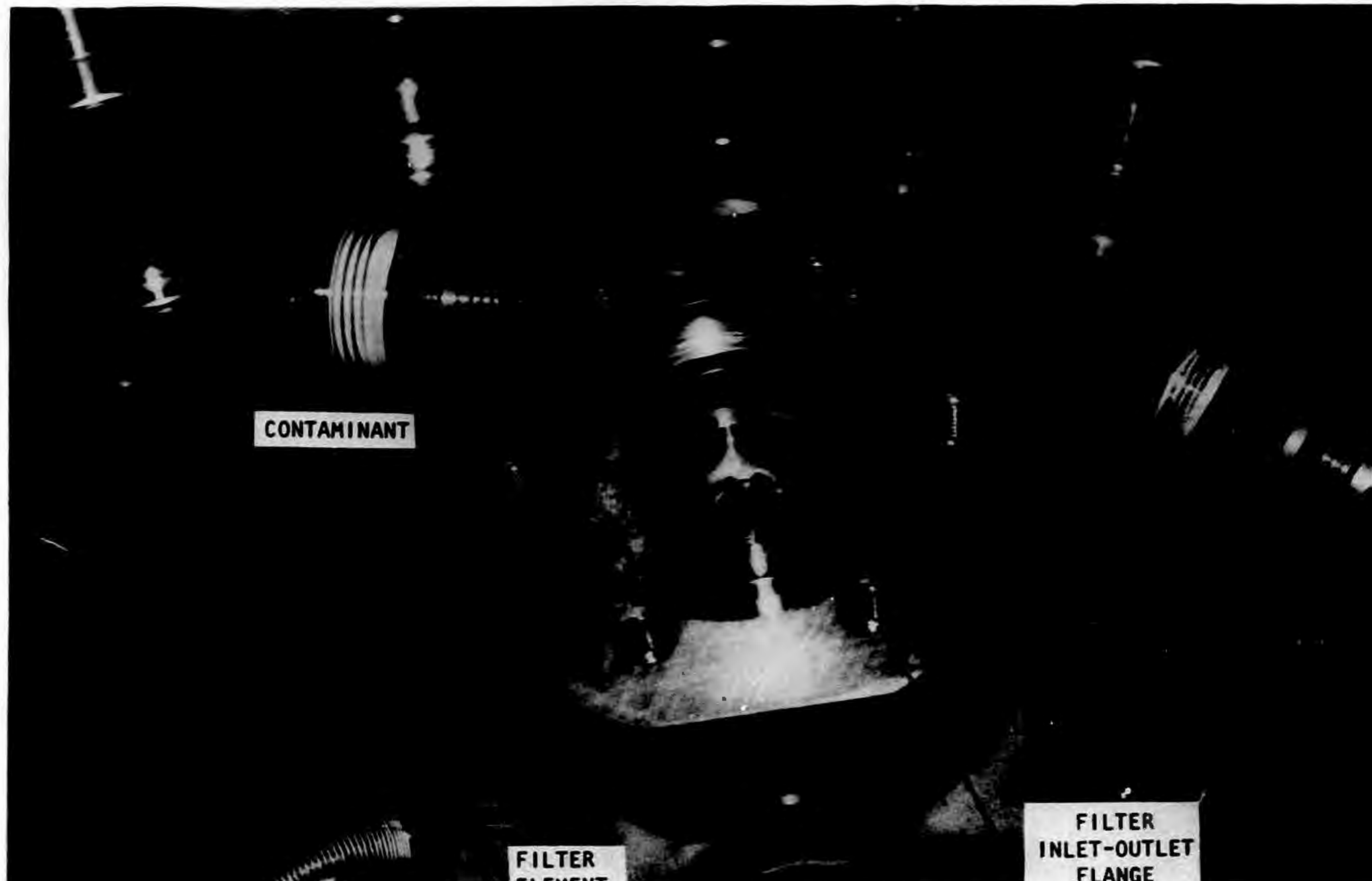

1HZ95-3/24/70-R1A*

Figure 101. Disassembled Facility Fluorine Filter (U)

CONFIDENTIAL

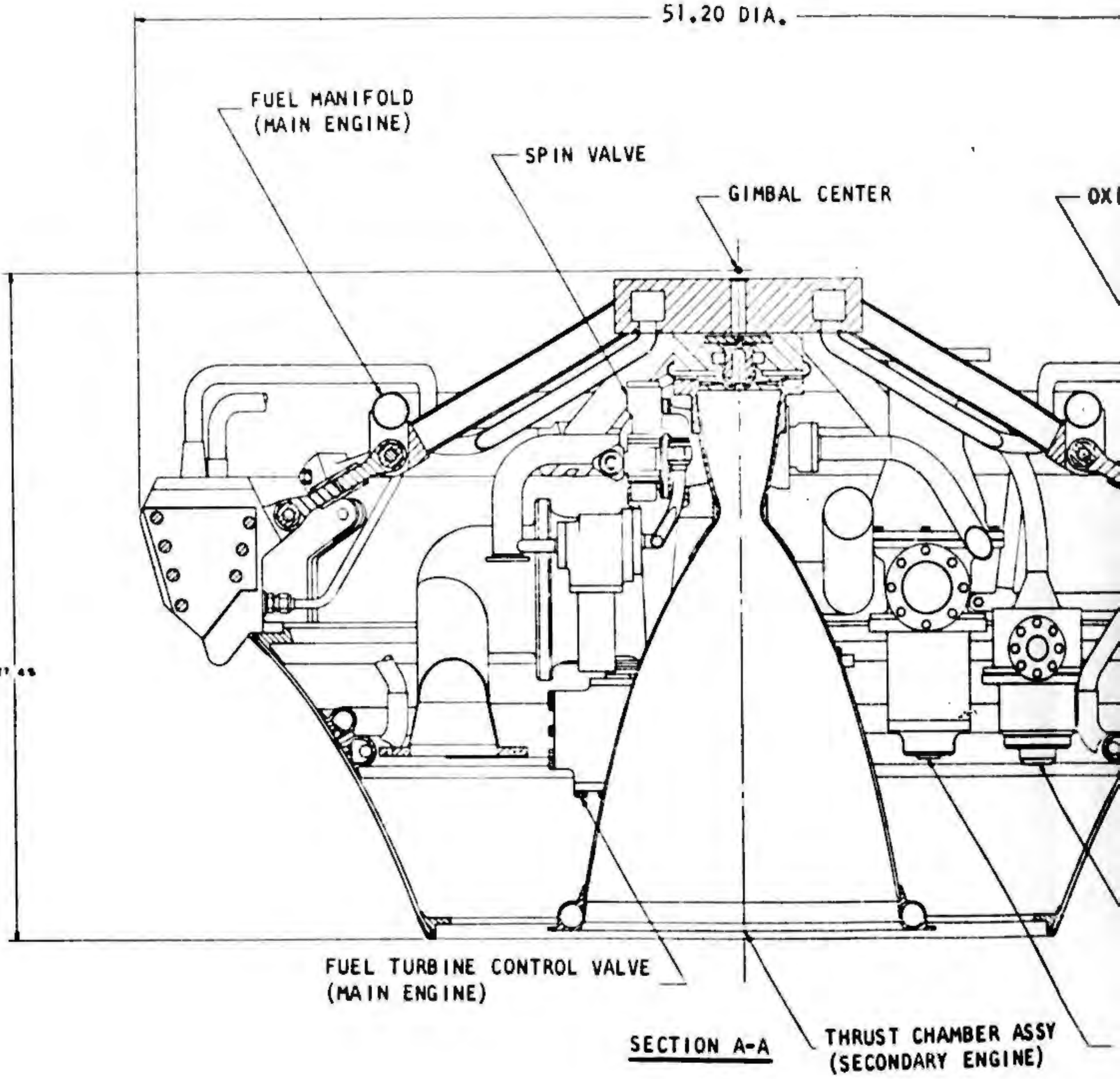

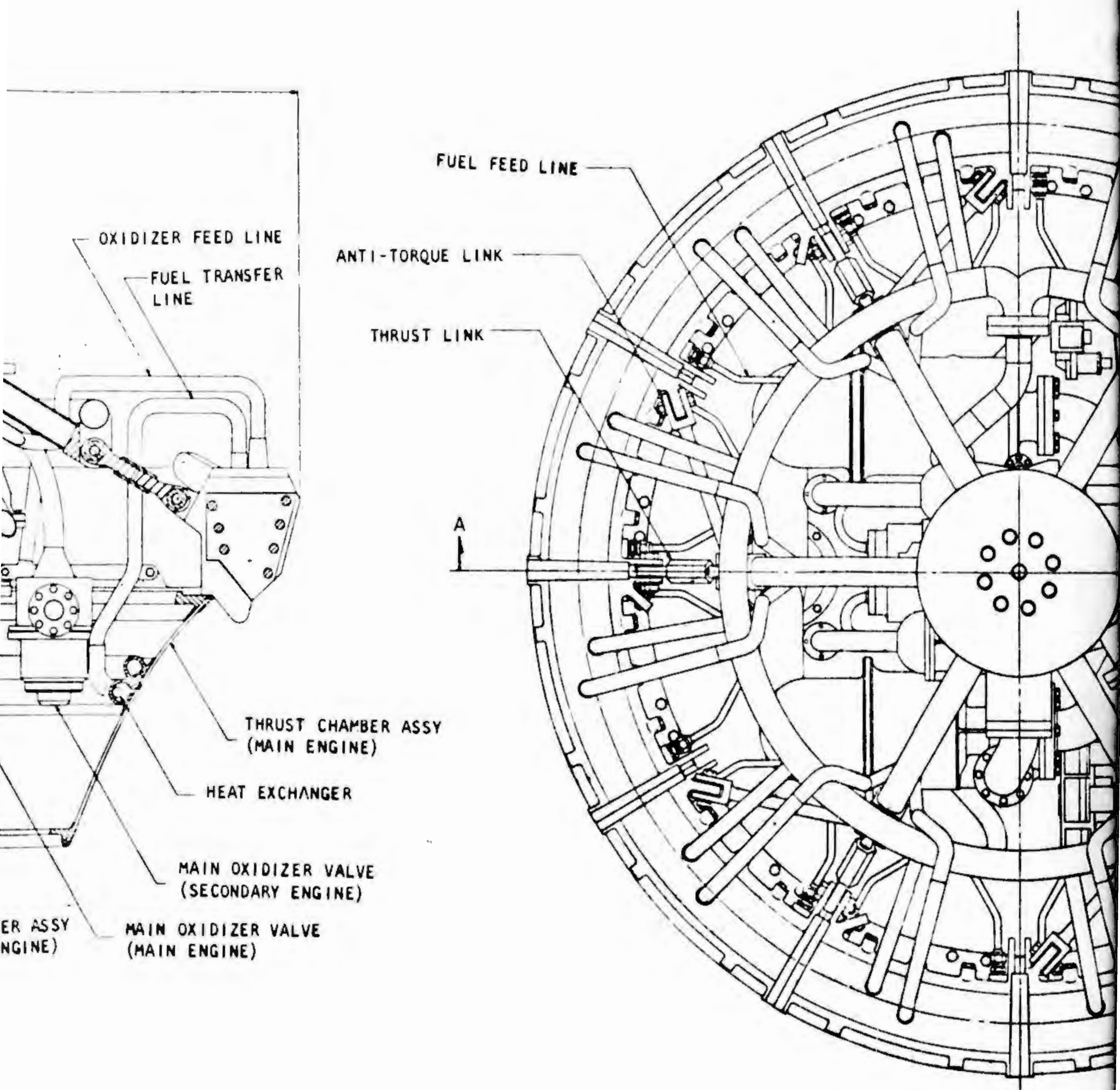

OXIDIZER FEED LINE
FUEL TRANSFER LINE
FUEL FEED LINE
ANTI-TORQUE LINK
THRUST LINK
A
THRUST CHAMBER ASSY (MAIN ENGINE)
HEAT EXCHANGER
MAIN OXIDIZER VALVE (SECONDARY ENGINE)
ER ASSY
NGINE)
MAIN OXIDIZER VALVE (MAIN ENGINE)

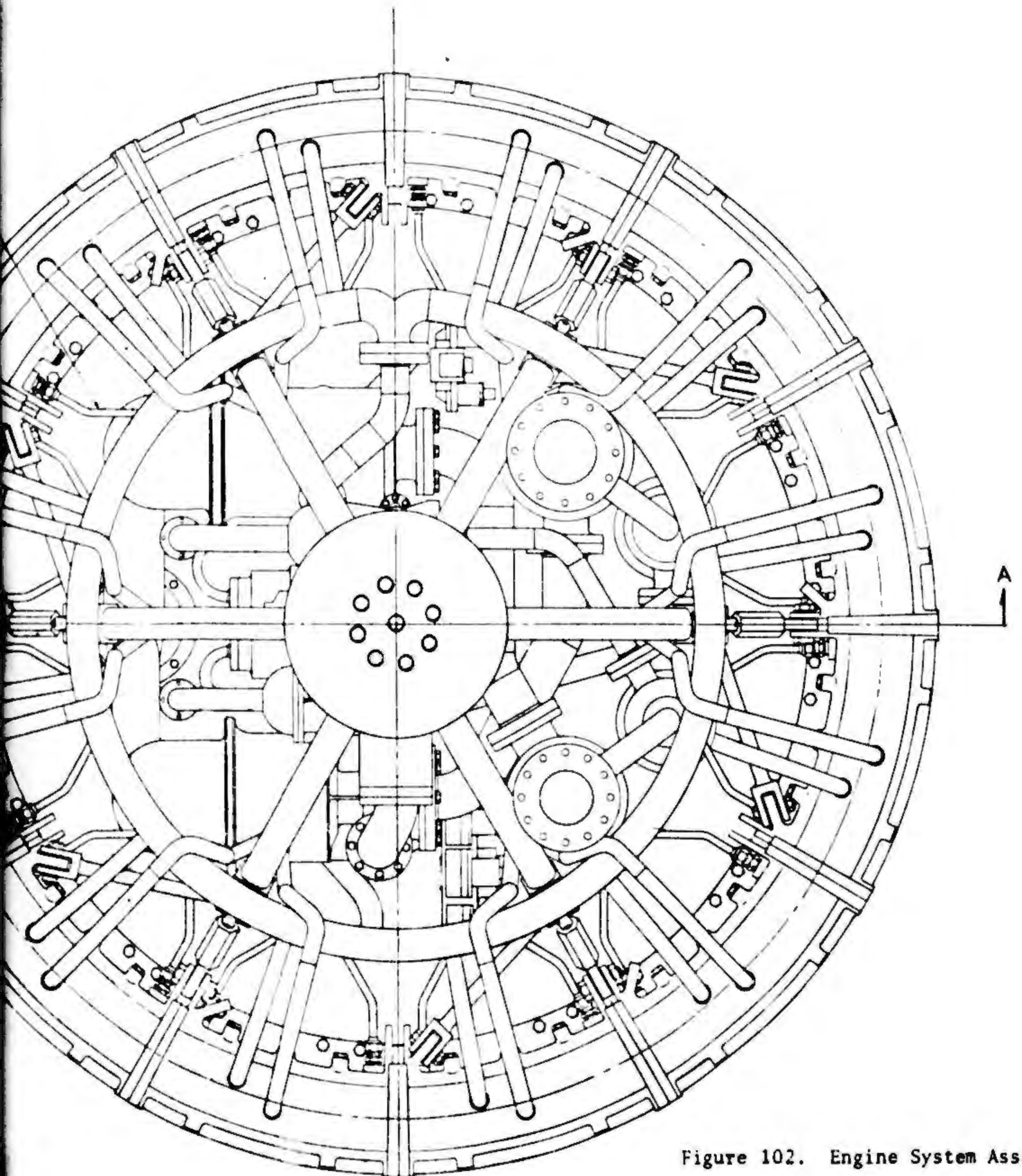

Figure 102. Engine System Assembly (U)

3

CONFIDENTIAL

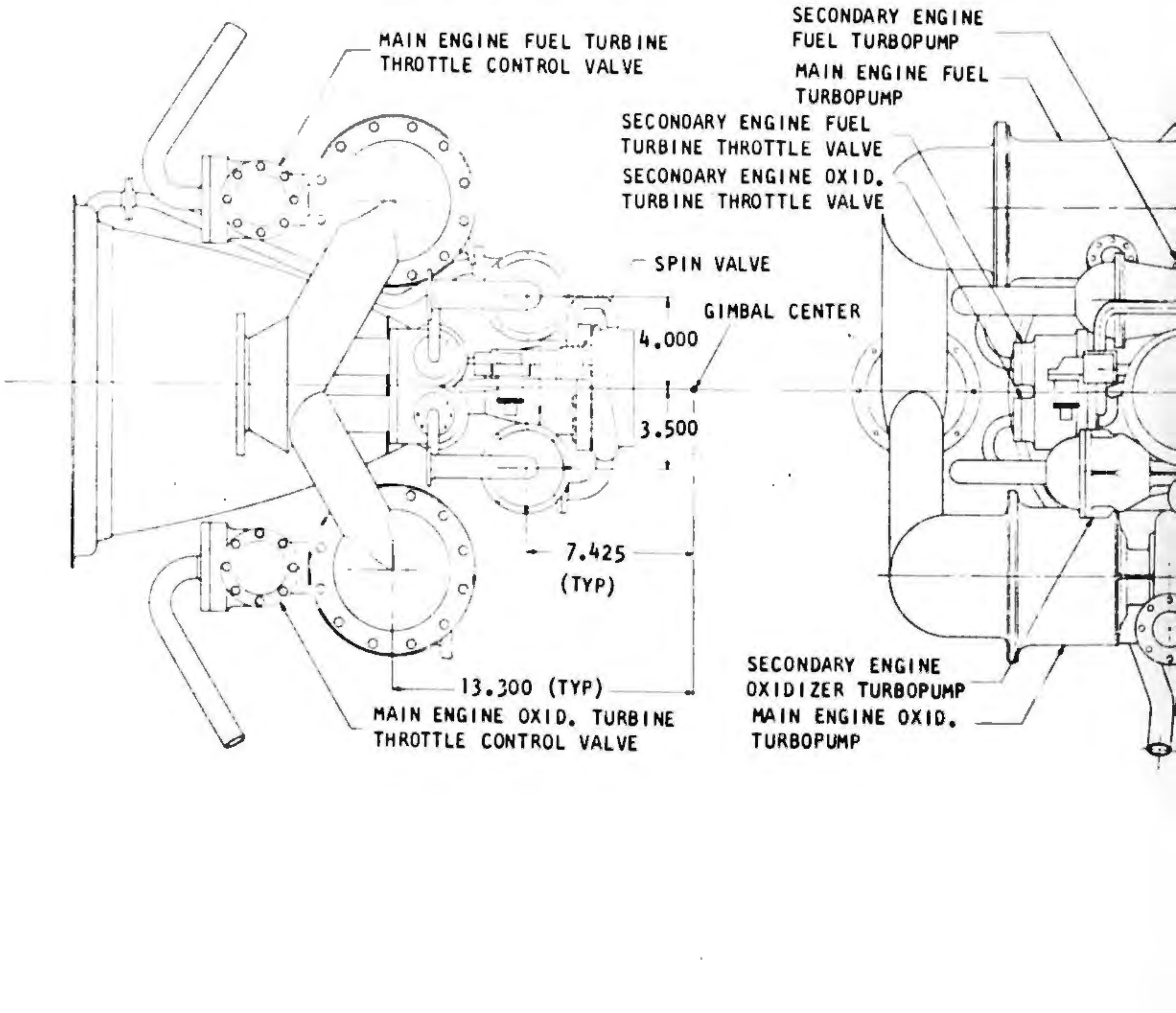

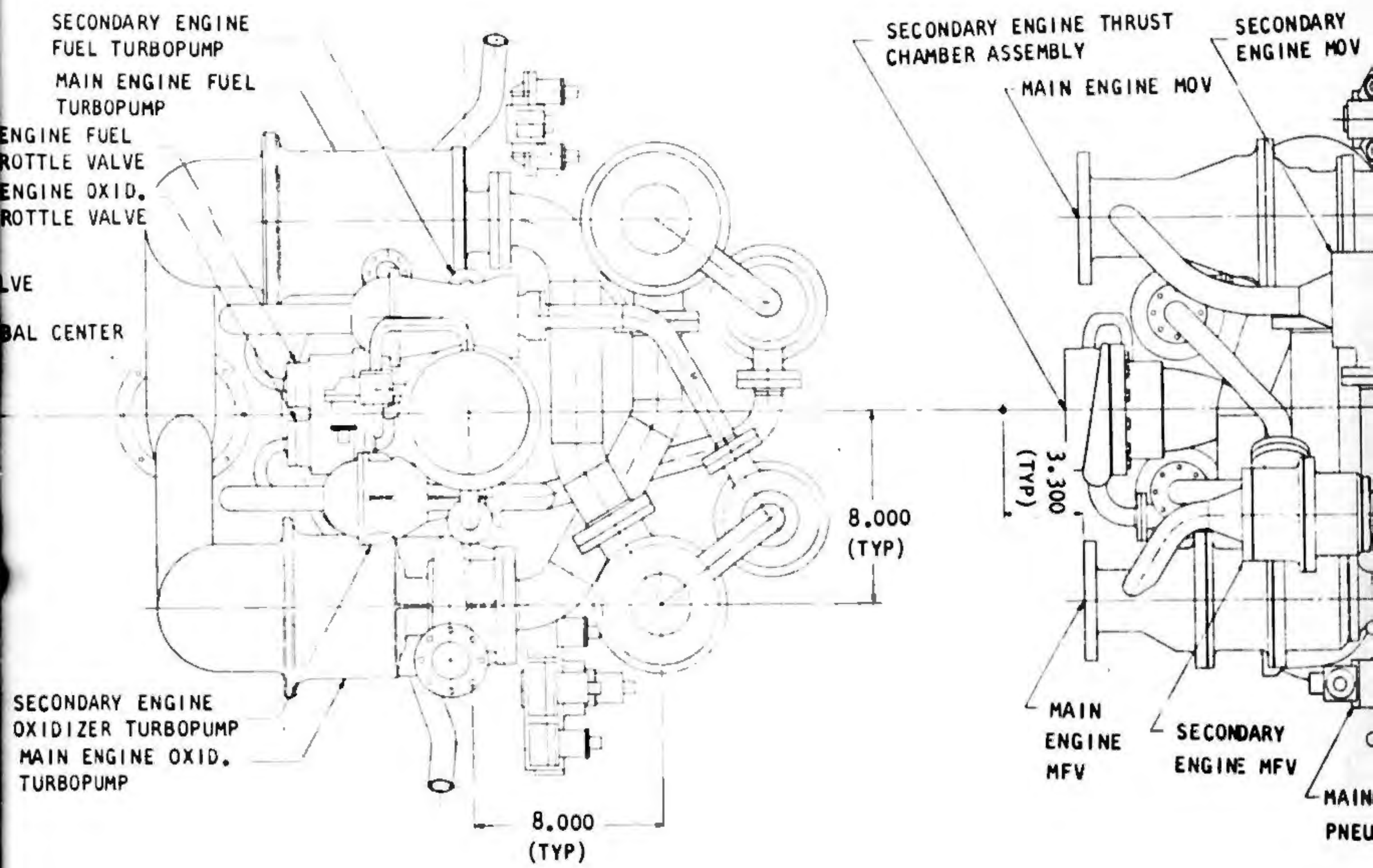
SECONDARY ENGINE
FUEL TURBOPUMP
MAIN ENGINE FUEL
TURBOPUMP
ENGINE FUEL
ROTTLE VALVE
ENGINE OXID.
ROTTLE VALVE
LVE
BAL CENTER
SECONDARY ENGINE
OXIDIZER TURBOPUMP
MAIN ENGINE OXID.
TURBOPUMP
8.000
(TYP)
8.000
(TYP)
3.300
(TYP)
SECONDARY ENGINE THRUST
CHAMBER ASSEMBLY
MAIN ENGINE MOV
SECONDARY
ENGINE MOV
MAIN
ENGINE
MFV
SECONDARY
ENGINE MFV
MAIN
PNEU

2

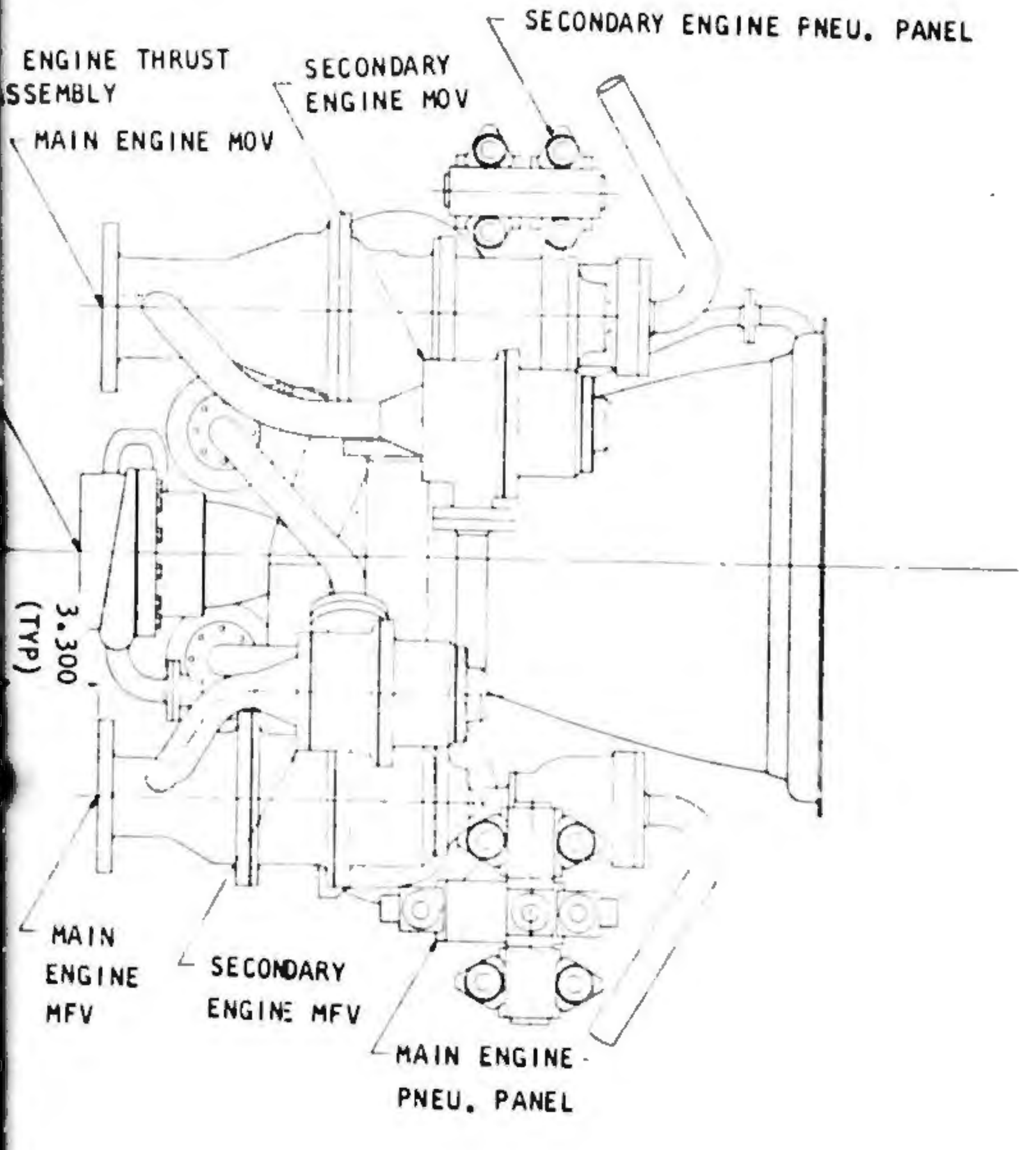

Figure 103. Engine System Packaging Layout (U)

CONFIDENTIAL

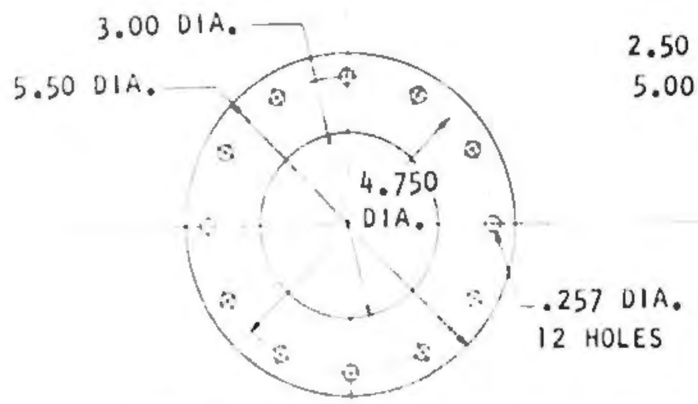

OXIDIZER INLET FLANGE DETAIL

FUEL

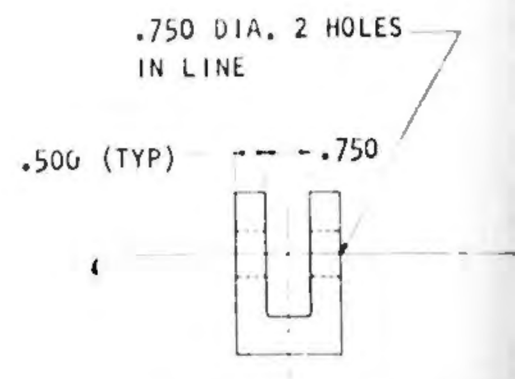

GIMBAL ACTUATOR ATTACHM

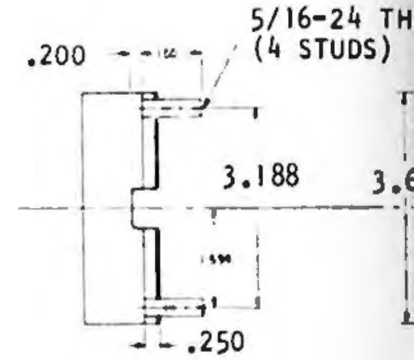

GIMBAL BEARING VEHIC

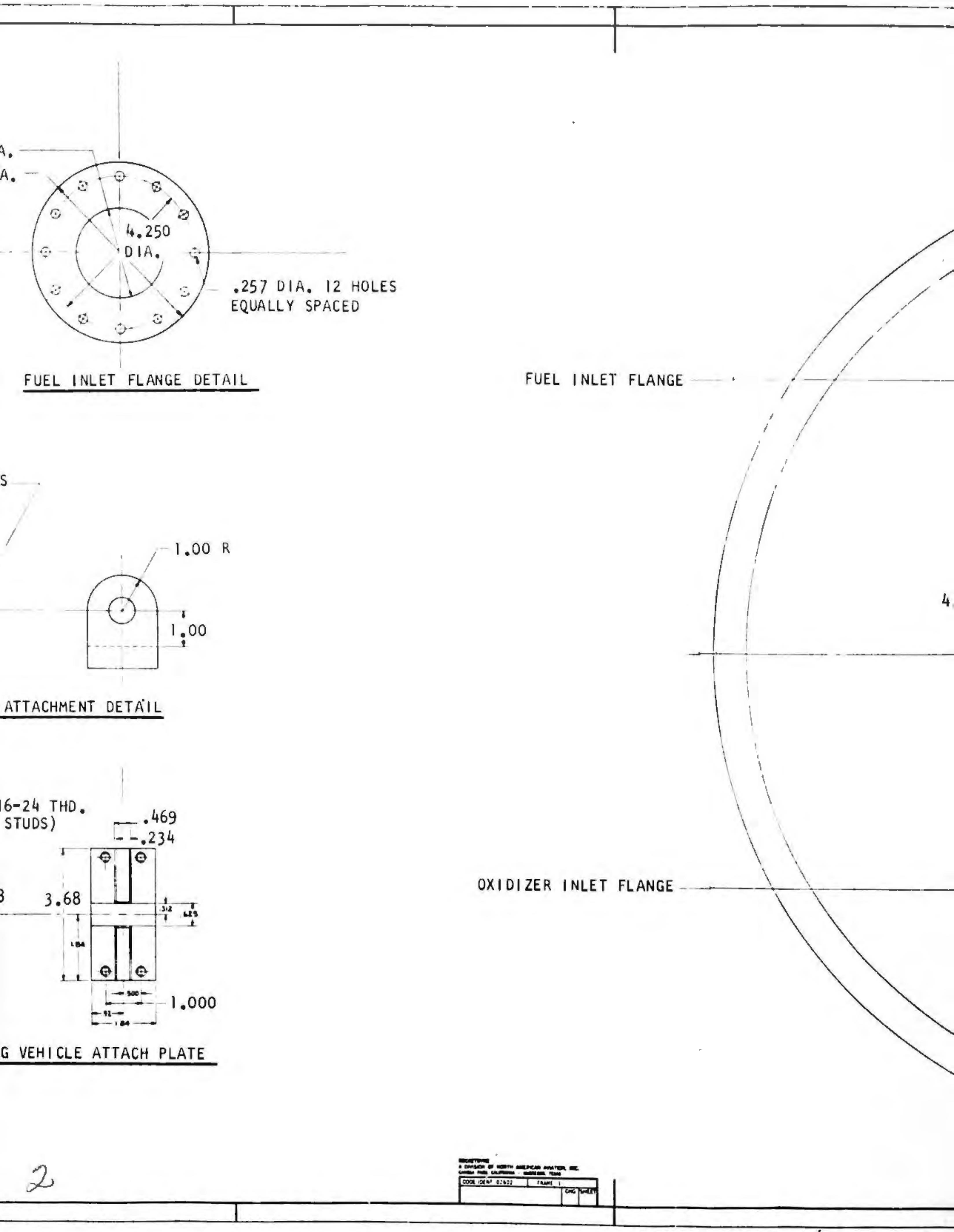

A.
A.
4.250
DIA.
.257 DIA. 12 HOLES
EQUALLY SPACED
FUEL INLET FLANGE DETAIL
FUEL INLET FLANGE
S
1.00 R
1.00
4
ATTACHMENT DETAIL
16-24 THD.
STUDS)
.469
.234
3
3.68
1.000
OXIDIZER INLET FLANGE
G VEHICLE ATTACH PLATE
2
FRAME 1

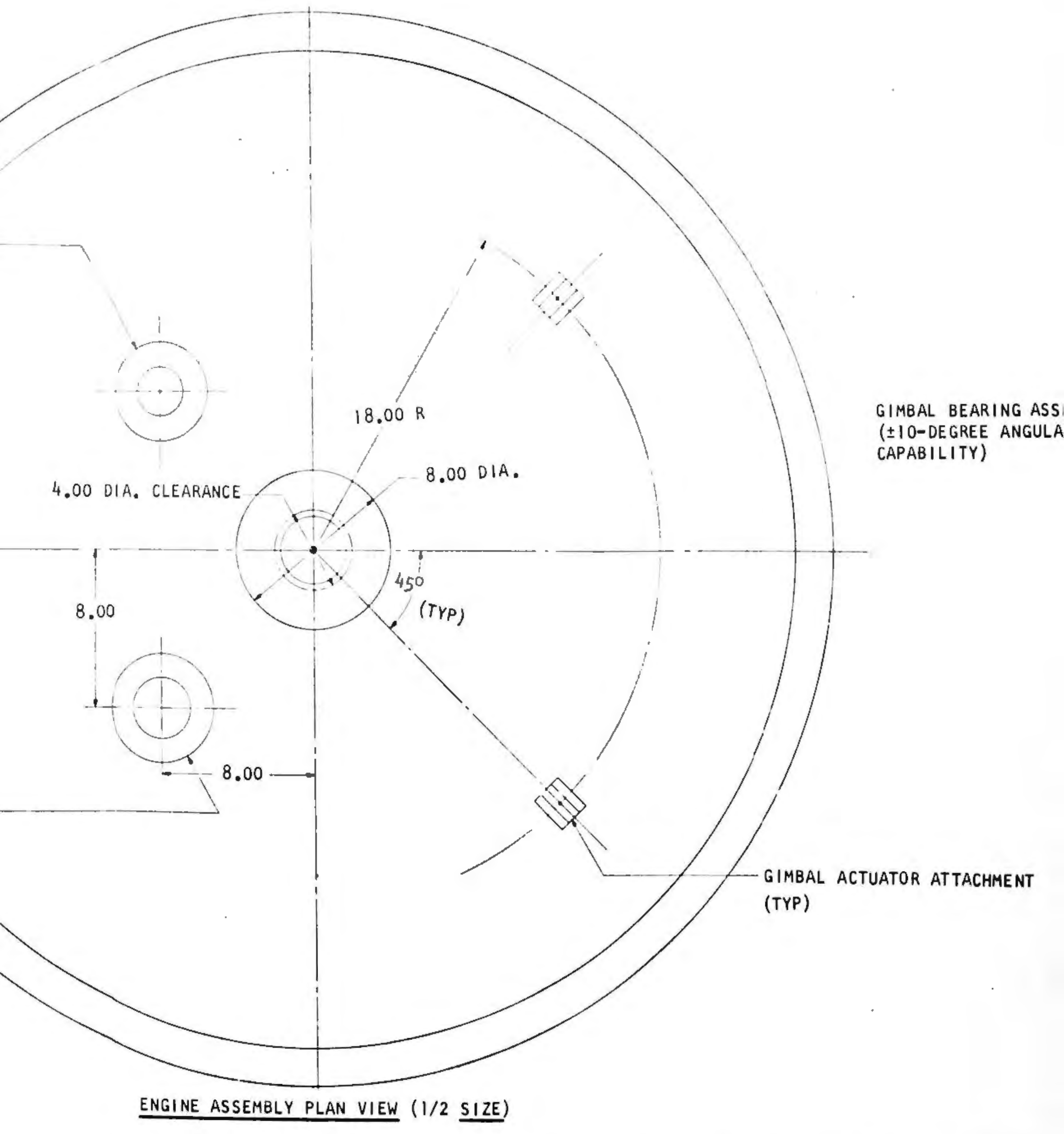

ENGINE ASSEMBLY PLAN VIEW (1/2 SIZE)

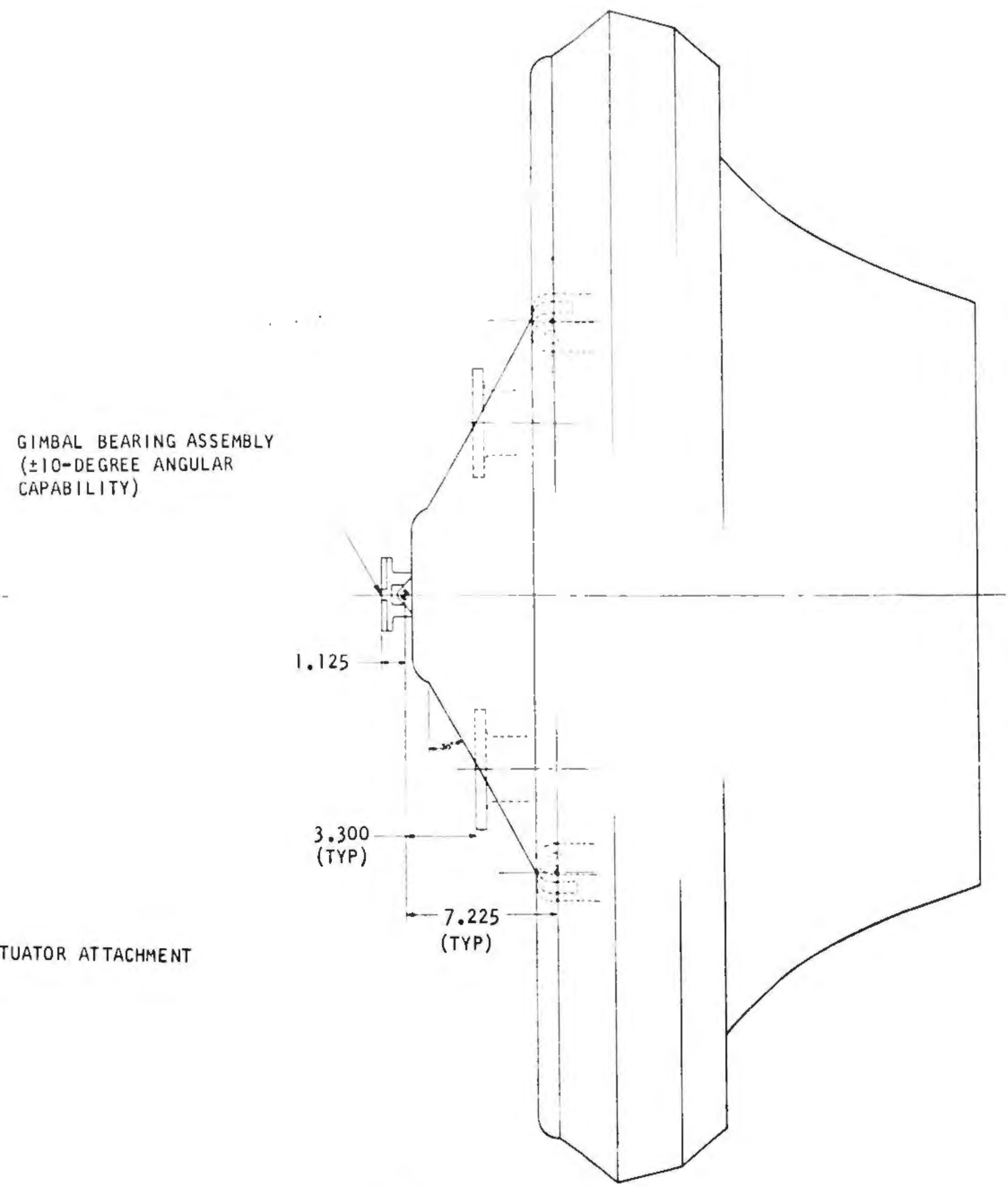
GIMBAL BEARING ASSEMBLY
(±10-DEGREE ANGULAR
CAPABILITY)
1.125
3.300
(TYP)
7.225
(TYP)
TUATOR ATTACHMENT

4

Figure 104. Engine-to-Vehicle Interfaces and Locations (U)

CONFIDENTIAL

5

(U) Single fuel and oxidizer ducts interface with the propellant feed system to deliver propellants to both engines. These interfaces are located at the main valve inlets upstream of the turbopumps.

(2) Thrust Mount

(U) The engine system thrust mount is a welded tubular assembly which includes the propellant manifolds for the main engine. The physical design is best described by referring to Fig. 102. In this illustration, a cross-sectional view and a plan view are shown. The thrust mount assembly extends from the thrust links to the gimbal interface.

(U) The six tubular members attached at the two propellant manifolds are the basic structural members of the assembly. To increase the stability of the assembly and prevent independent member bending, the fuel manifold was attached to the extreme ends of the structural members providing a tension tie. End clevis are welded to the member ends and the fuel manifold. These provide the means for attaching the thrust links and the antitorque rods.

(C) The thrust mount is designed to be structurally capable of withstanding a load of 7 g from any direction while simultaneously transmitting the maximum thrust load and maintain an overall safety factor of 1.3 with regard to the material yield strength. To be compatible with the design philosophy of minimum cost and neglecting the increased weight, the material selections favored the type 321 CRES. However, for the structural members and the oxidizer manifold,it was found to be advantageous to use the INCO 718 and heat treat it.

(U) The location of the oxidizer manifold was governed by the objective of obtaining the smallest manifold diameter, thereby minimizing the amount of upstream oxidizer at engine cutoff. Equal propellant distribution is achieved by contoured internal flow passages coupled with the inherent downstream resistance of the manifold fixed lines. To minimize flow disturbances at the manifold inlet, the entrance velocity was reduced to a minimum. Provisions for the mounting of a gimbal bearing to the interface surface of the manifold plate include recessing the bearing approximately 1-1/2 inches

(U) within the plate. Because of the negative thermal growth which is expected to be encountered, the manifold fixed oxidizer delivery lines are designed to deflect.

(U) The fuel manifold is designed as a constant-area torus with 24 outlets. Flow resistance is less than 1 percent of the total cooling jacket resistance.

(3) Main Valve Supports

(C) To prevent excessive propellant boiloff by heat conducted to the valves, the valve support system adopted by each main valve was designed as a thermal resistor. An investigation indicated the most suitable approach was a series of struts fabricated from a low thermal conductive material. Teflon FEP (fluorinated ethylene propylene) was chosen as the material, because it possesses a low thermal conductivity and is usable over a temperature range of -420 to 500 F. (An average value of K over this temperature range is 0.012 Btu/hr-in.-F.) Structurally the system is designed to support each valve as a free body (7-g load) by arranging the struts of each valve support system to resist rotation in three planes and translation in three planes. Each system contains a grouping of three struts, two struts, and one strut to accomplish stability.

(U) Each strut is formed from Teflon tubing with end plugs of solid Teflon spin welded at the tube ends and to which CRES clevis are attached by riveting. Various methods and cements were investigated to join the tubing directly to the CRES, but each required some development to ensure its integrity.

(4) Heat Exchanger

(U) A vast difference in the requirements of the two feed system contractors for heated helium prevented the use of one heat exchanger design suitable for both systems. Heat input required by Lockheed is 17.5 Btu/sec and the Convair system requires 80.5 Btu/sec. An external heat exchanger fitted into the turbine exhaust ducting appears to be almost impossible when considering the Convair conditions. The design which appears most suitable is a single tube submerged in the collector manifold of the aerospike nozzle. Depending on the feed system being considered, the

(U) length of the submerged tube will vary. All of the ground rules and analyses were based on the engine operating at the full thrust condition.

(5) Propellant Inlet Ducts

(U) The propellant inlet ducting, located between the main valve discharge and the turbopump inlet, is designed to resist heat flow to the main engine valves in addition to transporting the fluid. Based on the desired heat barrier characteristic, the ducts were designed with a maximum length, and a minimum wall thickness, and fabricated from a material of low thermal conductivity. Material investigations resulted in the selection of Hastelloy tubing as the design material for the ducts. This material has a relatively low thermal conductivity when compared with most of the metals and is compatible with the oxidizer. Much consideration was given to a design which formed the ducting from a plastic material with an oxidizer-compatible metallic liner. The design was abandoned when the practical limitations of fabrication influenced the liner wall thickness to an extent that the thickness approached that of a metallic duct.

(U) Each inlet duct is subjected to the relative thermal growth of the turbopump and the corresponding main valve. Because the turbopumps supports include the turbine exhaust duct and the propellant discharge duct, the relative thermal growth to which the inlet ducts are subjected is sufficient to induce internal duct stresses which approach the material yield strength. To relieve these stresses, a section of flexible metal hose was included in each duct design. The flexible section is constructed from CRES as a one-ply convoluted metal hose.

(6) Turbine Exhaust Ducts

(U) In addition to functioning as the exhaust duct to service the turbopump, this component coupled with the discharge duct reacts the major turbopump loads as members in the turbopump mounting system. Therefore, the thermal

(U) growth of the two ducts must be compatible with respect to each other. A material investigation showed that, by using titanium as the exhaust duct material and CRES as the discharge duct material, the differential thermal growth of the two materials was made negligible. In addition, the titanium exhibits the desired mechanical properties required for the duct to serve as a mount member for the turbopump.

w. Engine Design Approach for a Manned Application

(U) A limited analysis was conducted to evaluate the AMPS engine system for manned application. The role of man in spacecraft during previous programs has been primarily for the purpose of exploring man's behavior and capabilities in a space environment. A logical assumption is that for the AMPS, the relationship of man to the engine can be made to be more functional, not only in a control mode, but also in troubleshooting and maintenance modes. In this respect, full advantage should be taken of the fact that there are certain tasks he can perform to improve the overall reliability of the engine.

(U) In previous programs, the pilot has been given some tasks to perform in engine control (X-15) and initiation of sequences (X-15 and Gemini), both of which have produced successful results. In the case of AMPS, situations will arise where an engine restart or other compensation could be achieved following a malfunction if proper diagnosis can be accomplished by the pilot. The important factor in this respect is time, in which the AMPS mission has an advantage of being several orders of magnitude longer than the X-15 mission. Tasks requiring this kind of time were performed by astronauts during the Gemini flights, and, in the case of one flight, equipment repair was accomplished. Because of this factor, considerable more reliance can be placed on the pilot and crew of the AMPS to evaluate, inspect, and possibly repair malfunctions experienced in the engine

(U) system. Maximum engine reliability is achieved only if the engine can be maintained operable throughout the entire mission (i.e., to start, control, and stop the engine safely on command). In other words, in the event of an engine component malfunction, the safety of the pilot and integrity of the engine and vehicle are dependent on the ability to shut the engine down safely so that a diagnosis can be made, corrective measures taken, and the engine restarted. With these ideas in mind, the following philosophy is presented as an approach to completing an engine design for the manned AMPS vehicle:

1. Redundancy will be considerable in all hardware that controls or performs critical functions, e.g., electrical control systems, pneumatic control systems, and check valves. However, redundancy, in itself, does not guarantee higher system reliability; therefore, care will be taken so that, by adding additional components, the overall system reliability is actually increased.

2. As an extension of the redundancy concept, methods will be considered in which valves can be actuated and controlled by secondary systems in the event the primary system is inoperable; e.g., in the event pneumatics are lost or the electrical system malfunctions in the main engine control system, a secondary system (possibly the secondary engine system) could be used to control the main engine.

3. Desensitize the effect of any one failure on the integrity of the engine as a whole, e.g., consider (1) a design for the turbopumps that can safely operate with excessive shaft seal leak (including adequate structural design and isolation of turbine seal and oxidizer seal leakage) and (2) fail-safe shutdown methods for the engine shutoff valves and secondary control methods for the turbines.

4. Evaluate alternate start, cutoff, or control procedures (in cases where particular components are inoperable) that can be safely substituted without serious compromise to the engine integrity. This capability may result in provisions for an override control shutoff and control valves.

5. Evaluate devices that would limit the possible operating range of the engine within the range of hardware integrity, e.g., (1) maximum engine thrust can be limited to a designated value over the full thrust point by limiting the wide open area of the oxidizer and fuel turbine control valves; (2) turbopump shaft speeds could be monitored for maximum speed conditions; and (3) maximum engine mixture ratio could be limited by making the appropriate feedback from the mixture ratio signal to the fuel and oxidizer turbine control valves.

6. Utilize component design concepts that are not only compatible with the advanced concept of the AMPS engine but also are proved concepts. For example, miniaturized electronic equipment (solid state) has been used successfully in other Rocketdyne engines and could be used in the AMPS engine to provide high reliability in redundant networks without significant weight penalty. Minimization of shutoff valve leakage is important to conserve propellant and, in the case of the oxidizer valve, not to compromise the engine integrity. Because of the nature of the oxidizer, some advancement of the state of the art will probably be accomplished in both actuators and seals; however, in the case of the fuel shutoff valve and turbine control valves, existing designs are to be considered from the standpoint of weight and reliability in similar applications. Potential leakage points are to be minimized through judicious selection of methods for joining components (welded where possible).

7. Pilot control of the engine requires an engine control panel in the cockpit with sufficient displays to make man a functional part of the engine. For example, engine start and cutoff sequence displays would provide the pilot with considerable information concerning functional behavior of the engine components. A display of this type would have to be simple. The panel would

contain the necessary controls to perform individual component or complete engine checkout. Also provided would be the capability for the pilot to override the automatic control system so that alternate procedures can be accomplished. Among these procedures are changing the opening sequence of the main valves, turbine control valves, and purge control valves. If the pilot can do nothing about the malfunction, however, there may be no good reason to provide a cockpit monitor of the particular function.

8. Malfunction warning devices are to be considered for engine components. In this respect, consideration must be given to the component failure mode and the most probable failures. These components and failure modes must not only be identified, but instrumented to provide a warning of the malfunction.

(U) Although the engine for the manned AMPS is of primary consideration in this discussion, most of the philosophies presented here are not necessarily unique to the manned application but, also, are applicable to any highly reliable engine. Aside from the equipment specifically attendant with the cockpit control, the basic engine for manned and unmanned applications will be interchangeable.

x. Engine System Components Failure Mode and Effect Analysis

(U) A failure mode and effect analysis was performed for all major component designs. The analysis is presented in the appendix and includes the results for the engine system as well as for the thrust chamber assemblies, turbopump assemblies, and controls.

SECTION IV
THRUST CHAMBER ASSEMBLIES

(U) The primary purpose of this effort was to conduct analyses and provide design layouts of the main and secondary thrust chamber assemblies for the engine system. A concurrent critical component development program was conducted within Task II to evaluate candidate main thrust chamber designs and provide experimental data and verification of selected concepts. Results of the Task II testing were incorporated into the Task I main thrust chamber analysis and design effort.

(U) This task consisted of two main items:

1. Main thrust chamber assembly analysis and design.
2. Secondary thrust chamber assembly analysis and design.

1. MAIN THRUST CHAMBER

(C) At the beginning of the program, a re-evaluation of the proposed main thrust chamber assembly design philosophy was conducted which resulted in the selection of a different design approach than that originally proposed. The review indicated several primary areas of concern: (1) that major development tasks would not be encountered until late in the Task II test program and potentially without time for subsequent action, (2) that the planned segment configurations of Task II resulted in limited possibility of reuse of hardware in subsequent complete thrust chamber testing, and (3) testing performed on an aerospike thrust chamber in another development program, concurrent with the initiation of the AMPS program, resulted in a circumferential mode of instability, apparently unrestrained by a short, subsonic baffle (tip upstream of throat configuration) (Ref. 22). In addition, the use of subsonic baffles on the AMPS main engine chamber design could result in boundary layer disturbance downstream of the baffle with resultant higher throat heat flux. To overcome the potential problems and simultaneously gain the flexibility inherent in a building-block approach to the full thrust chamber design, a segmented thrust chamber concept was adopted (Fig. 105).

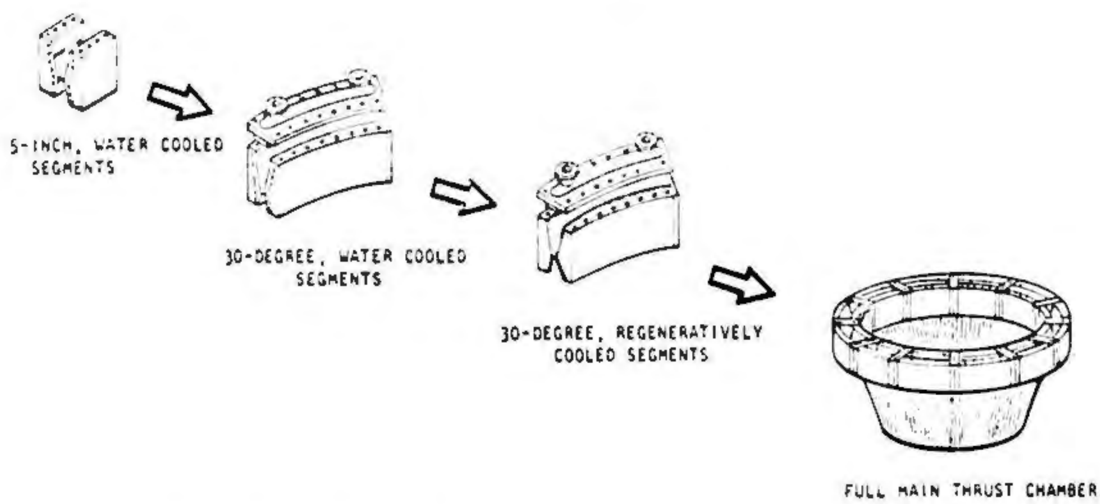

Figure 105. Main Thrust Chamber Hardware Development Sequence (U)

(U) The reconfigured thrust chamber consisted of 12 compartments, each representing 30 degrees of the 360-degree thrust chamber. A regeneratively cooled, supersonic baffle was utilized between compartments (thus precluding any possibility of circumferential instability). The 12 segments were to be bolted together to form the complete thrust chamber. Each of the 30-degree segments were to have its individual injector. Though the Task II test hardware for initially establishing performance, heat transfer and basic component durability was of the 5-inch length configuration because of schedule and economy, major emphasis was placed on the evaluation of the 30-degree segments as building blocks for the subsequent full thrust chamber. The results of the 5-inch-segment test program were applied directly to the 30-degree segments and, thus, the full thrust chamber design.

(U) The main thrust chamber analysis and design efforts accomplished in Task I included the following areas: (1) thrust chamber contour analysis, (2) thrust chamber cooling analysis, and (3) thrust chamber design.

(U) The major effort was devoted to the cooling analysis because this area represented the most critical design aspect of the chamber configuration.

a. Main Thrust Chamber Contour Analysis

(U) Preliminary design and analysis studies had been conducted prior to initiation of the contract to define the thrust chamber dimensions and nozzle and shroud contour for the main thrust chamber. Following the initial contract effort to establish the engine characteristics, modification of the thrust chamber description was incorporated to include the effects of the most recent refinements in the engine system design parameters.

(C) These system modifications included a change in the nominal engine design mixture ratio, the adoption of a hot-hydrogen tapoff turbine drive cycle, the use of 12 supersonic baffles in the combustion chamber, a full thrust design chamber pressure of 650 psia, and a slight increase in the engine diameter. Other system operational characteristics that influenced the thrust chamber design dimensions, i.e., pressure stresses and thermal growth, also were included. A summary of the major engine design parameters and design refinements that influenced the thrust chamber and nozzle contour dimensions is presented in Table 26. The geometric and aerodynamic throat area requirements were obtained from the engine balance information for the specific engine design point. The resulting thrust chamber design parameters are presented in Table 27.

(C) The throat gap value given for the initial tube-wall chamber included the open fillet area between adjacent tubes and is the dimension measured across the throat at the tube crown. The tube-wall throat gap calculation assumed a 0.076-inch tube OD and a total of 3788 tubes (inner and outer body). A fillet area was determined from previous experience.

(C) A correction also was included to account for the variation in throat area as a result of pressure and thermal stresses. An estimated

TABLE 26

MAIN THRUST CHAMBER DESIGN CONDITIONS (U)

CONFIDENTIAL

Chamber Pressure, psia	650
Engine Mixture Ratio	12:1
Chamber Diameter (at throat centerline), inches	45.83
12 Supersonic Baffles 1-inch thick at throat	Hot Hydrogen Tapoff Turbine Drive
Pressure Stress and Thermal Expansion Precicted fot Hot-Firing Conditions	Correction in Throat-Gap Dimension for Fillet Area Not Filled With Braze Between Adjacent Tubes

TABLE 27

THRUST CHAMBER DESIGN PARAMETERS (U)

Geometric Throat Area, sq in.	25.163
Aerodynamic Throat Area, sq in.	25.050
Chamber Diameter (at throat centerline), inches	45.836
Smooth Wall Throat Gap,* inches	0.187
Tube OD, inches	0.076
Tube-Wall Throat Gap,* inches	0.175
Resulting Expansion Area Ratio	
Geometric	59.30
Aerodynamic	59.57

CONFIDENTIAL

*Chamber at ambient temperature

1.66-percent net increase in throat area was calculated for the 12 supersonic baffle chamber configuration. The throat-gap values presented are for fabrication purposes and represent ambient chamber temperature conditions.

(U) The engine and thrust chamber design modifications resulted in refinement in the thrust chamber contour. A summary of the major geometrical parameters for the selected design configuration is presented in Table 28.

TABLE 28

AMPS DOUBLE-EXPANSION, SHROUDED AEROSPIKE GEOMETRICAL PARAMETERS (U)

Effective Throat Radius (R_t), inches	2.83013
Shroud Cowl Radius (ρ_2/R_t), inch	0.120
Centerbody Throat Radius (ρ_1/R_t), inch	0.300
Nozzle Radius to Throat (Y_t/R_t), inches	8.0978
Shroud Exit Radius (Y_e/R_t), inches	7.70656
Throat Gap (G/R_t), inch	0.06183
Throat Angle (θ_t), degrees CONFIDENTIAL	-1.7122

(U) The throat wall radius, $1/R_t$, was selected considering both kinetic and heat transfer aspects. Critical contour dimensions were identified with respect to the wall coordinates X/R_t and Y/R_t, where X is the axial coordinate and Y is the radial coordinate. The center of the shroud cowl radius, ρ_2 is located at $X/R_t = 0.0$, and $Y/R_t = 7.8265$. The center of the inner body throat radius, ρ_1 is located at $X/R_t = 0.8467$, $Y/R_t = 7.7671$.

b. Main Thrust Chamber Cooling Analysis

(U) The main thrust chamber cooling analysis was conducted in iterative steps as follows:

1. Preliminary tube-wall chamber analysis
2. Interim tube-wall chamber analysis
3. Final chamber configuration analysis

(U) The initial analysis (step 1) was conducted based on the heat transfer test results obtained from the previous contract (Ref. 23). As water-cooled segment heat transfer test data became available from Task II of the subject program, the cooling analysis was refined and updated (step 2). Subsequent heat transfer data from the 30-degree tube-wall segment tests indicated that other design approaches than the previous conventional tube-wall configurations were necessary. The final configuration analysis (step 3) was then accomplished.

(1) Preliminary Tube-Wall Chamber Analysis

(U) The preliminary design analysis considered main engine thrust chamber walls which were regeneratively cooled using Nickel 200, two-pass, fuel tubes on each body (inner and outer). The tubes were of 0.017-inch wall thickness with a minimum ID at the throat of 0.040 inch. The supersonic baffle sides were cooled by fuel bypassing the outer body and feeding into the coolant circuit upstream of the inner body. The flow paths through the thrust chamber are illustrated in Fig. 106 .

(U) The outer contour was cooled first using a two-pass flow circuit. The inner contour, from injector to shroud exit plane, was cooled next using a similar two-pass scheme. The nozzle portion of the thrust chamber was cooled last, again using a two-pass circuit. This coolant circuit selection was based on the desire to have the entire coolant flow available for the more severe conditions of the inner body.

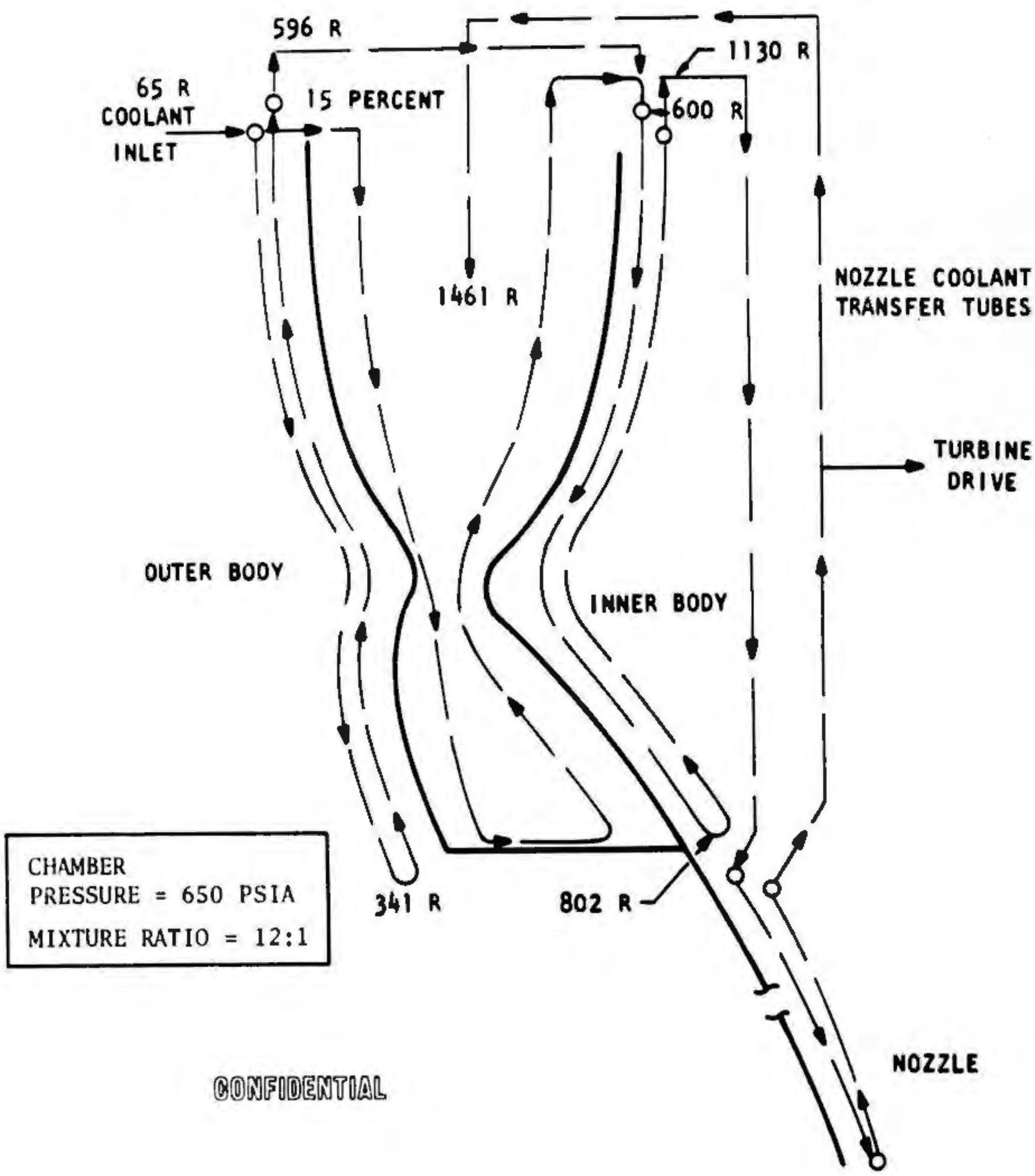

Figure 106. Preliminary Tube-Wall Thrust Chamber Cooling Circuit (Main Engine) (U)

(C) With 15 percent of the flow through the supersonic baffles, the fuel temperature profile for the thrust chamber was calculated to be as indicated in Fig. 106. The temperature of the fuel into the injector was predicted to be 1461 R.

(C) The basic constraint used in the cooling analysis was a nominal thrust level of 30,000 pounds at a chamber pressure of 650 psia. The engine diameter at the throat centerline was 45.7 inches, which resulted in an expansion area ratio of 60:1. An engine mixture ratio of 12:1 was used in the analysis.

(U) Various parameters of interest in the preliminary tube-wall chamber cooling circuit design are presented in Fig. 107 to 115. The convective film coefficient profiles used in the design are shown in Fig. 107 and 108 for the combustor and nozzle, respectively. The combustor film coefficient profile is based on experimental data obtained during a previous program (Ref. 23). The shroud and nozzle profiles were based on the throat film coefficient value and the combustion-gas flow-field analysis. The shroud exhibited higher coefficients than the inner wall because of the slower (controlled) expansion required by kinetic performance considerations.

(C) The convective film coefficient profiles were input to the Rocketdyne "Regenerative Cooling Design" digital computer program. A nominal tube-wall thickness of 0.017 inch was used for design purposes. This thickness was believed to have a greater margin of safety than the 0.012-inch thickness originally proposed even though the tubes operate at a slightly higher temperature. The resulting combustion-side wall temperature profiles are shown in Fig. 109 to 111 for the outer contour, inner contour, and nozzle, respectively. In the outer contour, the wall temperature at the throat was less than 1400 F. The peak temperature, however, was approximately 1500 F at a point 1 inch from the injector on the downpass leg of the circuit. This high temperature resulted from the poorer cooling characteristics of the hydrogen at low temperature ($\leq$ 120 R). The inner body and nozzle have maximum combustion-side wall temperatures of 1495 and 1450 F, respectively.

(C) Nominal heat flux profiles for the combustion chamber and nozzle are presented in Fig. 112 and 113.

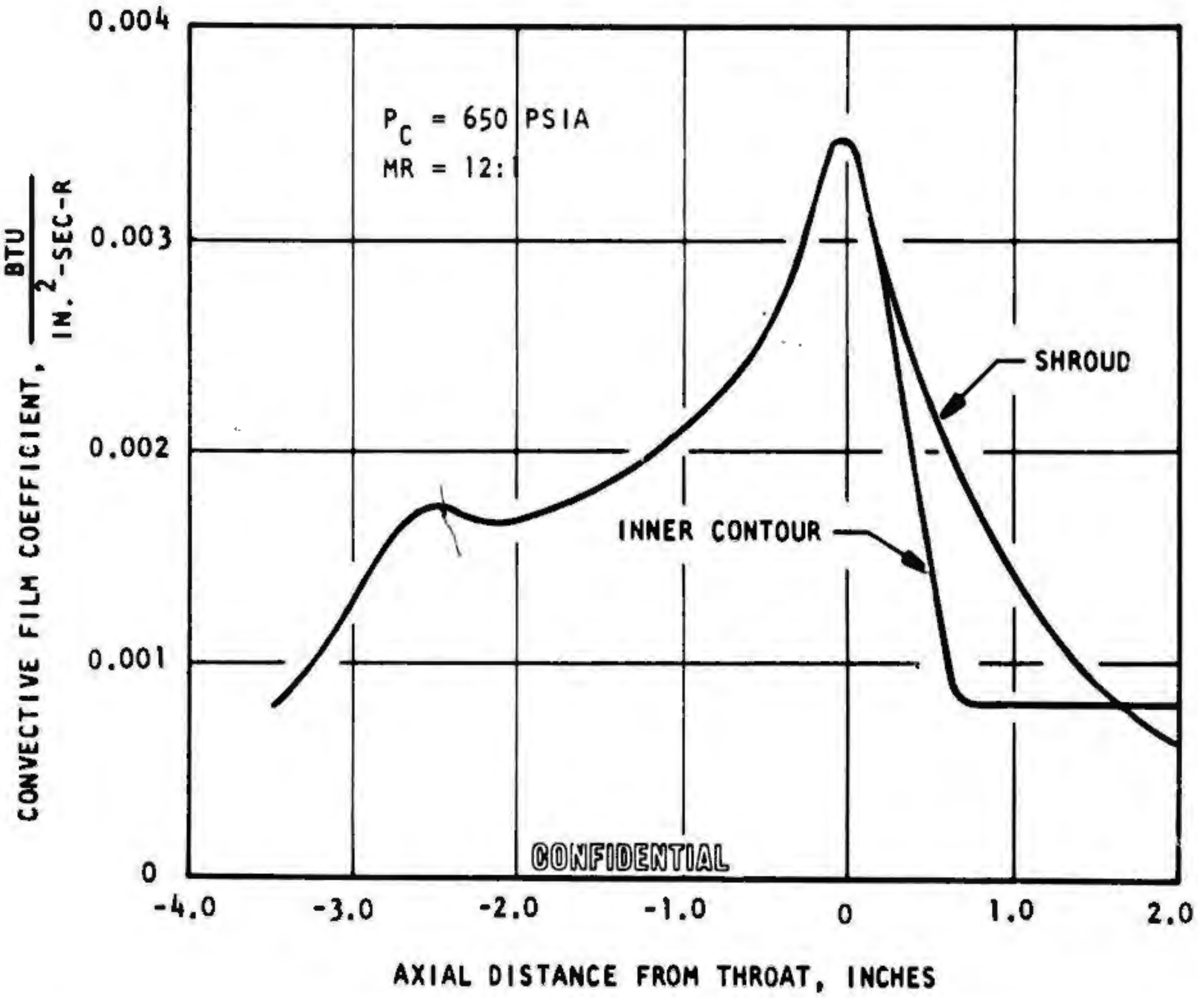

Figure 107. Convective Hot-Gas Side Film Coefficient Profile for the Combustor (Preliminary Tube-Wall Design) (U)

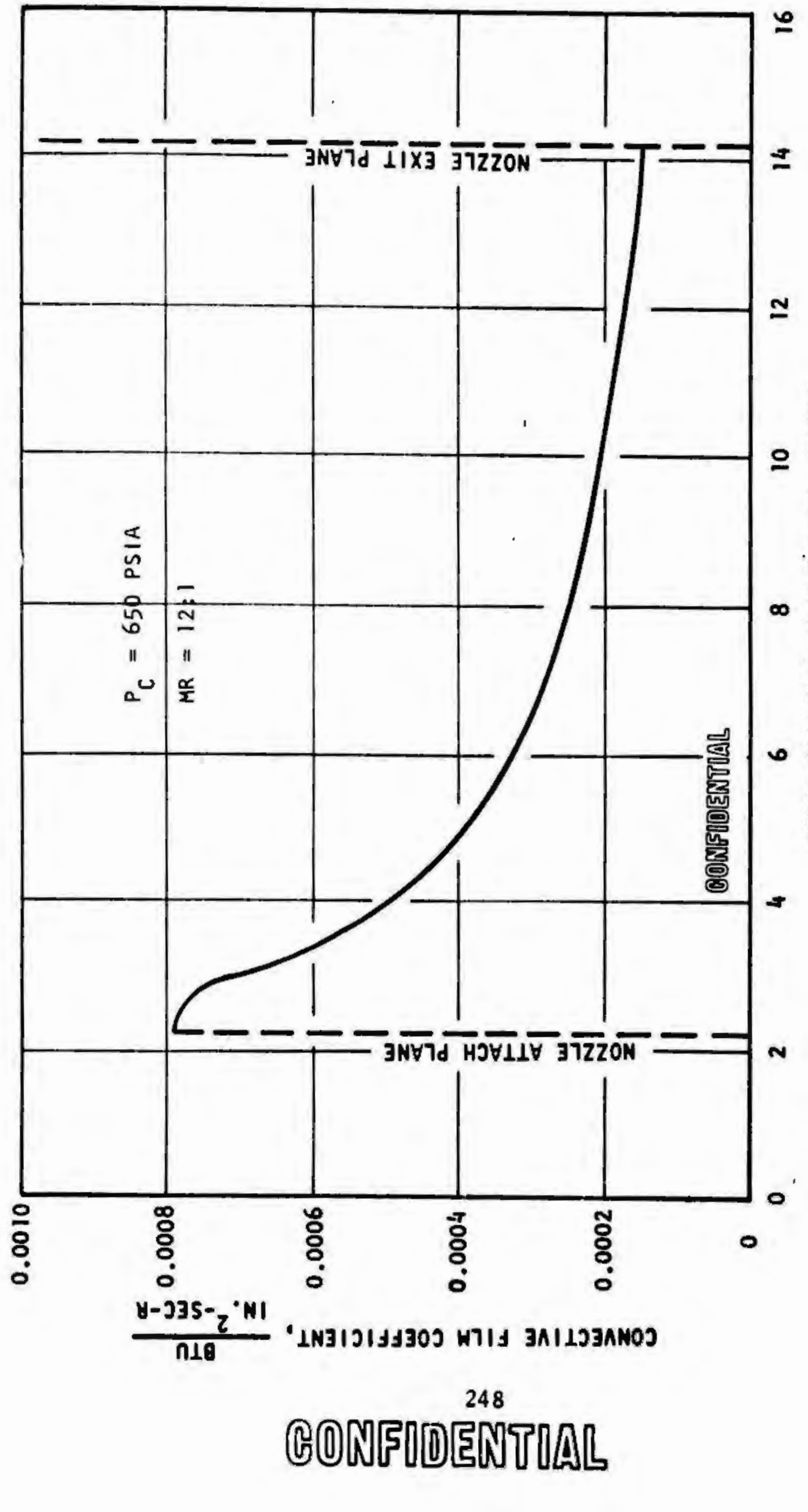

Figure 108. Convective Hot-Gas Side Film Coefficient Profile for the Nozzle (Preliminary Tube-Wall Design) (U)

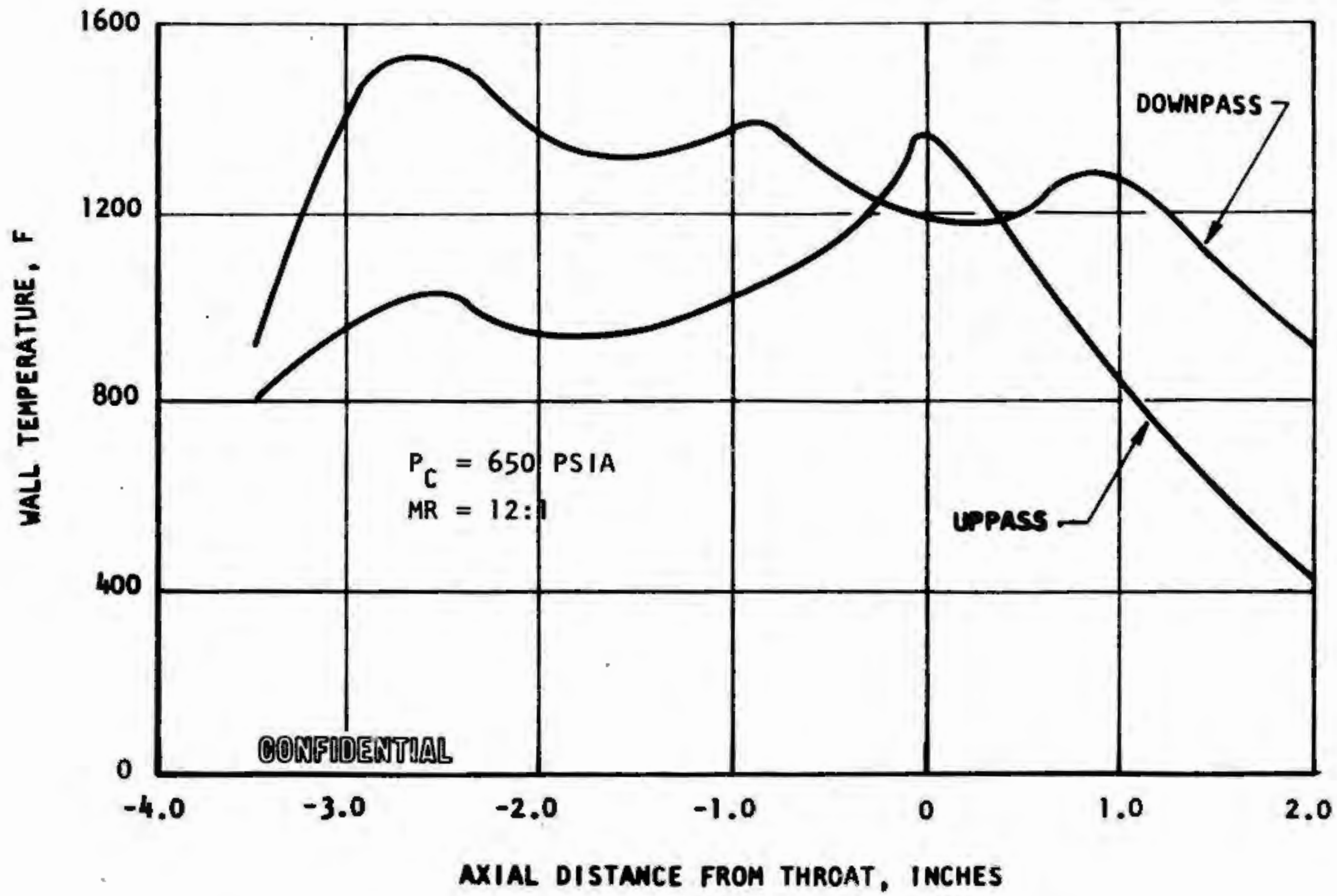

Figure 109. Surface Temperature Profile, Combustor Outer Contour (Preliminary Tube-Wall Design) (U)

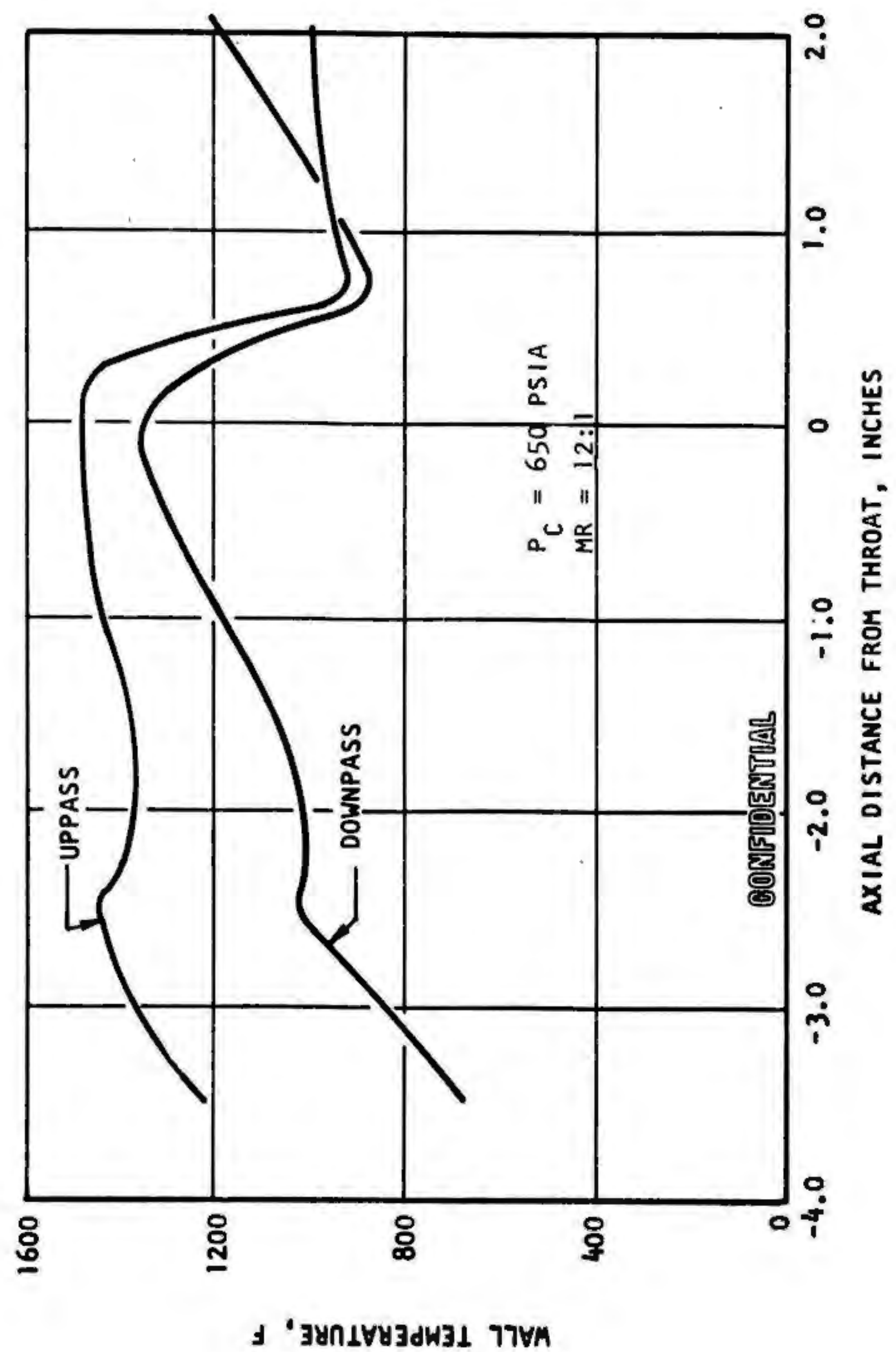

Figure 110. Surface Temperature Profile, Combustor Inner Contour (Preliminary Tube-Wall Design) (U)

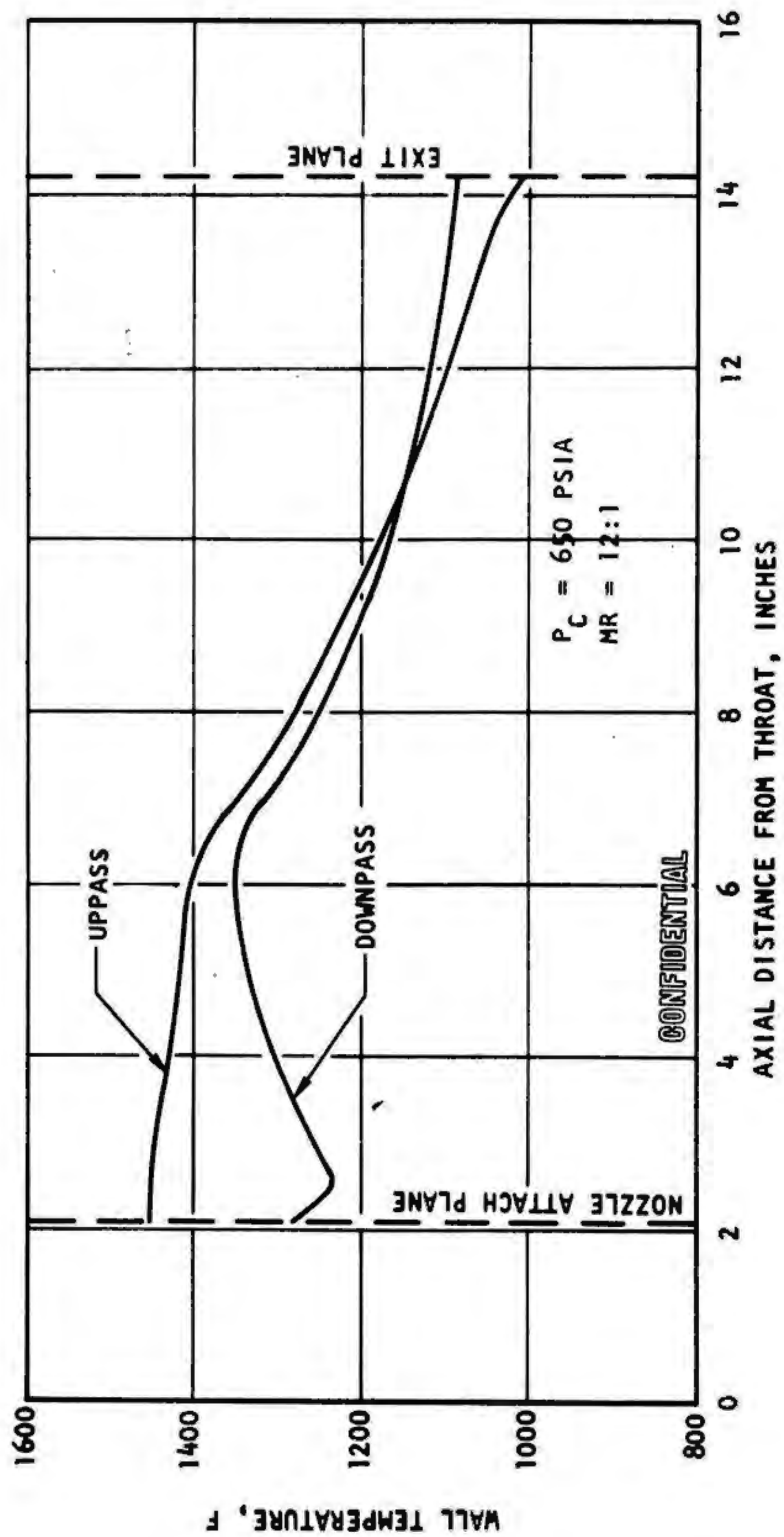

Figure 111. Surface Temperature Profile, Nozzle (Preliminary Tube-Wall Design) (U)

CONFIDENTIAL

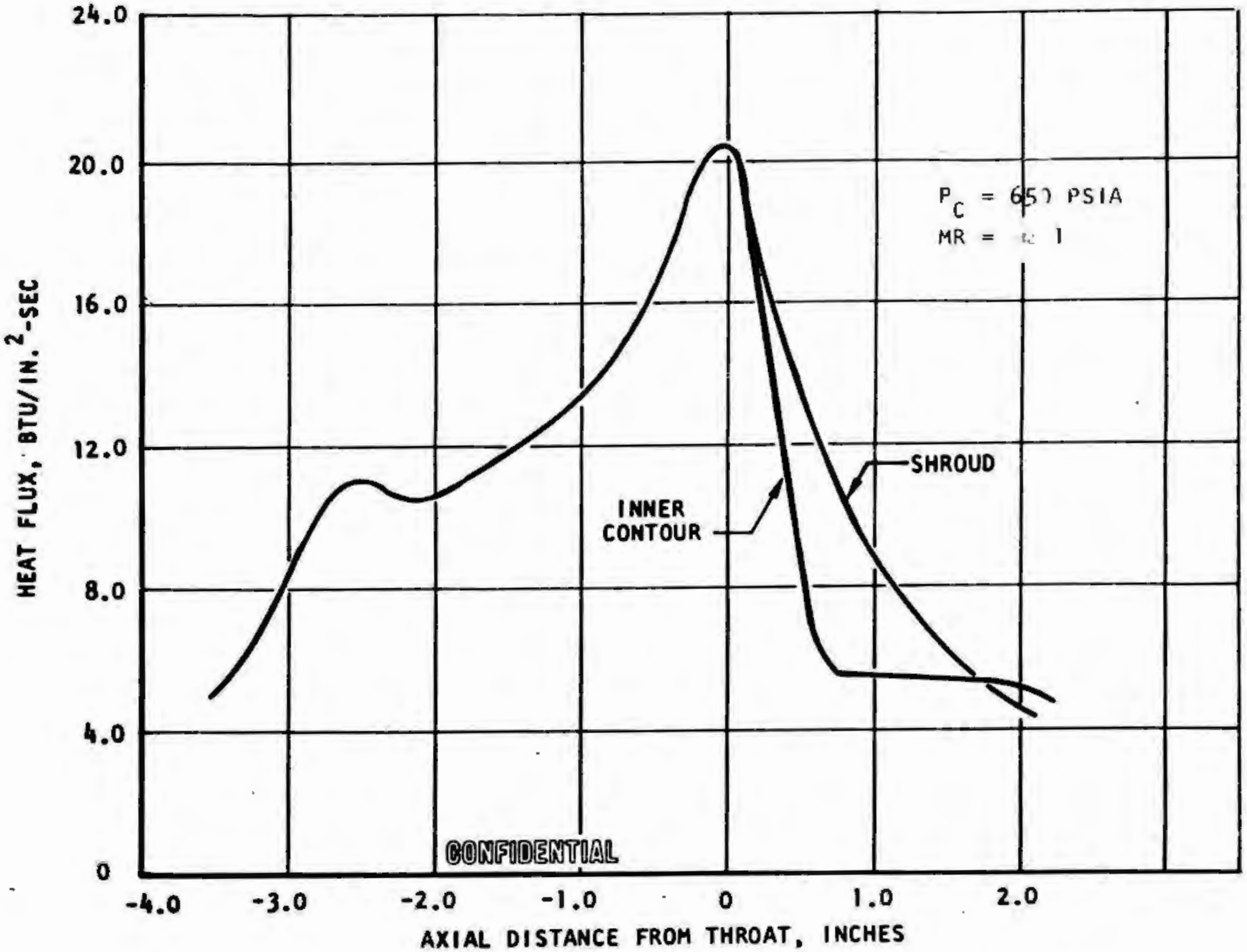

Figure 112. Combustion Chamber Heat Flux Profile (Preliminary Tube-Wall Design) (U)

CONFIDENTIAL

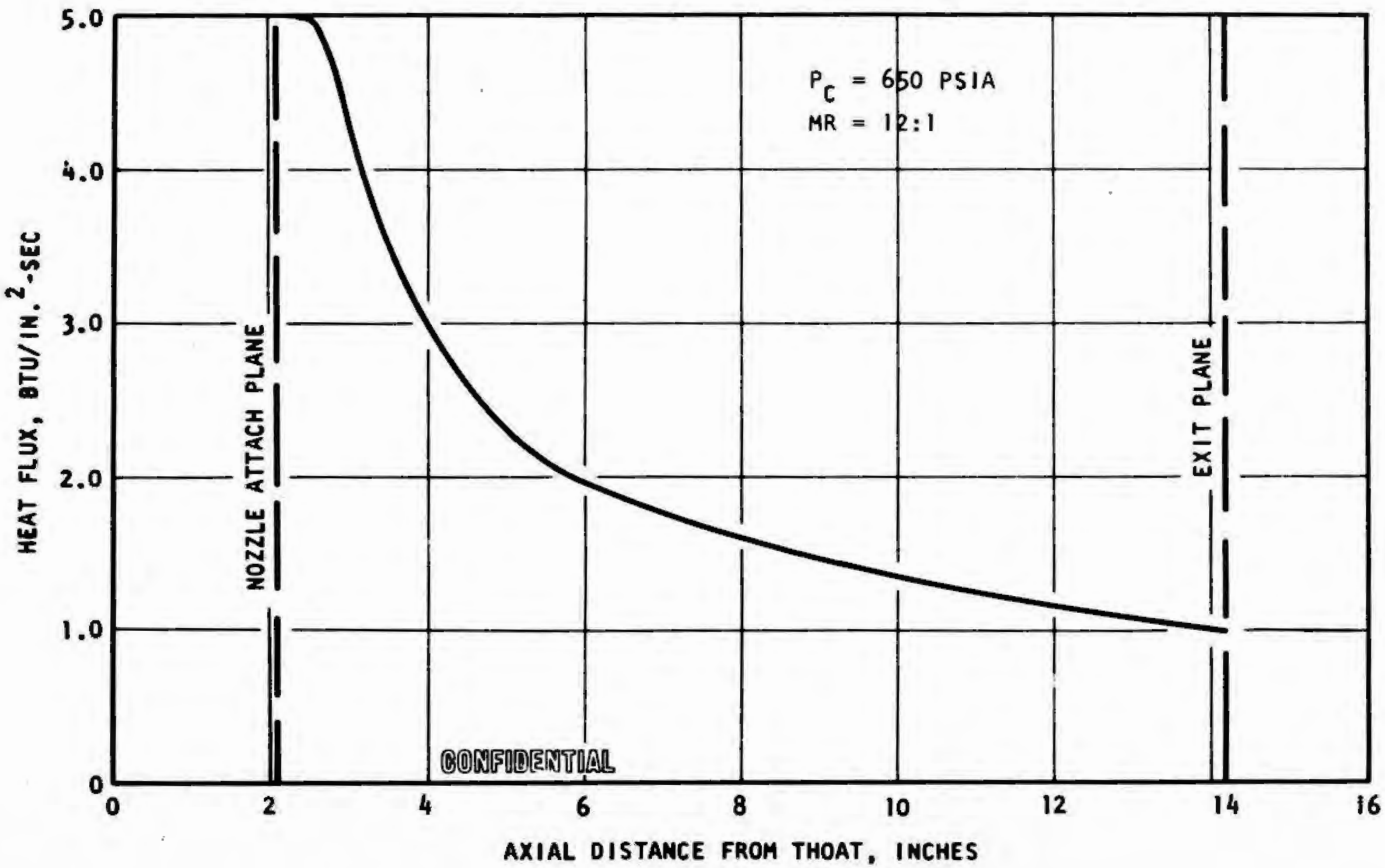

Figure 113. Nozzle Heat Flux Profile (Preliminary Tube-Wall Design) (U)

(C) The maximum (throat) heat flux was approximately 20 Btu/in.^{2}-sec at a wall temperature of 1500 F.

(C) The coolant tube geometries are presented in Fig. 114 and 115 for the combustor and nozzle sections, respectively. The minimum tube inner diameter occurs at the throat and is 0.040 inch. The flat length is seen to be zero at the throat, implying a round tube. The unformed tube diameter is the diameter (outer) of a round tube before forming to the desired shape.

(U) The preceding discussion presented the results of a single detailed regenerative-cooling design analysis based on previously obtained (Ref. 23) experimental heat transfer data.

(2) Interim Tube-Wall Chamber Analysis

(C) As experimental heat transfer data became available from the initial Task II 5-inch water-cooled segment testing, a reiteration of the main thrust chamber cooling analysis was conducted. The data (Vol. II, Table 4) were for chamber pressure levels of 370 and 650 psia.

(C) The thrust chamber cooling analysis again considered nickel tubes of 0.017-inch wall thickness having a minimum unformed tube outside diameter of 0.072 inch. Three cooling circuits were considered (Fig.116), all of which use 15 percent of the total engine fuel flow to pass through the baffles. In the parallel-series (P-S) and series-parallel (S-P) configurations, 85 percent of the flow has a parallel pass through the outer tube body (P-S) and inner tube body (S-P), respectively. The combined flow (100 percent) passes through all of the remaining tube circuits. In the all-parallel (ALL-P) configuration, 85 percent of the total fuel flow passes through both outer and inner bodies before recombining with the 15-percent baffle flow.

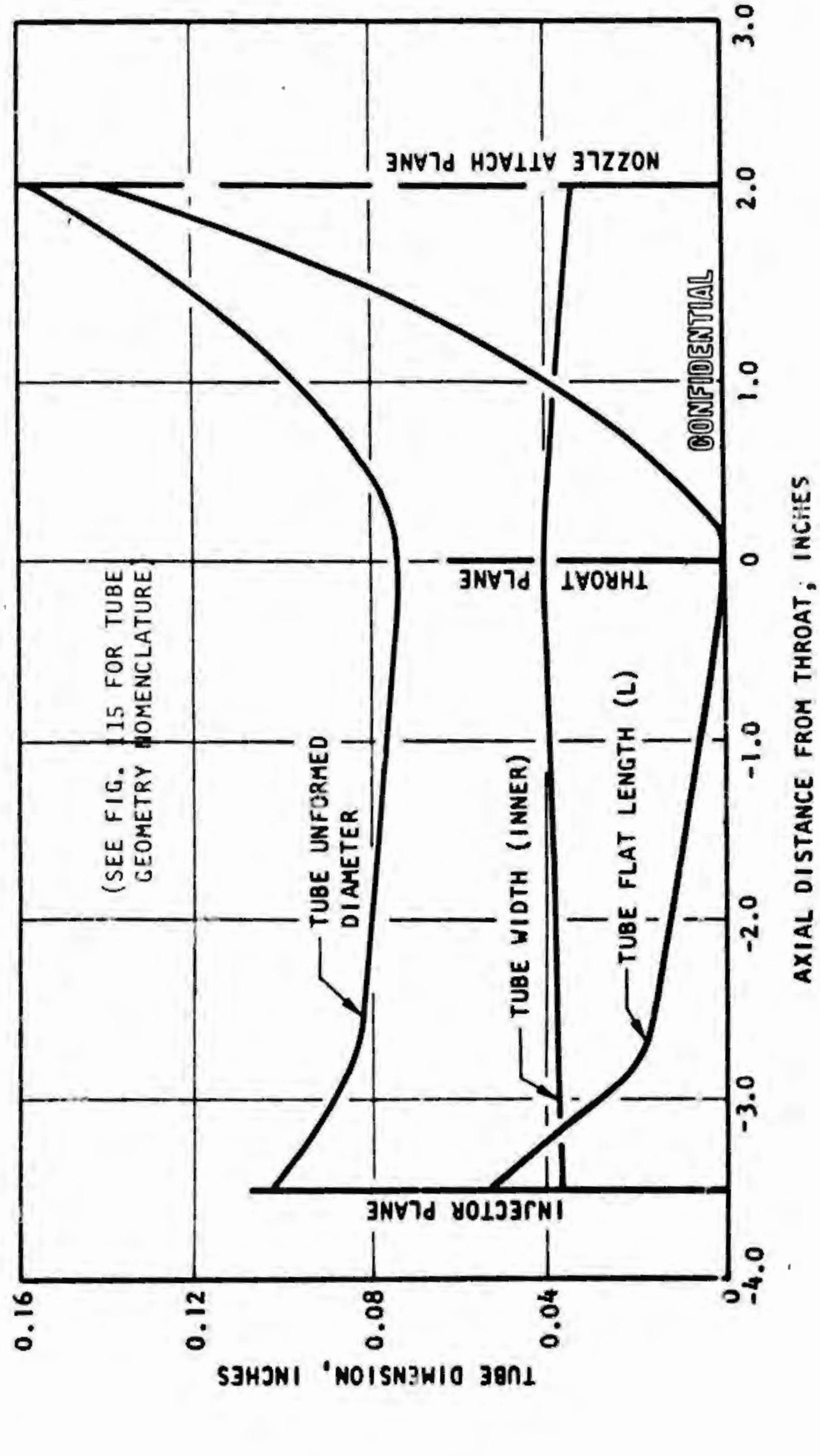

Figure 114. Combustion Chamber Tube Geometry Profiles (Preliminary Tube-Wall Design) (U)

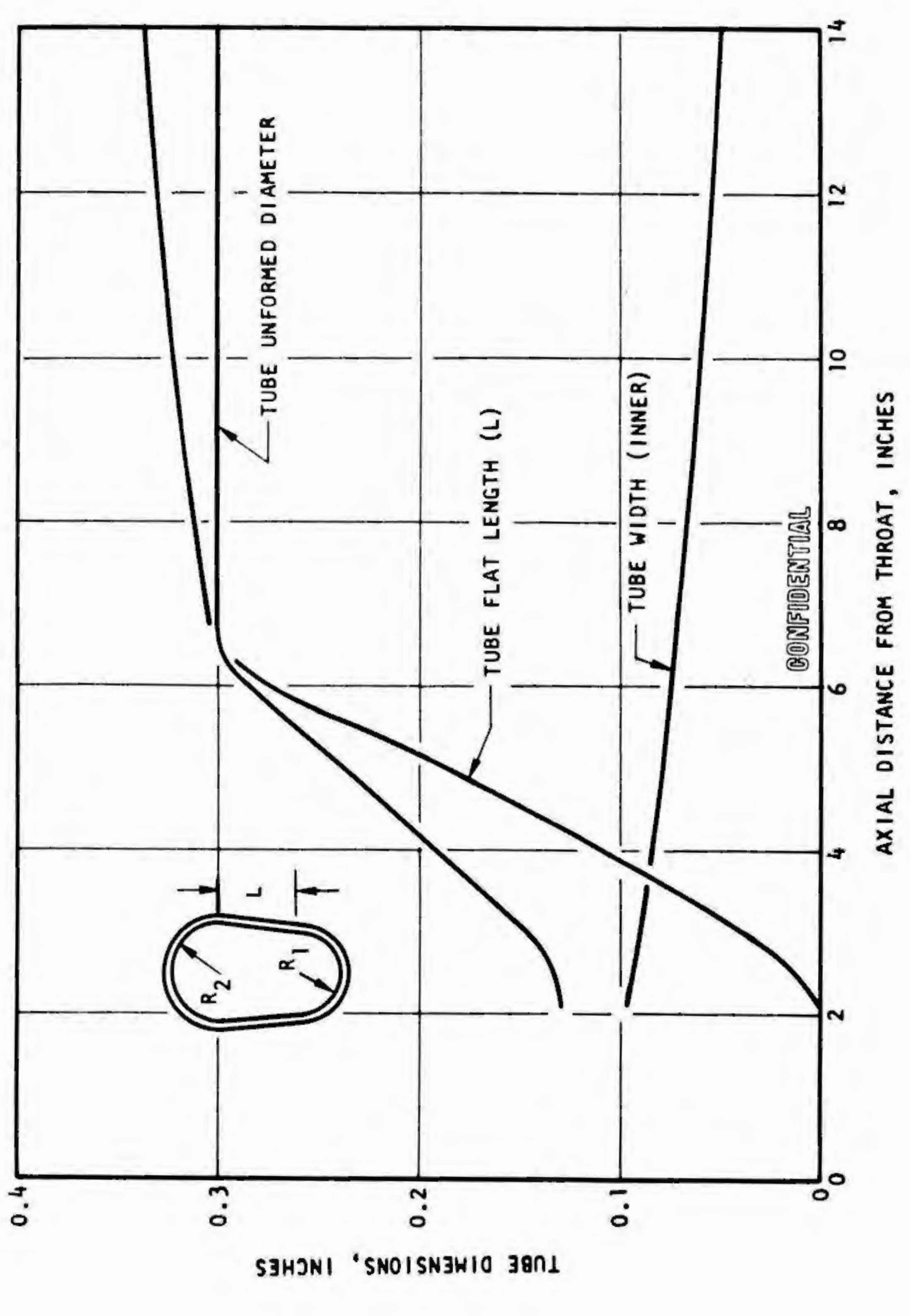

Figure 115. Nozzle Tube Geometry Profiles (Preliminary Tube-Wall Design (U)

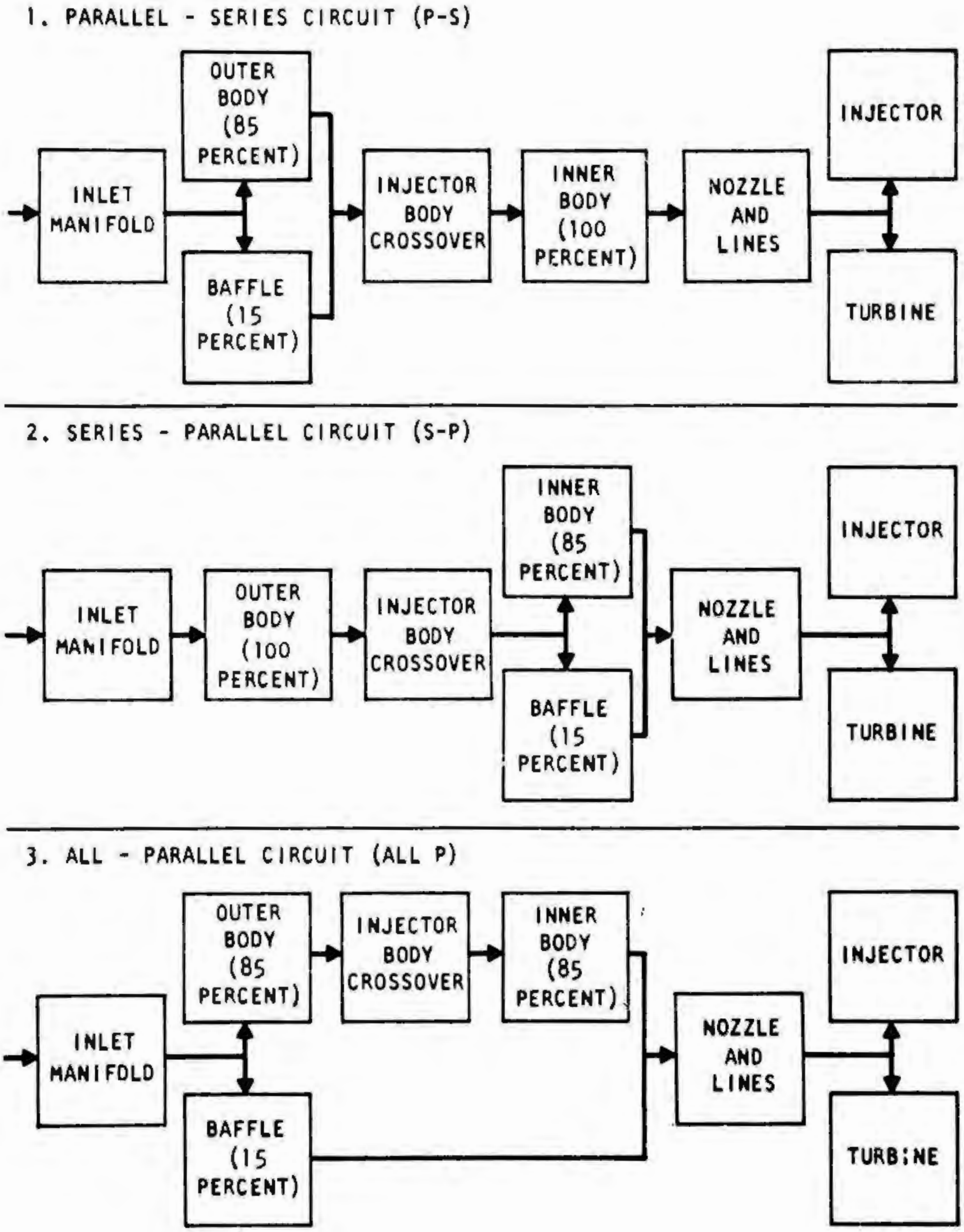

Figure 116. Candidate Cooling Paths for Main Engine Thrust Chamber (Interim Analysis) (U)

(C) The values of coolant flowrate used in the analysis are shown in Fig. 117 as a linear function of chamber pressure. The specific values for 370 psia and 650 psia chamber pressure are shown in Table 29. These values represent either 100 percent of the flow, or 85 percent of the flow corresponding to the particular flow path being considered.

(C) The surface heat transfer coefficient on the combustion side of the tubes was obtained by analyses of the experimental data. The observed heat fluxes and gas-side conditions were reduced to curves relating axial distance from the throat to Stanton Number (St) and Prandtl Number (Pr). These are shown in Fig. 118. The product, St x $Pr^{2/3}$, is relatively constant with changing chamber gas-side conditions because the relation reduces to St x $Pr^{2/3} = \frac{f}{2}$ where f = friction factor.

(U) The curve of St x $Pr^{2/3}$ vs axial position was used in the analysis to estimate surface heat transfer coefficients (h_g) on the combustion gas side of the inner and outer tube bodies using the relation $h_g \propto$ (St x $Pr^{2/3}$).

where

$$St = \frac{h_g}{\rho V C_p}$$

$$Pr = \frac{C_p \mu}{k}$$

k = thermal conductivity

C_p = specific heat

ρ = density

V = velocity

μ = viscosity

(U) The gas-side film coefficients (h_g) used in the analysis are shown in Fig. 119. Interpolation between the test data points was accomplished to complete the curves.

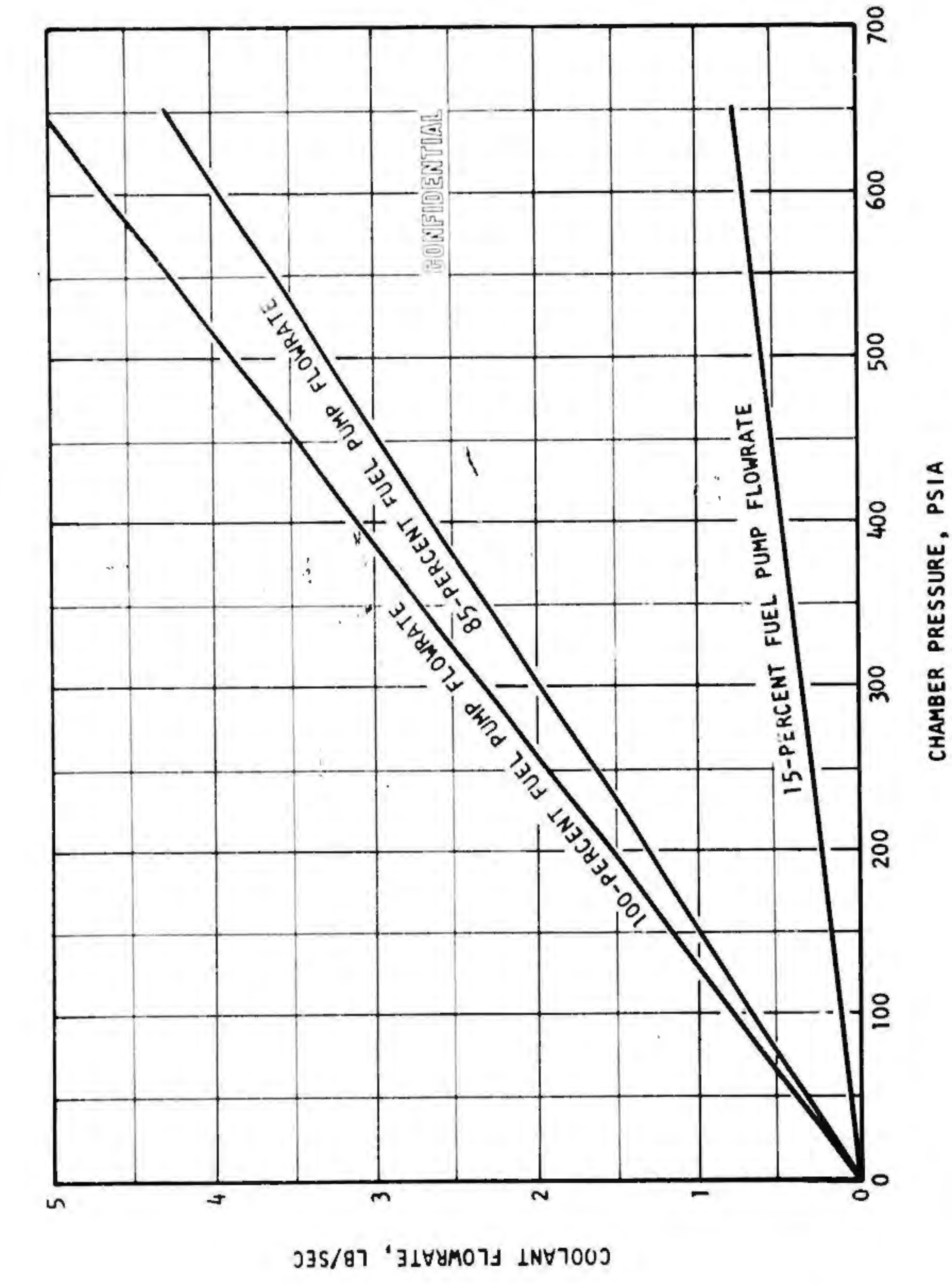

Figure 117. Coolant Flowrate vs Chamber Pressure (Interim Analysis) (U)

TABLE 29

COOLANT FLOWRATES FOR CANDIDATE
MAIN THRUST CHAMBER COOLANT CIRCUITS (U)

Chamber Pressure, psia	CONFIDENTIAL Configuration	Outer-Body Flowrate		Inner-Body Flowrate		Baffle Flowrate	
		lb/sec	Percent of Engine Flowrate	lb/sec	Percent of Engine Flowrate	lb/sec	Percent of Engine Flowrate
650	Parallel-Series	5.10	100	4.335	85	0.765	15
	Series-Parallel	4.335	85	5.10	100	0.765	15
	All-Parallel	4.335	85	4.335	85	0.765	15
370	Parallel-Series	2.903	100	2.467	85	0.436	15
	Series-Parallel	2.467	85	2.903	100	0.436	15
	All-Parallel	2.467	85	2.467	85	0.436	15

(Interim Analysis)

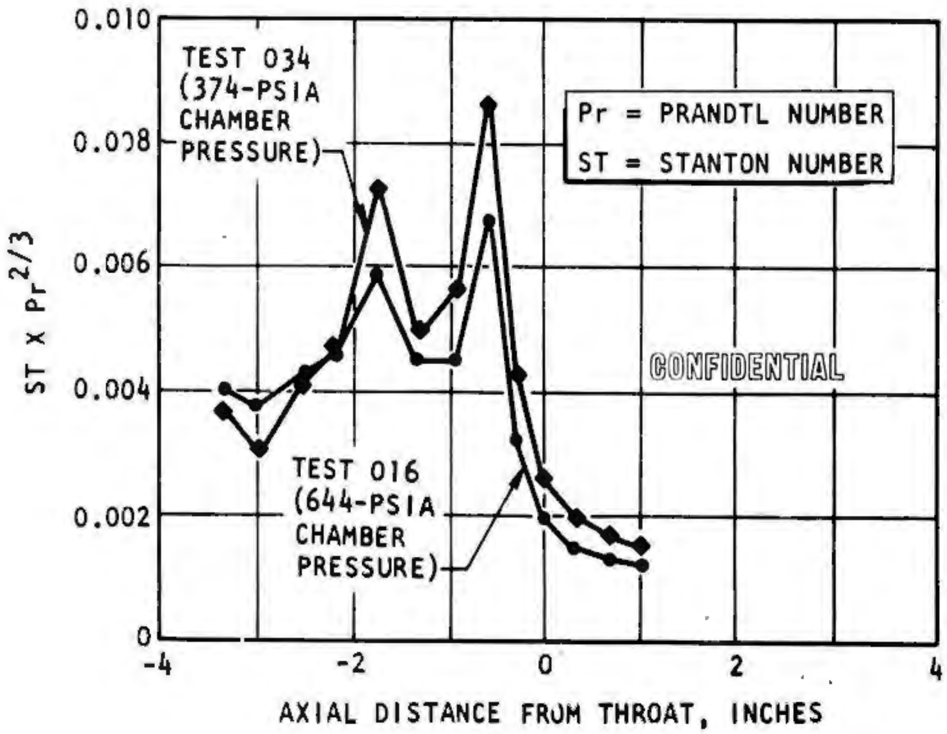

Figure 118. Relationship of Wall Position to Stanton and Prandtl Numbers (Tube-Wall Chamber Interim Analysis) (U)

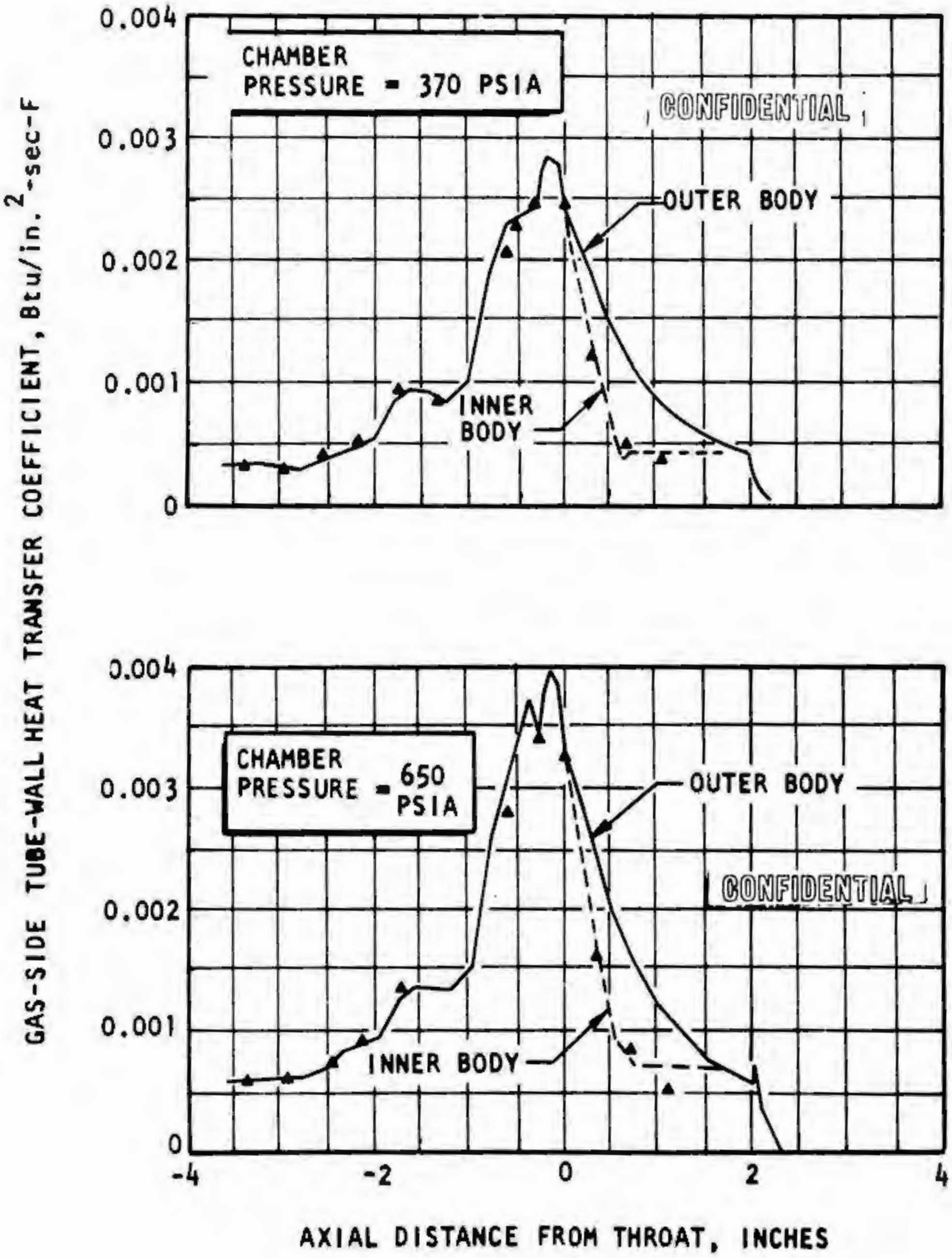

Figure 119. Heat Transfer Coefficient Profile at 370- and 650-psia Chamber Pressure (Tube-Wall Chamber Interim Analysis (C)

(C) Using the heat transfer coefficient profiles of Fig. 119, the tube gas-side wall temperature profiles of the outer and inner tube bodies for 650 psia chamber pressure are shown in Fig. 120 and 121 for the three candidate configurations (Fig. 116 and Table 29). The 5.10 lb/sec flow is for the series-parallel flow configuration and the 4.335 lb/sec flow is for the parallel-series and all-parallel flow configurations. Typical results of the 370 psia chamber pressure analyses are presented in Fig. 122 for the inner body.

(U) The effect of contouring the back side of the tubes where maximum tube-wall temperatures occurred also was analyzed. The concept, illustrated in Fig. 123 , was to increase the coolant side heat transfer coefficient locally by increasing the mass-velocity. The length of the contoured portions of the tubes was 0.6 inch or less. The effect of the contouring is shown in Fig. 121 for the inner body. As indicated, the peak wall temperature was reduced approximately 50 F as a result of the tube contouring.

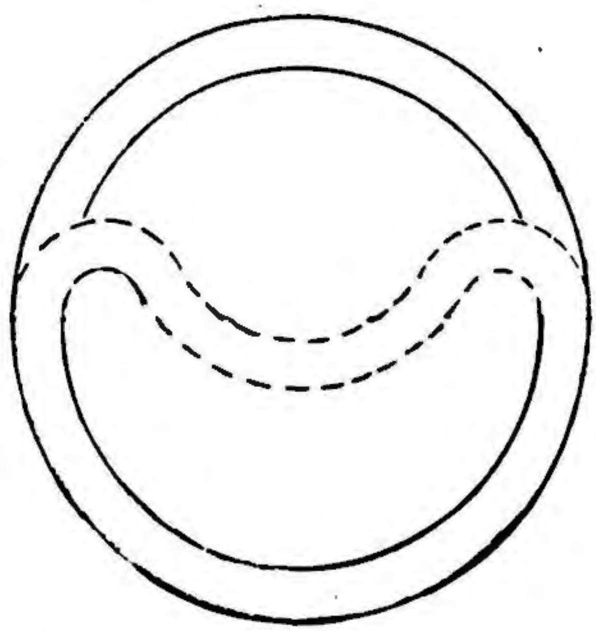

Figure 123 . Schematic of Contoured Tube Concept

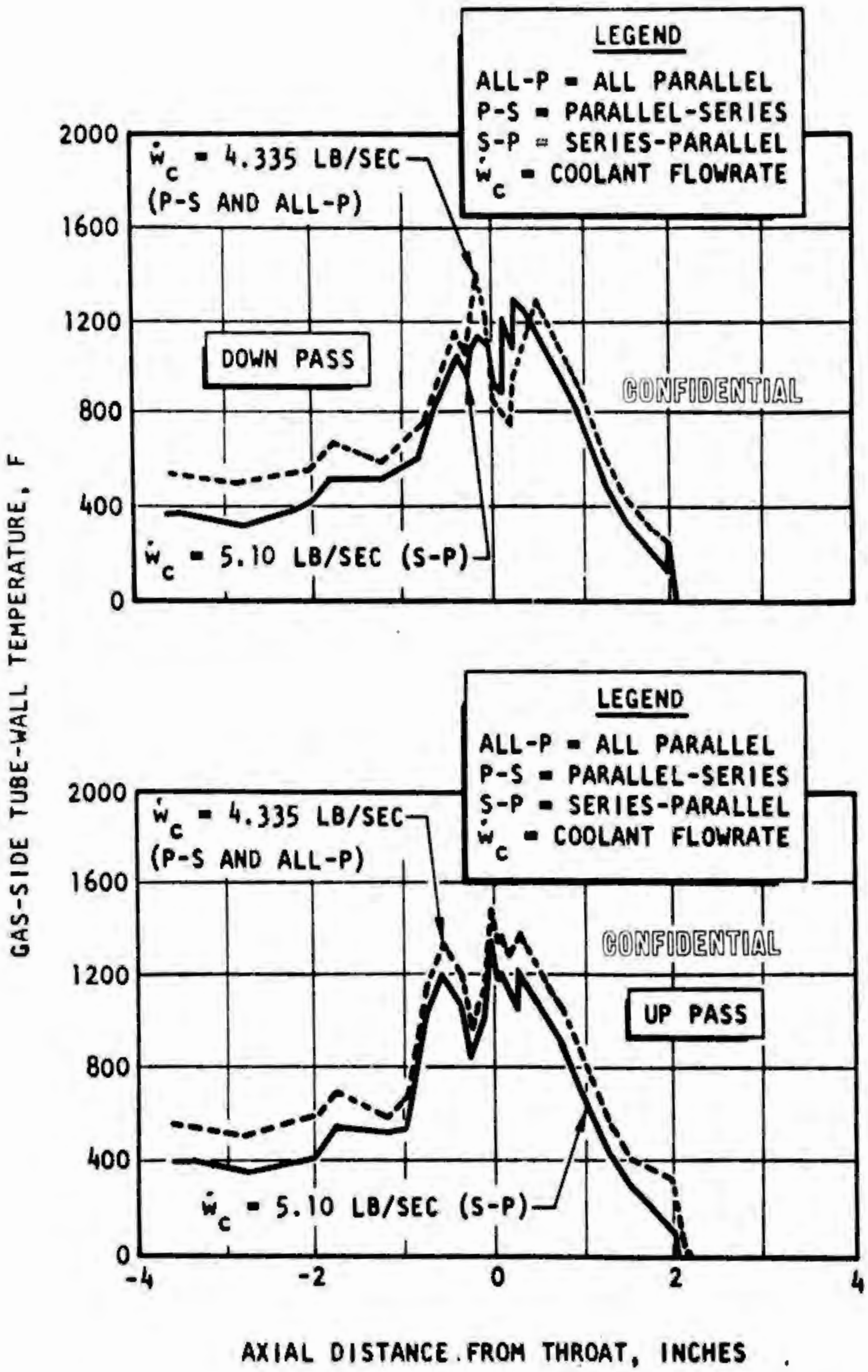

Figure 120. Temperature Profile for Tube Outer Body at 650-psia Chamber Pressure (Interim Analysis) (C)

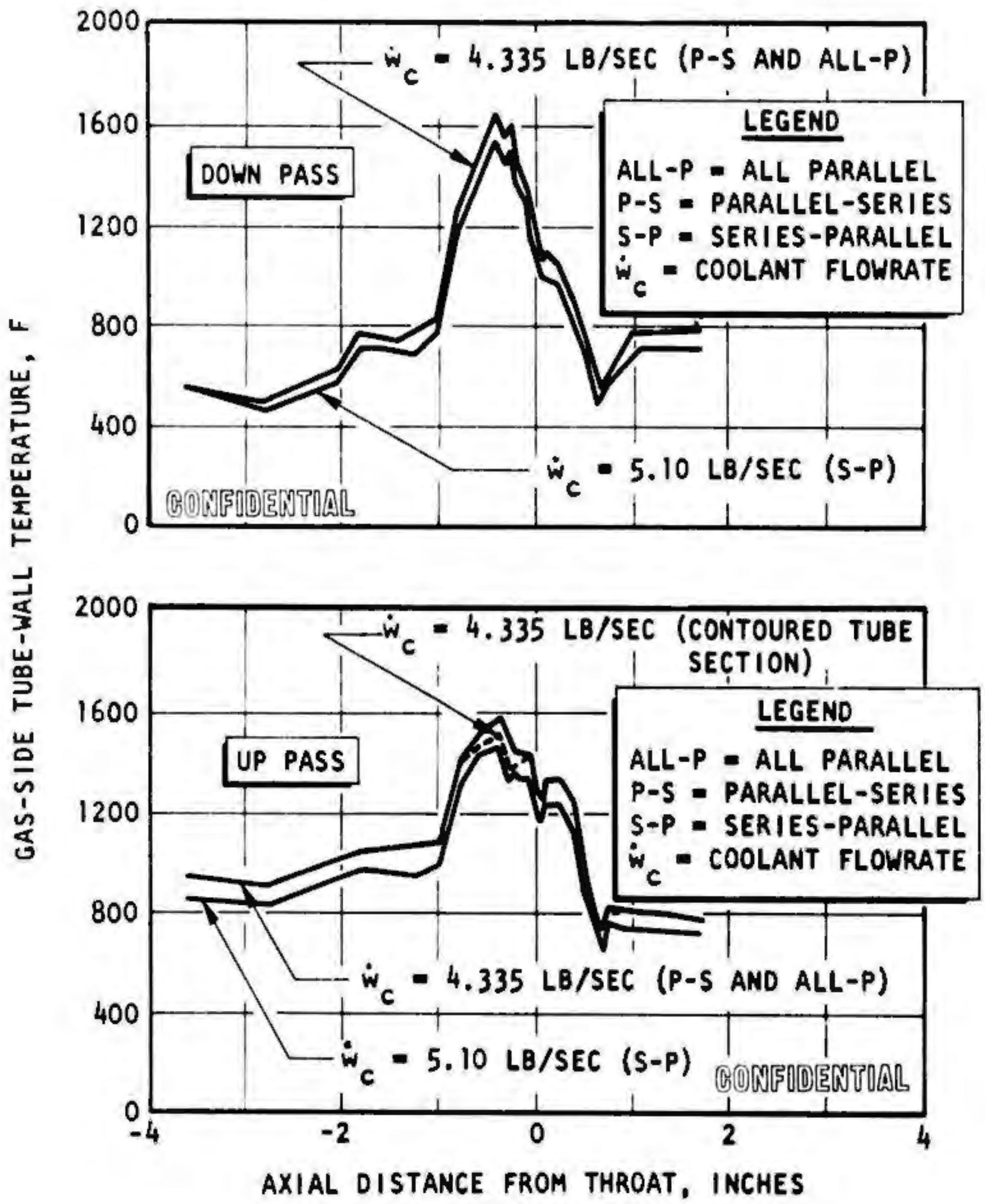

Figure 121. Temperature Profile for Tube Inner Body at 650-psia Chamber Pressure (Interim Analysis) (C)

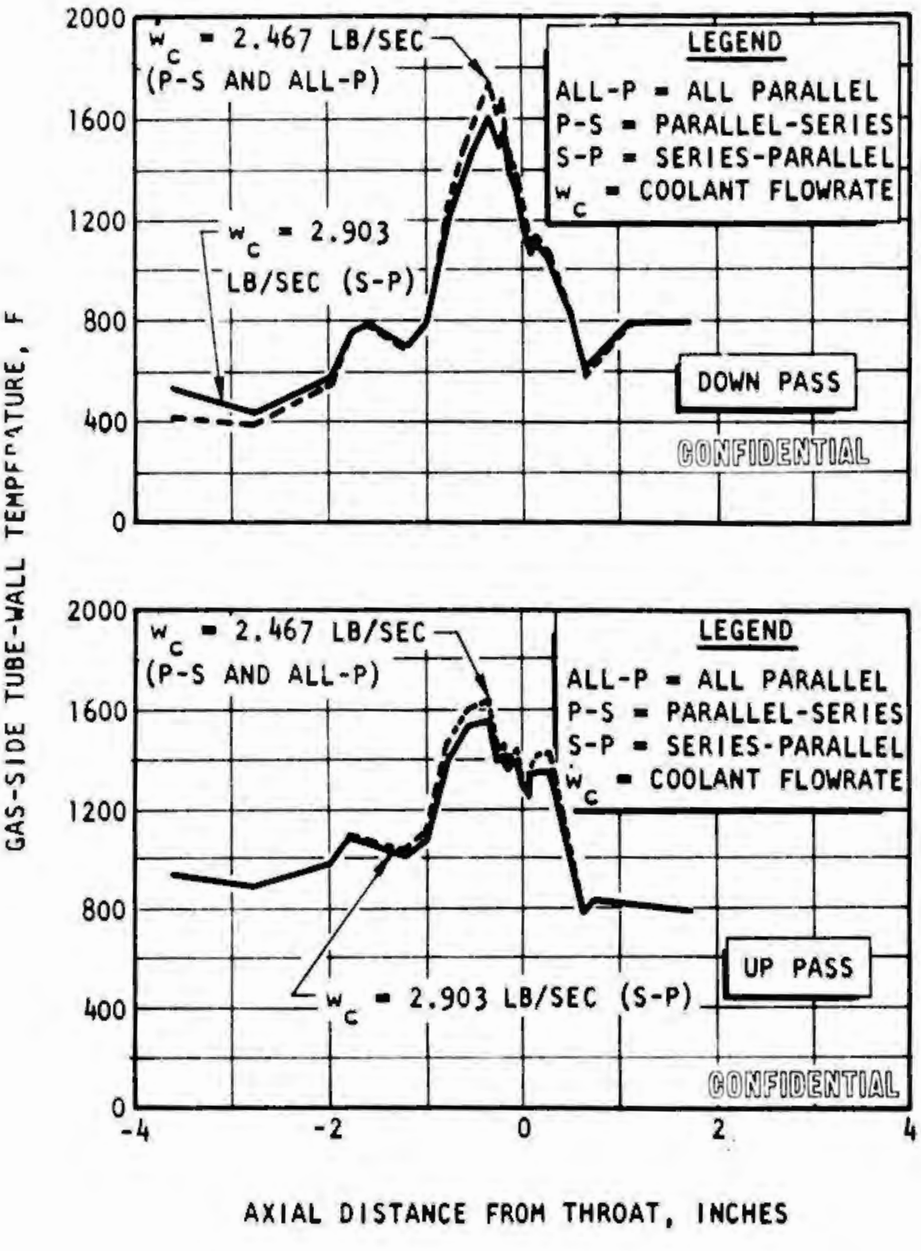

Figure 122. Temperature Profile for Tube Inner Body at 370-psia Chamber Pressure (Interim Analysis) (C)

(U) There are several characteristics common to all the profiles: (1) a peaking just prior to the throat that is a result of the input combustion side surface heat transfer coefficients peaking at that point, and (2) the improvement in coolant-side surface heat transfer coefficient due to curvature causing the large dip in the profiles for the first 0.35 inch downstream of the throat on the down-passes and the similar effect for 0.35 inch upstream of the throat on the up-passes. A third common characteristic of all the tube-wall temperature profiles are the steep gradients and sharp peaks near the throat. These results are due to a heat flux condition where heat flow is neglected in the axial direction of the tubes, and rapid changes are occurring axially in combustion gas and coolant properties. In the actual case, there is some axial heat transfer which would result in reducing the computed throat heat flux.

(U) The rise to a new peak downstream of the throat in the outer body down-pass profiles (Fig. 120) is a result of the coolant-side heat transfer coefficient being sensitive to the rapid increase in tube diameter (decreasing velocity) of this pass.

(C) The gas-side tube wall heat flux profiles for 650 psia and 370 psia chamber pressures (Fig. 124 and 125) are essentially of the same shape as the combustion-side surface heat transfer coefficient profiles shown in Fig. 119. This result is because 90 percent of the total heat flow resistance is contained in the heat transfer coefficient. The effect of the coolant-side heat transfer coefficient is evidenced in the small difference, for a given tube body, between the profiles of a down-pass and an up-pass. Coolant flowrate (over the range of from 85 to 100 percent of engine flowrate) has negligible effect on the heat flux profiles for a given chamber pressure.

(C) From these analyses several possible cooling circuits are indicated that result in suitable wall temperatures, heat loads, and pressure profiles. The series-parallel circuit, however, gave generally lower gas-side wall

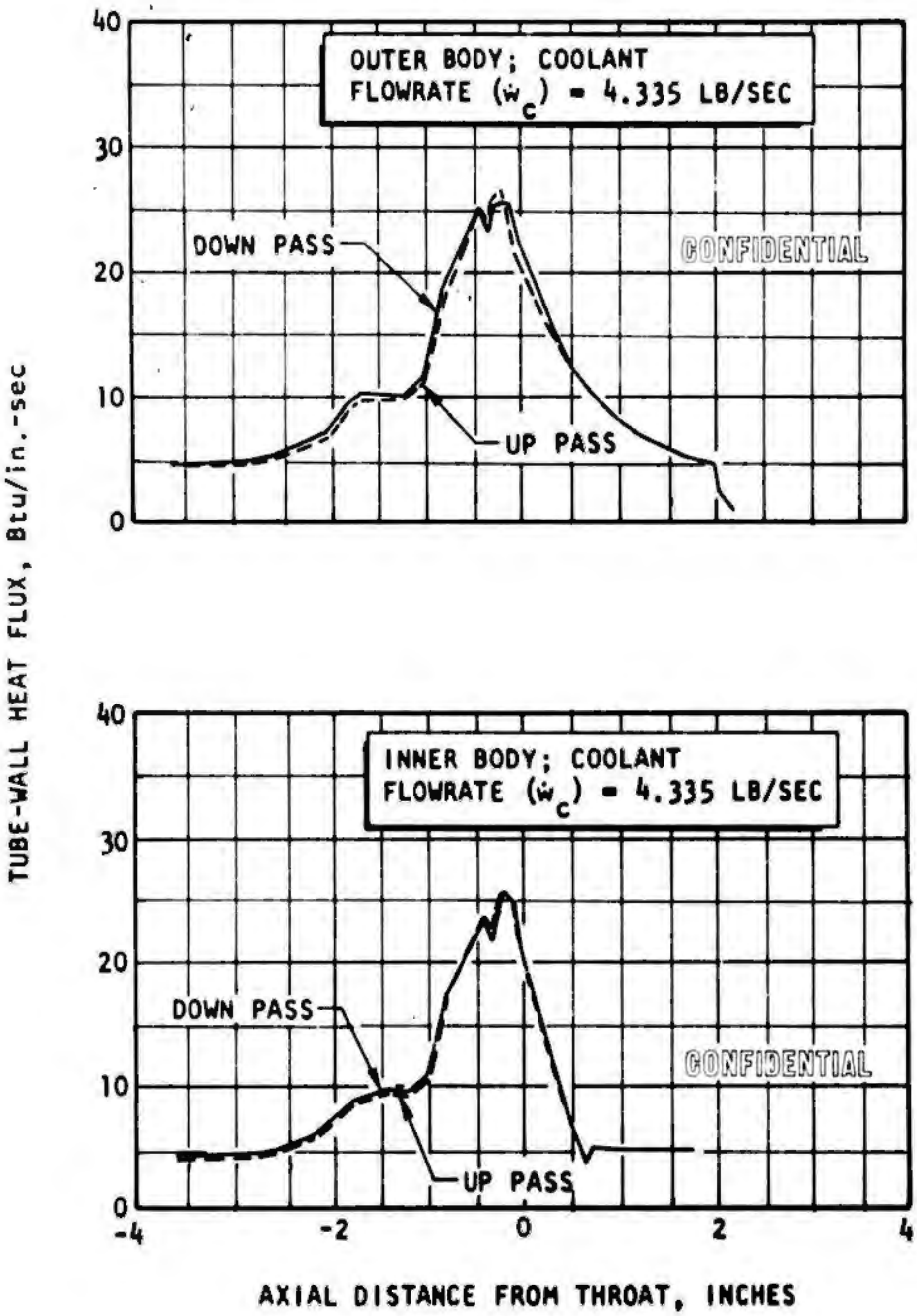

Figure 124. Heat Flux Profile for Tubes at 650-psia Chamber Pressure (Interim Analysis) (C)

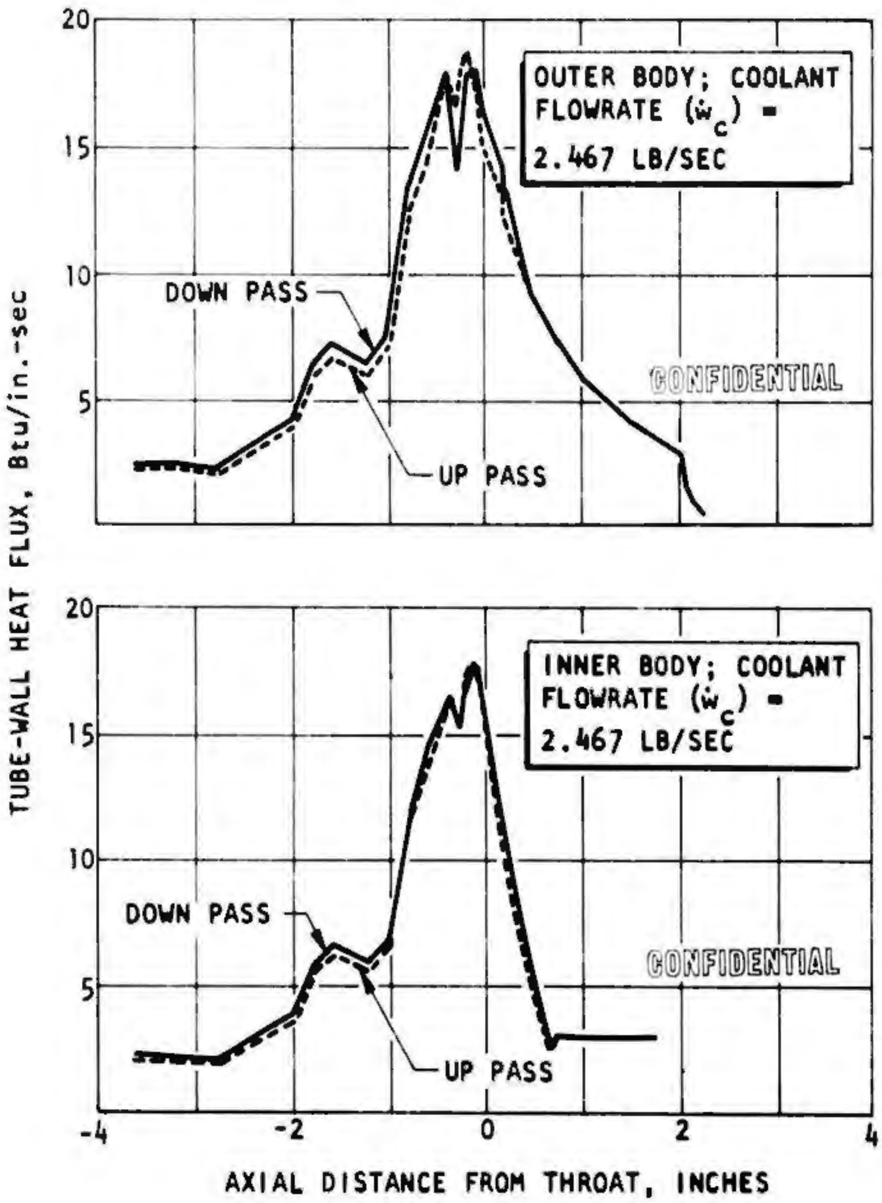

Figure 125. Heat Flux Profile for Tubes at 370-psia Chamber Pressure (Interim Analysis) (C)

(C) temperatures over the wall profile than the other cooling circuits. The pressure drop available to the injector is shown in Fig. 126 as a function of thrust chamber inlet pressure for the three cooling circuits at chamber pressures of 650 psia and 370 psia.

(U) Based on the above analysis, an interim selection of the tubular wall cooling circuit was made. The series-parallel circuit was chosen (Fig. 127). The major criteria considered in the selection were:

1. Minimum tube gas-side wall temperature over the throttle range
2. Minimum pressure drop
3. Minimum number of coolant tubes

(U) The series-parallel cooling circuit provided the maximum margin with regard to these three major selection criteria. This circuit provided the best hydrogen bulk temperature and cooling conditions at the critical locations of the circuit. The final coolant circuit selection, however, was to be made after completion of further analysis involving the full range of chamber pressure operation and data obtained from Task II tests of the tube-wall segments.

(C) After interim selection of the cooling circuit, the tube wall heat transfer analysis was refined to provide more accurate gas-side film coefficients. The straight line interpolation, which was used in the previous analysis, was changed to a curve fit interpolation of the $N_{St} \times N_{Pr}^{2/3}$ vs combustion gas Mach number. This refinement reduced the calculated maximum value of the throat gas-side film coefficient at 650 psia chamber pressure from a value of 0.00395 Btu/in.^{2}-sec-F to 0.00345 Btu/in.^{2}-sec-F. Reduction of the gas-side film coefficient resulted in changes in the predicted heat flux and tube wall temperature.

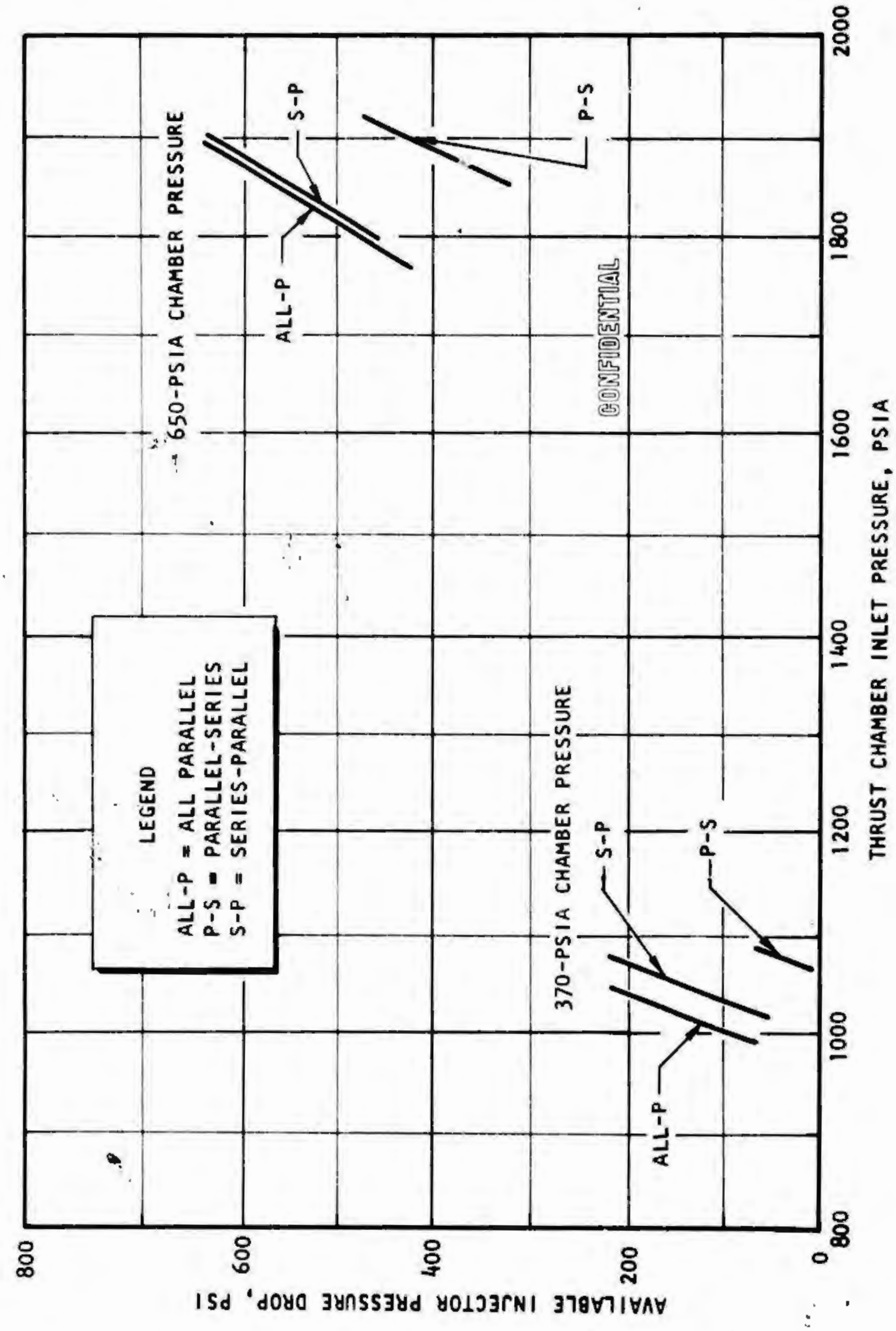

Figure 126. Available Injector Pressure Drop vs Thrust Chamber Inlet Pressure (Interim Analysis) (U)

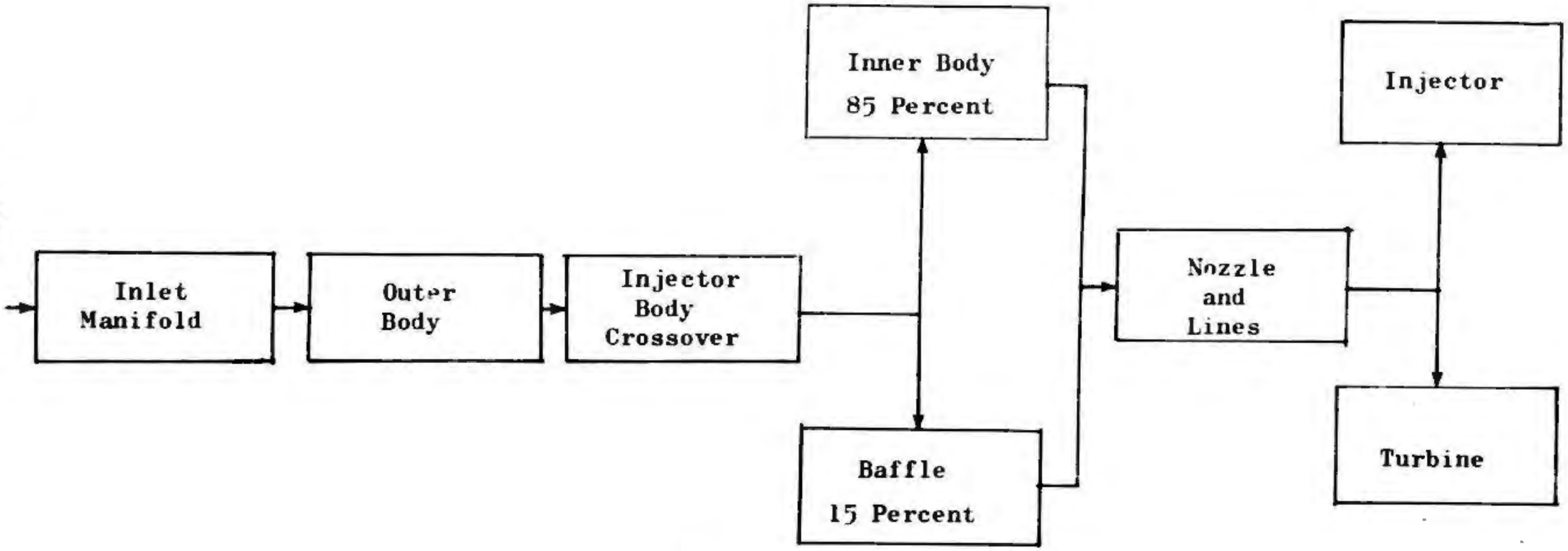

Figure 127. Main Engine Thrust Chamber Tube-Cooling Circuit (Interim Analysis) (U)

(U) The predicted maximum gas-side tube wall temperatures that resulted from the refined analysis are shown in Fig. 128 and 129. The significant change compared to the previous values presented in Fig. 120 and 121 was for the inner body where the peak gas-side wall temperature was reduced.

(U) Analytical studies were also conducted to investigate possible advantages that might be obtained with an unequal distribution of the number of coolant tubes in the downpass and uppass of the outer body. By decreasing the number of downpass tubes and increasing the coolant velocity, where the hydrogen is at its lowest bulk temperature and has relatively poor cooling properties, the gas-side wall temperature could be reduced. The approach would be to have a maximum of two adjacent tubes with coolant flow in the same direction to provide a near equal temperature distirbution. More nearly equalized maximum gas-side tube-wall temperatures of uppass and downpass tubes would result for the outer body. The study, however, indicated that the small heat transfer benefit derived was not commensurate with the additional manufacturing effort that would be required.

(C) An interim analysis of the main thrust chamber nozzle extension also was conducted. The nozzle configuration consisted of 900, 347 CRES tubes with a wall thickness of 0.012 inch. The unformed tube outside diameter was 0.145 inch. The tubes did not require tapering prior to forming. Furnace brazing was to be used to attach the tubes to the CRES backup structure consisting of two "hat bands" and an end frame. The predicted axial gas-side wall temperature distribution of the nozzle is shown in Fig. 130.

(3) Final Chamber Cooling Analysis

(U) As additional experimental heat transfer data became available from the Task II, 30-degree water-cooled and 30-degree tube-wall segment testing, the main thrust chamber cooling analysis was updated and refined. The results of this analysis predicted excessive pressure drop and gas-side wall temperature for the tube-wall configuration and led to the consideration of several alternate design approaches. The tube-wall analysis and

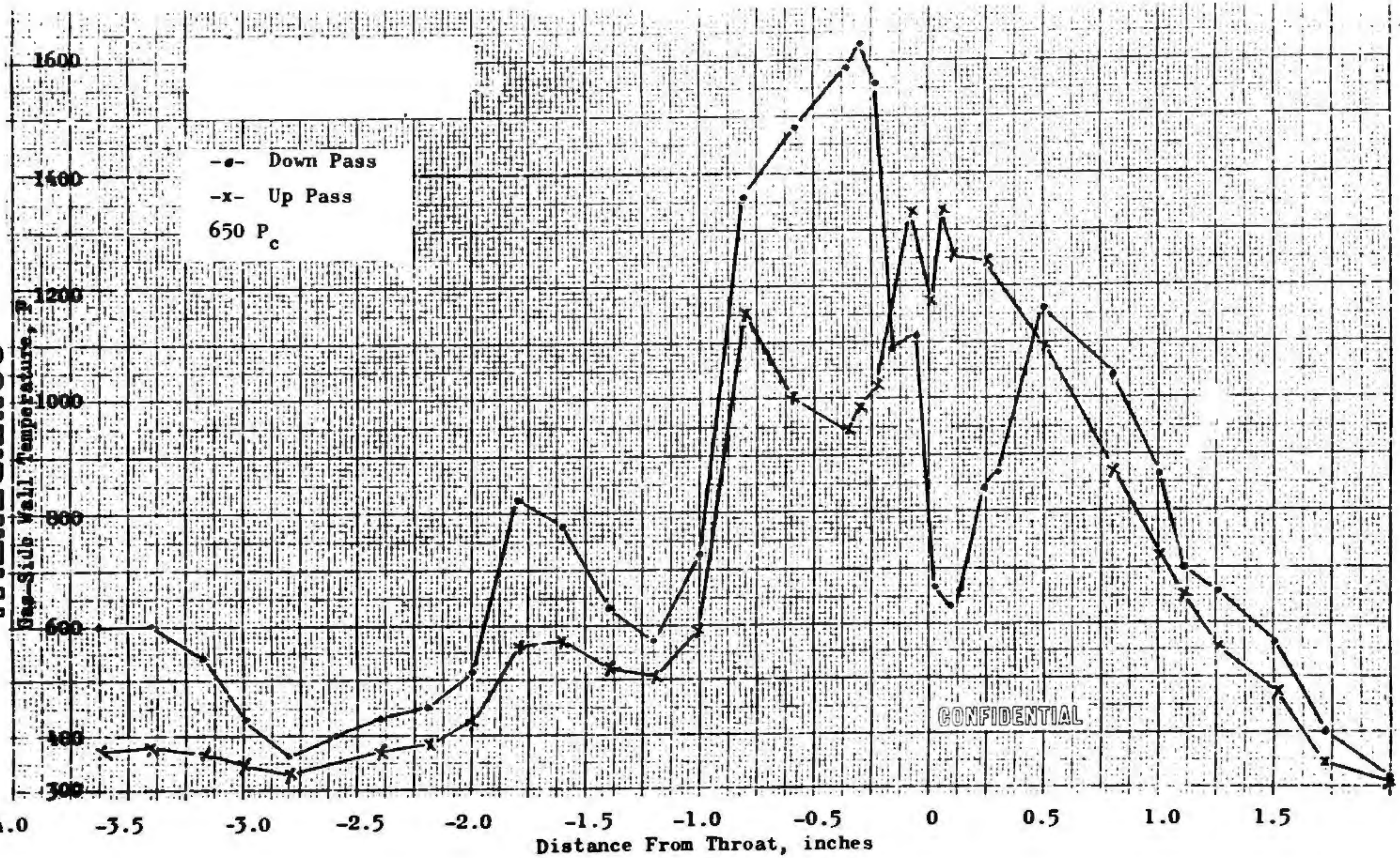

Figure 128. Outer Body Gas-Side Wall Temperature Profile (Refined Interim Analysis) (U)

CONFIDENTIAL

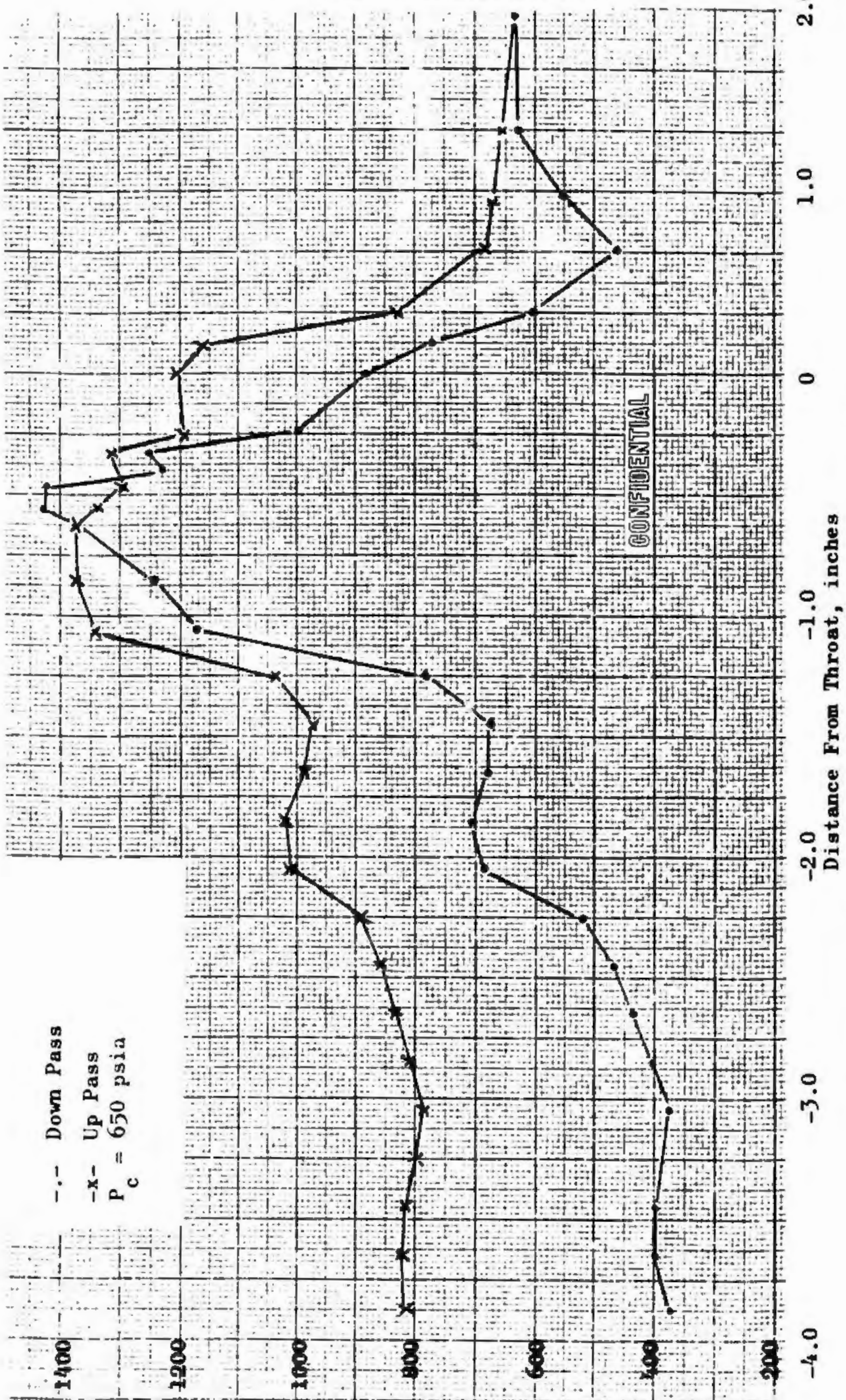

Figure 129. Inner-Body Gas-Side Wall Temperature Profile (Refined Interim Analysis) (U)

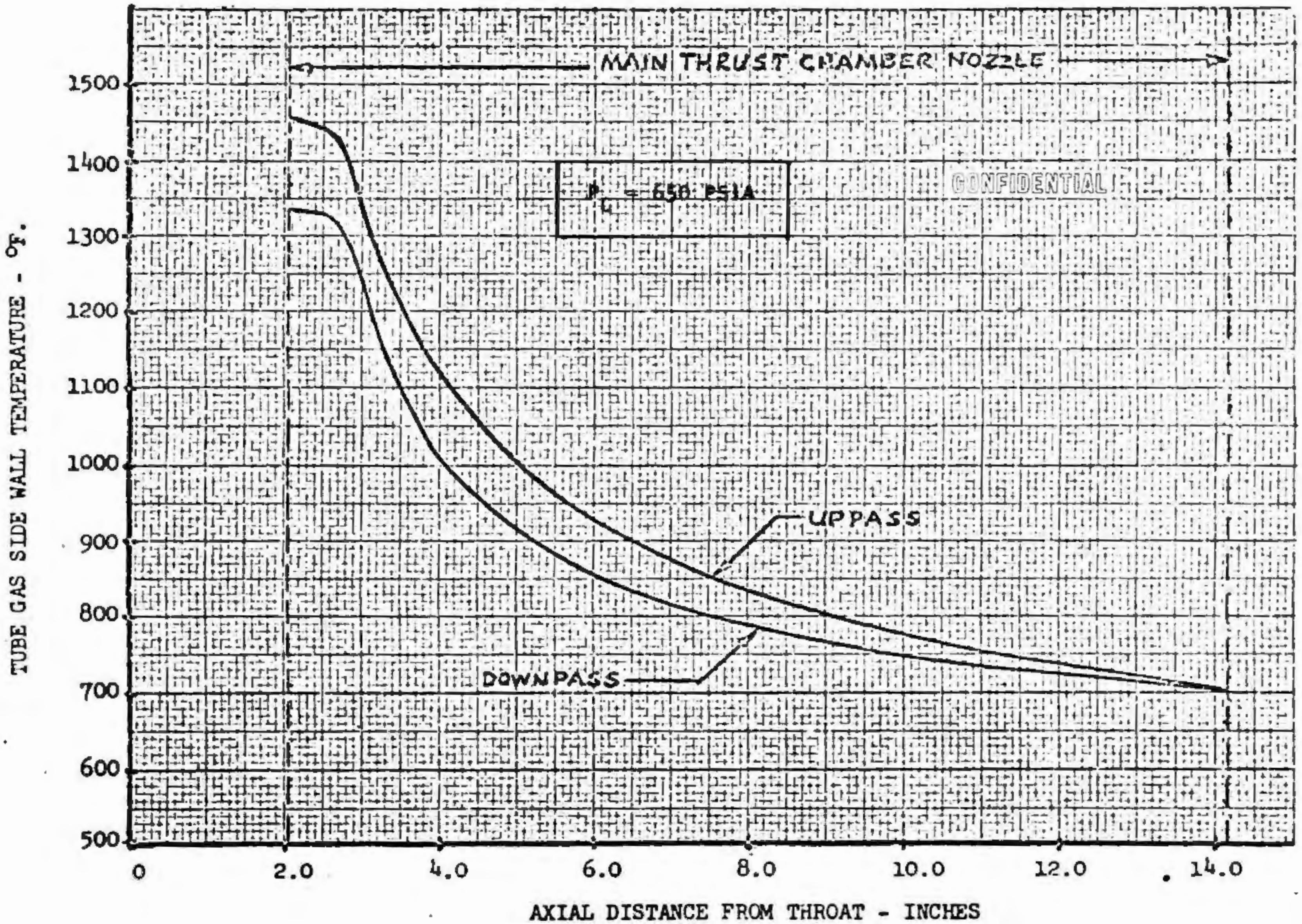

Figure 130. Temperature Profile of Main Thrust Chamber Nozzle Tube (Interim Analysis) (U)

(U) alternate approaches, which led to the final chamber cooling configuration, are discussed in the following paragraphs.

(a) Tube-Wall Analysis

(C) Using the heat transfer method of analysis described in the previous section, the gas-side heat transfer film coefficients were determined from tests of the 30-degree water-cooled thrust chamber segment. The heat transfer film coefficient profiles are shown in Fig. 131 through 133 for chamber pressures of 650, 342, and 90 psia, respectively. The three chamber pressures are for tests 078, 079, and 081 of Task II (Vol. II). The outer and inner body coefficients are shown to be the same in the converging part of the chamber. On the expansion nozzle, the outer body coefficients were higher than the inner body coefficients as a result of the hot-gas turning.

(U) The heat transfer coefficient profiles shown differ somewhat from the profiles shown in Fig. 119 which were obtained from earlier 5-inch segment experimental data. The coefficients of Fig. 131 through 133 were obtained from tests in which the prototype 30-degree injector design was utilized, while injector design variations were being made for the earler tests.

(U) The coolant-side heat transfer film coefficient was calculated using the techniques and equations developed in previous Rocketdyne studies (Ref. 23). The curvature enhancement factor was varied in the analysis from a value of 1.0 (no enhancement) at the beginning of curvature to a maximum of 1.5 in 10 equivalent tube diameters.

(U) The coolant exit pressure from the chamber must be sufficiently high to allow for pressure drop through the nozzle extension, interconnect lines, injector body, and injector orifices. Figure 134 shows the calculated exit pressure of the chamber, as well as the injector inlet pressure, as a function of chamber pressure.

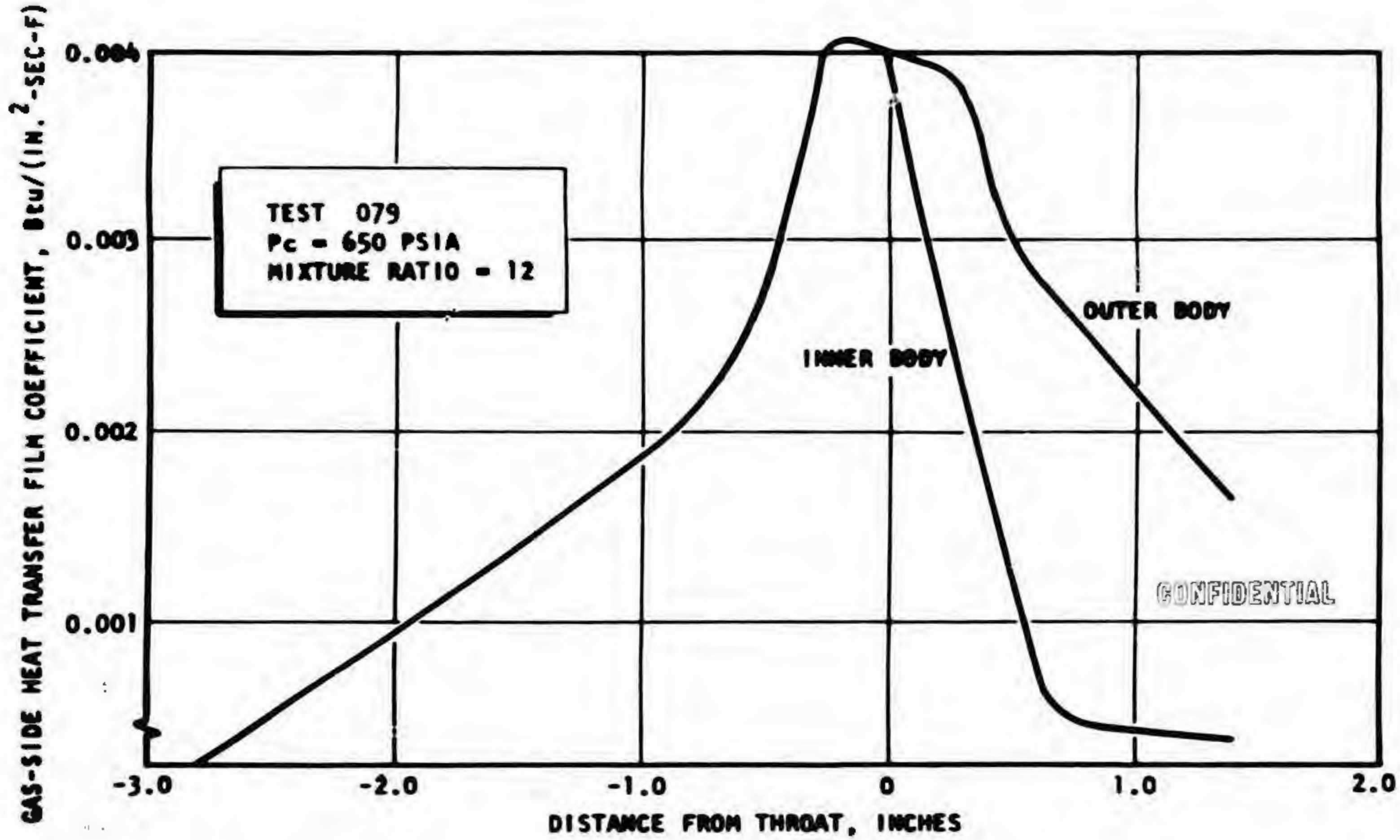

Figure 131 Gas-Side Heat Transfer Film Coefficient Profile of 30-Degree Water-Cooled Thrust Chamber (U)

CONFIDENTIAL

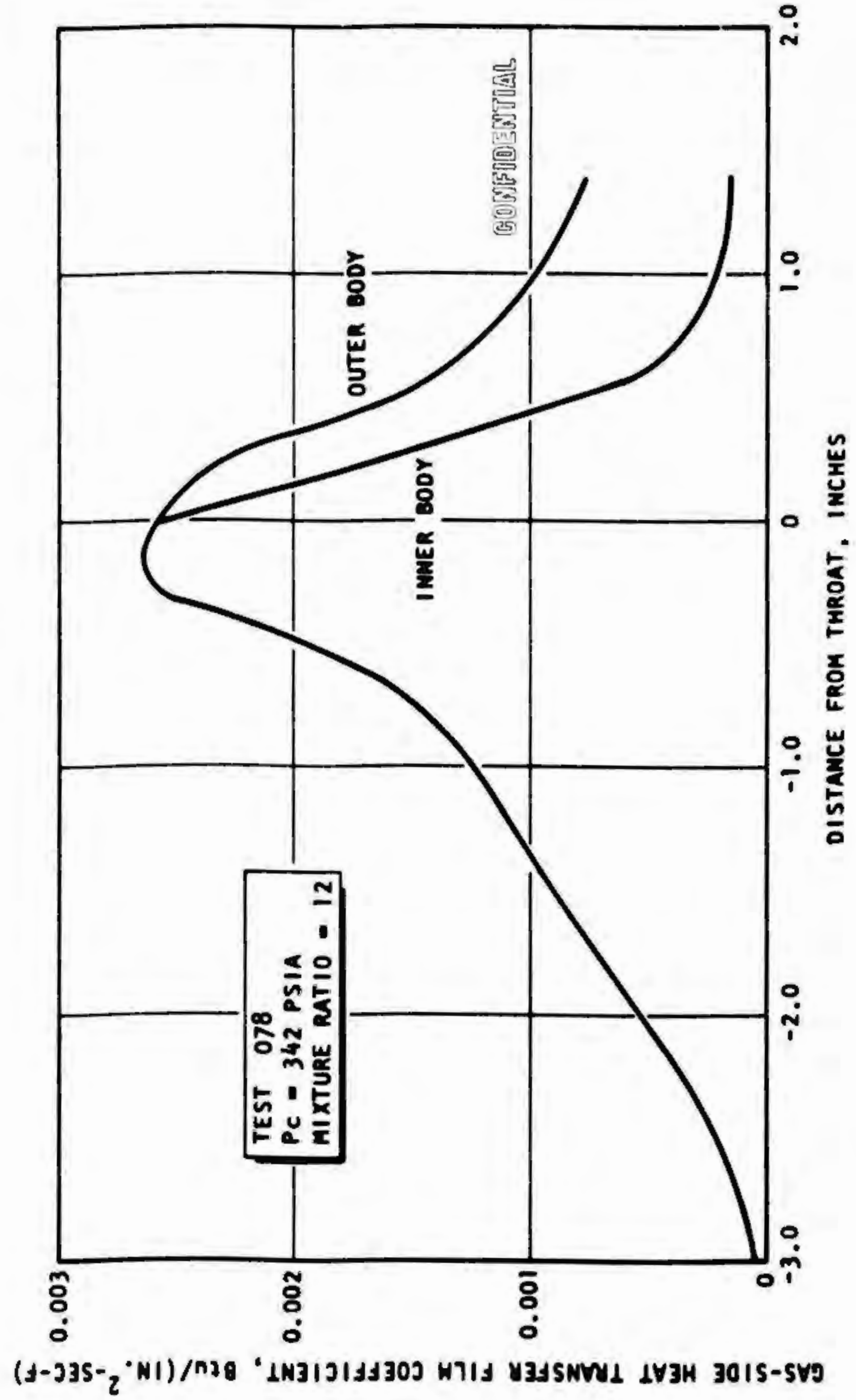

Figure 132. Gas-Side Heat Transfer Film Coefficient Profile of 30-Degree Water-Cooled Thrust Chamber (U)

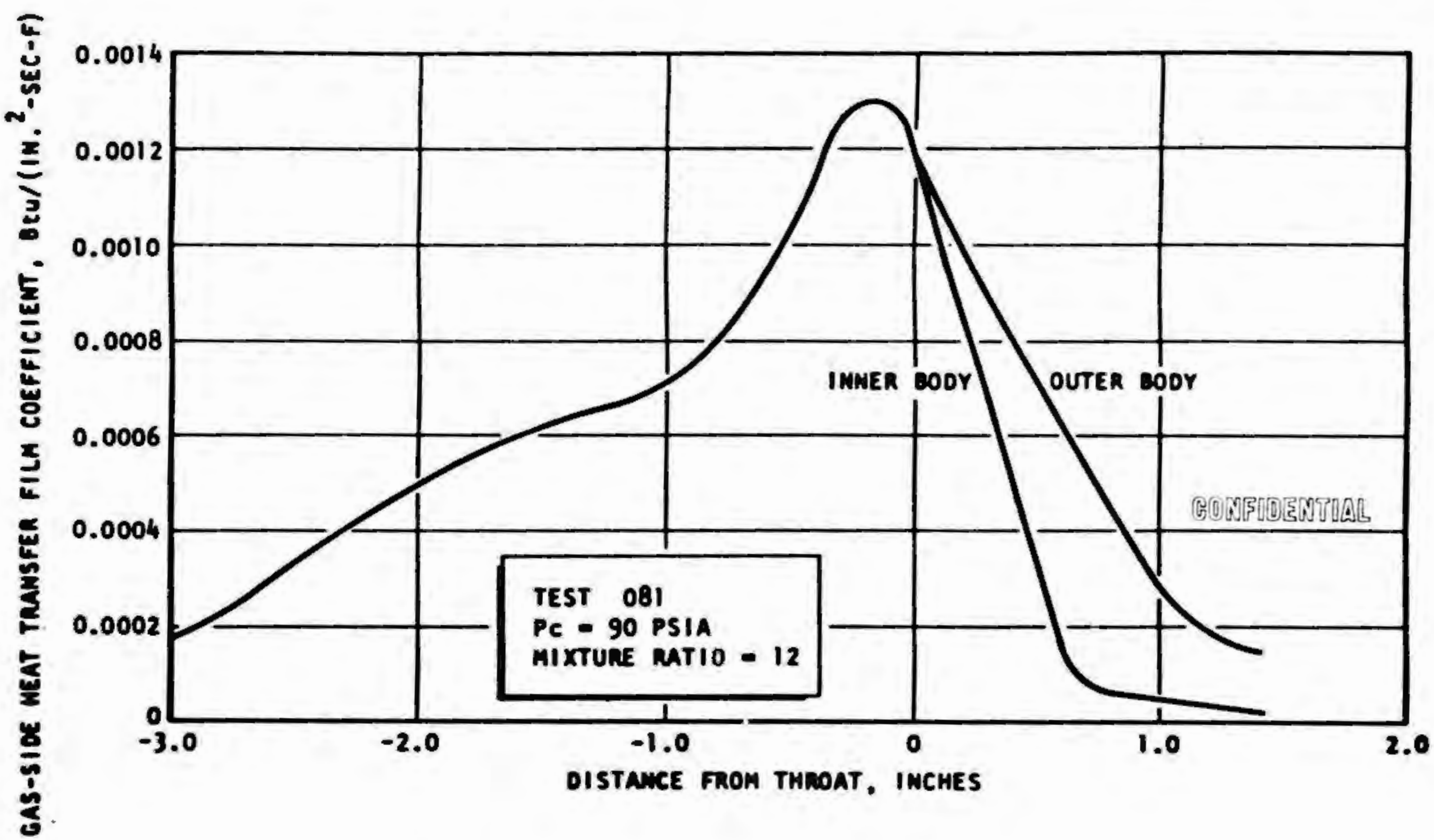

Figure 133. Gas-Side Heat Transfer Film Coefficient Profile of 30-Degree Water-Cooled Thrust Chamber (U)

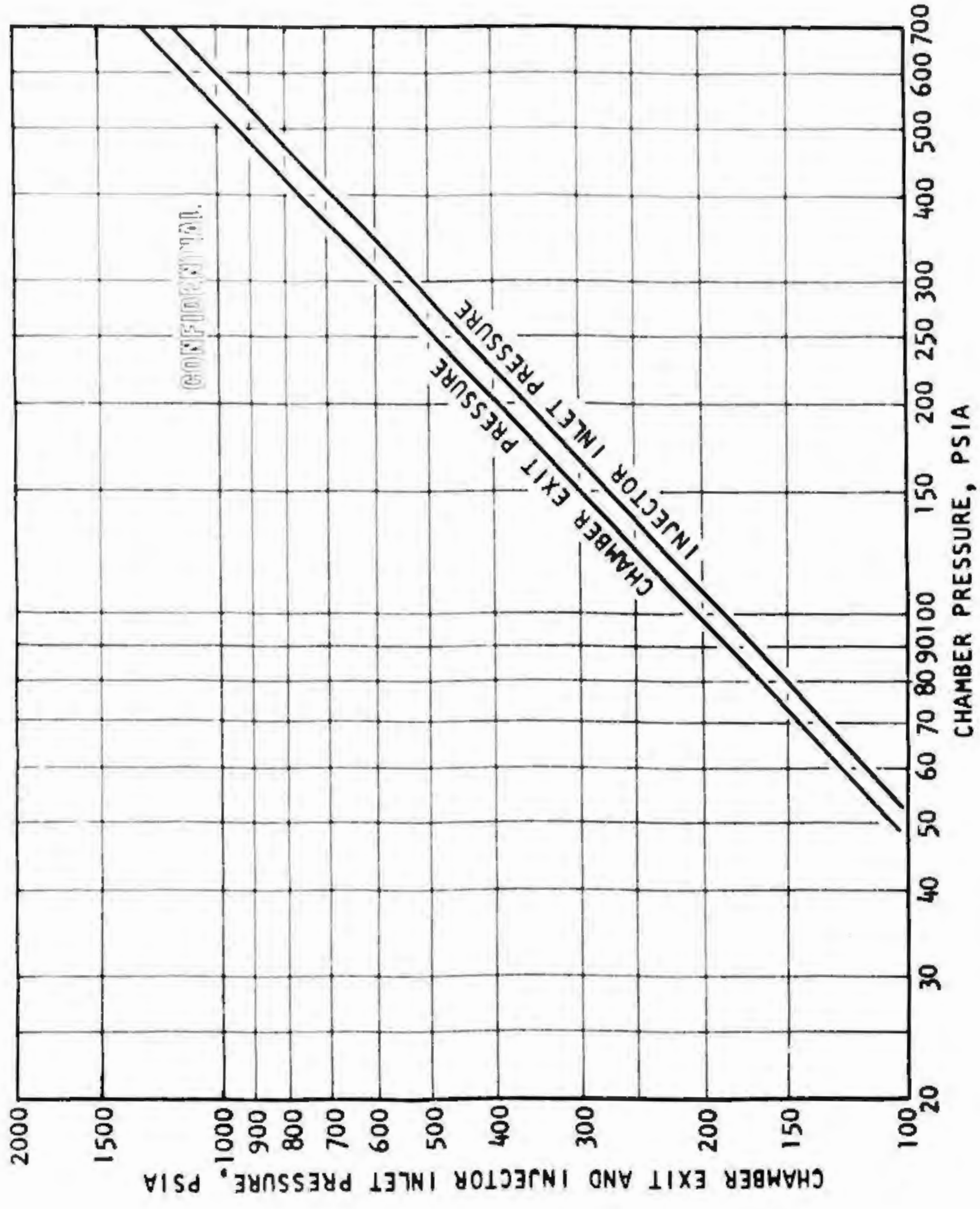

Figure 134. Chamber Exit and Injector Inlet Pressure as a Function of Chamber Pressure (Mixture Ratio = 12) (C)

CONFIDENTIAL

(C) Applying these data to the tubular wall segment design, and by making the appropriate corrections for rated coolant flowrate (design value), the projected coolant exit temperature, pressure drop of the coolant, and maximum gas-side wall temperature were determined for chamber pressures of 650 and 222 psia. These data are presented in Table 30, and represent an average of all the tube-wall testing. The calculations were not performed at chamber pressures below 222 psia because the predicted maximum hot-gas wall temperature of 2000 F (at 222-psia chamber pressure) was considered excessive, and even higher wall temperatures would occur at lower pressures. A maximum hot-gas wall temperature of 1600 F was the design goal to achieve a long-life chamber design.

TABLE 30

PREDICTED TUBE-WALL THRUST CHAMBER COOLING PARAMETERS
(Two-Pass Design - No Injector Oxidizer Bias) (U)

Configuration	650 psia				222 psia			
	Max. Wall Temp., F	Inlet Press., psia	Press. Drop, psi	Exit Bulk Temp., F	Max. Wall Temp., F	Inlet Press., psia	Press. Drop, psi	Exit Bulk Temp., F
Outer Body	1700	2300	835	1000	1750	1200	225	1310
Inner Body	1960				2000			

(U) The value of 2300-psia thrust chamber inlet pressure at 650-psia chamber pressure was the maximum value considered practical from consideration of the fuel pump design (Section V). In addition, choking of the coolant in the tube passages was predicted to occur at an inlet pressure of 2100 psia. The higher value of inlet pressure (2300 psia), however, caused a lower pressure drop of the coolant (compared to 2100-psia inlet pressure) by virtue of causing a high density of the coolant.

(U) One other important factor noted from the analysis was the high-pressure loss that occurred in regions other than the throat (in low heat flux regions). In these areas, the coolant mass flux was much higher than that required to cool the tubes adequately. Therefore, excessive pressure losses were encountered with little regard for optimum cooling at high chamber pressures. This factor also increased manifold pressure losses caused by high entrance and exit velocities to and from manifolds.

(C) Based on the above result, a new tube diameter profile was analyzed in an attempt to lower the heat transferred to the coolant and lower the pressure drop. The diameters of the tubes of the original tube-wall segment chamber are compared to the new tube design in Fig. 135. The diameter decrease of the tube in the throat area resulted in an increase of coolant mass flux from 4.1 to 4.83 lb/in.-sec.

(U) The design was made with the condition that the heat transfer to the coolant was equal to that of the original tube-wall chamber design. However, because of the lower coolant mass velocity in the combustion zone of the new tube design, the gas-side tube-wall temperature may increase and the heat transferred to the coolant may be lower than that measured in tests with the original tube-wall design.

(C) A comparison made of the old tube and new tube design parameters at the 650-psi chamber pressure level (on the basis of equal heat input) showed a reduction in pressure loss of 1150 psi while lowering the maximum gas-side wall temperature 150 F. This result was because the combustion zone and supersonic region were previously overcooled for the 650-psia chamber pressure condition. Lowering the mass velocity in the combustion zone and expansion nozzle reduced the friction loss in the tube and the manifold entrance and exit pressure losses sufficiently to allow for some increase of the mass flux in the throat region. This design approach, however, reduced the combustion zone cooling margin at reduced chamber pressures.

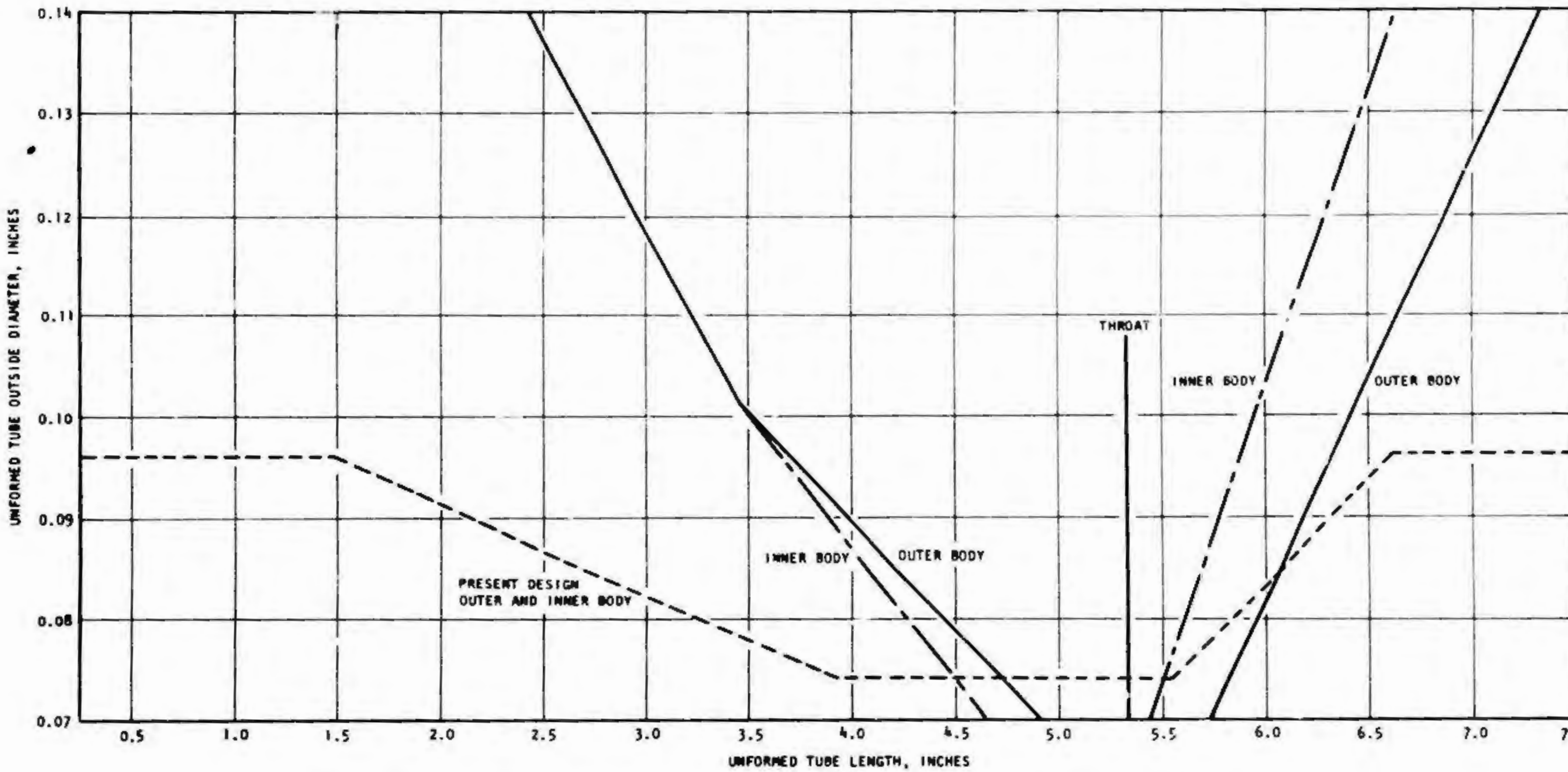

Figure 135. Unformed Tube Outside Diameter vs Tube Length (2300-psia inlet at P_c = 650 psia (C)

(U) The calculated gas-side tube-wall temperatures cf the new tube design are given as a function of the distance from the throat in Fig. 136. Little additional improvement in reducing the gas-side wall temperature can be expected except by using smaller diameter tubes with a great deal more pressure drop.

(C) The inlet pressure to the thrust chamber with the new tube profile was 2300 psia. As the result of the relatively high wall temperatures and pressure requirement for the two-pass tubular wall chamber design, an analysis of a one-pass inner body design was performed. Coolant tube sizes and pressure drops were determined for the single-uppass cooling circuit as a function of coolant inlet temperature and various maximum (one-dimensional) tube-wall temperatures. A two-dimensional heat transfer analysis of the tube in the throat region was conducted to obtain the necessary temperature corrections resulting from the use of a thick-walled tube. A nominal nickel wall thickness of 0.0165 inch was used in the analysis.

(C) The analysis showed that for the expected hydrogen inlet temperature of 800 R to the inner body, the tube size necessary to maintain the combustion-side wall temperature at 1600 F was less than 0.016-inch inner diameter (0.049-inch outer diameter). This tube size results in approximately 2700 tubes for the inner body. The required coolant inlet pressure to prevent choking was determined to be in excess of 3000 psia. A larger tube (d_i = 0.028 inch, d_o = 0.061 inch, N = 2164 tubes) resulted in a lower pressure drop but had maximum tube-wall temperatures in excess of 2000 F based on a two-dimensional thermal analysis.

(U) A primary problem area results from the use of relatively thick-walled tubes because two-dimensional temperatures are about 300 to 500 F higher than those calculated on a one-dimensional basis (Refer to Vol. II, Section III, 4.0, b, (1) for a detail analysis of the two-dimensional heat transfer.) The use of a thinner wall was not considered because the

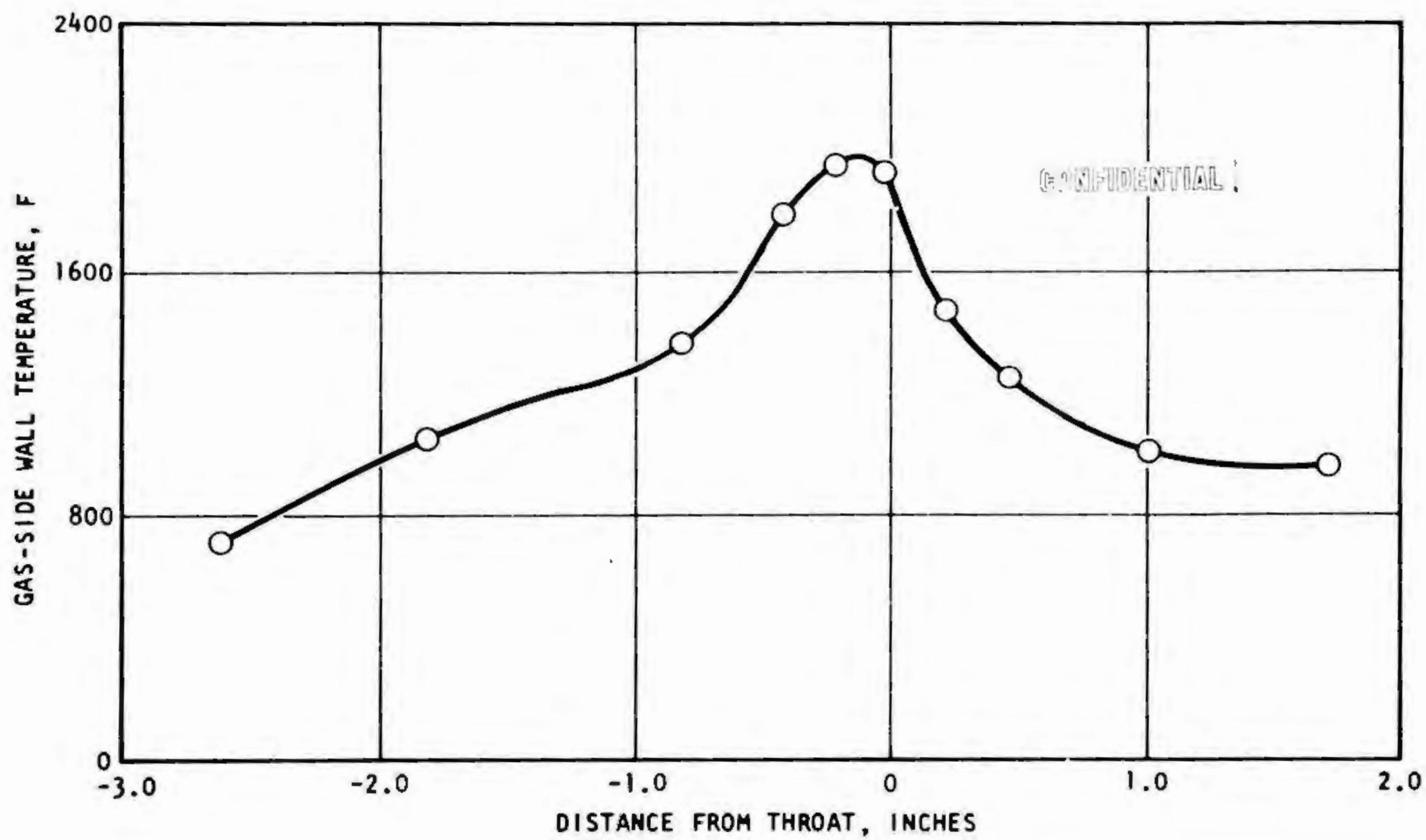

Figure 136. Tubular Inner Body Gas-Side Wall Temperatures as a Function of Distance From the Throat. (P_c = 650 psia) (C)

(U) estimated wall thickness of nickel tubes would have to be less than 0.008 inch to be of significant benefit in achieving acceptable wall temperatures and pressure drops. This tube thickness was considered not to be practical for manufacturing, handling, etc.. Based on the above results, the tube-wall design, with a single-pass coolant circuit for the inner body, was not considered a satisfactory solution for the excessive gas-side wall temperatures and pressure drop of the tube-wall thrust chamber. Alter·ate cooling concepts were required and are discussed in the next section.

(b) Alternate Cooling Design Approaches

(U) Analysis of the data from the Task II 30-degree tube-wall segment testing showed the tube-wall thrust chamber design was unsatisfactory because of excessive heat loads and associated required coolant circuit pressure drop. Several approaches for reducing the heat load and improving chamber cooling were considered. These approaches were:

1. Flattened Tubes
2. Filled or Dimpled Tubes
3. Shortened Combustion Chamber Length
4. Channel Coolant Passages (Channel-Wall)
5. Injector Mixture Ratio Bias (Film Cooling)

(U) Evaluation of the more promising approaches was conducted in Task II and are discussed in Vol. II, Section III, 5.0. The test evaluations of the channel-wall and mixture ratio bias concepts were successful in reducing the heat load and resulted in a satisfactory 30-degree prototype segment design. The analyses of these concepts, as they pertain to the main thrust chamber design,are discussed below.

(c) Channel-Wall Segment Thrust Chamber

(U) The design approach selected for the prototype regeneratively cooled 30-degree segment utilized channel coolant passages for all of the segment-wall cooling surfaces. This approach offered several potential advantages over the tubular-wall segment design which was previously evaluated. Principally, these advantages were reduced total integrated heat load and reduced fabrication cost and time.

(U) The fabrication improvements resulted from elimination of tooling for tube forming, as well as the handling of the large number of tubes for forming, stacking, brazing, etc.

(U) The advantage of reduced total integrated heat load resulted from having a flat hot-gas wall rather than the bumpy surface of a tube-wall design. The hot-gas wall heat transfer surface area of the channel-wall design was approximately 75 percent of that of the tube-wall design.

(U) An analysis was made to define the heat transfer characteristics of the channel-wall segment thrust chamber, using the gas-side film coefficients determined from the Task II water-cooled segment thrust chamber tests.

(U) Both two-pass and single-pass designs were analyzed. The single-pass chamber had 24 percent less pressure drop than the two-pass design. A comparison of one- and two-pass channel-wall designs is shown in Table 31. Also included are parameters for the tube-wall design.

(U) The channel-wall segment construction was analyzed for two-dimensional heat conduction. A chart of the isotherms for the channel-wall construction is shown in Fig. 137. The gas-side surface temperature of the single-pass channel-wall design, in general, was 500 F lower than the tube-wall thrust chamber. A comparison of two-dimensional effects for tubes and channels is shown in Table 32.

TABLE 31

THRUST CHAMBER SEGMENT COMPARISON OF CHANNEL-WALL AND TUBE-WALL DESIGNS

(no injector oxidizer bias) (U)

Configuration	650 psia				222 psia				90 psia			
	Max. Wall Temp., F	Inlet Press., psia	Press. Drop, psi	Exit Bulk Temp., F	Max. Wall Temp., F	Inlet Press., psia	Press. Drop, psi	Exit Bulk Temp., F	Max. Wall Temp., F	Inlet Press., psia	Press. Drop, psi	Exit Bulk Temp., F
One-Pass Channel Wall												
Outer Body	1370	2100	550	570	1270	1000	165	955	1520	500	71	1360
Inner Body	1500				1500				1670			
Two-Pass Channel Wall												
Outer Body	1530	2100	970	370	1490	1000	275	945	--	--	--	--
Inner Body	1650				1700				--			
Two-Pass Tube Wall												
Outer Body	1700	2300*	835*	1000	1750	1200	225	1310	--	--	--	--
Inner Body	1960				2000				--			

*Coolant will choke at 2100-psia inlet pressure. Low pressure drop of coolant is caused by higher density of coolant when introduced at a higher pressure. If an inlet pressure of 2300 psia were used in the channel wall designs, the computed loss would be well below the 835 value shown for the tube wall.

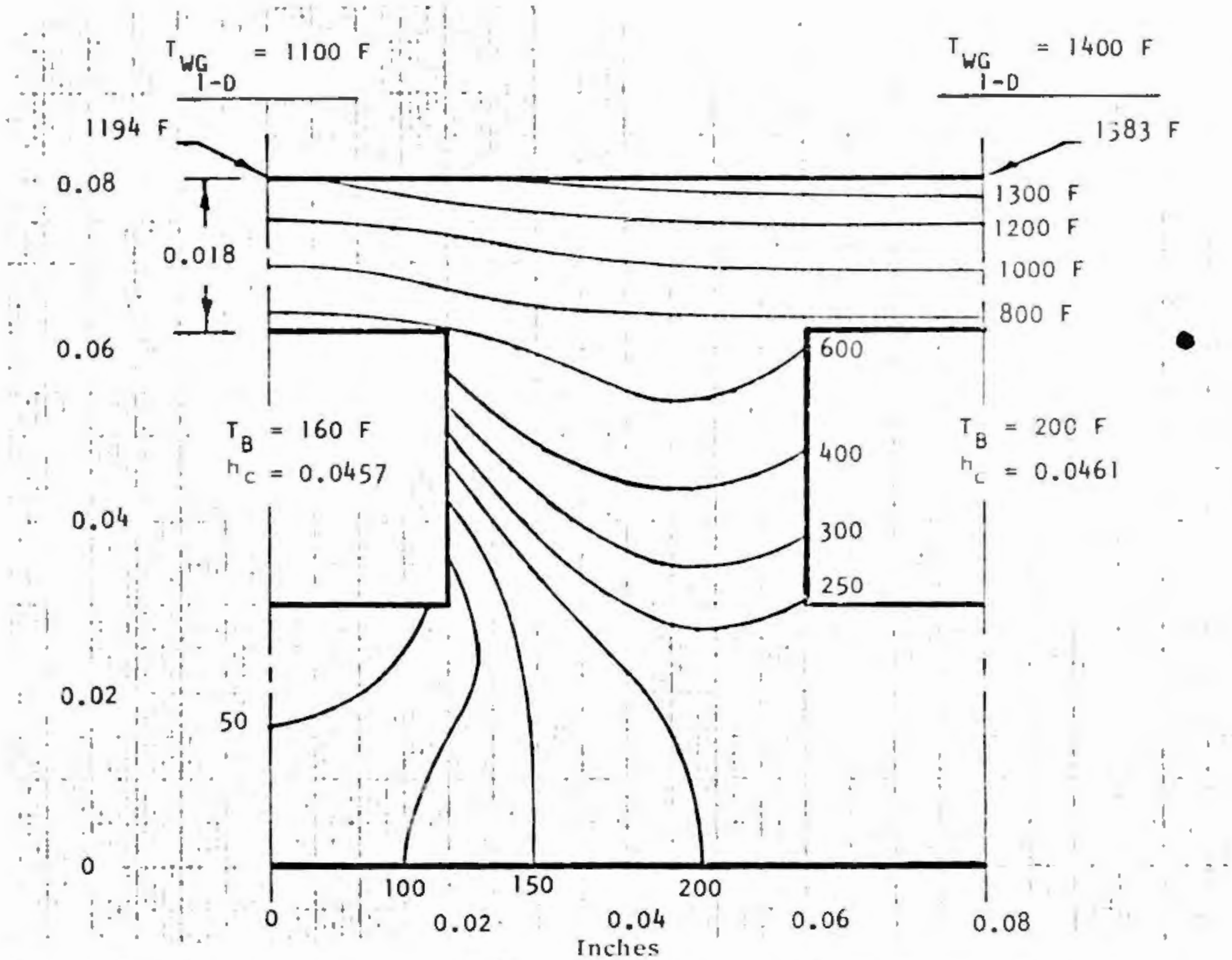

Figure 137. Typical Channel-Wall Segment Temperature Distribution (Outer Body) (P_c = 650 psia) (C)

TABLE 32

TWO-DIMENSIONAL EFFECT ON GAS-SIDE WALL TEMPERATURES
(COMPARISON OF TWO-PASS TUBE WALL AND ONE-PASS CHANNEL WALL) (U)

Gas-Side Heat Transfer Coefficient, (Btu/in.^{2}-sec-F)	Coolant Bulk Temperature, F	Difference Between Two- and One-Dimensional Wall Temperatures*, F ($T_{2-D} - T_{1-D}$)	
		Channel	Tubes
0.004	1000	200	400
	-200	50	400
0.001	1000	30	130
	-200	-200	-40
0.0002	1000	-180	-80
	-200	-350	-350

*The one-dimensional temperature is 1400 F in all cases.

(U) The two-dimensional wall temperature effect as a function of gas-side heat transfer coefficient and hydrogen temperature was analyzed for a 0.016- by 0.036-inch channel, with a 0.018-inch gas-side wall thickness and a 0.04-inch land width. All-nickel channels were used. The analysis used a 8000 F adiabatic wall temperature and assumed a 1400 F one-dimensional gas-side wall temperature for computing the coolant-side film coefficient. The results of this analysis are shown in Fig. 138 . The trend of maximum wall temperature was as expected, with two-dimensional effects causing increases at high heat transfer rates and decreases for low heat transfer rates. The maximum wall temperature obtained with the channel configuration was lower than that obtained using a tubular configuration because of the better two-dimensional temperature characteristics. At the nozzle throat (h_g = 0.00398 Btu/in.^{2}-sec-F), the maximum wall temperature increase from two-dimensional influences was approximately 180 F. The influence of the assumed one-dimensional gas-side wall temperature is shown in Fig. 139 . At low heat transfer rate (h_g = 0.0002), the maximum

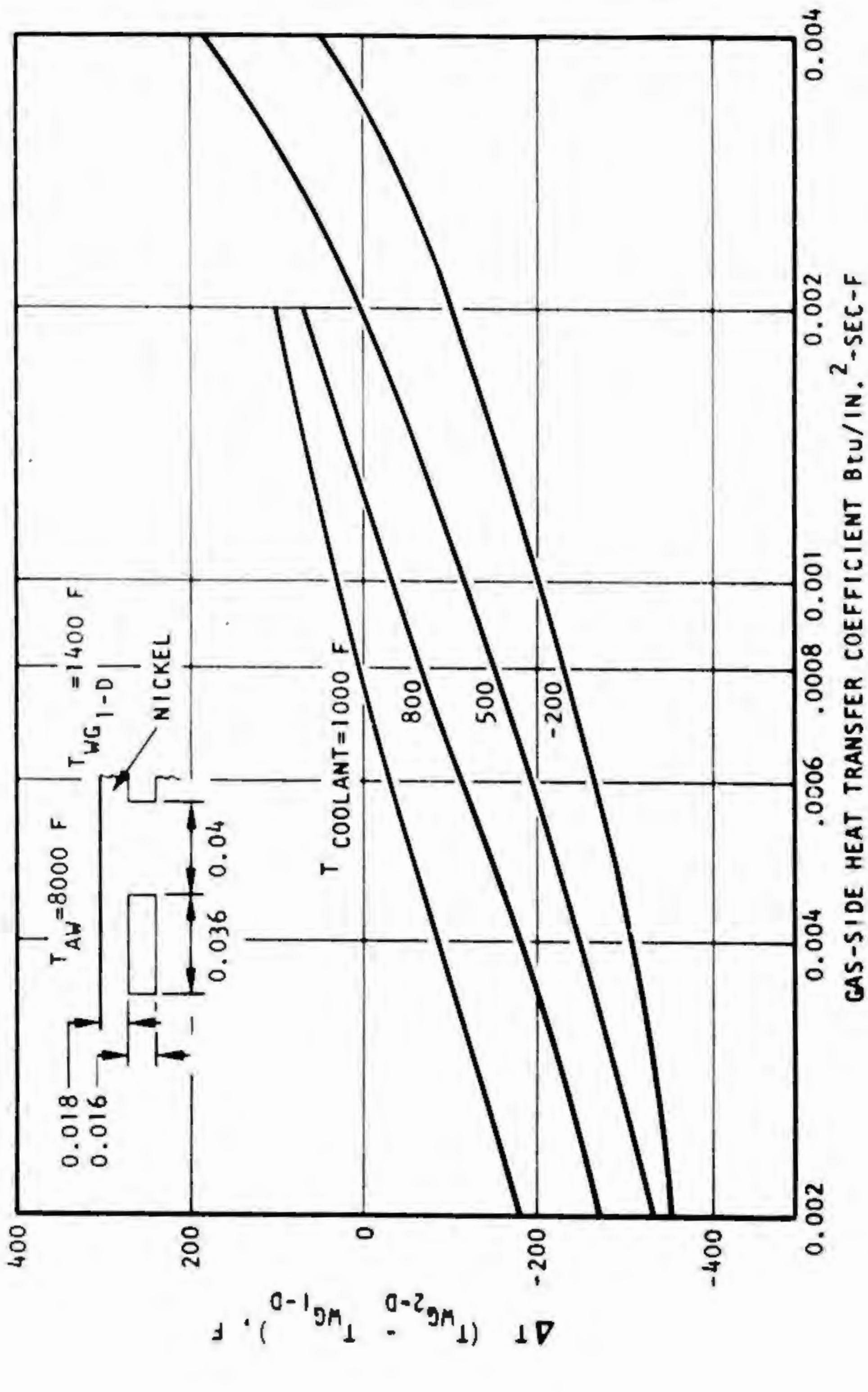

Figure 138. Chamber-Wall Segment Two-Dimensional Heat Transfer Influence (Single-Pass Channel Configuration) (U)

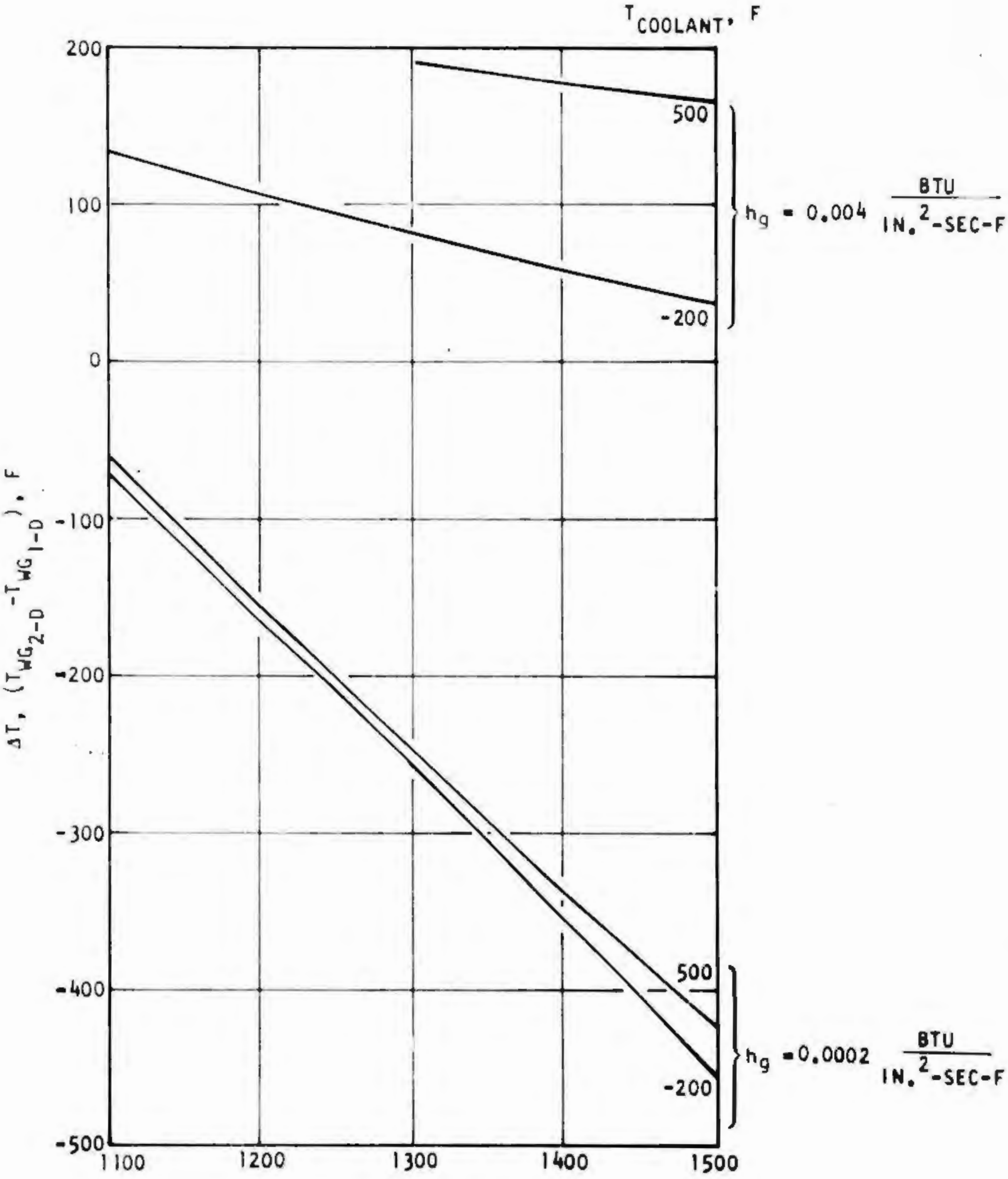

Figure 139. Influence of Assumed One-Dimensional Wall Temperature (Channel-Wall Segment) (U)

wall temperature varied 300 F for the 1100 to 1500 F one-dimensional temperatures. However, at high heat transfer rates, the maximum wall temperature varied approximately 50 F. For one-dimensional wall temperatures other than 1400 F, this analysis provides an indication of the resulting wall temperature.

(U) The effect of using a stainless-steel backup structure in low heat flux regions of the combustion chamber and nozzle is shown in Table 33. The stainless-steel backup structure resulted in approximately a 200 F increase in the maximum gas-side wall temperature over the all-nickel configuration because of the difference in thermal conductivities of the two materials.

(C) With a gas-side wall thickness of 0.018 inch and a channel width of 0.028 inch, the channel depth and land width were varied while maintaining a constant coolant mass velocity of 4.8 lb/in.^{2}-sec. For a throat gas-side heat transfer coefficient of 0.00398 Btu/in.^{2}-sec-F, representative coolant bulk temperature and coolant-side film coefficients were assumed for the inner and outer bodies. In general, the maximum gas-side wall temperature would be decreased as the channel depth is increased; an increase in the land width would result in a temperature increase. As shown in Table 34, the increased land width dominated the effect of the increase in channel depth, and the maximum wall temperature increased approximately 120 F from 0.0272- to 0.041-inch land width. All the channel configurations resulted in maximum gas-side wall temperatures less than 1600 F. The incorporation of stainless-steel backup, as shown in Table 35, resulted in a 140 to 250 F increase in maximum wall temperature (~1600 F). A throat channel size of 0.016 by 0.028 inch (all nickel) was selected based on this analysis.

(U) The predicted coolant discharge temperature for the channel-wall chamber is shown as a function of chamber pressure in Fig. 140. The gas-side surface temperature of the channel-wall thrust chamber was determined for the design condition, and a plot of the maximum gas-side surface temperature

TABLE 33

SINGLE-PASS CHANNEL (STAINLESS-STEEL BACKUP STRUCTURE VS NICKEL BACKUP STRUCTURE) (U)

T_{AW} = 8000 F, h_g = 0.00167 Btu/in.^{2}-sec-F

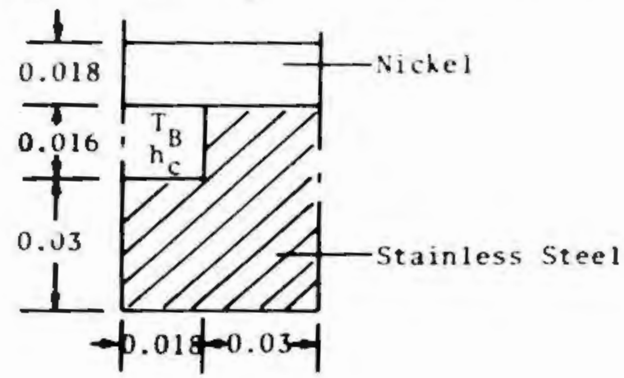

	T_{Bulk}, F	h_g Btu/in.^{2}-sec-F	$(T_{wg_{1-D}})$, F	Stainless Steel $(T_{wg_{2-D}})_{max}$, F	Nickel $(T_{wg_{2-D}})_{max}$, F
Outer Body	-260	0.005	1989	1883	1654
	↓	0.010	1157	1222	980
		0.015	949	827	704
Inner Body	110	0.01	1464	1496	1265
	↓	0.02	978	1110	879
		0.03	799	969	738

TABLE 34

CHANNEL DEPTH AND LAND WIDTH INFLUENCE (ALL NICKEL) (U)

P_c = 650 psia
T_{AW} = 8000 F
h_g = 0.00398 Btu/in.^{2}-sec-F

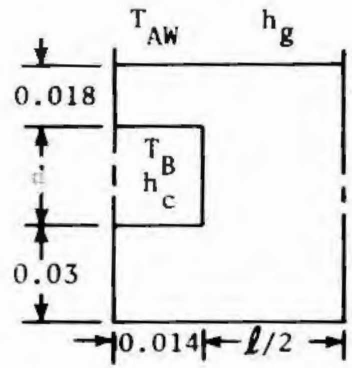

Land Width, inch	Channel Depth, inch	Outer Body			Inner Body		
		T_{Bulk}, R	h_c, Btu/in.^{2}-sec-F	$T_{Wg_{max}}$, F	T_{Bulk}, R	h_c, Btu/in.^{2}-sec-F	$T_{Wg_{max}}$, F
0.0410	0.0192	413	0.0357	1451	815	0.0621	1577
0.0370	0.0181			1411			1538
0.0333	0.0171			1377			1512
0.0301	0.0162			1346			1485
0.0272	0.0154			1321			1463

TABLE 35

CHANNEL DEPTH AND LAND WIDTH INFLUENCE (STAINLESS STEEL BACKUP) (U)

P_c = 650 psia
T_{AW} = 8000 F
h_g = 0.00398 Btu/in.^{2}-sec-F

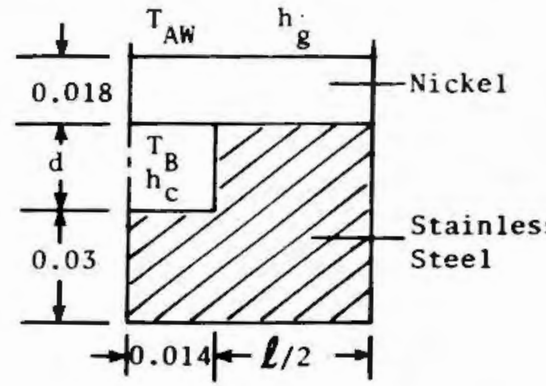

		Outer Body			Inner Body		
Land Width, inch	Channel Depth, inch	T_{Bulk}, R	h_c, Btu/in.^{2}-sec-F	$T_{Wg_{max}}$, F	T_{Bulk}, R	h_c, Btu/in.^{2}-sec-F	$T_{Wg_{max}}$, F
0.0410	0.0192	413	0.0357	1705	815	0.0621	1783
0.0370	0.0181			1644			1725
0.0333	0.0171			1589			1675
0.0301	0.0162			1548			1634
0.0272	0.0154			1504			1599

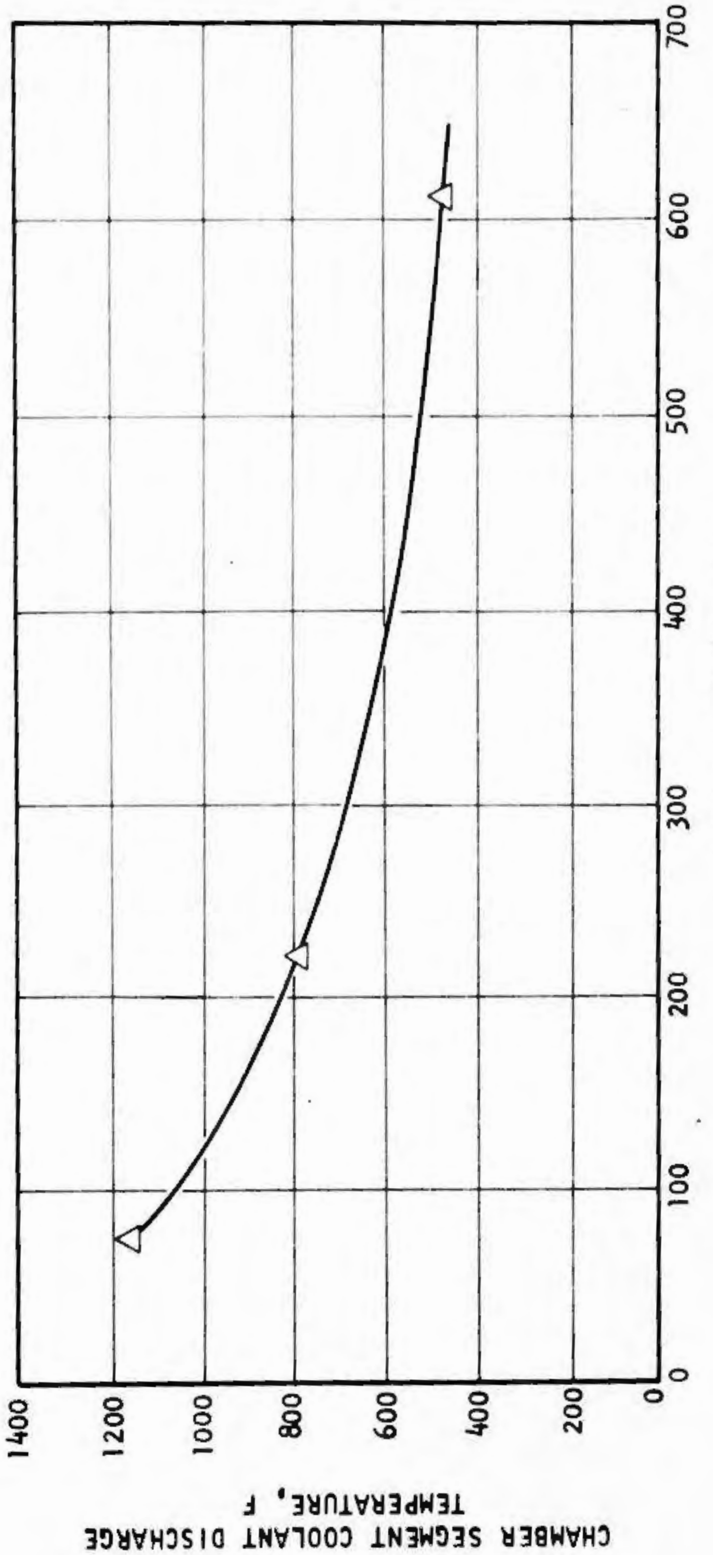

Figure 140. 30-Degree Regeneratively Cooled Prototype Chamber Segment, Predicted Coolant Discharge Temperature (U)

(U) as a function of chamber pressure appears in Fig. 141. This figure also compares the results of the one-dimensional and two-dimensional analyses.

(C) An additional design improvement which was incorporated into the channel-wall design was a revised coolant passage flow area profile (as compared to the previous tube-wall profile). The new profile increased the coolant passage flow area (reduced mass-velocity) in the overcooled regions of the chamber (upstream and downstream of the throat region). This change resulted in increased hot-gas wall temperatures in these regions, with associated reduced heat transfer and pressure drop. A plot of the channel-wall thrust chamber coolant flow area as a function of distance from the throat is given in Fig. 142. The channel width is kept at 0.025 inch, while the depth is varied. As shown in Fig. 142, the channel area varies from a maximum value of 5 in.^{2} at the outer body entrance to 1 in.^{2} at the throat. Also seen in Fig. 142 is a plot of the previous tubular thrust chamber design flow area which varied from 2.5 in.^{2} at the entrance to 1.2 in.^{2} at the throat.

(C) The calculated inlet pressure to the channel wall thrust chamber is given as a function of mixture ratio for three chamber pressure in Fig. 143. As shown, the pressure requirements for the chamber approaches 2200 psi for the extreme mixture ratio of 9:1.

(U) A study also was made to ascertain the effects of manufacturing defects on the heat transfer in the channel-wall thrust chamber. The study was performed on a two-dimensional heat transfer basis.

(C) The effect of a void in the land is shown in Fig. 144. This case was for the inner body at a chamber pressure of 650 psia. Only for gross voids (more than 50 percent of the braze over a long length of the land) do the temperatures become excessive. In this case, the chamber would fail during the prefiring pressure check.

(C) Figures 145 through 148 show the effect of reduction in coolant-side heat transfer coefficient for all channels on the wall temperature. Figure 146 shows, in addition, the effect of a single-channel reduction. Of significance is that, for total plugging of a single channel, a temperature well in excess

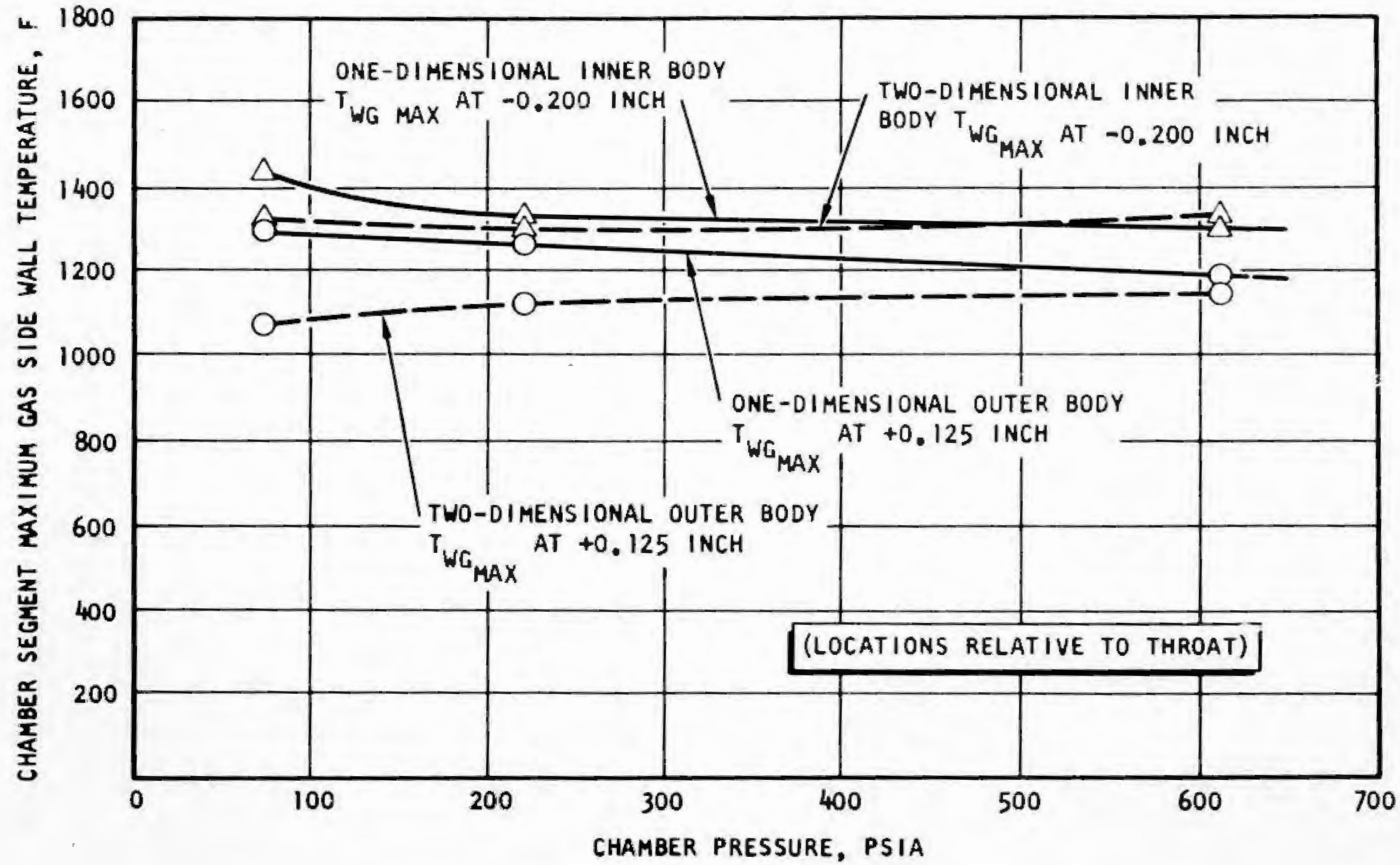

Figure 141. 30-Degree Regeneratively Cooled Prototype Chamber Segment, Predicted Maximum Gas-Side Wall Temperature (U)

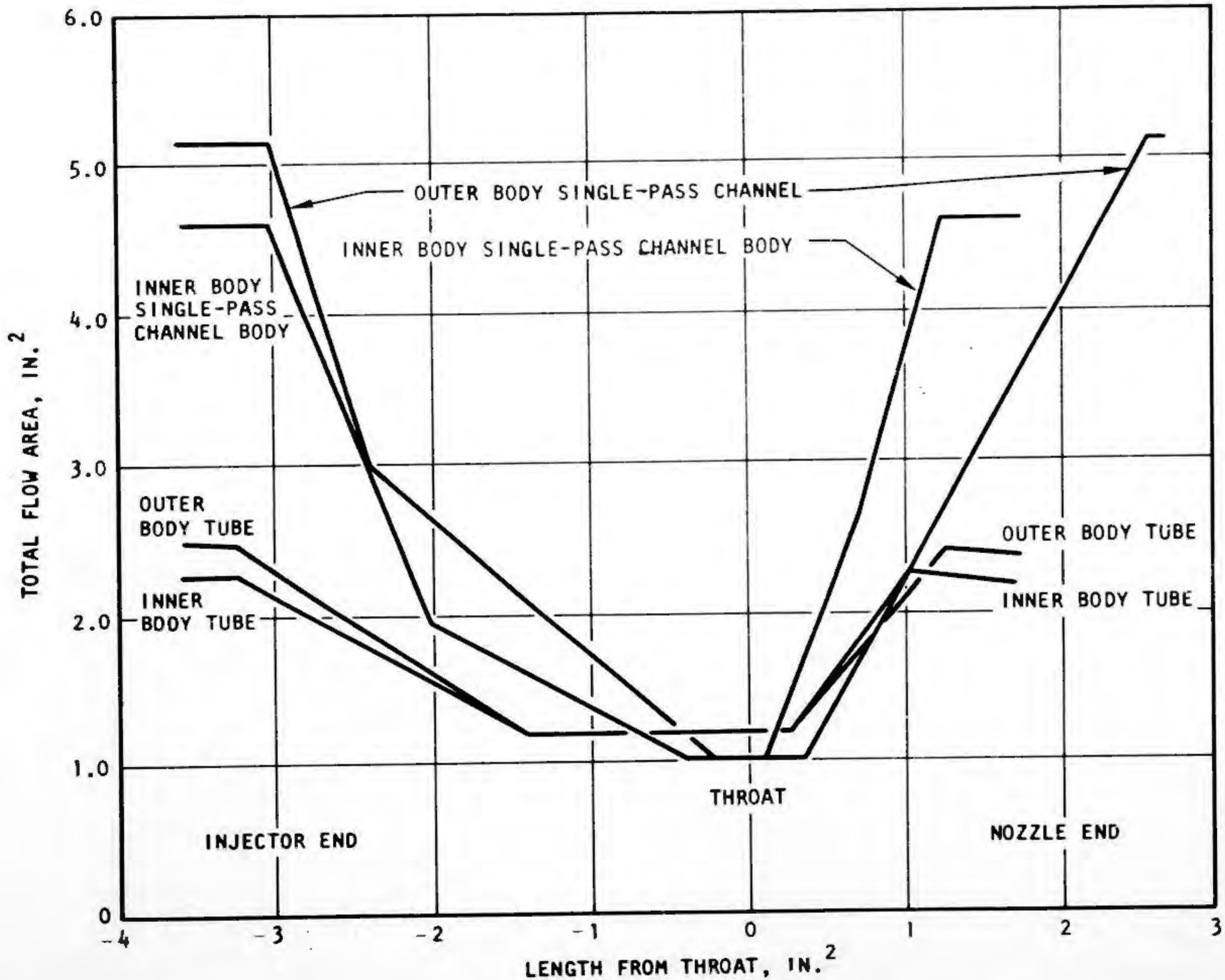

Figure 142. Outer and Inner Body Total Passage Area vs Length From Throat (Channel-Wall Segment) (U)

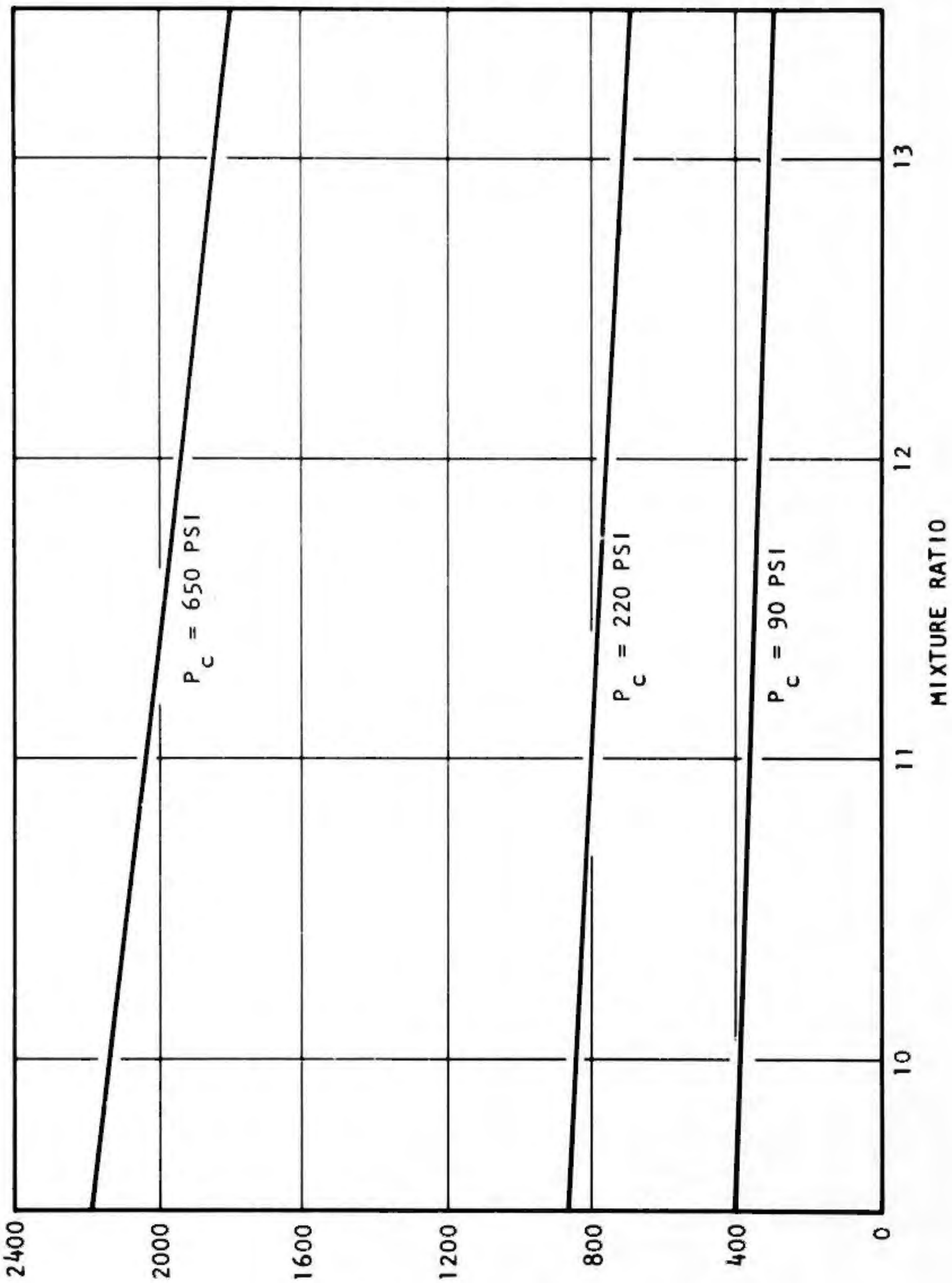

Figure 143. Effect of Mixture Ratio on Inlet Pressure (Channel-Wall Thrust Chamber) (U)

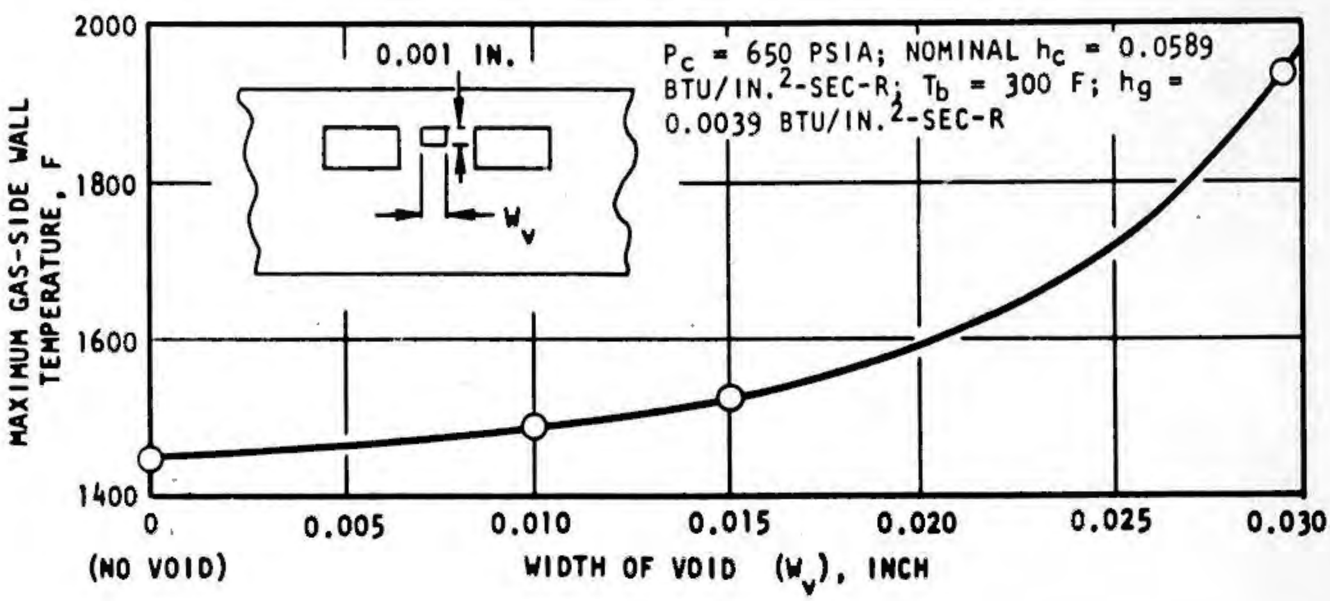

Figure 144. Effect of Void Width on Hot-Gas Side-Wall Temperature (Inner Body Channel-Wall Segment) (U)

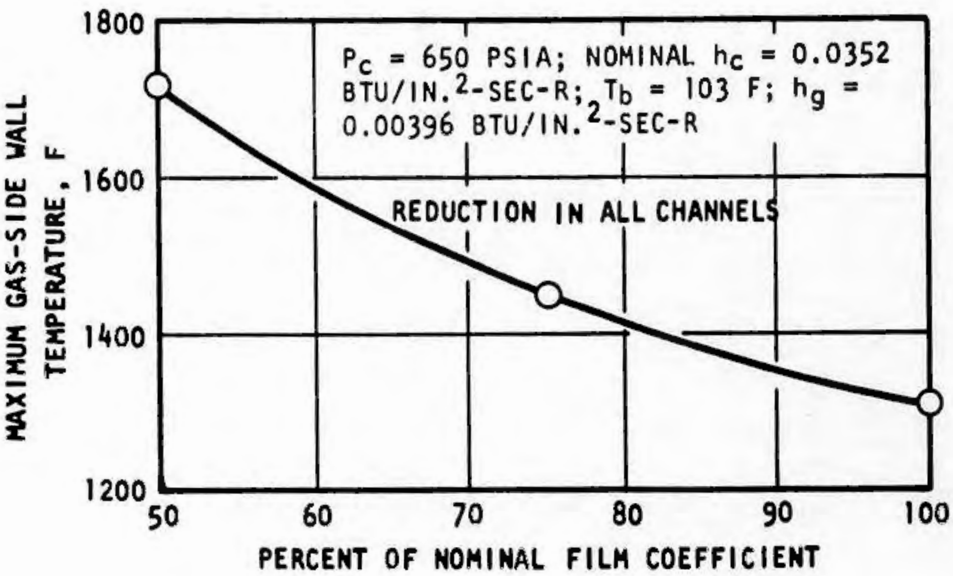

Figure 145. Effect of Reduced Coolant Film Coefficient, h_c, on Hot-Gas Side-Wall Temperature (Outer Body Channel-Wall Segment) (U)

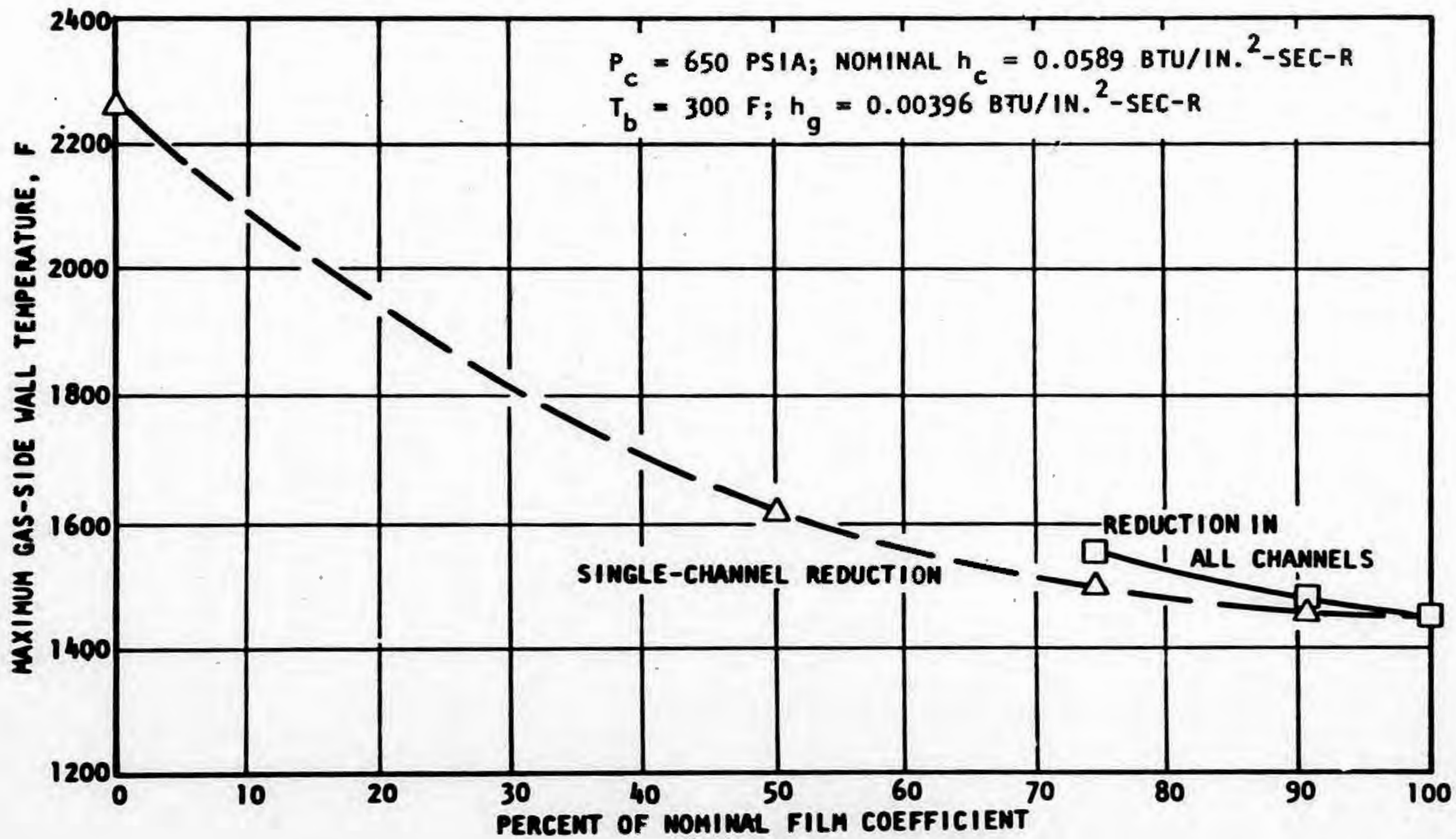

Figure 146. Effect of Reduced Coolant Film Coefficient, h_c, on Hot-Gas Side-Wall Temperature (Inner Body Channel-Wall Segment) (U)

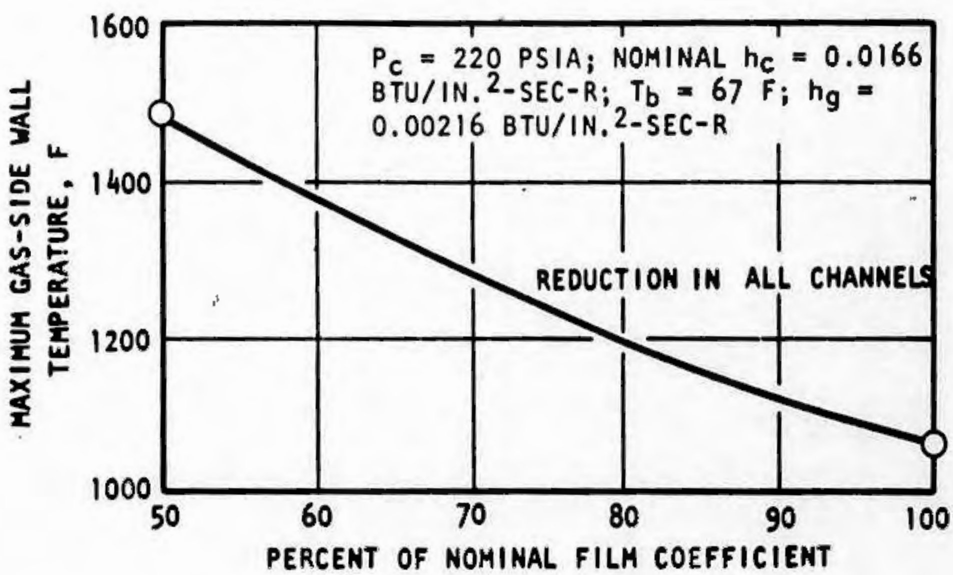

Figure 147. Effect of Reduced Coolant Film Coefficient, h_c, on Hot-Gas Side-Wall Temperature (Outer Body Channel-Wall Segment) (U)

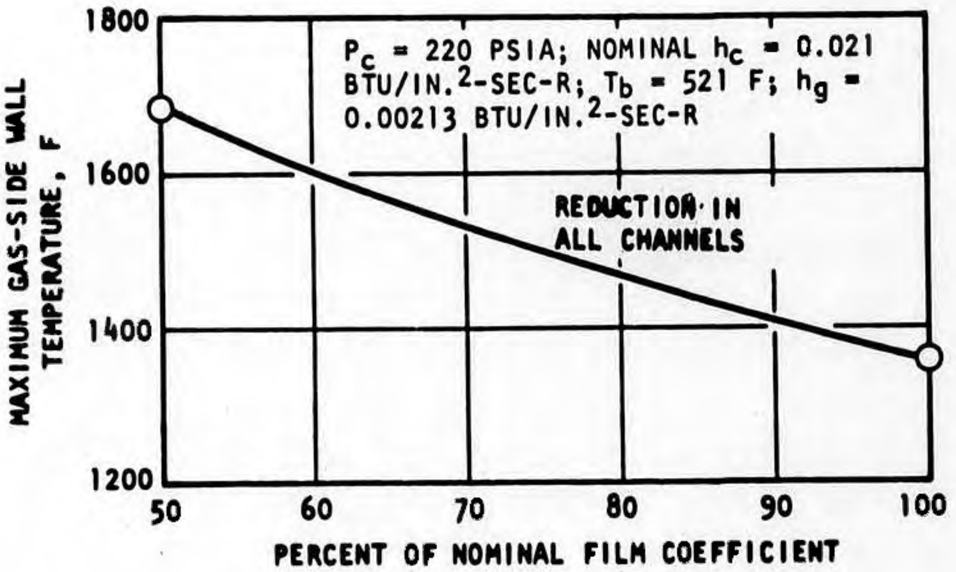

Figure 148. Effect of Reduced Coolant Film Coefficient, h_c, on Hot-Gas Side-Wall Temperature (Inner Body Channel-Wall Segment) (U)

(C) of 2200 F would be reached locally. This plugging condition could, however, be detected during the fabrication pressure checks.

(C) The effect of channel tolerances also was studied. The variation considered was +0.001 inch. At the throat of the chamber, the dimensions considered were:

Nominal	0.028 x 10.016 inch
With Tolerance	0.029 x 0.017 inch

(C) A 10-percent increase in passage area occurred at the throat with the larger dimension, and resulted in the following wall temperature increases:

Outer Body		Inner Body	
At P_c = 650 psia:	70 F	At P_c = 650 psia:	20 F
At P_c = 90 psia:	140 F	At P_c = 90 psia:	20 F

(C) The minus tolerance condition (-0.001 inch) was not analyzed because this condition would increase the local coolant mass velocity and result in a lowering of the wall temperature at that location.

(d) Influence of Mixture Ratio Bias

(U) Because of the favorable Task II test results obtained with mixture ratio bias (Vol. II, Section III, 3.0, b, (2)), a study was performed to ascertain the heat transfer effect of the oxidizer bias on the operation of the channel-wall (prototype) main thrust chamber. Three tests with oxidizer bias were evaluated in this study. The tests were conducted at chamber pressures of 612, 222, and 74 psia. The data were obtained with the water-cooled segment thrust chamber hardware and were utilized for determining the operating parameters for the prototype channel-wall segment configuration. The bulk temperature rise, hot-gas wall temperature, and pressure drop were determined.

(C) The effect of the oxidizer bias was analyzed by theoretically lowering the gas-side heat transfer film coefficient throughout the combustion zone and in the throat. As a result, the local heat flux and the overall bulk temperature rise were lowered. The lowered local heat flux and bulk temperature rise caused the maximum wall temperature to be lowered approximately 150 F compared to operation without oxidizer bias. Table 36 shows a summary of the conditions predicted for the prototype thrust chamber operation with oxidizer bias.

TABLE 36

MAIN THRUST CHAMBER OPERATION WITH OXIDIZER BIAS (U)

Chamber Pressure, psia	Coolant Inlet Pressure, psia	Coolant Exit Pressure, psia	Coolant* Exit Bulk Temperature, F
650	1940	1405	474
222	760	508	782
78	360	263	1330

*Chamber inlet temperature assumed to be -340 F

(U) Figure 149 compares the thrust chamber exit bulk temperature with and without injector oxidizer bias over the range of chamber pressures necessary for throttling. The significant improvements in pressure drop and heat load resulting from the oxidizer bias is apparent from the data of Table 36 and Fig. 149 .

(4) Main Thrust Chamber Pressure Drop and Coolant Temperature Distribution

(U) A parametric analysis was conducted to determine predicted hydrogen pressure drop and temperature rise for the various components of the final

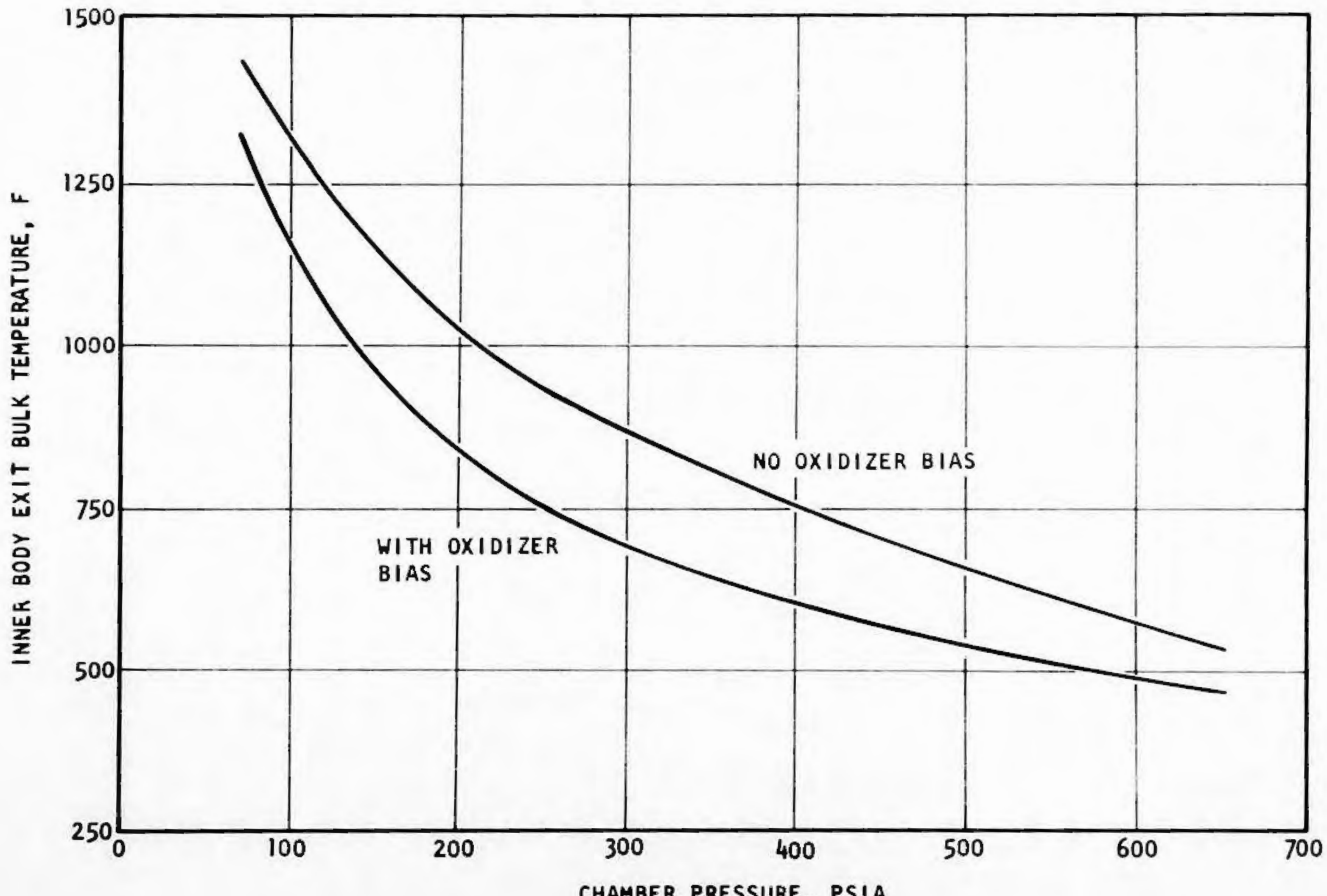

Figure 149. Main Thrust Chamber Segment Effect of Injector Oxidizer Bias on Inner Body Exit Bulk Temperature (C)

(U) main thrust chamber configuration over the intended operating conditions. The analysis utilized the Task II experimental test results for the prototype channel-wall segment chamber. The analysis was conducted for each of the thrust chamber subcomponents on a parametric basis to make the resulting data independent of any possible variations in future design or experimental results in other subcomponents in the thrust chamber assembly. The method of analysis consisted of a detailed heat transfer analysis based on specific test points. The hydrodynamic analysis performed for interconnecting ducts and other subcomponents where no heat addition takes place was based on the design details for the 30-degree prototype channel-wall segment assembly. The results of these detailed point design analyses were then extended on a parametric basis to cover the intended operating range with the use of scaling equations developed from the theoretical analysis.

(a) Chamber End Plate (Baffle)

(C) Heat transfer and fluid flow calculations were made for the baffle where the cooling circuit is divided into increments. For each increment, an iteration procedure was followed to determine the heat flux from the combustion gas to the coolant, the resulting temperature profile, and the coolant change of state until these parameters are compatible with the resulting friction and momentum pressure drop over the increment. This analysis was conducted for three operating chamber pressures (613, 222, and 74 psia) based on data obtained in solid-wall segment tests 014, 016, and 017 (Vol. II). The heat flux data obtained from these tests were used to predict the heat flux profile, gas-side wall temperatures, coolant bulk temperature rise, and coolant pressure drop for the prototype chamber baffles operating at an engine mixture ratio of 12:1 and a coolant inlet temperature of 65 R. The results of the detailed analysis for these three engine operating points were then used as the basis for an analytical scaling analysis to provide the same type of information over the entire engine system operating range. The scaling techniques were developed from the theoretical equations used in the analysis of the three basic

(C) operating points. These scaling methods were computerized to facilitate the rapid analysis of a wide range of parametric data. The computerized scaling methods also simplified the evaluation of the effects of newly acquired test data or design modifications. The results of the parametric analysis are shown in Fig. 150 through 152. The baffle coolant discharge temperature is shown in Fig. 150 versus chamber pressure for engine mixture ratios from 9:1 to 13:1. The bulk temperature rise of the coolant in the baffle is relatively insensitive to inlet pressure, and the curves shown in Fig. 150 are considered valid over a fairly wide range of coolant inlet pressures. The baffle coolant inlet versus exit pressure relationship is shown in Fig. 151 for each of the three selected operating chamber pressures and over the range of engine mixture ratios. The difference between the inlet and corresponding exit pressures is presented in Fig. 152 in the form of baffle pressure drop versus exit pressure.

(b) Chamber Segment--Outer and Inner Bodies

(C) The thrust chamber segment outer and inner body heat transfer and fluid dynamics calculations also were based on test data obtained in solid-wall segment tests 014, 016, and 017. The detailed analysis was performed for the three operating chamber pressures (613, 222, and 74 psia) used above for the end-plate analysis. The coolant enters the outer body and makes a single downpass through the coolant channels. The coolant then crosses through the lower portion of the baffle to the inner body, which is cooled by a single up-pass, and the coolant is then transferred to the nozzle. The results of the detailed studies for the three operating chamber pressures were used to generate parametric data describing coolant temperature rise and exit pressure for a range of inlet temperature and pressure conditions for both the outer and inner bodies. The coolant discharge temperature versus operating chamber pressure is shown in Fig. 153 for mixture ratios of 9:1 to 13:1. The outer body coolant inlet temperatures were obtained from the baffle coolant discharge temperature (Fig. 150) and the outer body discharge temperature becomes the inner body inlet temperature for the corresponding chamber pressure and mixture ratio values.

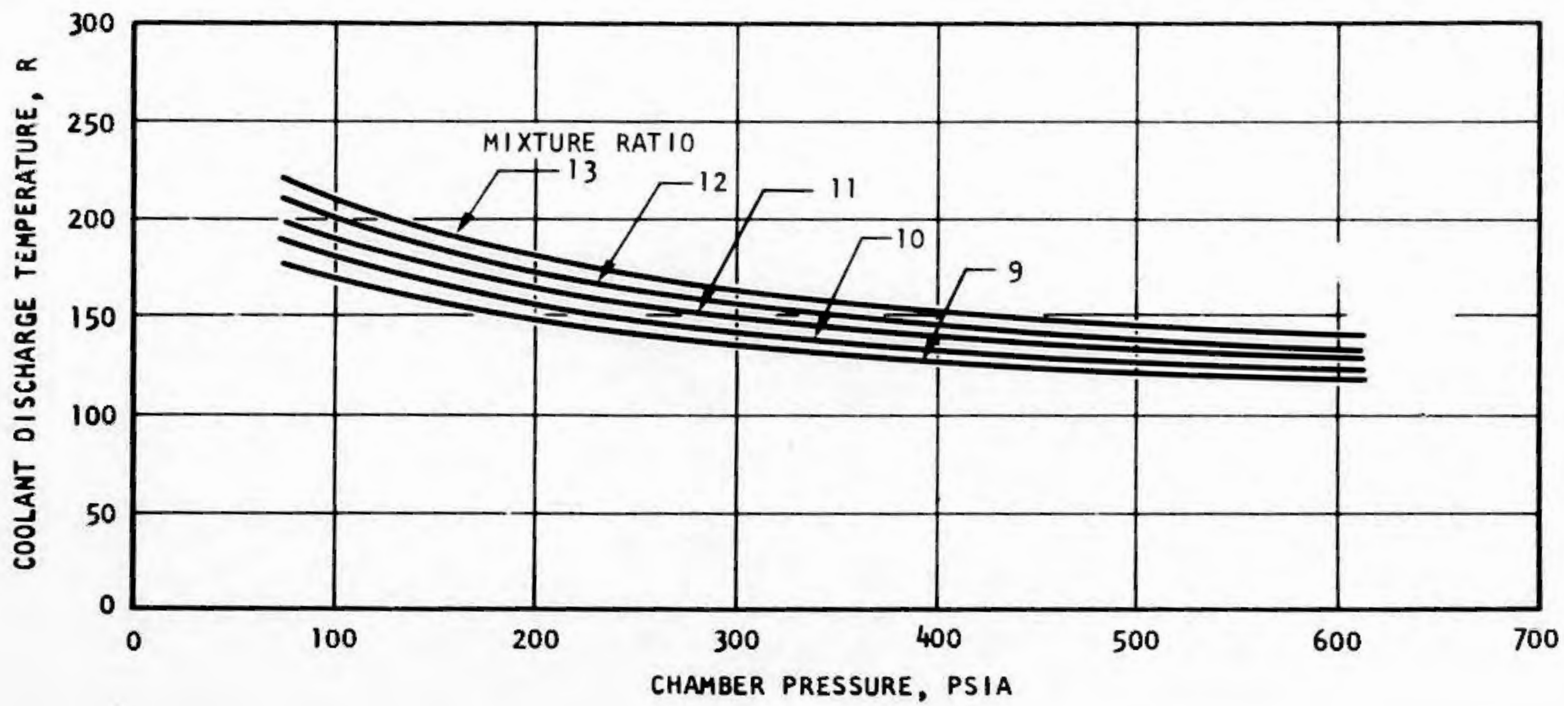

Figure 150. Baffle Coolant Discharge Temperature (U)

CONFIDENTIAL

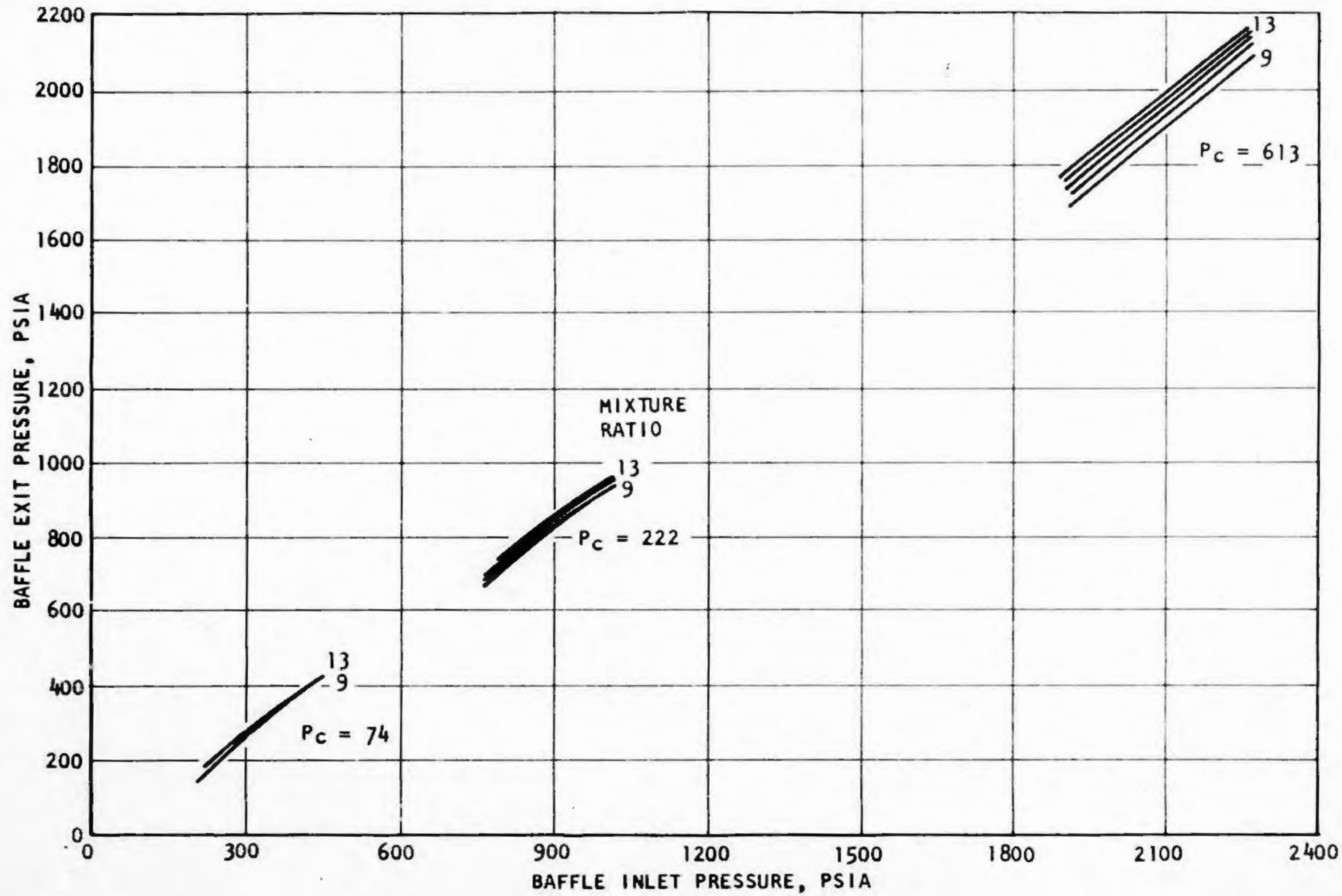

Figure 151. Baffle Coolant Pressures (U)

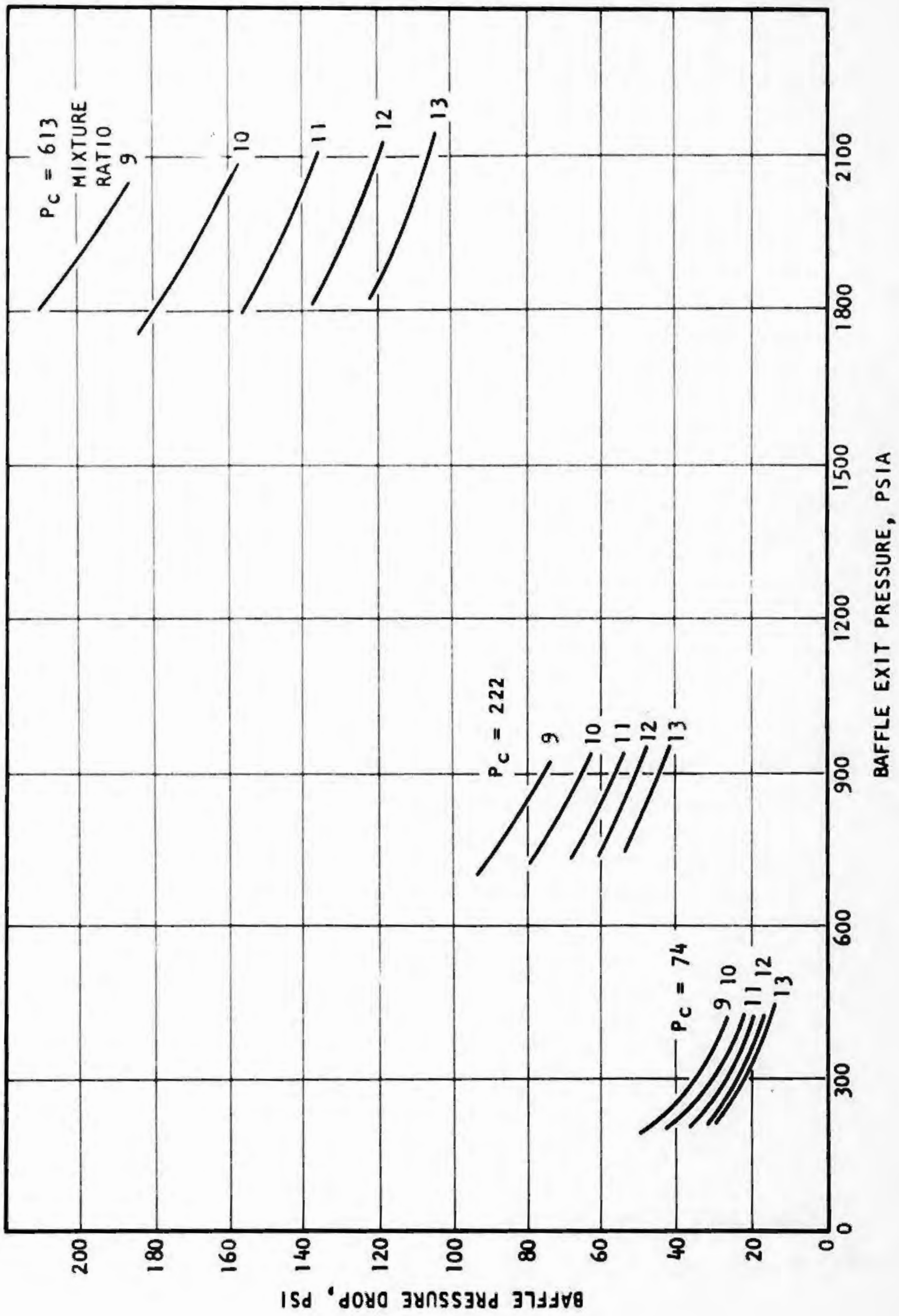

Figure 152. Baffle Coolant Pressure Drop (U)

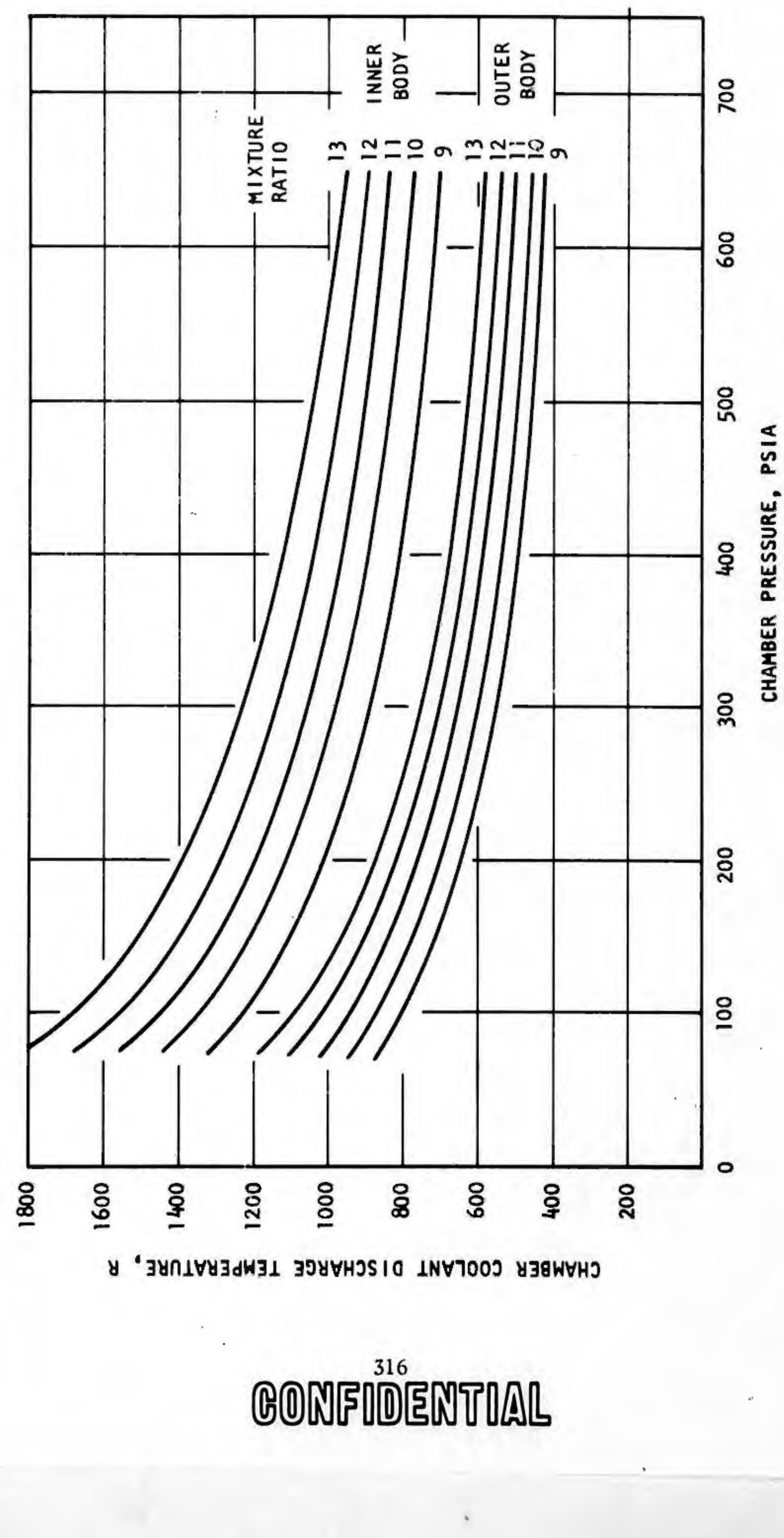

Figure 153. Channel-Wall Chamber Discharge Temperature (U)

(C) Chamber inner and outer body exit versus inlet pressure are shown in Fig. 154 for operating chamber pressures of 613, 222, and 74 psia and engine mixture ratios from 9:1 to 13:1. Inlet temperature for each engine mixture ratio was obtained from Fig. 150 and 153 for the outer and inner bodies, respectively. The pressure drop versus exit pressure is shown in Fig. 155 and 156 for the outer and inner bodies, respectively. Note that the outer body exit pressure is not equal to the inner body inlet pressure; an additional pressure drop occurs in the crossover duct within the lower portion of the baffle. Estimates of this crossover duct pressure loss are presented in the next section. The pressure losses shown for the outer body include all losses from the baffle exit to the entrance of the crossover duct. The pressure drop values shown for the inner body include all losses from the crossover duct exit to the exit of the inner body coolant channels. Heat addition was assumed to occur only in the coolant channels.

(c) Outer-to-Inner Body Crossover Duct

(U) The pressure losses that occur in the crossover duct between the outer body and inner body were estimated for a range of engine fuel flowrates and for inlet conditions dictated by the outer body discharge flow conditions for the indicated values of operating chamber pressure and mixture ratio. The results are shown in Fig. 157.

(d) Transfer From Inner Body Channels to Nozzle Tubes

(U) The coolant is transferred from the inner body channels to the nozzle tube bundle through a series of collection and distribution manifolds and transfer ducts. The total pressure loss incurred in this portion of the cooling circuit has been estimated versus engine system fuel flowrate for the transfer system inlet conditions (inner body discharge) dictated by the indicated operating chamber pressure and mixture ratio values. The results are shown in Fig. 158.

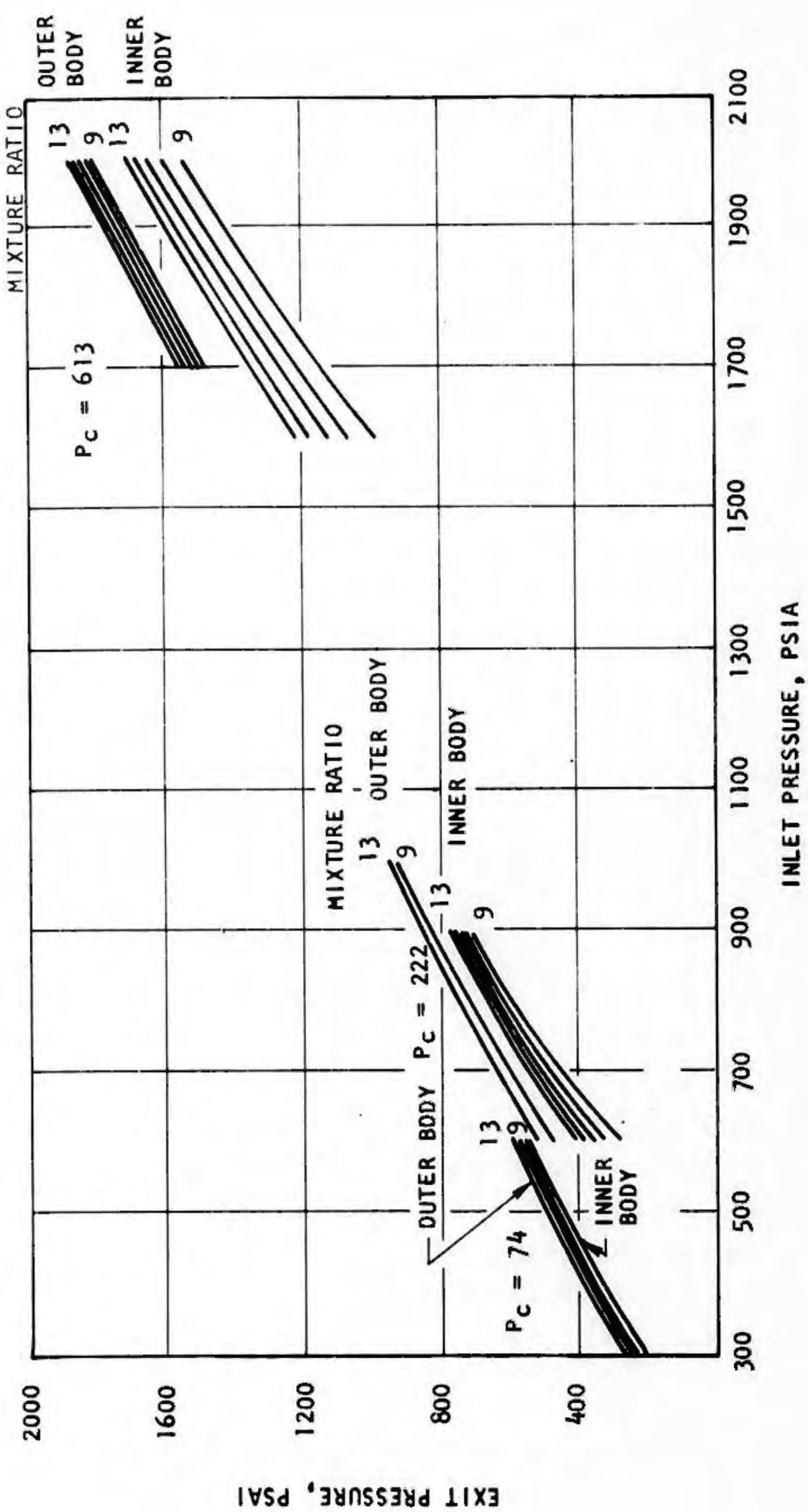

Figure 154. Chamber Inner and Outer Body Inlet/Exit Pressure Relationship (U)

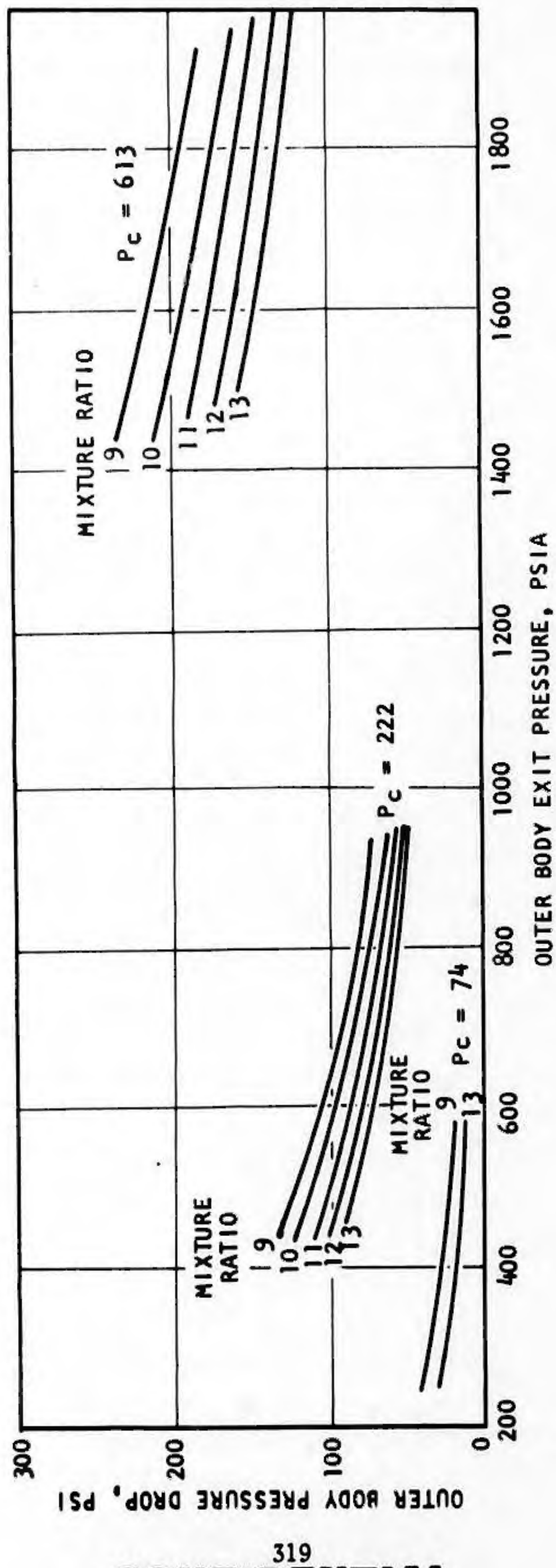

Figure 155. Outer Body Channel-Wall Chamber Pressure Drop (U)

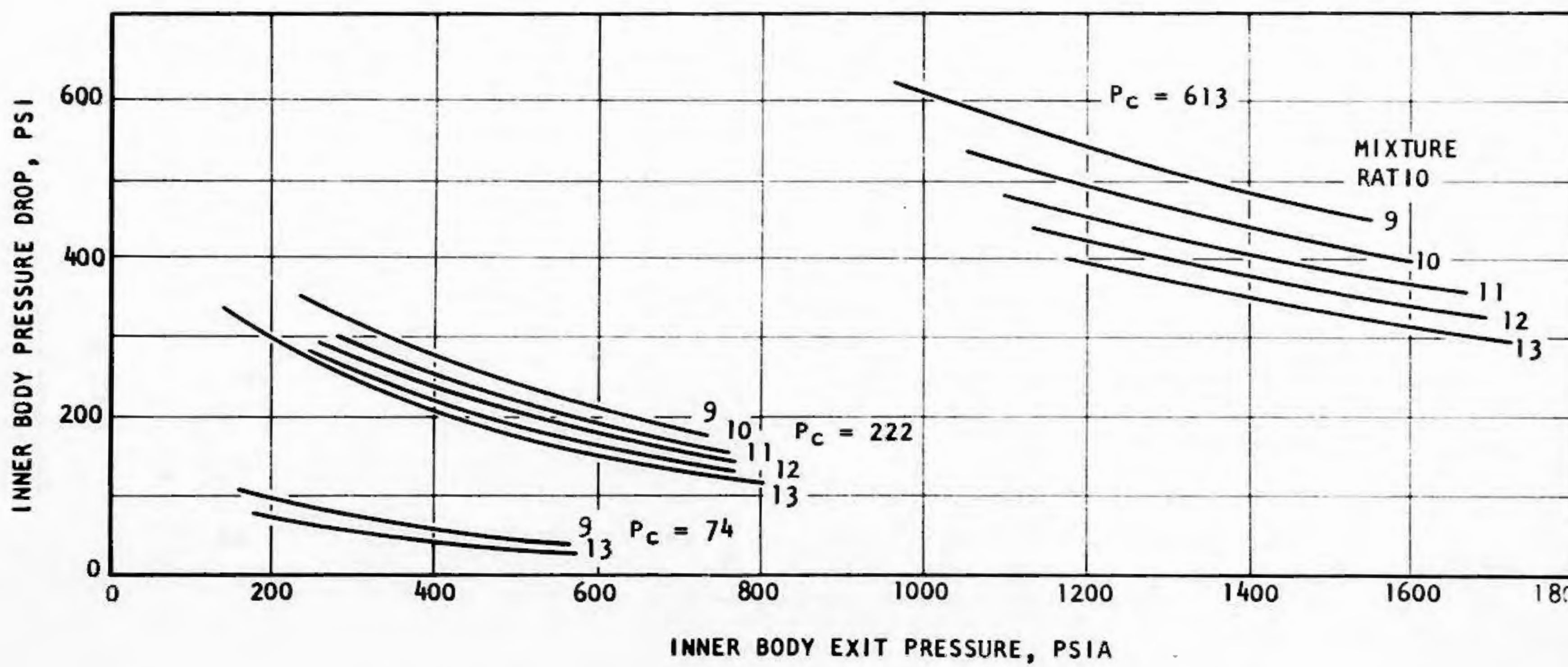

Figure 156. Inner Body Channel-Wall Chamber Pressure Drop (U)

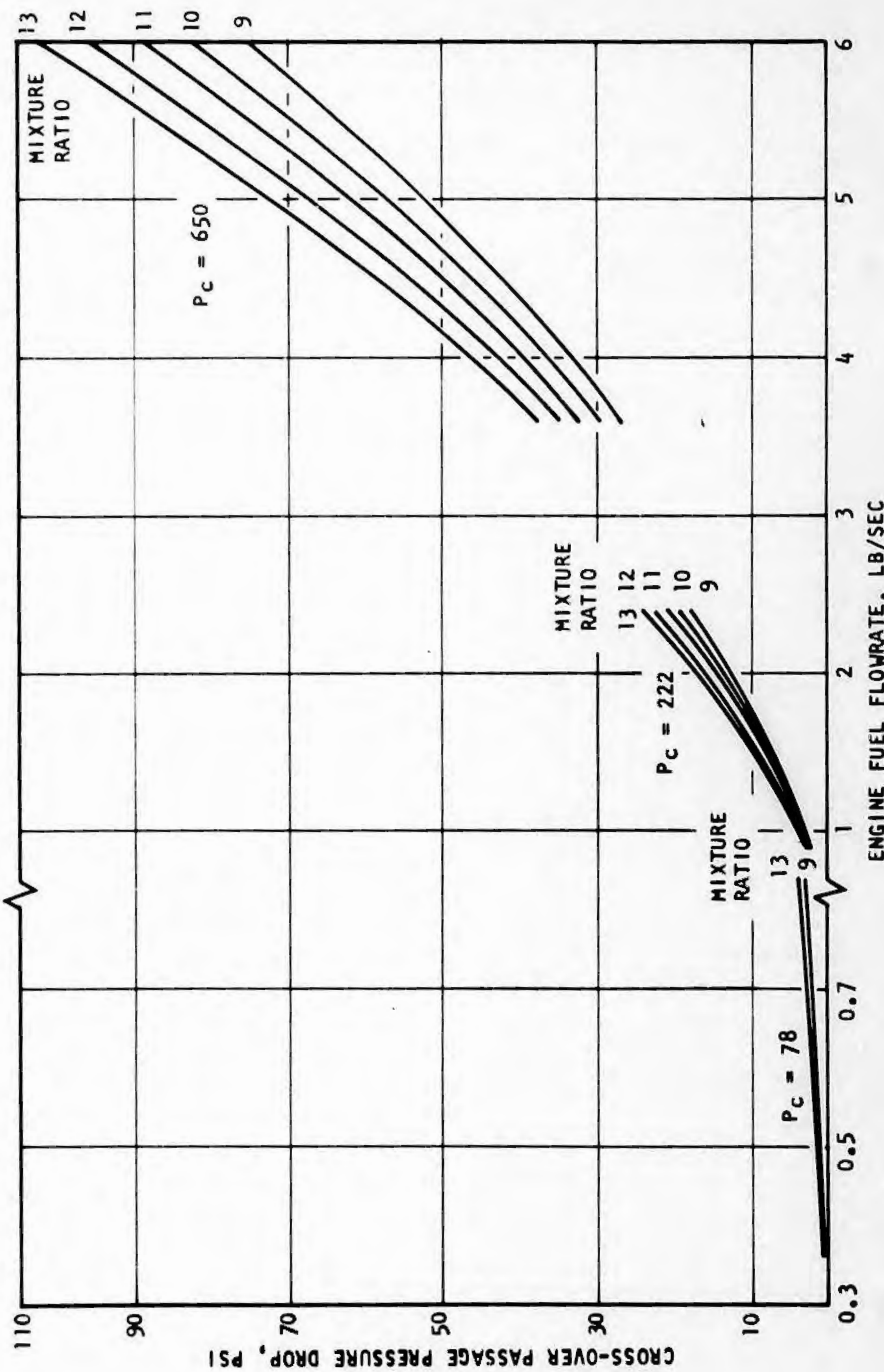

Figure 157. Inner Body-to-Outer Body Crossover Duct ΔP (U)

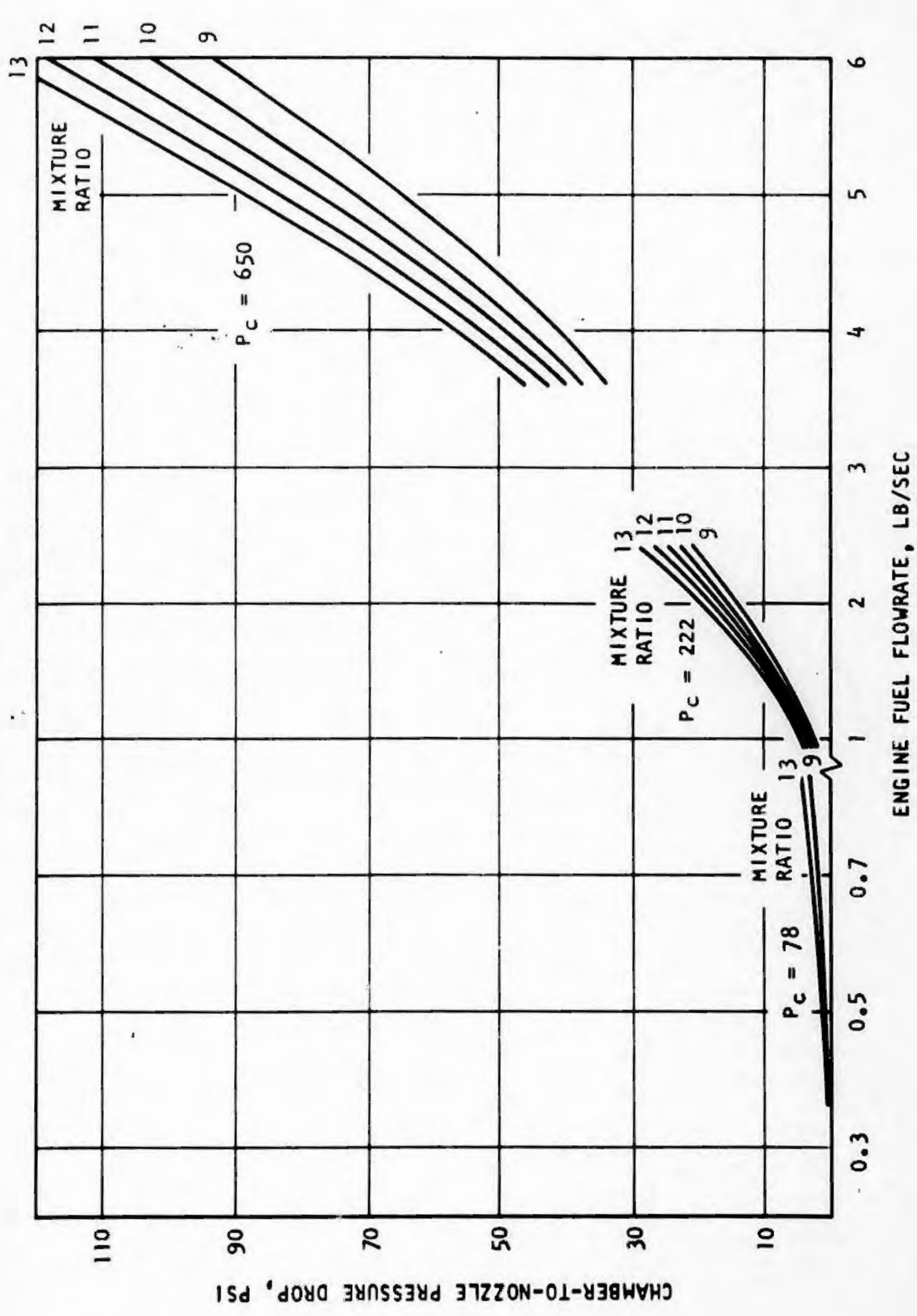

Figure 158. Coolant Pressure Drop From Inner Body Channels to Nozzle Tubes (U)

(e) Nozzle Extension Tube Bundle

(U) Parametric heat transfer and fluid flow calculations also were conducted for the nozzle extension. The cooling circuit was divided into increments, and heat flux, wall temperature, and coolant conditions were evaluated for each increment. The method balances heat flux with the friction and momentum pressure drop over each increment. The coolant enters the nozzle tube assembly at a location 6 inches (measured axially) below the leading edge of the nozzle extension (Fig.159). This nozzle extension manifold location was chosen to simplify the attachment flange design by not having the manifolds located at the flange location.

(C) The analysis was conducted for estimates of nozzle tube bundle inlet conditions for operating chamber pressures of 650, 222, and 90 psia. The results were then scaled to cover a range of inlet pressures, inlet temperatures, and mixture ratios. Nozzle coolant inlet temperatures were obtained from the inner body exit temperatures (Fig. 153). The resulting nozzle coolant exit temperatures are shown in Fig. 160 as a function of operating chamber pressure and mixture ratio. Coolant inlet versus exit pressures and pressure drop versus exit pressures are shown in Fig. 161 and 162, respectively.

c. Main Thrust Chamber Design

(U) Based on the work discussed above, design guidelines were defined for the major components of a flight-type thrust chamber and are presented in Table 37. The flight-type thrust chamber design was not intended to be the final flightweight configuration but, rather, an intermediate step with the purpose of demonstrating performance and regenerative cooling. Each of the design areas of Table 37 is briefly discussed below.

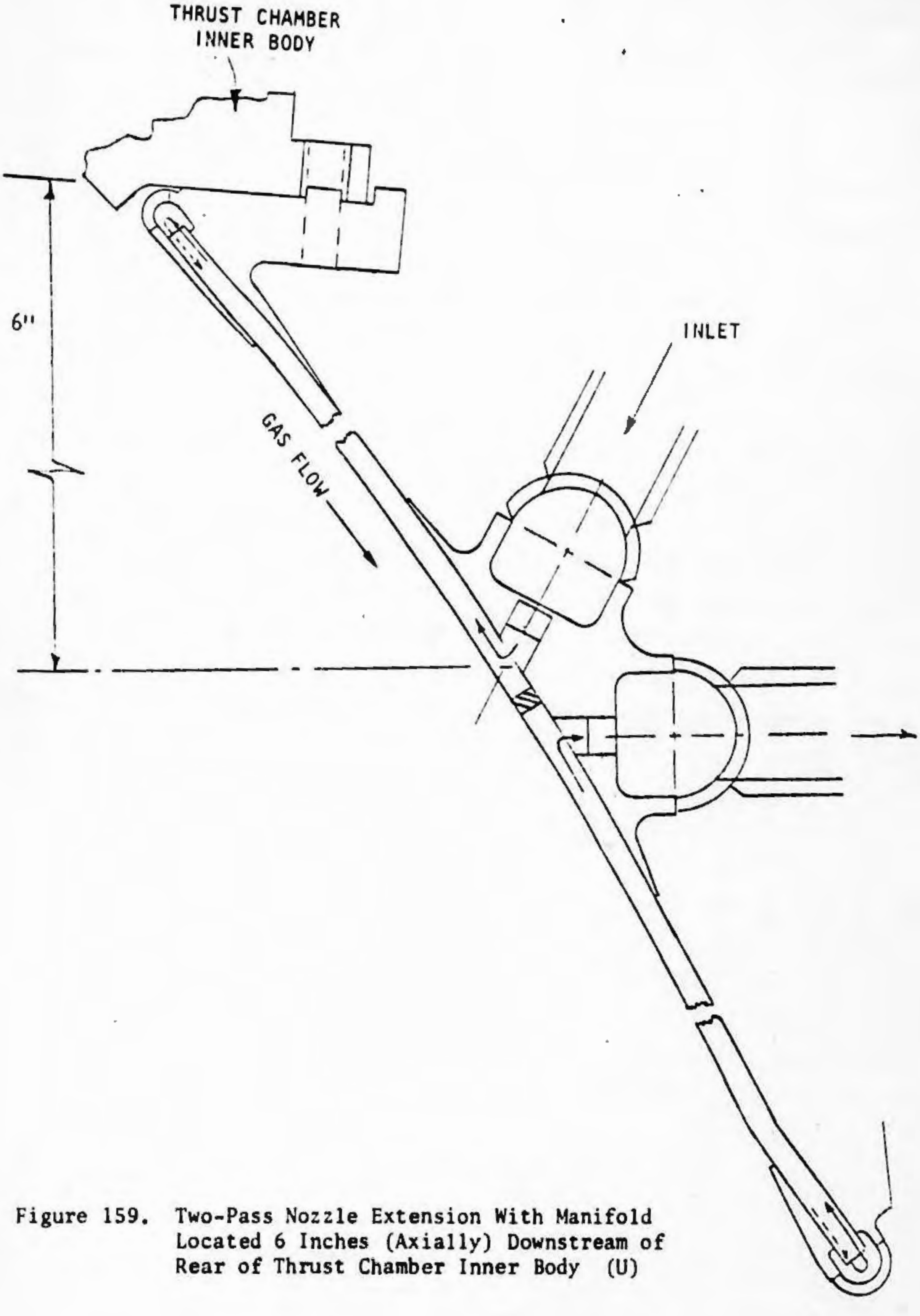

Figure 159. Two-Pass Nozzle Extension With Manifold Located 6 Inches (Axially) Downstream of Rear of Thrust Chamber Inner Body (U)

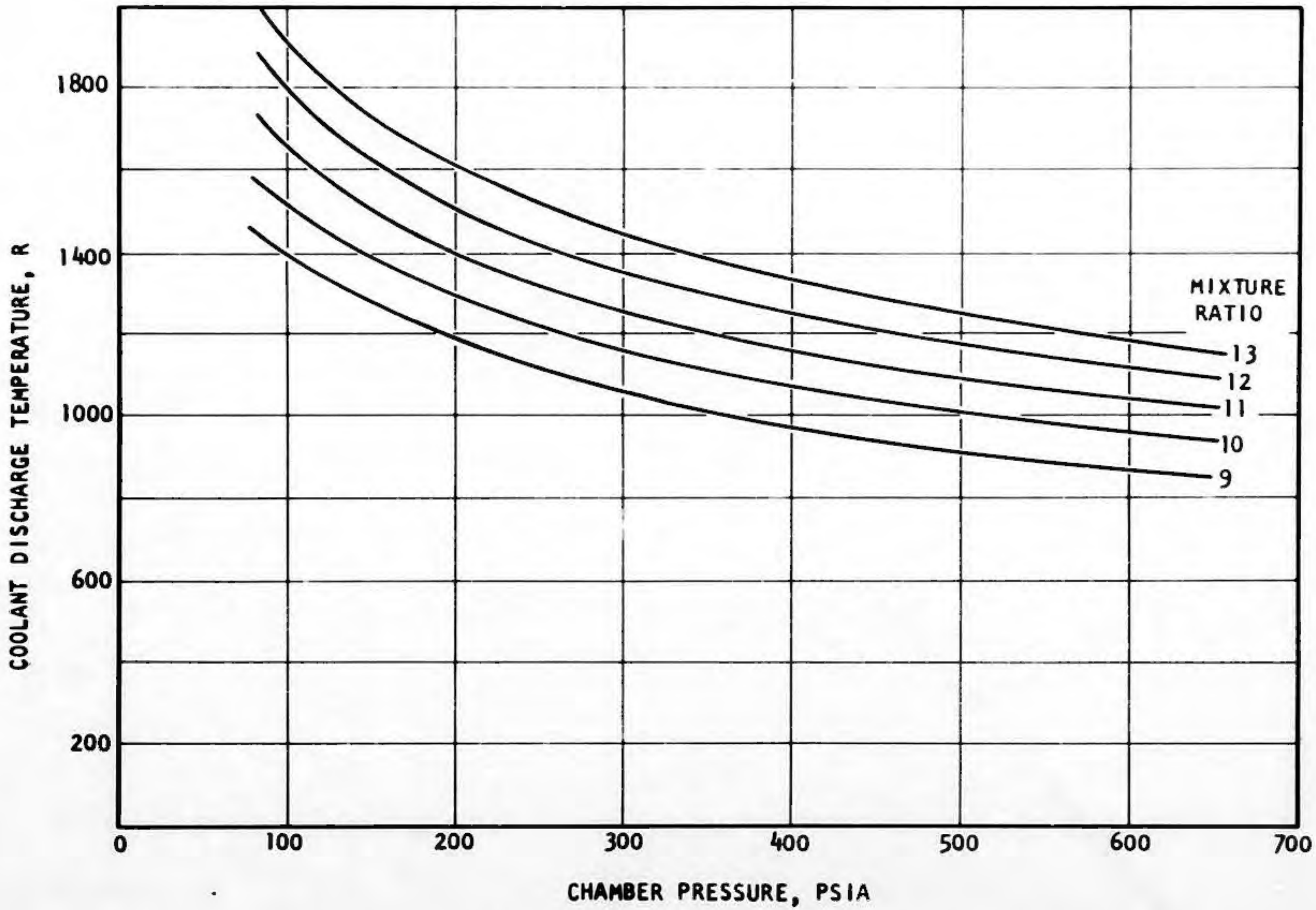

Figure 160. Chamber and Nozzle Coolant Discharge Temperature (U)

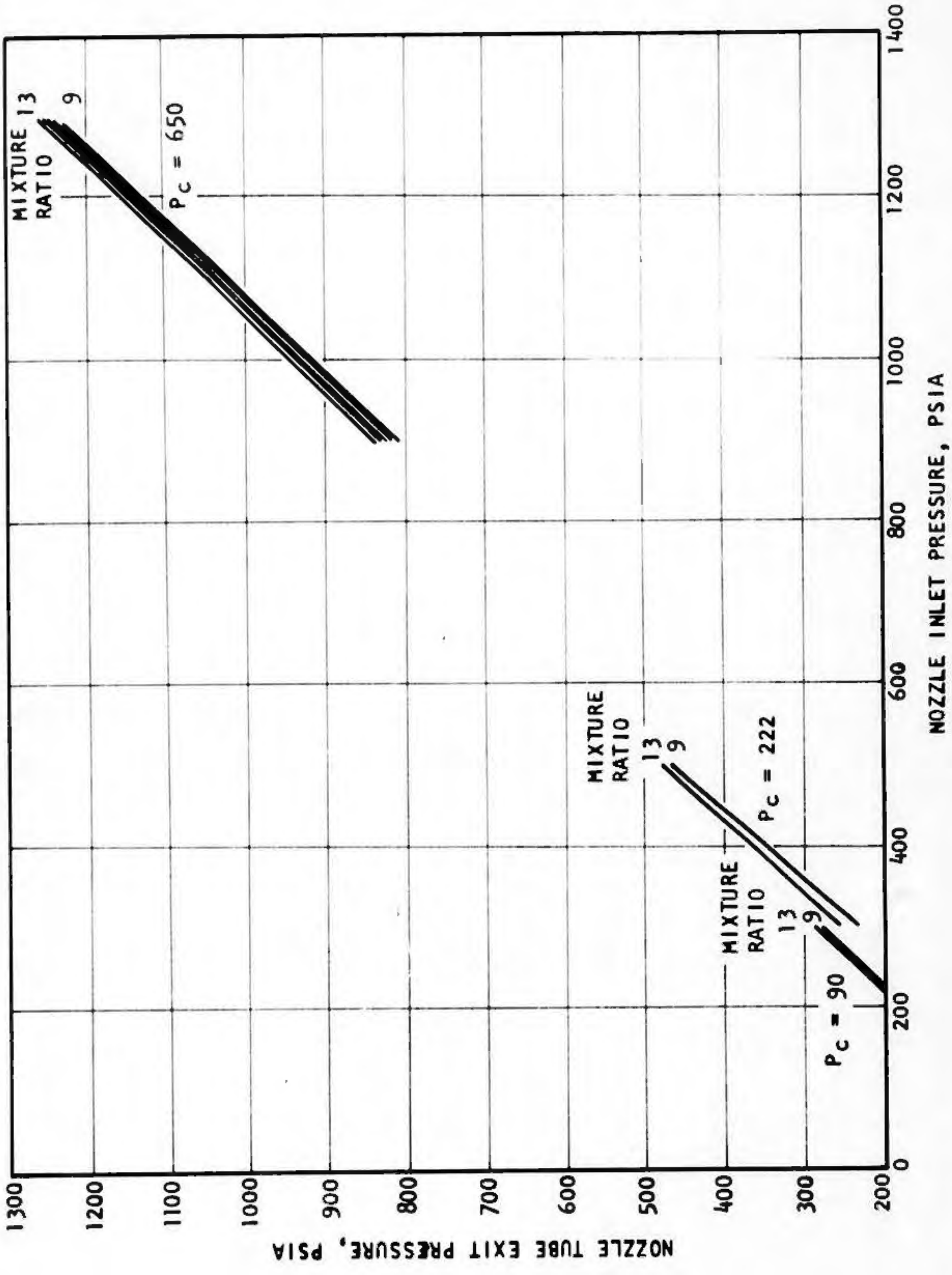

Figure 161. Nozzle Tube Inlet vs Exit Pressure (U)

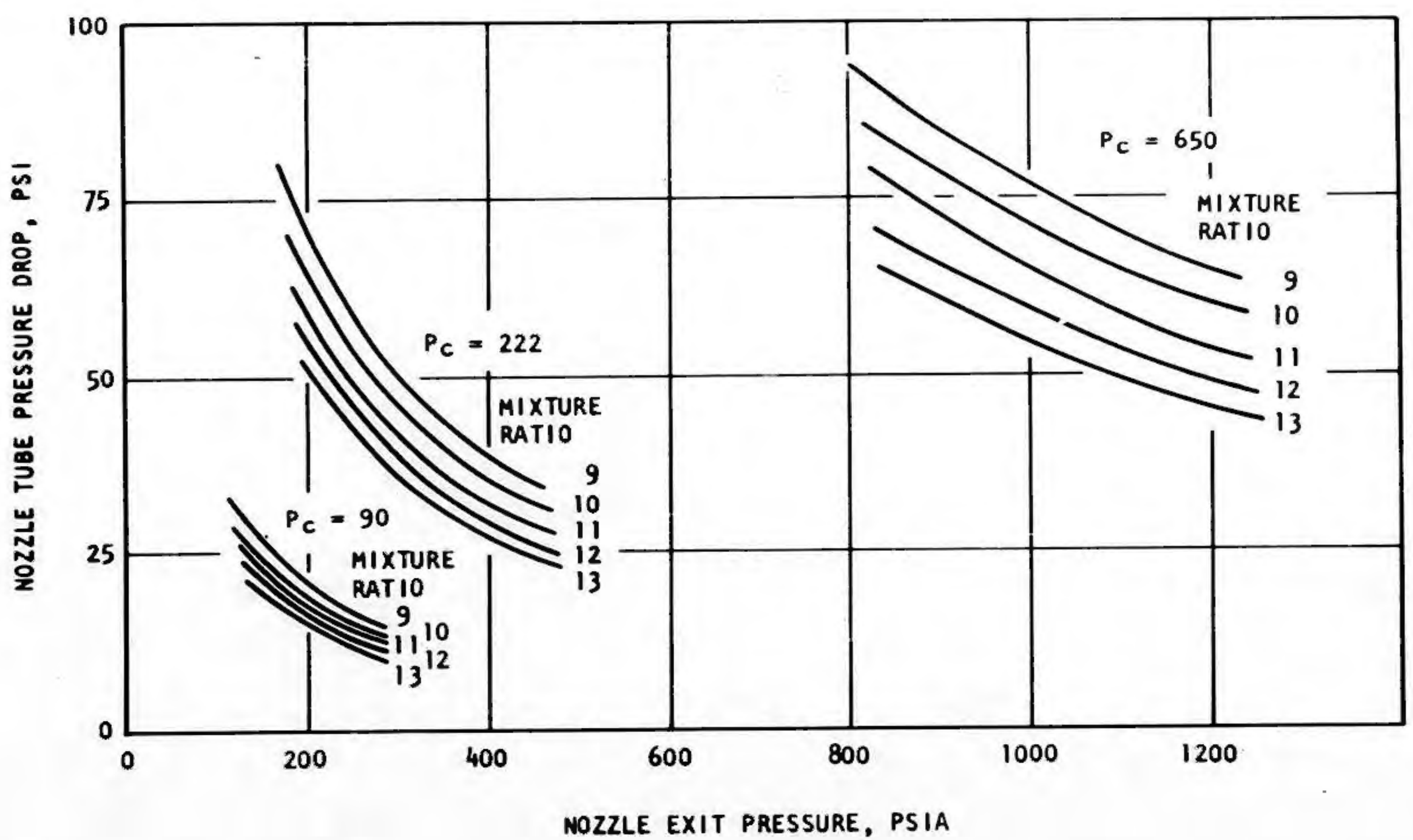

Figure 162. Nozzle Tube Pressure Drop vs Exit Pressure (Does Not Include Inlet or Exit Manifold) (U)

TABLE 37

THRUST CHAMBER ASSEMBLY DESIGN GUIDELINES (U)

THRUST CHAMBER SEGMENTS	
Guide Lines	**Remarks**
Use lightweight segment support structure.	Engine starting and throttling characteristics will be influenced by the transient heating and cooling of the thrust chamber structure. Test evaluation of these characteristics should be done on a structure that approaches a flightweight configuration.
Segments are to be bolted at the segment-to-segment interface.	The use of bolts at the segment-to-segment interface, in lieu of a serviceable weld joint, will permit greater freedom in the removal and installation of new segments. Welding on future configurations, however, would result in a weight savings.
Segments should be identical in configuration.	This provides interchangeability of a spare segment with a segment in the assembly regardless of its position in the assembly.
Coolant circuitry and channel configuration should be based on Phase I design.	The Phase I coolant channel configuration and coolant circuitry should be adhered to, except in the end coolant panel where Delta P's can be reduced with minor modifications.

TABLE 37
(Continued)

THRUST CHAMBER SEGMENTS (CONTINUED)	
Guide Lines	Remarks
Hot gas wall contour same as Phase I Design.	Changes in the hot gas contour for potential weight savings would require additional segment testing to evaluate.
Hot gas face sheet and substrate same as Phase I Design.	Present configuration uses electroformed nickel substrate and brazed-on wrought nickel "200" face sheet. The nickel substrate is a functional part of the heat transfer capabilities because of two-dimensional heat transfer effects. The best process for applying the substrate is to be determined.
Throat area change should be maintained to within 10 percent of the nominal design value.	Both pressure and temperature loading causes deflections which result in throat area variations.
INJECTOR SEGMENT	
Use lightweight injector body construction.	Response of the injector to temperature changes should be evaluated for future flightweight configurations.

TABLE 37
(Continued)

INJECTOR SEGMENT (CONTINUED)	
Guide Line	**Remarks**
Use same injector face strip configuration as Phase I injector.	Performance, stability, and durability has been demonstrated in Phase I segment testing.
Use a serviceable weld joint to provide sealing and a structural tie to thrust chamber.	Sealing the injector to thrust chamber segment on the Phase I design has been demonstrated. The method employed uses two seals and pressurizing the cavity between them to eliminate external combustion gas leakage. This approach, however, is not compatible with lightweight construction and does not provide for maximum structural usage of the injector as a tension tie between the inner and outer bodies of the thrust chamber. Installation, removal and reinstallation of the injector will be made possible by using a serviceable weld joint.
NOZZLE EXTENSION	
Nozzle is to be detachable from thrust chamber segments.	Bolted flange similar to Phase I design will be used to facilitate segment removal and re-installation.

TABLE 37

(Concluded)

NOZZLE EXTENSION (CONTINUED)	
Guide Lines	Remarks
Coolant inlet and outlet lines rerouted for maximum engine hardware accessibility and clearance.	This was not a requirement of the Phase I nozzle extension.
Outlet manifold redesign to incorporate a propellant feed system tank pressurant heat exchanger.	Heat exchanger was not required on the Phase I design.
Aft manifold-base closure mounting flange modified for attachment of lightweight base closure.	An integrated base closure and secondary engine simulator was used on Phase I for evaluation of optimum base flow cooling and performance.
THRUST MOUNT AND BASE CLOSURE	
Thrust mount similar to Phase I design.	Modification of oxidizer and fuel feed lines are anticipated, but basic design will be similar to Phase I design.
Base closure of lightweight construction.	Detail design considerations for a lightweight base closure will be based on the test results of the present Phase I thrust chamber.

(1) Thrust Chamber Segment

(a) Support Structure

(U) The basic design considerations for the structural support were to restrain the throat deflection within acceptable limits, to effectively use materials to minimize the weight, and to use known manufacturing techniques to facilitate their fabrication. A stress analysis tradeoff study was made which considered weight, number of segments, and throat deflection. The results indicated that the throat deflection would be less than 2.0 percent of the throat gap. Various designs for aerospike thrust chamber support structures, such as "C" clamp, hoop tension, subsonic baffles, and supersonic baffles have previously been investigated. Studies of the backup structure for the aerospike thrust chamber conducted (Ref. 23) indicated that either a rib- or honeycomb-type structure would provide adequate rigidity to the assembly to control throat gap. Fabrication and weight of the two assembly types were comparable. The analysis, however, indicated that loads predicted for the backup structure were greater than those in which honeycomb designs are generally used.

(U) The use of supersonic baffles as structural ties between the inner-to-outer body can effectively control throat area changes. The supersonic baffle design basically consists of an inner and outer ring joined together with equally spaced radial ties. The combustion chamher pressure acts between the two rings, applying radial outward loading on the outer ring and radial inward loading on the inner ring. The pressure loads between the supersonic radial baffle ties are restrained by the ring segments acting as fixed-end beams. The loads transfer through the ring and react as a tension load across the baffle ties. The use of 12 such baffles results in a good basic structural ring design. In addition to controlling throat deflection, the design is lightweight and is conducive to several conventional manufacturing techniques.

(U) Two basic design approaches were studied for the flightweight support structure: precision investment casting using INCO 718C material and a weld-fabricated, ribbed structure using INCO 718 wrought material. The welded, ribbed structure is similar in configuration to the support structure fabricated and structurally tested in Ref. 23.

(U) Design layout drawings of two versions of the cast support structure have been made, and a comparative stress analysis was completed to determine the most optimum approach. The first design used an open-faced rib construction with integrally cast manifolds. The axially oriented beams spanned from the forward manifold to the shroud manifolds on the outer body and to the nozzle-mounting flange on the inner body. A main load-carrying, circumferential I-beam located at the throat plane on each body transfers the separating load due to chamber pressure into the structural end plates. The main I-beam was welded to the casting to maintain simplicity of the open-face casting.

(U) The second cast support structure design used an open-faced casting with four circumferential beams on the outer body and three beams on the inner body. The mainfolding is cast integral with the support structure.

(U) Both design approaches indicated adequate structural rigidity for equivalent weights. The circumferential beam configuration, however, eliminates the necessity for secondary welding, affords better structural continuity at the segment-to-segment interface, and provides more freedom for weight reduction than the combined axial-main I-beam configuration. For these reasons, the cast approach is considered more desirable for the circumferential beam configuration. A preliminary design layout of the circumferential beam cast support structure thrust chamber segment is shown in Fig. 163.

(U) The welded-rib structure approach offers a possibility for a lightweight segment but with a somewhat greater cost than the cast approach. The

(U) fabrication of the welded structure is complicated by the segment approach. Attachment of the support structure to the segment-to-segment flanges must be done in intervals as the overall support structure is built up. Further difficulties are anticipated in controlling distortion due to welding. The consequences of the above discussion will be evaluated in continuing studies. A layout drawing of the welded-rib structure approach is shown in Fig. 164.

(2) Mechanical Interfaces

(U) Seven, 7/16-inch-diameter, high-strength bolts form the segment-to-segment structure tie. The aft bolt on the outer body and the top bolt on the inner body also serve as a shear joint to react the torsional loads between segments. The nozzle is attached to the segments at the aft flange of the inner body. The injector-to-thrust chamber joint is tentatively planned for a serviceable weld joint, i.e., the injector can be removed and reinstalled without damage to either component. The weld will be a full penetration, hand fusion weld. To remove the injector, an EDM electrode conforming to the weld joint contour will cut a 0.020- to 0.030-inch slot through the weld material and free the injector. To reinstall the injector, the weld joint is remachined and the injector rewelded in place. Thrust mount attach points are integrally cast on the inner body structure.

(3) Cooling Circuitry

(U) The cooling circuitry for the flight-type thrust chamber was identical to the design for the Task II thrust chamber except for the direction of fuel coolant flow in the end plates. In the Task II thrust chamber design, the end plates are cooled by a single downpass and the coolant is transferred through external tubes to the outer body forward end for a single downpass. The flight-type thrust chamber coolant inlet was located at the aft portion of the end plate. The coolant flowed up the end plate and was internally

CONFIDENTIAL

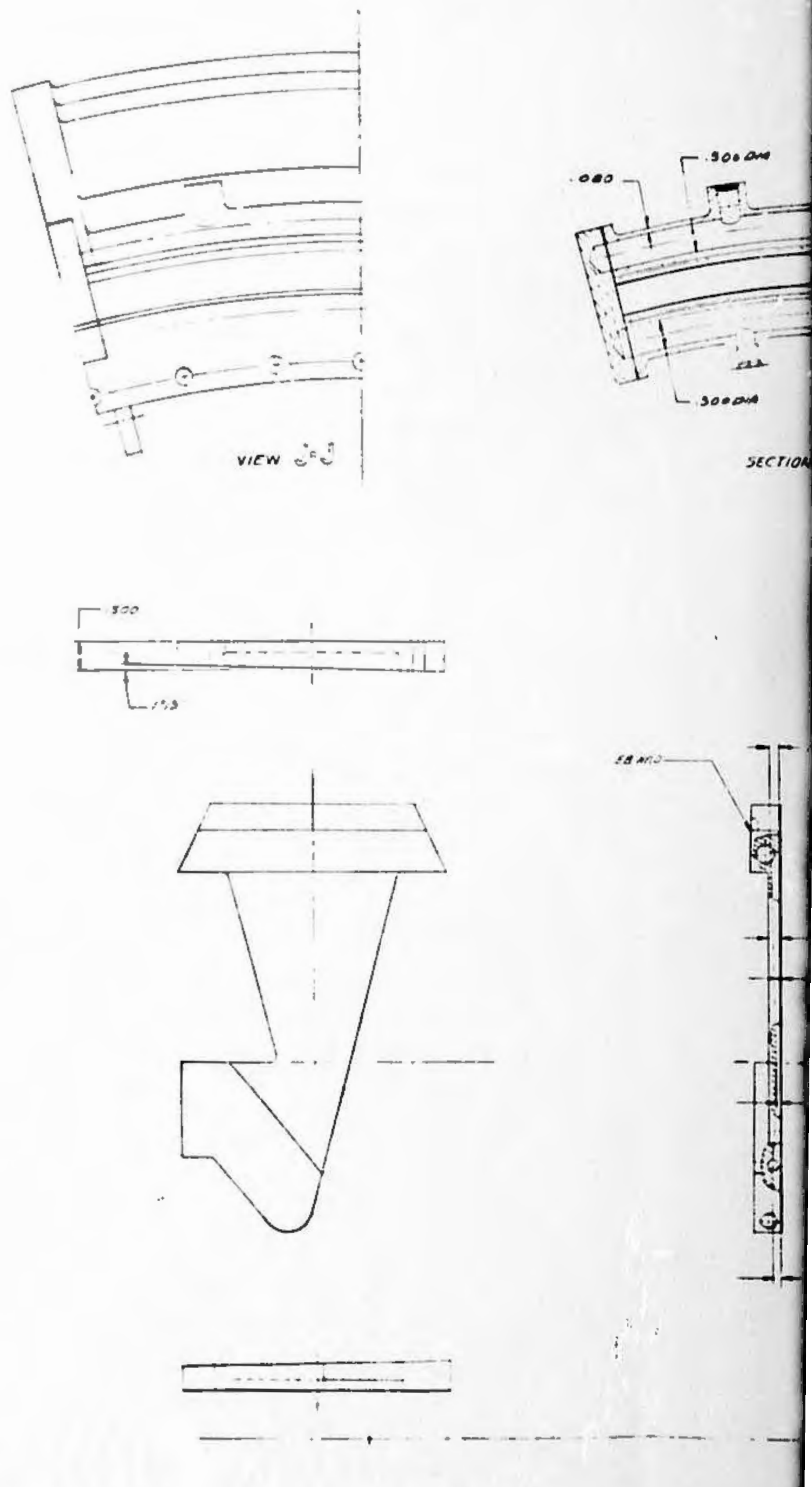

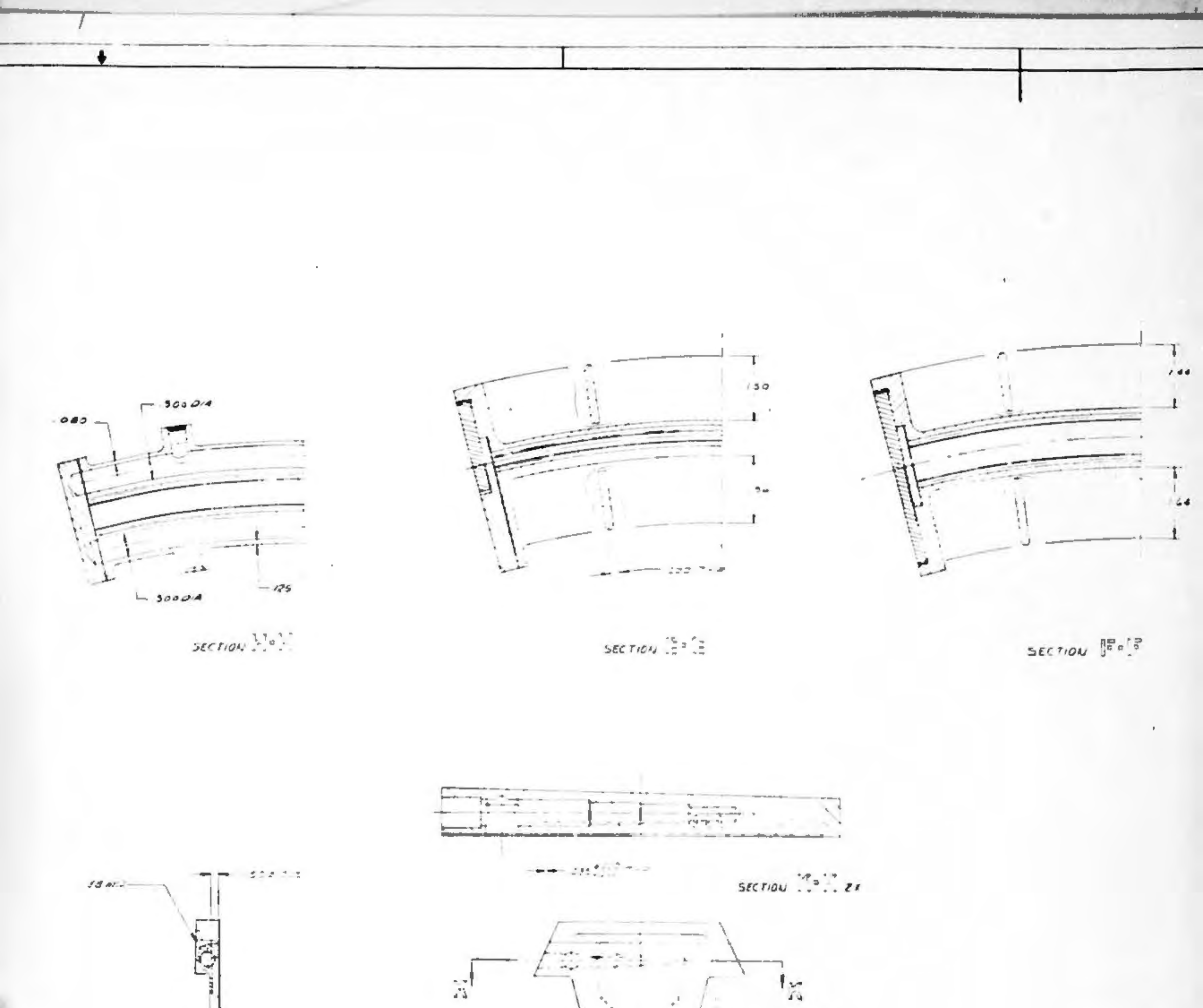
.500 DIA
.080
.500 DIA
.125
.150
COOLANT FLOW DIRECTION
COOLANT INLET PORT
DIRECTION OF FLOW IN CROSS OVER PASSAGE
DETAIL OF COOLANT END PLATE

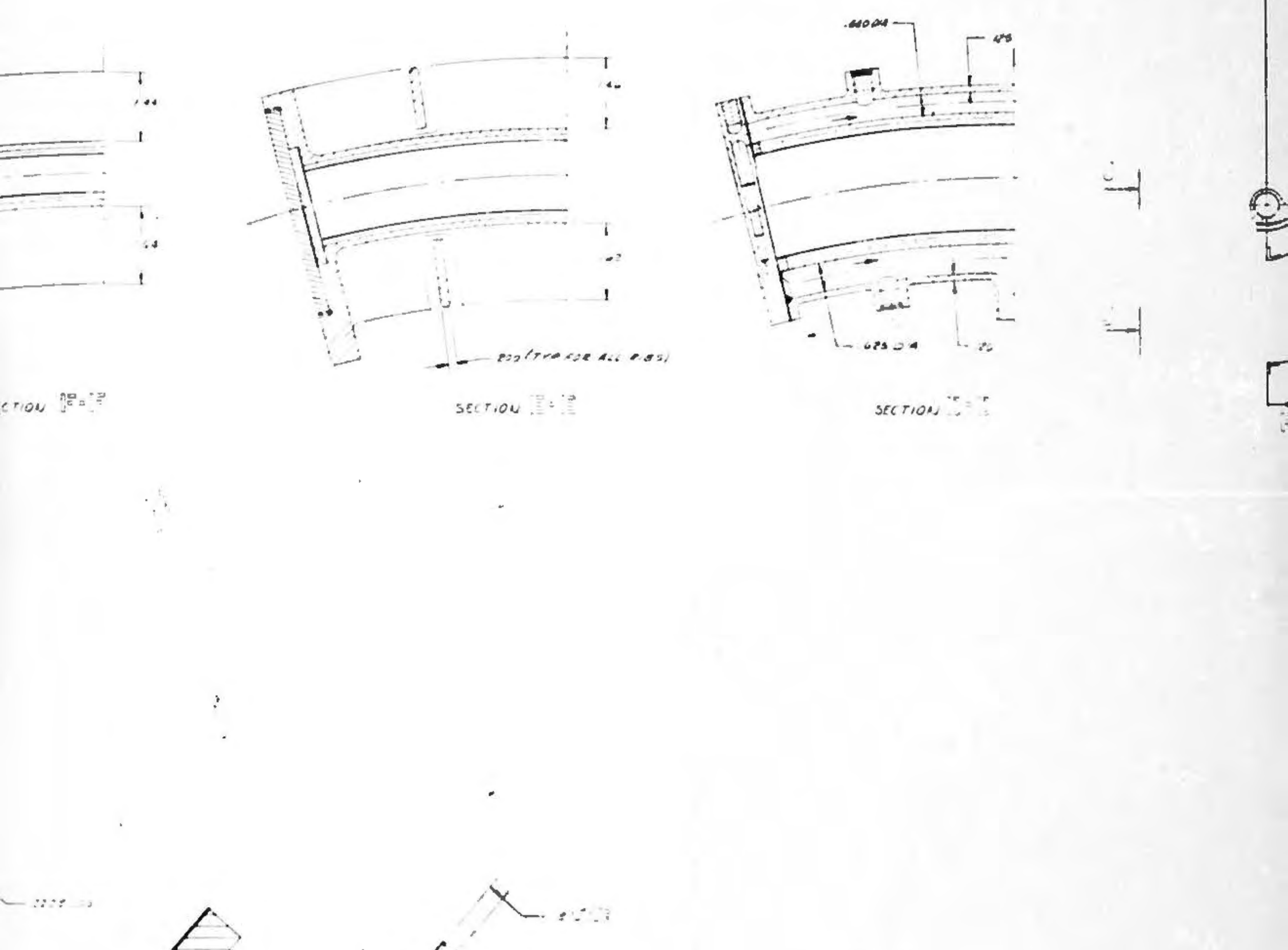
.660 DIA
.625 DIA
.200 (TYP FOR ALL RIBS)
SECTION
SECTION
SECTION
SECTION N-N 2:1

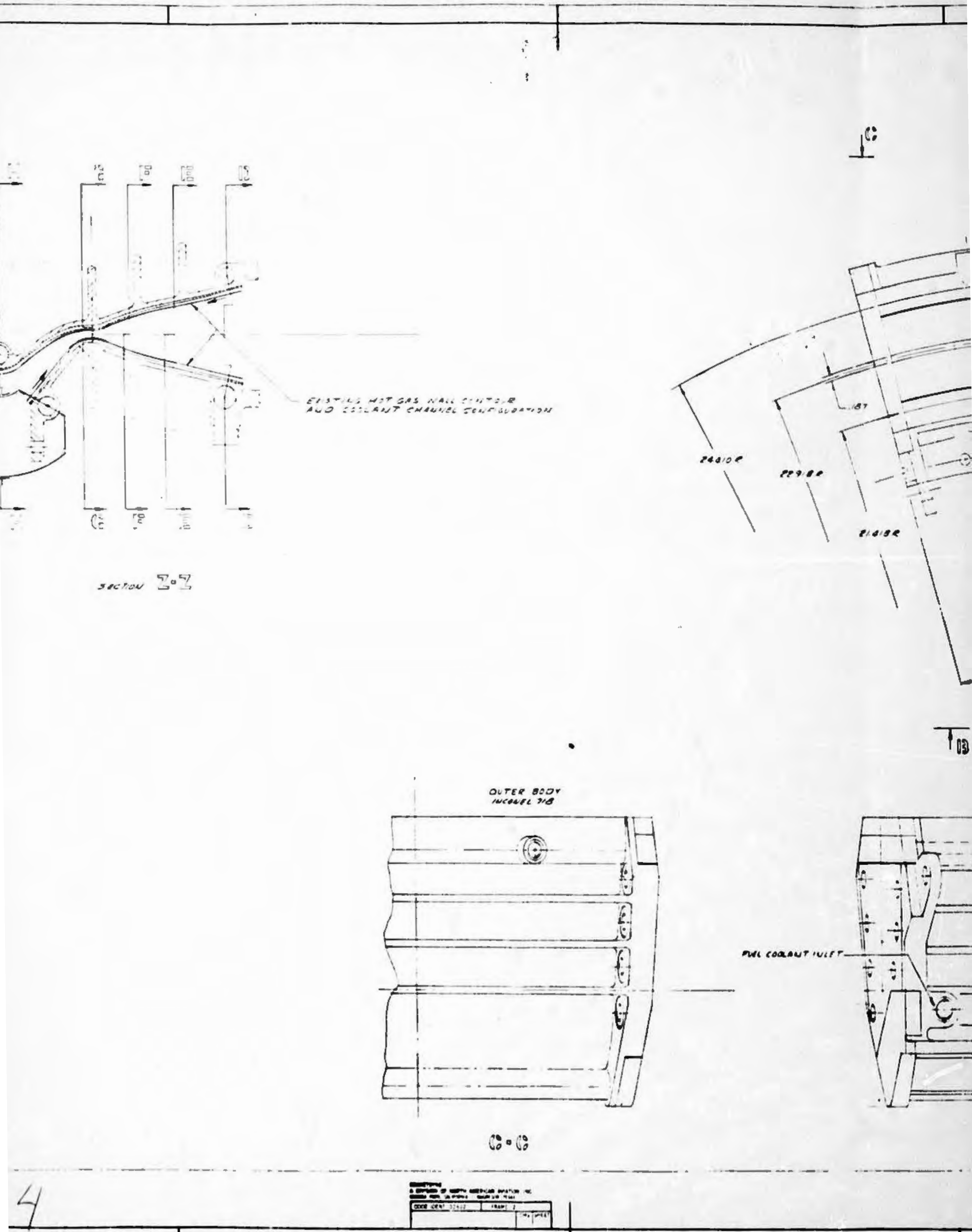

EXISTING HOT GAS WALL CONTOUR AND COOLANT CHANNEL CONFIGURATION
SECTION Z-Z
24.610 R
22.918 R
21.418 R
.187
OUTER BODY INCONEL 718
FUEL COOLANT INLET
C-C
CODE IDENT
FRAME
SHEET

4

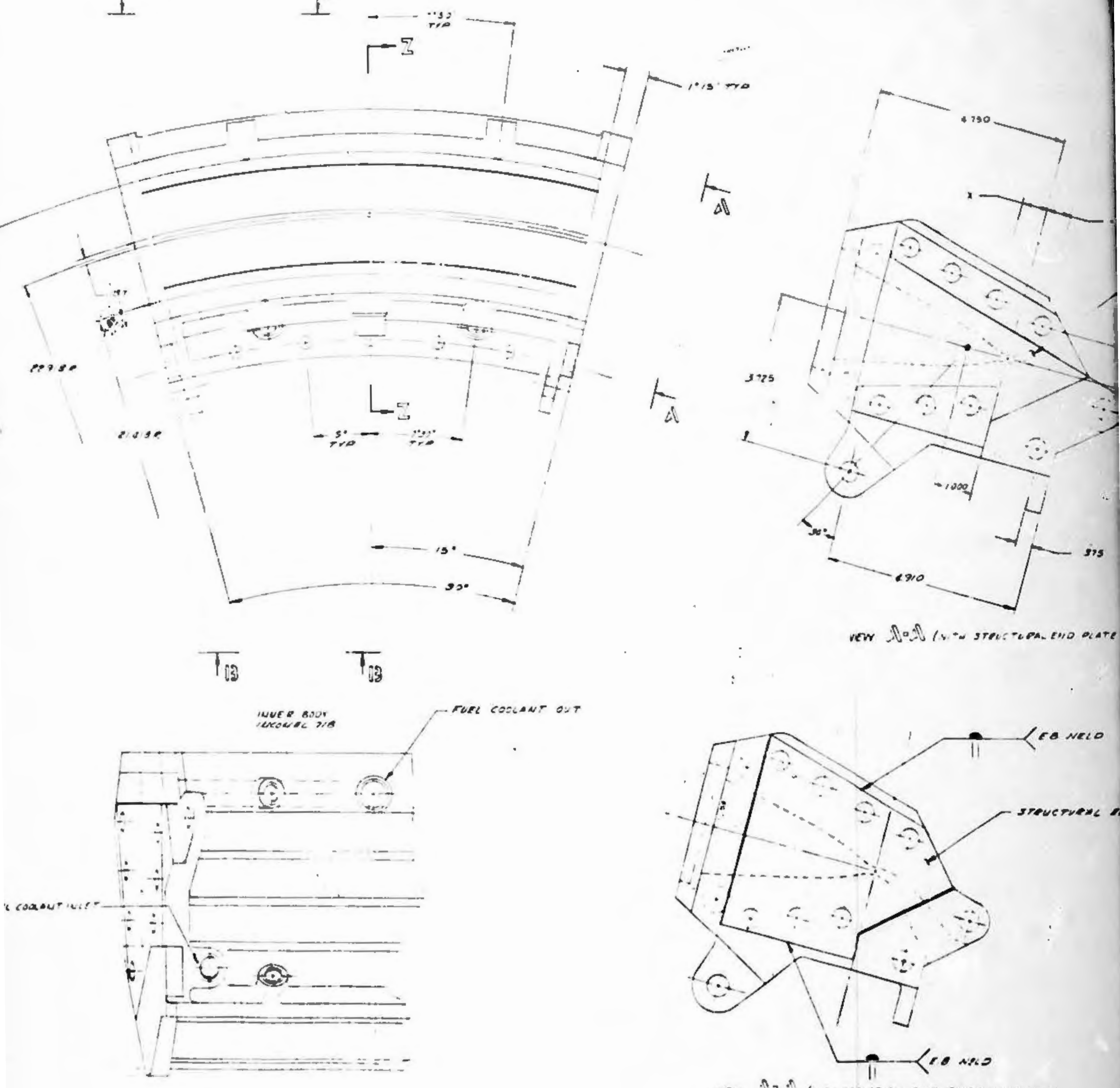

Figure 1

5

335/336 CONFID

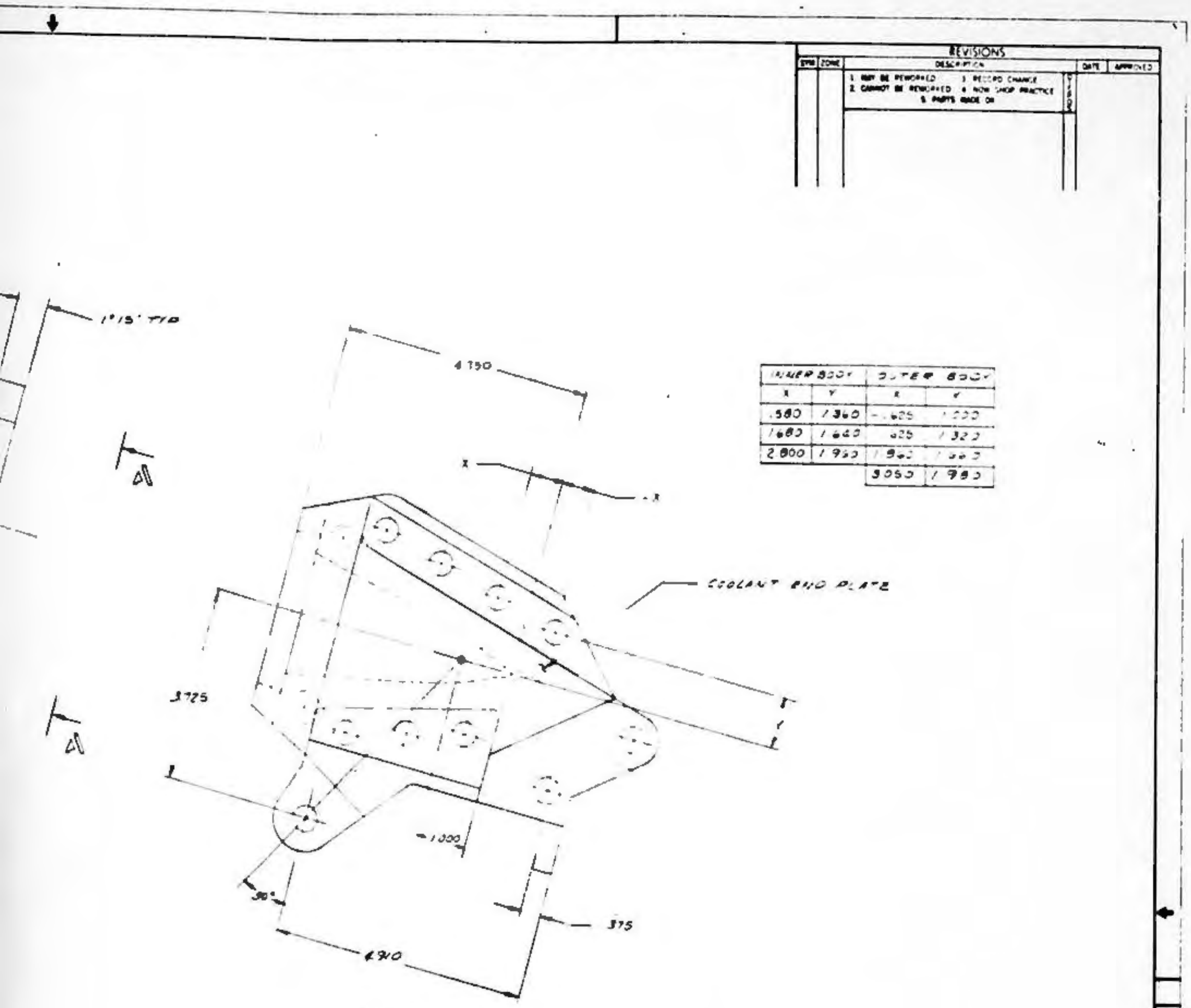

Figure 163. Circumferential Beam Cast Support Structure Layout (U)

CONFIDENTIAL

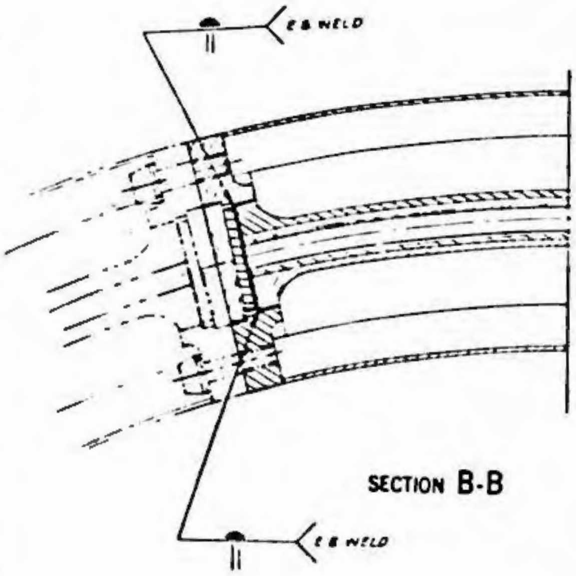

SECTION B-B

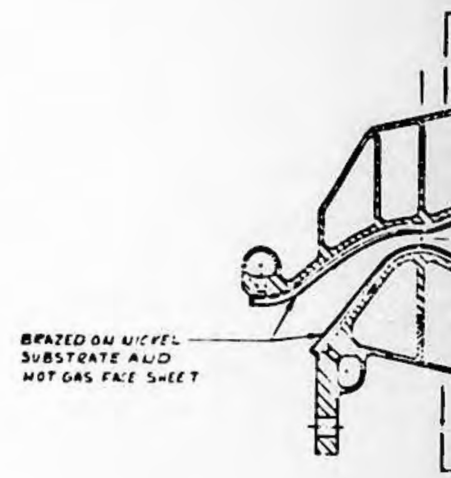

SECTI

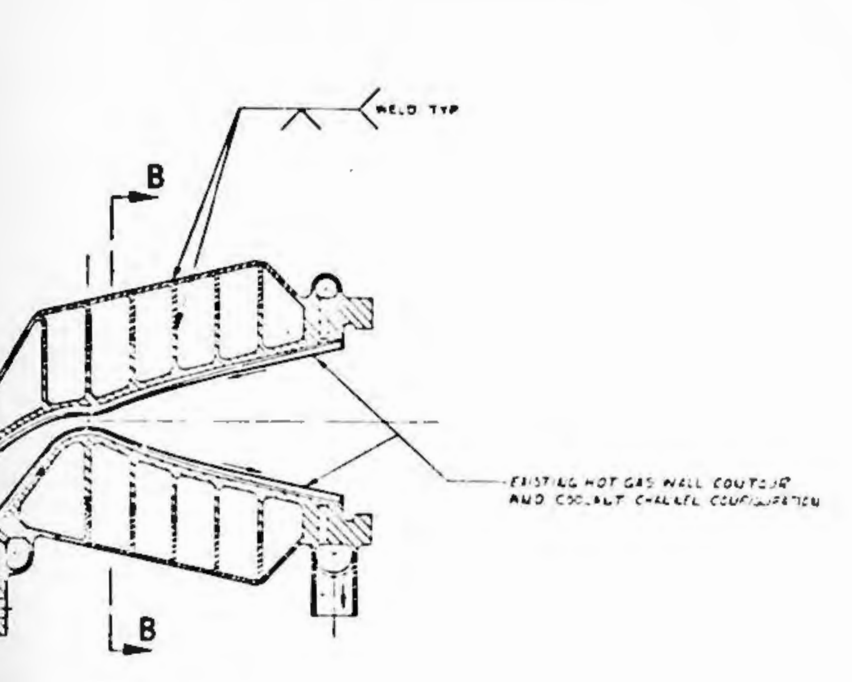

SECTION A-A

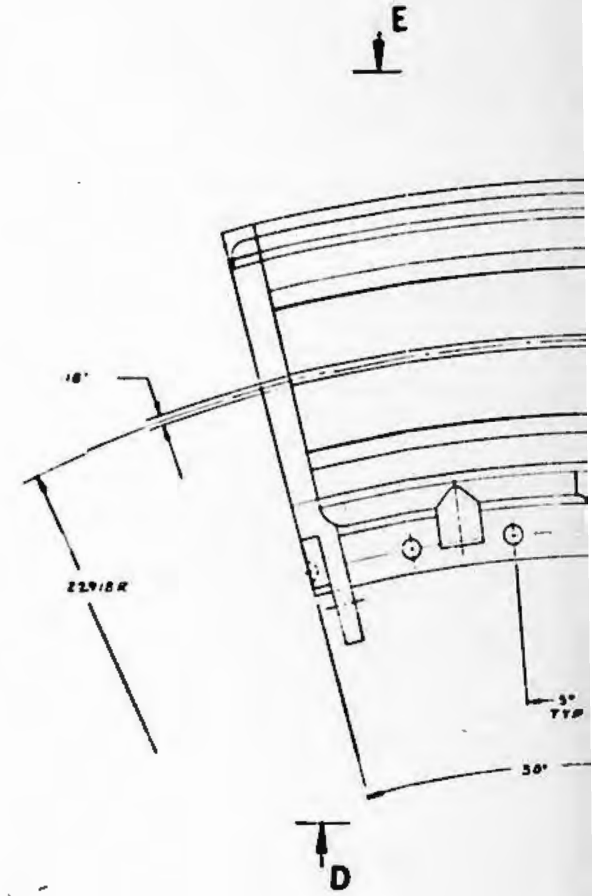

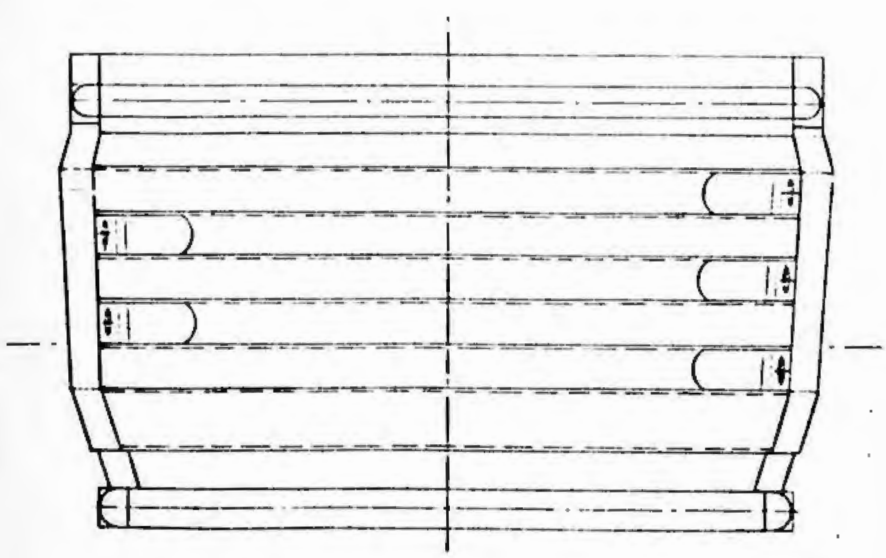

VIEW E-E (OUTER BODY LOOKING INBOARD)

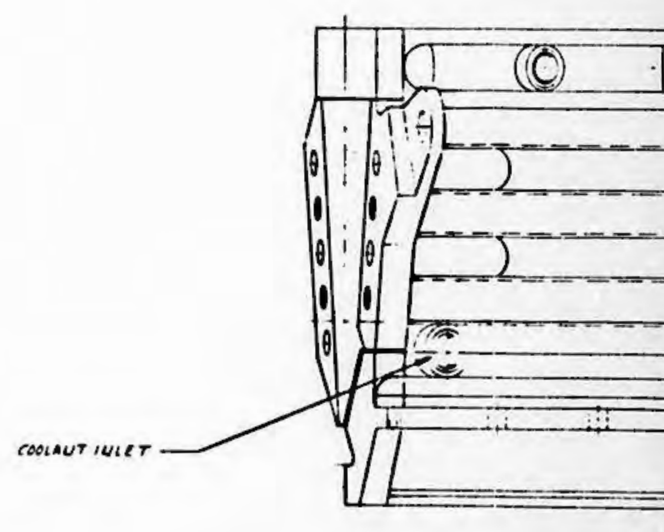

VIEW D-D (INNER BODY LO

2

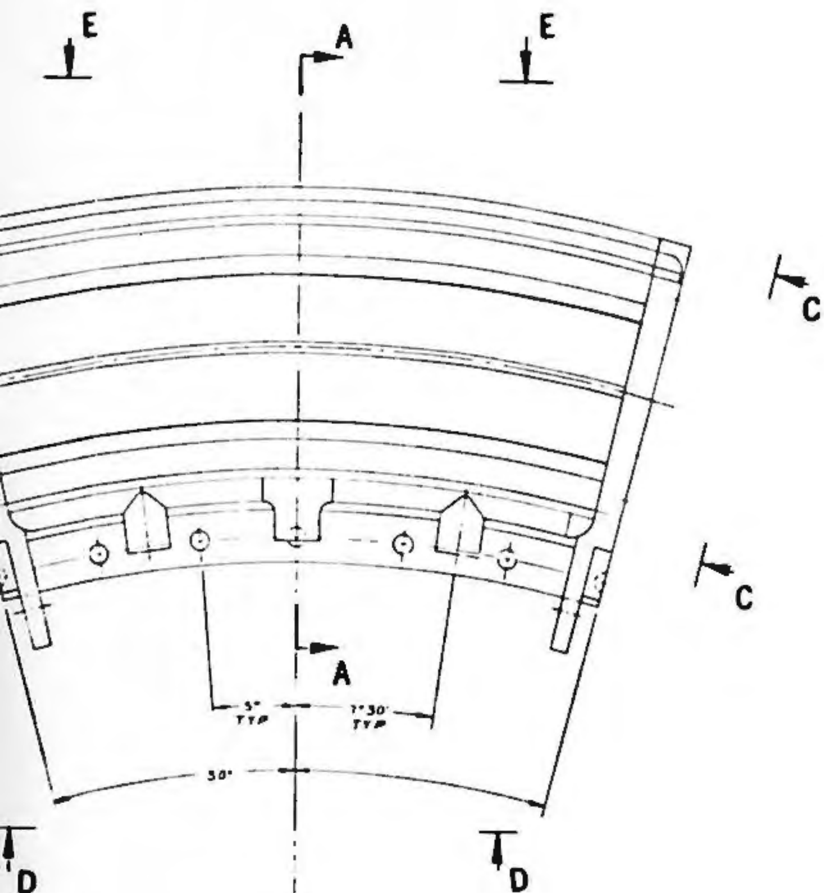

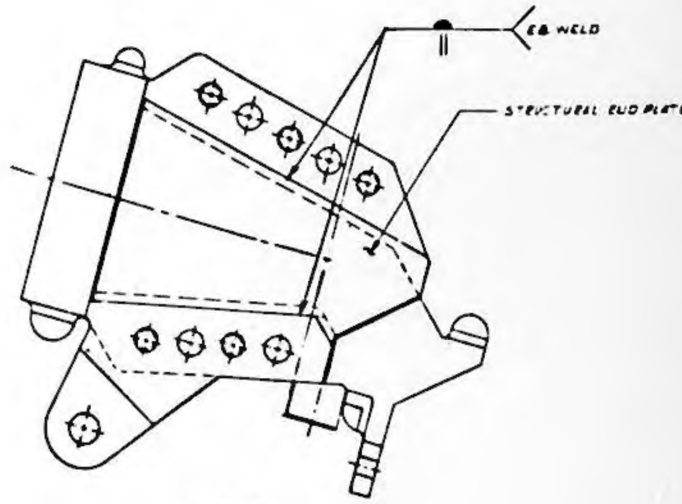

VIEW C-C

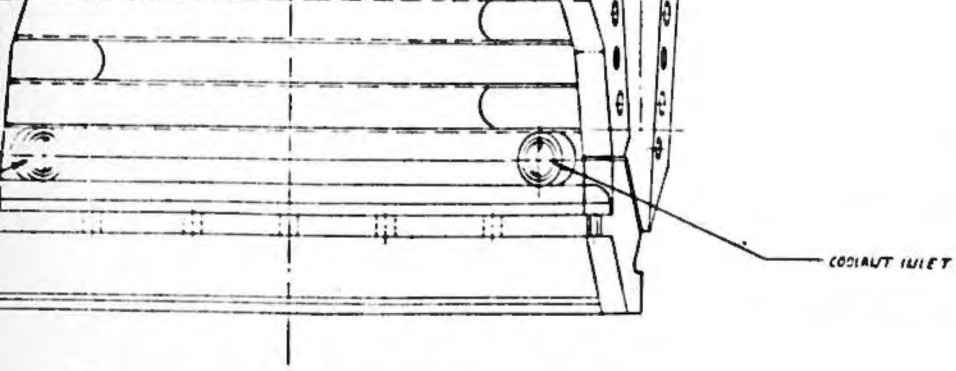

VIEW D-D (INNER BODY LOOKING OUTBOARD)

3

REVISIONS

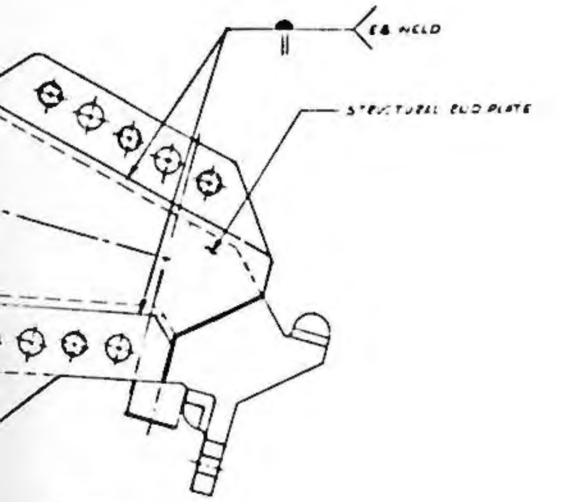

VIEW C-C

Figure 164. Welded-Rib Structure Layout (U)

THRUST CHAMBER SEGMENT (MACHINED AND WELDED SUPPORT STRUCTURE)

J 02602

4

(U) manifolded to the forward end of the outer body for a single downpass. This coolant circuitry modification simplified manifolding and resulted in a more compact and lighter weight thrust chamber segment.

(4) Coolant Channels and Hot-Gas Face Sheet

(U) The coolant channel configuration was the same as that used on the Task II segments. The heat transfer capabilities of these channels have been adequately demonstrated during the segment testing. The nickel substrate was necessary in the throat region of both the inner and outer bodies to reduce the maximum gas-side wall temperature and the face sheet-to-land braze joint temperature. Two methods of applying the nickel substrate to the support structure were considered. One method uses electroformed nickel deposited directly on the backup structure (as done in Phase I), and the other method would be to explosively form a wrought-nickel sheet and braze it to the backup structure.

(U) The hot-gas face sheet was wrought-nickel 200 sheet and would be either explosively or stretch formed to fit the hot-gas wall contour as used on the Task II segments.

(5) Coolant End Plates

(U) Coolant plates use wrought-nickel 200 bodies and brazed-on nickel 200 hot-gas face sheets. The coolant channels are electrical-discharge machined into the body. The manifolding and crossover passages are drilled in the body. Direction of coolant flow is upward as indicated in Fig. 163.

(6) Structural End Plates

(U) The structural end plates would be fabricated form INCO 718, inset, and electron-beam welded to the end flanges of the support structure.

(7) Injector

(U) The injector face strip incorporated in the design was the same as used in the final Task II segments. The body of the injector was designed for fabrication by investment casting using INCO 718C material.

(8) Nozzle Extension

(U) The nozzle extension design incorporated the same tube design as used on the Task II nozzle. Inlet and outlet coolant lines were rerouted to provide maximum clearance for engine hardware. The outlet manifold incorporated a heat exchanger for the propellant feed system tank pressurant. Both the nozzle-to-thrust segment flange and the base closure attachment flange required some redesign to meet the requirements of a flight-type engine design.

2. SECONDARY ENGINE THRUST CHAMBER DESCRIPTION

(U) The secondary engine thrust chamber is a bell-type configuration and is based on previous optimization studies of Ref. 1 . Basic design parameters are shown in Table 38 and additional parameters are shown in Table 2 .

TABLE 38

SECONDARY THRUST CHAMBER PARAMETERS (U)

Thrust (max), pounds	3330
Chamber Pressure (max nozzle stagnation), psia	750
Expansion Area Ratio	60:1
Engine Mixture Ratio	12:1
Throttling Ratio	9:1

CONFIDENTIAL

(U) The Task I analysis and design work accomplished on this component consisted of the following three areas:

1. Chamber Contour Selection
2. Injector Design
3. Chamber Design

(U) Each of these areas is discussed in the following sections.

a. Chamber Contour Selection

(C) The results of previous bell chamber and toroidal segment hot-firing tests indicated that high combustion efficiencies could be obtained with chambers having a combustion chamber length of 6 inches and a characteristic length (L*) of approximately 22 inches. To meet these requirements and also to

(C)

ensure good boundary-layer attachment for low throat heat transfer, the combustion chamber should have a contraction ratio of 4:1 and a contoured tapered into the throat. The combustion chamber shape was important in that the throat, and combustion zone heat transfer rates, could be significantly affected by different combustion chamber shapes. The range of combustion chamber shapes considered for the secondary engine bell chamber as shown in Fig. 165. These shapes varied from a conventional bell combustion chamber shape (contour A) to a conical shape (contour C).

(C) Significant reductions in combustion chamber heat transfer rates are achieved through the use of gradual convergence combustion chambers. These reductions have been shown to be the result of the boundary-layer growth behavior within the combustion chamber. When the integrated length from the start of the boundary layer to the nozzle throat is long, the throat heat flux is lower. Consequently, for a fixed combustion chamber length, as in the case of the secondary engine, the combustion chamber shape in conjunction with the injector, determines the boundary-layer attachment point and thus the integrated boundary-layer development length. Early boundary-layer attachment (close to the injector face) results in low throat heat flux. However, this method of reducing the throat heat flux increases the combustion chamber heat fluxes and this, in turn, increases the integrated heat input.

(C) Analytical predictions of the gas-side heat transfer coefficient and the combustion chamber integrated heat input were performed for contours A and B using the solution of the integral energy boundry-layer equation with a semi-empirical relationship between the energy boundary-layer thickness and the Stanton number. For the predicted boundary-layer

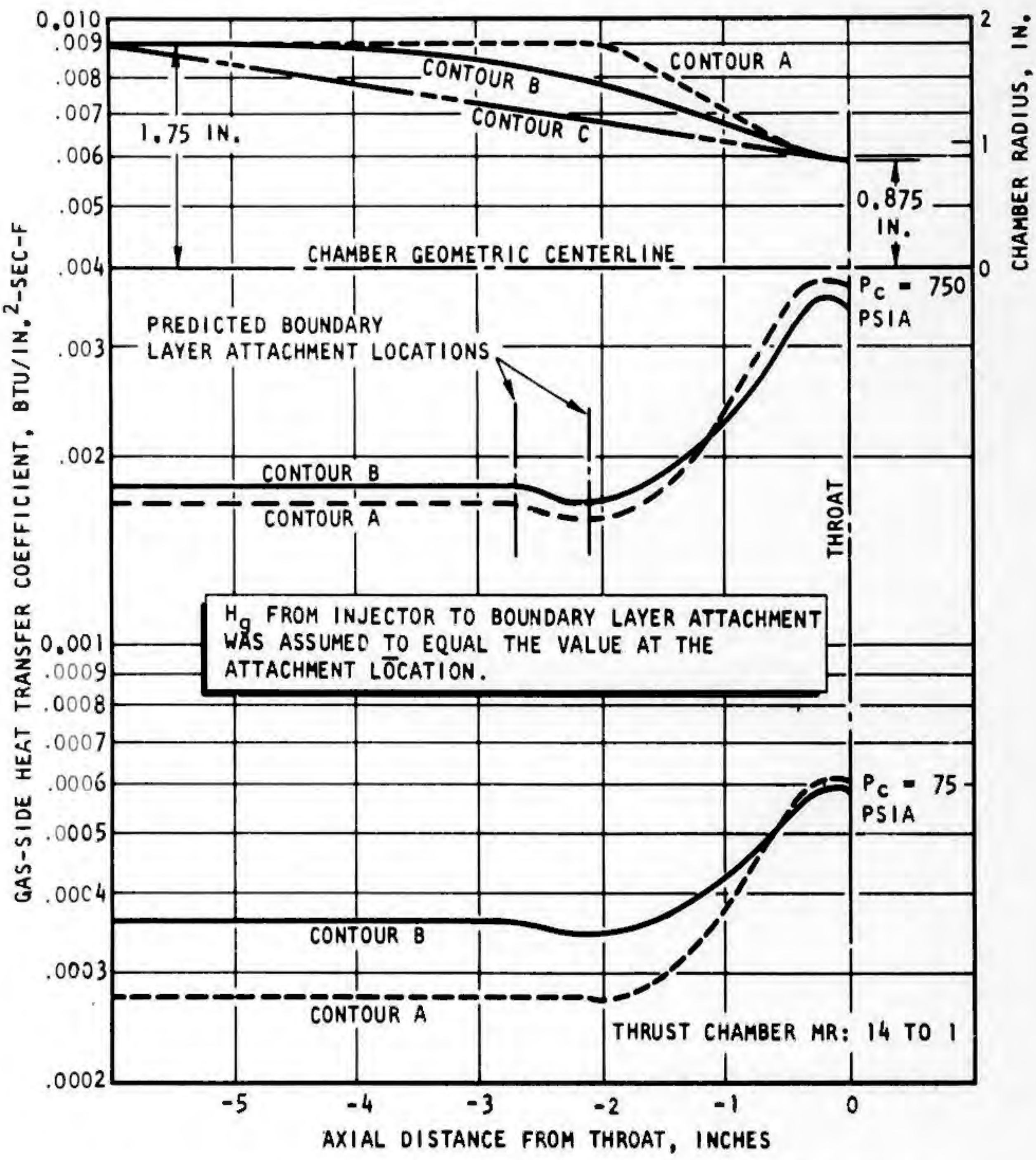

Figure 165. Predicted Gas-Side Heat Transfer Coefficient as a Function of Contour

(C) attachment locations shown in Fig.165 contour B reduced the throat heat approximately 3 percent lower than contour A and resulted in approximately a 10-percent increase in heat input at both 75 psia and 750 psia chamber pressure.

(U) Independent of the injector configuration, contour A would result in boundary-layer attachment near the start of the contraction and utilizes only 30 percent of the available boundary-layer growth length. The boundary-layer attachment location for contour B, depending on the injector configuration, could move closer to the injector, which would further reduce the throat heat flux. Also, the predicted 10-percent increase in heat input was a liberal estimate since a constant heat flux from the injector face to the boundary-layer attachment was assumed; normally, the heat flux is at a lower level than at the boundary-layer attachment location.

(U) Contour C (Fig.165) would provide the most efficient use of the available boundary-layer growth length (i.e., lowest throat heat flux); however, the highest integrated heat input would result and on an uppass coolant circuit, contour C would not achieve the most efficient coolant curvature enhancement. The conclusion was that either of the three contours could be used with satisfactory results on the secondary engine.

(C) As a compromise to reduce the throat heat flux with minimum increase in integrated heat input, contour B was selected for the secondary engine thrust chamber and is shown dimensionally in Fig.166. The coordinates shown for the contour were based on a 13.402-inch radius which is tangent to both the 1.313-inch throat radius and the 3.500-inch-diameter cylinder as indicated in the table shown in Fig. 166. The 1.00-inch dimension from the injector face location to the end of the chamber was based upon existing injector designs similar to the one being considered for the secondary engine chamber.

(C) Although this study did not consider, in detail, the contour aft of the throat plane, previous studies (Ref. 1) indicated that a constant 1.313-inch throat radius results in negligible performance losses and reduces fabrication complexity.

CONFIDENTIAL

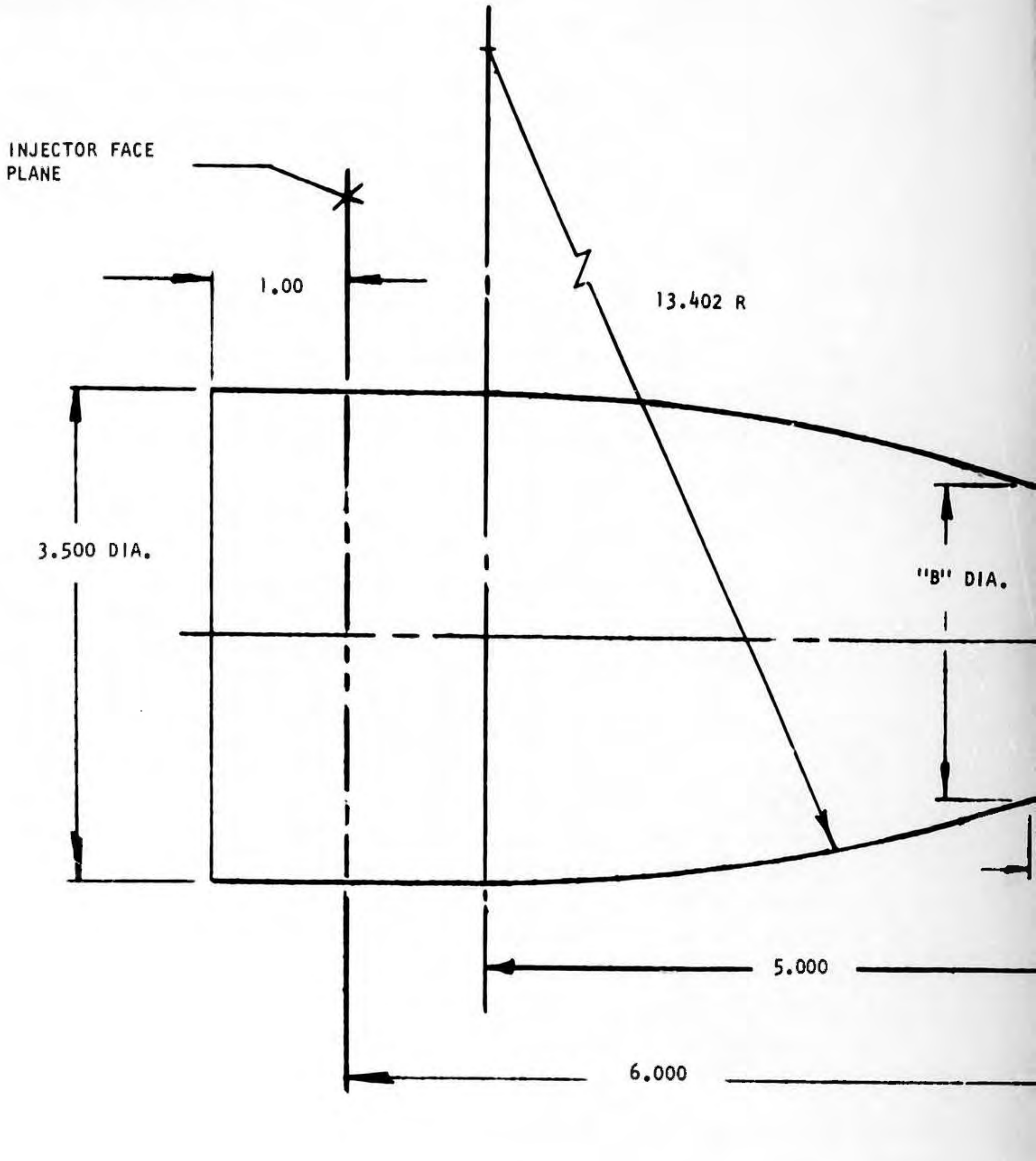

"A"	"B" DIA.
0.000	1.750
0.455	1.900
1.000	2.396
1.500	2.592
2.000	2.816
2.500	3.026
3.000	3.196
3.500	3.326
4.000	3.426
4.500	3.476
5.000	3.500

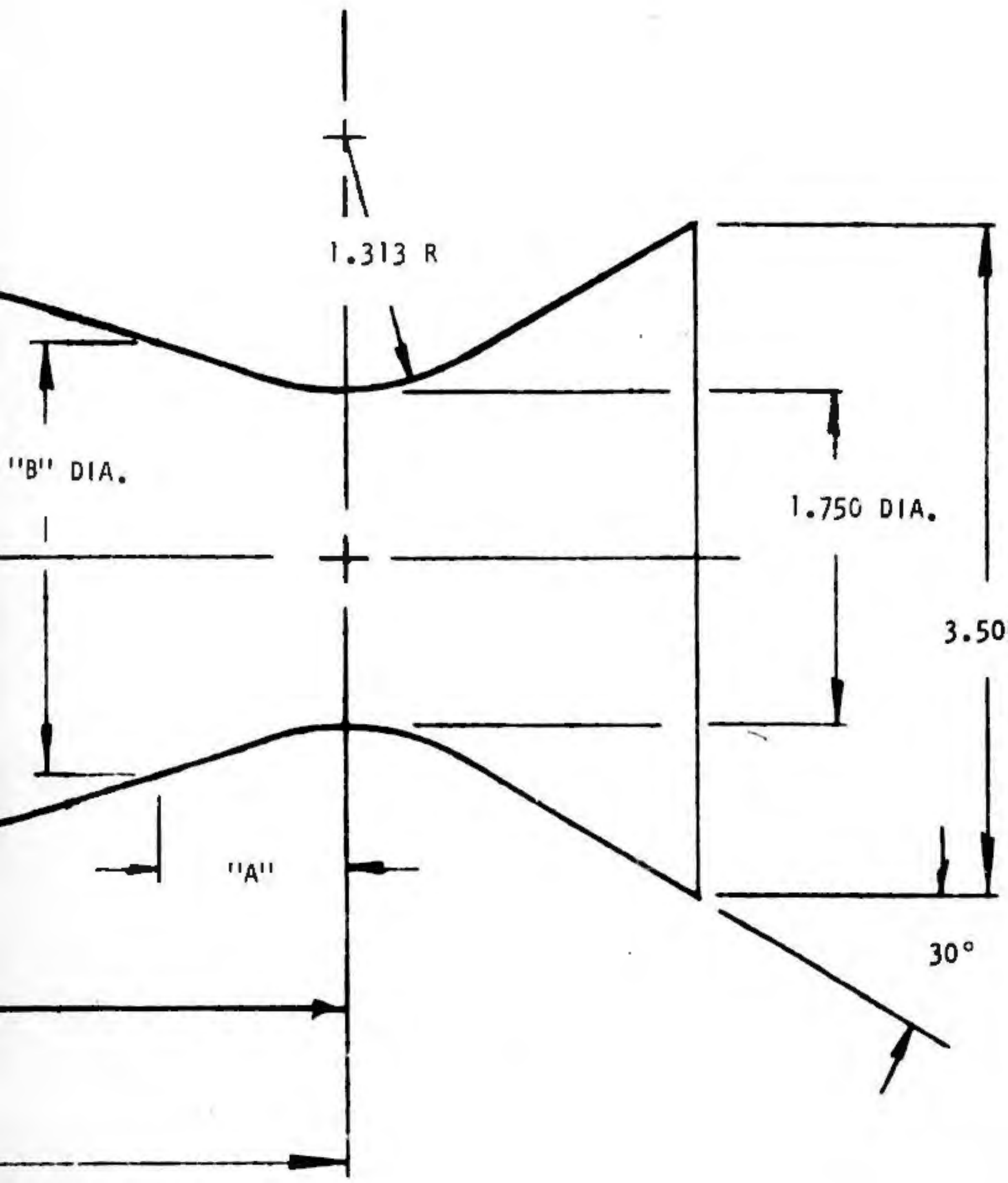

Figure 166. Secondary Engine Thrust Chamber Contour

 2

b. Secondary Injector Design

(C) The preliminary design of the secondary thrust chamber injector is shown in Fig. 167, and the injector ring set is shown in Fig. 168. The basic injector design criteria established during the main thrust chamber injector development program were used for the design. Some specific design features are:

1. Impinging fan pattern with orifice sizes to obtain required injection velocities for maximum η_{c*}
2. Nickel face
3. High oxidizer ring groove velocities (40 ft/sec) for good face cooling
4. Injector face provides for central hot-gas tapoff and diluent system

(C) A three-dimensional, steady-state conduction heat transfer analysis was conducted to determine the isothermal temperature distribution in the injector body and rings and on the hot-gas surfaces. The analysis was based on face heat fluxes of 3 Btu/sec, which was considerably greater than the values that could be inferred from the experimental results obtianed during 30-degree segment testing at 650 psia. In those tests, the actual face heat flux was not measured but was assumed to be equal to the measured wall heat flux immediately below the injector face. A maximum gas-side wall temperature of 1910 R was predicted.

(U) The analysis required the assumption of heat transfer conditions in the central tapoff region because of a lack of experimental data (Fig. 167). Development versatility, however, was provided in the design to allow the necessary cooling, as required.

c. Secondary Chamber Design

(U) The secondary thrust chamber was designed as a nickel channel-wall combustion zone that mates with a tubular wall nozzle (Fig. 169). The

CONFIDENTIAL

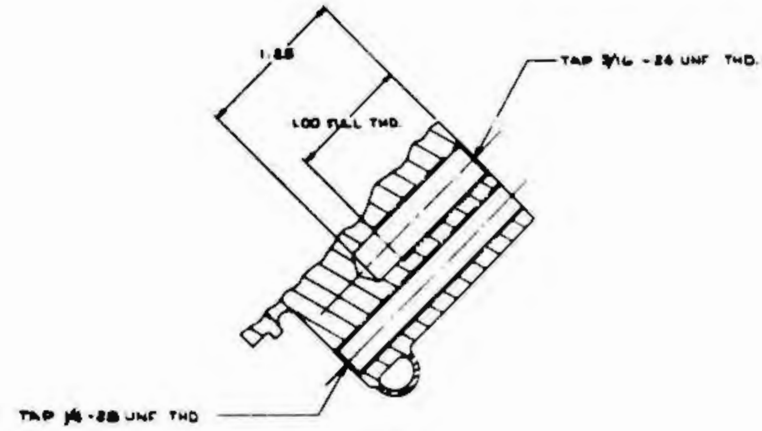

SECTION D-D

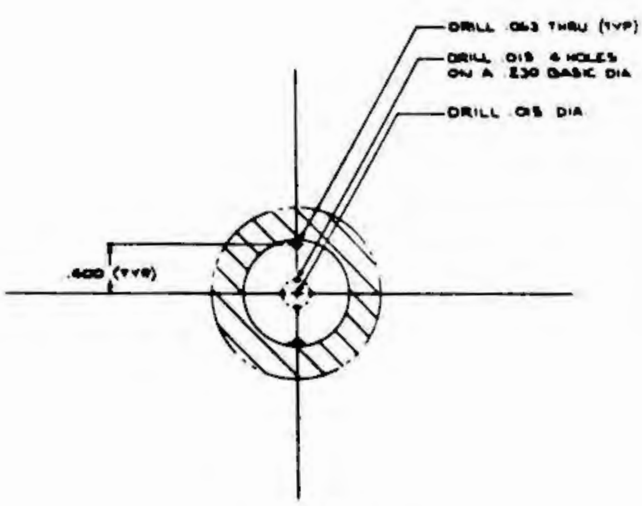

SECTION E-E

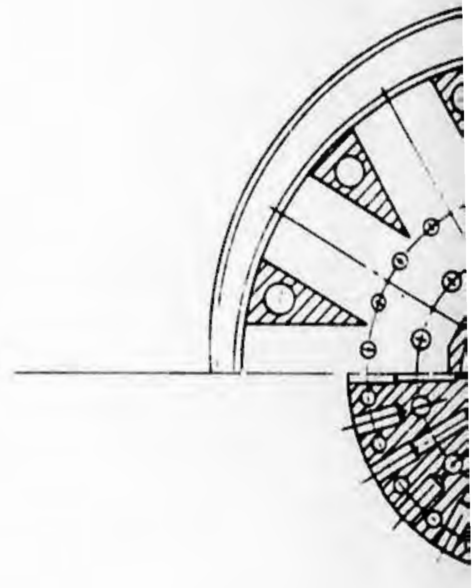

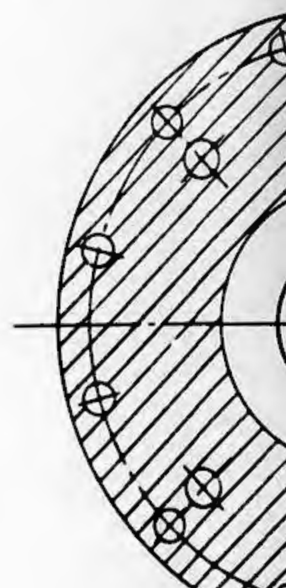

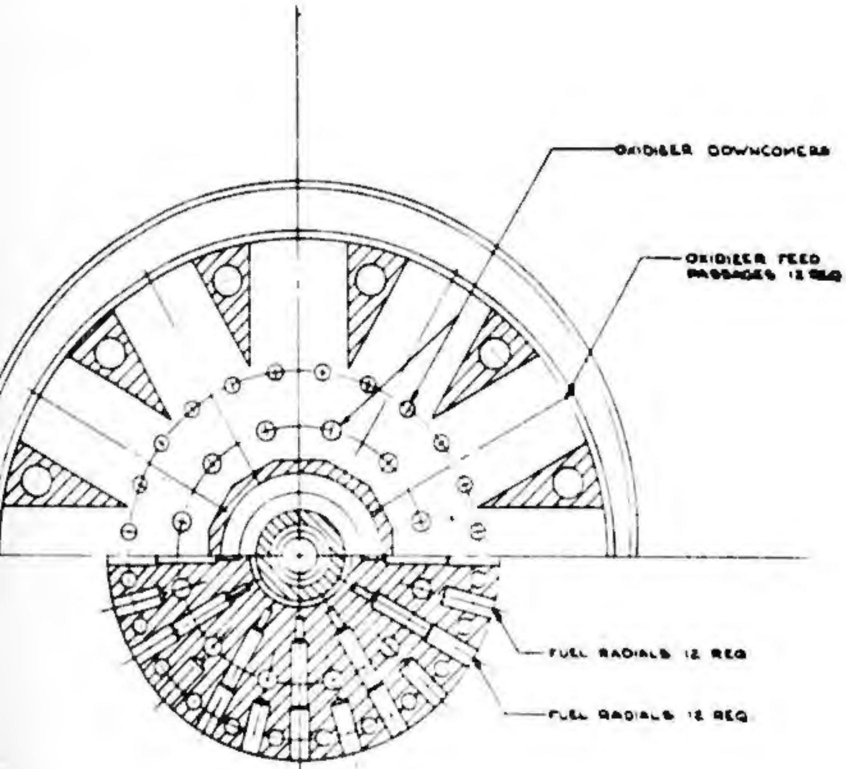

SECTION A-A

SECTION B-B

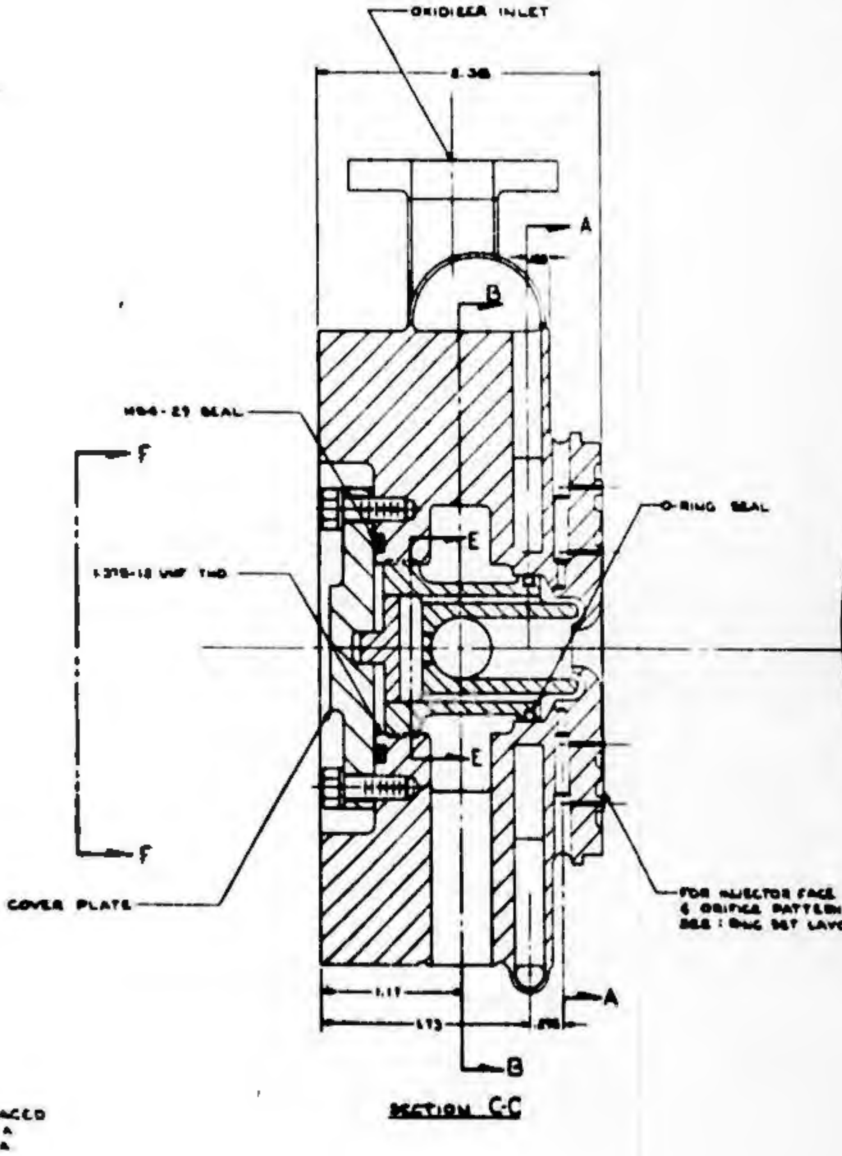

SECTION C-C

VIEW F-

2

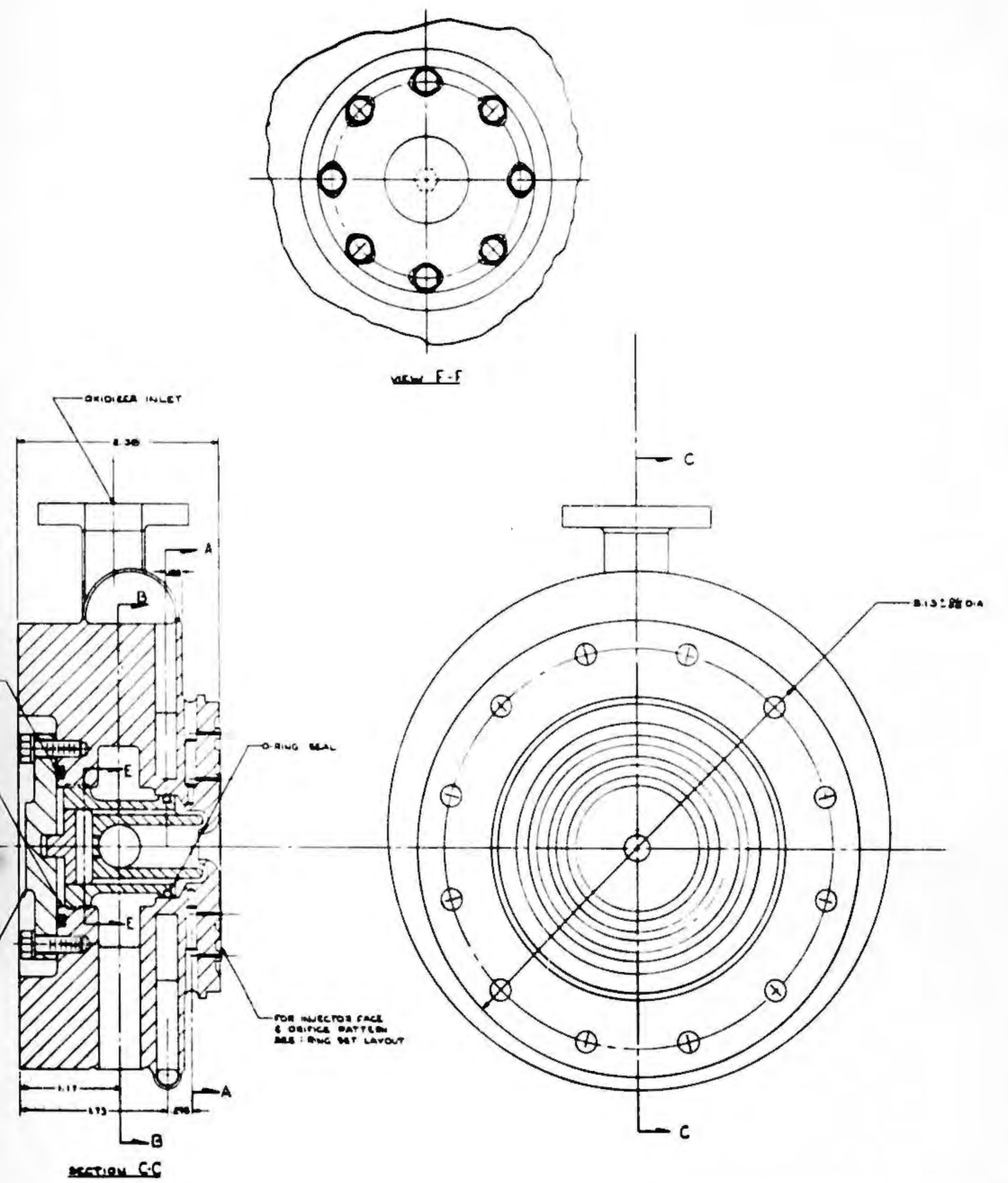

Figure 167. Secondary Engine Injector Layout (U)

CONFIDENTIAL

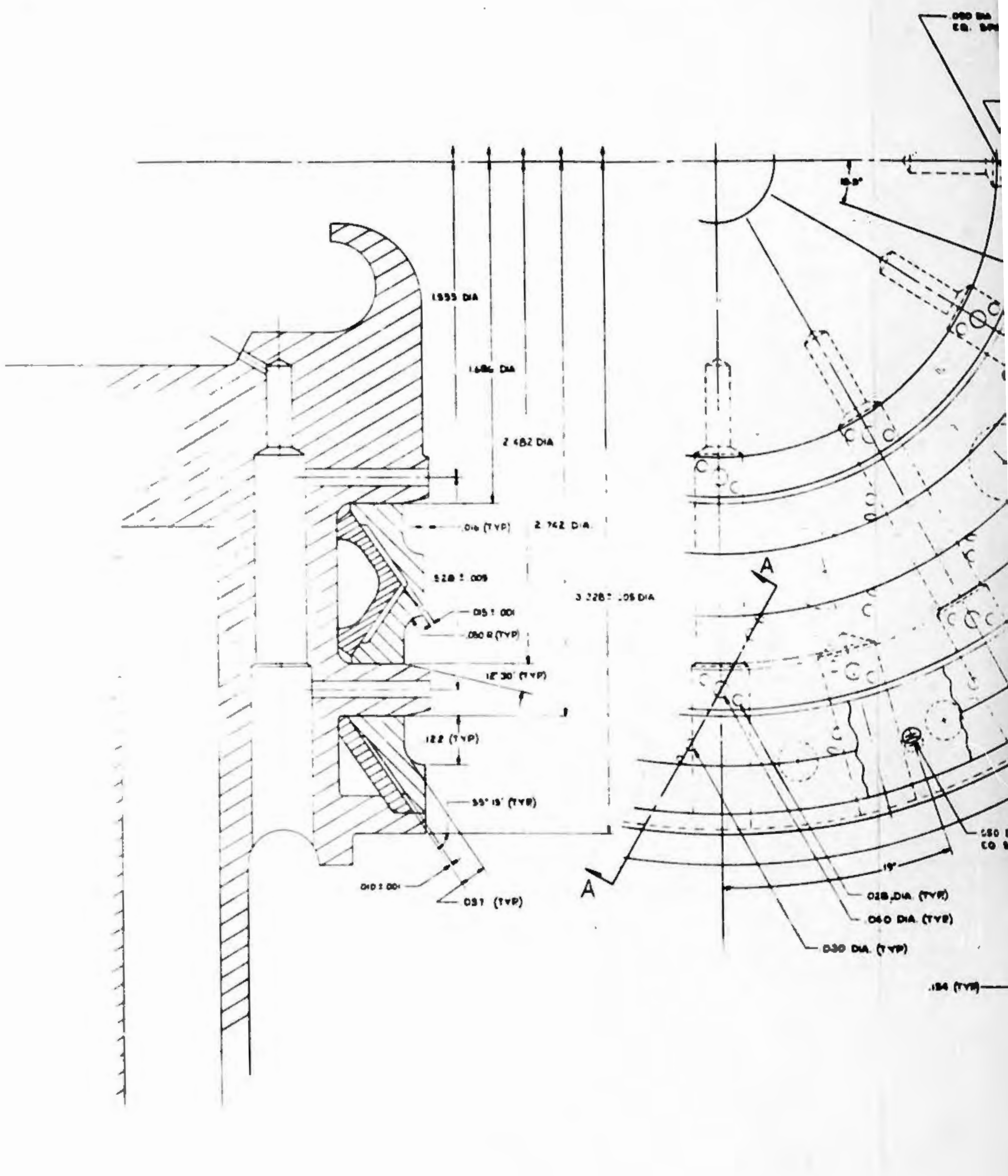

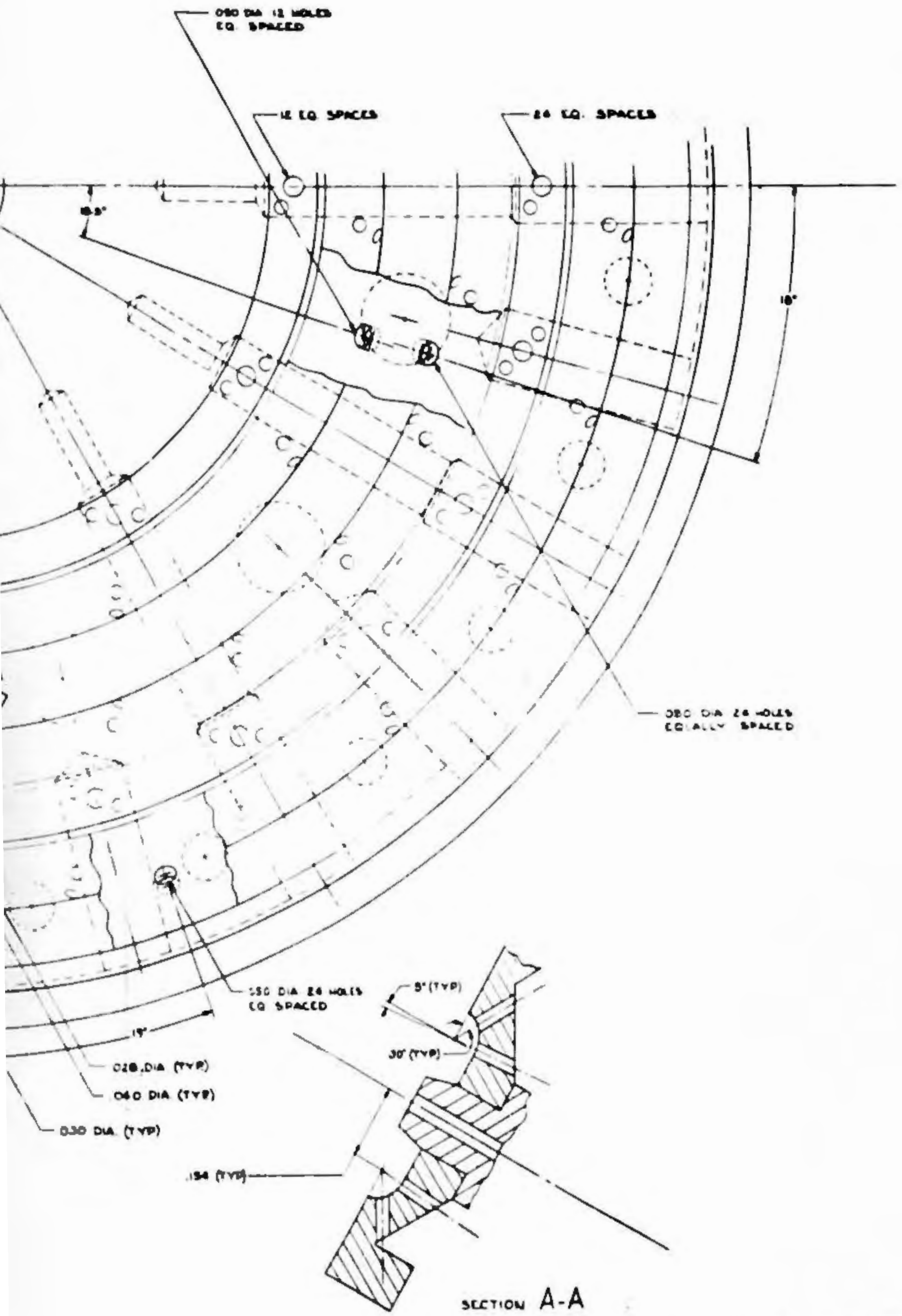

Figure 168. Secondary Engine Injector Ring Set (U)

CONFIDENTIAL

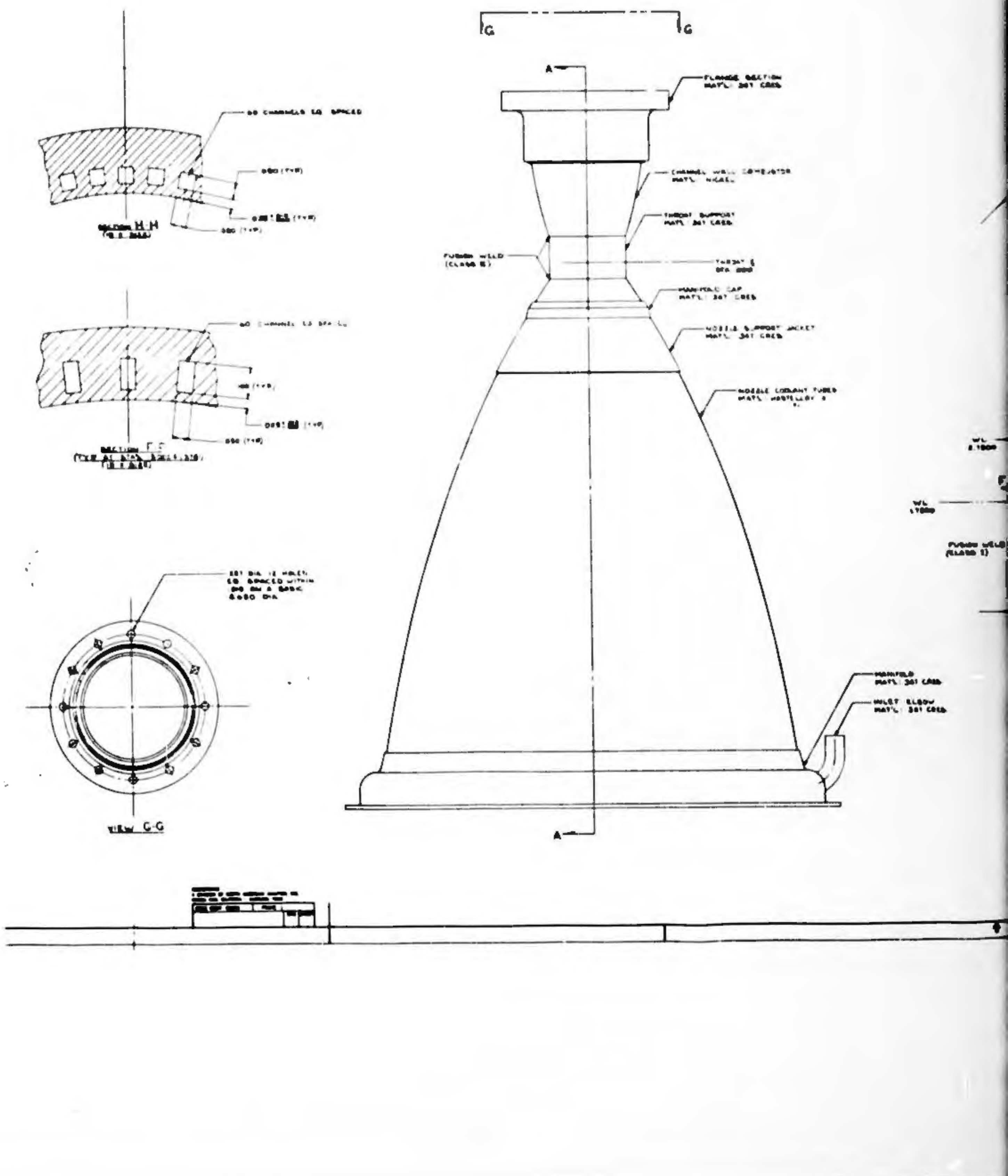

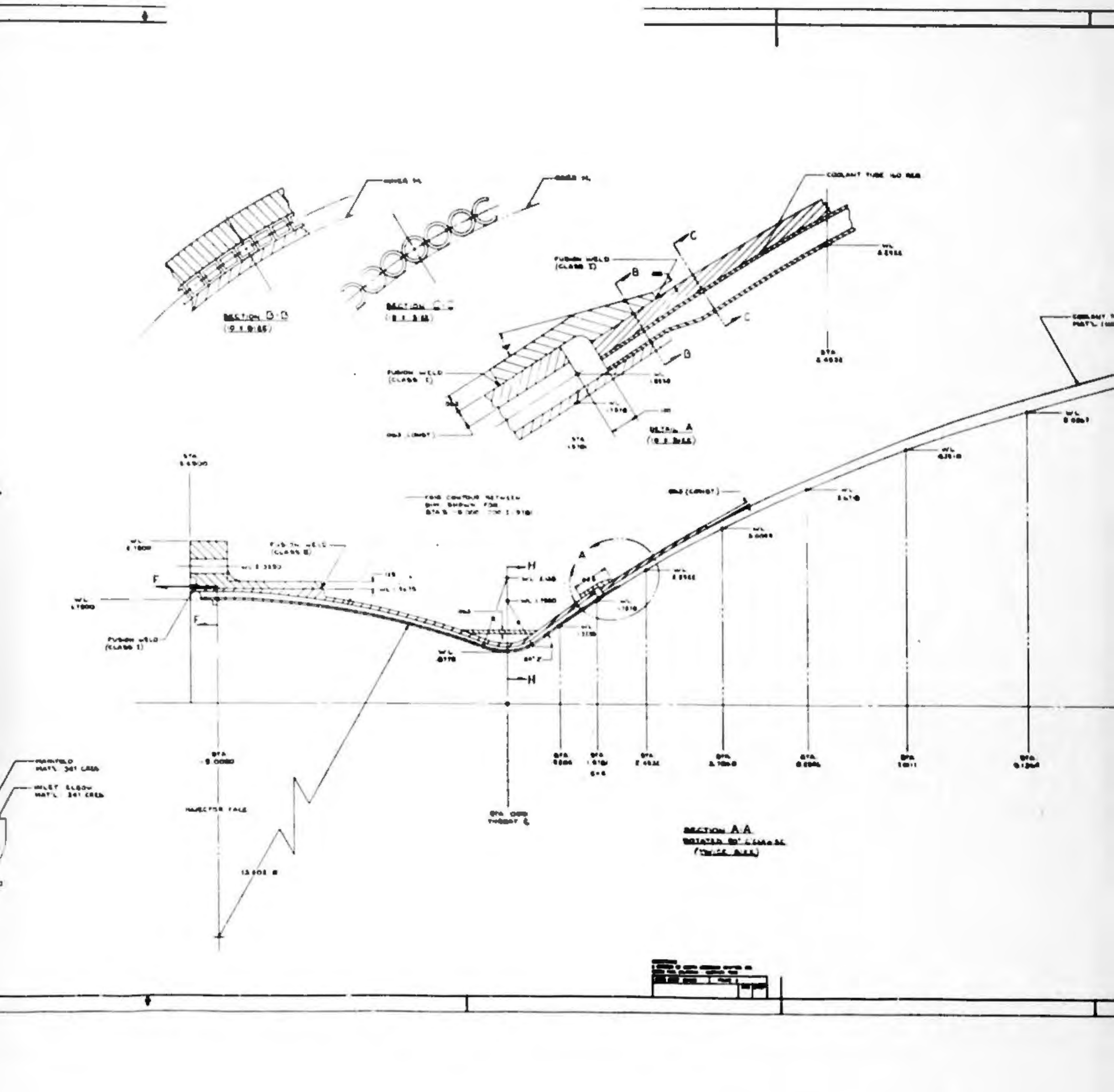

COOLANT TUBE
FUSION WELD
(CLASS I)
SECTION B-B
SECTION C-C
DETAIL A
STA
W.L.
FUSION WELD
(CLASS I)
MANIFOLD
INLET ELBOW
INJECTOR FACE
THROAT
SECTION A-A

2

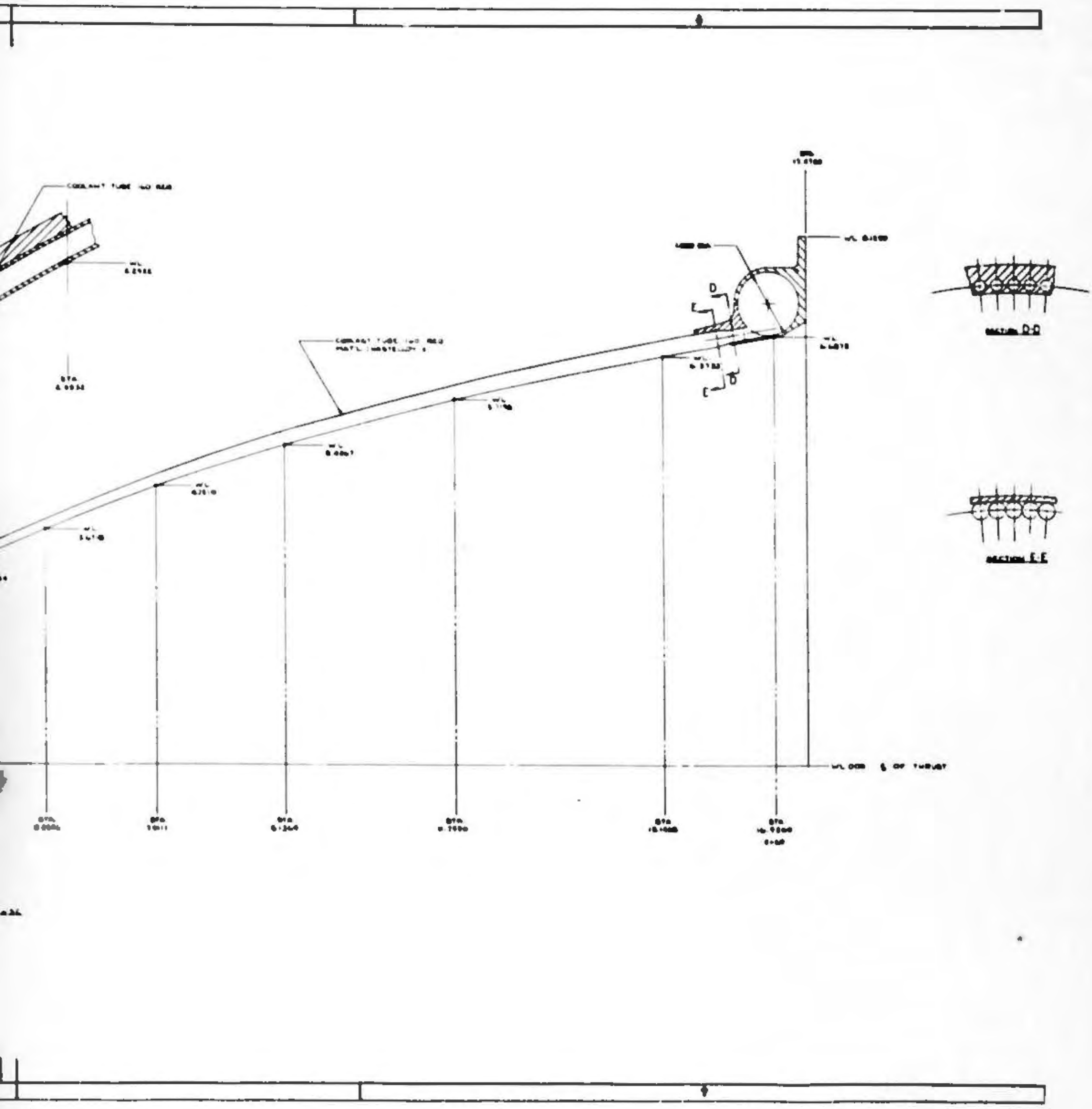

Figure 169. Secondary Thrust Chamber Design (U)

3

(C) channel-wall construction and design were not finalized. Sintered nickel, spun nickel, electroformed nickel, and brazed nickel sheet are all possible construction methods. The chamber is to be regeneratively cooled by a single-pass system with the coolant entering at the nozzle exit plane. Unlike other tubular designs the tubes for the nozzle are singular, i.e., there is no splitting of the flow from one tube to two tubes, and the cross section of the tubes is circular, instead of eliptical, at all stations. The nozzle design utilizes a 360-degree manifold at the forward end of the tubes to receive the fuel coolant from the tubes and distribute the fuel to the channel passages (Fig. 169). A layout of the assembled thrust chamber and injector is shown in Fig. 170.

(C) The expansion ratio of the nozzle is 60:1, and the nozzle is designed as an 80-percent bell contour.

CONFIDENTIAL

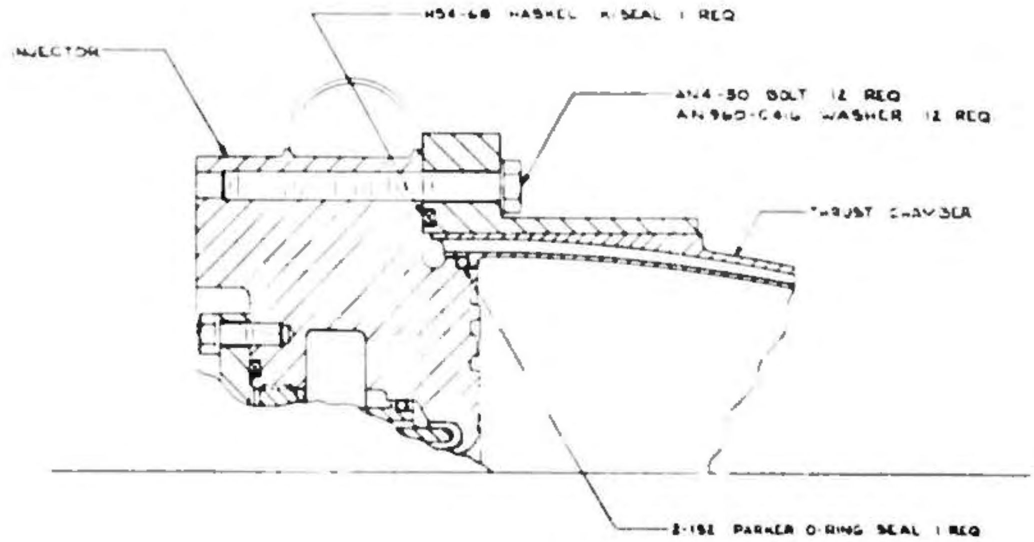

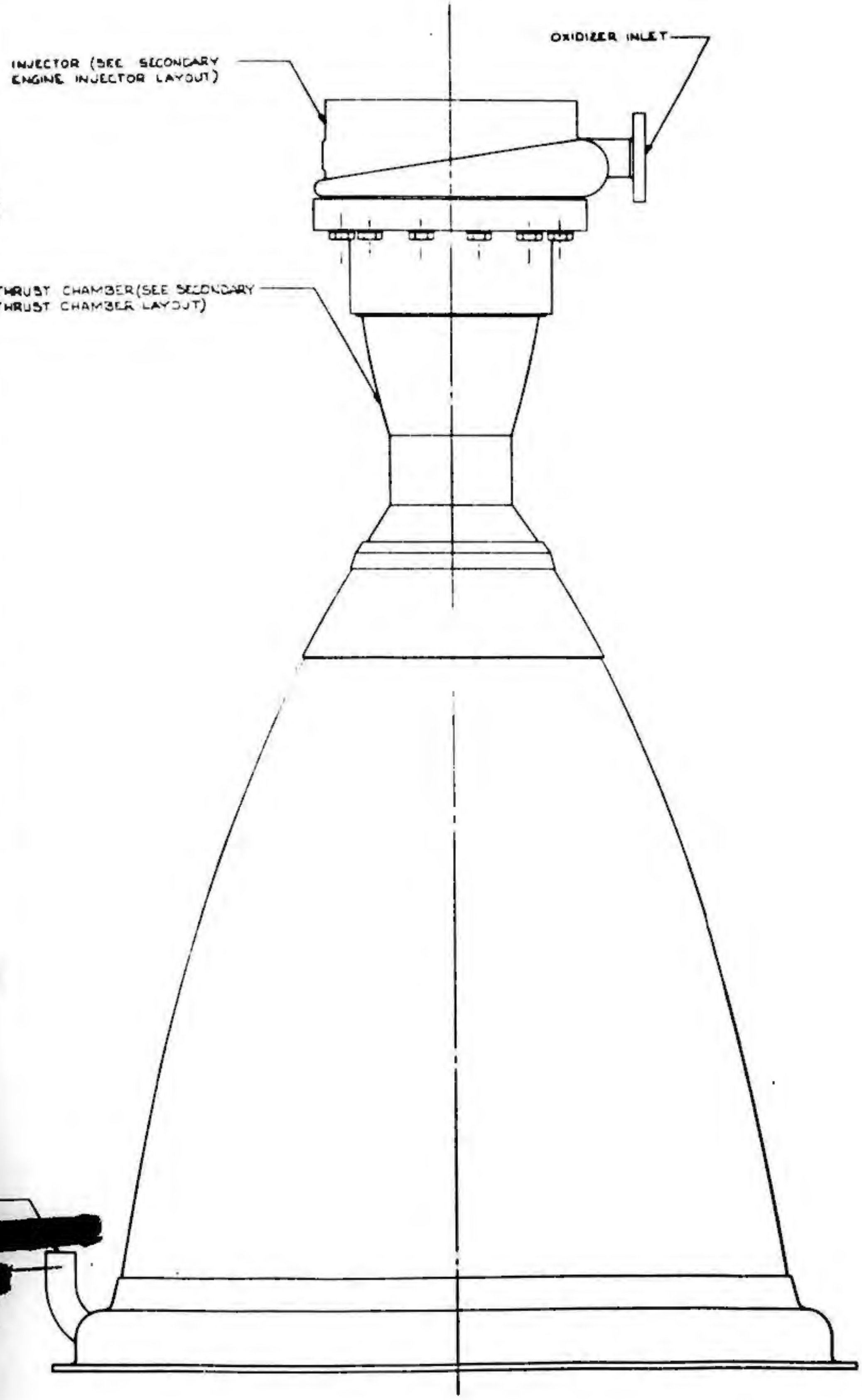

Figure 170. Secondary Engine Thrust Injector Assembly Layout (U)

SECTION V

TURBOPUMPS

1. GENERAL DESIGN DESCRIPTION

(U) The design of the main and secondary engine turbopumps was the result of trade studies, incorporation of new technology, and previous experience. Typical trade studies included (1) an evaluation of the Barske-type pump which showed the shrouded centrifugal pump to have a higher efficiency potential and fewer mechanical problems, and (2) an evaluation of vaneless versus vaned diffusers which showed improved performance for the vaned diffuser. The incorporation of new technology included the utilization of material compatibility data obtained from the Task II bearing and seal tester program. The utilization of previous experience included the scaling of empirical data from Rocketdyne's Mark-15 LO_2 pump and the Mark-29 LH_2 turbopumps to establish head, flow, and efficiency maps for the AMPS turbopumps.

(U) The design parameters for the four turbopumps are presented in Table 39.

a. Inducers

(C) All four inducers have a cylindrical tip and a tapered hub. The purpose of the cylindrical configuration, in addition to better performance, is to eliminate the dependence of tip clearance on axial location. Each inducer has three blades, a tip solidity (blade cord length/blade spacing) of about 2.5, a leading edge sweepback of 90 degrees, and a 30-degree sweep forward at the trailing edge. The fuel inducer cant angle is zero degrees, and the oxidizer inducer cant angle is 15 degrees. In each case, the inducer required head is quite low, with head coefficients much lower than 0.100.

TABLE 59

PUMP DESIGN PARAMETERS (U)

Parameter	Main LH_2 Pump	Secondary LH_2 Pump	Main LF_2 Pump	Secondary LF_2 Pump
Flowrate, gpm	500	55.8	289	32.2
Head, feet	65,000	43,400	1370	1920
Speed, rpm	75,000	138,000	27,500	75,000
Specific Speed (per stage)	700	570	2100	1470
Inducer				
Tip Diameter, inch	2.2	0.86	2.2	0.85
Inlet Hub Diameter, inch	1.0	0.35	0.44	0.27
Number of Blades	3	3	3	3
Inlet Blade Angle (tip), degree	7.5	7.5	9.5	7.5
Impeller				
Number of Stages	2	2	1	1
Tip Diameter, inch	3.88	1.8	3.25	1.15
Eye Diameter, inch	2.2	0.86	2.2	0.85
Hub Diameter, inch	1.5	0.46	0.875	0.404
Number of Blades	5+5+10	5+5+10	6	6
Discharge Tip Width, inch	0.075	0.042	0.120	0.0763
Discharge Blade Angle, degree	50	40	30	25
Volute and Crossover				
Volute Area at Tongue, sq in.	0.365	0.052	1.03	0.0782
Number of Crossover Vanes	14	--	--	--
Diffuser Outer Diameter, inch	5.0	2.3	--	--
Diffuser Inlet Blade Angle, degree	14.3	7.4	--	--
Diffuser Outlet Blade Angle, degree	19.3	14	--	--
Diffuser Vane Number	14	13	--	--

b. Impellers

(U) Both oxidizer pumps are single stage and both fuel pumps have two stages. The two stages have the effect of increasing the very low specific speed by the factor of the square root of 2, so that the fuel pump efficiency will be higher.

(U) The fuel impellers on both the main and secondary pump designs have five full vanes running from the inlet to the discharge. Part way through the impeller, the passages between these vanes split with partial vanes and then, farther on, these passages split again, giving a total of 20 vanes at the discharge. The reason for the large number of vanes is the relatively high required head coefficient per stage of 0.65 and 0.60 for the main and secondary pumps, and the high discharge blade angle requires more guidance (reduced passage aspect ratio).

(U) Because the oxidizer impeller tip diameters are small and the eye diameters large, the head coefficients are necessarily low and the discharge blade angles are lower than on the fuel impellers. Six full vanes are used with no partial vanes.

(U) The discharge flow coefficients are lower on the fuel impellers than on the oxidizer impellers to keep the discharge width from getting too small.

c. Diffusers and Volutes

(C) The fuel pump designs are equipped with diffuser vanes at the impeller discharge because of the high fluid velocities. The main and secondary diffusers have diffusion factors of 0.561 and 0.402, respectively. The diffusion factor is defined by:

$$D = 1 - \frac{C_3}{C_2} + \frac{Cu}{2\sigma C_2}$$

where

C_2 = inlet velocity

C_3 = outlet velocity

Cu = change in tangential component of velocity

σ = solidity = chord length/spacing

(U) The diffusers were designed so that the leaving velocity is roughly two-thirds that of the entering velocity.

d. Turbines

(U) As a result of a trade study of optimum turbines versus identical turbines for both main turbopumps and both secondary turbopumps, the designs incorporate the identical turbines. The value of minimum development costs outweighed the very small performance penalty.

e. General

(U) The designs incorporate the basic philosophy of similarity of construction in all areas where size and function will allow; e.g., identical turbines for both the fuel and oxidizer turbopumps, identical hydrodynamic passages for both stages of the hydrogen pump, similarity in arrangement and function between the main and secondary turbopumps, and similar fabrication concepts.

2. MAIN FUEL TURBOPUMP

(U) The general design layout for the main fuel turbopump is shown in Fig. 171.

(U) The pump housing arrangement eliminates all high-pressure external joints, except the pump discharge flange. The volute inlet, just aft of the second-stage diffuser vanes, incorporates a relief on both volute walls

CONFIDENTIAL

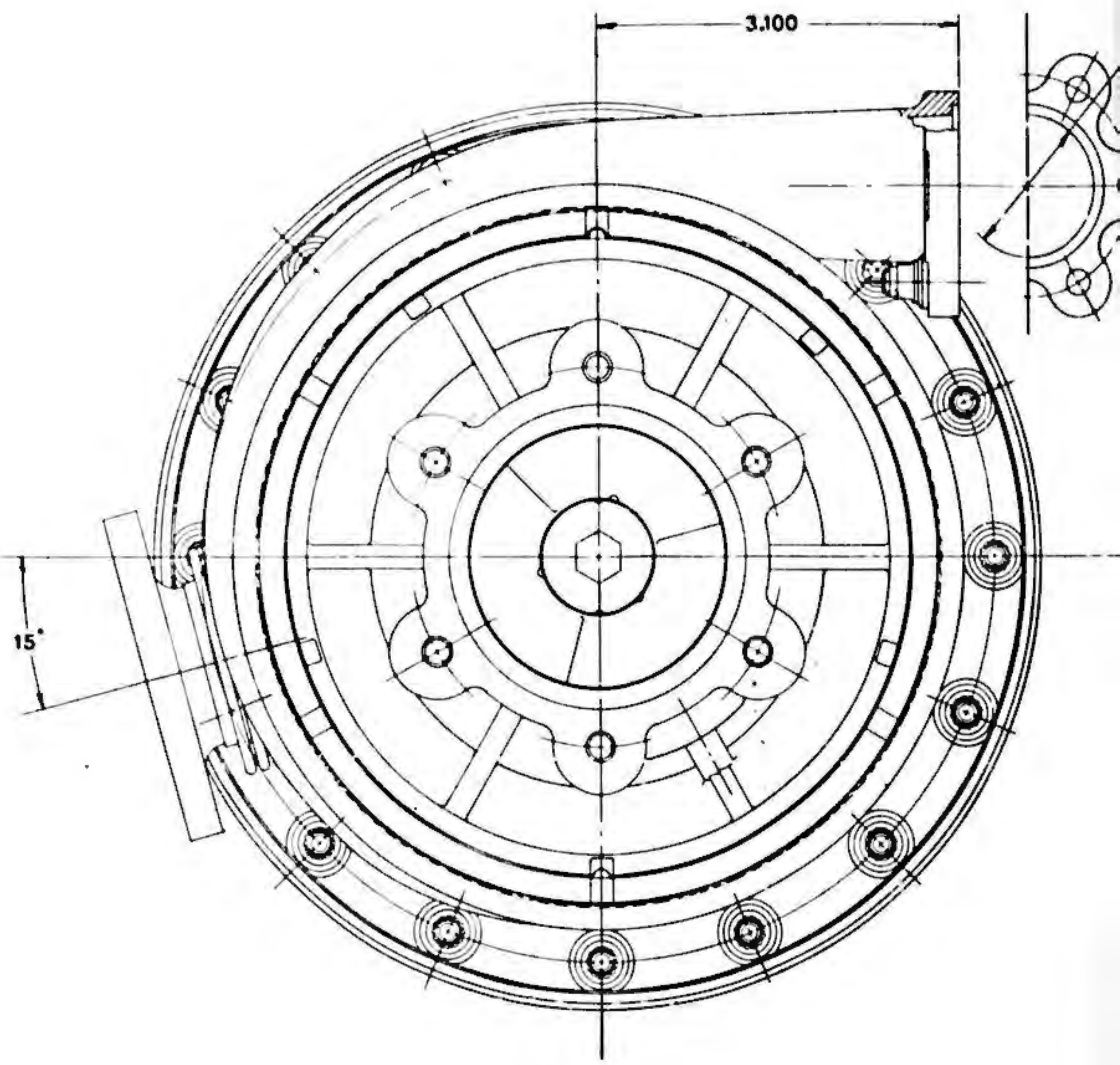

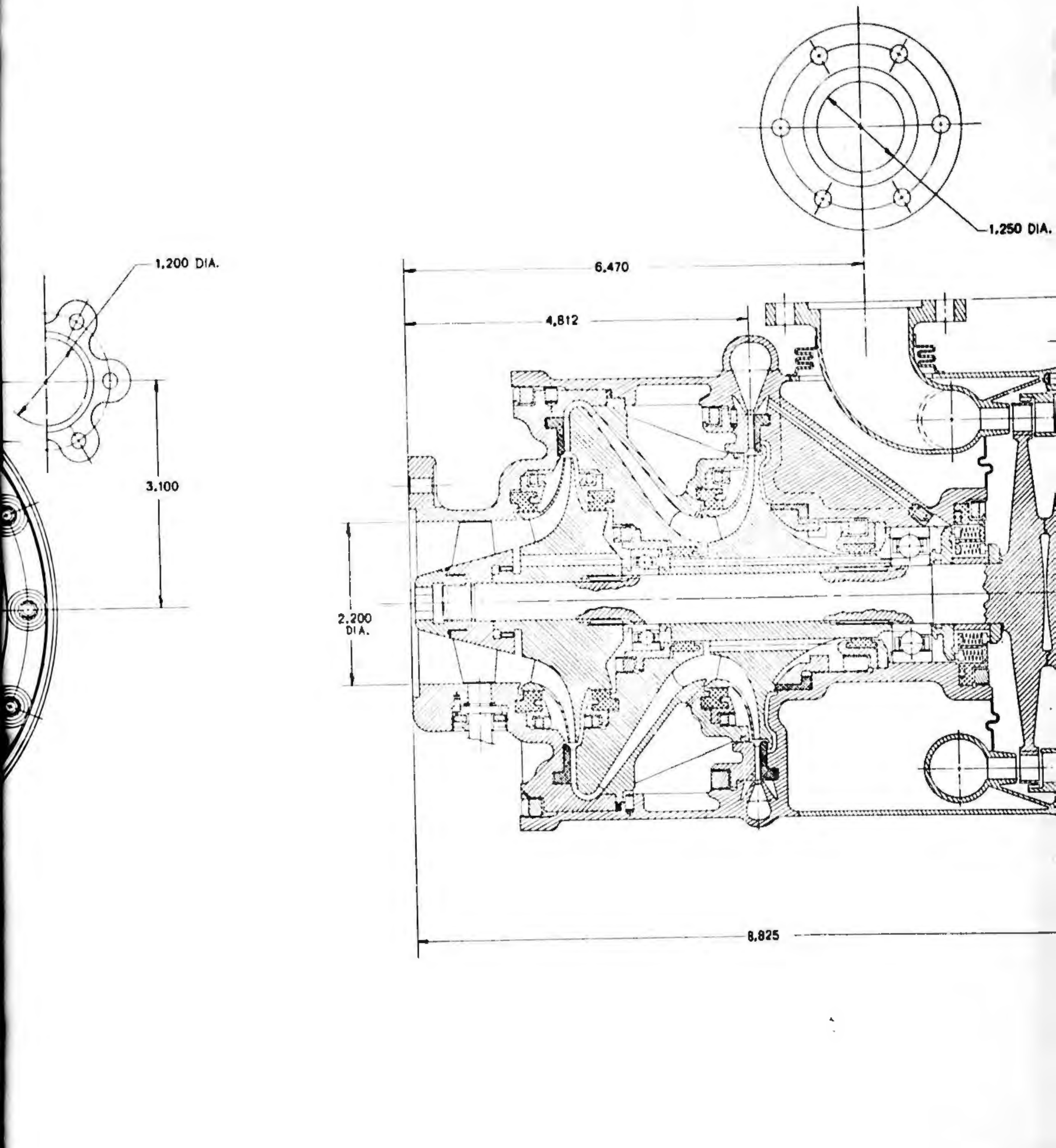

2

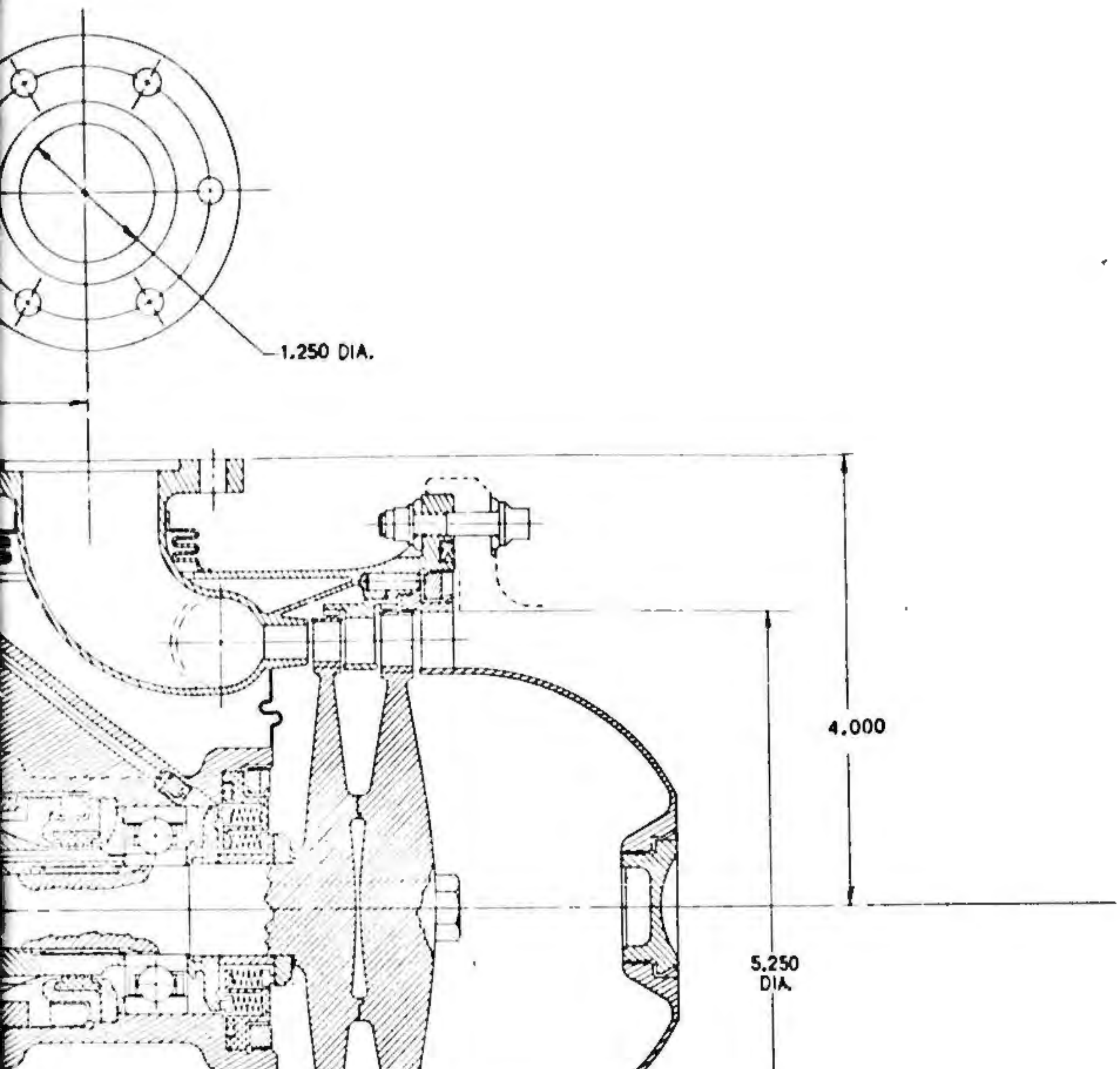

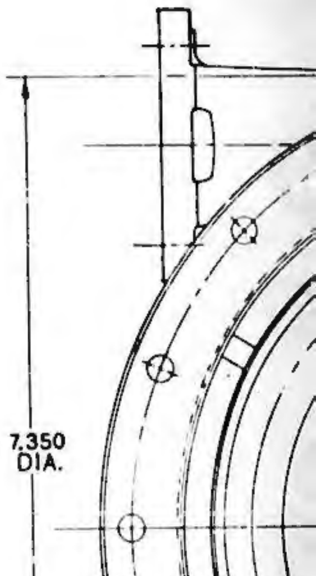

3

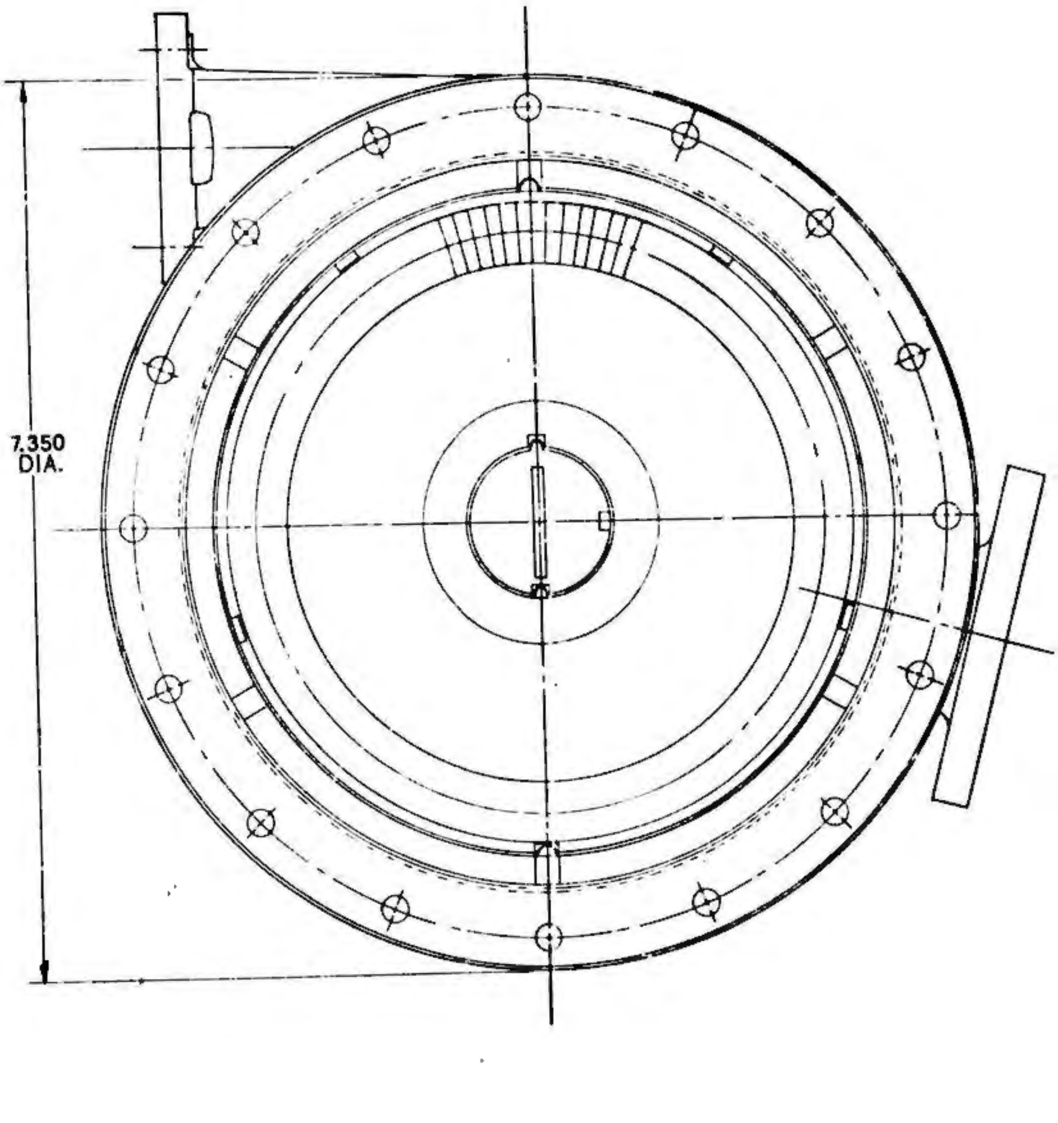

Figure 171. Main Fuel Turbopump (U)

(U) for a full 360 degrees. This relief was incorporated to pressure balance the volute side walls and, thus, relieve the tensile stress in the volute tongue area. Figure 172 shows the hydrodynamic layout of the volute passage. The impeller dynamic seal material final selection was not made. The relative size of this pump, in comparison with previous hydrogen pumps, may influence the selection of material. Materials including plastics and sintered materials would be considered for the impeller dynamic seal.

(U) Both first- and second-stage impellers for the main fuel pump would be machined from identical INCO 713C castings. The stress analysis was completed on the machined configuration of both impeller back plates. The first-stage impeller is pressure balanced to minimize the axial loading. The variable turbine axial thrust loading encountered during throttling is compensated for by the balance piston incorporated on the second-stage impeller.

(U) The crossover vanes for the main fuel pump direct the fluid from the first-stage diffuser vane discharge to the second-stage impeller inlet. This part would be cast from INCO 713C material. The first-stage diffuser vanes would be machined as an integral part of this casting. The second-stage diffuser vanes would be machined from an INCO 718 ring and held in place by a retention nut. The tips of both first- and second-stage diffuser vanes would be pressed against a soft material (Bearium B-10) with sufficient force to yield the material locally, and thus, restrain the vanes from vibration. Bearium B-10 was also selected as the sealing surface for the balance piston at the second-stage diffuser vane location. This soft material has been used in Rocketdyne's Mark-29 pump in similar applications. The hydrodynamic layout of the crossover is shown in Fig. 173 .

(U) Figures 174 and 175 show the main fuel pump predicted performance based on scaled empirical data from Rocketdyne's Mark-29 pump.

CONFIDENTIAL

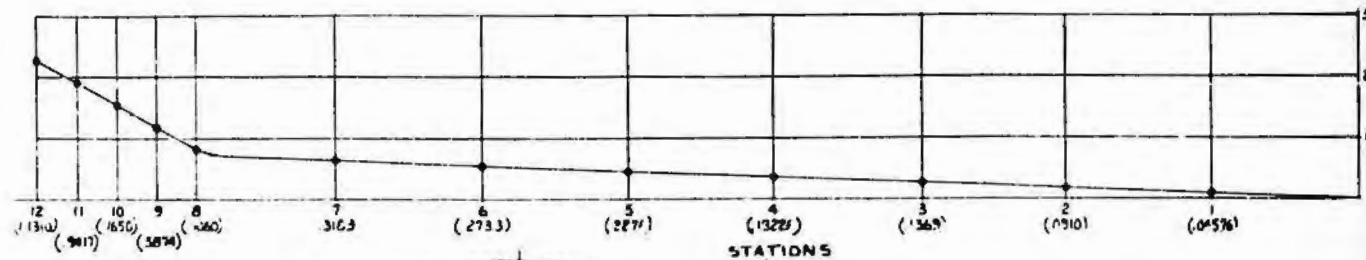

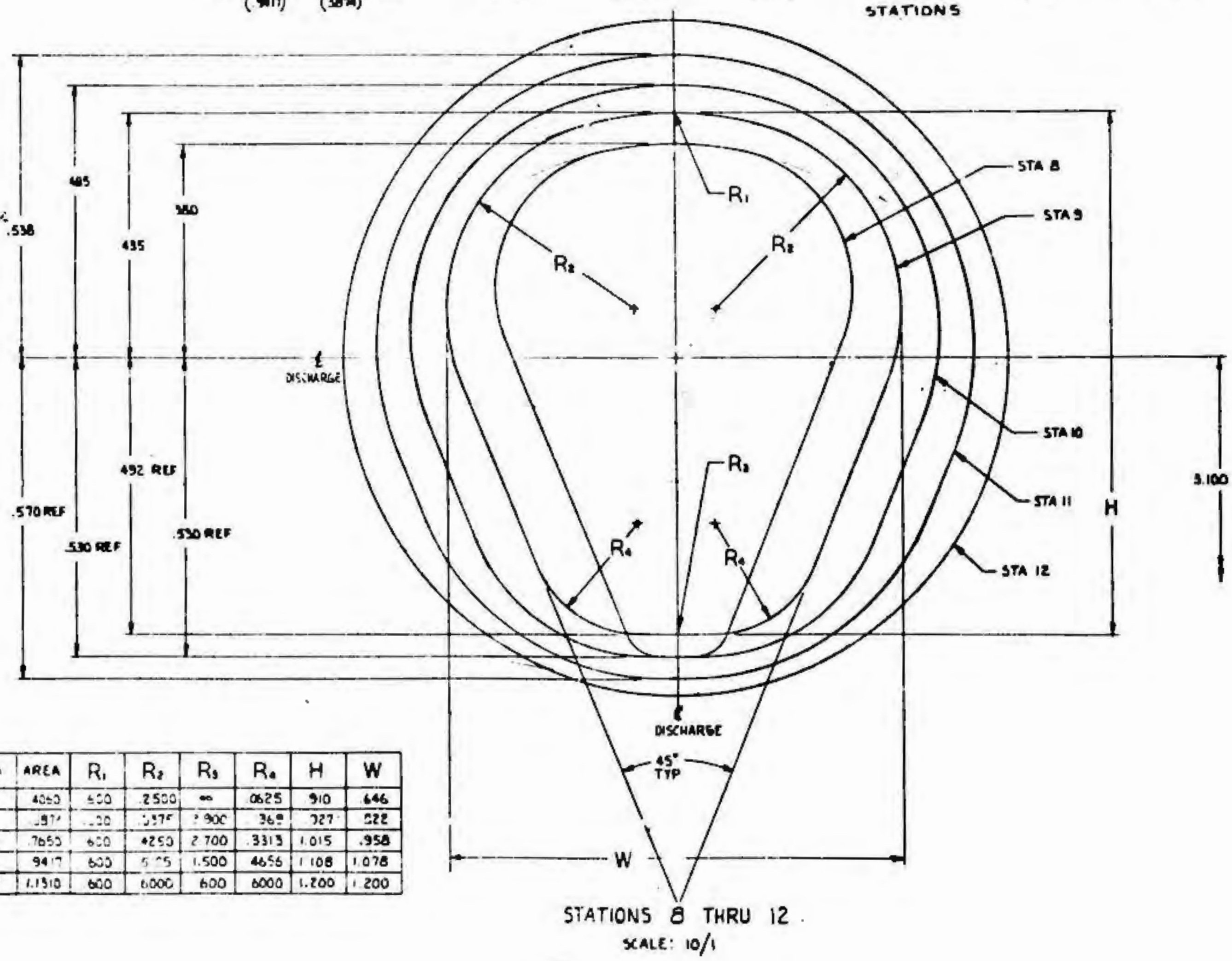

STA	AREA	R_1	R_2	R_3	R_4	H	W
8	4060	600	.2500	∞	.0625	910	.646
9	.587[illegible]	[illegible]	.537[illegible]	[illegible]900	369	927	922
10	.7650	600	4250	2.700	.3313	1.015	.958
11	9417	600	5[illegible]25	1.500	4656	1.108	1.078
12	1.1310	600	6000	600	6000	1.200	1.200

STATIONS 8 THRU 12

SCALE: 10/1

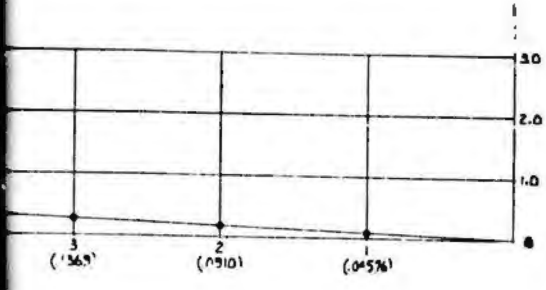

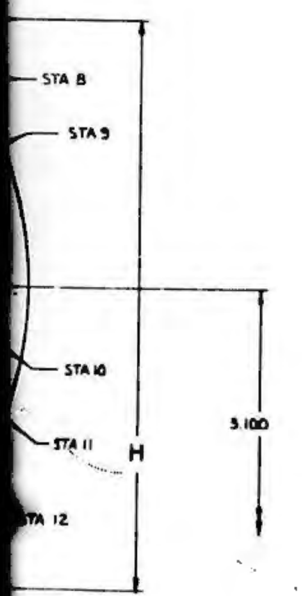

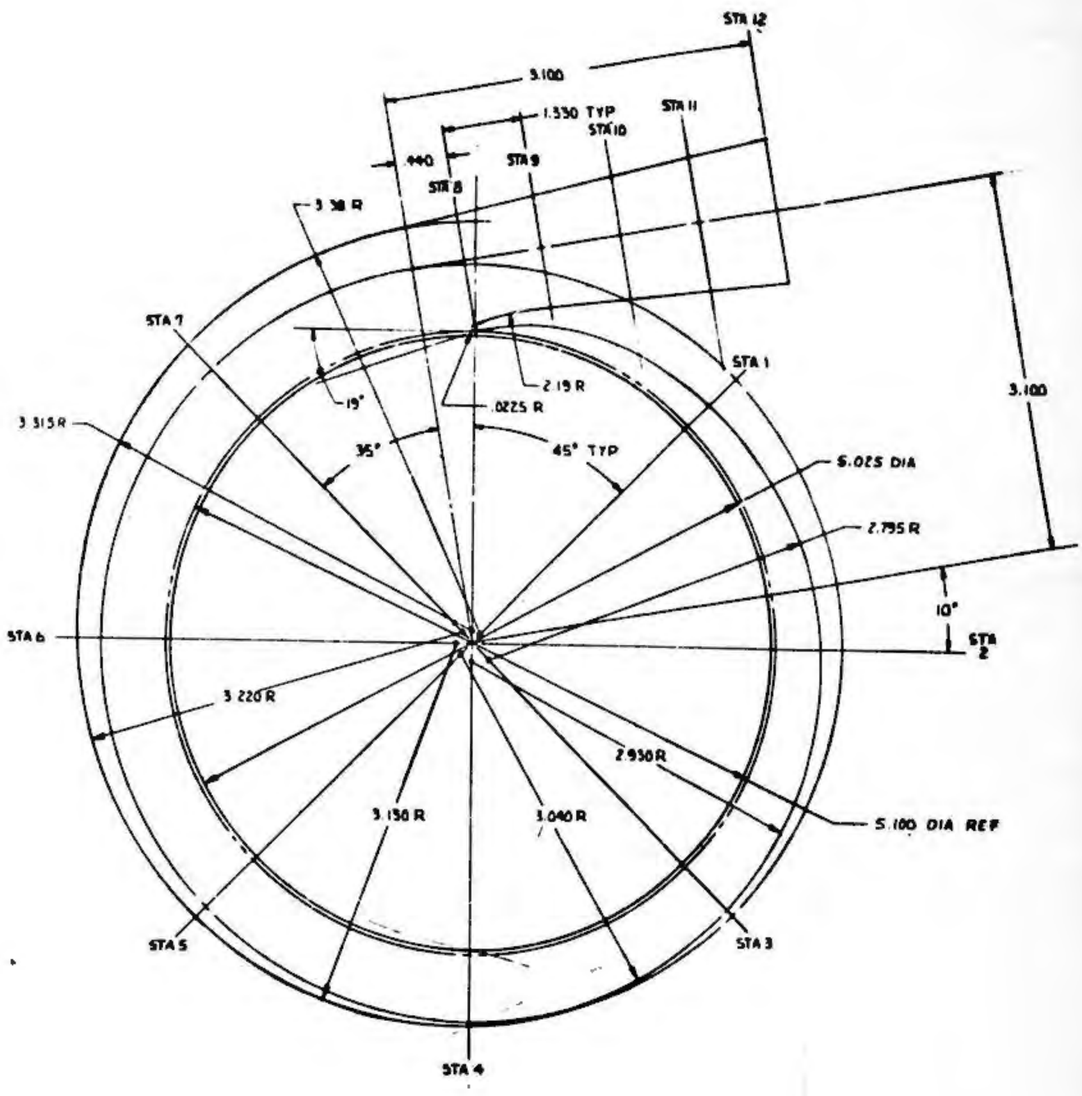

VOLUTE PROFILE
SCALE: 2/1

STA	AREA IN²
1	.04576
2	.0910
3	.1369
4	.18226
5	.2276
6	.2733
7	.3189
8 REF	.4560

2

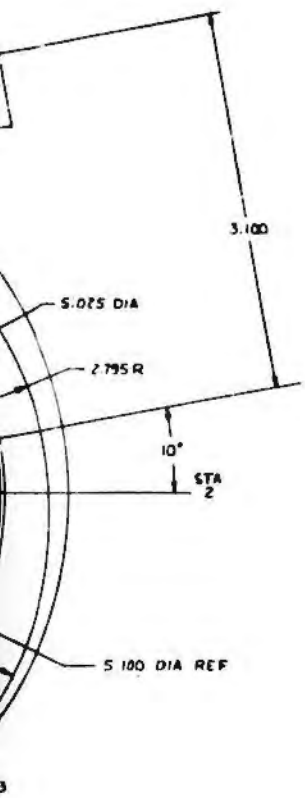

STA	AREA IN²	H	R_1	R_2
1	.04576	240	10.50	.0625
2	.0910	381	8.50	.0900
3	.1369	489	6.95	.1180
4	.18226	.582	5.50	.1425
5	.2276	.670	4.20	.1700
6	.2733	.752	2.90	.1925
7	.3189	.828	1.65	.2250
8 REF	.4[illegible]60	.910	.50	.2[illegible]00

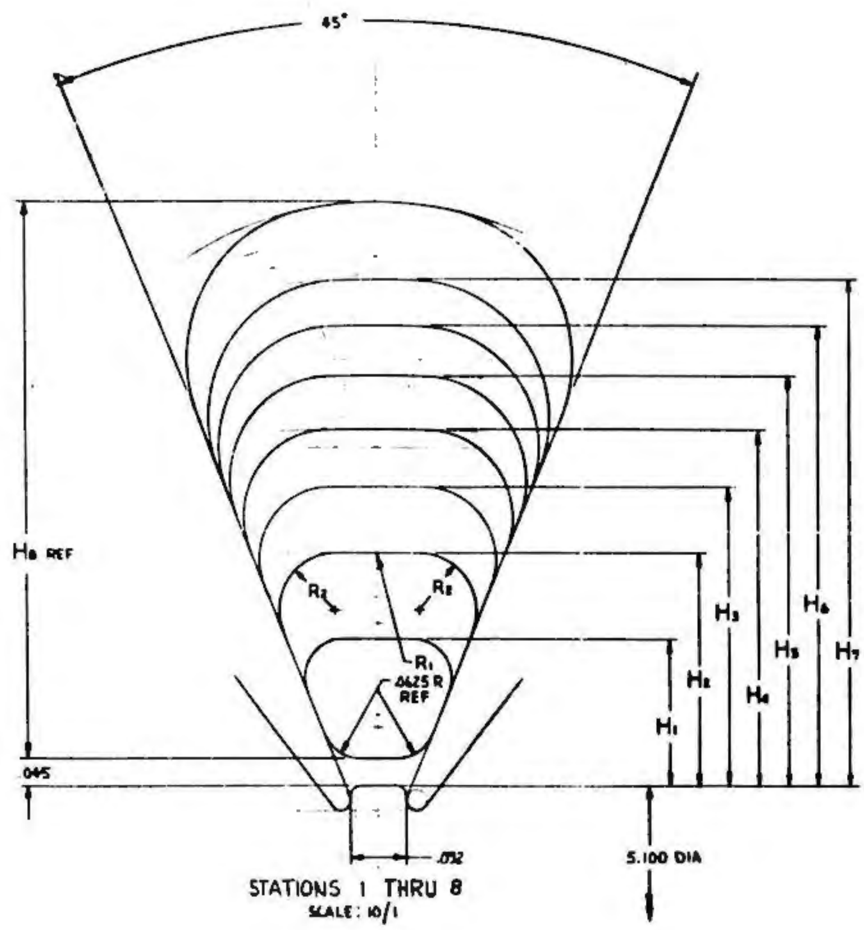

Figure 172. Main Fuel Turbopump Volute Passage Layout (U)

3

CONFIDENTIAL

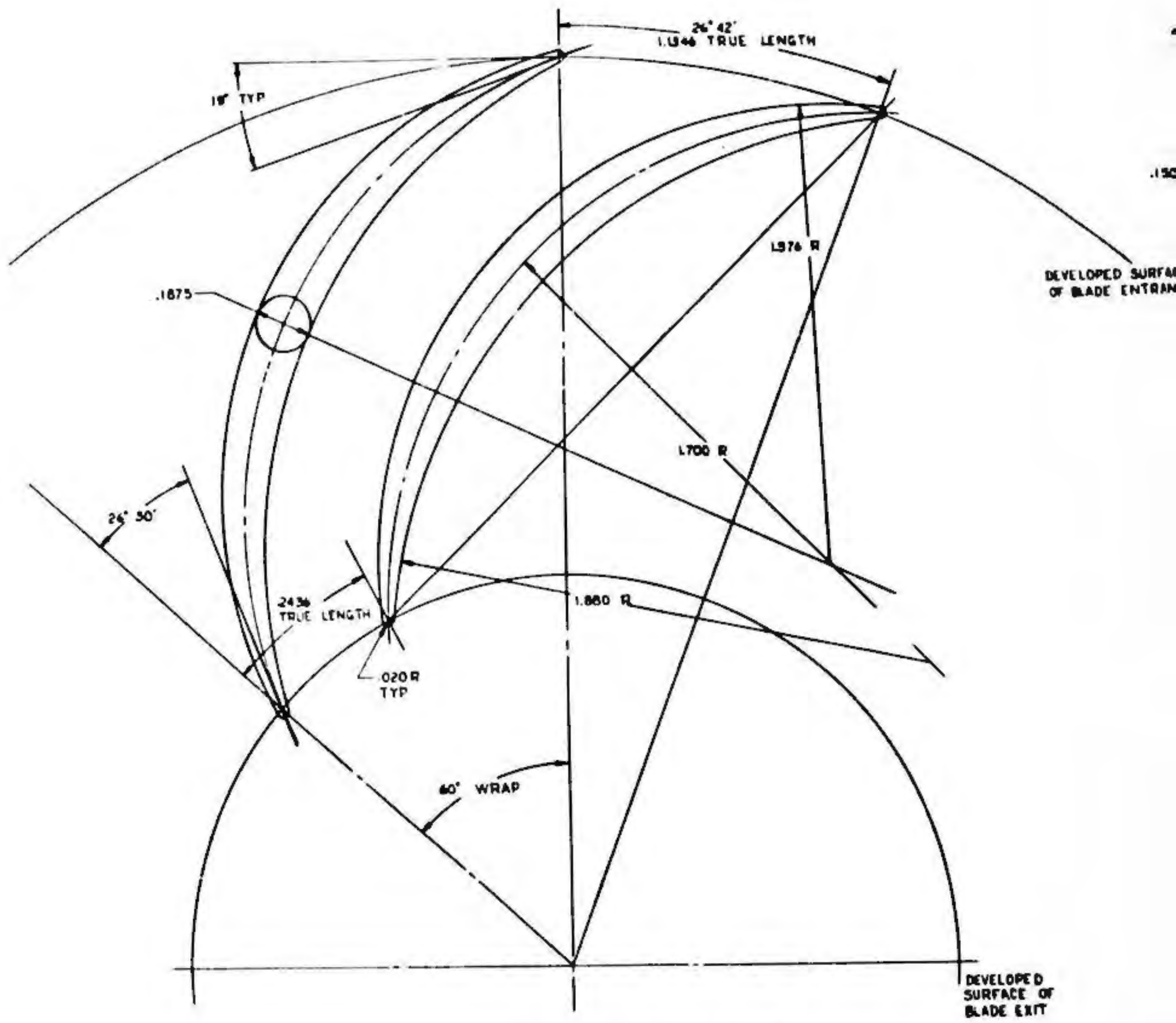

DEVELOPED VIEW OF SECTION **A-A**

14 BLADES

UP[illegible] SHROUD [illegible]NATES	
R_L	L
2.530	.440
2.500	.518
1.900	.914
1.590	1.170
1.500	1.246
1.400	1.336
1.300	1.430
1.250	1.490
1.200	1.554
1.160	1.630
1.110	1.810

LOWER SHROUD COORDINATES	
R_L	L
2.530	.320
2.500	.384
1.900	.714
1.590	.900
1.500	.980
1.400	1.056
1.300	1.116
1.250	1.148
1.200	1.181
1.160	1.216
1.110	1.260
1.000	1.356
.900	1.476
.850	1.554
.800	1.646
.766	1.810

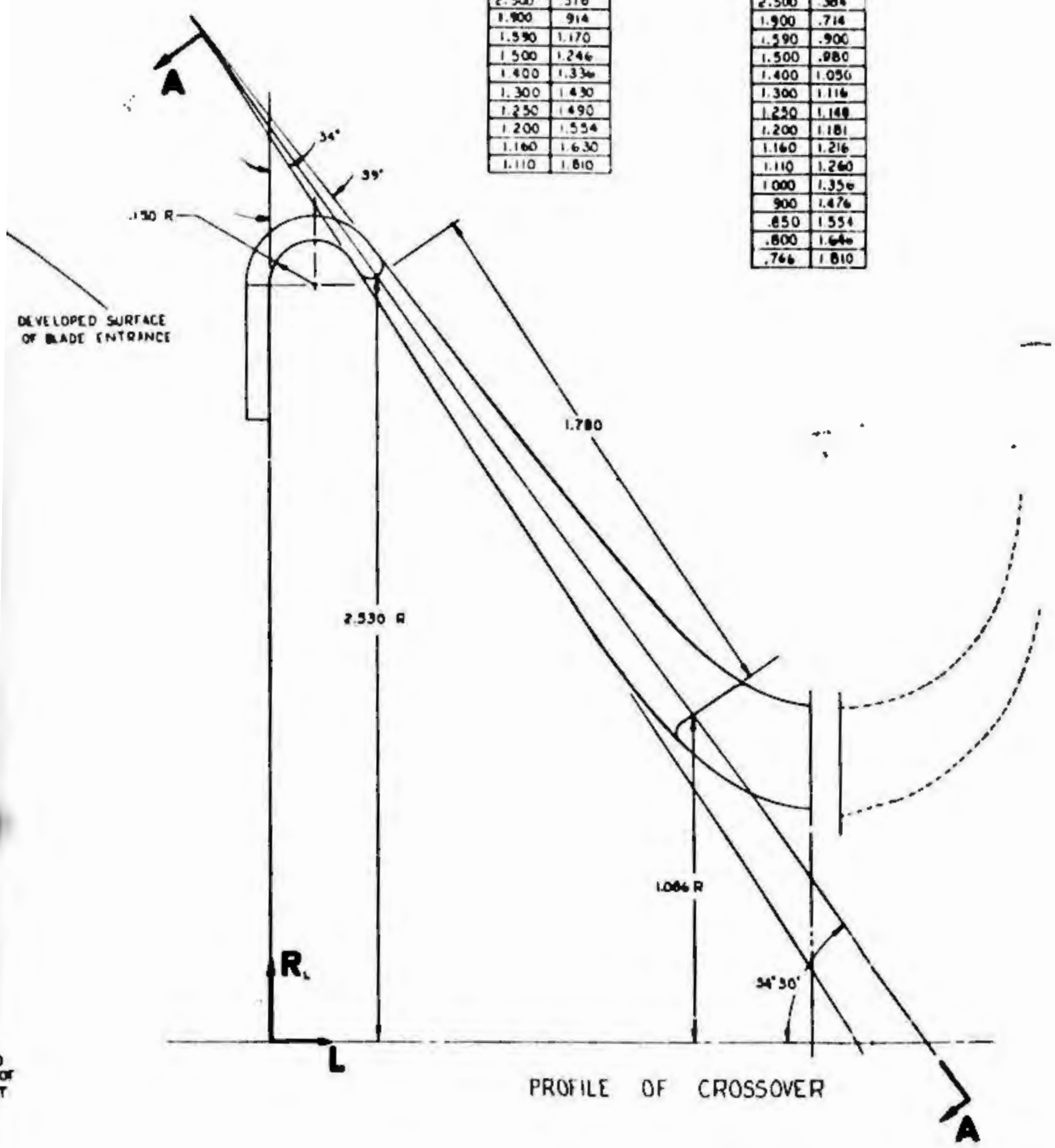

PROFILE OF CROSSOVER

Figure 173. Main Fuel Pump Crossover Layout (U)

2

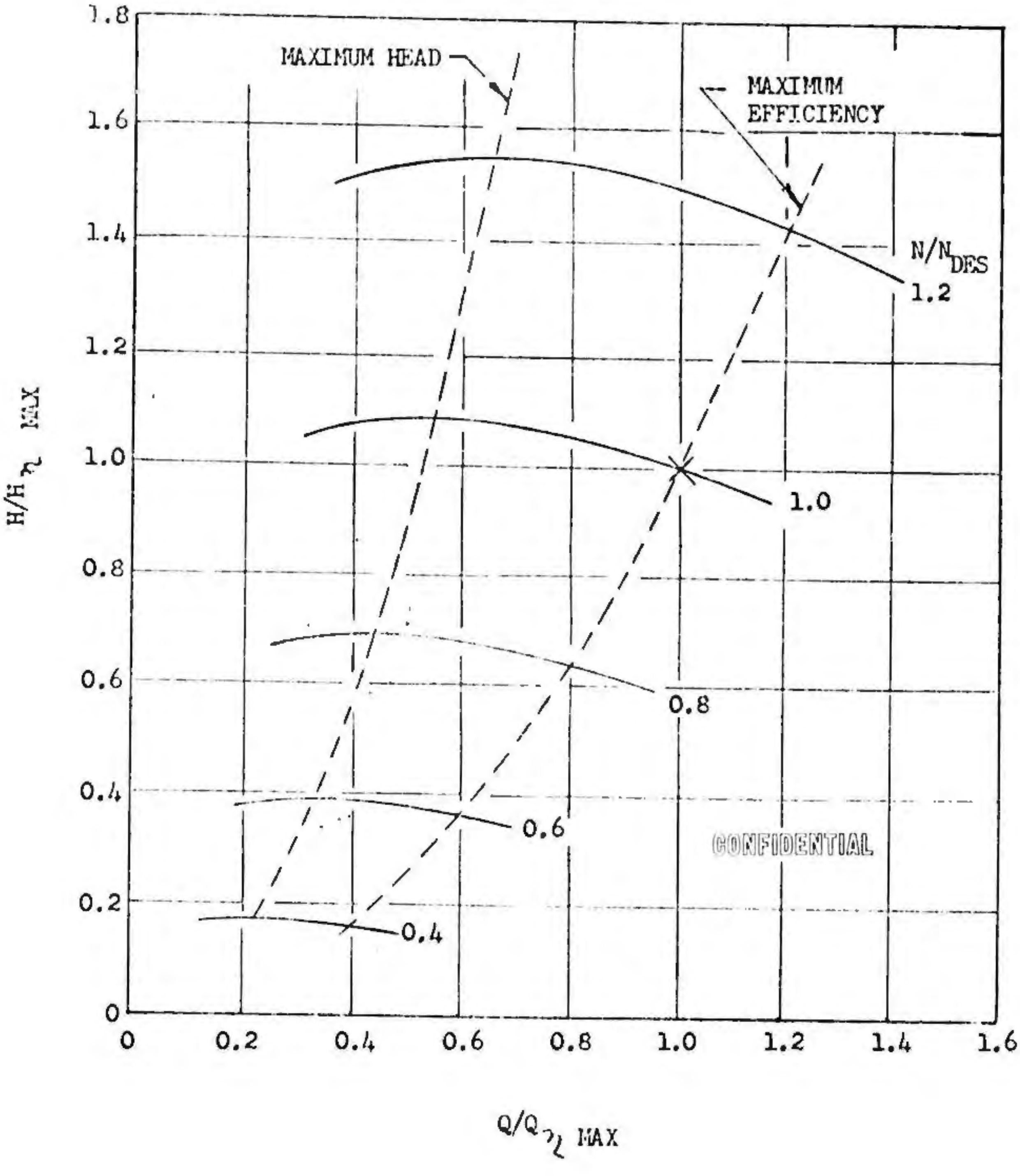

Figure 174. Predicted Main Fuel Pump Performance Based on Mark-29 Pump (U)

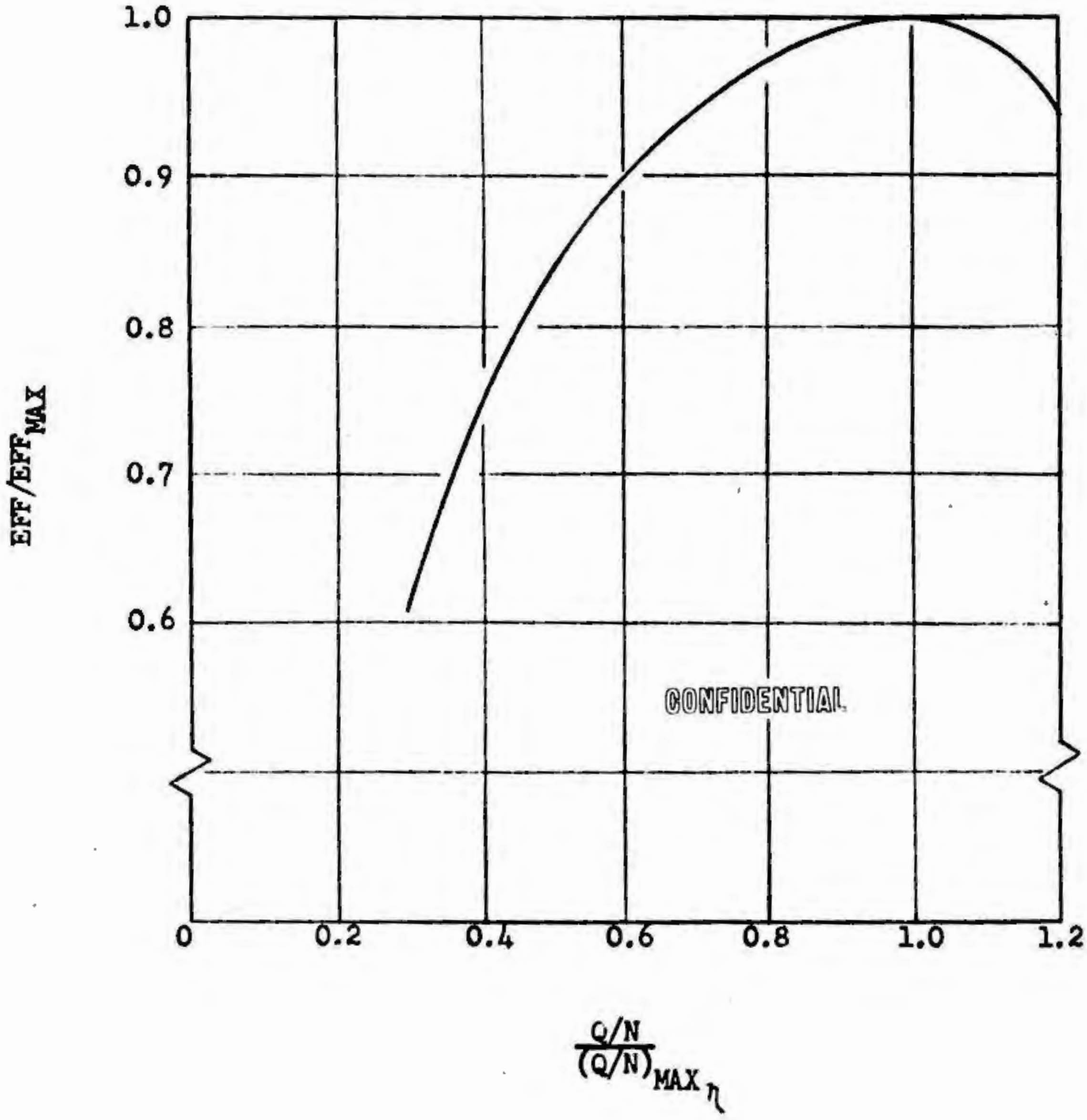

Figure 175. Predicted Main Fuel Pump Efficiency Based on Mark-29 Pump Efficiency (U)

3. SECONDARY FUEL TURBOPUMP

(U) The general design layout for the secondary fuel turbopump is presented in Fig. 176. The general arrangement is similar to the main fuel turbopump except for the impeller and shaft seals which are different in mounting or design as indicated by the small size. The volute and crossover hydrodynamic layouts are shown in Fig.177 and 178.

4. MAIN OXIDIZER TURBOPUMP

(U) The general design layout for the main oxidizer turbopump is presented in Fig. 179. The design is that of a conventional centrifugal turbopump and incorporates a single shaft mounted on two hall bearings. The pump inducer and impeller are overhung on one end of the shaft outboard of the pump bearing. The turbine disks are overhung on the other end of the shaft with the dynamic seals, outboard of the turbine bearing. The pump portion consists of an inducer, impeller, volute or scroll, and a discharge diffuser cone. The seal package is of the conventional design and incorporates a primary face-riding turbine seal. The pump is small in size, requiring closer tolerances than in previous turbopump designs. Similar materials will be used in the major components and where cose tolerances are required so that the differential contraction and/or expansion of the two components will not affect the design clearances.

(U) INCO 718 material and variations of this material would be used as the basic material for the main oxidizer turbopump. This material was used for a liquid fluorine pump which was built for a NASA-sponsored experimental program (Ref. 9).

(U) The impeller would be machined from a lost wax investment casting of INCO 713C material. Dynamic seals are incorporated on the front and rear side of the impeller to reduce recirculation; the diameter of the rear impeller seal is selected to compensate for the axial load of the turbine.

CONFIDENTIAL

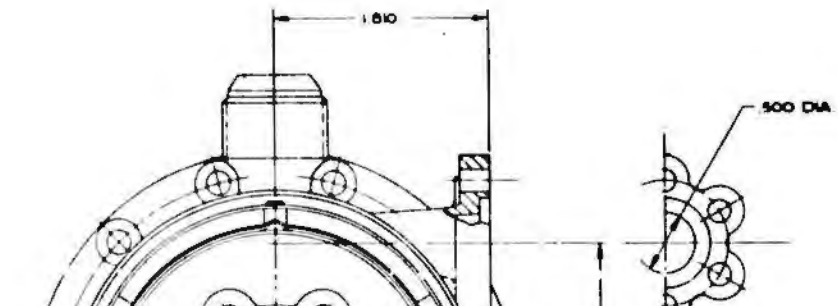

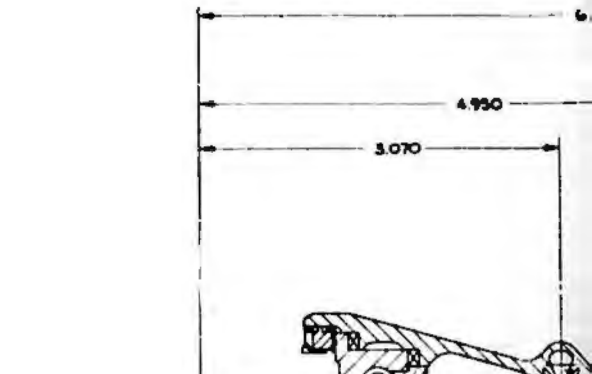

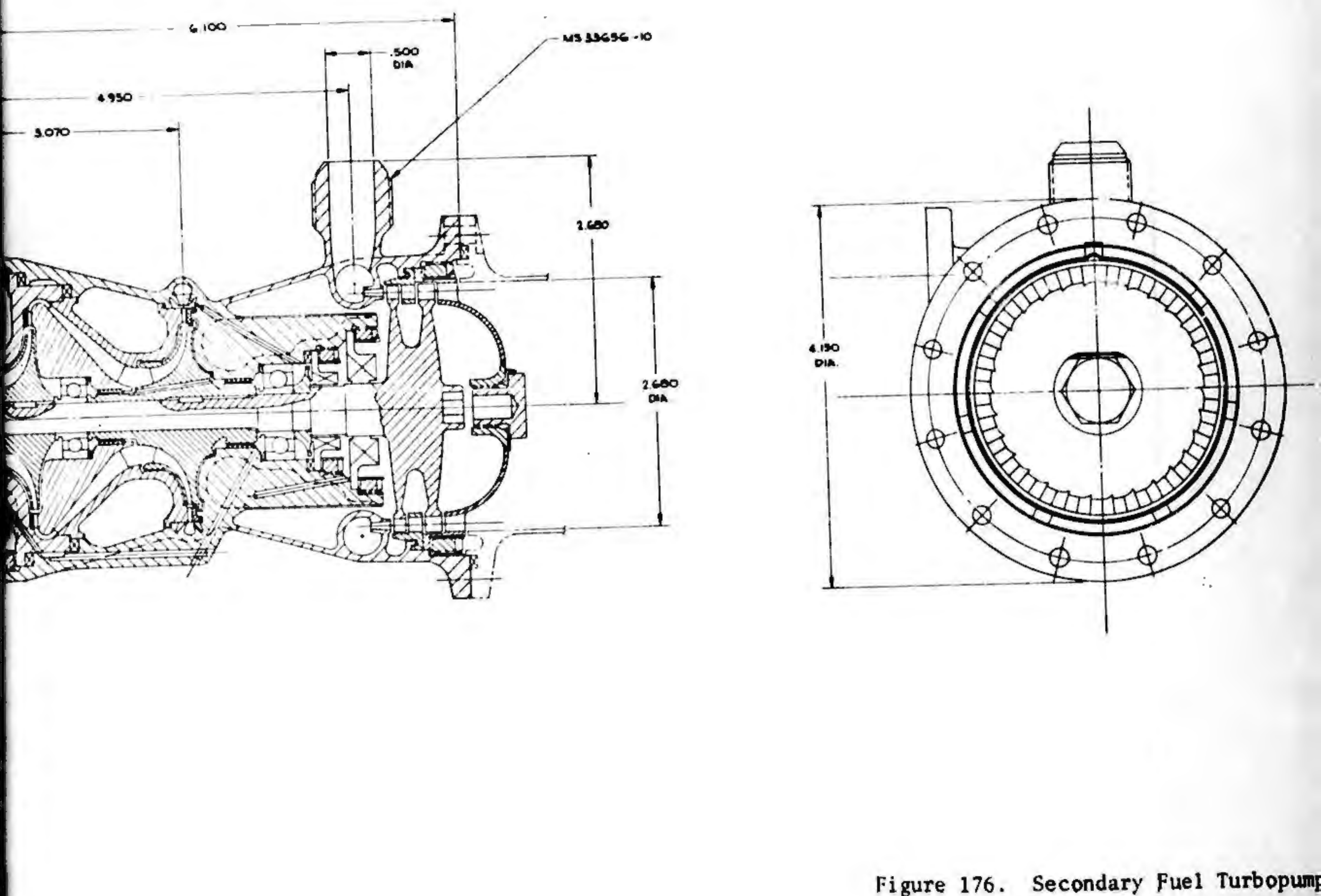

Figure 176. Secondary Fuel Turbopump

CONFIDENTI

2

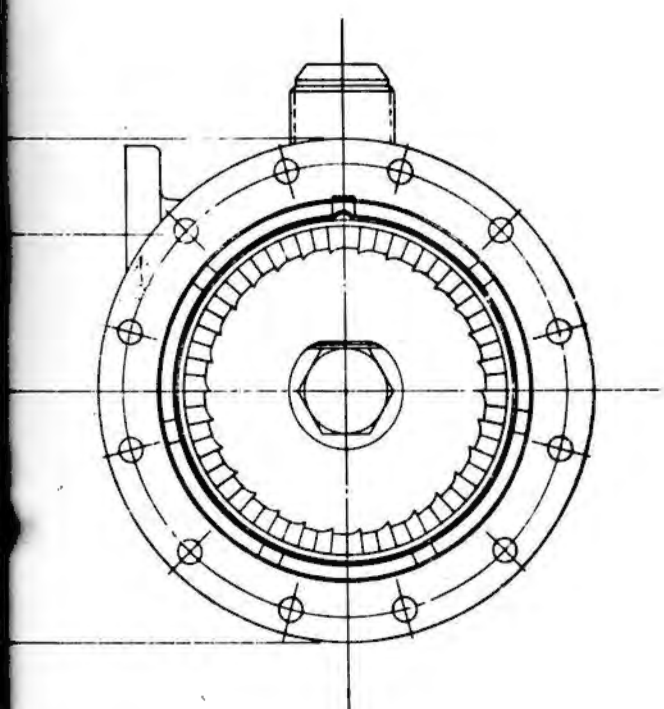

Figure 176. Secondary Fuel Turbopump (U)

3

CONFIDENTIAL

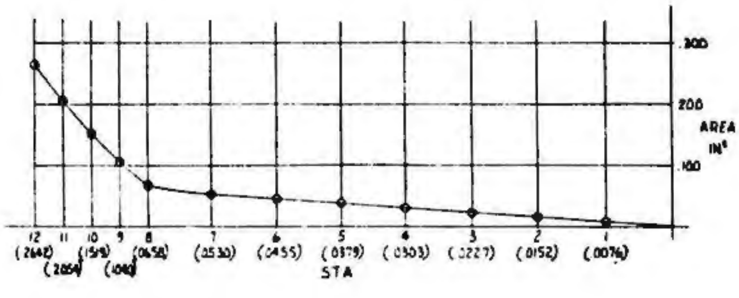

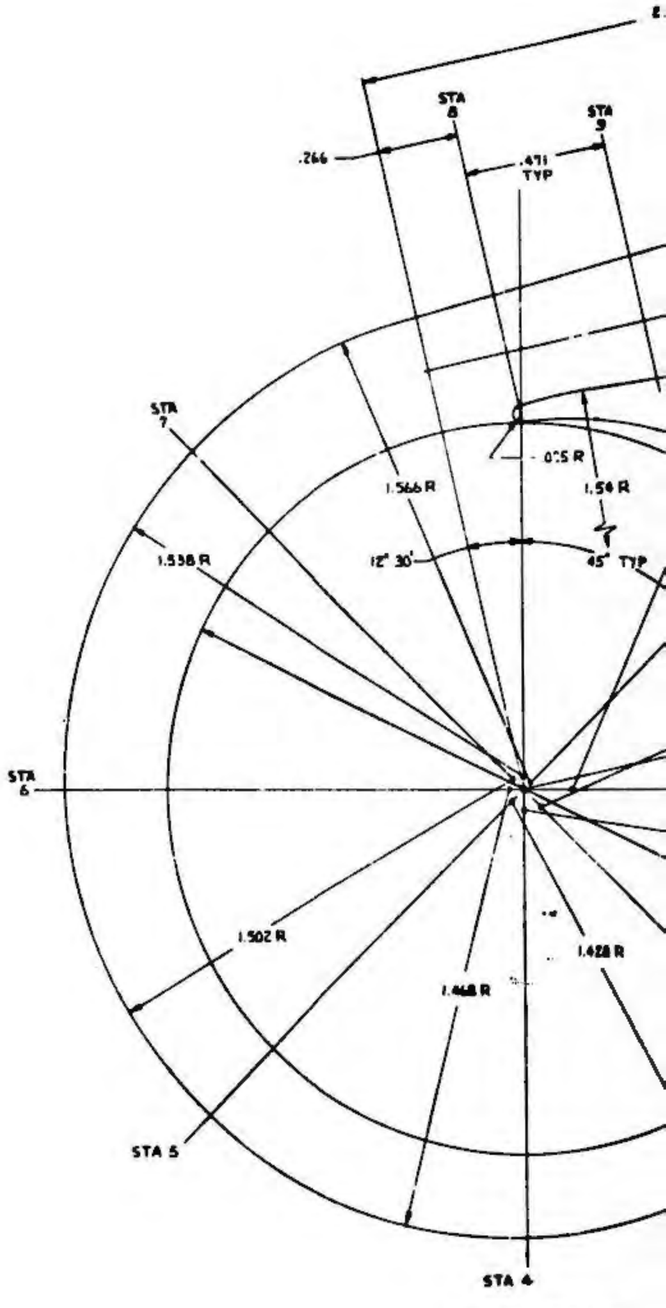

VOLUTE PROFILE
SCALE: 5/1

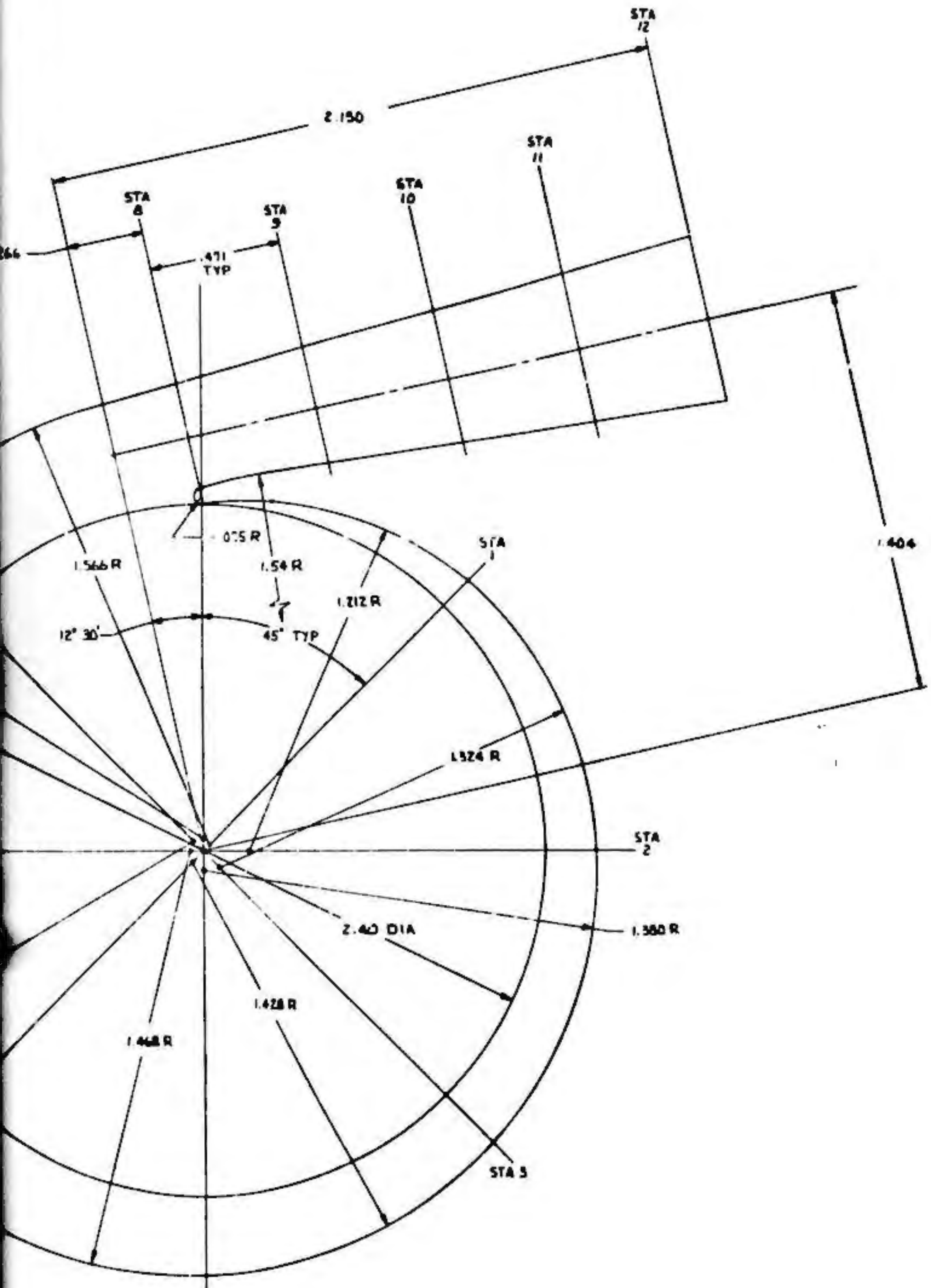

VOLUTE PROFILE
SCALE: 5/1

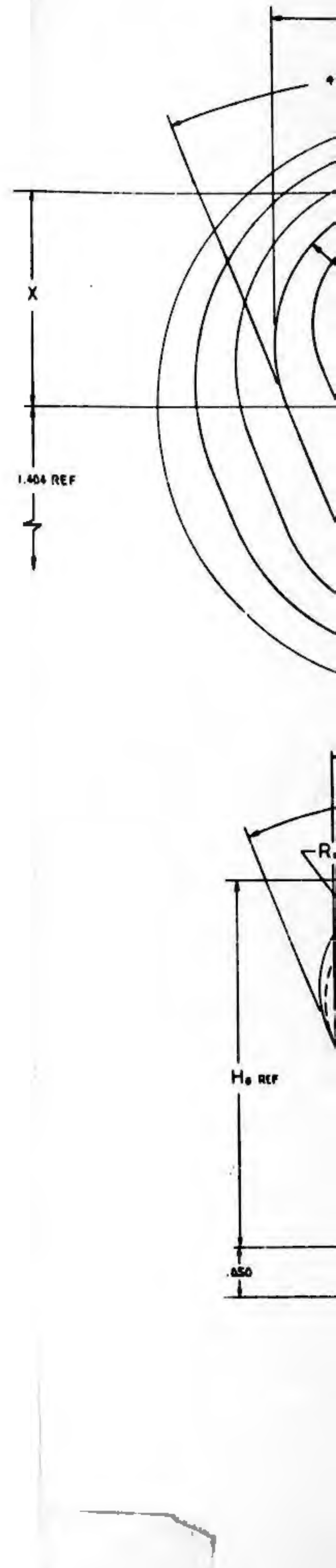

2

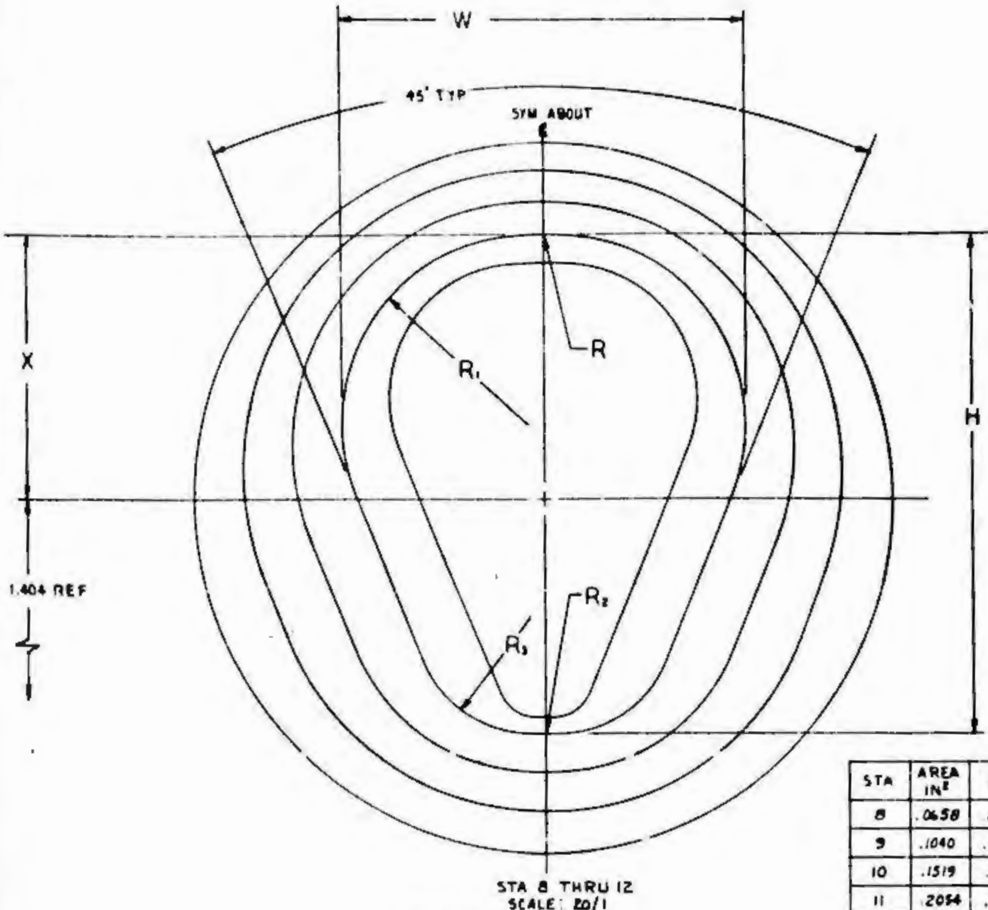

STA	AREA IN^2	R	R_1	R_2	R_3	H	X	W
8	.0658	290	109	—	.030	.370	.192	.255
9	.1040	.290	.154	475	.095	.408	.215	.335
10	.1519	.290	199	.385	.160	.466	.242	.418
11	.2054	.290	.244	330	.225	.524	.267	.499
12	.2642	.290	290	.290	.290	.580	.290	.290

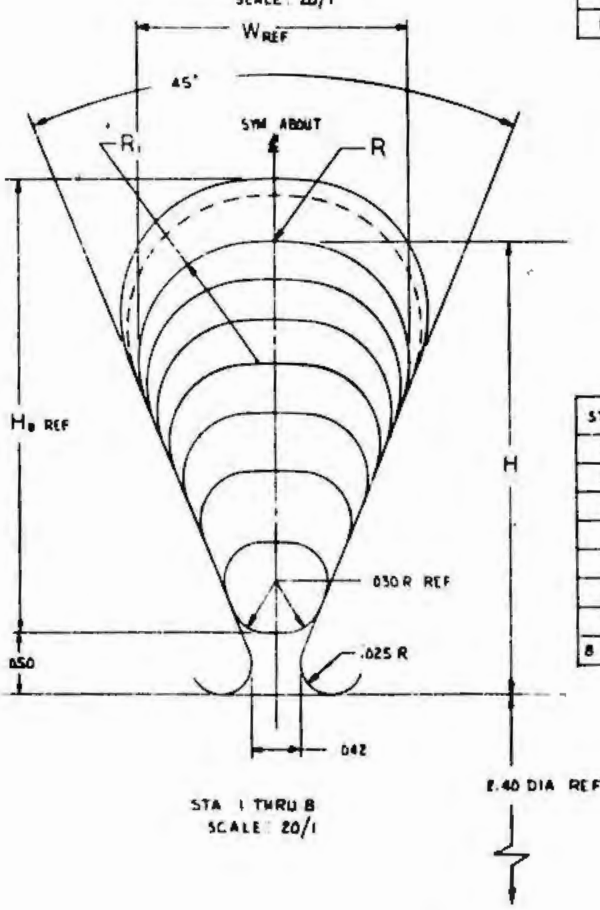

STA	AREA IN^2	R	R_1	H	W_{REF}
1	.0076	.523	.031	.125	.087
2	.0152	.461	042	181	.125
3	0227	.418	.053	.229	.153
4	.0303	.385	.064	.269	.175
5	.0379	.356	.075	.305	.194
6	.0455	331	.086	.338	.210
7	.0530	.310	.098	.349	.224
8 REF	.0658	.290	.109	.370	.255

Figure 177. Secondary Fuel Turbopump Volute Layout (U)

CONFIDENTIAL

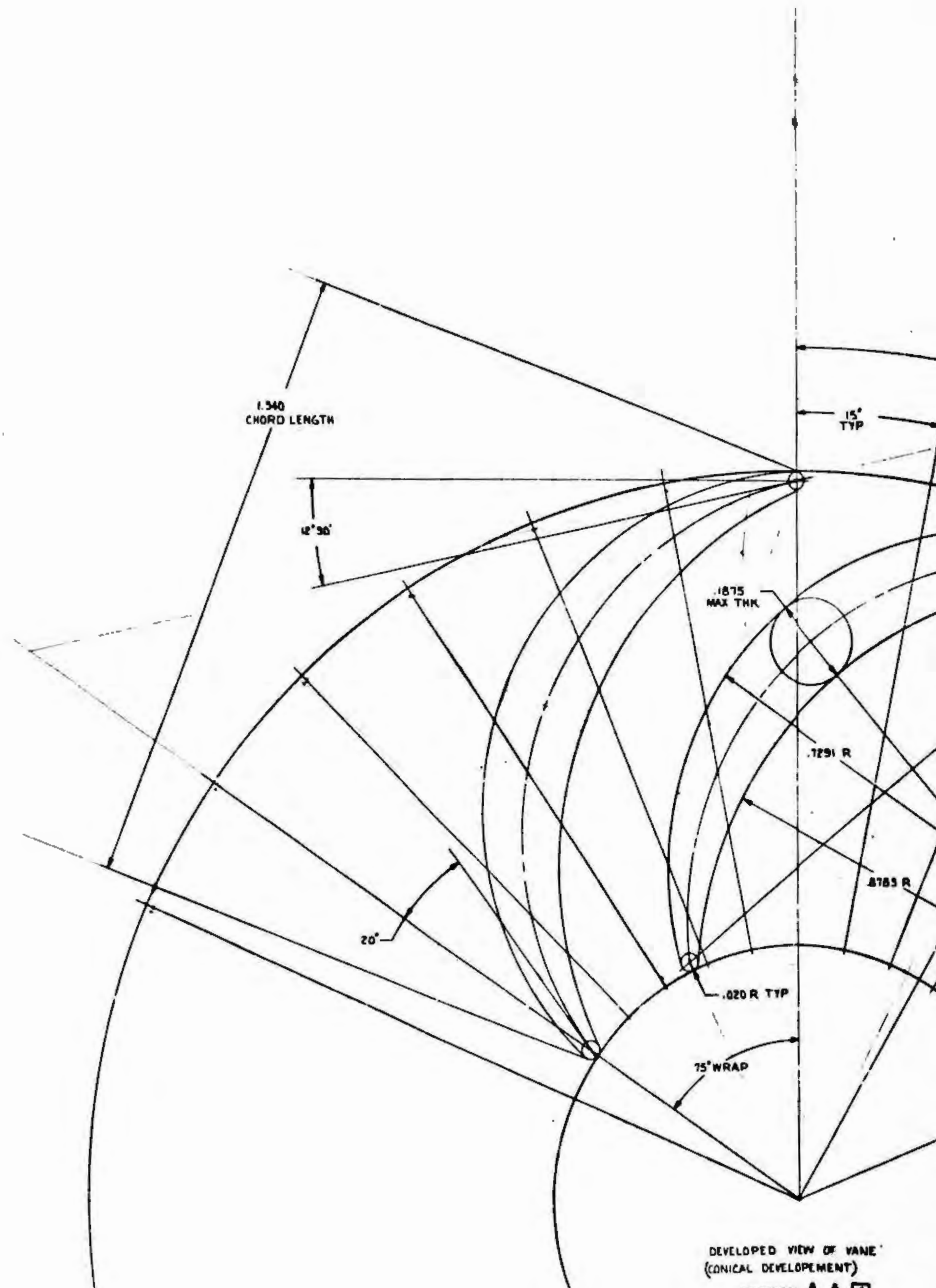

DEVELOPED VIEW OF VANE
(CONICAL DEVELOPEMENT)

SECTION A-A 4

5 VANES EQUALLY SPACED

13 12 11 10 9 8

MICROFILM OVERLAP AREA

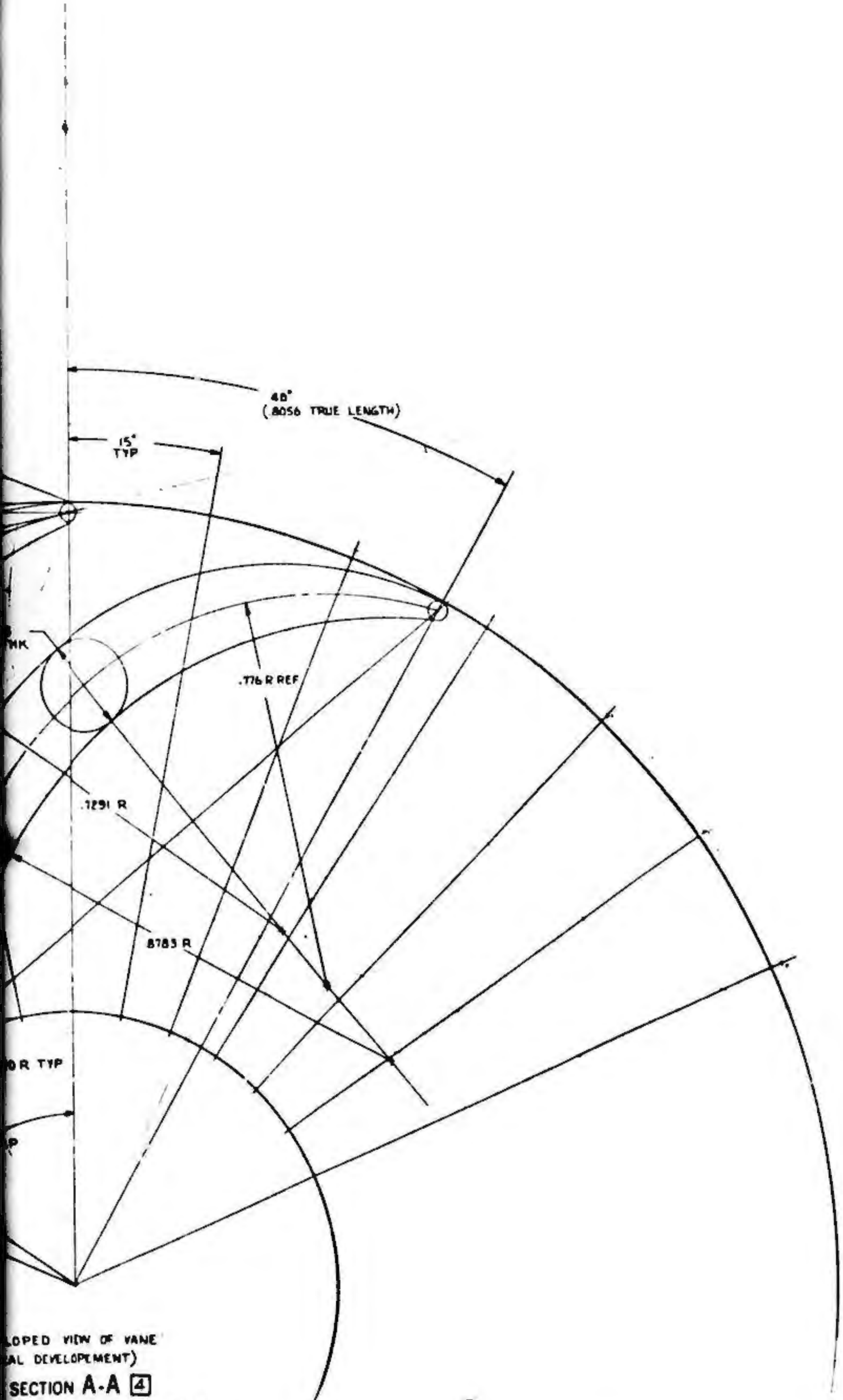

LOPED VIEW OF VANE
AL DEVELOPEMENT)

SECTION A-A 4

9 VANES EQUALLY SPACED

2

367/368

CODE IDENT 03507

FRAME 1

13 12 11 10 9 8

MICROFILM OVERLAP AREA

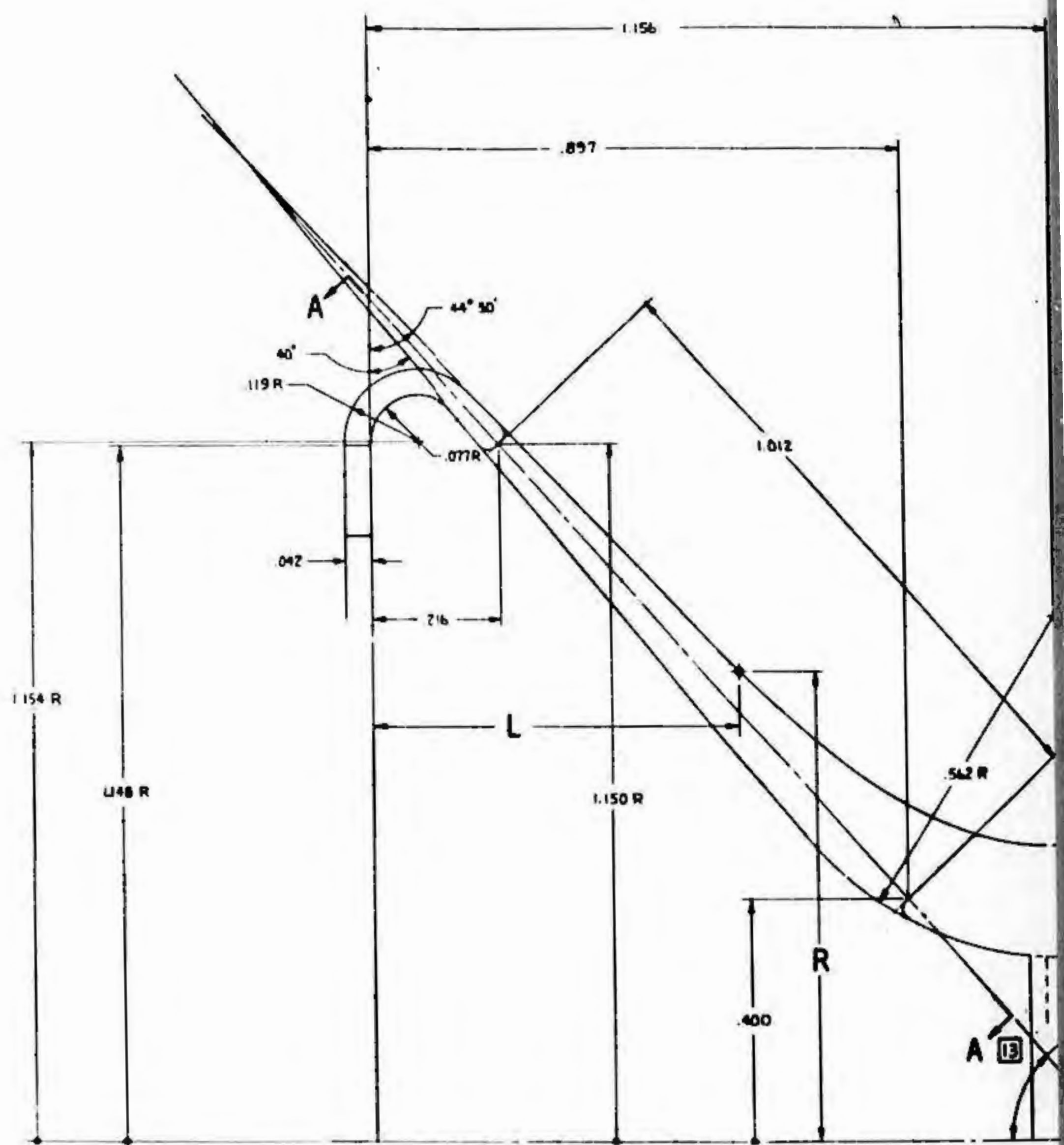

UPPER SHROUD COORDINATES

L	R
.300	1.098
.400	.996
.500	.894
.600	.792
.700	.695
.800	.615
.900	.552
1.000	.509
1.100	.487

PROFILE OF CROSSOVER

1368

3

1. ALL DIMS. SHOWN ARE BASIC

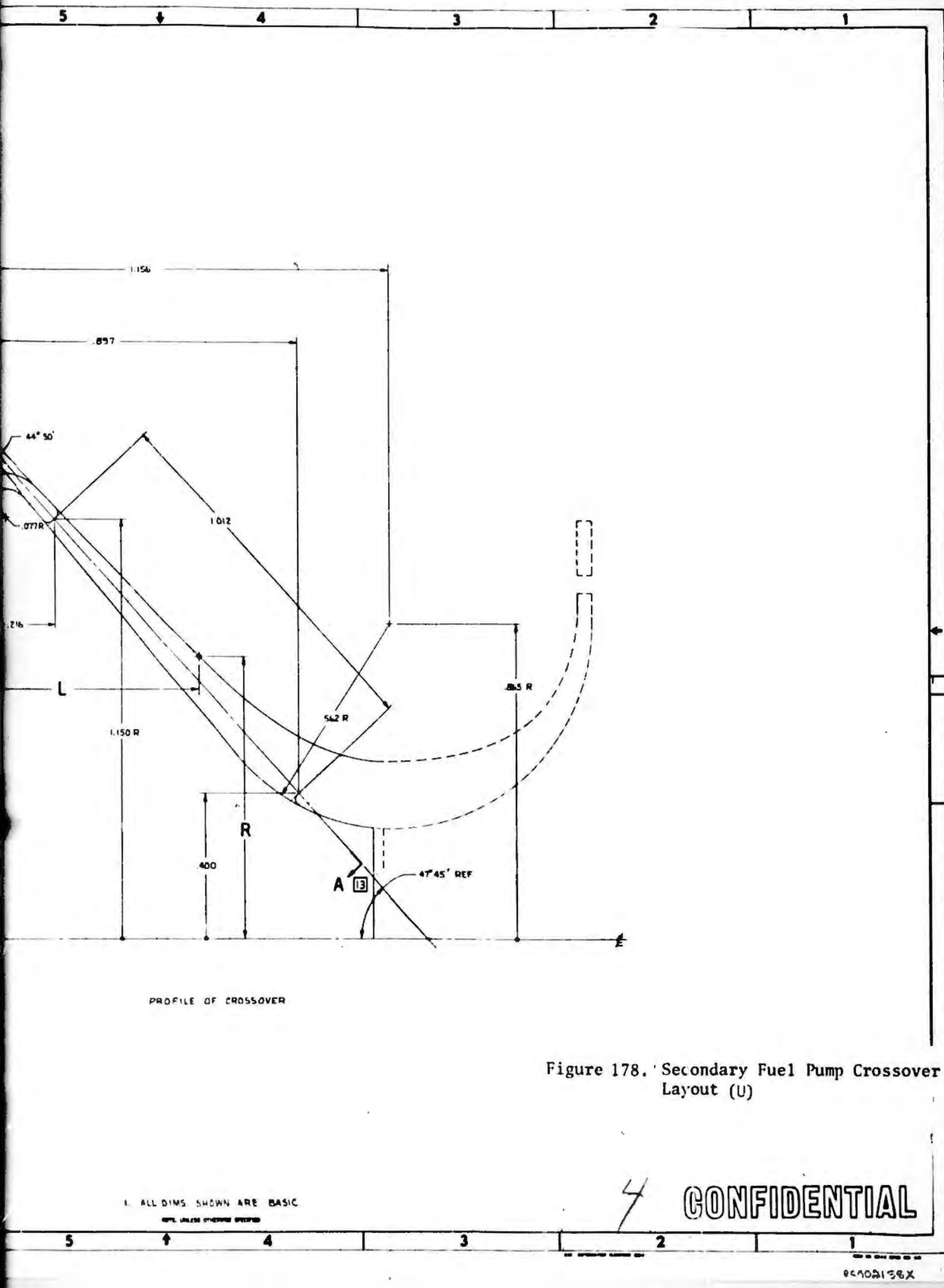

Figure 178. Secondary Fuel Pump Crossover Layout (U)

4

CONFIDENTIAL

CONFIDENTIAL

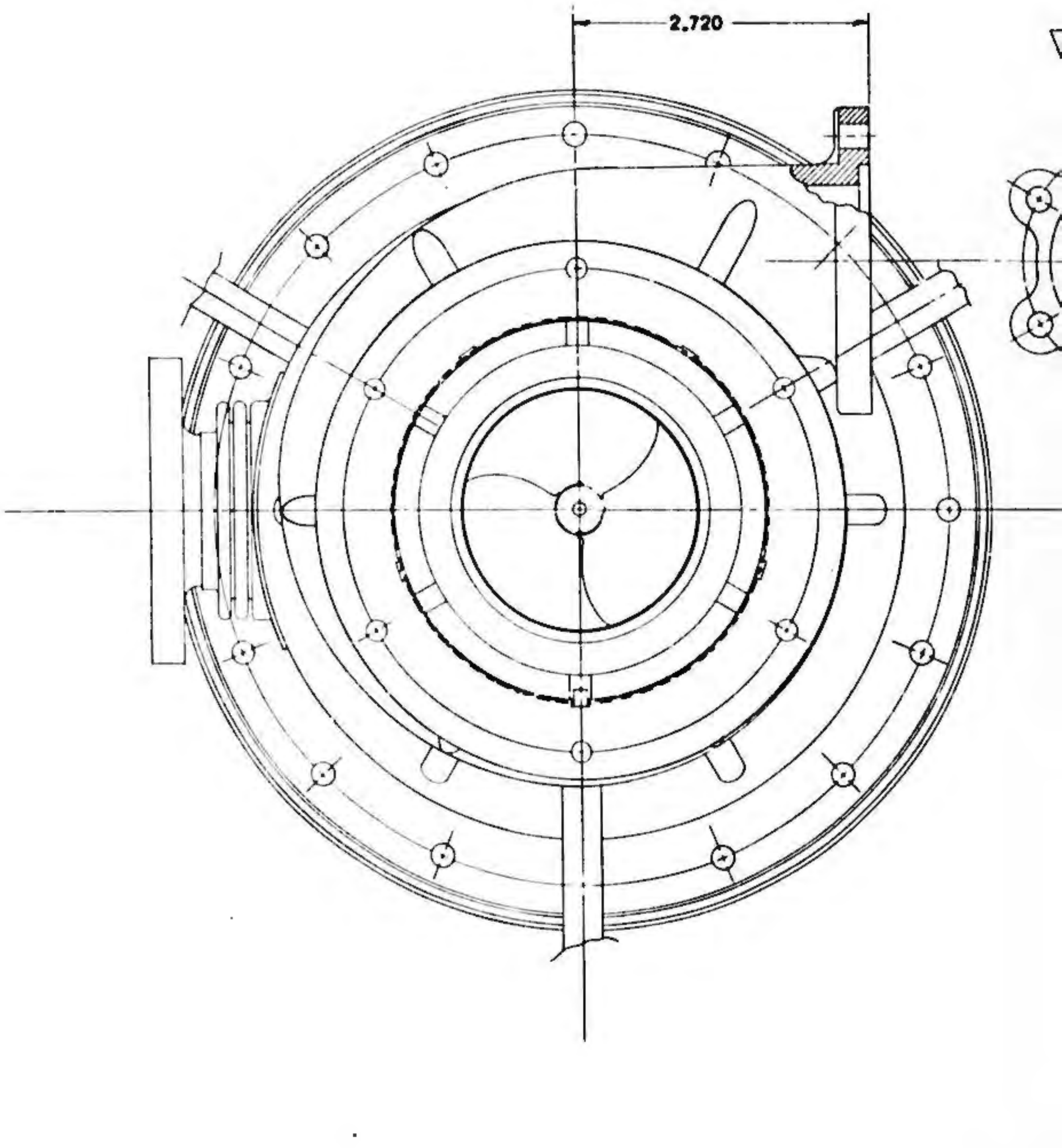

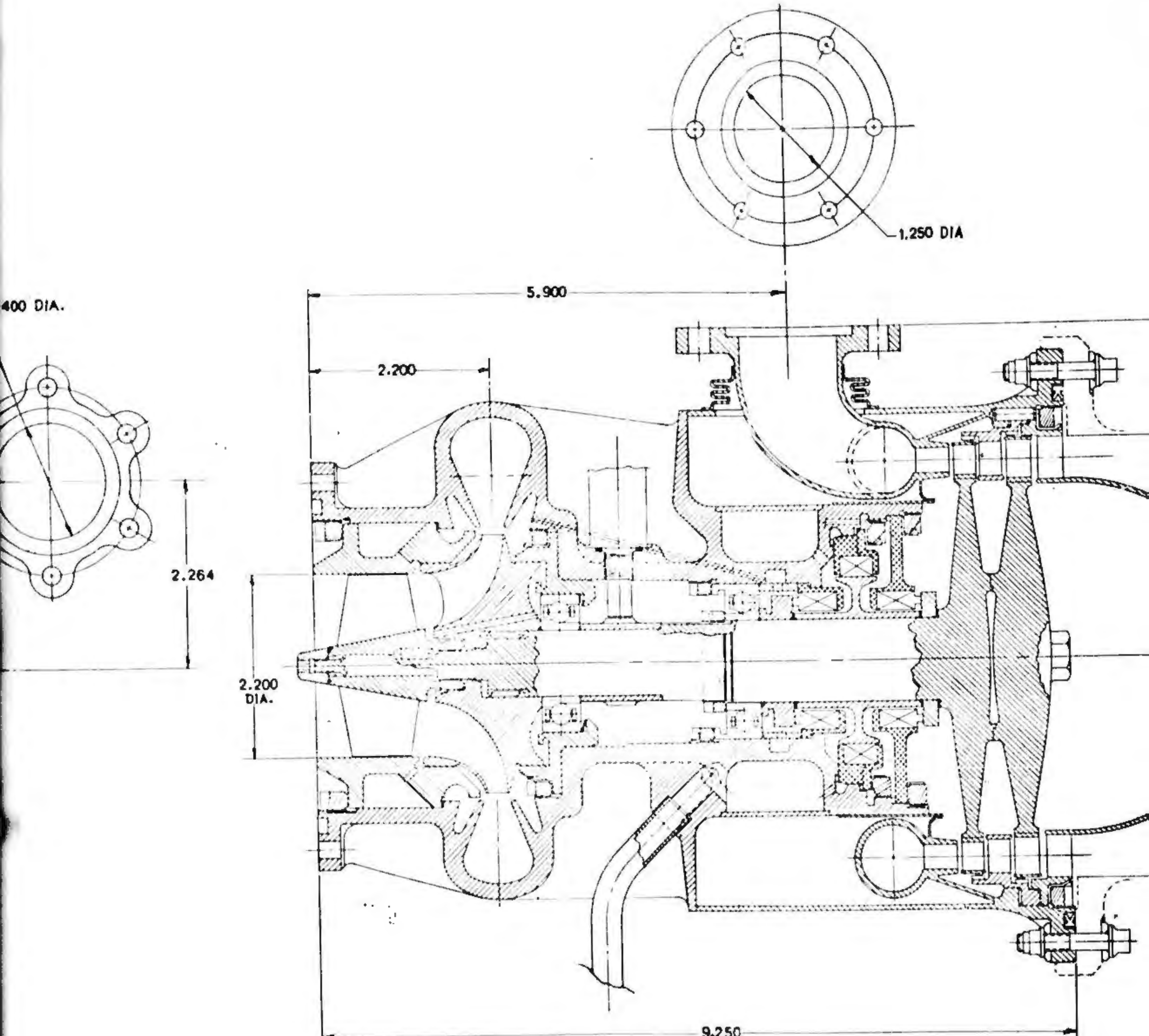

2

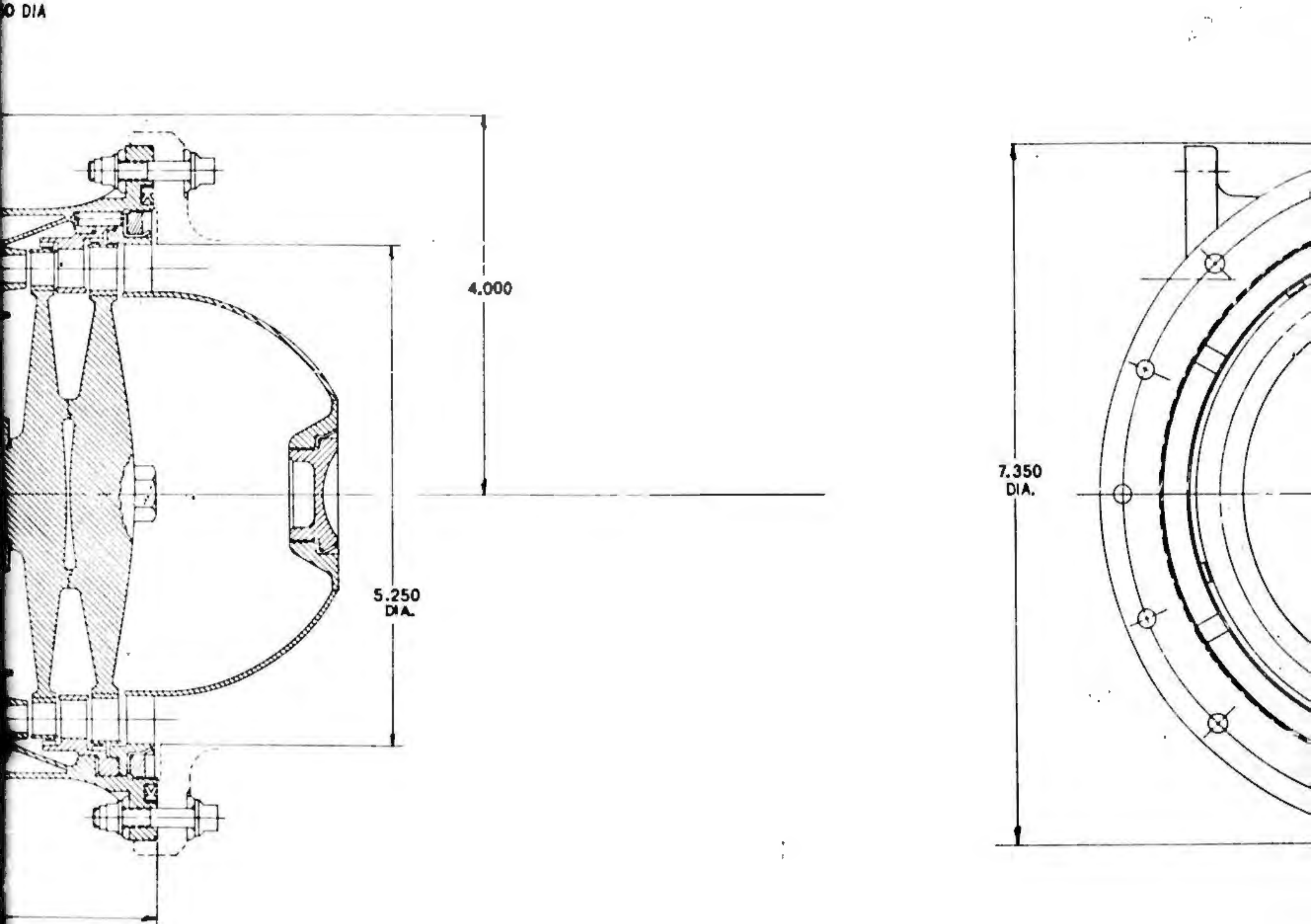

3

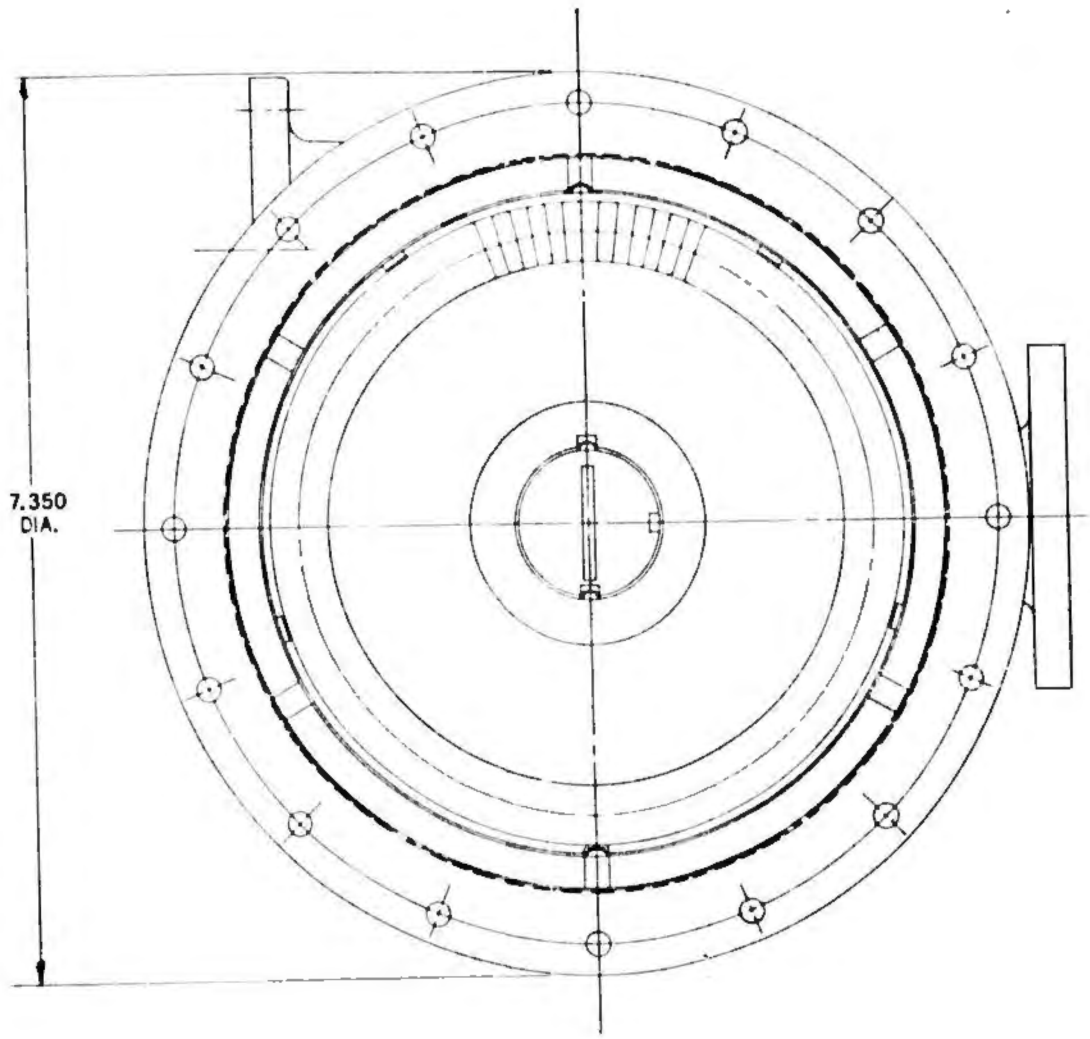

Figure 179. Main Oxidizer Turbopump (U)

4

(U) The volute would be an investment casting and, as in the case of the fuel pump, the volute has a relief 360 degrees around each side wall to balance the pressure and, thus, reduce the volute tongue loads.

(U) Figures 180 and 181 show the main oxidizer pump predicted performance based on scaling empirical data from the Rocketdyne Mark-15 LO_2 pump.

(U) The hydrodynamic layout drawing of the volute passage is shown in Fig. 182.

5. SECONDARY OXIDIZER PUMP

(U) The design layout drawing for the secondary oxidizer pump is shown in Fig. 183. The general arrangement is similar to this main oxidizer pump except for the dynamic seal package which, due to its small size, has a modified design. This design is similar to a LF_2 pump design which is in the feasibility testing phase under a NASA contract with Rocketdyne (Ref. 10).

(U) The volute hydrodynamic layout drawing is shown in Fig. 184.

6. TURBINE DESIGN

(U) The turbine operating parameters are shown in Table 40 . As stated previously, identical turbines are used on the main fuel and oxidizer turbopumps, and identical turbines are used on the secondary fuel and oxidizer turbopumps.

(U) The main turbopump manifold assemblies would be fabricated using lightweight sheet metal construction with a machined nozzle. A sheet metal construction appears to be feasible for this size manifold. The manifold for the secondary turbines would be machined from a forging or made from an investment casting; in either case, the nozzles would be welded into place.

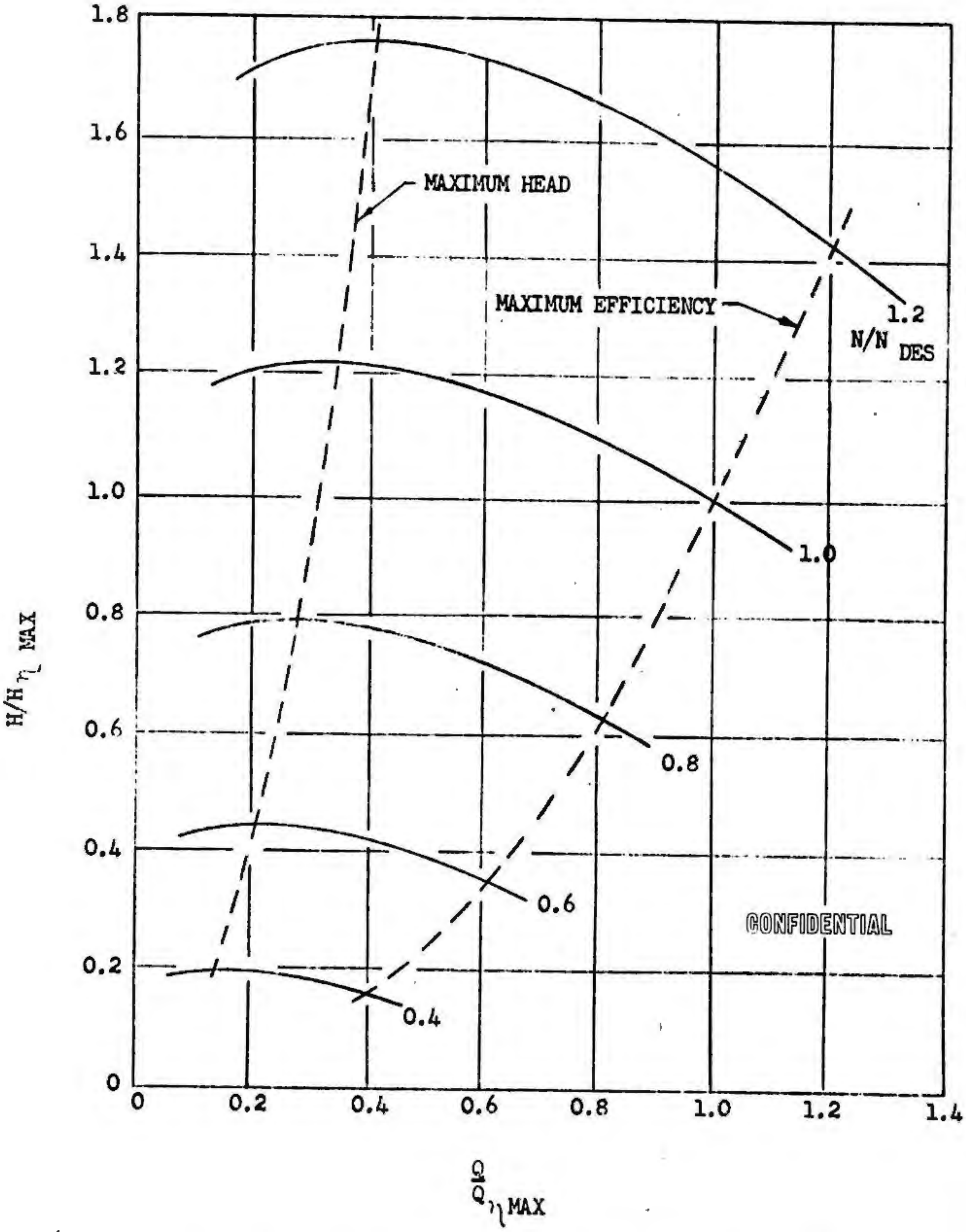

Figure 180. Predicted Main Oxidizer Pump Performance (U)

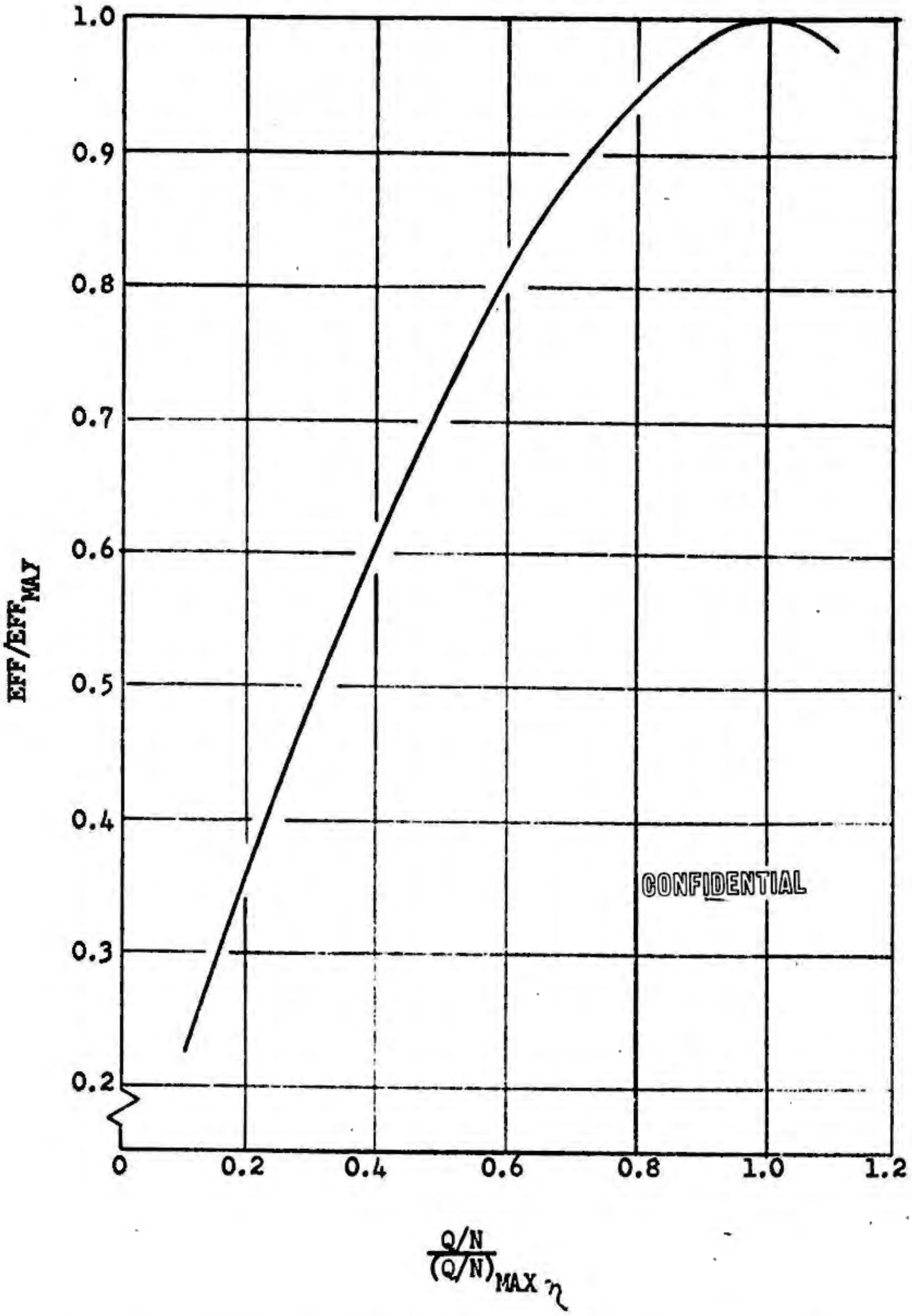

Figure 181. Predicted Main Oxidizer Pump Efficiency Based on Mark-15 LO_2 Pump Efficiency (U)

CONFIDENTIAL

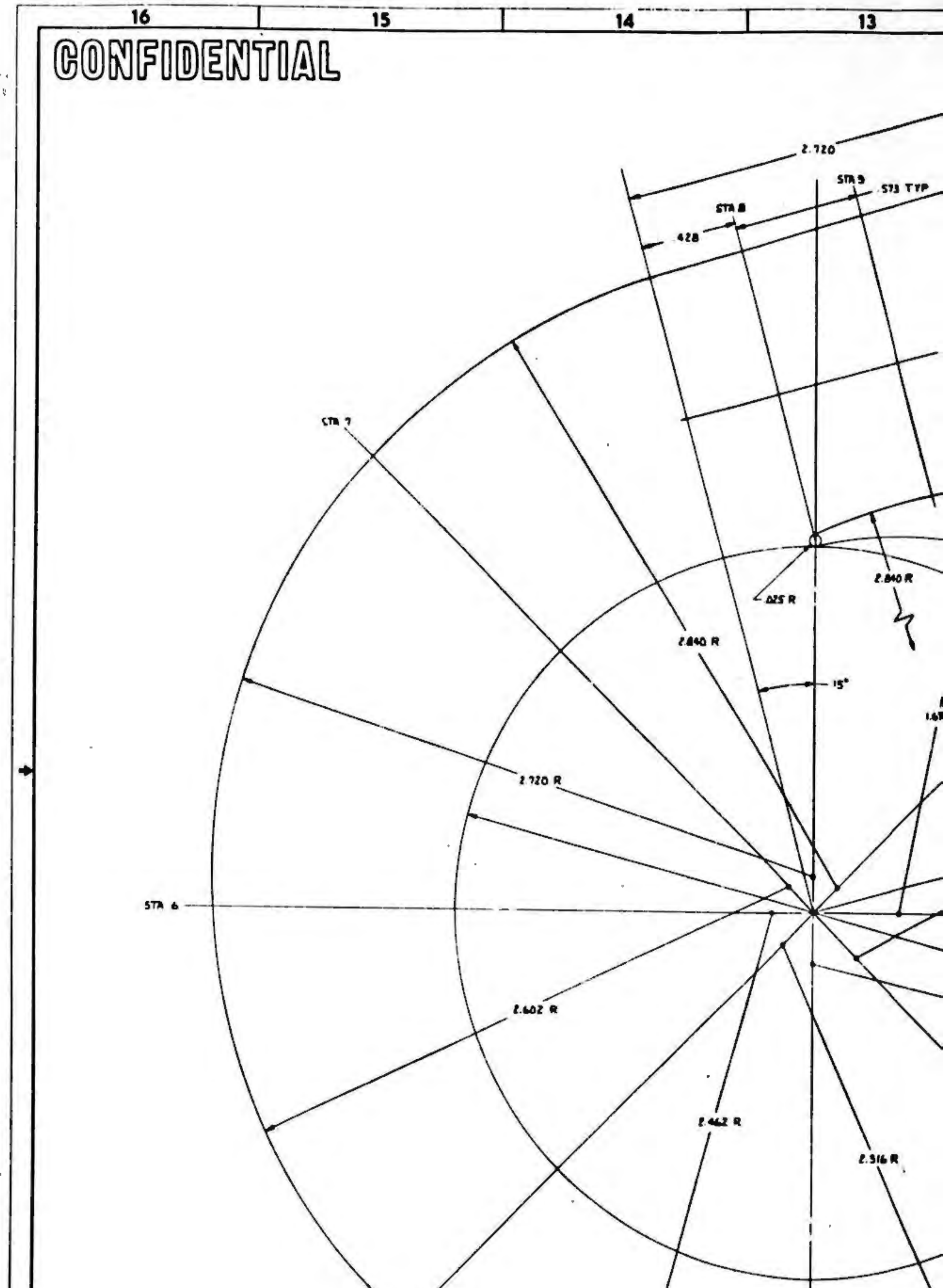

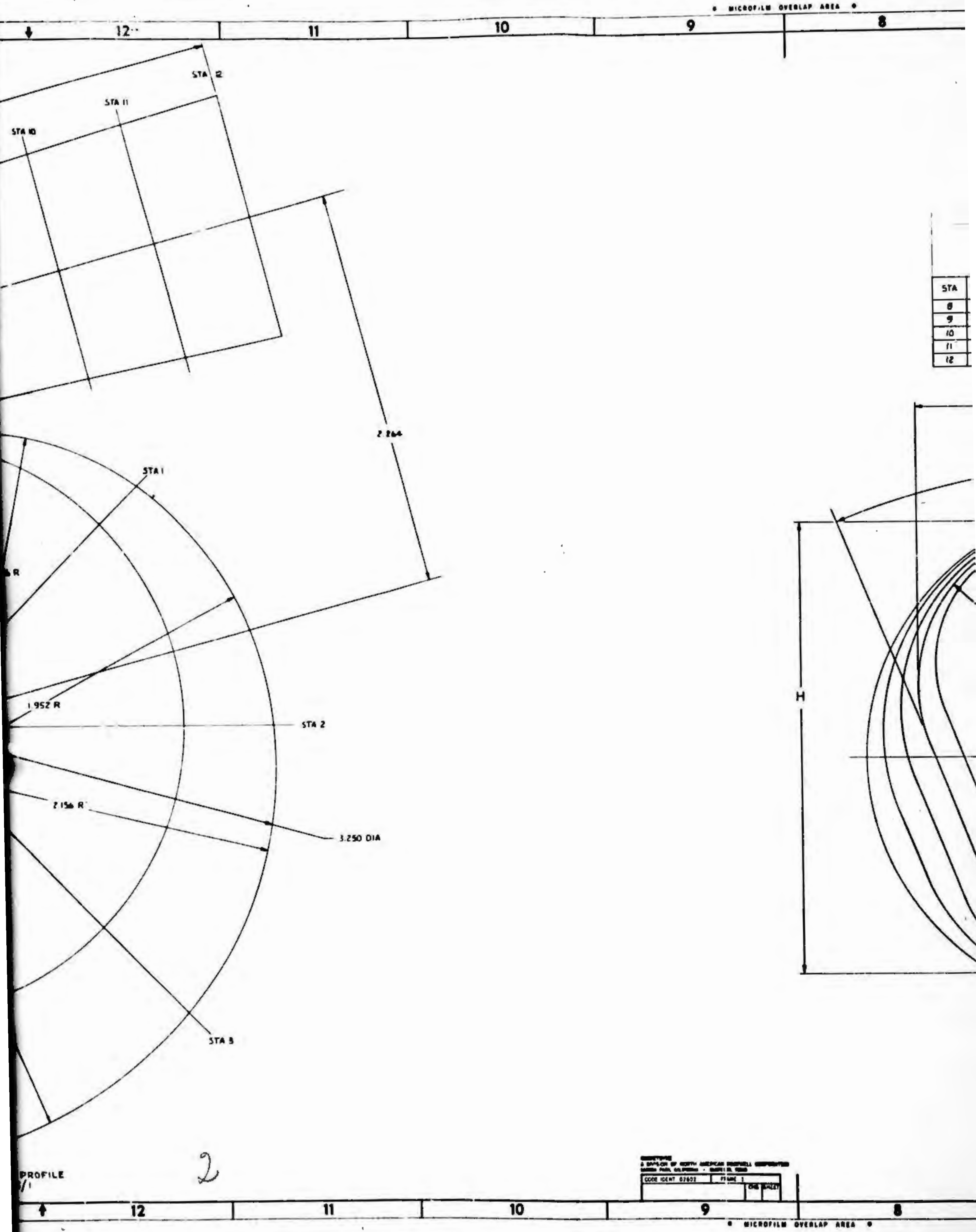

MICROFILM OVERLAP AREA
12
11
10
9
8
STA 12
STA 11
STA 10
2.264
STA 1
1.952 R
STA 2
2.156 R
3.250 DIA
STA 3
STA
8
9
10
11
12
H
PROFILE
2
CODE IDENT 02602
FRAME 1
12
11
10
9
8
MICROFILM OVERLAP AREA

8	7	6	5	4

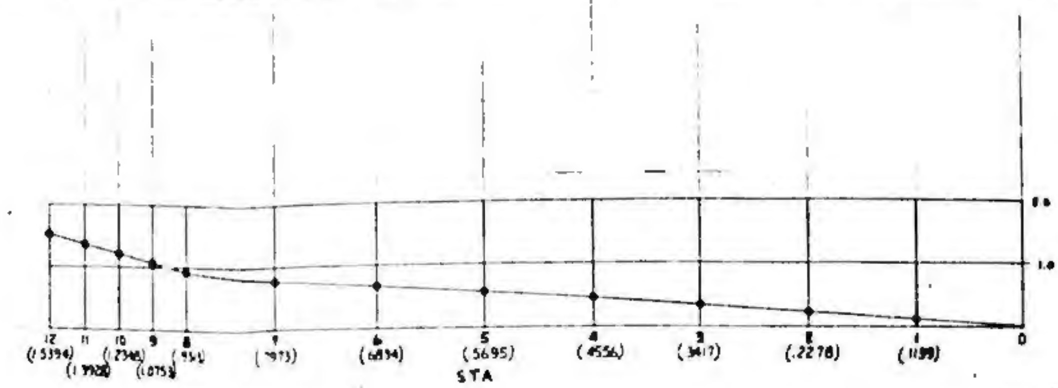

STA	AREA IN^2	R	R_1	R_2	R_3	W	X	H
8	.9313	.700	.350	∞	.063	1.004	.648	1.296
9	1.0753	↓	.458	.863	.222	1.105	.665	1.276
10	1.2348		.525	.783	.381	1.203	.678	1.318
11	1.3928	↓	.613	.733	.541	1.303	.691	1.362
12	1.5394	.700	.700	.700	.700	1.400	.700	1.400

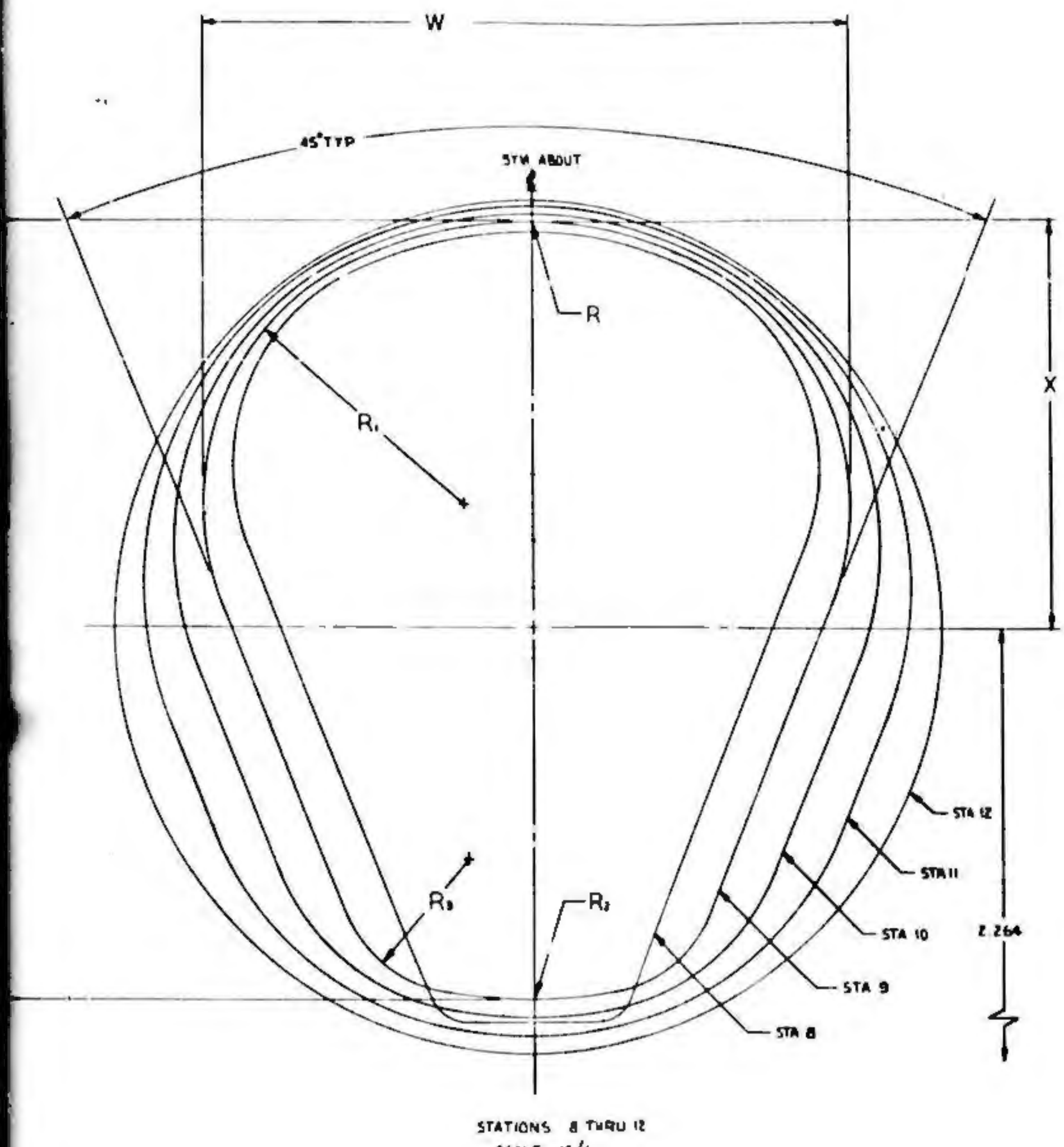

STATIONS 8 THRU 12
SCALE 10/1

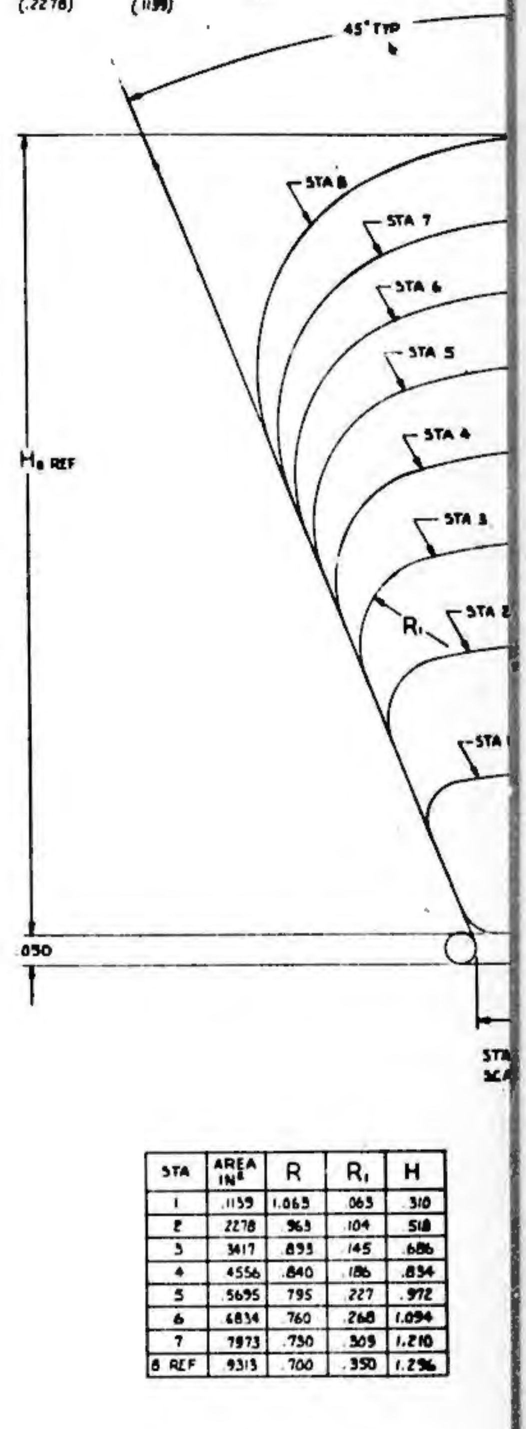

STA	AREA IN^2	R	R_1	H
1	.1159	1.063	.063	.310
2	.2278	.963	.104	.518
3	.3417	.893	.145	.686
4	.4556	.840	.186	.834
5	.5695	.795	.227	.972
6	.6834	.760	.268	1.094
7	.7973	.730	.309	1.210
8 REF	.9313	.700	.350	1.296

3

1. ALL DIMS SHOWN ARE BASIC

NOTE, UNLESS OTHERWISE SPECIFIED

8	7	6	5	4

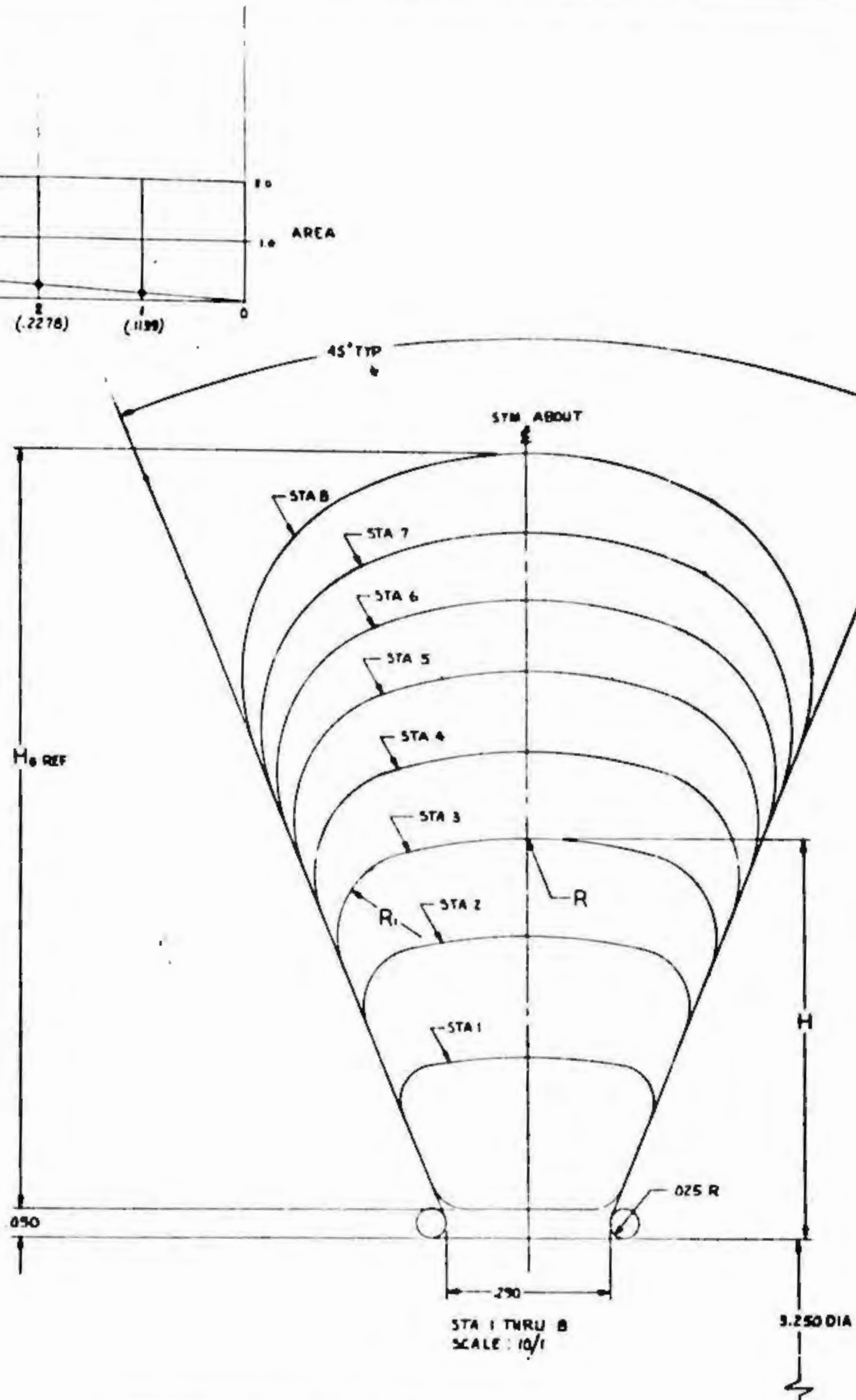

STA	AREA IN^2	R	R_1	H
1	1139	1.065	.063	310
2	2278	963	104	518
3	3417	895	145	686
4	4556	.840	186	.834
5	5695	795	227	.972
6	6834	760	.268	1.094
7	7973	730	.309	1.210
8 REF	9313	700	.350	1.296

1. ALL DIMS SHOWN ARE BASIC

Figure 182. Main Oxidizer Pump Volute Layout (U)

CONFIDENTIAL

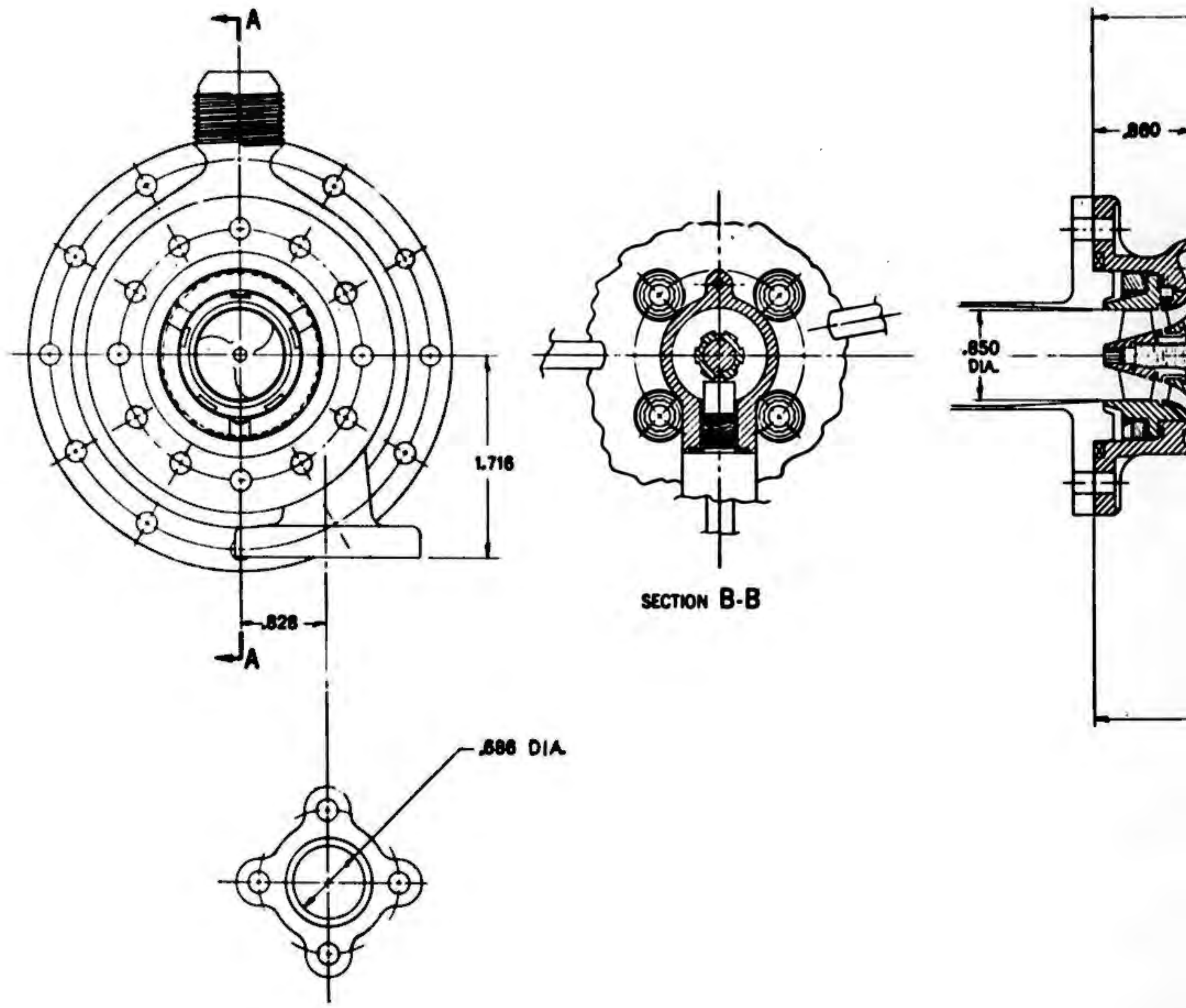

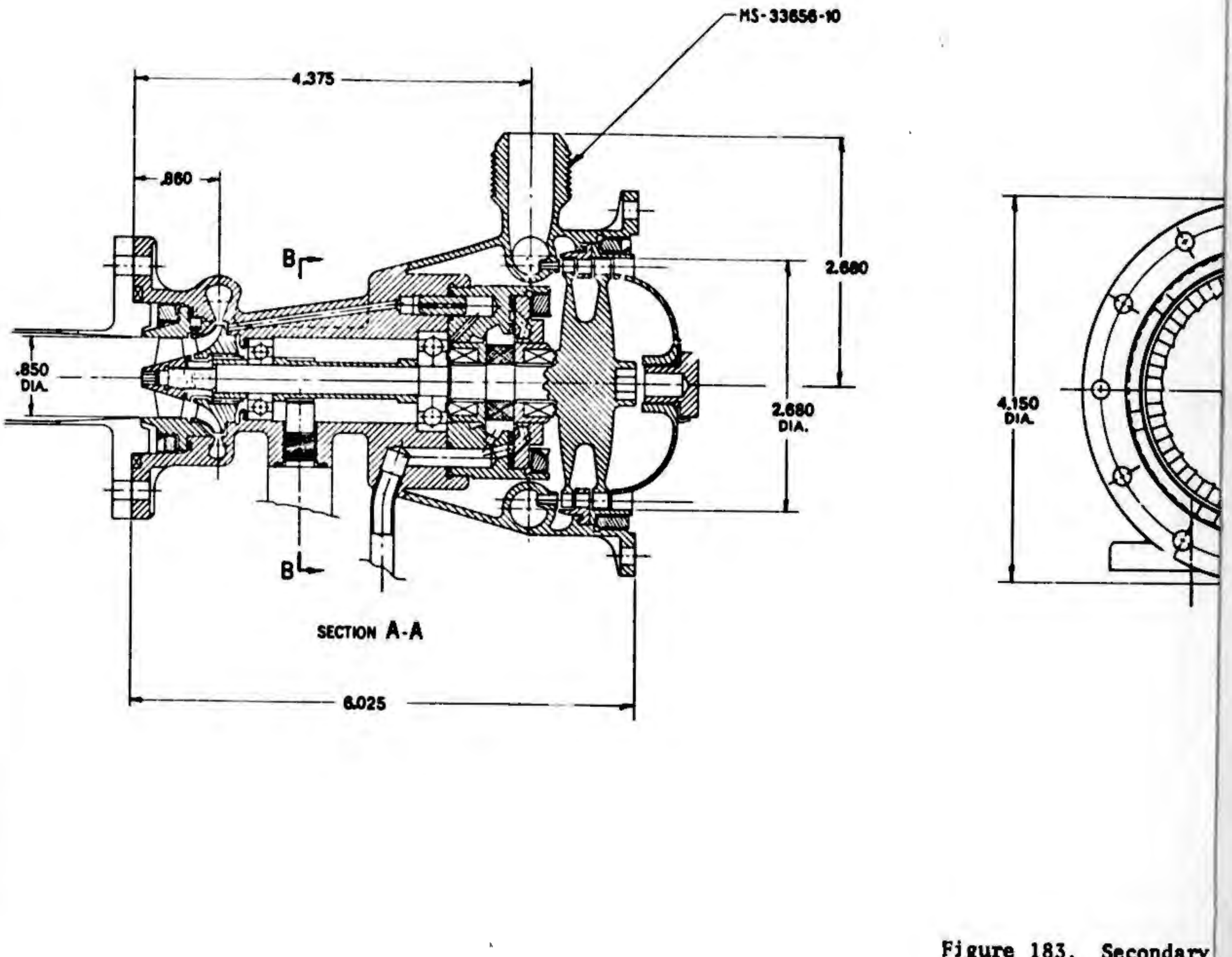

Figure 183. Secondary
(U)

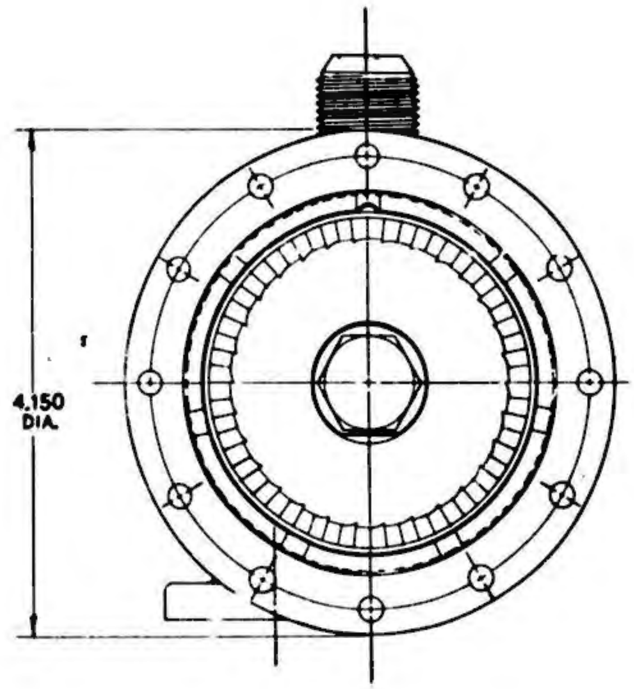

Figure 183. Secondary Oxidizer Turbopump (U)

3

CONFIDENTIAL

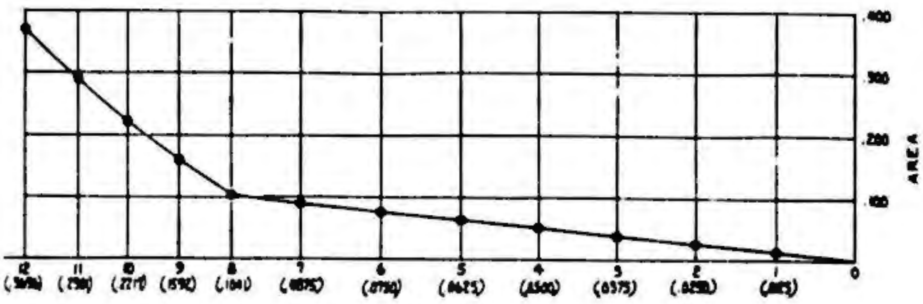

AREA DISTRIBUTION CURVE

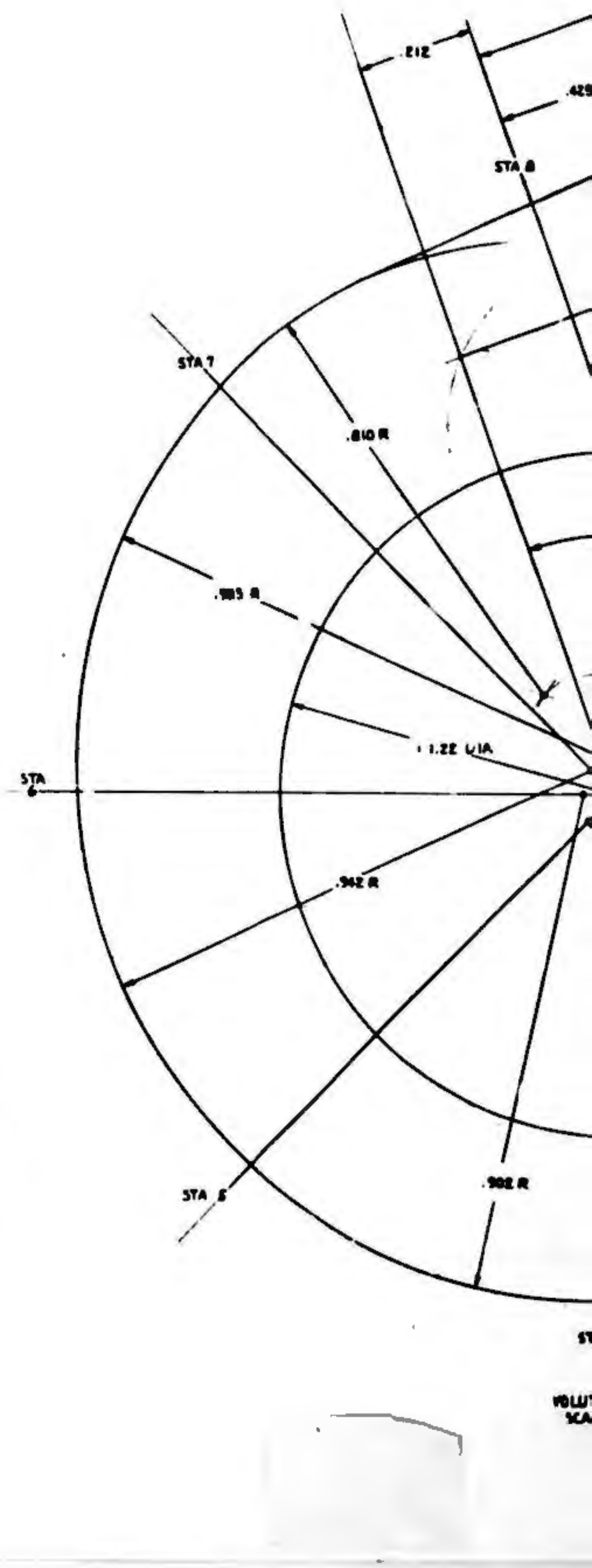

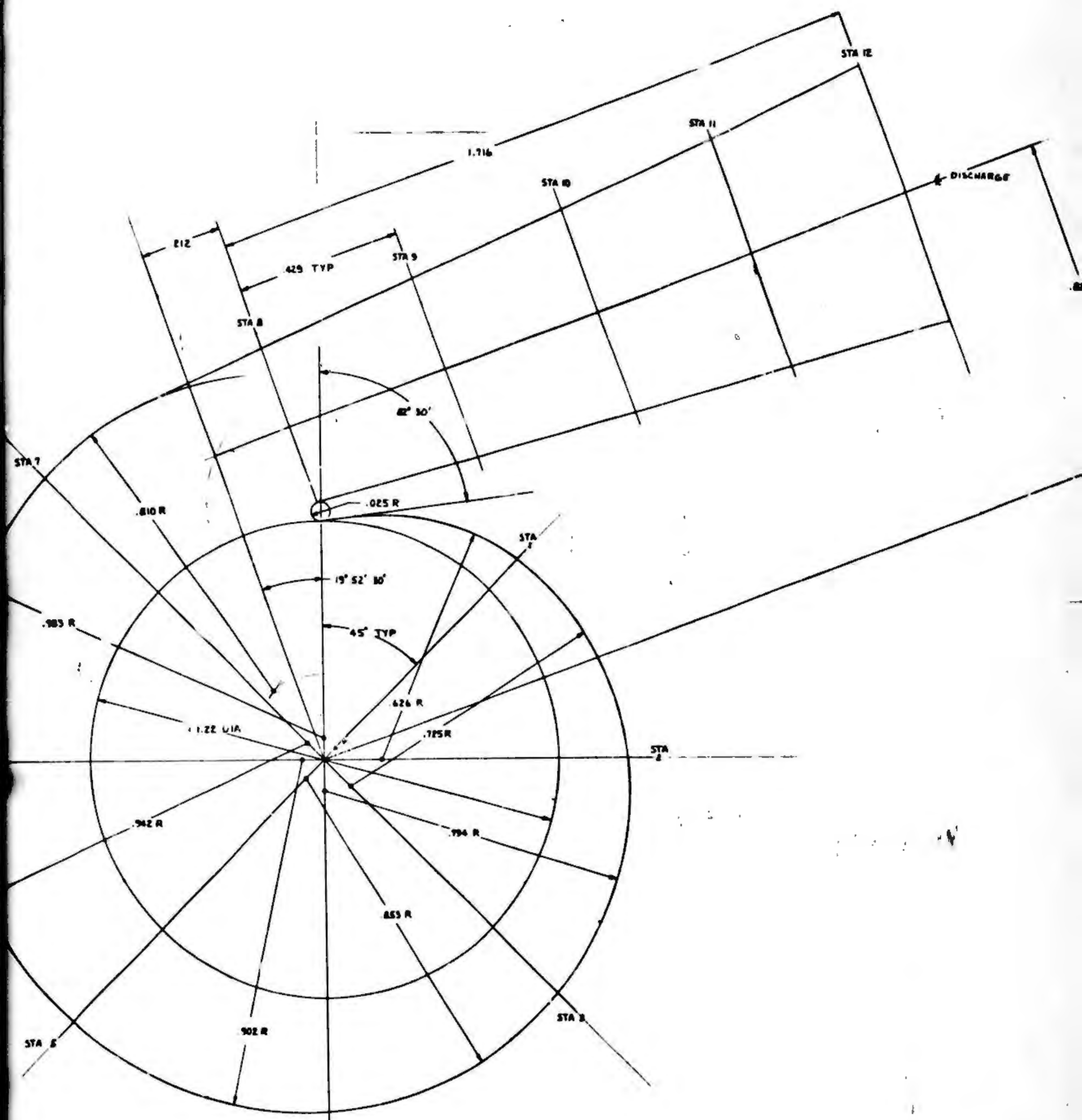

VOLUTE PROFILE
SCALE: 10/1

2

3

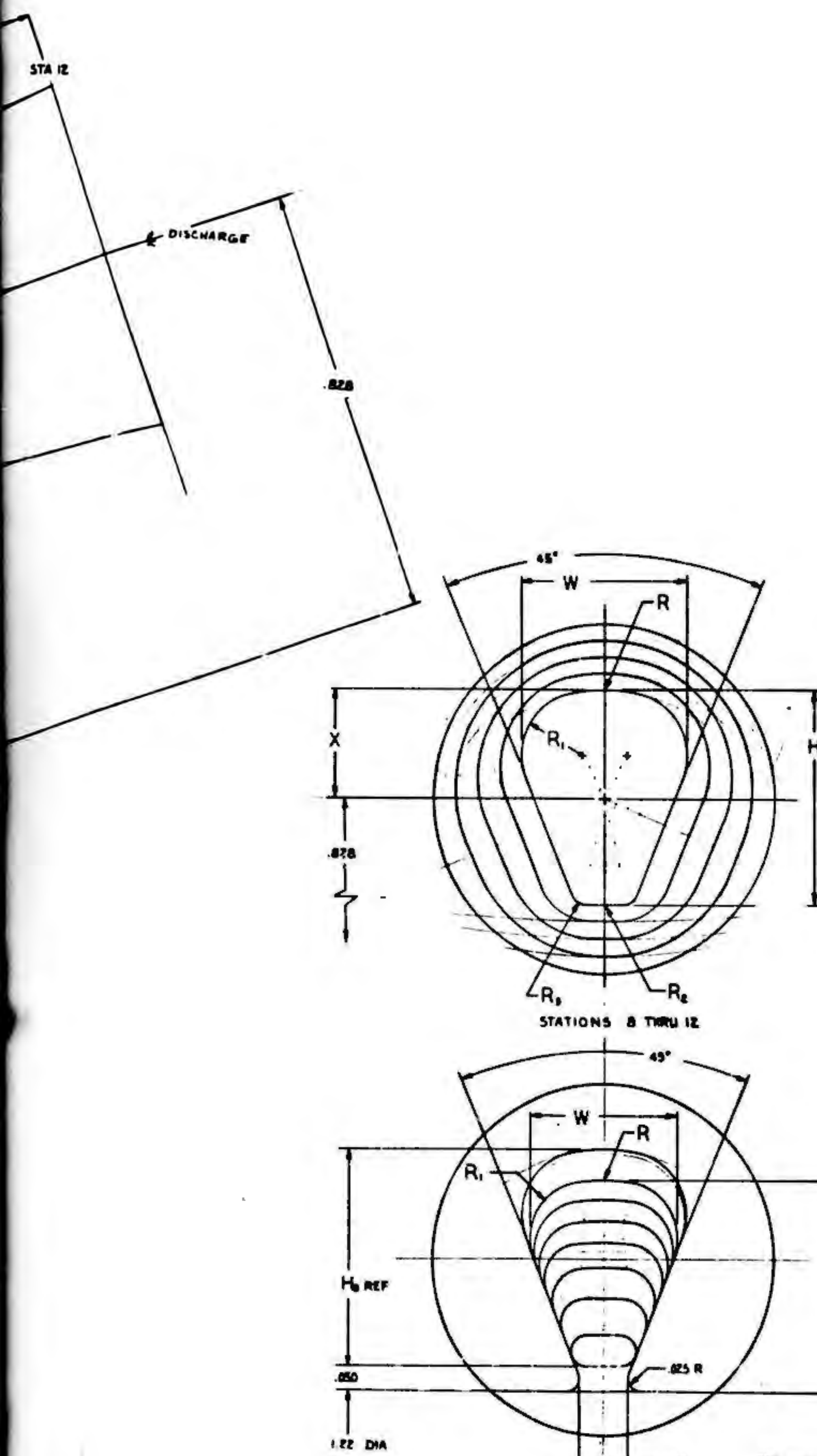

STA	AREA	H	R	R_1	R_2	R_3	W	X
8	.1041	.421	.343	.125	∞	.081	.338	.218
9	.1592	.485	↕	.180	3.60	.109	.424	.246
10	.2217	.551		.234	2.15	.187	.512	.278
11	.2901	.618		.289	1.15	.265	.595	.310
12	.3696	.686	.343	.343	.343	.343	.686	.343

STA	AREA	H	R	R_1	W_{REF}
1	.0125	.110	.860	.081	.153
2	.0250	.180	.710	.045	.174
3	.0375	.239	.610	.058	[illegible]
4	.0500	.288	.530	.072	[illegible]
5	.0625	.330	.470	.085	.263
6	.0750	.372	.420	.098	.292
7	.0875	.410	.380	.112	.302
8 REF	.1041	.421	.343	.125	.338

Figure 184. Secondary Oxidizer Pump Volute Layout (U)

TABLE 40

TURBINE PARAMETERS (U)

Parameter	Main Engine		Secondary Engine	
	Oxidizer	Fuel	Oxidizer	Fuel
Inlet Temperature, R	1038	1038	1660	1660
Inlet Pressure, psia	225	360	200	200
Pressure Ratio	7.5	12	10	10
Discharge Pressure, psia	30	30	20	20
Speed, rpm	27,500	75,000	75,000	138,000
Flowrate, lb/sec	0.336	0.535	0.055	0.059
Efficiency CONFIDENTIAL	0.27	0.575	0.32	0.50
Horsepower	202	810	43.6	73.8
Mean Diameter, inch	4.75	4.75	2.50	2.50
Mean Blade Velocity, ft/sec	570	1555	818	1505

(U) Because of the high turbine gas temperature encountered with both main and secondary turbines at the full-throttled condition, the preferred material, INCO 718, is inadequate. INCO 718 age hardens at the elevated temperature. A material investigation showed INCO 625 to be the best candidate.

(U) Manufacturing and cost studies, together with an evaluation of the hot-gas passage for the secondary turbines, showed that the best turbine design was achieved by machining the blading as an integral part of a forged disk. A vibration analysis was made on the blade geometry and showed that shrouds would not be required for vibration damping. The shrouded blade configuration was required for the main engine turbopumps to provide the necessary vibration damping.

7. CRITICAL SPEED ANALYSIS

(U) Synchronous critical speed characteristics were defined for the fuel and oxidizer pump designs and are shown in Fig. 185.

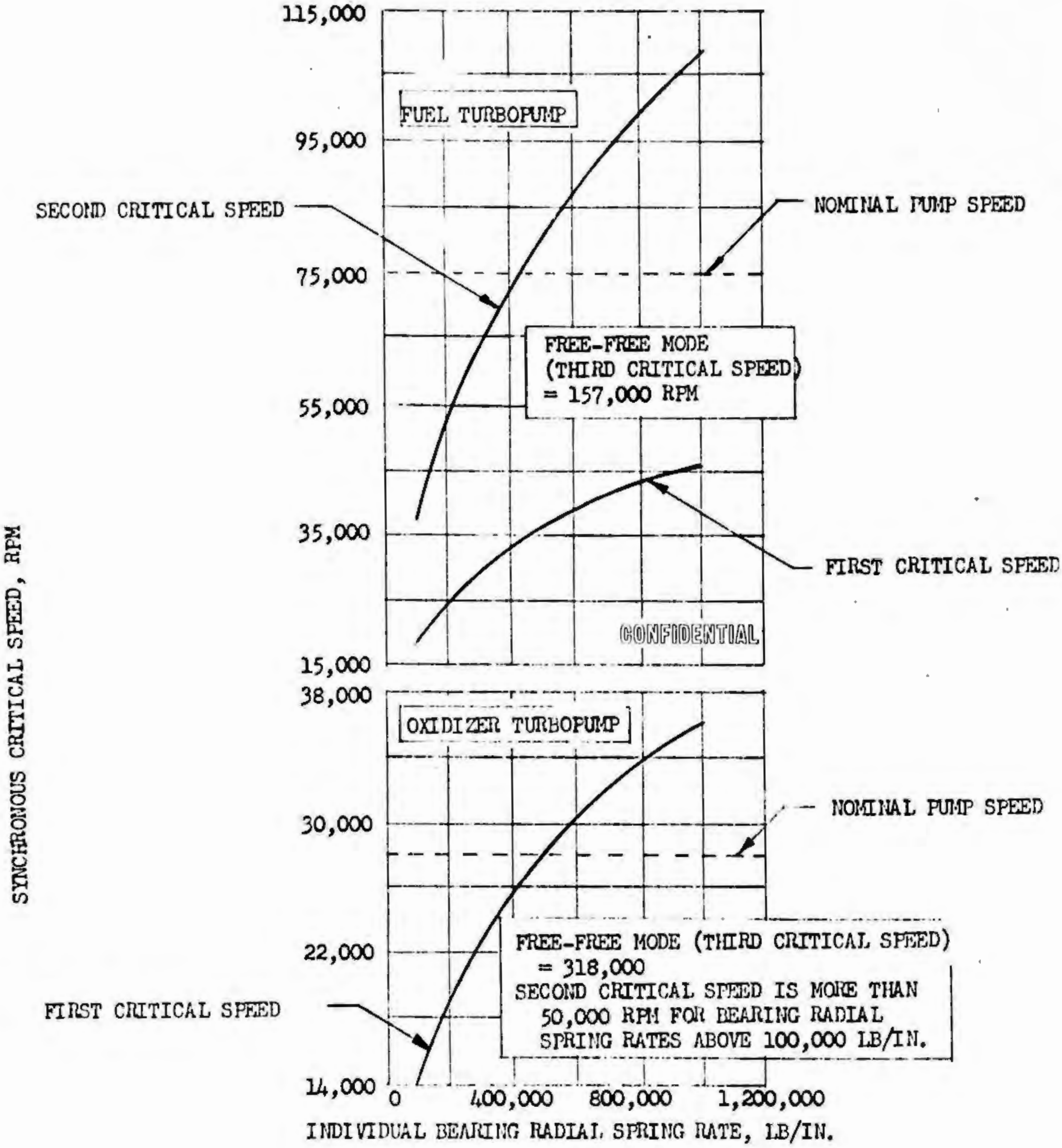

Figure 185. Main Engine Turbopump Critical Speed Versus Bearing Spring Rate (U)

(C) For the main engine primary fuel and oxidizer turbopumps there are two speed areas which were investigated. The first area was the "free-free" mode synchronous critical speed in which the bearings are not loaded and the shaft rotates within the bearing clearance in its bent shape about the bearing geometric centerline. The free-free mode is a function of shaft stiffness and weight only. The free-free critical speed was maintained above maximum operating speed by securing maximum shaft stiffness and minimum weight. The free-free synchronous critical speeds are estimated to be 318,000 rpm for the oxidizer turbopump and 157,000 rpm for the fuel turbopump. These free-free modes are sufficiently above the operating speeds to avoid problems.

(C) There are two other synchronous critical speeds, both well below the free-free critical speed. The main oxidizer pump can have its first synchronous critical speed below, at, or above the engine full-thrust operating speed of 27,500 rpm, depending upon bearing radial spring rate. The design provides sufficiently high spring rate in order to place the first synchronous critical mode well above 27,500 rpm.

(C) The main fuel turbopump will have its first two synchronous critical speeds below the nominal speed of 75,000 rpm, for any reasonable value of spring rate. The bearings and mounting are designed with sufficient flexibility to keep both criticals well below 75,000 rpm but rigid enough to prevent excessive bearing load.

8. STRUCTURAL ANALYSIS

a. Main Fuel Pump

(C) A maximum operating speed of 78,750 rpm was used in the structural analysis of the main fuel turbopump.

(1) Impellers

(C) The calculated first- and second-stage pump impeller burst speeds are 104,000 rpm and 100,900 rpm, respectively. These speeds are sufficiently in excess of the maximum operating speed such that impeller failure will not occur. The most severe condition with regard to burst speed occurs at an operating temperature of -100 F (Table 41). The material elongation to ultimate strength ratio is unfavorable at this temperature. Impeller stress distributions at maximum operating speed (78,750 rpm) are shown in Fig.186 and 187.

TABLE 41

MAIN FUEL PUMP IMPELLER BURST SPEED(U)

Stage	Operating Temperature, F	Burst Speed, rpm
First	Room	107,600
	-100	101,300
	-423	104,000
Second	Room	103,900
	-110	92,000
	-423	100,900

(2) Turbine Disks

(C) The turbine rotor disks were sized for the required center thicknesses of 0.50 and 0.54 for the first and second stages, respectively. The profiles are based on maintaining an average tangential stress level of approximately 68,000 psi which is sufficiently low to provide an adequate safety margin.

(3) Turbine Rotor Blades

(C) Airfoil stresses were calculated based on the selected blade shapes. The designs were structurally adequate. The blade root stresses for the first- and second-stage shrouded blades are listed below (Table 42) for the maximum operating speed of 78,750 rpm.

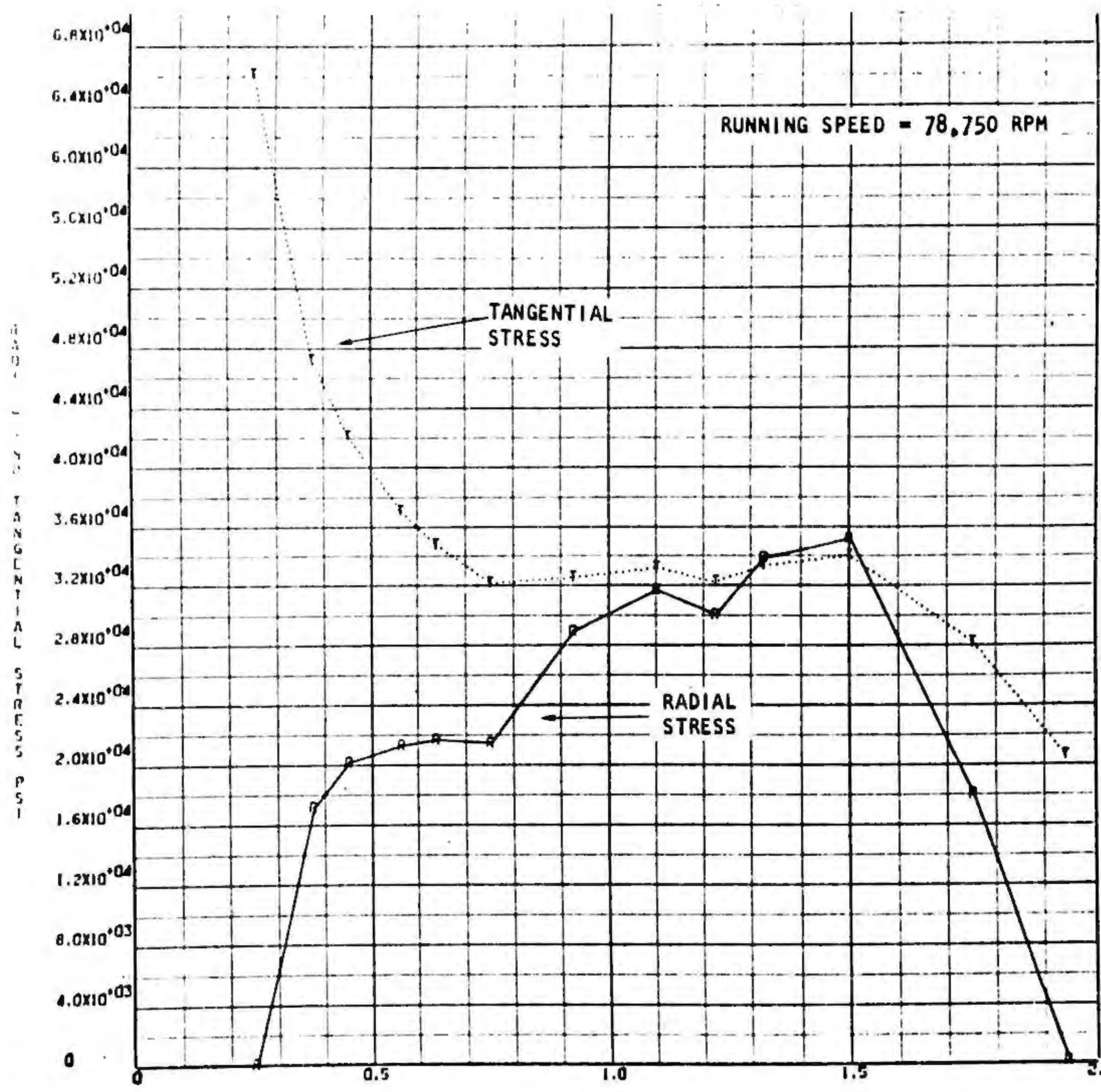

Figure 186. Main Fuel Pump First-Stage Impeller Stress Distributions (U)

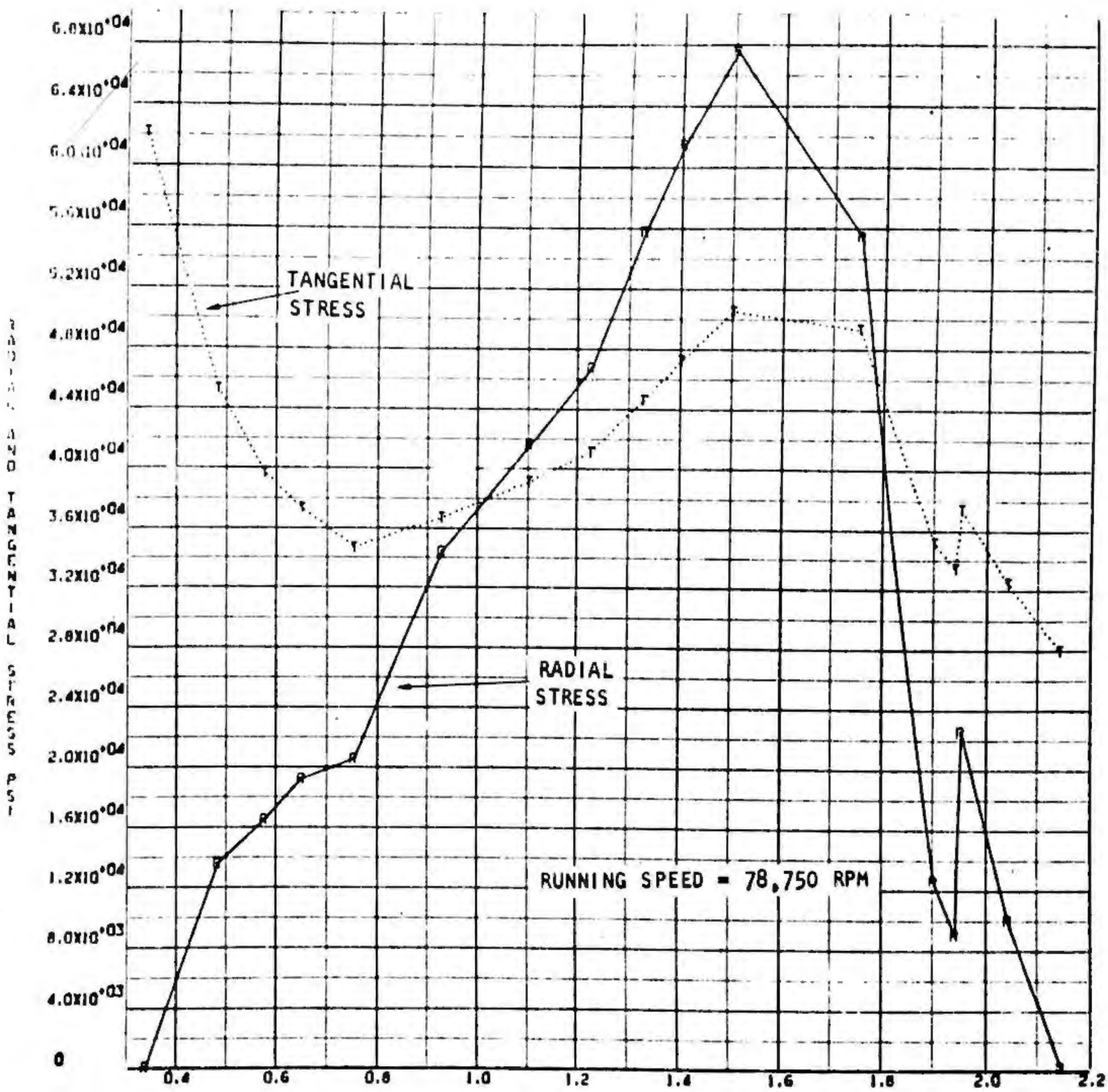

Figure 187. Main Fuel Pump Second-Stage Impeller Stress Distributions (U)

TABLE 42

MAIN FUEL TURBINE ROTOR BLADE STRESS (U)

Blade Root Stress, psi	First Stage	Second Stage
Direct Centrifugal	54,500	71,500
Power Bending	1,700	1,300

CONFIDENTIAL

b. Secondary Fuel Pump

(C) A maximum operating speed of 145,000 rpm was used in the structural analysis of the secondary fuel pump.

(1) Impellers

(C) The calculated first- and second-stage pump impeller burst speeds are 185,900 rpm and 192,300 rpm, respectively. These speeds are sufficiently in excess of the maximum operation speed such that impeller failure will not occur. Impeller stress distributions at maximum operating speeds are presented in Fig. 188 and 189.

(2) Turbine Disks

(C) Sizing of the turbine disks was accomplished for a required center thicknesses of 0.32 and 0.38 inch for the first and second stages, respectively. The profiles are based on maintaining an average tangential stress level of 68,000 psi which is sufficiently low to provide an adequate safety margin.

c. Oxidizer Turbopumps

(U) Both the primary and secondary oxidizer turbopumps are subjected to less severe operating conditions and present no major structural problems.

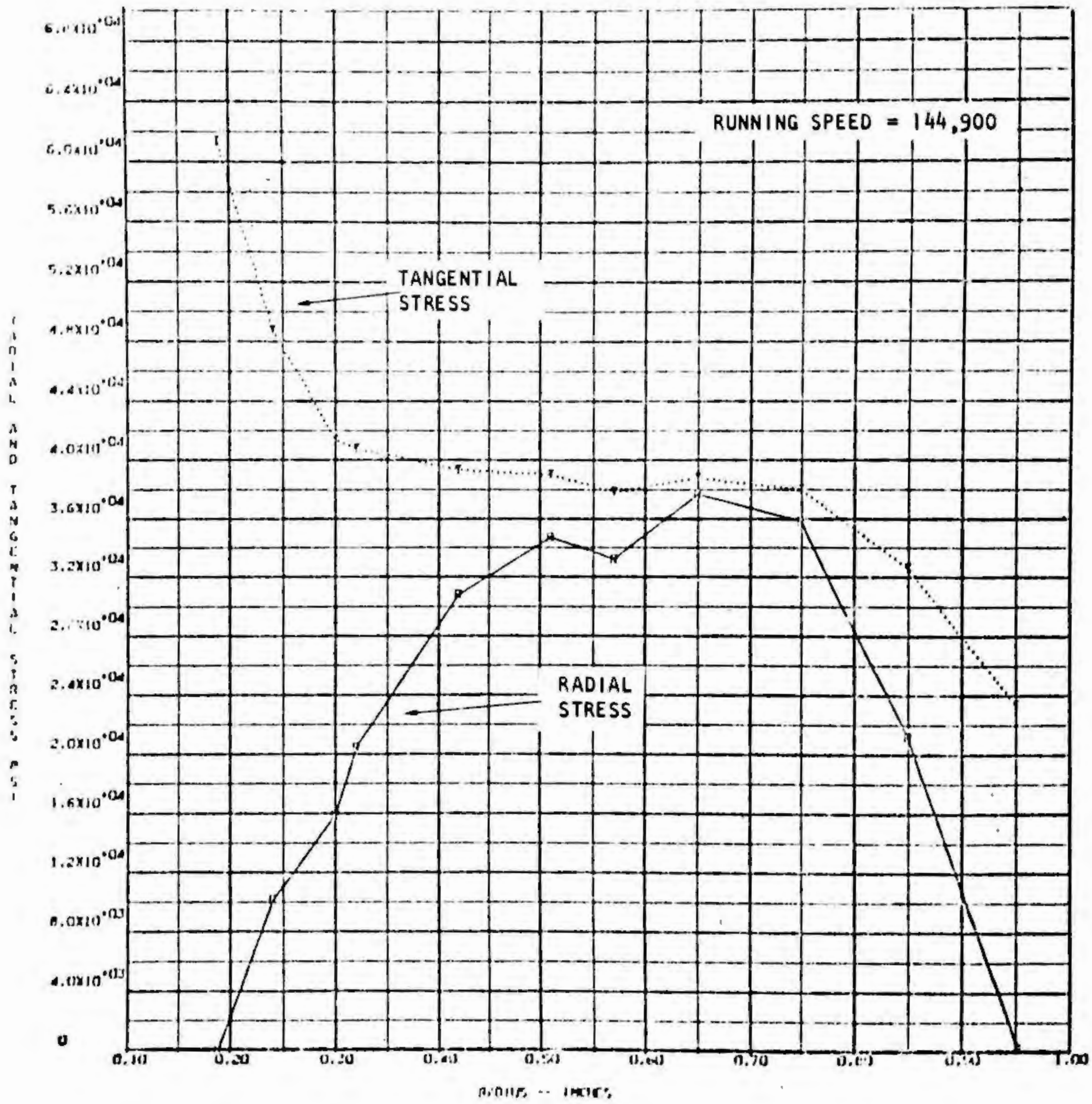

Figure 188. Secondary Fuel Pump First-Stage Impeller Stress Distributions (U)

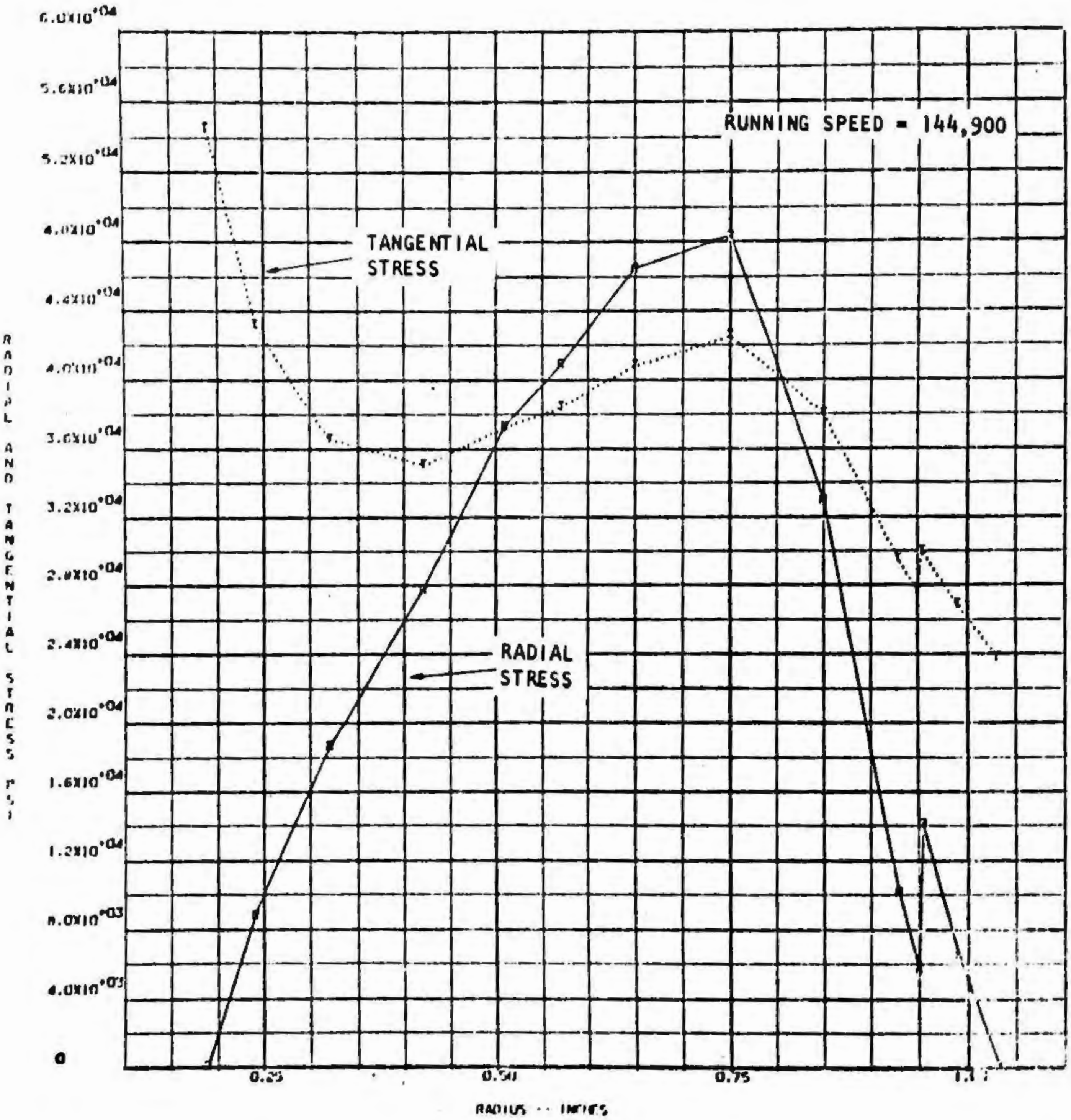

Figure 189. Secondary Fuel Pump Second-Stage Impeller Stress Distributions (U)

SECTION VI

CONTROLS

1. CONTROL SYSTEM COMPONENT DESIGN

(U) Analysis and design of the main and secondary engine control system components included the following: turbine throttle valves, main propellant valves, main and secondary control logic, main and secondary pneumatic control assemblies, turbine spin valve, electrical control system, and engine performance controller. The design features of each of the components are described below.

a. Turbine Throttle Valves

(U) These valves control the flow of hot gas to the oxidizer and fuel pump turbines on the main and secondary engines. One valve controls each turbine and, consequently, four different valves are used. The designs, which are similar, are ball-type valves actuated by a-c motors through planetary gear systems. Position feedback potentiometers are provided for control and instrumentation. Figures 190 through 193 show the design details.

(U) A ball-type throttle valve was selected rather than a poppet type because of its inherent simplicity and lower pressure drop. The rotary actuation eliminated the need for a long stroke bellows as an external dynamic seal.

CONFIDENTIAL

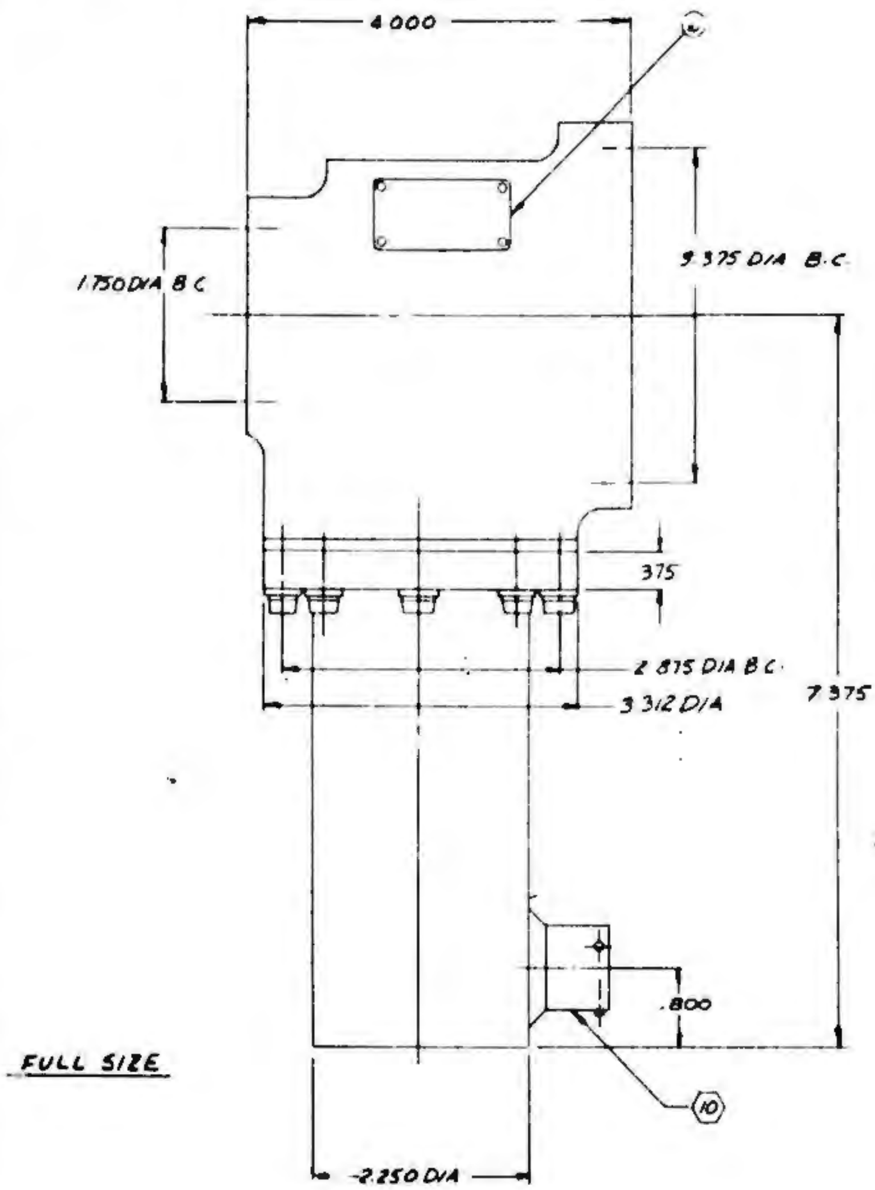

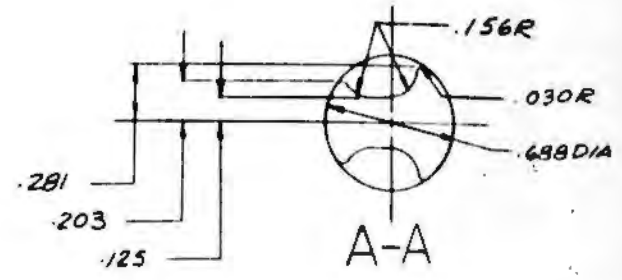

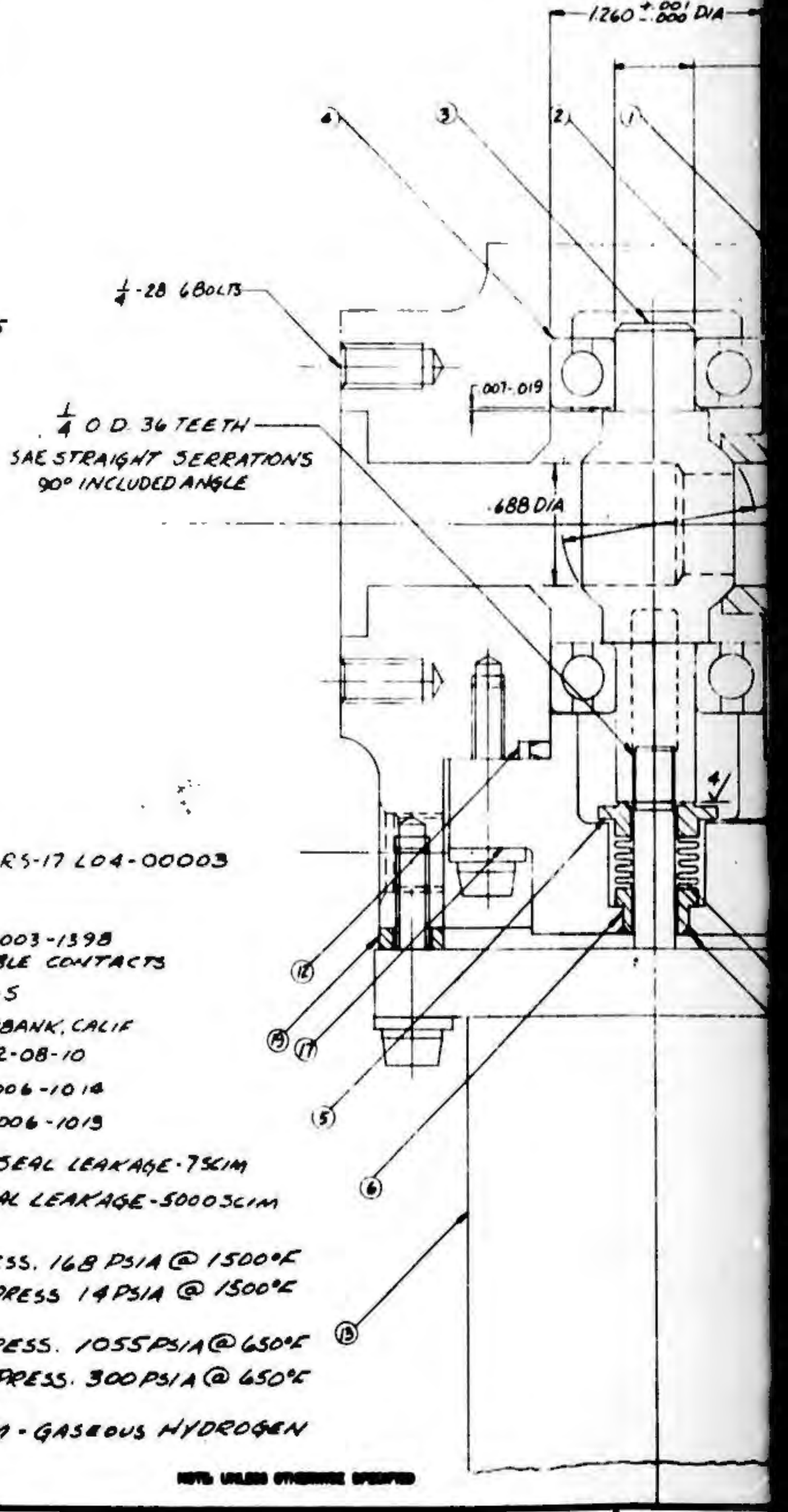

FULL SIZE

12. DESIGN PER DRS RY RS-17 L04-00003
(11) SIMILAR TO 550176
(10) SIMILAR TO RD 414-8003-1398
EXCEPT USE BRAZEABLE CONTACTS
(9) SIMILAR TO MRC 201-S
(8) HARRISON MFG CO. BURBANK, CALIF
(7) SIMILAR TO NAS 1102-08-10
(6) SIMILAR TO RD 111-3006-1014
(5) SIMILAR TO RD 111-3006-1013
4. ALLOWABLE SHAFT SEAL LEAKAGE - 75CIM
ALLOWABLE BALL SEAL LEAKAGE - 5000SCIM
3. MAXIMUM INLET PRESS. 168 PSIA @ 1500°F
MAXIMUM OUTLET PRESS 14 PSIA @ 1500°F
2. MAXIMUM INLET PRESS. 1055 PSIA @ 650°F
MAXIMUM OUTLET PRESS. 300 PSIA @ 650°F
1. OPERATING MEDIUM - GASEOUS HYDROGEN

(16) WELD PER RAO 107-027
15. MAX. BALL TO MOTOR MISALIGNMENT ± 5°
14. BURST PRESS - 1950 PSIG
13. PROOF PRESS - 1300 PSIG

NOTE: UNLESS OTHERWISE SPECIFIED

ACTUATOR CHARACTERISTICS	
RUNNING TORQUE	15 IN.LBS.
STALL TORQUE	60 IN.LBS.
MAX TRAVEL	90°
SLEW RATE	1.0 SEC
HORSE POWER	.0036
DUAL POTENTIOMETER	
EACH POT.	0.3K TO 5K
FIXED PHASE VOLTAGE 110VAC 400~	

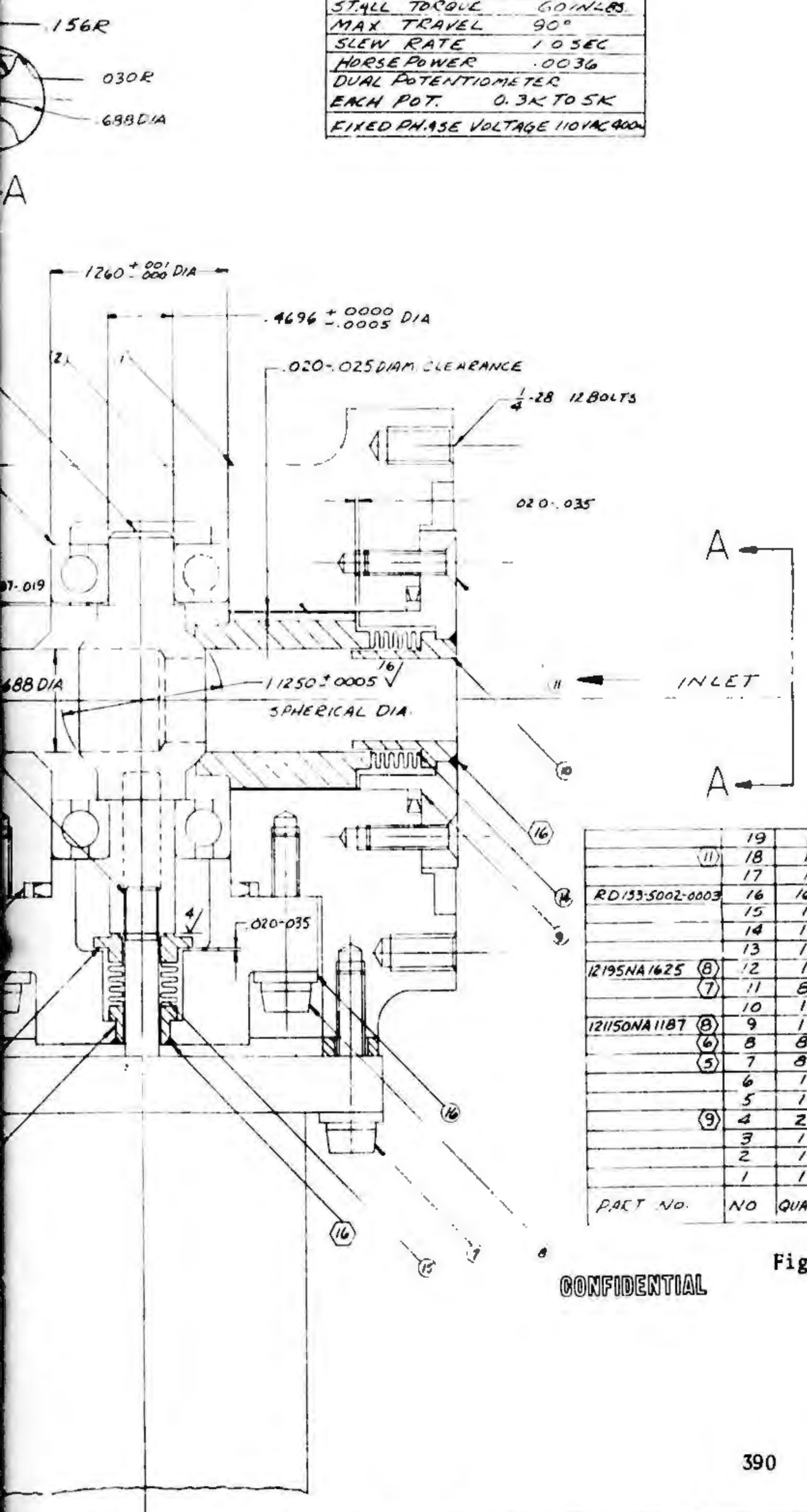

BELLOWS DATA		
PART NO	(14)	(15)
OUTSIDE DIA	.930	.470
INSIDE DIA	.690	.310
WALL THICKNESS	.005	.005
ACTIVE CONV.	8	7
INST. LENGTH	.375	.281
LOAD @ INST LGTH (LBS)	10	30
RATE (LBS/IN)	250	400

BEARING LOADS (LBS)		
TEMPERATURE °F	650	1500
RADIAL	107	14
THRUST	36	2

	19	1	INSULATOR	MICA PLATE	———
(11)	18	1	NAMEPLATE	302 CRES	PASSIVATE
	17	1	CAP	INCO 718	PASSIVATE
RD133-5002-0003	16	16	WASHER	A 286	PASSIVATE
	15	1	FORMED BELLOWS	INCO 625	PASSIVATE
	14	1	FORMED BELLOWS	INCO 625	PASSIVATE
	13	1	AC ELECT. ACTUATOR	COMMERCIAL	———
12195NA1625 (8)	12	1	K SEAL 12195	INCONEL X 750	GOLD PLATED
(7)	11	8	SCREW (8-32)	RENE 41	PASSIVATE
	10	1	RETAINER	INCO 718	PASSIVATE
12115ONA1187 (8)	9	1	K SEAL 121150	INCONEL X 750	GOLD PLATED
(6)	8	8	BOLT (10-32)	RENE 41	PASSIVATE
(5)	7	8	BOLT (10-32)	RENE 41	PASSIVATE
	6	1	RETAINER	INCO 718	PASSIVATE
	5	1	SEAL	INCO 718	FLAME PLATE
(9)	4	2	BALL BEARING	STELLITE	PASSIVATE
	3	1	SHAFT	RENE 41	PASSIVATE
	2	1	SEAL	INCO 718	FLAME PLATE
	1	1	HOUSING	INCO 718	PASSIVATE
PART NO.	NO	QUANT.	DESCRIPTION	MATERIAL	FINISH

CONFIDENTIAL

Figure 190. Main Engine Fuel Turbine Throttle Valve (U)

2

CONFIDENTIAL

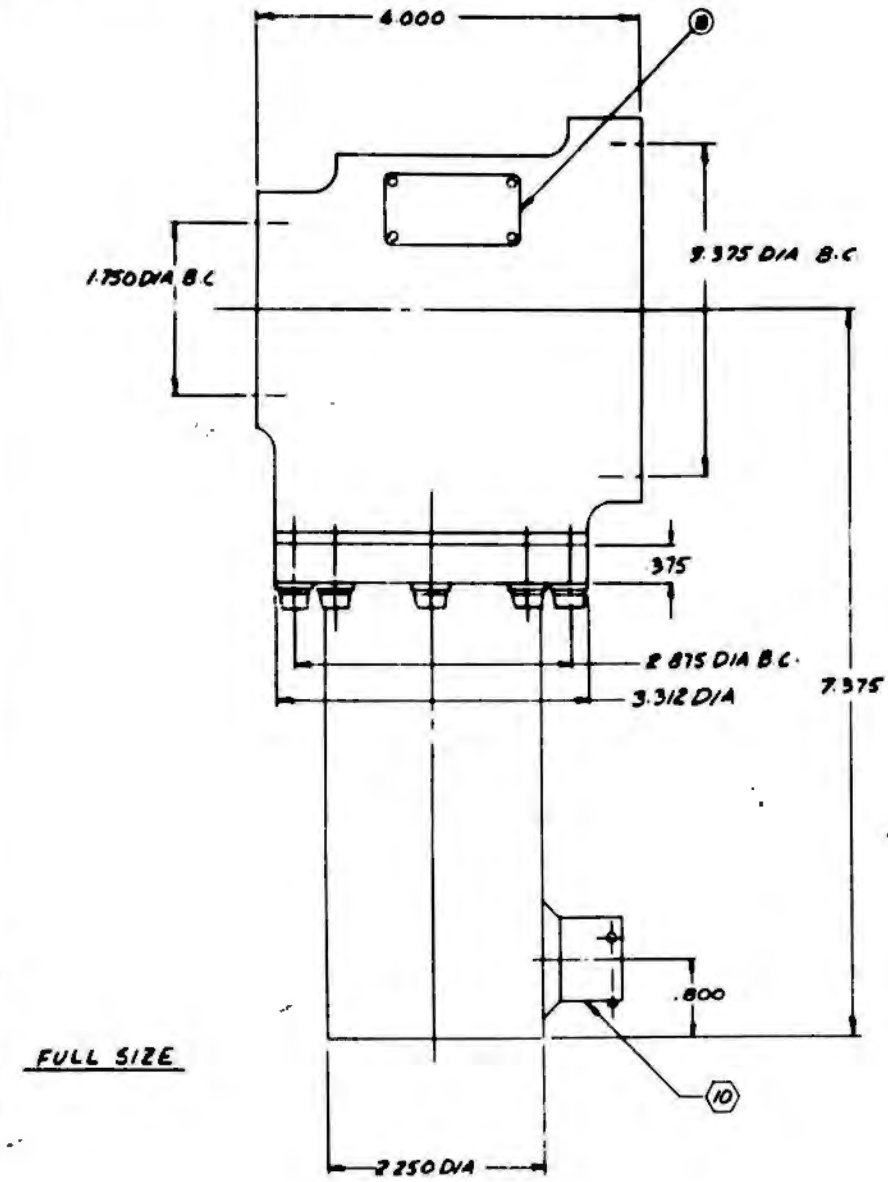

FULL SIZE

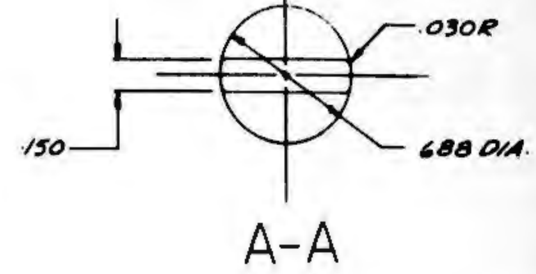

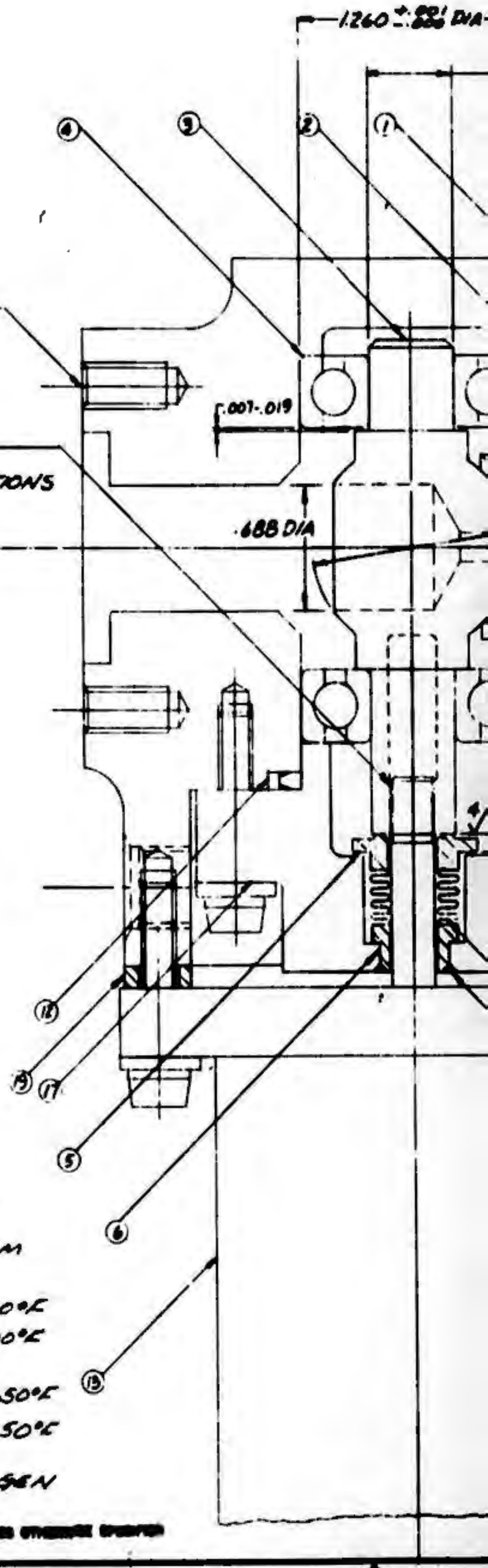

12. DESIGN PER DRS RY RS-17 L04-00004

(11) SIMILAR TO 550176

(10) SIMILAR TO RD 414-8003-1398
EXCEPT USE BRAZEABLE CONTACTS

(9) SIMILAR TO MRC 201-5

(8) HARRISON MFG CO. BURBANK, CALIF

(7) SIMILAR TO NAS 1102-08-10

(6) SIMILAR TO RD 111-3006-1014

(5) SIMILAR TO RD 111-3006-1013

4. ALLOWABLE SHAFT SEAL LEAKAGE - 7SCIM
ALLOWABLE BALL SEAL LEAKAGE - 5000SCIM

3. MAXIMUM INLET PRESS. 168 PSIA @ 1500°F
MAXIMUM OUTLET PRESS 12 PSIA @ 1500°F

2. MAXIMUM INLET PRESS. 1055 PSIA @ 650°F
MAXIMUM OUTLET PRESS. 273 PSIA @ 650°F

1. OPERATING MEDIUM - GASEOUS HYDROGEN

(16) WELD PER RAO 107-027

15. MAX BALL TO MOTOR MISALIGNMENT ± 5°

14. BURST PRESS - 1950 PSIG

13. PROOF PRESS - 1300 PSIG

NOTE: UNLESS OTHERWISE SPECIFIED

ACTUATOR CHARACTERISTICS	
RUNNING TORQUE	15 IN. LBS.
STALL TORQUE	60 IN. LBS.
MAX. TRAVEL	90°
SLEW RATE	1.0 SEC
HORSE POWER	.0036
DUAL POTENTIOMETER	
EACH POT.	0.3K TO 5K
FIXED PHASE VOLTAGE 110 VAC 400~	

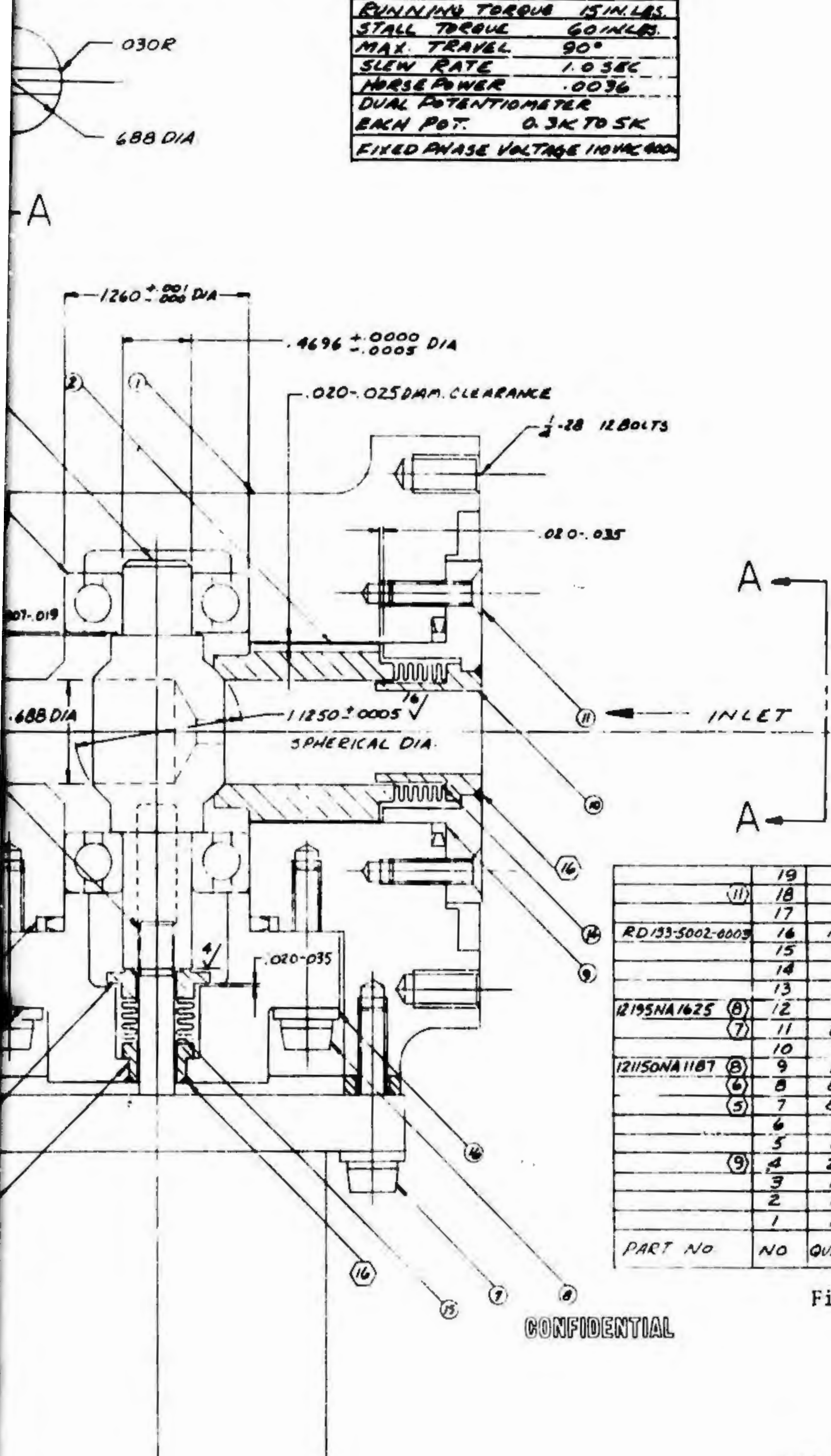

BELLOWS DATA		
PART NO	14	15
OUTSIDE DIA	.930	.470
INSIDE DIA	.690	.310
WALL THICKNESS	.005	.005
ACTIVE CONV.	8	7
INST. LENGTH	.375	.281
LOAD @ INST LGTH (LBS)	10	30
RATE (LBS/IN)	250	400

BEARING LOADS (LBS)		
TEMPERATURE °F	650	1500
RADIAL	107	14
THRUST	36	2

PART NO	NO	QUANT.	DESCRIPTION	MATERIAL	FINISH
	19	1	INSULATOR	MICA PLATE	——
11	18	1	NAMEPLATE	302 CRES	PASSIVATE
	17	1	CAP	INCO 718	PASSIVATE
RD133-5002-0003	16	16	WASHER	A 286	PASSIVATE
	15	1	FORMED BELLOWS	INCO 625	PASSIVATE
	14	1	FORMED BELLOWS	INCO 625	PASSIVATE
	13	1	AC ELECT. ACTUATOR	COMMERCIAL	——
12195NA1625 8	12	1	K SEAL 12195	INCONEL X 750	GOLD PLATED
7	11	8	SCREW (8-32)	RENE 41	PASSIVATE
	10	1	RETAINER	INCO 718	PASSIVATE
121150NA1187 8	9	1	K SEAL 121150	INCONEL X 750	GOLD PLATED
6	8	8	BOLT (10-32)	RENE 41	PASSIVATE
5	7	8	BOLT (10-32)	RENE 41	PASSIVATE
	6	1	RETAINER	INCO 718	PASSIVATE
	5	1	SEAL	INCO 718	FLAME PLATE
9	4	2	BALL BEARING	STELLITE	PASSIVATE
	3	1	SHAFT	RENE 41	PASSIVATE
	2	1	SEAL	INCO 718	FLAME PLATE
	1	1	HOUSING	INCO 718	PASSIVATE

Figure 191. Main Engine Oxidizer Engine Throttle Valve (U)

CONFIDENTIAL

2

CONFIDENTIAL

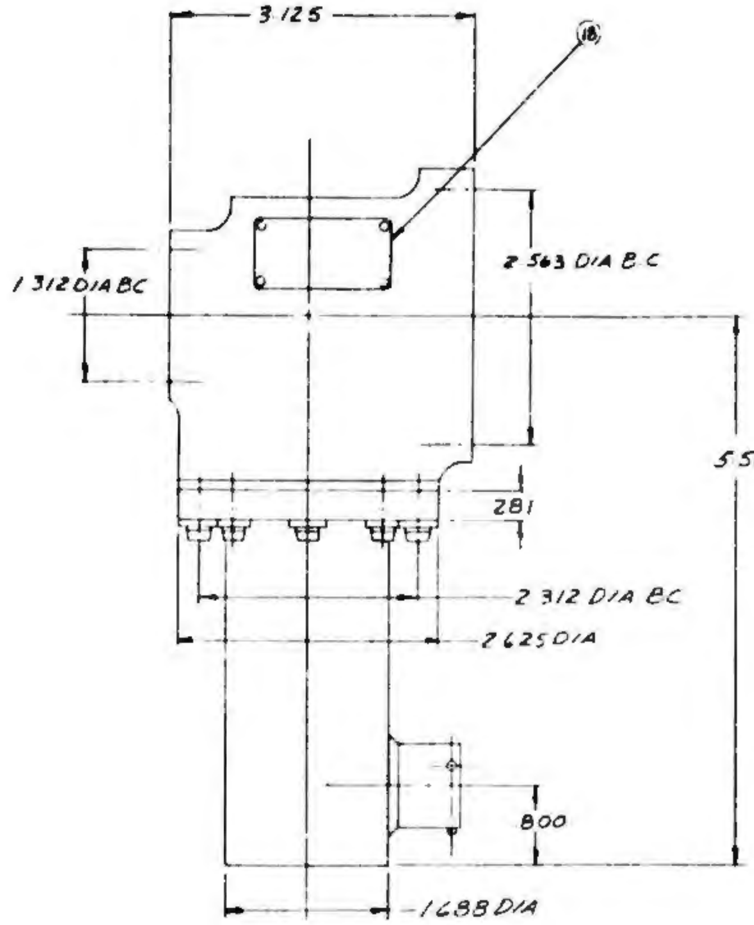

FULL SIZE

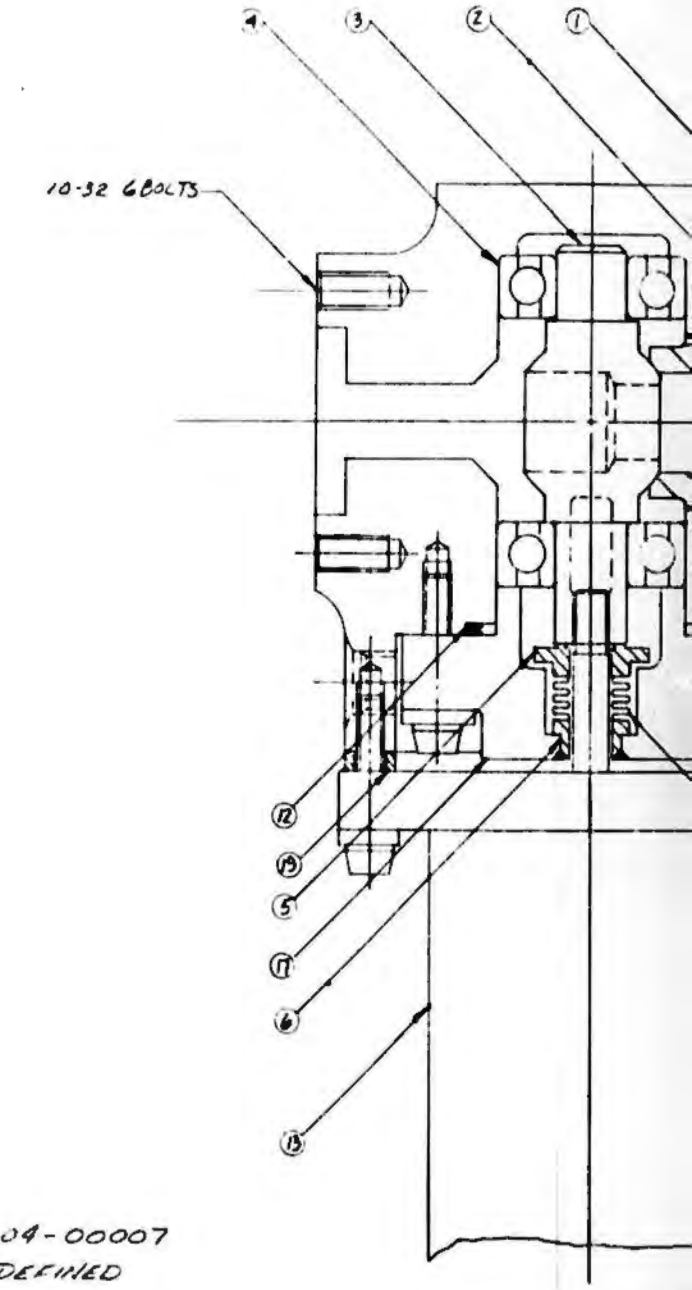

4 DESIGN PER DRS RY RS-17 L04-00007

3. SHAPING OF THROTTLE NOT DEFINED

2 OPERATING MEDIUM - GASEOUS HF

1 DESIGN SIMILIAR TO MAIN ENGINE FUEL TURBINE THROTTLE VALVE SEE LAYOUT RS000901L

/

NOTE: UNLESS OTHERWISE SPECIFIED

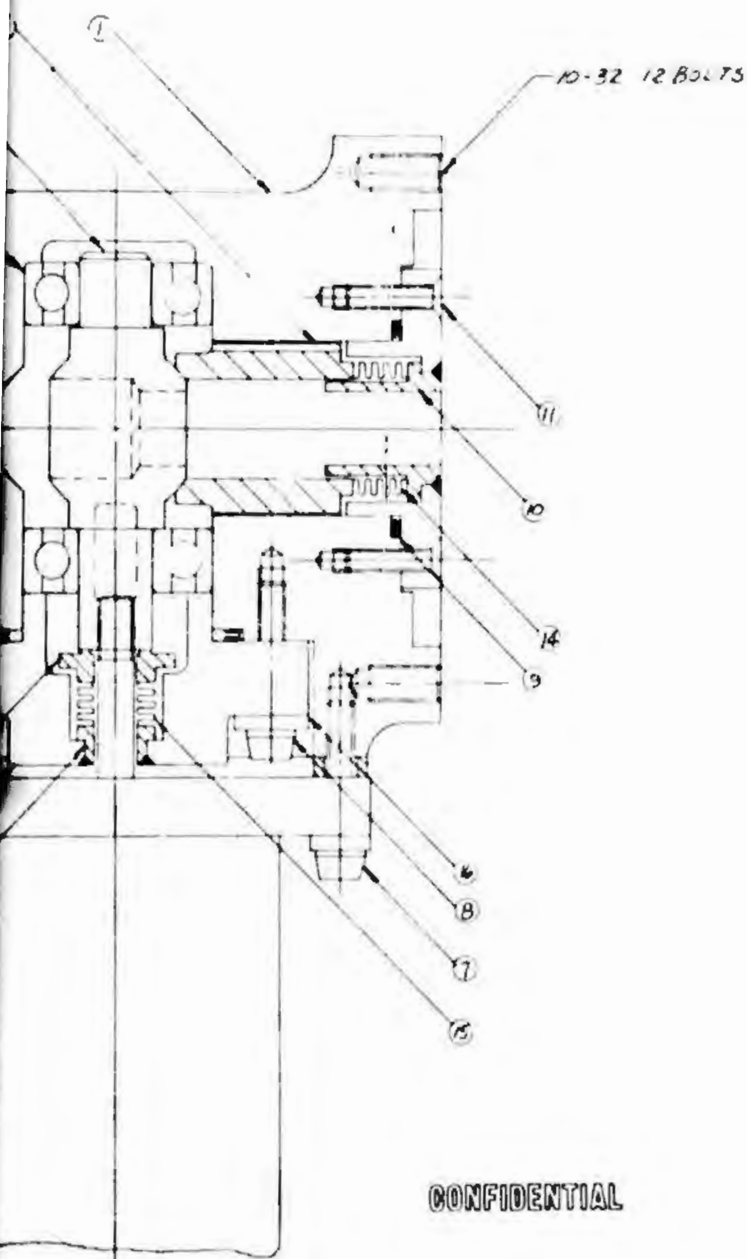

19	1	INSULATOR	MICA PLATE	————
18	1	NAMEPLATE	302 CRES	PASSIVATE
17	1	CAP	INCO 718	PASSIVATE
16	16	WASHER	A 286	PASSIVATE
15	1	FORMED BELLOWS	INCO 625	PASSIVATE
14	1	FORMED BELLOWS	INCO 625	PASSIVATE
13	1	AC ELECT ACTUATOR	COMMERCIAL	————
12	1	KSEAL 12130	INCONEL X 750	GOLD PLATED
11	8	SCREW (4-40)	RENE 41	PASSIVATE
10	1	RETAINER	INCO 718	PASSIVATE
9	1	KSEAL 121100	INCONEL X 750	GOLD PLATED
8	8	BOLT (8-32)	RENE 41	PASSIVATE
7	8	BOLT (8-32)	RENE 41	PASSIVATE
6	1	RETAINER	INCO 718	PASSIVATE
5	1	SEAL	INCO 718	FLAME PLATE
4	2	BALL BEARING	STELLITE	PASSIVATE
3	1	SHAFT	RENE 41	PASSIVATE
2	1	SEAL	INCO 718	FLAME PLATE
1	1	HOUSING	INCO 718	PASSIVATE
NO	QUANT	DESCRIPTION	MATERIAL	FINISH

Figure 192. Secondary Engine Fuel Turbine Throttle Valve (U)

CONFIDENTIAL

RS00903L

CONFIDENTIAL

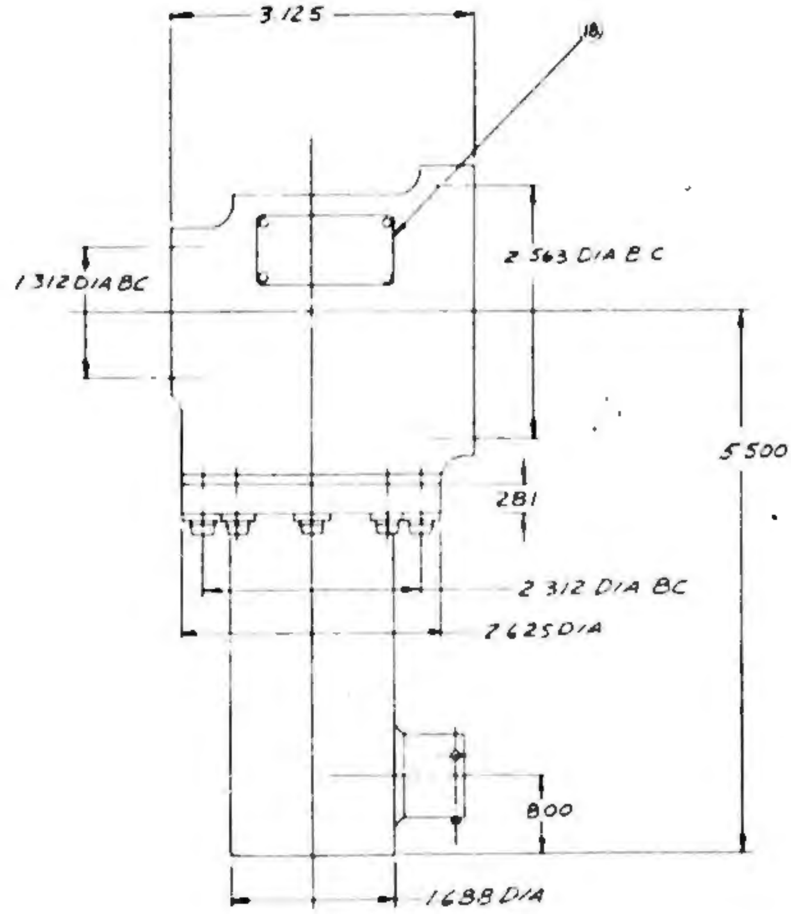

FULL SIZE

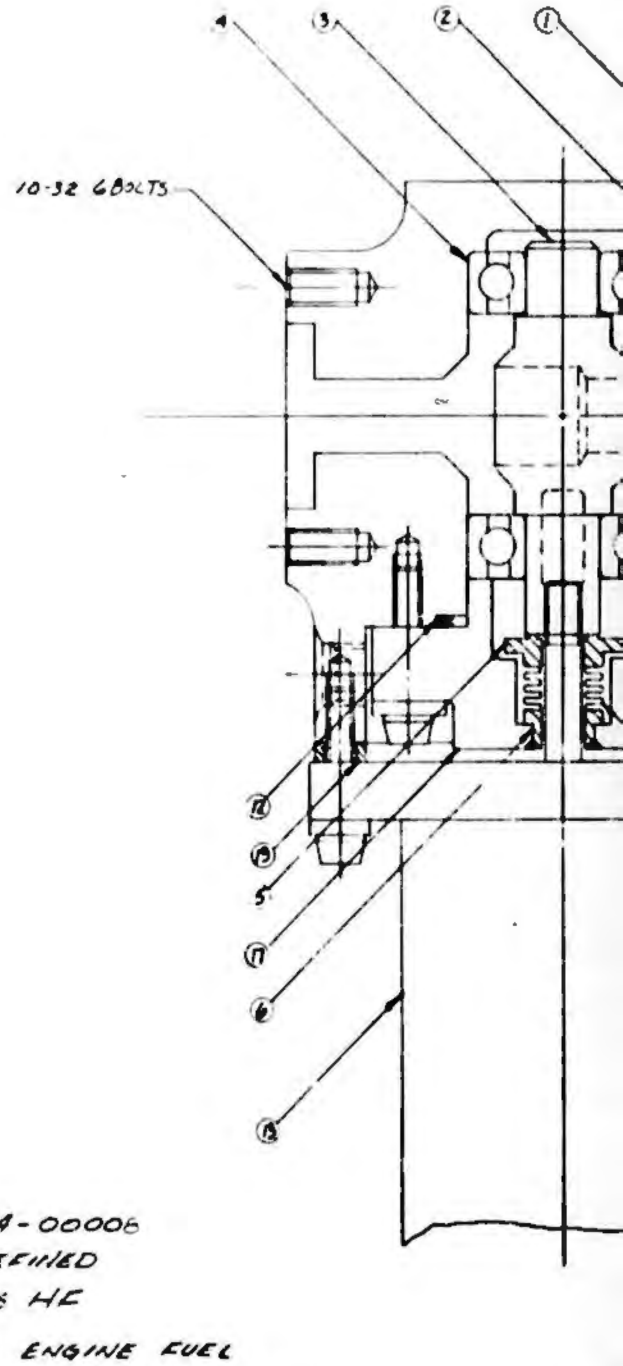

4 DESIGN PER DRS RY RS-17 L04-00006
3. SHAPING OF THROTTLE NOT DEFINED
2 OPERATING MEDIUM - GASEOUS HF
1 DESIGN SIMILIAR TO MAIN ENGINE FUEL TURBINE THROTTLE VALVE. SEE LAYOUT RS00C 90[illegible]

NOTE: UNLESS OTHERWISE SPECIFIED

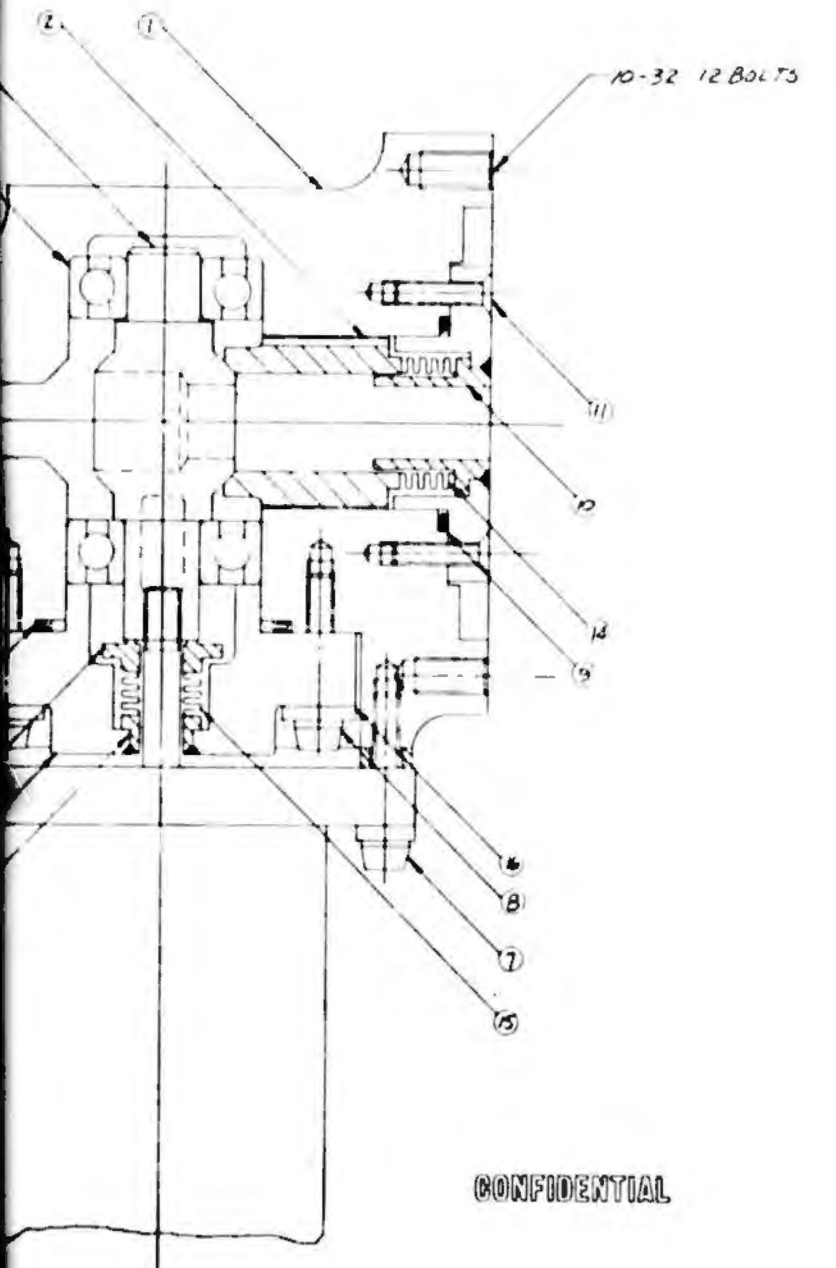

19	1	INSULATOR	MICA PLATE	————
18	1	NAME PLATE	302 CRES	PASSIVATE
17	1	CAP	INCO 718	PASSIVATE
16	16	WASHER	A 286	PASSIVATE
15	1	FORMED BELLOWS	INCO 625	PASSIVATE
14	1	FORMED BELLOWS	INCO 625	PASSIVATE
13	1	AC ELECT ACTUATOR	COMMERCIAL	————
12	1	KSEAL 12130	INCONEL X 750	GOLD PLATED
11	8	SCREW (4-40)	RENE 41	PASSIVATE
10	1	RETAINER	INCO 718	PASSIVATE
9	1	KSEAL 121100	INCONEL X 750	GOLD PLATED
8	8	BOLT (8-32)	RENE 41	PASSIVATE
7	8	BOLT (8-32)	RENE 41	PASSIVATE
6	1	RETAINER	INCO 718	PASSIVATE
5	1	SEAL	INCO 718	FLAME PLATE
4	2	BALL BEARING	STELLITE	PASSIVATE
3	1	SHAFT	RENE 41	PASSIVATE
2	1	SEAL	INCO 718	FLAME PLATE
1	1	HOUSING	INCO 718	PASSIVATE
NO	QUANT	DESCRIPTION	MATERIAL	FINISH

Figure 193. Secondary Engine Oxidizer Turbine Throttle Valve (U)

CONFIDENTIAL

2

(U) The design features an integral ball and shaft which has a shaped flow passage and is easily replaced for modification of throttling characteristics. Thrust and radial loads on the shaft produced by the flow of the hot gas are transmitted to the housing by means of ball bearings so that friction is kept to a minimum.

(U) The shaft seal is a rotary face seal welded to a stationary, short-stroke, hydroformed bellows. The shaft seal is on the low-pressure side of the throttle valve so that leakage is reduced to a low level. The leakage past the shaft seal is routed overboard.

(U) The throttle valve is positioned by means of an electrical rotary actuator. The actuator is compact, utilizing an electric motor and a planetary gear system with open and closed stops and dual position potentiometers for feedback. The electric motor is an a-c servomotor requiring no brushes to avoid radio frequency interference, and no permanent magnets which may be weakened by high temperatures. The actuator is coupled to the throttle shaft through a spline. There is an additional seal on the actuator shaft to prevent hot gas from seeping into the motor.

(U) The ball seal serves a dual purpose. In the closed throttle position, it reduces the flow to an acceptable level. In the semi-open position, the seal forms part of the throttling area. The ball seal also is welded to a stationary, short-stroke, hydroformed bellows which, in turn, is protected by a shield from the eroding effects of a high-velocity hot-gas stream. Both the shaft seal bellows and the ball seal bellows are protected from overdeflection during the assembly procedure or possibly during valve operation transients.

(U) Heat transfer from the valve into the electrical actuator has been reduced to a tolerable level by minimizing the heat transfer area and providing an insulator between the valve housing and the electrical actuator base.

(U) The design utilizes high heat-resistant nickel alloys with matching coefficients of expansion. Sufficient clearances have been provided between moving parts, including the ball bearings, so that during the initial moments of hot firing, thermal gradients will not cause the valve to bind. Sealing surfaces have been flame plated to ensure minimum wear, low friction, antigalling characteristics, and good surface finish. Valve torque has been reduced by throttling at the ball inlet only, and allowing the ball outlet to be open to downstream pressure. Maximum valve torque including friction is approximately one-fourth of the stall torque of the electrical actuator. This ratio will provide sufficient acceleration capability for adequate transient response when the throttle valve is part of a closed servoloop.

(U) The valve design permits ease of assembly and disassembly with no special tools required.

b. Main Propellant Valves

(U) These valves are two-position, poppet-type valves that control the flow of oxidizer and fuel to the main and secondary engines. They are located immediately downstream of the propellant feed system interface and upstream of the turbopumps. Figures 194 through 197 show the design details, and Fig. 198 and 199 show the inlet manifold configurations.

(C) The following discussion presents the technical approach associated with the design of the main propellant valves for the AMPS engine. The most stringent design requirements are generated by system requirements for low shutoff leakage in a flightweight valve controlling corrosive propellant at cryogenic temperatures. The solution to these design problems incorporated the most advanced state-of-the-art concepts acquired through Rocketdyne's poppet and seat development program, NASA's component and system programs, and the Air Force's metal bellows analysis and test program (Ref. 10 through 18).

CONFIDENTIAL

BELLOWS DATA	
OUTSIDE DIA	1.40
INSIDE DIA	.980±.020
NO. PLYS	1
WALL THICKNESS	.008
ACTIVE CONVOLUTIONS	40
INSTALLED LENGTH	2.71
INSTALLED LOAD (LB)	72.4
RATE (LB/IN.)	60

(21) SPRING DATA	
OUTSIDE DIA	3.875
WIRE DIA	.375
ACTIVE COILS	3.5
TOTAL COILS	5.5
RATE (LB/IN.)	191
LOAD, VALVE CLOSED	350
LOAD, VALVE OPEN	473

(11) SPRING DATA	
OUTSIDE DIA	.688
WIRE DIA	.100
ACTIVE COILS	2
TOTAL COILS	4
RATE (LB/IN.)	353
LOAD, VALVE CLOSED	40
LOAD, VALVE OPEN	46

GENERAL NOTES
1. DESIGN PER ORS RY RS-17106-
2. PROPELLANT SECTION
NOMINAL INLET PRESS: 55 P
MAXIMUM INLET PRESS: 160
PROOF PRESS: 200
BURST PRESS: 300
ΔP (60.1 SLB/SEC, 93.8 LB/FT³): 8 P
3. ACTUATOR
NOMINAL PRESS: 750
MAX OPERATING PRESS: 900
PROOF PRESS: 1100
BURST PRESS: 1650
4. PROPELLANT LEAKAGE (MAX. F
EXTERNAL: 10^{-4} SCIM
INTERNAL: 0.1 SCIM
5. ACTUATOR LEAKAGE:
150 SCIM MAX. TOTAL HE. AT
(A) TU CARBIDE FLAME PLATE STE
(B) SILVER-COPPER FURNACE BRA
(C) SEE LAYOUT DWG. R5000
HOUSING CONFIGURATION

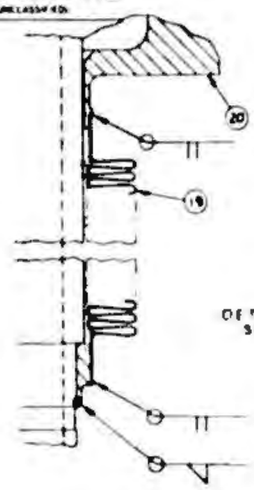

DETAIL D SCALE 4

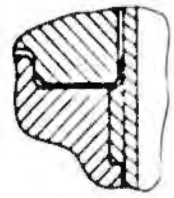

DETAIL G SCALE 4

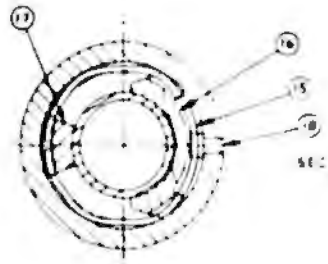

SECTION C-C SCALE 4

(15) SPRING DEVELOPED VIEW

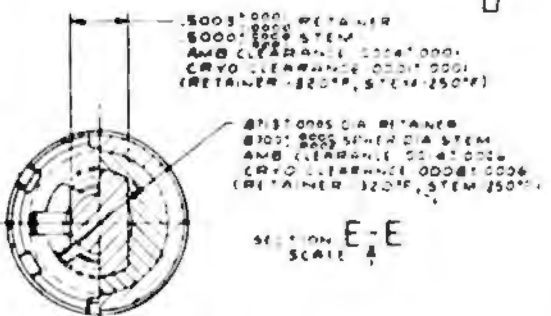

SECTION E-E SCALE 4

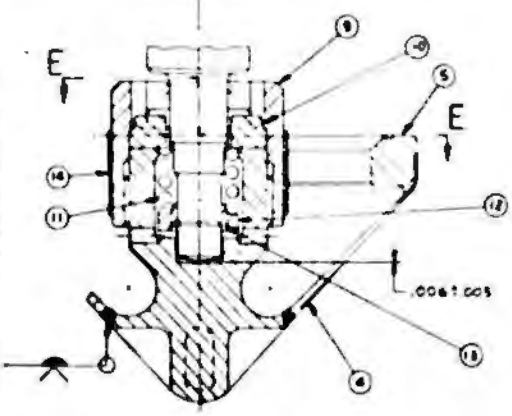

SECTION B-B SCALE 4

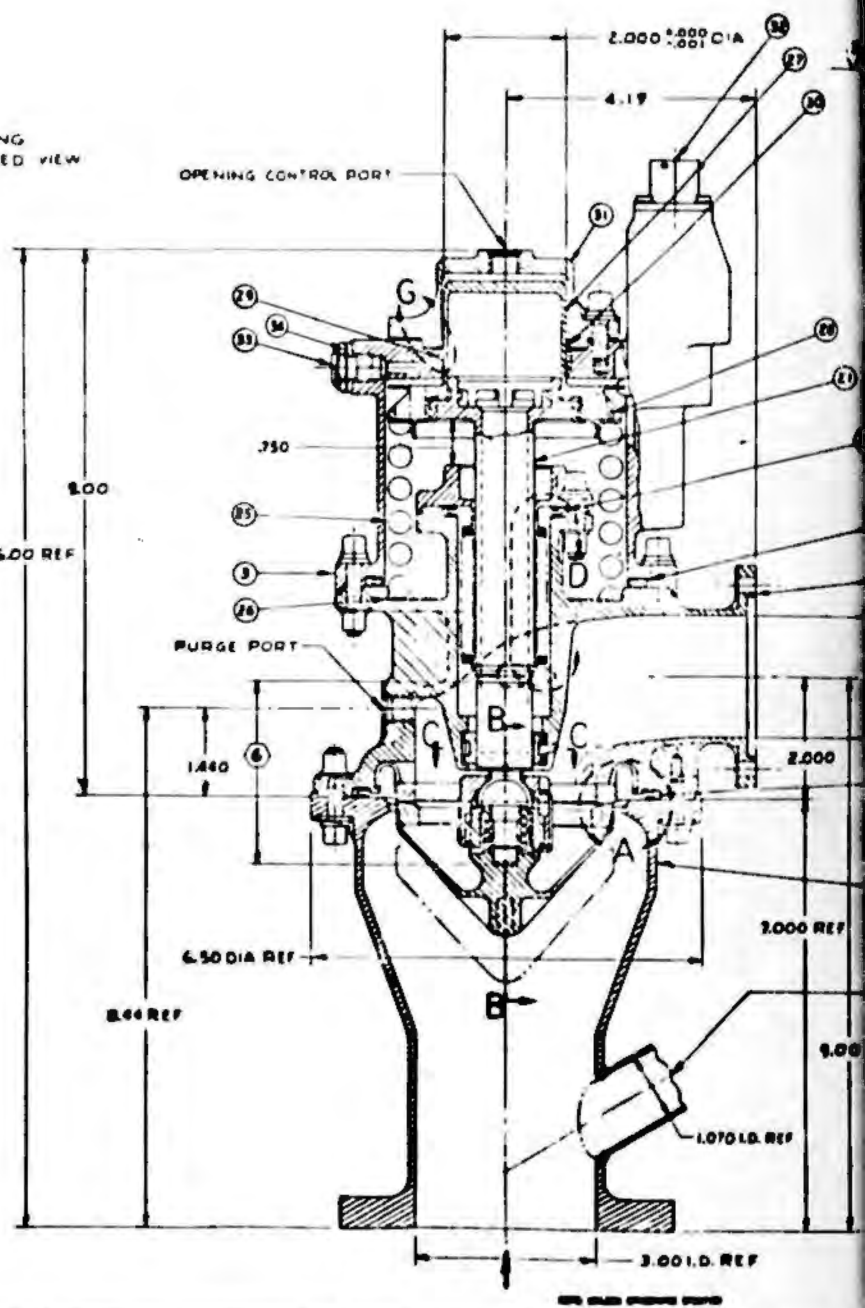

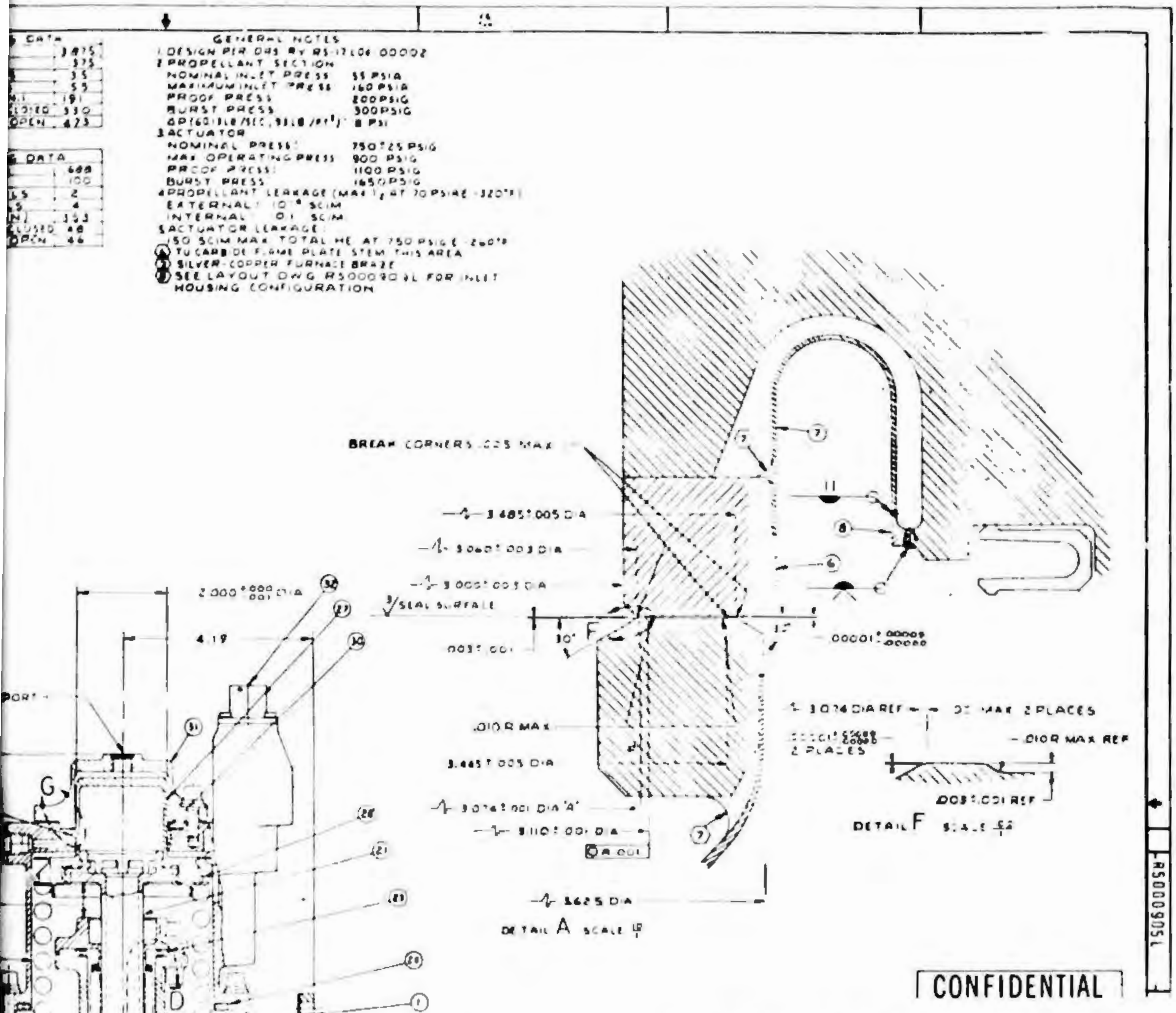

CONFIDENTIAL

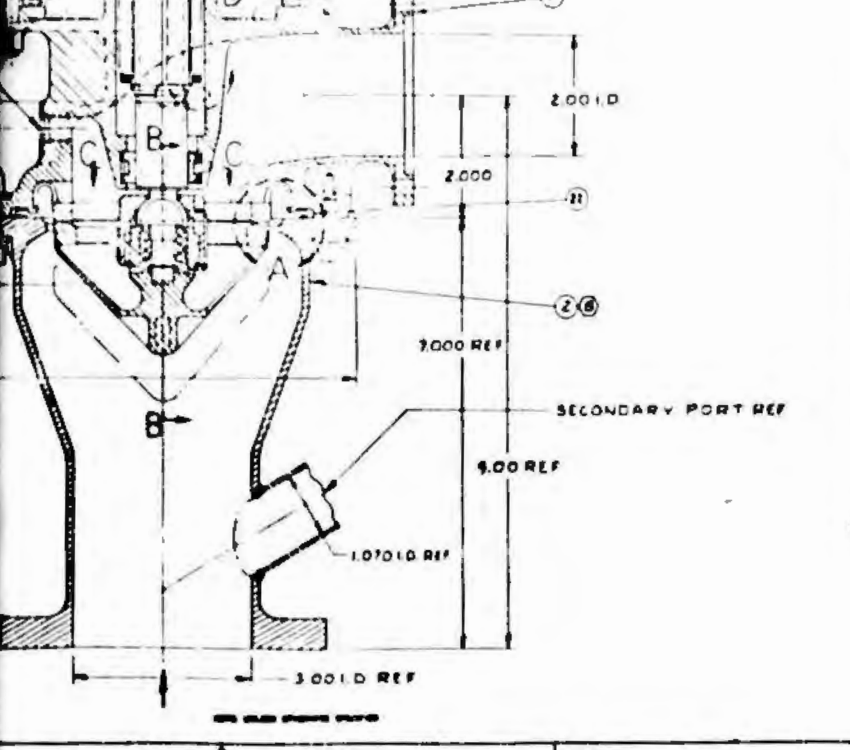

34	SEAL, HARRISON P/N 1210024		
33	VALVE, VENT P/N 552994		
32	POSITION INDICATOR		
31	CAP	6061 AL ALLOY	ANODIZE
30	SEAL	MYLAR	
29	GUIDE	FEP TEFLON	
28	RING, TAB LOCKING	302 CRES	PASSIVATE
27	PISTON	A 286 CRES	
26	WASHER	302 CRES	
25	SPRING	INCO 718	PASSIVATE
24	SEAL, NAFLEX	INCO 718	TEFLON DISPERSION
23	SEAL, NAFLEX	INCO 718	GOLD PLATE
22	SEAL, NAFLEX	INCO 718	GOLD PLATE
21	STEM	INCO 718	PASSIVATE
20	FLANGE	INCO 718	
19	BELLOWS	INCO 718	
18	PIN	303 CRES BAR	PASSIVATE
17	BEARING	BERYLLIUM COPPER	GOLD PLATE
16	BEARING	BERYLLIUM COPPER	GOLD PLATE
15	SPRING, RADIAL	BERYLLIUM COPPER	
14	SLEEVE, LOCK	347 CRES TUBE	PASSIVATE
13	RING	BERYLLIUM COPPER	
12	RETAINER	303 CRES BAR	PASSIVATE
11	SPRING	INCO 718	PASSIVATE
10	RETAINER, POPPET	BERYLLIUM COPPER	
9	BEARING, POPPET	BERYLLIUM COPPER	GOLD PLATE
8	RING	INCO 718	PASSIVATE
7	DIAPHRAGM	INCO 718	
6	SEAT, BODY	TITANIUM CARBIDE	
5	SEAT, POPPET	TITANIUM CARBIDE	
4	SHELL, POPPET	INCO 718	PASSIVATE
3	HOUSING, ACTUATOR	6061 AL ALLOY	ANODIZE
2	HOUSING, INLET	6061 AL ALLOY	ANODIZE
1	BODY, VALVE	MONEL INCO 718 CRES	PASSIVATE
NO	DESCRIPTION	MATERIAL	FINISH

Figure 194. Main Engine Oxidizer Valve (U)

CONFIDENTIAL

2

CONFIDENTIAL

BELLOWS DATA	
OUTSIDE DIA	1.40
INSIDE DIA	.990±.010
NO PLYS	1
WALL THICKNESS	.008
ACTIVE CONVOLUTIONS	20
INSTALLED LENGTH	1.56
INSTALLED LOAD (LB)	38.5
RATE (LB/IN)	86

SPRING DATA	[illegible]	[illegible]
OUTSIDE DIA	1.875	.438
WIRE DIA	.375	.090
ACTIVE COILS	2	2.5
TOTAL COILS	4	4.5
RATE (LB/IN)	[illegible]	212
LOAD, VALVE CLOSED	211	31
LOAD, VALVE OPEN	473	30

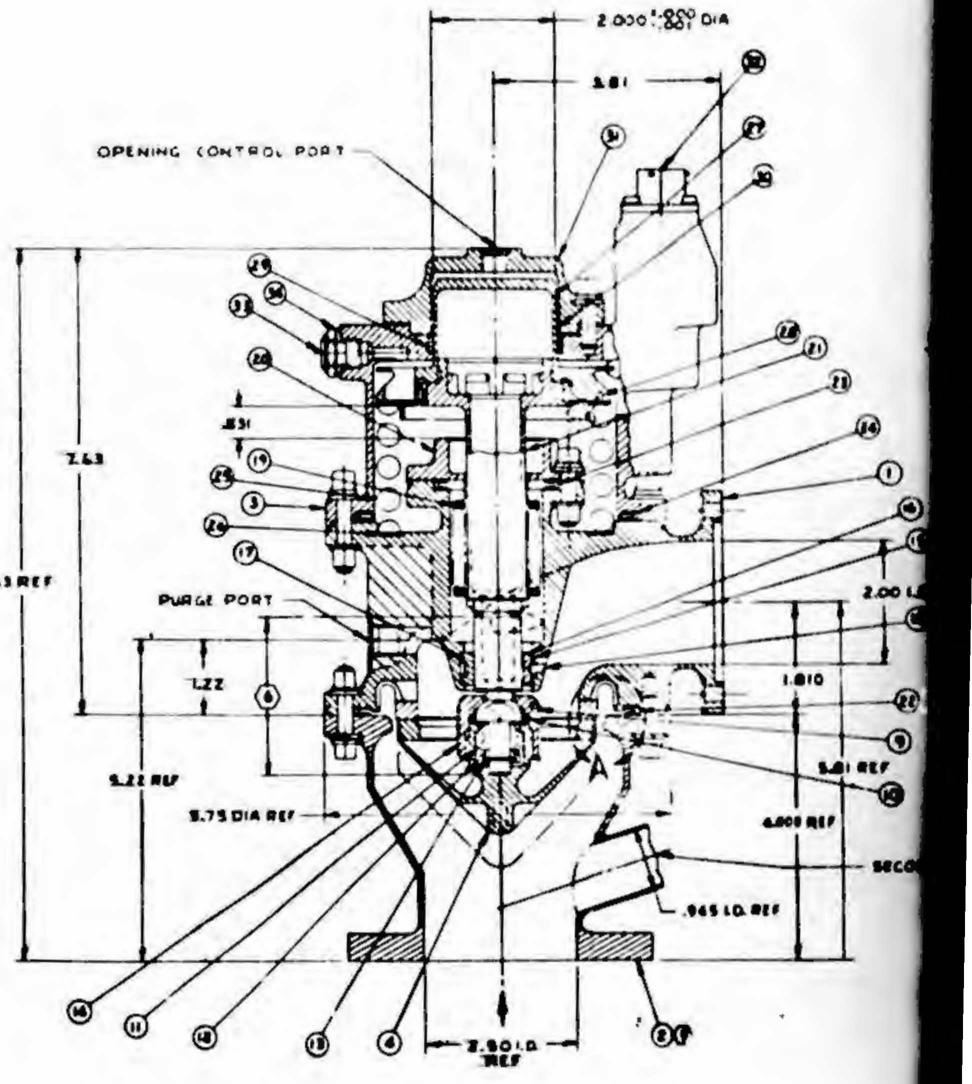

SEE LAYOUT DWG R5000910L FOR INL
HOUSING CONFIGURATION
SEE LAYOUT DWG R5000905L FOR L/M &
SILVER COPPER FURNACE BRAZE
TU CARBIDE FLAME PLATE STEM THI
ACTUATOR LEAKAGE:
150 SCIM MAX. TOTAL HE AT 750 PSIG
4. PROPELLANT LEAKAGE: MAX. H_2 AT 75
EXTERNAL: 7 SCIM
INTERNAL: 100 SCIM
3. ACTUATOR
NOMINAL PRESS: 750±25 PS
MAX. OPERATING PRESS: 900 PSIG
PROOF PRESS: 1100 PSIG
BURST PRESS: 1650 PSIG
2. PROPELLANT SECTION
NOMINAL INLET PRESS: 65 PSIA
MAXIMUM INLET PRESS: 100 PSIA
PROOF PRESS: 130 PSIG
BURST PRESS: 195 PSIG
ΔP (5.01 LB/SEC., 3.86 LB/FT.³): 5 PSI
1. DESIGN PER DRS RY RS-17L04-00001

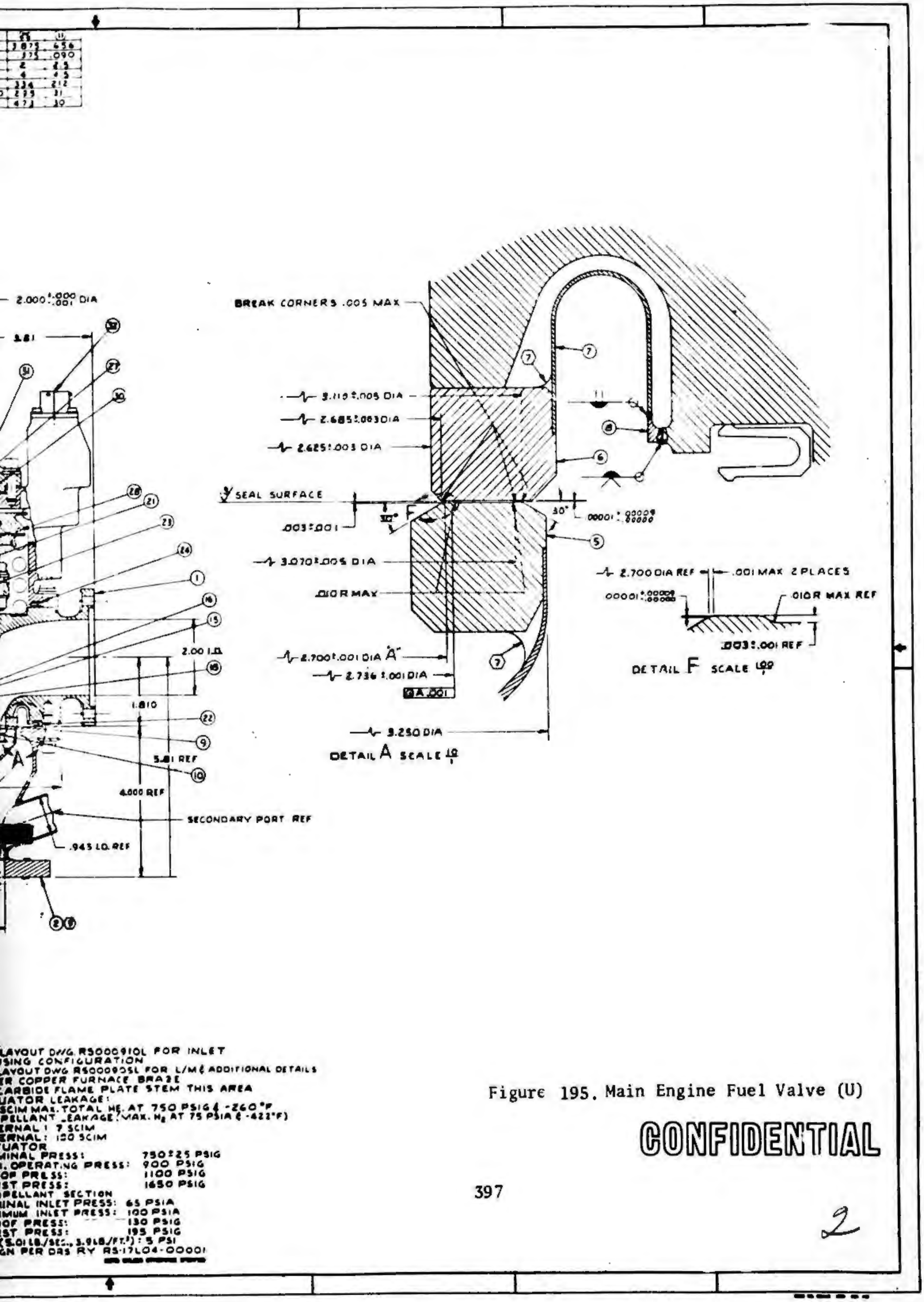

Figure 195. Main Engine Fuel Valve (U)

CONFIDENTIAL

2

CONFIDENTIAL

BELLOWS DATA	
OUTSIDE DIA	.75
INSIDE DIA	.485±.020
NO. PLYS	1
WALL THICKNESS	.005
ACTIVE CONVOLUTIONS	13
INSTALLED LENGTH	.870
INSTALLED LOAD	13.6
RATE (LB./IN.)	68

SPRING DATA	25	11
OUTSIDE DIA	3.000	.375
WIRE DIA	.3125	.063
ACTIVE COILS	2	2
TOTAL COILS	4	4
RATE (LB./IN.)	352	360
LOAD, VALVE CLOSED	235	17
LOAD, VALVE OPEN	323	15

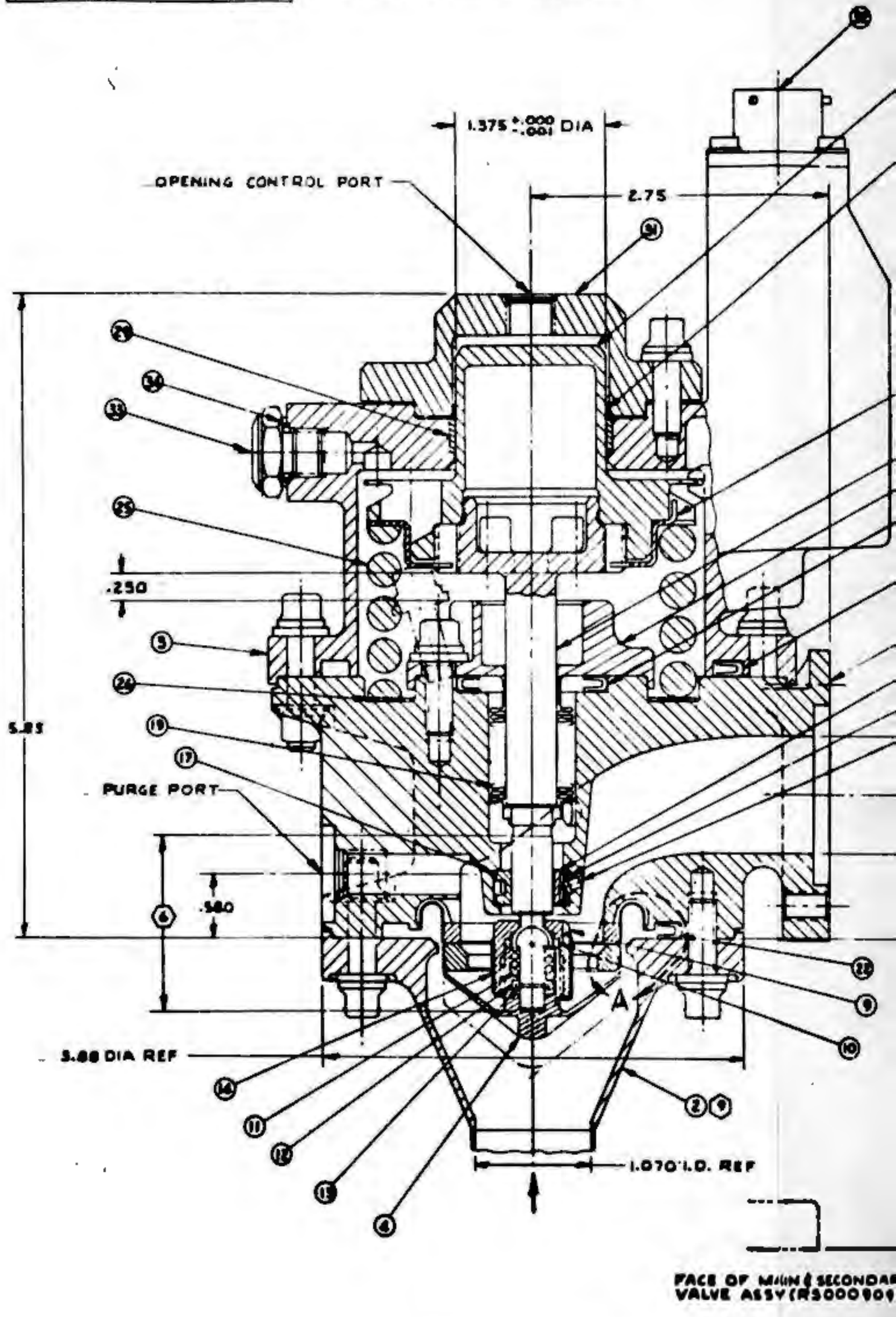

SEE LAYOUT DWG RS00090L FOR INLET HSG. CONF
SEE LAYOUT DWG RS00090SL FOR L/M & ADDITIONAL
SILVER COPPER FURNACE BRAZE
TU CARBIDE FLAME PLATE STEM THIS AREA
5. ACTUATOR LEAKAGE:
150 SCIM MAX. TOTAL HE. AT 750 PSIG & -260°F
4. PROPELLANT LEAKAGE (MAX. F_2 AT 70 PSIA & -320°
EXTERNAL: 10^{-4} SCIM
INTERNAL: 0.1 SCIM
3. ACTUATOR
NOMINAL PRESS: 750±25 PSIG
MAX. OPERATING PRESS: 900 PSIG
PROOF PRESS: 1100 PSIG
BURST PRESS: 1650 PSIG
2. PROPELLANT SECTION
NOMINAL INLET PRESS: 55 PSIA
MAXIMUM INLET PRESS: 160 PSIA
PROOF PRESS: 200 PSIG
BURST PRESS: 300 PSIG
ΔP (6.71 LB./SEC., 93 LB./FT.^{3}): 5 PSI
1. DESIGN PER DRS RY RS-17L04-00006

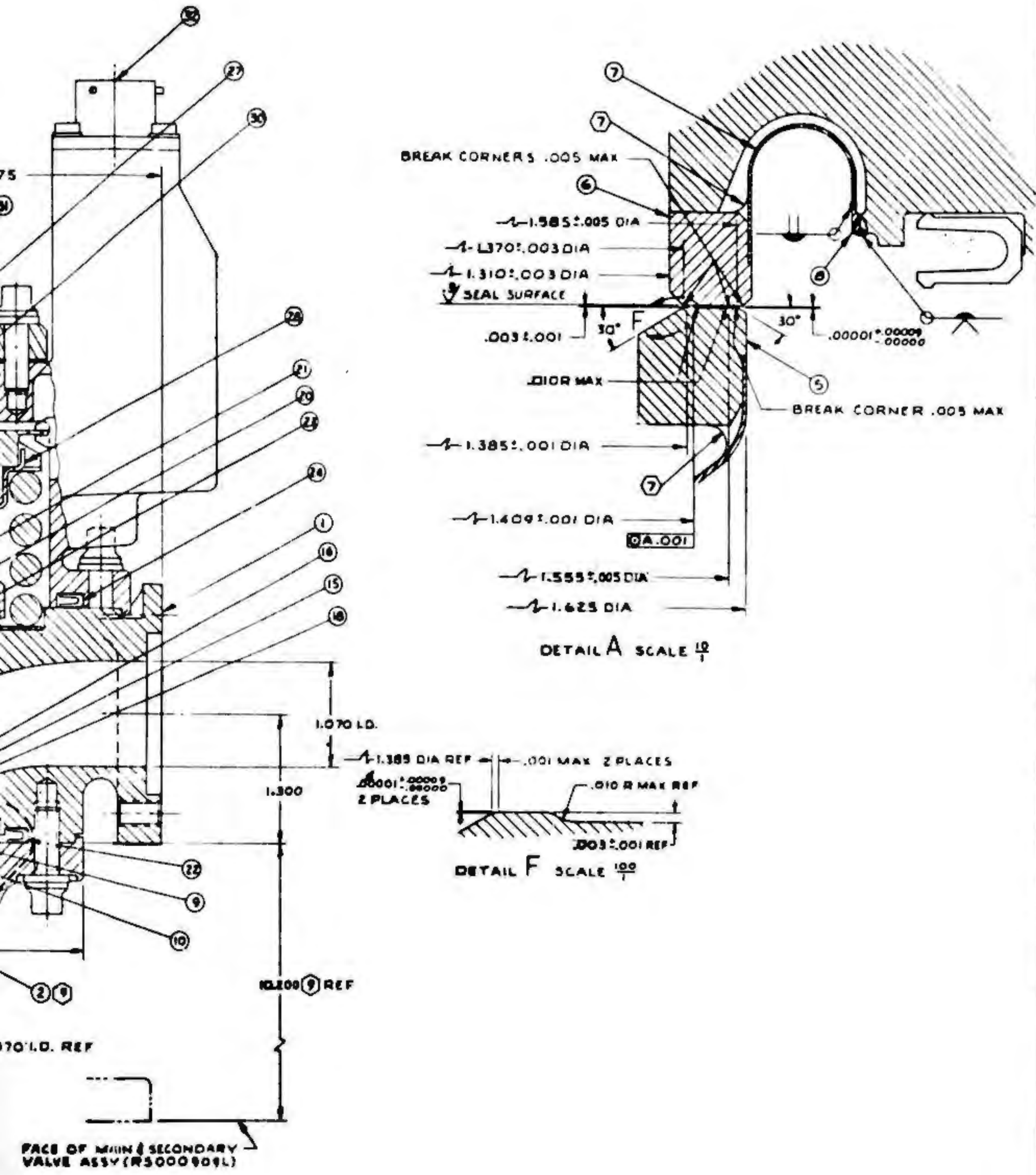

Figure 196. Secondary Engine Oxidizer Valve (U)

2

CONFIDENTIAL

BELLOWS DATA	
OUTSIDE DIA	.75
INSIDE DIA	.4857.020
NO. PLYS	1
WALL THICKNESS	.005
ACTIVE CONVOLUTIONS	13
INSTALLED LENGTH	.870
INSTALLED LOAD	13.6
RATE (LB/IN)	68

SPRING DATA	8	11
OUTSIDE DIA	1.000	.375
WIRE DIA	.1125	.063
ACTIVE COILS	2	2
TOTAL COILS	4	4
RATE (LB/IN)	152	360
LOAD,VALVE CLOSED	235	17
LOAD,VALVE OPEN	323	19

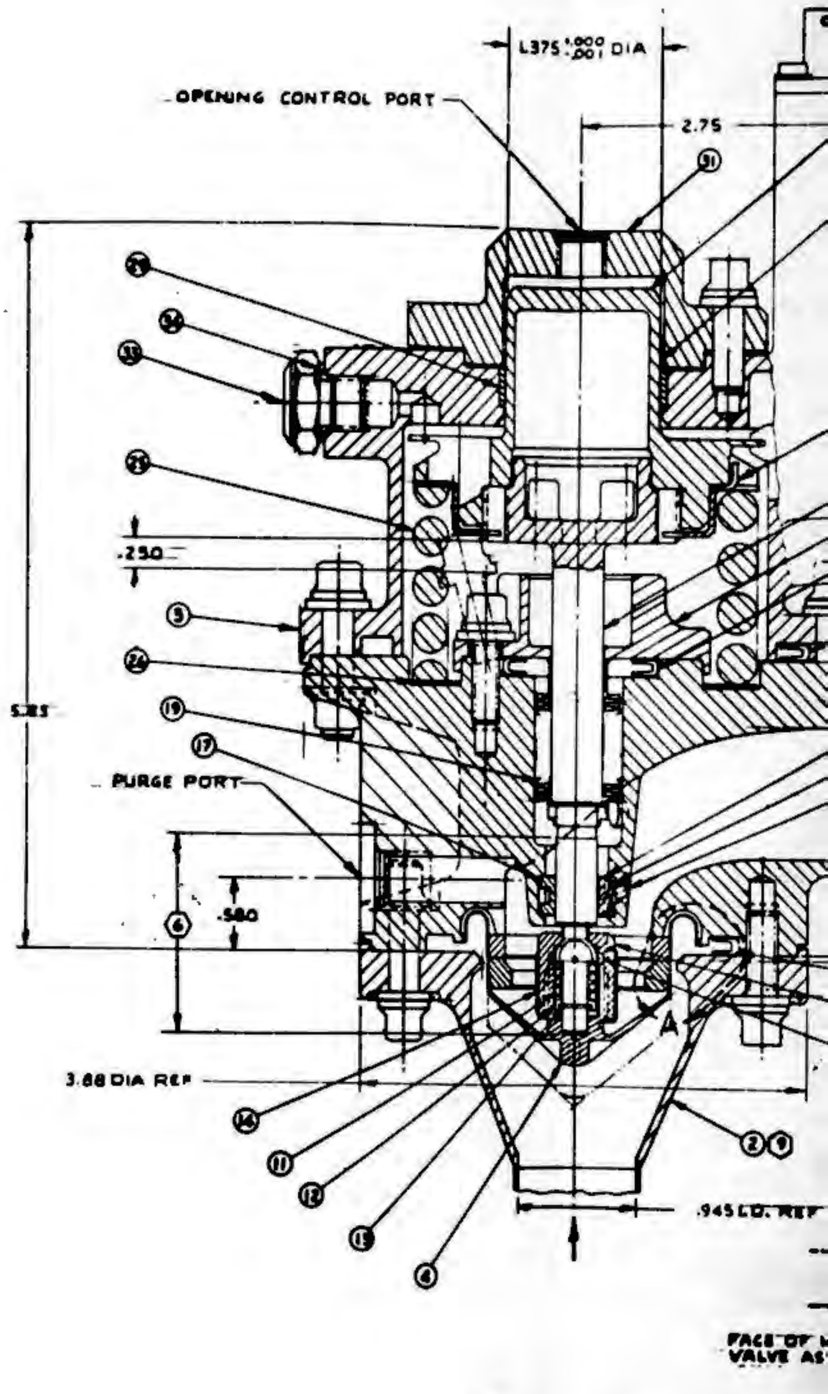

FACE OF
VALVE AS

SEE LAYOUT DWG RS000910L FOR IN
SEE LAYOUT DWG RS000905L FOR L/
SILVER COPPER FURNACE BRAZE
TU CARBIDE FLAME PLATE STEM
5. ACTUATOR LEAKAGE:
150 SCIM MAX. TOTAL HE. AT 750 P
4. PROPELLANT LEAKAGE (MAX. H_2 AT
EXTERNAL : 7 SCIM
INTERNAL : 100 SCIM
3. ACTUATOR
NOMINAL PRESS: 750±25
MAX. OPERATING PRESS: 900 PS
PROOF PRESS: 1100 PS
BURST PRESS: 1650 PS
2. PROPELLANT SECTION
NOMINAL INLET PRESS: 65 PSIA
MAXIMUM INLET PRESS: 100 PSIA
PROOF PRESS: 130 PSIG
BURST PRESS: 195 PSIG
ΔP (.55 LB./SEC., 3.9 LB./FT.³): 5 P
1. DESIGN PER DRS RY RS-17L04-000

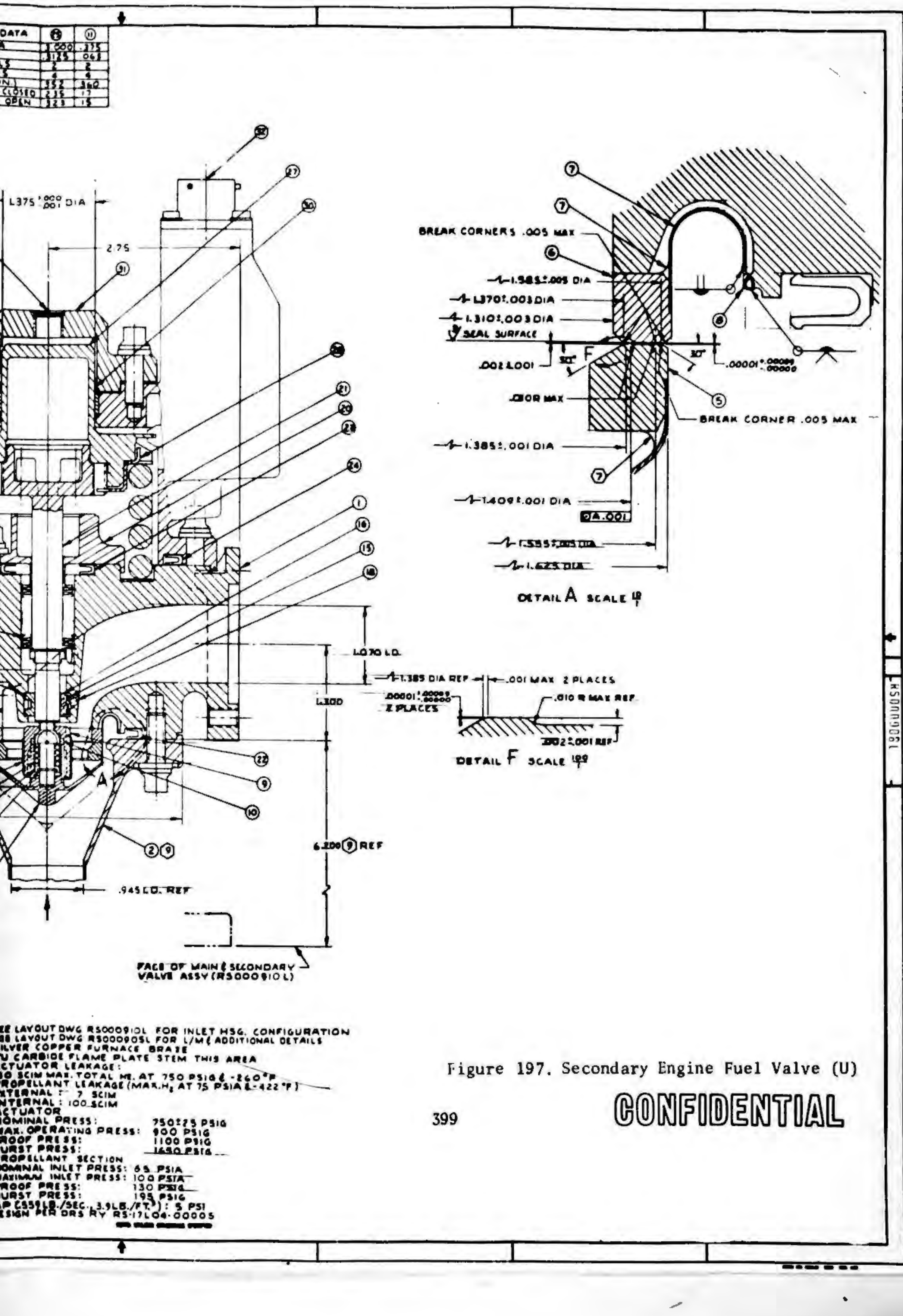

Figure 197. Secondary Engine Fuel Valve (U)

CONFIDENTIAL

2

CONFIDENTIAL

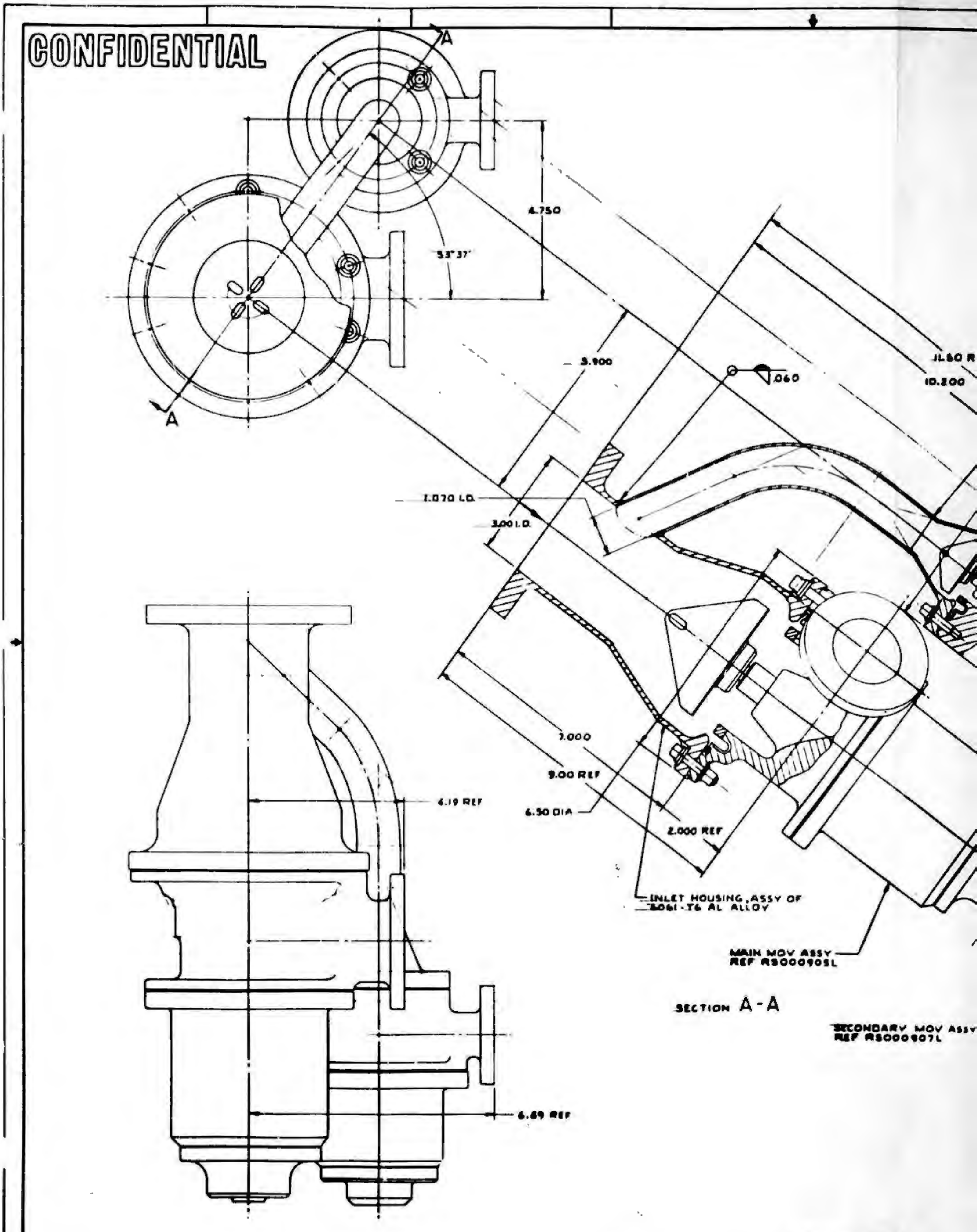

SECTION A-A

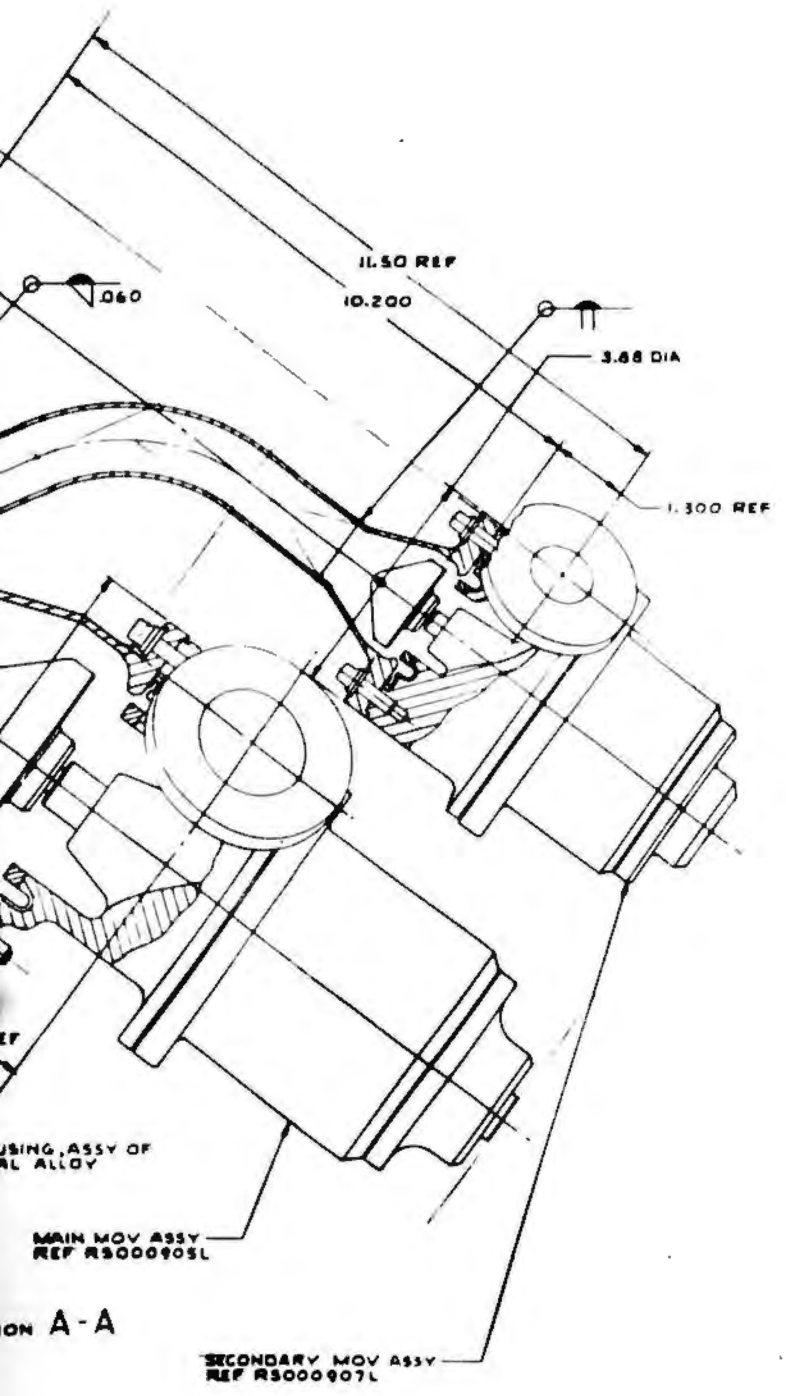

RS000909L

Figure 198. Main Oxidizer Valve Assembly Inlet Manifold Configuration (U) (U)

CONFIDENTIAL

2

CONFIDENTIAL

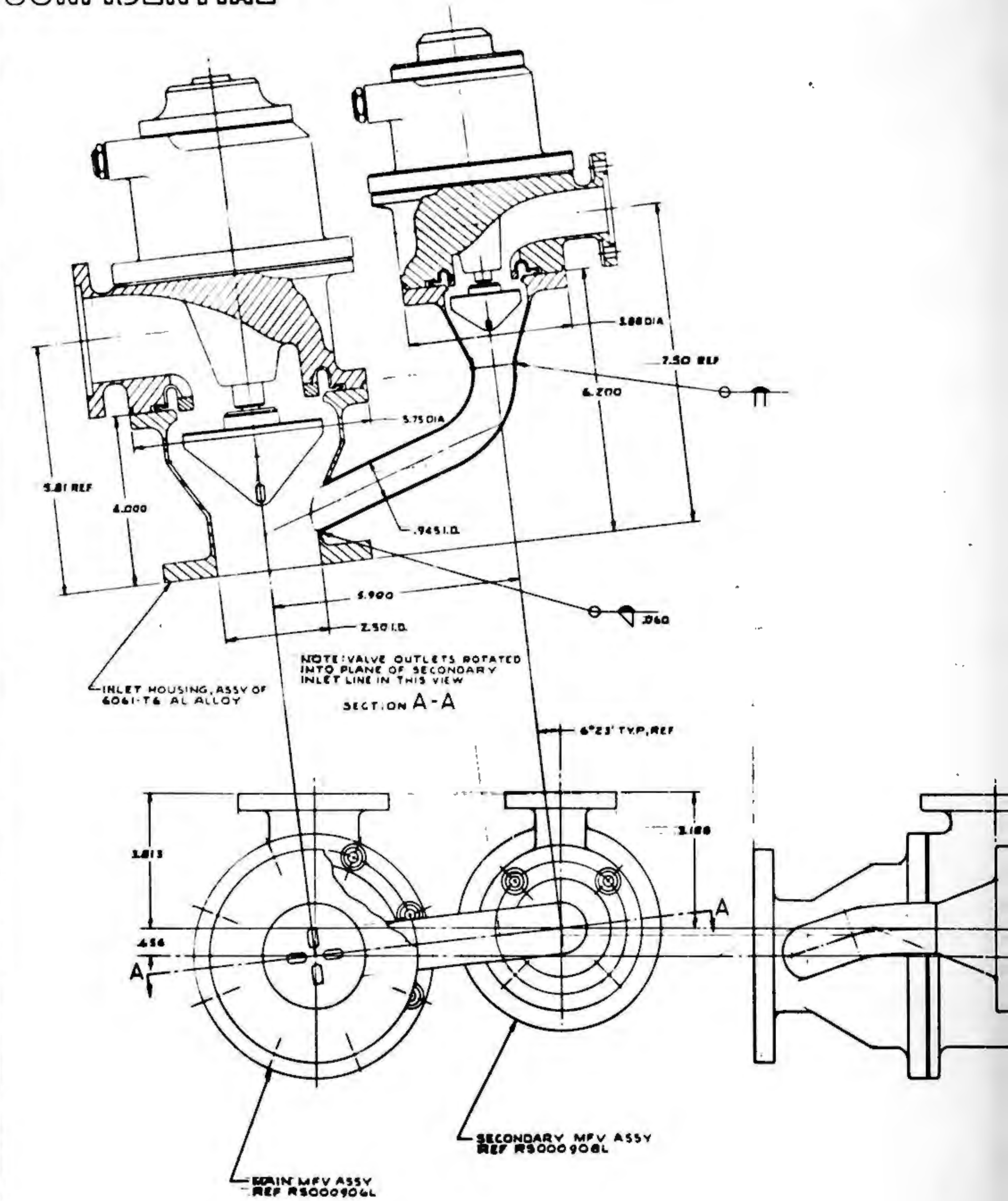

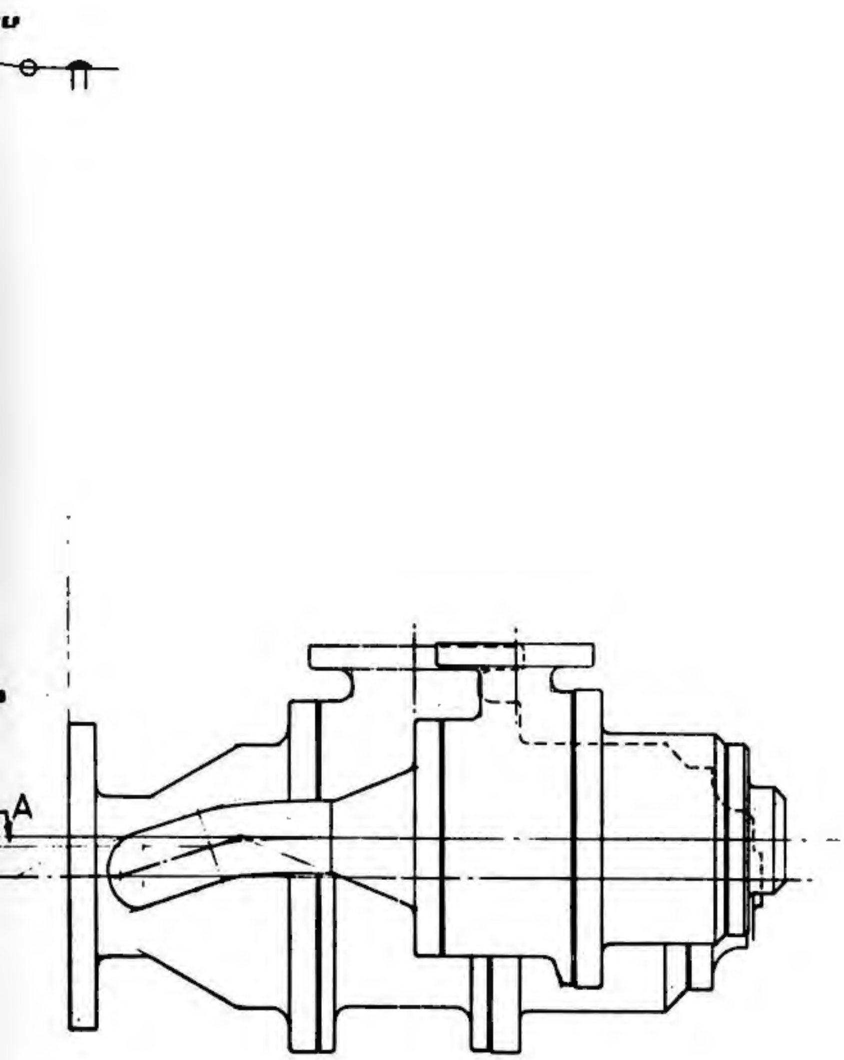

Figure 199. Main Fuel Valve Assembly
Inlet Manifold Configuration (U)

2

(C) The poppet-type valve was selected because, compared with ball, butterfly, gate, slide, or other valve types, it is the only valve in which sliding between the valving elements at valve closure can be held to the minimum required to maintain acceptable shutoff leakage. Three different valve sizes are used (1, 2-1/2, and 3 inches), all of which incorporate the same basic design features scaled to the individual valve requirements.

(C) The basic approach to the subject valve design was dictated primarily by the engine system requirement for low shutoff leakage of a corrosive, cryogenic propellant, throughout a relatively long duty cycle with a minimum-weight valve. Rocketdyne's Nomad system experience and NASA's various liquid fluorine system test programs (Ref. 19 and 8) dictated that all valving elements exposed to the propellant be metal. Rocketdyne's poppet and seat development program (Ref. 10) has shown that, for lightly loaded seats, the only metal-to-metal type that will operate without scrubbing or degradating the seat is the flat-faced poppet. In the preliminary design concept study, a "flow-to-close," "push-off" type of poppet configuration was selected for the following reasons: (1) "flow-to-close" provides higher seat loading (lower leakage) with higher propellant inlet pressures than the "flow-to-open" design, (2) it permits placing the poppet stem guide close to the poppet for a minimum of overhang when seat contact is made, thereby reducing poppet-to-seat scrubbing, and (3) pressure drop through the valve is lower when the stem is on the downstream side of the poppet because the stem provides better continuity of flow area throughout the valve and, correspondingly, less turbulence.

(U) Other basic design principles considered critical to successful performance are a minimum of rubbing surfaces in the propellant and the elimination of propellant traps which cannot be drained or purged. Details of these features in the subject valve design are treated in the following discussion.

(1) Valve Seat Design

(U) A basic seat configuration was derived in a preliminary design concept study (Ref. 11). Details of seat land configuration (width, finish, edge condition, etc.) were designed utilizing concepts developed in the poppet and seat development program and summarized in Ref. 10. The only other details were poppet and seat materials and the method of mounting poppet and seat to limit poppet-to-seat scrubbing.

(C) Titanium carbide material was selected for both the poppet and seat based on three significant considerations:

1. Compatibility with liquid fluorine has been demonstrated by Rocketdyne in the Nomad main oxidizer valve, by Pratt and Whitney in liquid fluorine pump shaft seals, and by NASA in materials compatibility tests (Ref. 8 and 19).
2. Exceptional hardness tolerates more scrubbing between poppet and seat without degradation of the sealing surface.
3. Exceptional hardness also has greater resistance to damage from contaminant impingement and propellant erosion. The material has further advantages for a poppet and seat design in that the material is a very fine grained, homogeneous, and easily finished by diamond lapping to the 0.3-microinch surface finish required for the subject valve seat. The relatively low density (approximately 70 percent that of steel) of the material reduces the inertia forces in the poppet, and the relatively high modulus of elasticity (approximately twice that of steel) enhances the rigidity of poppet and seat against deflection under load. The material cannot be welded, but it is readily brazed with a variety of alloys which are compatible with liquid fluorine.

(U) Reference 10 delineates the amount of relative lateral motion between poppet and seat which can be tolerated: 0.002 inch radially and 0.002 inch circumferentially.

(2) Seat Installation

(U) The valve seat is held in the housing by means of a diaphragm brazed to the seat and welded to the valve housing. This arrangement provides a positive seal against internal leakage between seat and housing and virtually isolates valve body thermal and structural deflections from the seat. The seat is supported in the axial direction by lands machined in the valve body and installed with a slight preload on these lands to eliminate fretting between seat and housing when the valve is open and propellant is flowing. The body-to-seat configuration is so arranged that the seat sealing surface projects outside the body to allow flat lapping of the seat without special tooling. This feature is designed as an aid in both fabrication of new valves and servicing of used valves where only lapping is required. Complete seat replacement may be readily accomplished by cutting out the diaphragm and rewelding a new diaphragm seat brazed assembly. Braze and weld joints are designed to eliminate cracks which cannot be cleaned. The body diaphragm cavity downstream of the seat is adequately relieved between support lands to allow propellant drainage and purge.

(3) Poppet Installation

(U) Dominant features of the poppet design and installation include a lightweight poppet shell, ball loading, and control of radial clearance, rotation, and cocking. A flexure between stem and poppet was originally considered. The flexure was dropped in favor of the ball-loading device

(U) primarily because of its eccentric load characteristics and fastener design problems. Eccentric loading of the poppet by the flexure is created by off-nominal parallelism and normality conditions in the flexure and its several retaining details. The resultant nonparallel condition between poppet and seat is reflected as an eccentric load into the seat from the poppet flexure which, under low seat loading conditions, introduces a wide variation in seating pressure around the periphery of the seat. The fastener problem has to do with the space available (especially in the 1-inch valve), and the number and reliability of locking devices required.

(U) The poppet loading device was designed to meet the lateral motion restriction and also provide substantially concentric transfer of stem load to the poppet by use of the ball joint. (Note that the requirement for a centered stem load exists at low line pressures where seat stresses are generated almost entirely by actuator forces applied through the stem, i.e., little contribution from propellant inlet pressure.)

(C) The basic elements of the poppet include the INCO 718 poppet body, a beryllium copper retainer, and a beryllium copper bearing. The bearing is threaded to the poppet body, firmly locking the three parts together, and is positively locked against loosening by a tab-locking sleeve. Clearance between the beryllium copper retainer and stem is designed to permit a 70 F temperature difference while limiting relative motion between poppet and seat to 0.002 inch, both in the radial and circumferential direction. Cocking between poppet and stem is limited to that required to allow the poppet to seat without restraint by a controlled diametral clearance at the lower end of the stem. A coil spring between the beryllium copper retainer and stem preloads the poppet against the end of the stem when the valve is open to prevent excessive poppet flutter. The clearance between the end of the stem and poppet, in turn, allows free self-alignment of the poppet. Fretting between poppet and stem is prevented by flame plating with tungsten carbide and grinding the stem bearing surfaces.

(U) Poppet assembly to the stem is accomplished by holding the valve open and, working between poppet and seat, torquing the bearing to the poppet and bending the locking tabs. Special protective devices would be provided to protect the seating surfaces during this operation.

(C) A feature of the ball-loading detail pertains to the location of the center of the ball, which is located in the plane of the seat sealing surface. This allows cocking of the poppet to occur for self-alignment without introducing radial scrubbing between the poppet and seat. The internal part of the poppet body, however, is below the titanium carbide sealing surface, which allows flat lapping of the seat after fabrication without tooling limitations. A large opening between the titanium carbide portion of the poppet and internal details and drilled cross holes in the inner portion of the poppet body permits propellant drainage and purge.

(4) Poppet Stem Guide

(C) Design of the poppet stem guide was intended to provide the minimum possible lateral motion of the poppet and the minimum number of bearing surfaces in the propellant. Virtual elimination of lateral motion is accomplished by providing a spring-loaded guide close to the seat and a close fitting guide at the other end of the stem on the actuator piston. This feature also results in only one guide operating in the propellant and, because of the long span between guides, relatively low bearing loads. Segmented beryllium copper inserts operate on a flame-plated portion of the stem to provide a trouble-free installation.

(5) Stem Sealing Bellows

(C) The single-ply, INCO 718 bellows which functions as a dynamic stem seal was conservatively designed for a life of 10,000 cycles using the advanced design technology developed in Ref. 16. The bellows is used

(C) in compression for approximately 85 percent of its stroke, and in extension for approximately 15 percent of its stroke. The bellows is butt welded at each end to provide the cleanest possible configuration and adequately vented to the valve outlet to permit propellant drainage and purge. A bolted flange utilizing a gold-plated Naflex seal provides a seal to the valve body which may be removed for valve servicing.

(6) Actuator

(U) A double-acting piston actuator was originally considered. This design was revised to a single-acting piston utilizing helium pressure to open and a spring to close. A stronger spring was incorporated which provides safety factors of approximately 3 on closing and 10 on opening over the maximum anticipated friction (safety factor = net available actuator force ÷ maximum friction; no line pressure assist on closing, opening against 160 psig).

(U) The double-acting actuator has additional seal friction and in the event of a loss of closing control pressure (fail-safe closing), has a safety factor of only approximately 2 for the same spring. Further arguments against the double-acting actuator include the larger, heavier, more complicated actuator in addition to control system complexity, particularly the four-way control valves required for a double-acting actuator as compared to three-way valves for a single-acting actuator.

(U) The spring is located outside the propellant cavity to reduce cleaning and corrosion problems and to allow for ease of installation without entering the propellant cavity. The moving end of the spring is located on a flange of the actuator piston which is installed and locked to the poppet stem while thespring is held compressed. The piston is attached to the poppet stem with a large thread and locked with a tab-locking ring. A pilot diameter is provided and bearing faces held normal to provide alignment for the poppet. Lightening holes in the piston and stem flanges

(U) reduce the poppet inertia loads. The overall weight reduction in the poppet-stem-piston assembly eliminated the need to provide a flexible coupling between the stem and piston as considered in the conceptual design study.

(U) The dynamic piston seals are formed from Mylar sheet, this design having been successfully used in main propellant valves for the J-2 and F-1 engines for both linear piston and rod seals. The Teflon guide provides support for the seal and a guide for the poppet stem. Its location in the actuator cylinder provides a long span between stem guides to reduce radial loads and poppet radial motion.

(U) Valve stroke is established by the gap between the poppet stem flange and bellows flange. Piston loads at the full-open position, therefore, are taken through a relatively heavy section of the bellows flange to the valve body.

(U) The actuator spring cavity is sealed against external pressure to prevent entrance of moisture and contamination. A relief valve allows venting of any piston seal leakage and normally holds a slight positive pressure in the spring cavity.

(7) Static Seals

(U) Two Naflex-type, pressure-actuated seals are used on the propellant section. They are fabricated from INCO 718 and are gold plated. Deep flange sections at the seals and conservative bolting keep flange deflections to a minimum for a reliable seal. Naflex seals were selected in comparison to other designs such as crush gaskets, Conoseals, or bobbin seals because of Rocketdyne's extensive experience with them and their relative ease of replacement.

(U) The purge port is machined for use with a Harrison metal-plated K seal or equivalent.

(U) The actuator spring housing is sealed with a Teflon-coated Naflex seal for positive isolation of moisture and contamination. The spring housing vent valve is sealed with a Teflon-coated K seal.

(8) Position Instrumentation

(U) Position switches are used to show the full-open and full-closed valve position and are operated by a direct mechanical link to the actuator piston. The switche are mounted in a portion of the actuator spring cavity which isolates them from the propellant and control atmosphere. The electrical connector is per MIL-C-27599.

(9) Inlet Housing--Manifold Assembly

(U) The inlet housing is part of the manifold assembly which connects the engine system inlet to the propellant feed system. This design yields the best configuration for minimum pressure drop, weight and number of connections, while allowing independent replacement of valves on the engine.

(10) Internal Leakage vs Contamination and Life

(C) The seat for the subject valves has been designed to maintain exceptionally low leakage after a relatively long duty cycle. The main engine oxidizer valve, in particular, must not exceed 0.1 scim after 1530 cycles, including 31 engine firings spread intermittently over a 14-day period. Scrubbing of the seating surfaces on impact and liftoff is the most important factor to be considered in the seat designed to meet this requirement. A large, highly loaded seat is unacceptable because of weight and space limitations. Rocketdyne's poppet and seat development program has demonstrated that the seat incorporated in this valve will meet the leakage and life cycle requirements as long as contamination is held

(C) within definite limits. The titanium carbide seat hardness prevents degradation or erosion from any anticipated particles flowing past the seat. Particle entrapment, however, is a possibility which may be, within reasonable probability limits, calculated by statistical methods.

(U) A simplified statistical examination of the main engine oxidizer valve seat was made, based on two level of particulate contamination considered to represent "clean" (level 4) and "dirty" (level 8) conditions (Ref. 20). The intent was to gain a better understanding of anticipated performance. The probability of the seat trapping a large (greater than 240 microns) particle and permitting catastrophic leakage (greater than 38,000 scim) is only one actuation in 1300 for level 4 and one actuation in 500 for level 8. At the other end of the scale, the probability of the seat trapping a small (10 to 20 microns) particle is approximately one actuation in 320 for level 4, and one actuation in 32 for level 8, and would result in approximately 50-scim maximum leakage. It would appear that the valve and the associated engine propellant system must be maintained somewhere between levels 4 and 8 to ensure satisfactory operation.

(U) Particulate contamination smaller than 10 microns is not expected to have a significant effect on leakage. The contamination anticipated is relatively soft compared to the seat and will not cause damage; furthermore, the contaminant will be washed away upon valve actuation under flow conditions. Also, all sliding bearing surfaces in the valve are downstream of the seat, and under flow conditions, wear particles are washed away from the seat.

(U) Results from the AFRPL Poppet and Seat Contamination Program (Ref. 17) have shown that a hard-on-soft combination of poppet and seat materials is much more able to envelop contaminants and maintain low leakage. This result was considered during initial design phase but attendant potential problems in fabricating ultra-smooth, soft metal surfaces (and also obtaining basic cyclic operation to meet the required low leakage) led to the more conservative choice of the hard carbide materials.

(C) The design for the propellant valves for the AMPS engine represents the latest state of the art in the development of low-leakage valves for high-performance systems using liquid fluorine and liquid hydrogen. The design is a poppet-type valve with an extremely hard, flat-faced poppet and seat. All parts exposed to the propellant are metal, with a single bellows used for the dynamic stem seal. Actuation is by pneumatic pressure to open, with spring and line pressure to close. No heaters are required for cryogenic operation.

c. Main Engine Pneumatic Control Assembly

(U) The main engine pneumatic system consists of a pressure regulator, a low-pressure high-capacity relief valve, a solenoid-operated isolation valve, two solenoid-operated three-way valves to control the main engine propellant valves, two solenoid-operated two-way valves to purge the propellant ducts, two filters to protect the solenoid valves, and one filter at the regulator inlet. Figure 200 shows the design details.

(C) The pneumatic pressure regulator is designed to regulate downstream pressure to 750 ±50 psig with flow demands from 0 to 0.12 lb/sec at an inlet pressure from 3600 to 900 psia.

(C) The downstream pressure is controlled by a pressurized bellows which is supplied by inlet pressure. The correct control pressure is obtained by orificing the flow into and out of the bellows cavity. The orifices were sized to provide a control pressure that compensates for the changes in supply pressure. The control pressure opposes outlet or regulated pressure; thus, if outlet pressure decreases below 750 psig the inlet flow area increases to correct the pressure decrease and, inversely, if outlet pressure increases, the inlet flow will decrease to reduce the outlet pressure.

CONFIDENTIAL
(LEGEND UNCLASSIFIED)

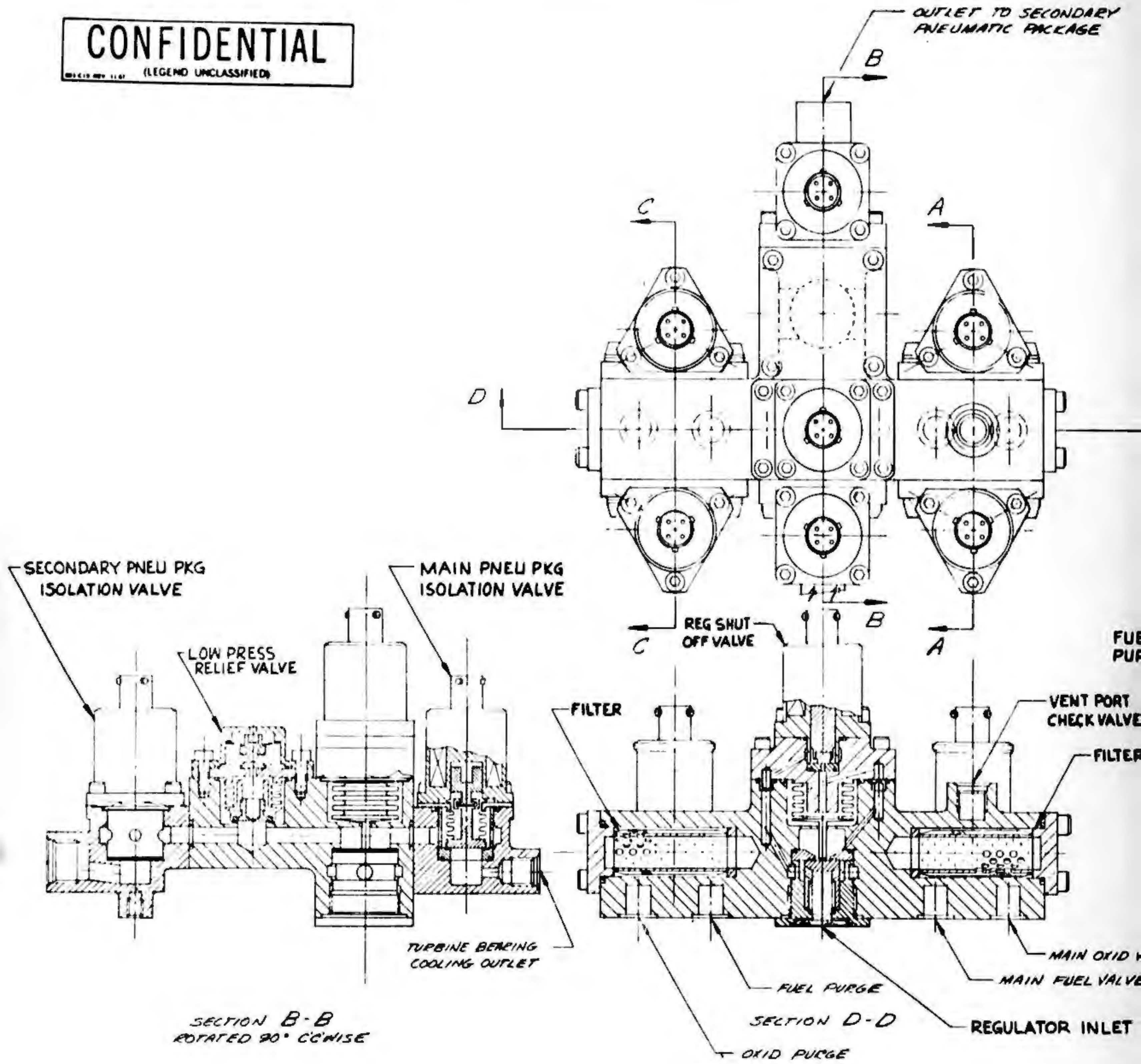

SECTION B-B
ROTATED 90° CC'WISE

SECTION D-D

LAYOUT APPROVAL BLOCK (DETAILS MUST CONFORM)		DATE
SECTION CHIEF		10/1
GROUP LEADER		
DESIGN SUPERVISOR	D.O. Kraum	9-30-69
[illegible] ENGINEER	W.A. Mayfield	9-30-69
[illegible] ENGINEER		
[illegible]		
REL ABILITY		
DESIGN REVIEW REP.		
DEVELOPMENT LAB ENGINEER		
LAYOUT STARTED		
LAYOUT COMPLETED		

1. DESIGN PER DRS RS17 L04-00009
NOTE: UNLESS OTHERWISE SPECIFIED

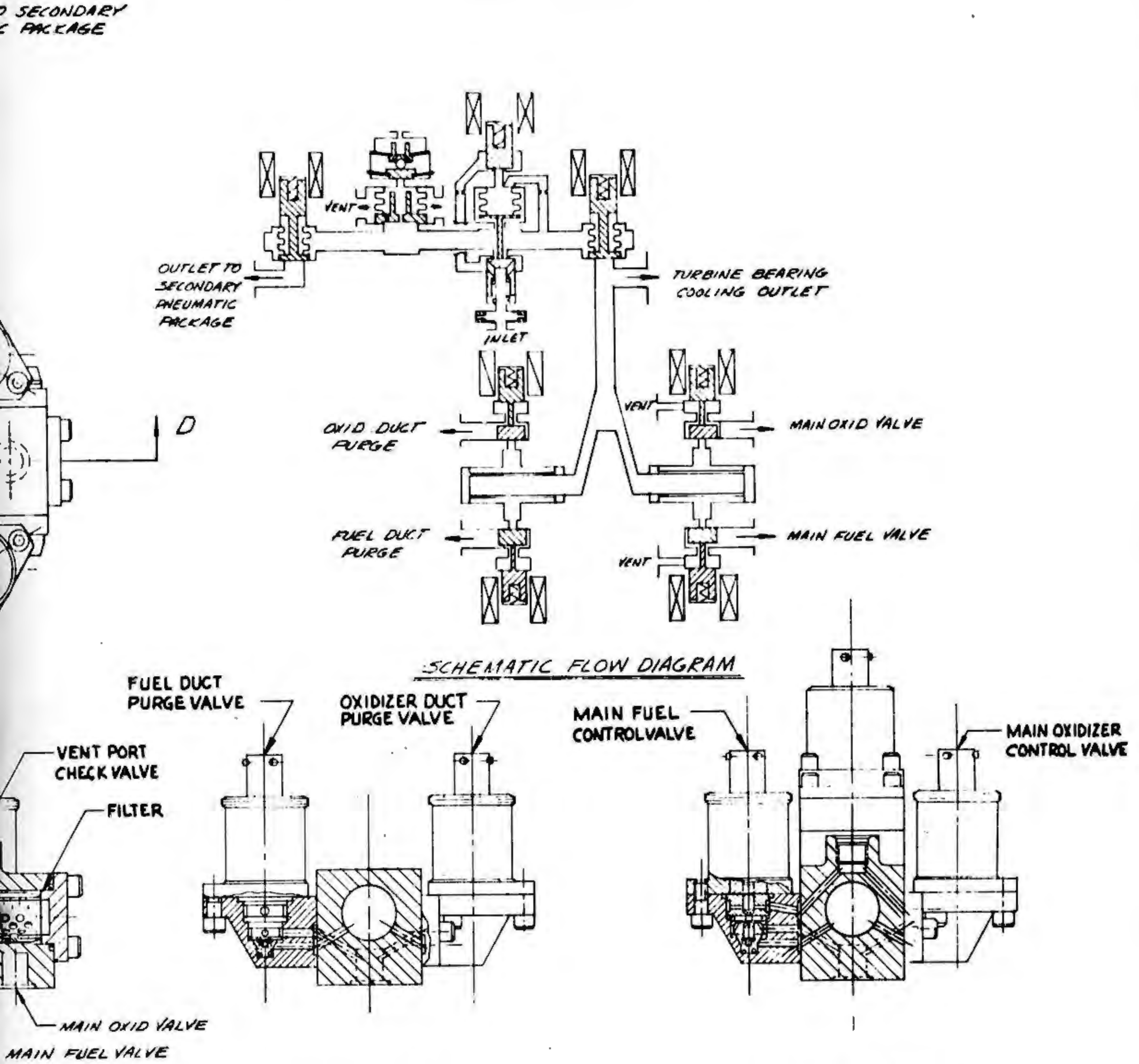

GULATOR INLET

SECTION C - C
ROTATED 90° C'WISE

SECTION A - A
ROTATED 90° C'WISE

Figure 200. Main Engine Pneumatic Control Package (U)

ONFORM)	DATE
[illegible]	10/1
[illegible]	9-30-69
[illegible]	9-30-69

R50009111

2

(U) The regulator is of all-metal construction. The materials selected are similar to those used on the J-2 regulator, which is also designed for cryogenic service. The J-2 regulator is fully qualified and has proved to be very successful on numerous flights. The poppet and seat are flat-lapped to achieve low leakage. The solenoid valve shuts off the regulator control pressure upon electrical command, thus closing the poppet to shut off downstream pressure. The poppet and seat are flat-lapped to achieve low leakage.

(C) The low-pressure relief valve is located directly downstream of the pressure regulator. The relief valve was designed to crack or start to open at 825 psig, and be fully open at 900 psig, with the flow area sufficient to expel the flow through a failed-open regulator with an upstream pressure of 3600 psia. The downstream system pressure will not exceed 900 psig even if the regulator fails wide open.

(U) The relief valve utilizes a pilot valve which relieves the balance pressure within the bellows at the crack pressure, thus unbalancing the main poppet to open.

(U) The isolation valves are located downstream of the relief valve. Their purpose is to shut off flow to the system not in use (i.e., main or secondary).

(U) The secondary isolation valve is mounted on the main engine pneumatic package for two considerations: (1) the secondary package can be shut off at the regulator to prevent an interconnect leak between the main and the secondary package from depleting the helium supply, and (2) the secondary package becomes a simple manifold mounting four solenoid valves.

(U) The isolation valves are pressure balanced by metal bellows. This design allows a large flow area, keeping the valve pressure drop to a minimum.

(U) The three-way solenoid valves supply pressure to, and vent, the main propellant valve actuating piston cavities; one for the fuel and one for the oxidizer. The valves have metal seats and poppets that are flat lapped to achieve low leakage.

(U) The two-way solenoid valves supply flow to purge the propellant ducts during engine shutdown. These valves are identical to the three-way propellant valve control valves except the vent port is blocked off.

d. Secondary Engine Pneumatic Control Assembly

(C) The secondary engine pneumatic system consists of two three-way solenoid-operated valves to control the secondary engine propellant valves, and two solenoid-operated two-way valves to purge the propellant ducts. These valves are identical to those on the main engine package except for size. The valve size has been designed, fabricated, and qualified for cryogenic service on existing Rocketdyne engine production programs; Fig. 201 shows the design details.

e. Turbine Spin Valve

(C) The turbine spin valve controls the flow of helium and hot gas to the turbine on the secondary engine. The valve is solenoid operated and, on electrical command, opens a helium port and closes a hot-gas (combustion

CONFIDENTIAL

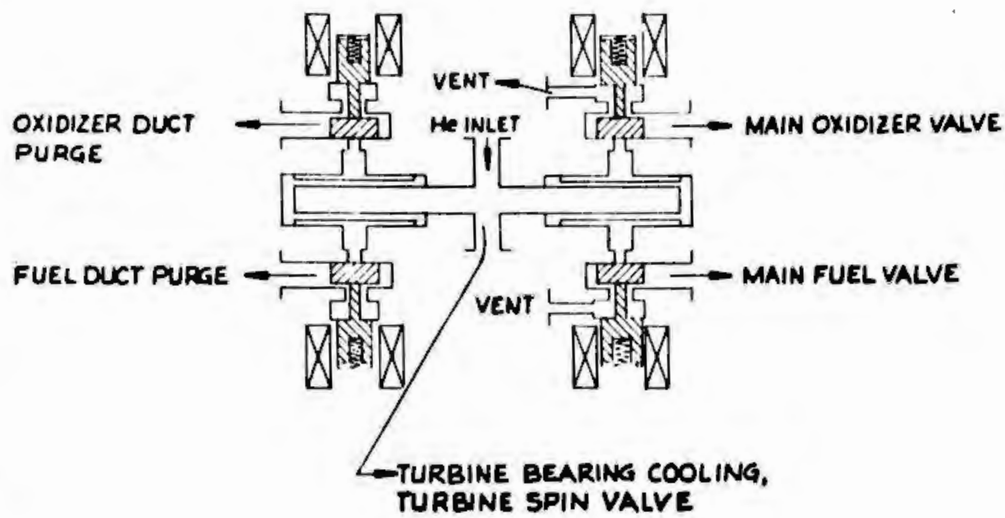

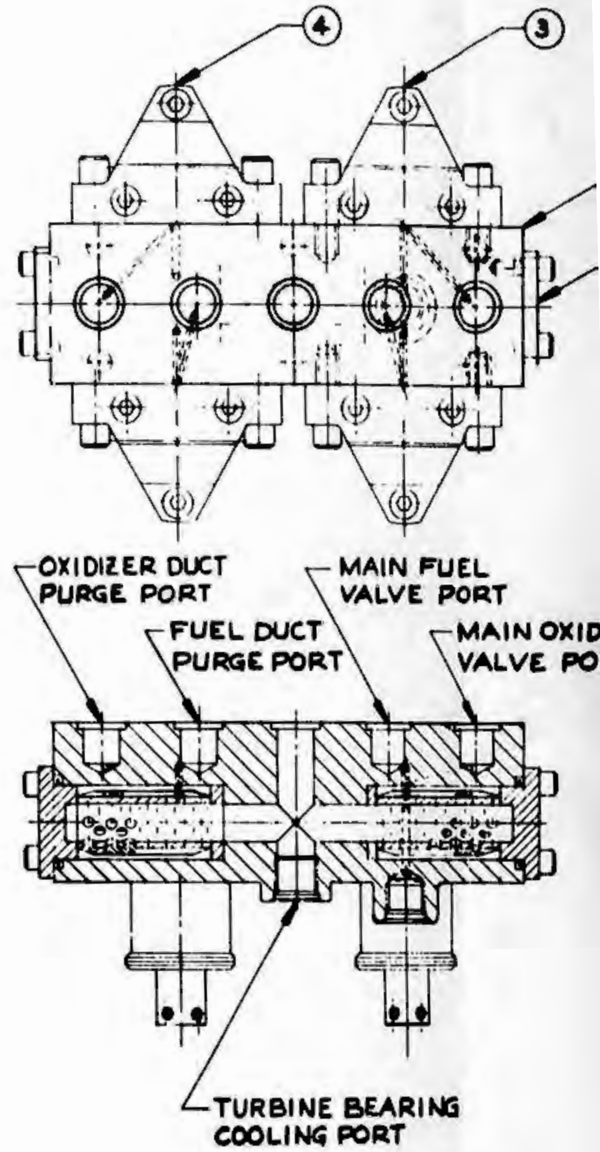

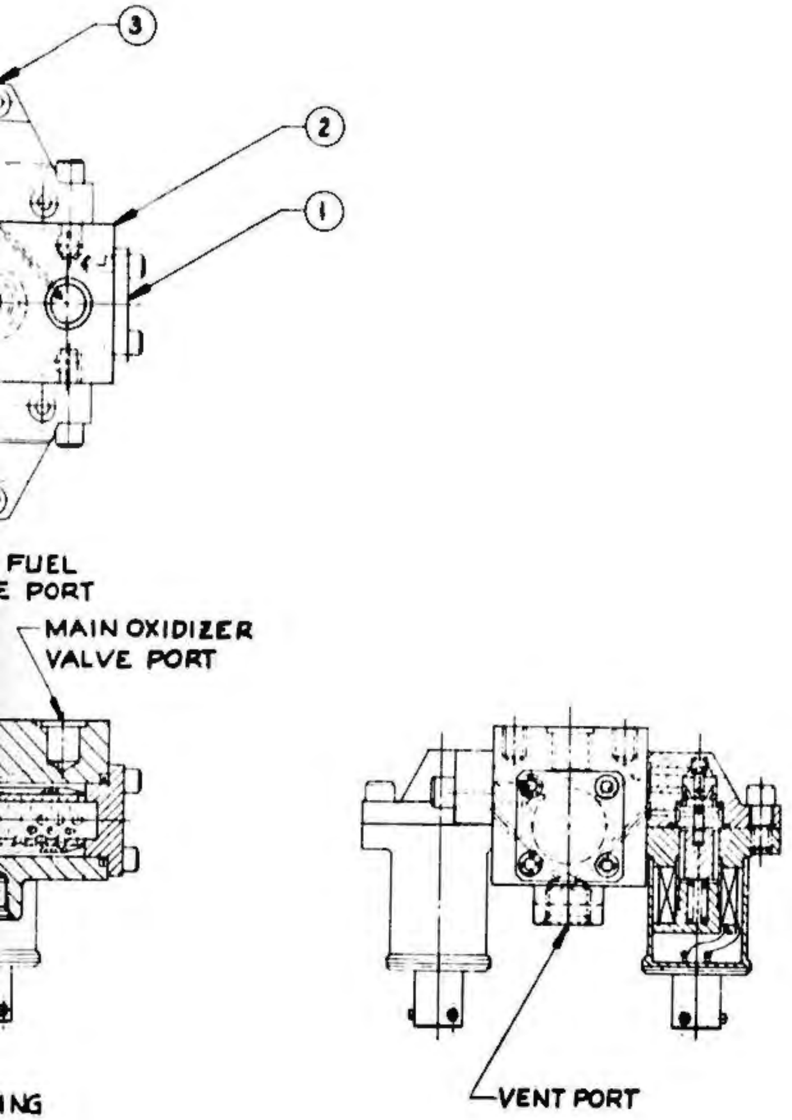

RS0009121

Figure 201. Secondary Engine Pneumatic Control Package (U)

4	2	2 WAY VALVE		
3	2	3-WAY VALVE		
2	1	MANIFOLD	347 CRES	PASSIVATE
1	2	FILTER	304L CRES	PASSIVATE
ITEM	REQD	DESCRIPTION	MATERIAL	FINISH

CONFIDENTIAL

2

(C) products) port to a common duct to the turbine control valve. Upon removal of the electrical signal, the helium port will close and the hot-gas port will open and the turbine will be powered by the thrust chamber gas. Figure 202 shows the design details.

(U) The valve is actuated by means of a three-way solenoid-operated pilot valve which, when electrically actuated, directs pressure to an expanding bellows, thus closing the hot-gas port while simultaneously opening the helium port. Upon removal of electrical signal from the pilot valve solenoid, the pilot blocks pressure and opens the bellows cavity to vent. The spring load of the bellows closes the helium port while simultaneously opening the hot-gas port.

(U) The materials used in this valve are consistent with those used in the turbine control valves which are subjected to the same hèlium and hot-gas media.

f. Electrical Control System

(U) The electrical control system provides for start and shutdown of the main and secondary engines. Command signals for thrust and mixture ratio are the principal activating signals. Provision also exists for emergency shutdown of either engine on receipt of a sustained cutoff command. Additional signals are given to the control system by pressure switches which sense the progress of the commanded sequence. These signals are distinct from those which provide feedback for the thrust and mixture ratio servosystems. This approach provides advantages during engine development and in maintainability of the ultimate system. Rapid anomaly investigation is possible because of limited interrelationships and, for the same reason, replacement of a sensor or servocontroller is permitted without the necessity of overall elaborate rebalancing.

(U) Electrical control system outputs activate solenoid valves to direct regulated pneumatic energy for initial drive of the secondary engine turbines, main propellant valve actuation, and required purges. Electrical control

CONFIDENTIAL

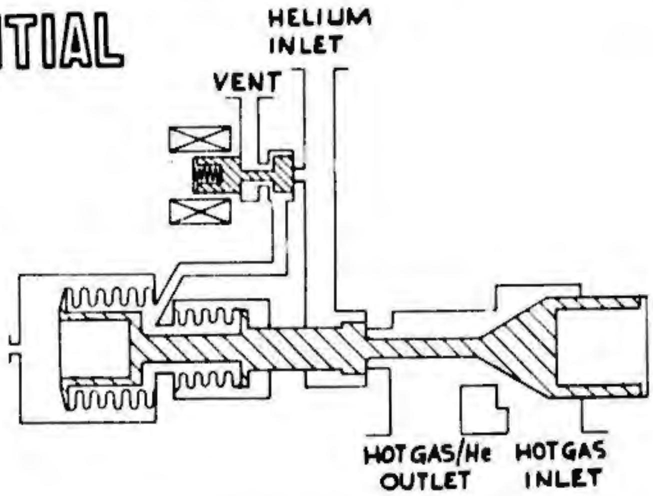

SCHEMATIC FLOW DIAGRAM

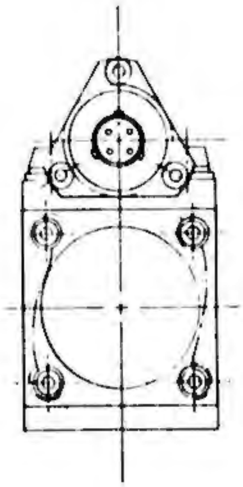

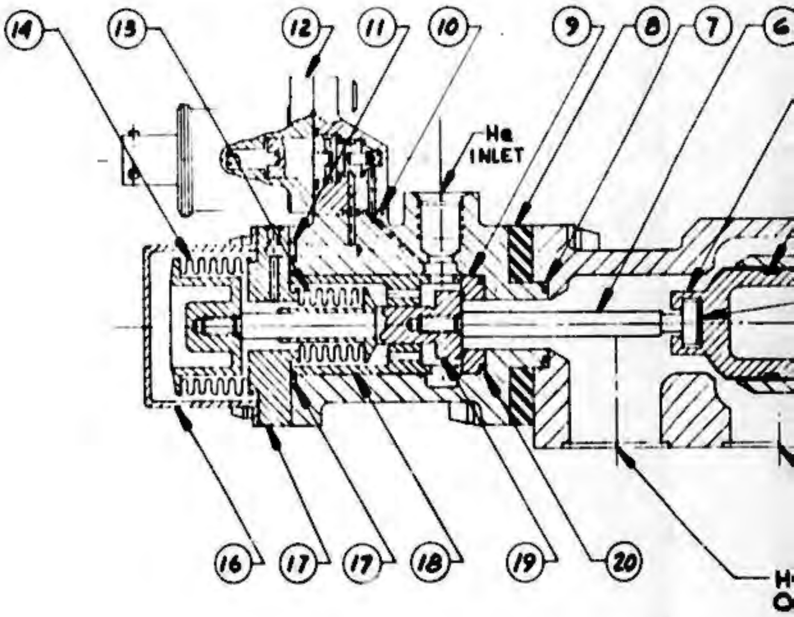

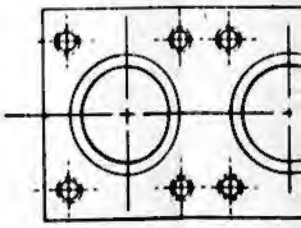

R50009131L

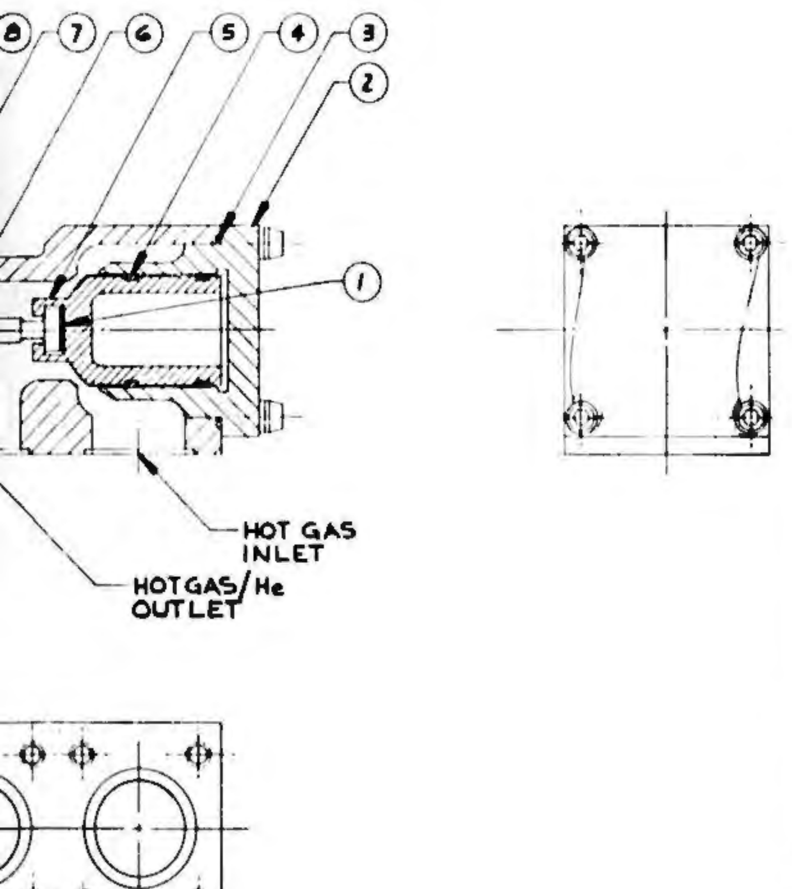

NO.	REQD		DESCRIPTION	MATERIAL	FINISH
20	1		K-SEAL	INCO X 750	GOLD PL.
19	1		POPPET	INCO 718	FLAME PLT
18	1		GUIDE	INCO 718	PASSIVATE
17	1		K-SEAL	INCO X 750	GOLD PLT
16	1		PLATE	INCO 718	PASSIVATE
15	1		CAP	321 CRES	PASSIVATE
14	1		BELLOWS	INCO 625	PASSIVATE
13	1		BELLOWS	INCO 625	PASSIVATE
12	1		3 WAY VALVE	———	———
11	1		K-SEAL	INCO X 750	GOLD PLT
10	2		K-SEAL	INCO X 750	GOLD PLT
9	1		SEAT	INCO 718	PASSIVATE
8	1		INSULATOR	MICA PLATE	———
7	1		K-SEAL	INCO X 750	GOLD PLT
6	1		STEM	RENE 41	PASSIVATE
5	1		POPPET	INCO 718	FLAME PLT
4	2		PISTON RING	CARBON	———
3	1		K-SEAL	INCO X 750	GOLD PLT
2	1		CAP	INCO 718	PASSIVATE
1	1		SPRING	INCO 718	PASSIVATE

Figure 202. Turbine Spin Valve (U)

2

(U) system outputs also control the time and mode of operation of the thrust controller and mixture ratio controller. The mode of operation may be to perform their named function or to hold the turbine valves at specific positions.

(U) Logic for the electrical control system is largely derived from the main and secondary engine start and shutdown sequences. These sequences are portrayed in Fig. 77 , 80 , 83 , and 85 in a manner that is convenient for following the main engine logic circuit diagram and the secondary engine logic circuit diagram, shown in Fig. 203 through 205. Each logic diagram is composed of lines and symbols. A line represents a path between symbols. This path, when translated into hardware, may be a single conductor, a shielded conductor, or a multiconductor cable, depending on the requirements of the components represented by the symbol. Symbol meaning is shown in Fig. 206.

(U) The OR symbol defined in Fig. 206 shows two inputs and one output. Either input causes an output. Diodes connected together at the output provide the physical hardware. These diodes are presently in use in the J-2S program.

(U) The AND symbol defined in Fig. 207 shows two inputs and one output. One input must be present and the other absent (not high level) to cause an output. A switch module, consisting of transistors, diodes, and resistors, is usable without modification. This switch module is a developed item presently in use in the J-2S program.

(U) Other AND symbol functions are obtainable by interconnecting switch modules with leads and diodes. In each case, a line into the straight side of the symbol represents an input that must be present to have an output. A line terminating in a small circle on the straight side of the symbol indicates an input which must be absent (not high level) to have an output.

CONFIDENTIAL

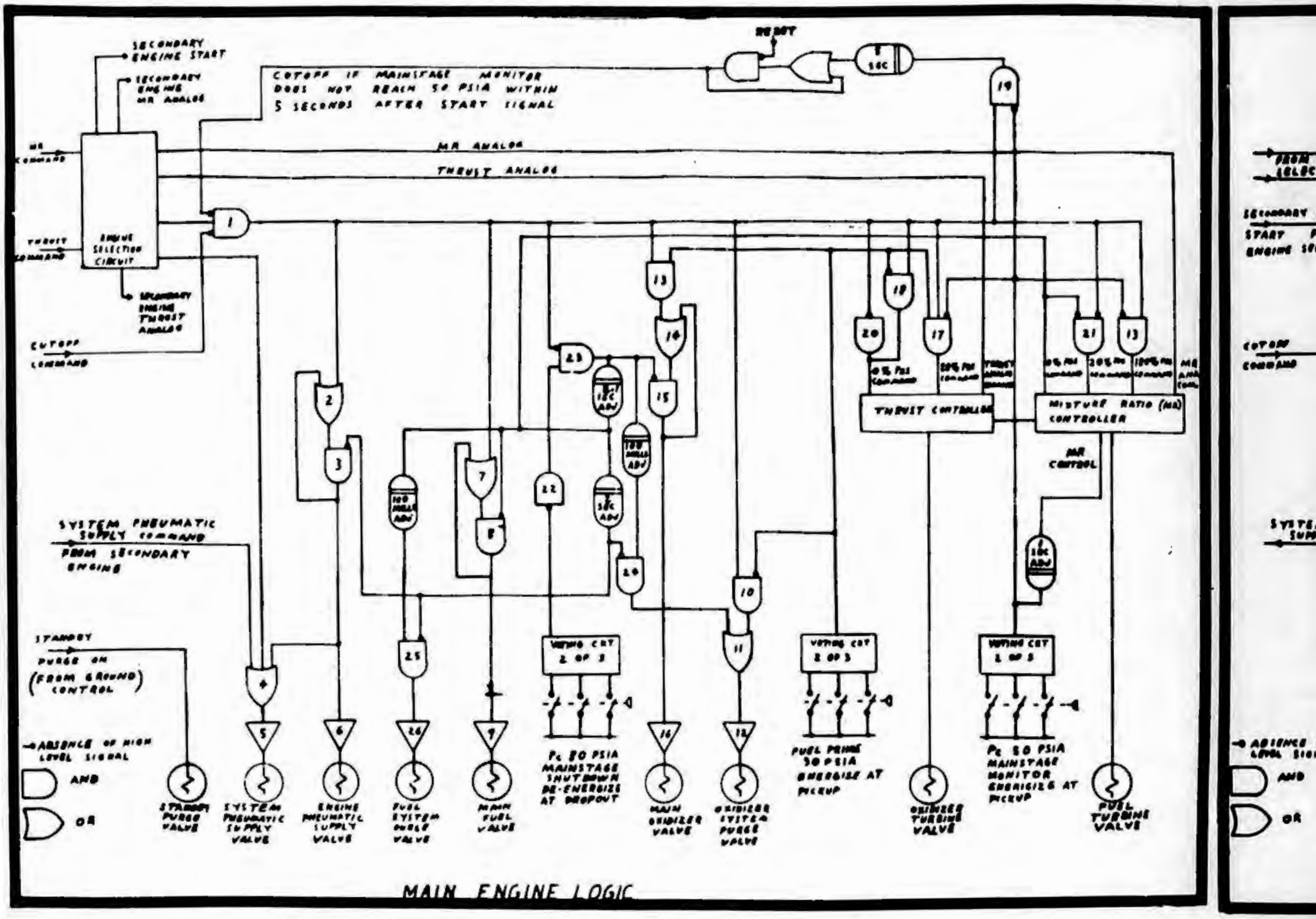

Figure 203. Main Engine Logic Diagram (U)

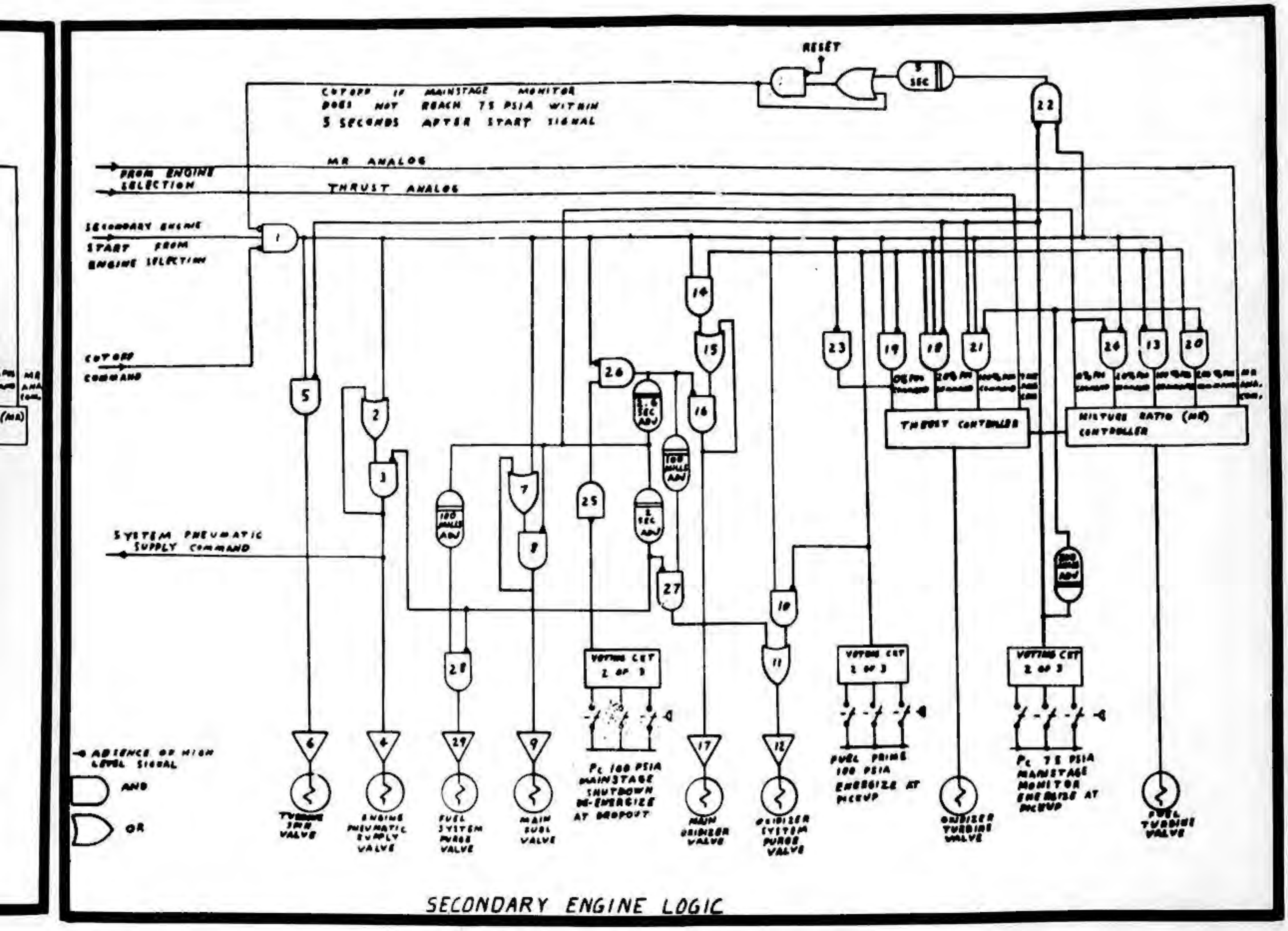

Figure 204. Secondary Engine Logic Diagram (U)

2

CONFIDENTIAL

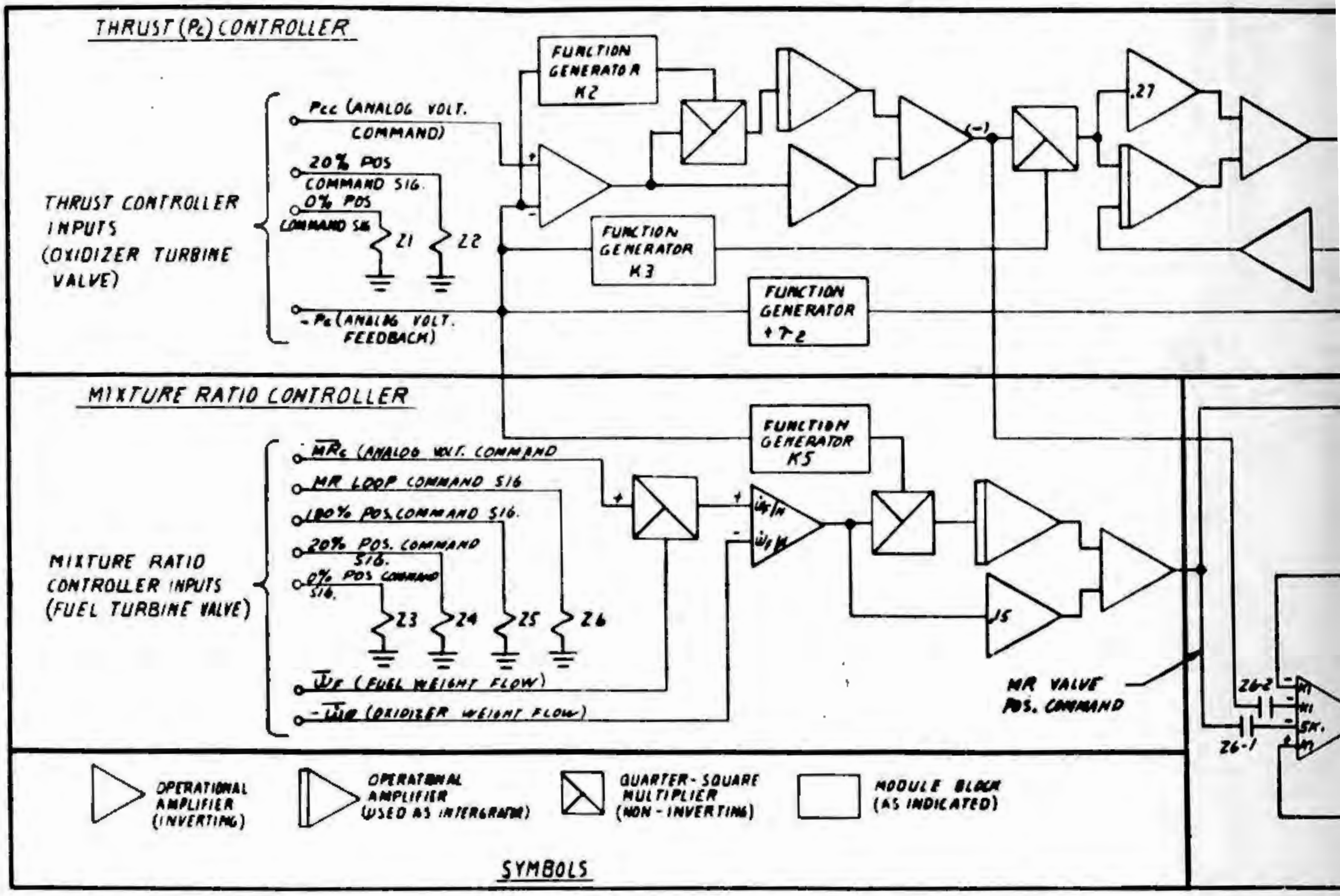

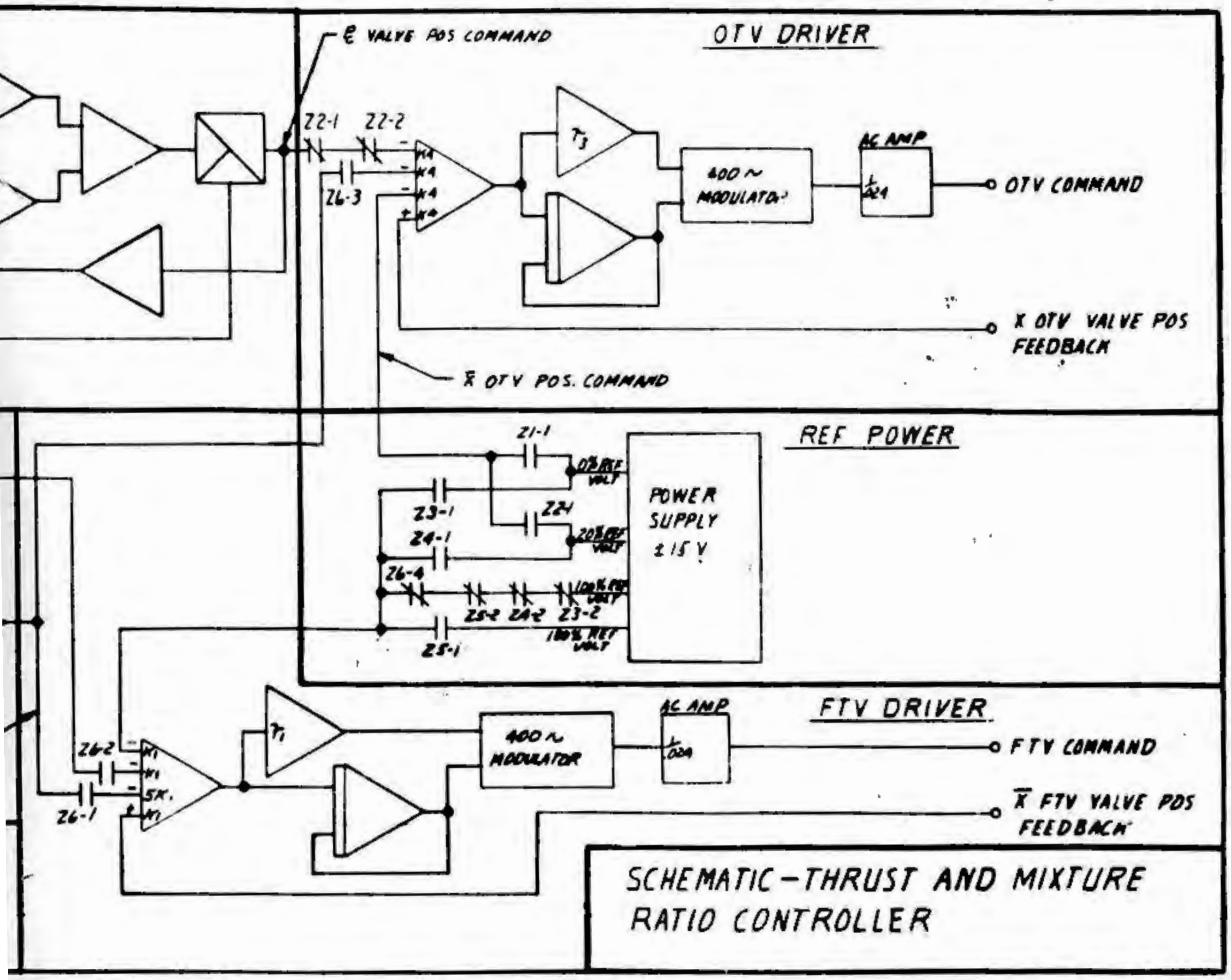

Figure 205. Thrust and Mixture Ratio Control Schematic (U)

2

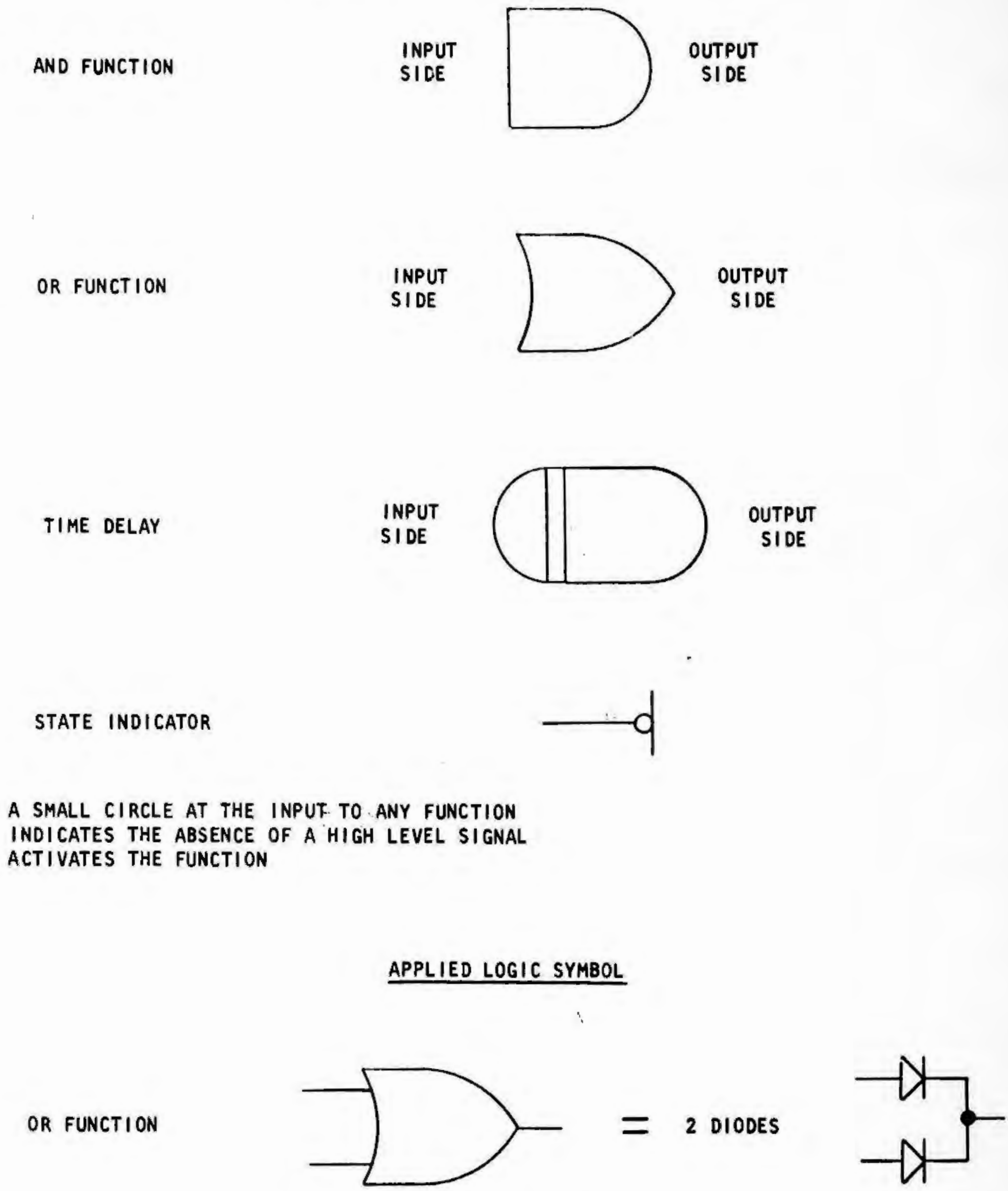

Figure 206. Logic Symbols (U)

AND FUNCTION 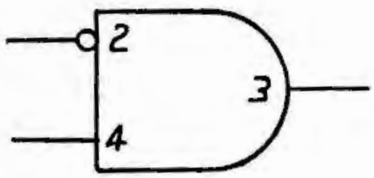 = J2S STANDARD SWITCH (501313)

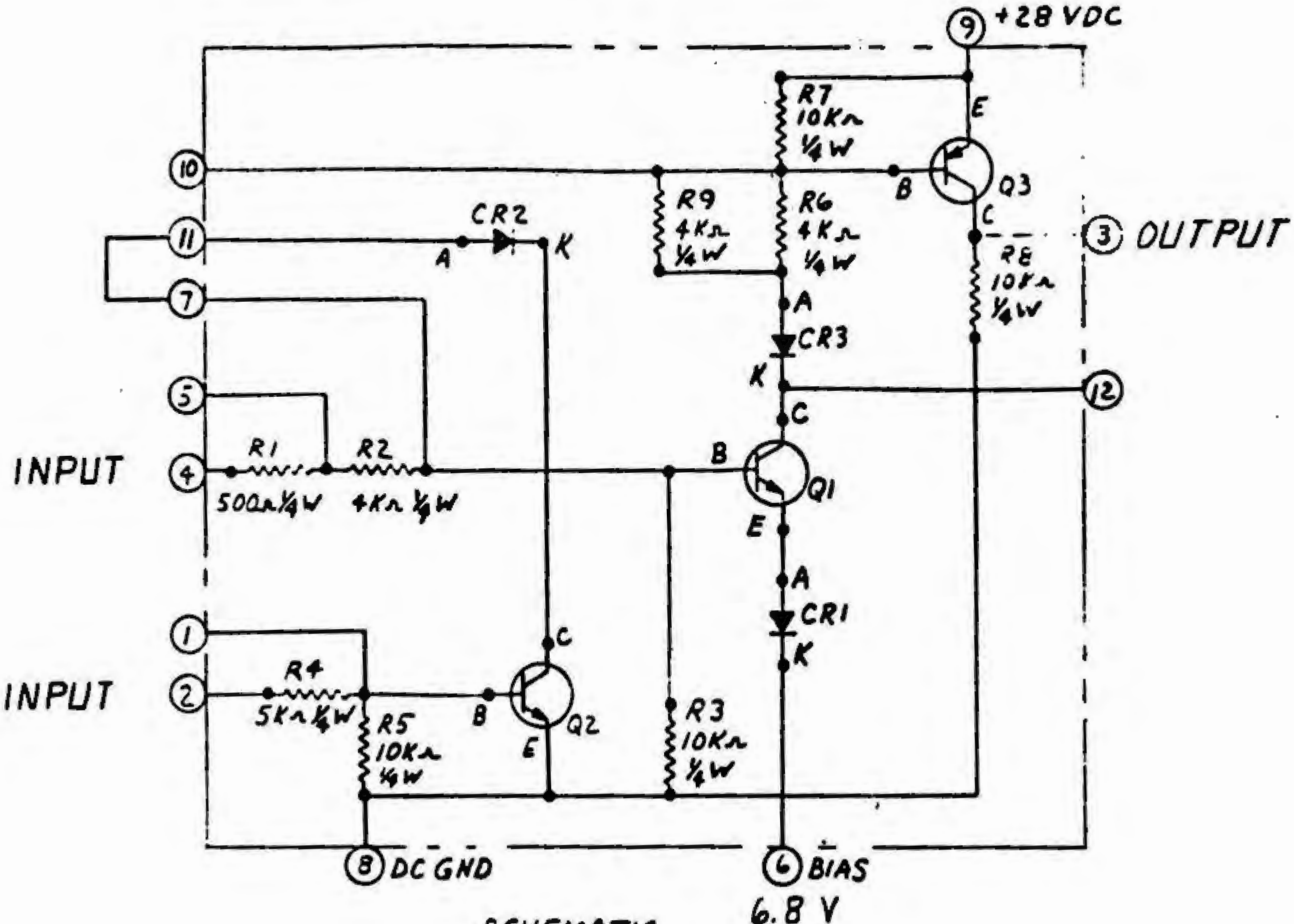

SCHEMATIC

Figure 207. Applied AND Logic Symbol (U)

(U) Timing function symbols represent timers similar to those used in the J-2S electrical control system.

(U) The current amplifier or driver symbol defined in Fig. 208 shows a low current input and a high current output. Power switch part number 503662 provides this function. In addition, this power switch provides inductive surge suppression and a path to accept an isolated component test signal.

(U) Major logic portions of the electrical control system will be potted, welded assemblies. Nickel leads and nickel component terminations with controlled characteristics will ensure uniform connections of high reliability with a minimum number of weld schedules. To avoid excessive throwaway cost, the major logic portions will have plug-in connectors with redundant paths and provision for bolted retention.

(C) Electrical control assemblies composed of potted modules have been successfully tested at random vibration levels of 2.5 g^2/cps. Vibration capability of the individual modules is approximately 70 g. In addition to providing vibration capability, the potting material conducts heat from the electronic components to the exterior of the assembly. This is important in a zero gravity environment where convection cooling is unusable.

(U) Temperature range of the electrical control system is largely a function of location in the vehicle and conditions encountered during a long hold period. Although neither of these is exactly defined, the temperature range of -130 C to +60 C appears reasonable and is the design temperature range of the J-2S electrical control system. Commonalities of the engines support reasonableness of this temperature range.

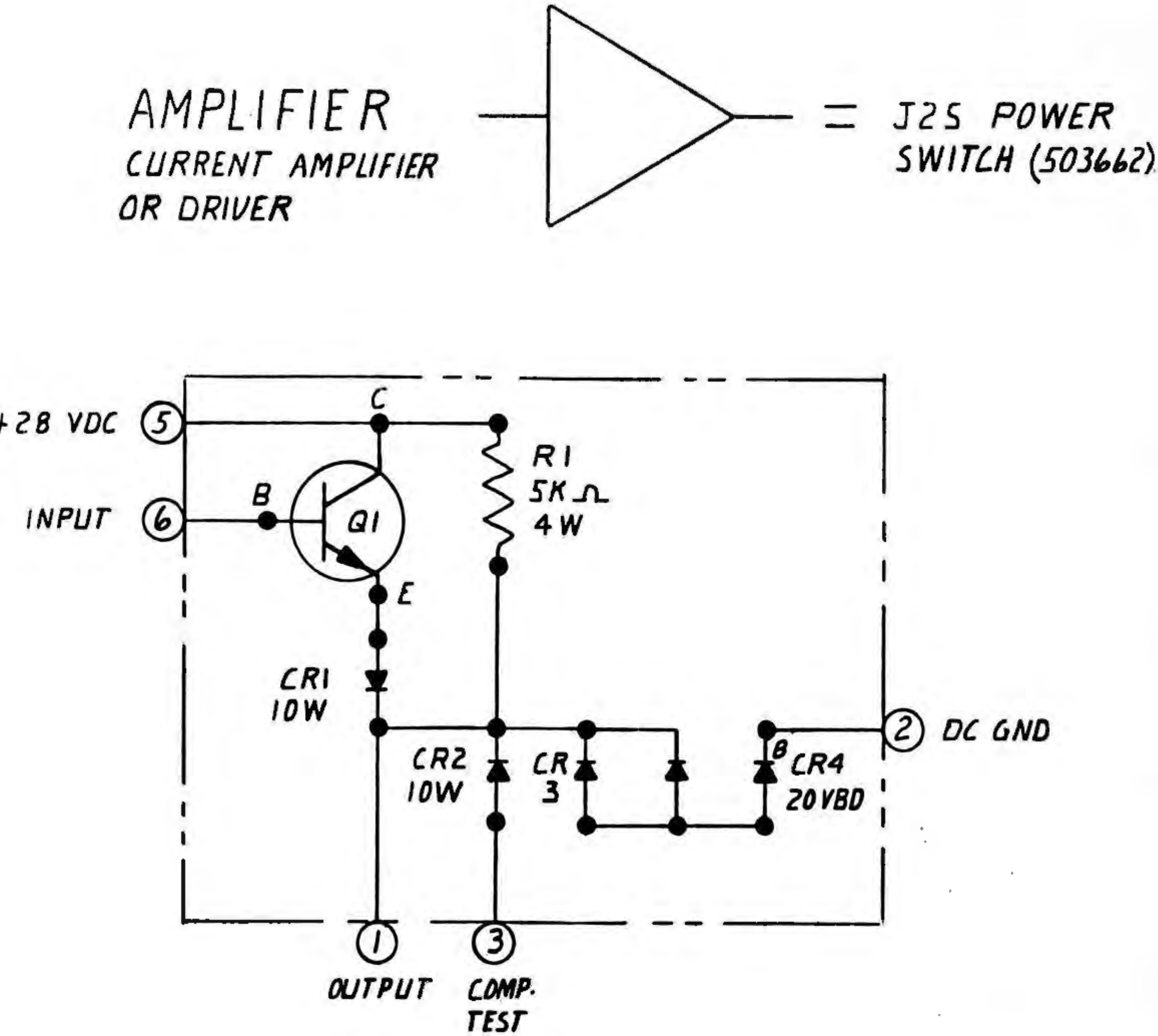

Figure 208. Applied Amplifier Logic Symbol (U)

(U) Protection from moisture and other atmospheric contaminants is given to the electrical control system by enclosing it in a pressurized, sealed container. Experience with electrical connectors, seals, and valves used on electrical packages of other engine systems would result in a minimum of required development effort. Final selection of the exact exterior configuration is largely dependent on space availability within the engine system. A single large package would provide the most convenient electrical layout, but more than one package of smaller sizes may be more practical to locate.

(U) Self-checking features for preflight checkout have not been included in the logic diagrams; however, they would be added prior to initial circuit development. These features must be part of the first physical circuit.

(U) A combined malfunction analysis of the engine and electrical control system is required before meaningful fail-safe features can be defined. This malfunction analysis also will indicate where redundancy techniques would be most applicable.

(1) Main Engine Logic

The engine selection circuit (Fig. 203) receives thrust and mixture ratio commands from a vehicle source.

(a) Start

(U) When commands indicate required operation of the main engine, a start signal from the engine selection circuit is sent to the succeeding AND (L)*. If cutoff signals are not present at its inputs, it gives an output. This output passes through OR (2) to AND (3). Output of AND (3) passes through OR (4) to driver (5) which energizes the system

*The numbers in parentheses refer to logic symbols in Fig. 203.

(U) pneumatic supply solenoid valve. Output of AND (3) also causes driver (6) to energize the engine pneumatic supply solenoid valve. Output of AND (3) enters OR (2), consequently providing an electrical lockin.

(U) Output of AND (1) also passes through OR (7) to AND (8). Output of AND (8) provides for lockin through OR (7) and causes driver (9) to energize the solenoid valve to open the main fuel valve.

(U) AND (10) input also receives the output of AND (1). Output of AND (10) passes through OR (11) to driver (12). Driver (12) energizes the oxidizer system purge solenoid valve.

(U) Output of AND (1) enters the input of AND (13). AND (13) gives an output to the servosystem to open the fuel turbine valve to the 180-percent position.

(U) Progression of the starting sequence is sensed by redundant fuel prime pressure switches. Output of the pressure switches passes through a voting circuit to an input of AND (10). This causes the output of AND (10) to cease, thereby removing the input from OR (11) and driver (12). The oxidizer system purge solenoid valve is consequently de-energized.

(U) Output of the fuel prime pressure switches enters the input of AND (13). The other input of AND (13) is already energized by the output of AND (1). Therefore, AND (13) gives an output which passes through OR (14) to the input of AND (15). Output of AND (15) goes to the input of driver (16). Driver (16) output energizes the solenoid valve to open the main oxidizer valve.

(U) Fuel prime pressure switch output also reaches an input of AND (17). AND (1) is also providing an input to AND (17), but the input from the mainstage monitor pressure switches is not present. Consequently, AND (17) provides an output to the servosystem to position the oxidizer

(U) turbine valve at the 20-percent position. The previous command to position the oxidizer turbine valve at the 0-percent position is removed when the fuel prime pressure switch output reaches an input of AND (18).

(U) Operation of the mainstage monitor pressure switches cause an output which goes to the input of AND (13). AND (13) output ceases and the command to hold the fuel turbine valve at the 180-percent position is removed from the servosystem.

(U) Output of the mainstage monitor pressure switches also is sensed by an input of AND (17). The output of AND (17) ceases to command the servosystem to hold the oxidizer turbine valve at the 20-percent position. Previously, the command to hold the oxidizer turbine valve at the 0-percent position had been removed. Absence of these position commands causes the servosystem to operate for thrust control.

(U) The mainstage monitor pressure switch signal to the input of AND (19) causes its output to cease and return the 5-second timer to zero. If the mainstage monitor pressure switch signal had not been received within 5 seconds from start, a locked-in cutoff signal would have resulted. A reset signal could remove this cutoff signal.

(U) A 1-second timer is started by the output of the mainstage monitor pressure switches. Output of the 1-second timer is given to the servosystem. This causes MR control to operate; thrust control remains. Main engine start is complete.

(b) Shutdown

(U) When commands indicate shutdown of the main engine, the engine selection circuit removes the start signal from AND (1). Output from AND (1) is removed from the input of AND (20). AND (20) then gives an output which commands the servosystem to hold the oxidizer turbine valve at the 0-percent position.

(U) Output from AND (1) also is removed from the input of AND (21). Output of AND (21) then commands the servosystem to hold the fuel turbine valve at the 20-percent position.

(U) Operation of the mainstage shutdown pressure switches causes their output to be removed from the input of AND (22). AND (22) then gives an output to AND (23). AND (23) sends its output to an input of AND (15). AND (15) then removes its output from OR (14), interrupts the lockin circuit, and also removes its output from the input of driver (16). Driver (16) ceases to energize the solenoid valve which controls the main oxidizer valve and the valve closes.

(U) Output of AND (23) also activates a 100-millisecond timer. AND (24) senses the output of the 100-millisecond timer and gives an output which passes through OR (11) to the input of driver (12). Output of driver (12) energizes the oxidizer system purge solenoid valve.

(U) Output of AND (23) energizes a 2.1-second timer. The 2.1-second timer gives an output to AND (21). AND (21) ceases to give a command to the servosystem to hold the fuel turbine valve at the 20-percent position.

(U) An output of the 2.1-second timer enters a servosystem input and commands the holding of the fuel turbine valve at the 0-percent position.

(U) Output of the 2.1-second timer enters an input of AND (8). AND (8) ceases to give an output to OR (7), interrupting the lockin circuit, and ceases to send its output to the input of driver (9). Driver (9) stops energizing the main fuel valve control solenoid valve and the main valve closes.

(U) A 100-millisecond timer also is signaled by the output of the 2.1-second timer. The 100-millisecond timer sends its output to an input of AND (25). AND (25) output goes to the input of driver (26). Driver (26) energizes the fuel system purge solenoid valve.

(U) The 2.1-second timer output starts a 2-second timer.

(U) Output of the 2-second timer enters an input of AND (24). AND (24) ceases to given an output through OR (11) to driver (12). Driver (12) de-energizes the oxidizer system purge solenoid valve.

(U) An input of AND (25) senses the output of the 2-second timer. AND (25) ceases to give an output to driver (26). Driver (26) de-energizes the fuel system purge solenoid valve.

(U) AND (3) receives an input from the 2-second timer. AND (3) ceases to give an output to OR (2), interrupting the lockin circuit, and ceases to give a signal to driver (6). Driver (6) stops energizing the engine pneumatic supply solenoid valve. Engine shutdown is complete.

(U) Output of AND (3) also ceases to pass through OR (4) to driver (5). Unless an output from the engine selection circuit is passing through OR (4), driver (5) de-energizes the system pneumatic supply solenoid valve.

(U) When the engine selection circuit intends to follow shutdown of an engine with start of the other engine, it provides an output through OR (4) to driver (5) to prevent de-energizing of the system pneumatic supply solenoid valve. This prevents unnecessary cycling of the pneumatic regulation system.

(2) Secondary Engine Logic

(U) The secondary engine logic diagram (Fig. 204) contains the sequencing for the start and shutdown.

(a) Start

(U) When commands indicate required operation of the secondary engine, a start signal from the engine selection circuit is sent to AND (1). If cutoff signals are not present at its inputs, it gives an output. This output passes through OR (2) to AND (3). Output of AND (3) passes through OR (2) to provide a lockin. Output of AND (3) is sent to cause energizing of the system pneumatic supply.

(U) Output of AND (3) also goes to driver (4). Driver (4) output energizes the engine pneumatic supply solenoid valve. AND (5) receives an input from AND (1). AND (5) output is sent to driver (6). Driver (6) output energizes the turbine spin valve solenoid.

(U) Output from AND (1) passes through OR (7) to AND (8). Output of AND (8) passes through OR (7) to provide a lockin, it also goes to the input of driver (9). Output of driver (9) energizes the control solenoid valve to open the main fuel valve.

(U) Output of AND (1) goes to the input of AND (10). Output of AND (10) passes through OR (11) to the input of driver (12). Output of driver (12) energizes the oxidizer system purge solenoid valve.

(U) Output of AND (1) also goes to the input of AND (13). Output of AND (13) commands the servosystem to hold the fuel turbine valve at the 100-percent position.

(U) When the fuel prime pressure switches operate, they send an output to AND (14). AND (14) sends its output through OR (15) to AND (16). Output of AND (16) goes through OR (15) to provide a lockin. Output of AND (16) reaches the input of driver (17). Driver (17) output energizes the solenoid valve which opens the main oxidizer valve.

(U) AND (10) receives an input from the fuel prime pressure switches. Output of AND (10) ceases to pass through OR (11) to driver (12). Driver (12) de-energizes the oxidizer system purge solenoid valve.

(U) Fuel prime pressure switch output goes to an input of AND (18). AND (18) gives an output which commands the servosystem to hold the oxidizer turbine valve at the 20-percent position.

(U) Output of the fuel prime pressure switches at an input of AND (19) cause AND (19) to stop commanding the 0-percent position of the oxidizer turbine valve.

(U) Fuel prime pressure switch output also reaches an input of AND (13). AND (13) ceases to command the servosystem to hold the fuel turbine valve at the 100-percent position.

(U) AND (20) senses the output of the fuel prime pressure switches and its output commands the servosystem to hold the fuel turbine valve at the 200-percent position.

(U) Actuation of the mainstage monitor pressure switches causes an output which goes to an input of AND (5). AND (5) ceases to provide an output to driver (6). Driver (6) de-energizes the turbine spin valve solenoid.

(U) Output of the mainstage monitor pressure switches goes to an input of AND (18). AND (18) ceases to command the 20-percent position of the oxidizer turbine valve.

(U) AND (21) senses output of the mainstage monitor pressure switches. Output of AND (21) commands the servosystem to hold the oxidizer turbine valve at the 100-percent position.

(U) The mainstage monitor pressure switch signal to the input of AND (22) causes its output to cease and return the 5-second timer to zero. If the mainstage monitor pressure switch signal had not been received within 5 seconds from start, a locked-in cutoff signal would have resulted. A reset signal could remove this cutoff signal.

(U) Fuel prime pressure switches also send their output to an 800-millisecond timer. Output of the 800-millisecond timer reaches AND (21), causing it to stop commanding the 100-percent position of the oxidizer turbine valve.

(U) AND (20) senses the output of the 800-millisecond timer. This causes AND (20) to stop commanding the 200-percent position of the fuel turbine valve.

(U) Without turbine valve position commands, the servosystem provides thrust control and MR control.

(b) Shutdown

(U) When commands indicate shutdown of the secondary engine, the engine selection circuit removes the start signal from AND (1). Loss of AND (1) output is sensed by AND (23). AND (23) gives an output to command the servosystem to hold the oxidizer turbine valve at the 0-percent position.

(U) Loss of AND (1) output is also sensed by AND (24). AND (24) commands the servosystem to hold the fuel turbine valve at the 20-percent position.

(U) Loss of output of the mainstage shutdown pressure switches is sensed by AND (25). AND (25) gives an output to AND (26). AND (26) gives an output to AND (16). AND (16) ceases to give an output to OR (15), interrupting the lockin circuit. Output loss from AND (16) also is sensed at the input of driver (17). Driver (17) de-energizes the main oxidizer valve control solenoid valve.

(U) A 100-millisecond timer is activated by output from AND (26). Output of this timer is sensed at the input of AND (27). Output of AND (27) passes through OR (11) to driver (12). Driver (12) energizes the oxidizer system purge valve.

(U) AND (26) also activates a 2.6-second timer. Output of the 2.6-second timer goes to AND (24). This causes AND (24) to cease commanding the servosystem to hold the fuel turbine valve at the 20-percent position.

(U) Output of the 2.6-second timer directly commands the servosystem to hold the fuel turbine valve at the 0-percent position.

(U) AND (8) senses the output of the 2.6-second timer. This causes AND (8) to cease providing an input to OR (7), thereby interrupting the lockin circuit. Driver (9) senses loss of output from AND (8) and causes the main fuel valve control solenoid valve to de-energize.

(U) The 2.6-second timer also activates a 100-millisecond timer. Output of the 100-millisecond timer is sent to AND (28). AND (28) provides an output to driver (29). Driver (29) energizes the fuel system purge valve.

(U) A 2-second timer receives its activation from the 2.6-second timer. Output of the 2-second timer is sensed at an input of AND (27). AND (27) ceases to send an output through OR (11) to driver (12). Driver (12) stops energizing the oxidizer system purge valve.

(U) Output of the 2-second timer is sent to an input of AND (28). AND (28) ceases to give a signal to driver (29). Driver (29) de-energizes the fuel system purge valve.

(U) AND (3) also receives an input from the 2-second timer. AND (3) ceases to pass a lockin signal through OR (2). Driver (4) senses loss of output from AND (3). Driver (4) de-energizes the engine pneumatic supply valve.

(U) AND (3) removes the system pneumatic supply command. Engine shutdown is complete.

g. Engine Controller

(U) The performance controller interface consists of several logical input signals dependent on the mode of engine operation. The signals include power output to two valves (fuel turbine throttle valve and oxidizer turbine throttle valve) and feedback from elements consisting of chamber pressure transducer(s), mass flow transducers, and valve position transducers for the two controlled valves. These signals are conditioned in an analog computer type of control circuit to perform the control functions , while avoiding regions of engine operation that are undesirable (such as excessively high mixture ratio excursions). The controller design is shown schematically in Fig. 205.

(1) Control System Components

(U) The command signal components consist of provisions for a valve position control mode, used principally for start and shutdown (but also available for other purposes, such as calibration, checkout, etc.), and certain variable command signals to generate the desired thrust and mixture ratio. Logic to generate shut position, full open (180 percent of nominal value), and nominal value is required for the fuel turbine throttle valve; logic to generate shut position, 10 percent of nominal value, and nominal value also is required for the oxidizer turbine valve during start. For shutdown, the only new position required is the 20 percent of nominal position for the fuel turhine throttle valve. During engine operation, the position command mode may be continued on the ground for checkout purposes, but for flight (and probably most of the time on the ground) the closed-loop operation mode will be used. Logic signal inputs will close the required relay contacts to bring about the various valve positions or operation modes required.

(C) Control over the engines is effected by two hot-gas valves, the fuel turbine throttle valve (FTV), and the oxidizer turbine throttle valve (OTV). A current input to the valve motor causes the valve to move in either direction depending on the polarity at a maximum rate of full travel in 1 second, and a position transducer is provided each valve for position information to the controller. An alternating current servomotor is used to position the valve; potentiometric feedback will be used.

(U) Feedback signal input consists of the valve position potentiometers and the performance control signals. Chamber pressure feedback will be used instead of thrust. This signal will probably utilize several transducers positioned around the chamber to provide a good average value and to increase the reliability of the system. Mass flow will be computed from volumetric flow as measured by turbine-type flowmeters with frequency to direct current conversion, temperature bulb measurement, and pressure correction from the chamber pressure measurement.

(2) Valve Position Mode of Control

(U) When the appropriate relays are actuated, the control loop is on valve position only. This mode of operation is required to hold the turbine throttle valves at intermediate positions for either start or shutdown. This feature may also have other uses, such as initial checkout of the control systems, test stand calibration of the engines, or safety backup in case of a failure in the performance control loops.

(U) The signal from the valve position indicating element is compared with the valve position command signal (which may be generated by either the performance controls or by the relay logic during start or shutdown), and any error is used to drive a lead compensation network to improve

(U) response characteristics of this inner control loop. This network drives a modulator package which, in turn, provides a signal of the proper magnitude and phase to the servomotor that drives the valve. All of the valve position control loops are assumed to be similar; later different response characteristics may require different compensation networks to be used to get the required response characteristics.

(U) The schematic shows the control signals to both valves on the right (OTV and FTV driven). The nomenclature is such that the nominal value (100 percent) is the valve position for full thrust at nominal mixture ratio. This value is not a limit; it may be exceeded during start or during mixture ratio excursions at nominal thrust.

(3) Closed Loop Mode of Control

(U) Operation in this mode of control consists of using commanded thrust (chamber pressure) and mixture ratio signals for comparison with measured chamber pressure and mixture ratio signals, and generating the appropriate valve position command. Proper dynamic compensation dictates that certain parameters must vary with power level (or with chamber pressure). Four terms require function generation varying with power level: both integral terms in proportion plus integration compensation, and the gain and lag time constant of the lead-lag network for chamber pressure control of the oxidizer turbine throttle valve. These variables (labeled K_2, K_3, K_5, and τ_2 in the diagram) are multiplied by the appropriate signals to produce proper compensation as a function of power level.

(U) Nominal values of command inputs and feedback inputs are again indicated by the diagram, with nominal being the full thrust at nominal mixture ratio condition (nominal equals 100 percent). The chamber pressure

(U) command signal can be directly compared with the feedback signal to generate the error signal that drives the control loop. In the case of the mixture ratio control loop, the commanded value of mixture ratio is multiplied by the normalized value of fuel flow generating a commanded normalized oxidizer flow. This is compared with the normalized oxidizer flow measured, and the resulting error signal is used to position the valves. The nominal value of fuel flow must be used as a gain multiplier for this configuration shown. The numerical gain figures given in the schematic were found to produce suitable transient response characteristics in the analog model.

(U) The numbers presented in the schematic are for the main engine. For the secondary engine, the assumption was made that loop gains will stay the same to obtain equivalent response characteristics; this means that only those factors that have a dimension of time (or its reciprocal) need be changed. Accordingly, K_3 should be the same for both engines because the ratio of turbomachinery time constants is approximately the same. The factors that will vary from the primary engine analysis are K_2, K_5, τ_2, and the time constant cross transfer function. This time constant is the reciprocal of the oxidizer turbopump frequency or 1/4 (= 0.25). The value of τ_2 and K_2 is directly related to the ratio of the fuel turbomachinery time constants for the main to secondary engines or 1.7/3.18 or about 1/2 the value of the main engine. The value of K_5 is directly related to the ratio of the oxidizer turbomachinery time constants for the main to secondary engine or 4.00/9.08 or 4/9 the value of the main engine. Adequate corroboration of these extrapolations were found by comparison of several preliminary analog computer runs of the secondary engine to the present closed-loop control model. The variation of these functions with power level are shown in Fig. 209 for the main engine and Fig. 210 and 211 for the secondary engine.

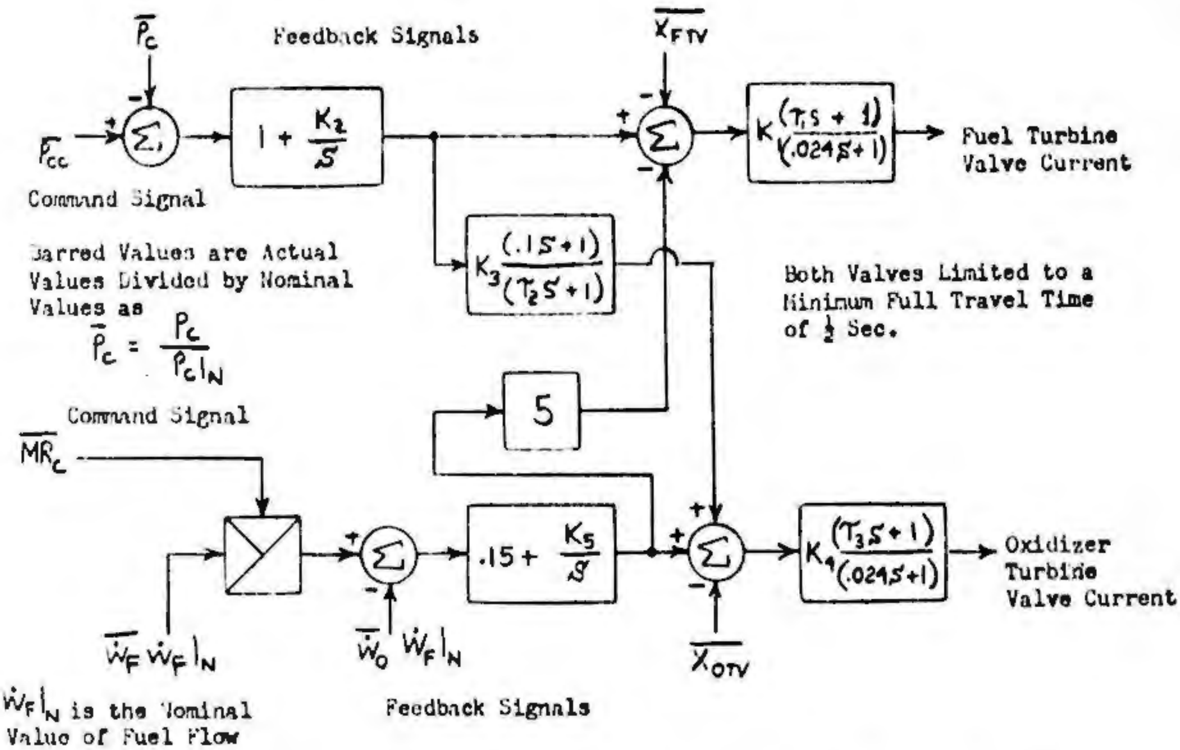

$K_1 = \dfrac{21.6\ X_{FTV}|_N}{K_{FTV}}$, K_{FTV} = Fuel Turbine Valve Poppet Slew Rate Response to Current (Small signal Steady-State)

τ_1 = First Order Approximation to Fuel Turbine Valve Time Constant (Small signal)

$K_4 = \dfrac{21.6\ X_{OTV}|_N}{K_{OTV}}$, K_{OTV} = Oxidizer Turbine Valve Poppet Slew Rate Response to Current (Small signal Steady-State)

τ_3 = First Order Approximation to Oxidizer Turbine Valve Time Constant (Small signal)

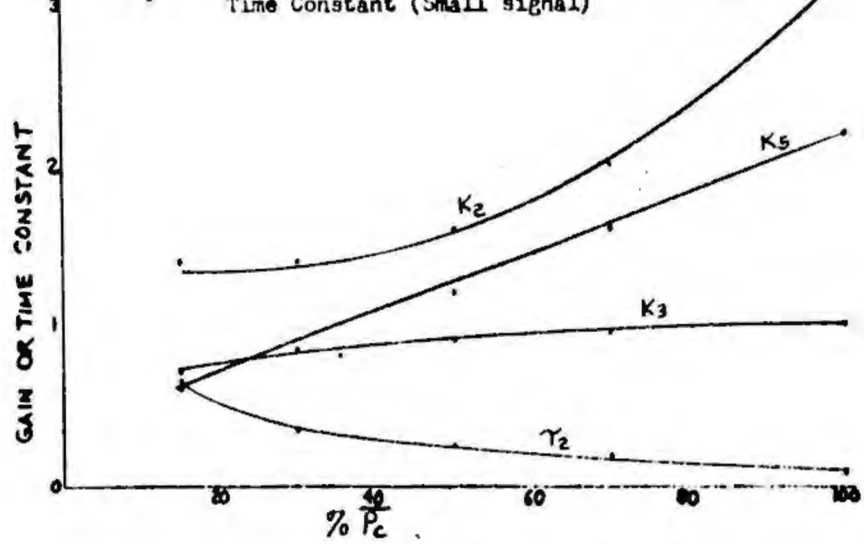

Compensation Parameters as a Function of Power Level

Figure 209. Main Engine Control System Compensation (U)

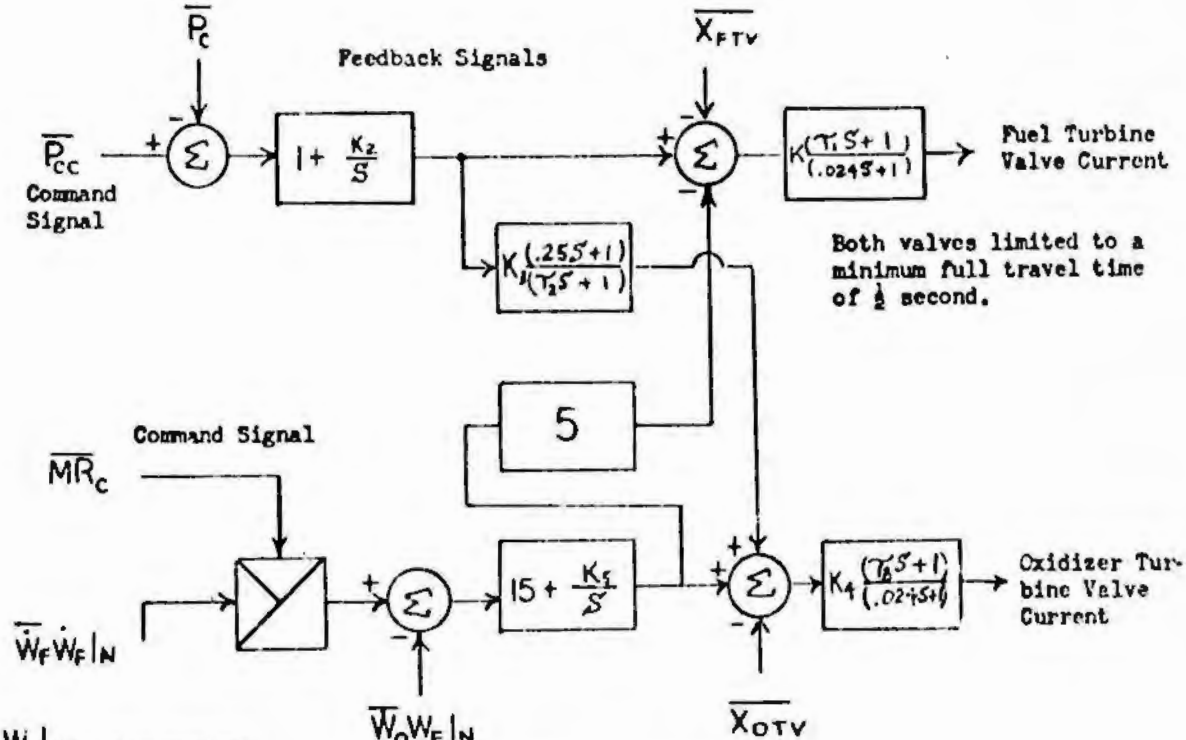

$W_F|_N$ is the nominal value of fuel flow.

$$K_1 = \frac{21.6\ X_{FTV}|_N}{K_{FTV}}$$

$$K_4 = \frac{21.6\ X_{OTV}|_N}{K_{OTV}}$$

$$\boxed{\begin{array}{l} K_1 = K_4 = .216 \\ \tau_1 = \tau_3 = .024 \end{array}}$$

K_{FTV} = Fuel Turbine Valve Slew Rate Response to Current

τ_1 = First Order Approximation to Fuel Turbine Valve Time Constant (Small Signal)

K_{OTV} = Oxidizer Turbine Valve Slew Rate Response to Current

τ_3 = First Order Approximation to Oxidizer Turbine Valve Time Constant (Small Signal)

Note: Barred variables refer to decimal fractions of nominal value, as $\overline{P_c}$ may take on values from 0 to 1.0 (or more).
The $'_N$ designation means nominal value.

Figure 210. Control System Compensation for Secondary Engine (U)

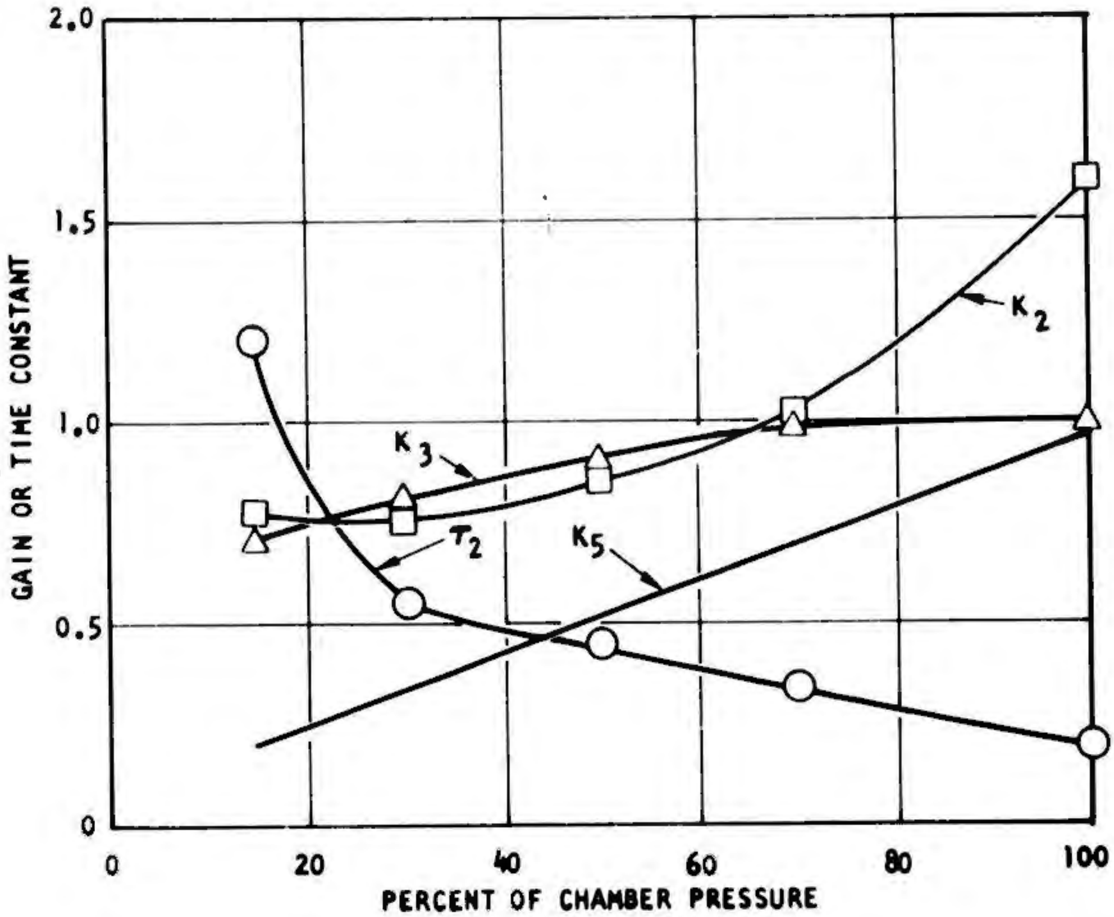

Figure 211. Compensation Parameters as a Function of Power Level (Secondary Engine) (U)

(4) Controller Assembly Construction

(U) For engine testing, the thrust and mixture ratio controller assemblies would be located in the control center. Therefore, they would be packaged for conventional rack mounting using high-quality commerical or military specification components. To provide for ease of servicing and modification, modular assembly techniques would be used wherever possible. Components required in the controller assemblies also are shown in the schematic.

(U) An operational amplifier module would contain two amplifiers and associated components mounted on a printed circuit (PC) board. The amplifier would be a Data Device Corporation model D-16 or equivalent. These amplifiers provide ±11 volts at ±2.2-milliampere output with a d-c open-loop gain of 100 decibels. Multiplier modules would contain two quarter-square multipliers per PC board. Multipliers used would be Burr-Brown Research Corporation model 4029/25 or equivalent. These multipliers have an accuracy of 0.25 percent and an output of ±5 milliamperes at 10 volts. Switching logic would be accomplished with sealed-contact reed relays similar to C. O. Clare & Co. model CR4MB-1007. The relays would be mounted four to a PC card. Nonlinear function generation would be performed using combinations of the previously described amplifiers, multipliers, and conventional Zener diodes. All module assemblies would be the same size and would plug into commercially available card racks.

(U) The valve driver subassemblies would provide the 400-cycle power for the valves and should be located at or near the test stand (within 100 yards of the valve if possible). The driver assemblies will require approximately 100 watts of 115 volts, 400-Hz power (single phase) per valve. A Westamp Incorporated model S-212 (or equivalent) modulator would be used to convert the d-c valve position error signal to a 400-cycle signal suitable to drive the valve servomotor. Power amplification (ac) would be provided by a Singer Company (Diehl Division) model TA-060-OA-500, 60-watt transistorized servoamplifier or equivalent.

SECTION VII

REFERENCES

1. AFRPL-TR-65-252, Maneuvering Satellite Propulsion System Optimization Study, Vol. I through III, Contract AF04611-10745, Rocketdyne, a division of North American Rockwell Corporation, Canoga Park, California, CONFIDENTIAL.

2. AFRPL-TR-66-301, Advanced Thrust Chamber for Space Maneuvering Propulsion--Task I: System Studies, Contract AF04611-11617, H. G. Diem, Rocketdyne, a division of North American Rockwell Corporation, Canoga Park, California, September 1966, CONFIDENTIAL.

3. RPL-TDR-64-120, Analysis of an Optimum Thrust Modulated Propulsion System for Use in a Space Maneuvering Vehicle, The Bell Aerosystems Company, Vol. 1 through 3, Contract AF04(611)-8163, June 1964, CONFIDENTIAL.

4. AFRPL-TR-68-20, Advanced Maneuvering Propulsion Technology Program (Second Quarterly Report) R-7380-2, Rocketdyne, a division of North American Rockwell Corporation, Canoga Park, California, June 1968, CONFIDENTIAL.

5. AFRPL-TR-68-154, Advanced Maneuvering Propulsion Technology Program (Third Quarterly Report) R-7380-3, Rocketdyne, a division of North American Rockwell Corporation, Canoga Park, California, September 1968, CONFIDENTIAL.

6. AFRPL-TR-70-103, Advanced Maneuvering Propulsion System (Convair Propellant Feed System Design), September 1970, CONFIDENTIAL.

7. AFRPL-TR-70-104, Advanced Maneuvering Propulsion System (Lockheed Propellant Feed System Design), September 1970, CONFIDENTIAL.

8. NASA-CR-72543, Development and Demonstration of Criteria for Liquid Fluorine Feed System Components, Douglas Aircraft Company, October 1967.

9. NASA 3-12022, Rotating and Positive-Displacement Pumps for Low-Thrust Rocket Engines.

10. AFRPL-TR-66-147, Poppet and Seat Design Data for Aerospace Valve, Rocketdyne, a division of North American Rockwell Corporation, Canoga Park, California, July 1966.

11. RPL-TDR-64-68, Rocket Engine Valve Poppet and Seal Design Data, Rocketdyne, a division of North American Rockwell Corporation, Canoga Park, California, May 1964.

12. AFRPL-TR-68-3, Liquid Fluorine Shutoff Valve Development, K. L. Beard, A. W. Brown, J. M. H. Langlois, The J. C. Carter Company, January 1968.

13. AFRPL-TR-69-41, Liquid Fluorine Shutoff Valve Development Program, H. D. Samuel, Jr., McDonnell Douglas Astronautics Company, April 1969.

14. Fluorine Systems Handbook, Douglas Aircraft Company, 1967.

15. NASA-TN-D-2453, Friction, Wear, and Dynamic Seal Studies in Liquid Fluorine and Liquid Oxygen, W. F. Hardy, et al., August 1964.

16. AFRPL-TR-68-22, Final Report on the Development of Analytical Techniques for Bellows and Diaphragm Design, March 1968.

17. AFRPL-TR-70-1, Poppet and Seat Design Criteria for Contaminant-Particle Resistance, Rocketdyne, a division of North American Rockwell Corporation, Canoga Park, California.

18. NASA-SP-3037, Handling and Use of Fluorine and Fluorine-Oxygen Mixtures in Rocket Systems, Schmidt, 1967.

19. AF04(647)-171, Nomad Engine Development Program.

20. AFRPL-TR-67-290, Survey of Contamination in Rocket Propulsion Fluid Systems, Rocketdyne, a division of North American Rockwell Corporation, Canoga Park, California, November 1967.

21. NASA-CR-72074, H_2-F_2 Propulsion System Final Report, 21 October 1966.

22. AFRPL-TR-67-280, Final Report, Advanced Cryogenic Rocket Engine Program, Aerospike Concept, Rocketdyne, a division of North American Rockwell, 1967.

23. AFRPL-TR-67-214, Advanced Thrust Chamber for Space Maneuvering Propulsion, H. G. Diem and R. P. Pauckert, July 1967.

APPENDIX I

ENGINE SYSTEM COMPONENTS FAILURE MODE AND EFFECT ANALYSIS (FMEA)

1. INTRODUCTION

(U) A failure mode and effect analysis (FMEA) was performed for all the major component designs completed within the Task I effort. The results of these analyses are presented herein.

(U) The purpose of the analysis is to investigate the adequacy of a design to meet its requirements by an assessment of the consequences and potential seriousness of the possible occurrence of each of the failure modes on the successful operation of the engine and vehicle, and/or on the successful completion of the planned mission.

2. SUMMARY

(U) The FEMA's performed for the system components consist of four major steps: (1) component description and function, (2) a listing of potential failure modes, (3) a listing of the possible causes of each failure mode, and (4) an evaluation of the effect on engine system operation, vehicle functions, and/or mission completion. Because of the lack of test history on some of the components presented in this study, the analysis is less detailed in those areas.

(U) The probability of a potential failure mode occurring has not been included but could be assessed in the future as data and experience with these components become available.

3. SYSTEM DESCRIPTION

(U) The control system for each engine consists of two main propellant valves and two turbine control valves. The main propellant valves are located upstream of the turbopumps to afford extended coast capability in space.

(U) The turbine control valves provide both thrust and mixture ratio control. The main propellant valves are pneumatically actuated, while the turbine control valves are electrically actuated for position changes during engine operation as required by the closed-loop control system.

(U) Because of the reactive propellant combination, individual oxidizer and fuel system purges are required in addition to oxidizer pump seal purges. Oxidizer and fuel system helium purges are provided downstream of the main propellant valves on each engine to maintain the oxidizer system insert during start and to scavenge residual propellants during cutoff. For space coast capability, pneumatic system isolation solenoid valves have been incorporated to ensure minimum pneumatic losses.

(U) A schematic diagram of the overall engine system is shown in Fig. I-1.

4. ANALYSIS PROCEDURE

(U) The failure mode and effect analysis consists of five basic operations:

1. Identification of components
2. Description of component function
3. Identify possible failure modes
4. Identify possible causes for each failure mode
5. Prediction of possible failure effect on engine, vehicle, and mission, coordinated as applicable by time of occurrence during mission sequence

(U) The engine system subdivision that was used is shown below:

1. Engine subsystems

Propellant Inlet Ducts	Turbine Discharge Ducts
Propellant Discharge Ducts	Heat Exchangers
Turbine Inlet Ducts	Gimbal Bearing

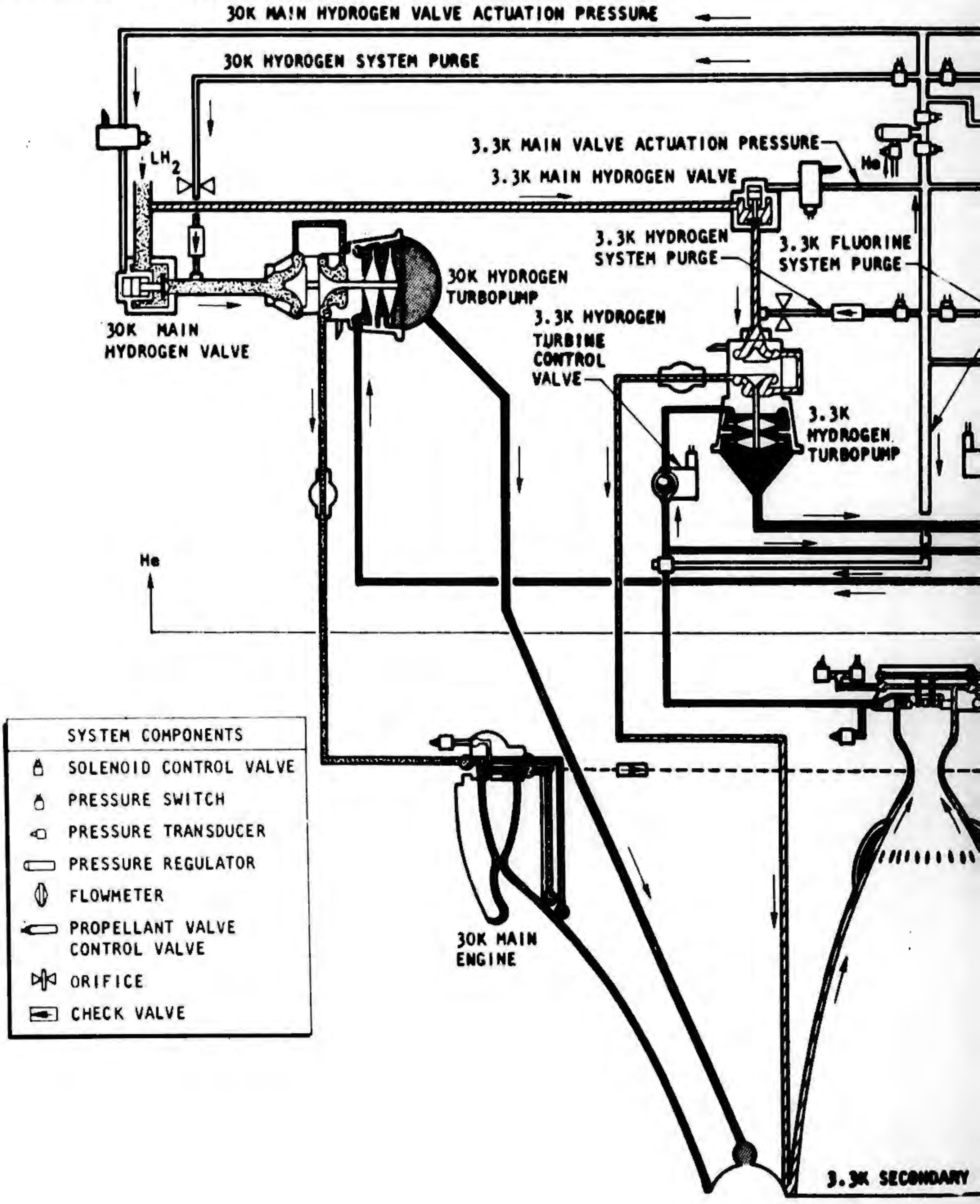
30K MAIN HYDROGEN VALVE ACTUATION PRESSURE
30K HYDROGEN SYSTEM PURGE
3.3K MAIN VALVE ACTUATION PRESSURE
He
3.3K MAIN HYDROGEN VALVE
LH2
3.3K HYDROGEN SYSTEM PURGE
3.3K FLUORINE SYSTEM PURGE
30K HYDROGEN TURBOPUMP
30K MAIN HYDROGEN VALVE
3.3K HYDROGEN TURBINE CONTROL VALVE
3.3K HYDROGEN TURBOPUMP
He
SYSTEM COMPONENTS
SOLENOID CONTROL VALVE
PRESSURE SWITCH
PRESSURE TRANSDUCER
PRESSURE REGULATOR
FLOWMETER
PROPELLANT VALVE CONTROL VALVE
ORIFICE
CHECK VALVE
30K MAIN ENGINE
3.3K SECONDARY

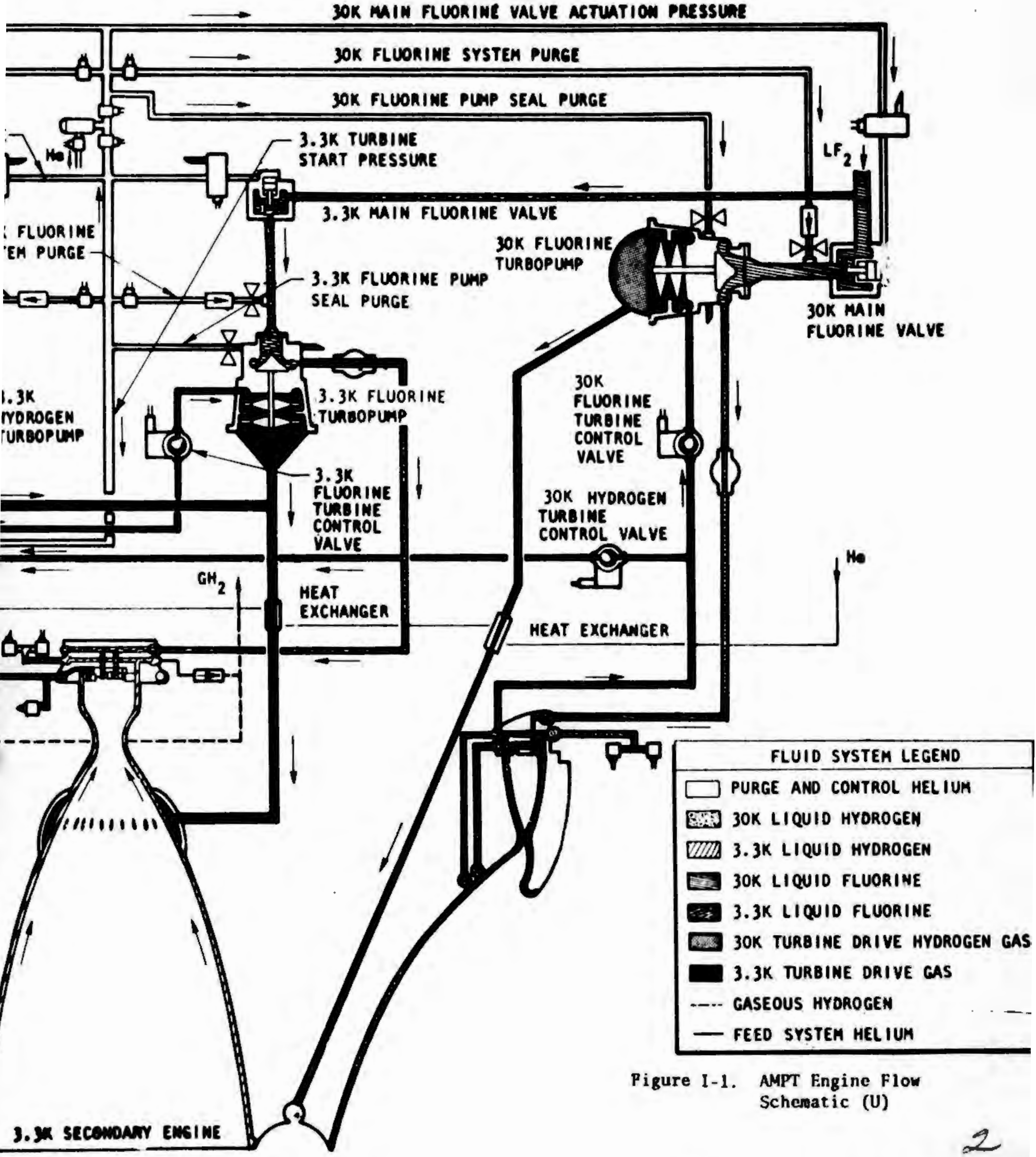

Figure I-1. AMPT Engine Flow Schematic (U)

2

(U) 2. Control System

Main Propellant Valves
Turbine Control Valves
Pneumatic System
Mainstage Controller
Start and Cutoff Controller

3. Turbopump Assemblies

Oxidizer Pump
Oxidizer Turbine
Fuel Pump
Fuel Turbine

4. Thrust Chamber Assemblies

Injector
Chamber
Nozzle

(U) The design of the various components accomplished did not provide sufficient detail to identify all possible failure modes that might be peculiar to the individual designs or fabrication techniques. Some of the possible failure modes can be determined only through detailed engine system design and development experience. Those failure modes that are identified are determined primarily from previous analysis of similar components designs. The possible causes are determined by a logical functional review of the design layout drawings.

(U) The following ground rules were adopted for implementation of the FMEA:

1. Structural failures and double failures are not considered.
2. The effects of the various failures are determined based on the results of the various engine system analytical and computer model studies.
3. Engine failure mode effects on the mission are based on the general mission requirements.
4. An engine restart subsequent to the failure is required.
5. Engine shutdown caused by the failure is considered a mission failure.

(U) The analysis for the main and secondary engines and their components is shown in Tables I-1 through I-8.

CONFIDENTIAL

TABLE I-1

MAIN ENGINE--SUBSYSTEM

Item and Part No.	Function	Possible Type of Failure	Possible Failure Cause	Seq.	Probable Failure Effect: Engine	Probable Failure Effect: Vehicle	Probable Failure Effect: Mission	Remarks
Duct; Oxidizer Pump Inlet	Inlet duct carries oxidizer from main valve to pump	Slight external leakage	Flange seal leakage	P	Detected and repaired during ground checks	None	None	Final configuration will be all welded construction
				S,C, M	Shift in control range	Propellant bias	Possible propellant depletion	
Duct; Oxidizer Pump Discharge	Discharge duct carries oxidizer from pump to injector oxidizer inlet manifold	Slight external leakage	Flange seal leakage	P	Detected and repaired during ground checks	None	None	Final configuration will be all welded construction
				S,C, M	Shift in control range	Propellant bias	Possible prolant depletion	
Duct; Fuel Pump Inlet	Inlet duct carries fuel from main valve to fuel pump	Slight external leakage	Flange seal leakage	P	Detected and repaired during ground checks	None	None	Final configuration will be all welded construction
				S,C, M	Shift in control range	Propellant bias	Possible propellant depletion	
Duct; Fuel Pump Discharge	Inlet duct carries fuel from pump to injector fuel inlet manifold	Slight external leakage	Flange seal leakage	P	Detected and repaired during ground checks	None	None	Final configuration will be all welded construction
				S,C, M	Shift in control range	Propellant bias	Possible propellant depletion	
Duct; Turbine Control Valve Inlet	Control valve inlet duct carries turbine drive gas from thrust chamber tapoff to TCV	Slight external leakage	Flange seal leakage	P	Detected and repaired during ground checks	None	None	Final configuration will be all welded construction
				S,C, M	Shift in control range	None	May limit capability	
Duct; Turbine Inlet	Turbine inlet duct carries turbine drive gas from TCV to turbine inlet	Slight external leakage	Flange seal leakage	P	Detected and reapired during ground checks	None	None	Final configuration will be all welded construction
				S,D, M	Shift in control range	None	May limit capability	

CONFIDENTIAL

CONFIDENTIAL

TABLE I-1

(Concluded)

Item and Part No.	Function	Possible Type of Failure	Possible Failure Cause	Seq.	Probable Failure Effect: Engine	Vehicle	Mission	Remarks
Duct; Turbine Discharge	Turbine discharge duct carries turbine exhaust from turbine to base manifold	Slight external leakage	Flange seal leakage	P	Detected and repaired during ground checks	None	None	
				S,C, M	None	None	None	
Heat Exchanger; Oxidizer Tank Pressurization	Heat exchanger heats oxidizer tank pressurization gas to minimize mass flow	Slight external leakage or	Flange seal leakage or contamination	P	Detected and repaired during ground checks	None	None	
				S,M	Possible pump cavitation	Loss of tank pressure	Possible abort	
Heat Exchanger; Fuel Tank Pressurization	Heat exchanger heats fuel tank pressurization gas to minimize mass flow	Slight external leakage or obstruction	Flange seal leakage or contamination	P	Detected and repaired during ground checks	None	None	
				S,M	Possible pump caviation	Loss of tank pressure	Possible abort	
Gimbal Bearing	Bearing transmits engine thrust to vehicle and provides for engine gimbaling	No applicable failure modes						

P = propellant checkout C = cutoff
S = start sequence O = orbital coast
M = mainstage

CONFIDENTIAL

TABLE I-2

(U) MAIN ENGINE--CONTROLS

Item & Part No.	Function	Possible Type of Failure	Possible Failure Cause	Seq.	Probable Failure Effect: Engine	Probable Failure Effect: Vehicle	Probable Failure Effect: Mission	Remarks
Main Oxidizer Valve	The main oxidizer valve is a normally closed, poppet type valve operated by pneumatic system pressure. The valve is located in the low-pressure propellant inlet duct and provides positive shutoff capability during periods when the engine is inoperative and during fuel lead portion of the engine start transient and at engine cutoff.	Fails to open	1. Insufficient actuator pressure	P	Detected and repaired during ground check	None	None	Prior to tanking propellants
			2. Excessive helium leakage around actuator piston	S	Engine will not start	None	Abort	
		Fails to close	Binding of actuator mechanism	P	Detected and repaired during ground check	None	None	
				C	Extended cutoff impulse; possible T/C burnout	Possible fire	Greater than targeted impulse would be obtained	
		Excessive oxidizer through leakage or accidental opening	Poppet seat damage or contamination	P	Detected and repaired during ground check	None	None	
				O	May accumulate oxidizer in T/C and interstage; possible fire	Loss of oxidizer Possible fire	Possible abort Possible abort	
		External oxidizer leakage	1. Defective Naflex seal	P	Detected and repaired during ground check	Possible fire	Possible abort	
			2. Defective bellows seal	O	Possible fire	Possible fire	Possible abort	
		Erroneous position indication	1. Malfunction in electrical system	P	Detected during preflight check	None	None	
			2. Faulty microswitch					
		Opens early Closes early	1. Malfunction in pneumatic system	S,C	Opens early or closes late; may cause high T/C mixture ratio and chamber damage	None	Uncertain	
		Opens late Closes late	2. Malfunction in start and cutoff controller		Opens late or closes early; no effect			

P = preflight checkout; S = start sequence; M = mainstage; C = cutoff; O = orbital coast

CONFIDENTIAL

CONFIDENTIAL

(This page is Unclassified)

TABLE 1-2

(Continued)

Item & Part No.	Function	Possible Type of Failure	Possible Failure Cause	Seq.	Probable Failure Effect: Engine	Vehicle	Mission	Remarks
Main Fuel Valve	The main fuel valve is a normally closed, poppet-type valve operated by pneumatic system pressure. The valve is located in the low-pressure propellant inlet duct and provides positive shutoff capability during periods when the main engine is inoperative and at cutoff.	Fails to open	1. Insufficient actuator pressure	P	Detected and repaired during ground check	None	None	Prior to tanking propellants
			2. Excessive helium leakage around actuator piston	S	Engine will not start	None	None	
		Fails to close	Binding of actuator mechanism	P	Detected and repaired during ground check	None	None	
				C	Extended cutoff impulse	Possible depletion of fuel supply	Possible abort of subsequent missions	
		Excessive fuel through leakage or accidental opening	Poppet seat damage or contamination	P	Detected and repaired during ground check			
				O	None	Possible depletion of fuel supply	Possible abort	
		External fuel leakage	1. Defective Naflex seal	P	Detected and repaired during ground check			
			2. Defective bellows seal	O	None			
		Erroneous position indication	1. Faulty micro-switch	P	Detected and repaired during ground check	None	None	
			2. Malfunction in electrical system	P	Detected and repaired during preflight check	None	None	
		Opens early Closes early	Malfunction in pneumatic system	S	No effect	None	None	
		Opens late Closes late	Malfunction in start and cutoff controller	C	Closes early: possible high T/C mixture ratio and chamber damage	None	Abort of subsequent missions	
					Closes late: excessive hydrogen usage at cutoff.	Excessive LH_2 usage	Possible propellant shortage	

P = preflight checkout; S = start sequence; M = mainstage; C = cutoff; O = orbital coast

TABLE I-2

(Continued)

Item & Part No.	Function	Possible Type of Failure	Possible Failure Cause	Seq.	Probable Failure Effect: Engine	Vehicle	Mission	Remarks
Turbine Control Valve (2 Req: 1 fuel and 1 oxidizer)	The turbine control valve is a variable position, ball-type valve actuated by an a-c motor through a planetary gear system. The valve provides flow control of turbine drive gas for thrust and mixture ratio control during mainstage and start and cutoff	Fails to close	1. Defective actuator	P	Detected and repaired during ground check	None	None	
			2. Excessive mechanical resistance in actuator drive	C	Engine cutoff transient will be extended--may damage T/P bearings	None	Restart may not be achieved	
			3. Loss of electrical power to actuator					
			4. Contamination					
		Fails to open	1. Defective actuator	P	Detected and repaired during ground check	None	None	
			2. Excessive mechanical resistance in actuator drive	S	Engine will not start	None	Abort	
			3. Loss of electrical power to actuator	M	Thrust or mixture ratio control cannot be accomplished	None	Possible abort	Depends on criticality of thrust and available propellants
		Excessive internal leakage	1. Faulty ball seal	P	Detected and repaired during ground check	None	Possible delay	
			2. Faulty ball seal bellows	S	Possible rotation of dry oxidizer pump; pump bearing damage	None	Possible abort	
				C	Extended cutoff transient; may damage T/P bearings	None	Restart may not be achieved	
		Excessive external leakage	1. Defective K seal	P	Detected and repaired during ground check	None	None	
			2. Defective actuator shaft bellows seal	S,M	Possible fire	None	Possible abort	
		Irregular response and failure to maintain position commands	1. Faulty potentiometer for feedback loop	P	Detected and repaired during ground check	None	None	
			2. Excessive mechanical resistance	S,C	Irregular start or cutoff transient; may damage engine	None	Uncertain	
				M	Irregular response to changes in thrust or mixture ratio	None	Uncertain	

P = preflight checkout; S = start sequence; M = mainstage; C = cutoff; O = orbital coast

CONFIDENTIAL

CONFIDENTIAL

(This page is Unclassified)

TABLE I-2

(Continued)

Item & Part No.	Function	Possible Type of Failure	Possible Failure Cause	Seq.	Probable Failure Effect			Remarks
					Engine	Vehicle	Mission	
Turbine Control Valve (continued)		Opens early	Faulty electrical or controller system	S	May cause oxidizer T/P overspeed and damage. Possible overshoot in thrust and mixture ratio. Possible T/C damage	None	Possible abort	No effect if fuel turbine control opens early
		Closes early	Faulty electrical or controller system	C	Fuel turbine control valve: may cause high T/C mixture ratio and chamber damage	None	Restart may not be accomplished	
				C	Oxidizer turbine control valve: no effect; early cutoff	None	None	
Pneumatic Regulator Shutoff Valve	Solenoid valve to provide positive shutoff of high-pressure helium supply to regulator actuating bellows	Fails to open	1. Loss of electrical power 2. Defective solenoid 3. Plugged inlet filter	P	Detected and repaired during ground check	None	None	
				S	Fails to activate pneumatic system; main valves will not open; engine will not start	None	Mission abort	
		Excessive leakage	1. Defective seat 2. Contamination	P	Detected and repaired during ground check	None	None	
				O	May activate pneumatic regulator continuously	None	None	
		Fails to close	Excessive mechanical resistance	P	Detected and repaired during ground check	None	None	
				C	Regulator would remain activated	None	None	

P = preflight checkout; S = start sequence; M = mainstage; C = cutoff; O = orbital coast

TABLE I-2

(Continued)

Item & Part No.	Function	Possible Type of Failure	Possible Failure Cause	Seq.	Probable Failure Effect: Engine	Probable Failure Effect: Vehicle	Probable Failure Effect: Mission	Remarks
Pneumatic System Regulator	This regulator controls helium downstream pressure to 750 ±50 psig with demands from 0 to 0.12 lb/sec with an inlet pressure from 3600 to 900 psia	High output	1. Ruptured bellows 2. Leaking poppet valve 3. Plugged compensating pressure port	S,M,C	High pressure would cause relief valve to open. Continued high pressure would cause helium depletion	Deplete ambient helium supply	Possible abort	
		Low output	Plugged inlet filter	S	Engine pneumatic system inoperative; engine would not start	None	Abort	
Low-Pressure Relief Valve	The relief valve is located directly downstream of the pressure regulator. The valve is designed to start to open at 825 psig and be fully open at 900 psig. This will ensure that the downstream pressure will not exceed 900 psig if the regulator fails	Fails to open and relieve	Ruptured bellows	P	Detected and repaired during ground check	None	None	
				S,M,C	Could cause line rupture and/or seal damage	Deplete helium supply	Possible abort	This would require a double failure
		Fails to close after relieving	Broken spring	P	Detected and repaired during ground check	None	None	
				S,M,C	Could cause depletion of helium supply and inoperative pneumatic system	Deplete helium supply	Possible abort	
		Excessive leakage	1. Damaged poppet seat	P	Detected and repaired during ground check	None	None	
			2. Contamination	S,M,C	Could cause depletion of helium supply and inoperative pneumatic system	Deplete helium supply	Possible abort	

P = preflight checkout; S = start sequence; M = mainstage; C = cutoff; O = orbital coast

TABLE I-2

(Continued)

Item & Part No.	Function	Possible Type of Failure	Possible Failure Cause	Seq.	Probable Failure Effect: Engine	Vehicle	Mission	Remarks
Engine Pneumatic System Isolation Valve	This valve provides a means of shutting off the helium flow to the engine not in use (i.e., main or secondary)	Fails to open	1. Faulty solenoid	P	Detected and repaired during ground check	None	None	
			2. Plugged bellows inlet port	S	Engine would not start	None	None	
		Opens prematurely	Faulty electrical controller	P	Detected and repaired during ground check			
				S	No effect	None	None	
				P	Detected and repaired during ground check	None	None	
		Fails to close or excessive through leakage	1. Damaged poppet 2. Contamination 3. Excessive mechanical resistance	M	Helium leakage would escape through the inoperative engine oxidizer turbopump seal cavity	Eventual loss of pneumatic helium supply	Possible abort	
				C	No effect; regulator shutoff valve would provide positive cutoff	None	None	
		Closes prematurely	1. Loss of electrical power	P	Detected and repaired during ground check	None	None	
			2. Faulty electrical controller	S,C	Insufficient purge; possible engine damage	None	Possible abort	
Fuel System Purge Solenoid Valve	The two-way solenoid valve controls the purge gas flow to the engine fuel system during start and cutoff	Fails to open	Faulty solenoid	P	Detected and repaired during ground check	None	None	
				C	Residual hydrogen in the thrust chamber would not be expelled	None	None	Hydrogen would vaporize and eventually be expelled. Fuel purge may not be necessary on flight engine
		Opens prematurely	Faulty delay timer	P	Detected and repaired during ground check	None	None	
				C	Purge injection pressure is higher than fuel tank pressure; therefore, the purge gas could stop the fuel flow and cause the helium purge to back up into the fuel tank. (continued)	Helium could be forced back into the main fuel tank	None	

P = preflight checkout; S = start sequence; M = mainstage; C = cutoff; O = orbital coast

CONFIDENTIAL

TABLE I-2

(Continued)

Item & Part No.	Function	Possible Type of Failure	Possible Failure Cause	Seq.	Probable Failure Effect: Engine	Vehicle	Mission	Remarks
Fuel System Purge Solenoid Valve (continued)					High T/C mixture ratio and T/C damage could occur			
		Fails to close	Excessive mechanical resistance	P	Detected and repaired during ground check	None	None	
				C	None	None	None	Regulator shutoff valve or engine isolation valve would provide shutoff
		Closes prematurely	Faulty delay timer	P	Detected and repaired during ground check	None	None	
				C	Insufficient purge; some residual hydrogen would remain	None	None	Residual hydrogen would vaporize
		Excessive leakage	1. Damaged seat 2. Contamination	M	Helium would leak into engine fuel flow	Eventual loss of helium purge gas	Uncertain	
Oxidizer System Purge Solenoid Valve	The two-way solenoid valve controls the purge gas flow to the engine oxidizer system during start and cutoff	Fails to open	Faulty solenoid	P	Detected and repaired during ground check	None	None	
				S	Loss of oxidizer purge could result in engine damage during start	None	Abort	
		Opens prematurely	Faulty delay timer	P	Detected and repaired during ground check	None	None	
				S	No effect	None	None	
		Fails to close	Excessive mechanical resistance	S	Higher pressure oxidizer system purge may hold back oxidizer flow and allow helium to back up into oxidizer tank. Engine would not start. Limiter switch would initiate cutoff	Helium purge gas would flow into oxidizer tank	Possible abort	
				C	No effect; engine system isolation valve would provide positive cutoff	None	None	

P = preflight checkout; S = start sequence; M = mainstage; C = cutoff; O = orbital coast

CONFIDENTIAL

TABLE I-2

(Concluded)

Item & Part No.	Function	Possible Type of Failure	Possible Failure Cause	Seq.	Probable Failure Effect: Engine	Vehicle	Mission	Remarks
Oxidizer System purge Solenoid Valve (continued)		Closes prematurely	Faulty delay timer	P	Detected and repaired during ground check	None	None	
				S,C	Insufficient purge; possible engine damage	None	Possible abort	
		Excessive leakage	1. Damaged seat 2. Contamination	M	Helium would leak into engine oxidizer flow	None	Uncertain	
Check Valves (2 required)	The check valves are located in the propellant purge lines downstream of the purge solenoid valves. The check valves protect the solenoid valves from exposure to the respective propellants	Fails to open	Excessive mechanical resistance	P	Detected and repaired during ground check	None	None	
				S,C	Engine purge gas will not flow; loss of oxidizer purge could cause engine damage	None	Possible abort	
		Fails to close	Excessive mechanical resistance	P	Detected and repaired during ground check	None	Possible abort	
				M	Propellants are allowed to flow back up to system purge solenoid valves; may damage oxidizer purge solenoid valve	None	None	

P = preflight checkout; S = start sequence; M = mainstage; C = cutoff; O = orbital coast

TABLE I-3

MAIN ENGINE--TURBOPUMPS

Item and Part No.	Function	Possible Type of Failure	Possible Failure Cause	Seq.	Probable Failure Effect			Remarks
					Engine	Vehicle	Mission	
Fuel Turbopump Assembly	Fuel turbopump is a centrifugal pump with direct turbine drive and is equipped with a seal purge and drain system. Pump is lubricated with the propellant and its function is to increase the pressure of the fuel and propel the fluid through the cooling jacket to the injector. The turbine is a two-stage velocity compounded Curtis type. The drive gas is heated hydrogen from the thrust chamber regenerative cooling jacket	Failure to start	1. High torque because of frozen or misaligned bearing shaft or seal	P	Detected and repaired during ground check	None	None	
				S	Engine will not start	None	Abort	
			2. Turbine control valve fails to open					
			3. Turbine spin valve fails to open					
		Fails to achieve design output in specified time	1. High torque	P	Detected and repaired during ground check	None	None	
			2. Turbine control valve fails to open completely	S	Engine may not start or may not achieve desired thrust and/or mixture ratio thrust chamber damage may occur			
			3. Excessive downstream fuel resistance					
			4. Excessive turbine flow resistance	M	Desired thrust and/or mixture ratio may not be achieved. Thrust chamber damage may occur	None	Possible failure	
			1. Oxidizer explosion or structural failure of pump or turbine	M	Engine will shutdown prematurely with certain damage to the thrust chamber due to lack of coolant flow	None	Possible failure	
			2. Turbine control valve closes prematurely					
			3. Turbine drive gas leakage					
			4. Bearing failure					

P - Preflight checkout; S - Start sequence; M - Mainstage; C - Cutoff; O - Orbital Coast

CONFIDENTIAL

TABLE I-3

(Continued)

Item and Part No.	Function	Possible Type of Failure	Possible Failure Cause	Seq.	Probable Failure Effect: Engine	Probable Failure Effect: Vehicle	Probable Failure Effect: Mission	Remarks
Fuel Turbopump Assembly (continued)		Overspeed	1. Loss of liquid fuel input 2. Ruptured high-pressure duct 3. Malfunction of engine start 4. Malfunction of overspeed cutoff network	S	Possible damage to fuel turbopump Possible spike in chamber pressure with subsequent structural damage to thrust chamber	Possible loss of Possible early depletion of tanked fuel	Possible abort Possible abort	Fuel pump speed must be limited during pump priming to assure proper bearing cooling and lubrication Control system will adjust to maintain command mixture ratio and thrust valve but depending on the seriousness of the failure, the required correction may exceed the control system component capability
		Underspeed	1. Loss of turbine blades 2. Hot gas leakage 3. Turbine control valve fails to open completely	S M	Slow engine start may occur. High thrust chamber mixture ratio may occur with subsequent damage to the thrust chamber High operating mixture ratio may occur with subsequent damage to the thrust chamber	None Possible early depletion of tanked oxidizer	Uncertain Possible abort	
		Internal shaft seal leakage	1. Damage turbopump seal package	S,M,C	Probable failure of turbopump	None	Possible abort	
		External hot-gas leakage	1. Damage duct or flange seal	S,M,C	Reduced turbine power available with subsequent reduction in thrust or mixture ratio	None	Possible abort	

TABLE I-3

(Continued)

Item and Part No.	Function	Possible Type of Failure	Possible Failure Cause	Seq.	Probable Failure Effect: Engine	Vehicle	Mission	Remarks
Oxidizer Turbopump Assembly	The oxidizer turbopump is a centrifugal pump with direct turbine drive and is equipped with a seal purge and drain system. The pump is self lubricated with the propellant and its function is to increase the pressure of the oxidizer and propel the fluid through the high-pressure ducting to the chamber. The turbine is a two-stage velocity compounded Curtis type. The drive gas is low mixture heated hydrogen from the thrust chamber regenerative cooling jacket	Failure to start	1. High torque because of frozen or misaligned bearing shaft or seal	P	Detected and repaired during ground check	None	None	
				S	Engine will not start	None	Abort	
			2. Turbine control valve fails to open completely					
			3. Turbine spin valve fails to open					
			1. High torque	P	Detected and repaired during ground check	None	None	
			2. Turbine control valve fails to open completely	S	Engine may not start or may not achieve desired thrust and/or mixture ratio	None	Possible abort	
			3. Excessive downstream oxidizer resistance	M	Desired thrust and/or mixture ratio may not be achieved	None	Possible failure	
			4. Excessive turbine flow resistance					
			1. Oxidizer explosion or structural failure of pump or turbine	M	Engine will shutdown prematurely with possible damage to oxidizer pump	None	Possible abort	
			2. Turbine control valve closes prematurely					
			3. Turbine drive gas leakage					
			4. Bearing failure					

CONFIDENTIAL

CONFIDENTIAL

TABLE I-3
(Concluded)

Item and Part No.	Function	Possible Type of Failure	Possible Failure Cause	Seq.	Probable Failure Effect: Engine	Vehicle	Mission	Remarks
Oxidizer Turbopump Assembly (continued)		Overspeed	1. Loss of liquid oxidizer input 2. Ruptured high pressure duct	S	Possible high thrust chamber mixture ratio during start transient and subsequent thrust chamber and/or oxidizer pump damage	Possible loss of tanked oxidizer	Possible abort	Control system will adjust to maintain command mixture ratio and thrust value, but with these failures the required correction may exceed the control system component capability
			3. Malfunction of engine start sequence or mainstage controller 4. Malfunction of overspeed cutoff network	M	Possible high thrust chamber mixture ratio and subsequent damage to thrust chamber and oxidizer pump	Possible loss of tanked oxidizer	Possible abort	
		Underspeed	1. Loss of turbine blades	S	Slow engine start may result	None	Uncertain	
			2. Hot-gas leakage 3. Turbine control valve fails to open fully	M	Low operating mixture ratio may occur	Possible early depletion of tanked fuel	Possible abort	
		Internal shaft seal leakage	1. Damaged turbopump seal package	S,M,C	Probable failure of turbopump	None	Probable abort	
		External hot-gas leakage	1. Damaged duct or flange seal	S,M,C	Reduced turbine power available with subsequent reduction in thrust or mixture ratio	None	Possible abort	

TABLE I-4

MAIN ENGINE--THRUST CHAMBER ASSEMBLY

Item and Part No.	Function	Possible Type of Failure	Possible Failure Cause	Seq.	Probable Failure Effect			Remarks
					Engine	Vehicle	Mission	
Thrust Chamber Assembly	Assembly consists of injector and regeneratively cooled thrust chamber whose function is to efficiency convert the products of combustion of the propellants into directed thrust	Slight internal leakage	Thermal fatigue or material deficiency	S	Delayed start	None	Possible abort	
				M	Shift in engine controls and thrust alignment	Propellant bias and reduced control capability	Possible propellant depletion	
				C	Shift in engine thrust alignment during cutoff	Reduced control capability	None	
		Slight external leakage	Material deficiency	S,C, M	Shift in engine controls	Propellant bias	Possible propellant depletion	
		Obstruction of one invector orifice	Contamination	S,C, M	None	None	None	

P - Preflight checkout
S - Start sequence
M - Mainstage

C - Cutoff
O - Orbital Coast

CONFIDENTIAL

CONFIDENTIAL

TABLE I-5

SECONDARY ENGINE--SUBSYSTEM

Item and Part No.	Function	Possible Type of Failure	Possible Failure Cause	Seq.	Probable Failure Effect			Remarks
					Engine	Vehicle	Mission	
Duct; Oxidizer Pump Inlet	Inlet duct carries oxidizer from main valve to pump	Slight external leakage	Flange seal leakage	P	Detected and repaired during ground checks	None	None	Final configuration will be all welded construction
				S,C, M	Shift in control range	Propellant bias	Possible propellant depletion	
Duct; Oxidizer Pump Discharge	Discharge duct carries oxidizer from pump to injector oxidizer inlet manifold	Slight external leakage	Flange seal leakage	P	Detected and repaired during ground checks	None	None	Final configuration will be all welded construction
				S,C, M	Shift in control range	Propellant bias	Possible propellant depletion	
Duct; Fuel Pump Inlet	Inlet duct carries fuel from main valve to fuel pump	Slight external leakage	Flange seal leakage	P	Detected and repaired during ground checks	None	None	Final configuration will be all welded construction
				S,C, M	Shift in control range	Propellant bias	Possible propellant depletion	
Duct; Fuel Pump Discharge	Inlet duct carries fuel from pump to injector fuel inlet manifold	Slight external leakage	Flange seal leakage	P	Detected and repaired during ground checks	None	None	Final configuration will be all welded construction
				S,C, M	Shift in control range	Propellant bias	Possible propellant depletion	
Duct; Turbine Control Valve Inlet	Control valve inlet duct carries turbine drive gas from thrust chamber tapoff to TCV	Slight external leakage	Flange seal leakage	P	Detected and repaired during ground checks	None	None	Final configuration will be all welded construction
				S,C, M	Shift in control range	None	May limit capability	
Duct; Turbine Inlet	Turbine inlet duct carries turbine drive gas from TCV to turbine inlet	Slight external leakage	Flange seal leakage	P	Detected and repaired during ground checks	None	None	Final configuration will be all welded construction
				S,C, M	Shift in control range	None	May limit capability	

TABLE I-5

(Concluded)

Item and Part No.	Function	Possible Type of Failure	Possible Failure Cause	Seq.	Probable Failure Effect			Remarks
					Engine	Vehicle	Mission	
Duct; Turbine Discharge	Turbine discharge duct carries turbine exhaust from turbine to base manifold	Slight external leakage	Flange seal leakage	P	Detected and repaired during ground checks	None	None	
				S,C, M	None	None	None	
Heat Exchanger; Oxidizer Tank Pressurization	Heat exchanger heats oxidizer tank pressurization gas to minimize mass flow	Slight external leakage or obstruction	Flange seal leakage or contamination	P	Detected and repaired during ground checks	None	None	
				S,M	Possible pump cavitation	Loss of tank pressure	Possible abort	
Heat Exchanger; Fuel Tank Pressurization	Heat exchanger heats fuel tank pressurization gas to minimize mass flow	Slight external leakage or obstruction	Flange seal leakage or contamination	P	Detected and repaired during ground checks	None	None	
				S,M	Possible pump caviation	Loss of tank pressure	Possible abort	

P - Preflight checkout
S - Start sequence
M - Mainstage
C - Cutoff
O - Orbital coast

CONFIDENTIAL

CONFIDENTIAL

TABLE I-6

SECONDARY ENGINE--CONTROLS

Item and Part No.	Function	Possible Type of Failure	Possible Failure Cause	Seq.	Probable Failure Effect: Engine	Vehicle	Mission	Remarks
Main Oxidizer Valve	The main oxidizer valve is a normally closed, poppet-type valve operated by pneumatic system pressure. The valve is located in the low pressure propellant inlet duct and provides positive shutoff capability during periods when the engine is inoperative and during fuel lead portion of the engine start transient and at engine cutoff	Fails to open	1. Insufficient actuator pressure	P	Detected and repaired during ground check	None	None	Prior to tanking propellants
			2. Excessive helium leakage around actuator piston	S	Engine will not start	None	Abort	
		Fails to close	Binding of actuator mechanism	P	Detected and prepaired during ground check	None	None	
				C	Extended cutoff impulse; possible thrust chamber burnout	Possible fire	Greater than targeted impulse would be obtained	
		Excessive oxidizer through leakage	Poppet seat damage or contamination	P	Detected and repaired during ground check	None	Possible delay	
				O	May accumulate oxidizer in thrust chamber and interstage	Loss of oxidizer	Possible abort	
					Possible fire	Possible fire	Possible abort	
		External oxidizer leakage	1. Defective Naflex seal	P	Possible fire	Possible fire	Possible abort	
			2. Defective bellows seal	O	Possible fire	Possible fire	Possible abort	
		Erroneous position indication	1. Malfunction in electrical system 2. Faulty microswitch	P	Detected during preflight check	None	None	
		Opens early Closes early	Malfunction in pneumatic system	S,C	Opens early or closes late; may cause high thrust chamber mixture ratio and chamber damage	None	Uncertain	
		Opens late Closes late	Malfunction in start and cutoff controller		Opens late or closes early; no effect			

P = preflight checkout; S = start sequence; M = mainstage; C = cutoff; O = orbital coast

CONFIDENTIAL

TABLE I-6

(Continued)

Item & Part No.	Function	Possible Type of Failure	Possible Failure Cause	Seq.	Probable Failure Effect: Engine	Vehicle	Mission	Remarks
Main Fuel Valve	The main fuel valve is a normally closed, poppet-type valve operated by pneumatic system pressure. The valve is located in the low-pressure propellant inlet duct and provides positive shutoff capability during periods when the main engine is inoperative and at cutoff.	Fails to open	1. Insufficient actuator pressure	P	Detected and repaired during ground check	None	None	Prior to tanking propellants
			2. Excessive helium leakage around actuator piston	S	Engine will not start	None	None	
		Fails to close	Binding of actuator mechanism	P	Detected and repaired during ground check	None	None	
				C	Extended cutoff impulse	Possible depletion of fuel supply	Possible abort of subsequent missions	
		Excessive fuel through leakage	Poppet seat damage or contamination	P	Detected and repaired during ground check			
				O	None	Possible depletion of fuel supply	Possible abort	
		External fuel leakage	1. Defective Naflex seal	P	Detected and repaired during ground check			
			2. Defective bellows seal	O	None			
		Erroneous position indication	1. Faulty microswitch	P	Detected and repaired during preflight check	None	None	
			2. Malfunction in electrical system					
		Opens early Closes early	Malfunction in pneumatic system	P	Detected and repaired during preflight check			
				S	No effect			
		Opens late Closes late	Malfunction in start and cutoff controller	C	Closes early-possible high T/C mixture ratio and chamber damage	None		
					Closes late-excessive hydrogen usage at cutoff	Excessive LH_2 usage	Possible propellant shortage	

P = preflight checkout; S = start sequence; M = mainstage; C = cutoff; O = orbital coast

CONFIDENTIAL

TABLE I-6

(Continued)

Item & Part No.	Function	Possible Type of Failure	Possible Failure Cause	Seq.	Probable Failure Effect: Engine	Probable Failure Effect: Vehicle	Probable Failure Effect: Mission	Remarks
Turbine Control valve (2 req: 1 fuel and 1 oxidizer	The turbine control valve is a variable position, ball-type valve actuated by an a-c motor through a planetary gear system. The valve provides flow control of turbine drive gas for thrust and mixture ratio control during mainstage and start and cutoff	Fails to open	1. Defective actuator	P	Detected and repaired during ground check	None	None	
			2. Excessive mechanical resistance in actuator drive	S	Engine will not start	None	Abort	
			3. Loss of electrical power to actuator	M	Thrust or mixture ratio control cannot be accomplished	None	Possible abort	Depends on criticality of thrust and available propellants
		Fails to close	1. Defective actuator	P	Detected and repaired during ground check	None	None	
			2. Excessive mechanical resistance in actuator drive	C	Engine cutoff transient will be extended--may damage turbopump bearings	None	Restart may not be achieved	
			3. Loss of electrical power to actuator					
			4. Contamination					
		Excessive internal leakage	1. Faulty ball seal	P	Detected and repaired during ground check	None	Possible delay	
			2. Faulty ball seal bellows	S	Possible rotation of dry oxidizer pump; pump bearing damage	None	Possible abort	
				C	Extended cutoff transient; may damage turbopump bearings	None	Restart may not be achieved	
		Excessive external leakage	1. Defective K-seal	P	Detected and repaired during ground check	None	None	
			2. Defective actuator shaft bellows seal	S,M	Possible fire	None	Possible abort	
		Irregular response and failure to maintain position commands	Faulty potentiometer for feedback loop	P	Detected and repaired during ground check	None	None	
				S,C	Irregular start or cutoff transient; may damage engine (continued)	None	Uncertain	

P = preflight checkout; S = start sequence; M = mainstage; C = cutoff; O = orbital coast

CONFIDENTIAL

TABLE I-6

(Continued)

Item & Part No.	Function	Possible Type of Failure	Possible Failure Cause	Seq.	Probable Failure Effect: Engine	Probable Failure Effect: Vehicle	Probable Failure Effect: Mission	Remarks
Turbine Control Valve (continued)				M	Irregular response to changes in thrust or mixture ratio commands	None	Uncertain	
		Opens early	Faulty electrical or controller system	S	May cause oxidizer turbopump overspeed and damage. Possible overshoot in thrust and mixture ratio. Possible T/C damage	None	Possible abort	No effect if fuel turbine control opens early
		Closes early	Faulty electrical or controller system	C	Fuel turbine control valve may cause high T/C mixture ratio and chamber damage	None	Restart may not be accomplished	
				C	Oxidizer turbine control valve: no effect; early cutoff	None	None	
Engine Pneumatic System Isolation Valve	This valve provides a means of shutting off the helium flow to the engine not in use (i.e., main or secondary)	Fails to open	1. Faulty solenoid	P	Detected and repaired during ground check	None	None	
			2. Plugged inlet port	S	Engine would not start	None	None	
		Opens prematurely	Faulty electrical controller	P	Detected and repaired during ground check			
				S	No effect	None	None	
		Fails to close or excessive through leakage	1. Damaged poppet	P	Detected and repaired during ground check	None	None	
			2. Contamination 3. Excessive mechanical resistance	M	Helium leakage would escape through the inoperative engine oxidizer turbopump seal cavity	Eventual loss of purge helium supply	Possible abort	
				C	No effect; regulator shutoff valve would provide positive cutoff	None	None	
		Closes prematurely	1. Loss of electrical power	P	Detected and repaired during ground check	None	None	
			2. Faulty electrical controller	S,C	Insufficient purge; possible engine damage	None	Possible abort	

P = preflight checkout; S = start sequence; M = mainstage; C = cutoff; O = orbital coast

CONFIDENTIAL

(This page is Unclassified)

CONFIDENTIAL

TABLE I-6

(Continued)

Item & Part No.	Function	Possible Type of Failure	Possible Failure Cause	Seq.	Probable Failure Effect: Engine	Probable Failure Effect: Vehicle	Probable Failure Effect: Mission	Remarks
Fuel System Purge Solenoid Valve	The two-way solenoid valve controls the purge gas flow to the engine fuel system during start and cutoff	Fails to open	Faulty solenoid	P	Detected and repaired during ground check	None	None	
				C	Residual hydrogen in the thrust chamber would not be expelled	None	None	Hydrogen would be vaporized and eventually be expelled. Fuel system purge may not be necessary on flight engine
		Opens prematurely	Faulty delay timer	P	Detected and repaired during ground check	None	None	
				C	Purge injection pressure is higher than fuel tank pressure. Therefore the purge gas could stop the fuel flow and cause the helium purge to back up into the fuel tank. High T/C mixture ratio and T/C damage could occur	Helium could be forced back into the main fuel tank	None	
		Fails to close	Excessive mechanical resistance	P	Detected and repaired during ground check	None	None	
				C	None	None	None	Regulator shutoff valve of engine and isolation valve would provide shutoff
		Closes prematurely	Faulty delay timer	P	Detected and repaired during ground check	None	None	
				C	Insufficient purge; some residual hydrogen would remain	None	None	Residual hydrogen would vaporize
		Excessive leakage	1. Damaged seat 2. Contamination	M	Helium would leak into engine fuel flow	Eventual loss of helium purge gas	None	

P = preflight checkout; S = start sequence; M = mainstage; C = cutoff; O = orbital coast

CONFIDENTIAL

TABLE I-6

(Continued)

Item & Part No.	Function	Possible Type of Failure	Possible Failure Cause	Seq.	Probable Failure Effect: Engine	Vehicle	Mission	Remarks
Oxidizer System Purge Solenoid Valve	The two-way solenoid valve controls the purge gas flow to the engine oxidizer system during start and cutoff	Fails to open	Faulty solenoid	P	Detected and repaired during ground check	None	None	
				S	Loss of oxidizer purge could result in engine damage during start	None	Abort	
		Opens prematurely	Faulty delay timer	P	Detected and repaired during ground check	None	None	
				S	No effect	None	None	
		Fails to close	Excessive mechanical resistance	S	Higher pressure oxidizer system purge may hold back oxidizer flow and allow helium to back up into oxidizer tank. Engine would not start. Limiter switch would initiate cutoff	Helium purge gas would flow into oxidizer tank	Possible abort	
				C	No effect, engine system isolation valve would provide positive cutoff	None	None	
		Closes prematurely	Faulty delay timer	P	Detected and repaired during ground check	None	None	
				S,C	Insufficient purge; possible engine damage	None	Possible abort	
		Excessive leakage	1. Damaged Seat 2. Contamination	M	Helium would leak into engine oxidizer flow	None	Uncertain	

P = preflight checkout; S = start sequence; M = mainstage; C = cutoff; O = orbital coast

TABLE I-6

(Concluded)

Item & Part No.	Function	Possible Type of Failure	Possible Failure Cause	Seq.	Probable Failure Effect: Engine	Probable Failure Effect: Vehicle	Probable Failure Effect: Mission	Remarks
Check Valves (2 req.)	The check valves are located in the propellant purge lines downstream of the purge solenoid valves. The check valves protect the solenoid valves from exposure to the respective propellants	Fails to open	Excessive mechanical resistance	P	Detected and repaired during ground check	None	None	
				S,C	Engine purge gas will not flow--loss of oxidizer purge could cause engine damage	None	Possible abort	
		Fails to close	Excessive mechanical resistance	P	Detected and repaired during ground check	None	Possible abort	
				M	Propellants are allowed to flow back up to system purge solenoid valves--may damage oxidizer purge solenoid valve	None	None	
Secondary Engine Turbine Spin Valve	The solenoid operated valve opens the helium port and closes the hot gas port to a common duct to the turbine control valves. The valve is actuated by a three-way solenoid pilot valve. An electrical command directs helium to a bellows-actuated spool valve and opens the helium port and closes the hot gas port. Upon removal of the electrical signal, the helium port is closed and the hot gas port is opened.	Hot gas port fails to close or excessive leakage	Damaged actuating shaft or poppet or seat	P	Detected and repaired during ground check	None	None	
				S	Helium would flow back into chamber and turbine speed buildup would be slower	None	None	
		Valve fails to actuate	1. Faulty solenoid 2. Ruptured closing bellows	P	Detected and repaired during ground check	None	None	
				S	Turbine starting energy would be dependent on the tapoff gases. Engine start would be much slower	None	None	
		Helium port fails to close or excessive leakage	1. Ruptured closing bellows 2. Damaged poppet seat	P	Detected and repaired during ground check	None	None	
				M	Helium would leak into the hot gas flow to the turbine	None	None	

P = preflight checkout; S = start sequence; M = mainstage; C = cutoff; O = orbital coast

CONFIDENTIAL

TABLE I-7

SECONDARY ENGINE--TURBOPUMPS

Item and Part No.	Function	Possible Type of Failure	Possible Failure Cause	Seq.	Probable Failure Effect: Engine	Probable Failure Effect: Vehicle	Probable Failure Effect: Mission	Remarks
Fuel Turbopump Assembly	Fuel turbopump is a centrifugal pump with direct turbine drive and is equipped with a seal purge and drain system. Pump is lubricated with the propellant and its function is to increase the pressure of the fuel and propel the fluid through the cooling jacket to the injector. The turbine is a two-stage velocity compounded Curtis type. The drive gas is low mixture ratio combustion gases tapped off from the thrust chamber	Failure to start	1. High torque because of frozen or misaligned bearing shaft or seal 2. Turbine control valve fails to open 3. Turbine spin valve fails to open	P	Detected and repaired during ground check	None	None	
				S	Engine will not start	None	Abort	
		Fails to achieve design output in specified time	1. High torque 2. Turbine control valve fails to open completely 3. Excessive downstream fuel resistance 4. Excessive turbine flow resistance	P	Detected and repaired during ground check	None	None	
				S	Engine may not start or may not achieve desired thrust and/or mixture ratio thrust chamber damage may occur			
				M	Desired thrust and/or mixture ratio may not be achieved. Thrust chamber may occur	None	Possible failure	
			1. Oxidizer explosion or structural failure of pump or turbine 2. Turbine control valve closes prematurely 3. Turbine drive gas leakage 4. Bearing failure	M	Engine will shutdown prematurely with certain damage to the thrust chamber due to lack of coolant flow	None	Possible failure	

P - Preflight checkout
S - Start sequence
M - Mainstage

C - Cutoff
O - Orbital coast

CONFIDENTIAL

TABLE I-7

(Continued)

Item and Part No.	Function	Possible Type of Failure	Possible Failure Cause	Seq.	Probable Failure Effect: Engine	Vehicle	Mission	Remarks
Fuel Turbopump Assembly (Continued)		Overspeed	1. Loss of liquid fuel input 2. Ruptured high-pressure duct 3. Malfunction of engine start sequence or mainstage controller 4. Malfunction of overspeed cutoff network	S	Possible damage to fuel turbopump	Possible loss of tanked fuel	Possible abort	Fuel pump speed must be limited during pump priming to assure proper bearing cooling and lubrication
					Possible spike in chamber pressure with subsequent structural damage to thrust chamber	Possible early depletion of tanked fuel	Possible abort	Control system will adjust to maintain command mixture ratio and thrust valve but depending on the seriousness of the failure, the required correction may exceed the control system component capability
		Underspeed	1. Loss of turbine blades 2. Hot-gas leakage 3. Turbine control valve fails to open completely	S	Slow engine start may occur. High thrust chamber mixture ratio may occur with subsequent damage to the thrust chamber	None	Uncertain	
				M	High operating mixture ratio may occur with subsequent damage to the thrust chamber	Possible early depletion of tanked oxidizer	Possible abort	
		Internal shaft seal leakage	1. Damaged turbopump seal package	S,M,C	Probable failure of turbopump	None	Possible abort	
		External hot-gas leakage	1. Damaged duct or flange seal	S,M,C	Reduced turbine power available with subsequent reduction in thrust or mixture ratio	None	Possible abort	

TABLE I-7

(Continued)

Item and Part No.	Function	Possible Type of Failure	Possible Failure Cause	Seq.	Probable Failure Effect: Engine	Vehicle	Mission	Remarks
Oxidizer Turbopump Assembly	The oxidizer turbopump is a centrifugal pump with direct turbine drive and is equipped with a seal purge and drain system. The pump is self-lubricated with the propellant and its function is to increase the pressure of the oxidizer and propel the fuel through the high pressure ducting to the chamber. The turbine is a two-stage velocity compounded Curtis type. The drive gas is low mixture ratio combustion gases tapped off from the thrust chamber	Failure to start	1. High torque because of frozen or misaligned bearing shaft or seal 2. Turbine control valve fails to open completely 3. Turbine spin valve fails to open	P	Detected and repaired during ground check	None	None	
				S	Engine will not start	None	Abort	
			1. High torque 2. Turbine control valve fails to open completely 3. Excessive downstream oxidizer resistance 4. Excessive turbine flow resistance	P	Detected and repaired during ground check	None	None	
				S	Engine may not start or may not achieve desired thrust and/or mixture ratio	None	Possible abort	
				M	Desired thrust and/or mixture ratio may not be achieved	None	Possible failure	
			1. Oxidizer explosion or structural failure of pump or turbine 2. Turbine control valve closes prematurely 3. Turbine drive gas leakage 4. Bearing failure	M	Engine will shutdown prematurely with possible damage to oxidizer pump	None	Possible	
		Overspeed	1. Loss of liquid oxidizer input 2. Ruptured high pressure duct	S	Possible high thrust chamber mixture ratio during start transient and subsequent thrust chamber and/or oxidizer pump damage	Possible loss of tanked oxidizer	Possible abort	Control system will adjust to maintain command mixture ratio and thrust valve but with these failures the required correction may exceed the control system component capability
			3. Malfunction of engine start sequence or mainstage controller 4. Malfunction of overspeed cutoff network	M	Possible high thrust chamber mixture ratio and subsequent damage of thrust chamber and oxidizer pump	Possible loss of tanked oxidizer	Possible abort	

CONFIDENTIAL

CONFIDENTIAL

TABLE I-7

(Concluded)

Item and Part No.	Function	Possible Type of Failure	Possible Failure Cause	Seq.	Probable Failure Effect: Engine	Vehicle	Mission	Remarks
Oxidizer Turbopump Assembly (continued)		Underspeed	1. Loss of turbine blades	S	Slow engine start may result	None	Uncertain	
			2. Hot-gas leakage 3. Turbine control valve fails to open fully	M	Low operating mixture ratio may occur	Possible early depletion of tanked fuel	Possible abort	
		Internal shaft seal leakage	1. Damaged turbopump seal package	S,M, C	Probable failure of turbopump	None	Probable abort	
		External hot-gas leakage	1. Damaged duct or flange seal	S,M, C	Reduced turbine power available with subsequent reduction in thrust or mixture ratio	None	Possible abort	

CONFIDENTIAL

CONFIDENTIAL

TABLE I-8

SECONDARY ENGINE--THRUST CHAMBER ASSEMBLY

Item and Part No.	Function	Possible Type of Failure	Possible Failure Cause	Seq.	Probable Failure Effect			Remarks
					Engine	Vehicle	Mission	
Thrust Chamber Assembly	Assembly consists of injector and regeneratively cooled thrust chamber whose function is to efficiently convert the products of combustion of the propellants into directed thrust	Slight internal leakage	Thermal fatigue or material deficiency	S	Delayed start	None	Possible abort	
				M	Shift in engine controls and thrust alignment	Propellant bias and reduced control capability	Possible propellant depletion	
				C	Shift in engine thrust alignment during cutoff	Reduced control capability	None	
		Slight external leakage	Material deficiency	S,C, M	Shift in engine controls	Propellant bias	Possible propellant depletion	
		Obstruction of one invector orifice	Contamination	S,C, M	None	None	None	

P - Preflight checkout
S - Start sequence
M - Mainstage
C - Cutoff
O - Orbital coast

CONFIDENTIAL

DISTRIBUTION LIST

	No. of Copies
HQ USAF (AFRDSD/Lt Colonel Wolfsberger) 5D166 Pentagon Washington, DC 20330	1
HQ AFSC (DLSP/Lt Colonel Weiss) Andrews AFB Washington, DC 20331	1
SAMSO (SMTAX/Lt Colonel Clark) Air Force Unit Post Office Los Angeles, CA 90045	1
AFRPL (RPRES) Edwards, CA 93523	3
Defense Documentation Center Cameron Station Alexandria, VA 22314	1
Chemical Propulsion Information Agency Applied Physics Laboratory Johns Hopkins University 8621 Georgia Avenue Silver Spring, MD 20910	1
HQ NASA Attn: RPX, Mr. Stephenson Washington, DC 20546	1
NASA-Lewis Research Center Attn: Library 21000 Brookpark Road Cleveland, OH 44135	1
Aerojet-General Corporation Attn: Technical Library P.O. Box 1947 Sacramento, CA 95809	1
Aerospace Corporation Attn: Library P.O. Box 95085 Los Angeles, CA 90045	1
Bell Aerospace Company Attn: Library P.O. Box 1 Buffalo, NY 14203	1

McDonnel Douglas Corporation 1
Western Division
Attn: Library
Huntington Beach, CA 92647

General Dynamics/Convair 1
Attn: Library
P.O. Box 1128
San Diego, CA 92112

General Dynamics/Convair 1
Attn: Mr. M. R. Barlow
P.O. Box 1128
San Diego, CA 92112

Grumman Aircraft Engineering Corporation 1
Attn: Library
Bethpage, Long Island, NY 11714

Jet Propulsion Laboratory 1
Attn: Library
4800 Oak Grove Drive
Pasadena, CA 91101

Lockheed Missiles and Space Company 1
Attn: Library
1111 Lockheed Way
Sunnyvalve, CA 94088

LTV 1
Astronautics Division
Attn: Library
P.O. Box 6267
Dallas, TX 75222

Martin Company 1
Attn: Library
Denver, CO 80201

North American Rockwell Corporation 1
Space Division
Attn: Library
12214 Lakewood Blvd.
Downey, CA 92042

North American Rockwell Corporation 2
Rocketdyne Division
Attn: Library
6633 Canoga Avenue
Canoga Park, CA 91304

TRW Space Technology Laboratories 1
Attn: Library
One Space Park
Redondo Beach, CA 90278

UNCLASSIFIED

CONFIDENTIAL

Security Classification

DOCUMENT CONTROL DATA - R & D

(Security classification of title, body of abstract and indexing annotation must be entered when the overall report is classified)

1. ORIGINATING ACTIVITY (Corporate author) Rocketdyne, a Division of North American Rockwell Corporation, 6633 Canoga Avenue, Canoga Park, California 91304	2a. REPORT SECURITY CLASSIFICATION CONFIDENTIAL 2b. GROUP 4

3. REPORT TITLE

Advanced Maneuvering Propulsion Technology Program--Interim Final Report (Volume I: Fluorine/Hydrogen Engine System Analysis and Design)

4. DESCRIPTIVE NOTES (Type of report and inclusive dates)

Interim Final (November 1967-June 1970)

5. AUTHOR(S) (First name, middle initial, last name)

Rocke i .ne Engineering

6. REPORT DATE	7a. TOTAL NO. OF PAGES	7b. NO. OF REFS
October 1970	502	23

8a. CONTRACT OR GRANT NO. F04611-67-C-0116	9a. ORIGINATOR'S REPORT NUMBER(S) R-8280 (Vol. I)
b. PROJECT NO.	
c.	9b. OTHER REPORT NO(S) (Any other numbers that may be assigned this report) AFRPL-TR-70-127
d.	

10. DISTRIBUTION STATEMENT

Qualified users may obtain copies of this report from the Defense Documentation Center

11. SUPPLEMENTARY NOTES	12. SPONSORING MILITARY ACTIVITY
	AFRPL AFSC USAF--Edwards AFB, California

13. ABSTRACT

(U) The analysis and design studies conducted on the fluorine/hydrogen engine system of the Advanced Maneuvering Propulsion System (AMPS) are presented. The work included the engine system, thrust chamber assemblies, turbopump assemblies, and controls. Design requirements, design tradeoffs, operating characteristics, and layout drawings are shown for the major components and system.

DD FORM 1 NOV 65 1473

CONFIDENTIAL

UNCLASSIFIED

Security Classification

14 KEY WORDS	LINK A		LINK B		LINK C	
	ROLE	WT	ROLE	WT	ROLE	WT
Maneuvering						
ΔV						
Liquid Fluorine						
Liquid Hydrogen						
High Performance						
Channel-Wall Cooling						
Centrifugal Pump						